UNIVERSITY OF LILLE

DOCTORAL THESIS

BIOLOGY AND HEALTH DOCTORAL SCHOOL

Doctorate speciality: Cellular and Molecular Aspects of Biology

Caroline MOLINARO

Mechanism of action of a new organometallic compound inhibitor of topoisomerase I in adenocarcinomas

JANUARY 18th 2023

Thesis Directors:
Dr. Katia CAILLIAU-MAGGIO (HDR) – Senior Lecturer at the University of Lille
Dr. Alain MARTORIATI (HDR) – Senior Lecturer at the University of Lille

JURY:

Rapporteurs:
Dr. Dennis GOMEZ (HDR) – Research Associate at the IPBS – Toulouse
Dr. Marie-Emilie TERRET (HDR) – Research Director at the Collège de France – Paris

Examiners:
Pr. Jean-François BODART (HDR) – Professor at the University of Lille (Jury President)
Dr. Céline GONGORA (HDR) – Research Director at the IRCM – Montpellier

Invited:
Pr. Lydie PELINSKI (HDR) – Professor at the University of Lille
Dr. Chann LAGADEC (HDR) – Senior Research Associate at CANTHER – Lille

Unité de Glycosylation Structurale et Fonctionnelle (UGSF – UMR 8576 CNRS) – University of Lille – Regulation of Early Development Team – Bâtiment SN3 – Cité Scientifique – Avenue Carl Von Linné – Villeneuve-d'Ascq 59650 – France

UNIVERSITÉ DE LILLE

THÈSE DE DOCTORAT

ÉCOLE DOCTORALE BIOLOGIE-SANTÉ

Spécialité de Doctorat : Aspects cellulaire et moléculaire de la Biologie

Caroline MOLINARO

Mécanisme d'action d'un nouveau composé organométallique inhibiteur des topoisomérases I d'adénocarcinomes

18 JANVIER 2023

Directeurs de thèse :
Dr. Katia CAILLIAU-MAGGIO (HDR) – Maître de Conférence à l'Université de Lille
Dr. Alain MARTORIATI (HDR) – Maître de Conférence à l'Université de Lille

JURY :

Rapporteurs :
Dr. Dennis GOMEZ (HDR) – Chargé de Recherche à l'IPBS – Toulouse
Dr. Marie-Emilie TERRET (HDR) – Directeur de Recherche au Collège de France – Paris

Examinateurs :
Pr. Jean-François BODART (HDR) – Professeur à l'Université de Lille (Président du Jury)
Dr. Céline GONGORA (HDR) – Directeur de Recherche à l'IRCM – Montpellier

Invités :
Pr. Lydie PELINSKI (HDR) – Professeur à l'Université de Lille
Dr. Chann LAGADEC (HDR) – Chargé de Recherche à CANTHER – Lille

Unité de Glycosylation Structurale et Fonctionnelle (UGSF – UMR 8576 CNRS) – Université de Lille – Regulation of Early Development Team – Bâtiment SN3 – Cité Scientifique – Avenue Carl Von Linné – Villeneuve-d'Ascq 59650 – France

REMERCIEMENTS

Mes remerciements vont aux **Pr. Christophe D'Hulst** et **Dr. Yann Guerardel**, précédent et actuel Directeurs de l'UGSF, pour avoir accepté mon inscription lors du M2 ainsi que de la thèse.

Je remercie **Dr. Marie-Emilie Terret** et **Dr. Dennis Gomez** d'avoir accepté d'être rapporteurs de cette thèse, **Dr. Céline Gongora** d'en être examinateur, malgré la distance à parcourir pour vous trois, ainsi que **Pr. Jean-François Bodart**, d'avoir accepté d'en être Président. De plus, je tiens à remercier **Dennis**, accompagné de **Dr. Chann Lagadec**, de m'avoir accompagné en tant que membres de mon comité de suivi de thèse durant ces trois ans, ainsi que pour votre bienveillance à mon égard et l'aide que vous m'avez apporté. Merci également à **Chann** pour la généreuse donation de cellule pour approfondir mes recherches. Enfin, merci à vous cinq pour le temps que vous m'avez accordé et votre expertise.

***

Je tiens à remercier mes directeurs de thèse **Dr. Katia Cailliau** et **Dr. Alain Martoriati**. Merci de m'avoir accepté en stage de L3 en 2017 et de m'avoir fait découvrir pour la première fois ce qu'est la recherche. Le stage m'avait conforté dans l'envie de continuer les études pour pouvoir devenir un jour moi-même chercheur. Ce stage s'est tellement bien passé que je suis revenue, deux ans plus tard, pour un stage de M2, avec cette fois l'idée en tête de postuler pour la bourse de thèse sous votre direction. Vous avez été des directeurs admirables, toujours disponibles si j'avais besoin d'aide, pour discuter sur des projets de manips et réfléchir ensemble à un protocole. En plus de votre accompagnement intellectuel, j'ai la chance que vous soyez deux personnes très sympathiques, sociables et drôles. Je reviendrais vous voir pour se faire un petit Burger King de temps en temps !

Je tiens également à remercier tous les membres du laboratoire, **Pr. Jean-François Bodart**, **Dr. Matthieu Marin**, **Dr. Ingrid Fliniaux**, **Dr. Yoshiko Uchimura** et **Guillaume Marchand**, la seule chose moins chaleureuse que vous est la température au laboratoire. Je remercie **Matthieu** et **Ingrid** pour leur extrême sympathie, **Yoshiko**, notre nouvelle recrue dans l'équipe, pour ses échanges sur le Japon, どうもありがとう, et **Guillaume**, avec qui nous avons des passions communes sur lesquelles nous pouvions échanger. Je te souhaite bon courage pour la suite de ta thèse. Je remercie également **Arlette Lescuyer**, qui m'a beaucoup appris et transmis ses connaissances en biologie moléculaire, à qui je souhaite une très belle et reposante retraite. Merci également à **Jean-François**, qui a chaleureusement accepté de présider ce jury de thèse.

Je remercie également les membres de l'UGSF avec qui j'ai pu collaborer durant mes trois années de thèses, **Pr. Tony Lefebvre** et **Dr. Anne-Sophie Edouart** pour nos discussions, l'aide avec le cytomètre et l'échange de cellules, **Dr. Corentin Spriet** pour la formation et son aide à la miscroscopie à fluorescence, **Dr. Jérôme de Ruyck** et **Dr. Julie Bouckaert**, pour la

modélisation et l'analyses docking du composé à venir, **Dr. Stéphan Hardivillé** pour les expériences sur les organoïdes, et **Pr. Jean-Marie Lacroix** et **Dr. Edwige Madek** pour l'accompagnement de l'analyse du composé sur les bactéries.

Merci au **Pr. Lydie Pelinski** pour les composés, pour les discussions que nous avons pu avoir sur le sujet et l'avancée de mes résultats, ainsi que pour votre sympathie.

Je remercie les stagiaires de L3 et BTS que j'ai pu encadrer durant ma thèse, **Claire Mikolajczak**, **Clémence Burnichon**, **Lucas Legrand**, **Julien Anquet**, ainsi que **Pauline Titran**, **Angèle Marquey** et **Marie Closset** avec qui j'ai pu partager mes connaissances lors de leur M2. Ça a été très agréable de partager ces moments avec vous. Votre encadrement m'a permis de renforcer mes connaissances et c'est en apprenant aux autres qu'on apprend soi-même.

***

Je remercie bien évidemment tout mes collègues de biologie depuis la L1, avec lesquels nos parcours se sont en grande partie éloignés. Un remerciement tout particulier à **Clément Fauvet**, **Mike Everaer** et **Mathilde Brulé** sans lesquels les études n'auraient pas été les mêmes. **Mathilde**, qu'auraient été mes années thèse sans toi. Je suis heureuse que nos chemins se soient croisés en L3, dès nos premiers travaux collectifs, nous avons su que nous étions faites pour travailler ensemble. En plus de partager notre amour pour la biologie, nous partageons les mêmes passions pour les parcs et autres licences… Merci d'avoir été là pour moi, j'espère que nous serons amenées à travailler de nouveau ensemble dans le futur. Je te souhaite toute la réussite du monde, tu le mérites, pour ton travail acharné, ainsi qu'une bonne dernière année de thèse.

Pour finir, je remercie bien évidemment tous les membres de ma famille, mes parents, qui m'ont toujours soutenu et ont toujours cru en moi. Je reconnais votre fierté et je vous en remercie. J'espère que papa pourra suivre ce travail de là-haut, j'aurais aimé pouvoir le partager avec toi, toi qui m'as transmis la soif de connaissances. Merci à toutes mes sœurs et mon frère, mes neveux, nièces, filleule, tantes, oncles, merci d'être là.

À mon Père, là-haut,

À ma Mère, qui a touché les étoiles.

Abstract: **Mechanism of action of a new organometallic compound, WN197, inhibitor of topoisomerases, inducer of cell cycle arrest and cell death.**

Keywords: Indenoisoquinoline, copper (II) complex, adenocarcinoma, topoisomerases, DNA Damage Response (DDR), cell cycle, autophagy.

Topoisomerases are the targets for inhibitors used in chemotherapy that induce DNA breaks accumulation leading to cancer cell death. A new copper (II) indenoisoquinoline complex was synthetized (WN197), and its activity and action mechanisms on cancer cells were determined. WN197 is cytotoxic below 0.5 µM, on MDA-MB-231 (triple-negative breast cancer), HeLa (cervical cancer), and HT-29 cells (colon cancer). At low doses, WN197 inhibits topoisomerase I. At higher doses, it inhibits topoisomerase IIα and IIβ and displays DNA intercalation properties. DNA damage, detected by the presence of γH2AX, is present in the three adenocarcinoma cell lines. The activation of the DNA Damage Response (DDR) occurs through the phosphorylation of ATM/ATR, Chk1/2 kinases, and an increase in p21 quantity, a p53 target. WN197 induces a G2 phase arrest characterized by the unphosphorylated form of histone H3, the accumulation of phosphorylated Cdk1, and an association of Cdc25C with 14.3.3. Cancer cells die by autophagy with Beclin-1 accumulation, LC3-II formation, p62 degradation, and RAPTOR phosphorylation in the mTOR complex. WN197 keeps its cytotoxic effect on multi-drug resistant cells, H69AR, with an IC_{50} below 0.7 µM, displays a higher IC_{50} on non-tumorigenic breast cells above 1 µM, and reveals no toxicity on Xenopus embryonic development. Finally, WN197, by inhibiting topoisomerase I at low concentration with high efficiency, is a promising agent for the development of future DNA damaging chemotherapies.

Résumé : **Mécanismes d'action d'un nouveau composé organométallique, WN197, inhibiteur des topoisomérases, inducteur d'arrêt dans le cycle cellulaire et de mort cellulaire.**

Mots-clés : Indénoisoquinoline, complexe cuivre (II), adénocarcinome, topoisomérases, DNA Damage Response (DDR), cycle cellulaire, apoptose, autophagie.

Les topoisomérases sont les cibles d'inhibiteurs en chimiothérapie induisant une accumulation de dommages à l'ADN, conduisant à la mort cellulaire. Un nouveau composé d'indénoisoquinoline cuivré a été synthétisé (WN197). Ses mécanismes d'action ont été déterminés sur trois lignées d'adénocarcinomes humains. WN197 est cytotoxique à des concentrations inférieures à 0,5 µM sur les lignées cancéreuses MDA-MB-231 (sein), HeLa (col de l'utérus) et HT-29 (côlon). À ces doses, WN197 inhibe les topoisomérases I. À des doses plus élevées (> 1 µM), il inhibe les topoisomérases IIα et IIβ et possède des propriétés intercalantes. Les dommages à l'ADN sont détectés par la présence de γH2AX, et La phosphorylation d'ATM/ATR et des kinases Chk1/Chk2 et l'augmentation des quantités de p53 et p21 démontrent l'activation du DDR dans les trois lignées. WN197 provoque un arrêt des cellules en phase G2 caractérisé par le maintien de Cdk1 inactif dû à l'association de Cdc25C à 14.3.3, et par la forme non-phosphorylée de l'histone H3. Les cellules cancéreuses meurent par autophagie avec une accumulation de Beclin-1, la formation de LC3-II, la dégradation de p62 et la phosphorylation de RAPTOR dans le complexe mTOR. WN197 s'avère cytotoxique sur des cellules H69AR « multi-drug resistant », avec un IC_{50} inférieur à 0,7 µM, et possède un IC_{50} supérieur à 1 µM sur une lignée du sein non-tumorigénique, et ne se révèle pas toxique pour le développement embryonnaire du Xénope. En inhibant les topoisomérases I à faible concentration avec une forte efficacité, WN197 est un agent prometteur pour le développement de futures chimiothérapies ciblant l'ADN.

Résumé substantiel en Français

RESUME SUBSTANTIEL FRANÇAIS DE LA THESE

Mécanismes d'action d'un nouveau composé organométallique, WN197, inhibiteur des topoisomérases, inducteur d'arrêt dans le cycle cellulaire et de mort cellulaire.

CONTEXTE SCIENTIFIQUE

Le cancer reste de nos jours un problème de santé mondial avec 19,3 millions de nouveaux cas et 9,96 millions de décès en 2020 (GLOBOCAN – WHO). Plusieurs traitements sont actuellement proposés aux patients, dont des chimiothérapies qui regroupent diverses molécules cytotoxiques, comme les agents alkylants (ex : cisplatine), des poisons du fuseau mitotiques (ex : nocodazole), ou encore des inhibiteurs des topoisomérases (ex : doxorubicine).

Les topoisomérases sont des enzymes de contrôle de la structure de l'ADN, dont elle diminue la torsion et l'enroulement afin de permettre la réplication, la transcription, et la séparation des chromosomes. Ces enzymes se lient à l'ADN puis génèrent des coupures transitoires avant de les refermer (Champoux, 2001 ; Pommier, 2013). Chez l'homme, les topoisomérases se classent dans les sous-groupes IA, IB et IIA. Les deux derniers groupes sont particulièrement ciblés dans le cadre des thérapies anticancéreuses. Leur inhibition provoque des cassures simples (type I) ou doubles (type II) brins de l'ADN, et est d'autant plus efficace que les topoisomérases sont surexprimées dans de nombreux cancers (Pommier, 2009 et 2013 ; Gouveris *et al*., 2011).

Ces inhibiteurs peuvent être des poisons qui se lient au complexe de clivage ADN-topoisomérase, formant un complexe tertiaire ADN-topoisomérase-inhibiteurs. Ils empêchent la religation des brins clivés de l'ADN. Ces dommages déclenchent une signalisation de réparation couplée à un arrêt dans le cycle ou une mort cellulaire s'ils sont trop étendus (Pommier, 2009 et 2013 ; Pommier *et al*., 2010 ; Ho Seo, 2015). Les inhibiteurs peuvent également être de types catalytiques (intercalants de l'ADN ; compétiteurs pour l'ATP ; inhibiteurs de l'hydrolyse de l'ATP), bloquer l'ADN et provoquer une activité anti-néoplasique (Larsen *et al*., 2003 ; Pommier 2013).

Parmi les inhibiteurs de topoisomérases I, le topotecan et l'irinotecan sont utilisés dans le traitement des cancers ovariens, de l'utérus et du côlon. La doxorubicine est un inhibiteur de topoisomérase II prescrits contre divers carcinomes, sarcomes et lymphomes. Néanmoins, les effets secondaires de ces molécules sont élevés (toxicité hématologique, vomissement, diarrhées, leucémies associées à la thérapie, cardiotoxicité), et elles provoquent des phénomènes de résistances des cellules cancéreuses, soit par augmentation de la production de transporteurs d'efflux (PGP, MRP, ABCG2…), soit par mutation des topoisomérases

(Pommier, 2009). Limiter au maximum les effets secondaires et contourner les phénomènes de résistances nécessitent la recherche permanente de nouvelles molécules toujours plus efficaces pour traiter ces cancers.

CONTEXTE DE RECHERCHE

Quatorze organométalliques dérivés de l'indénoisoquinoline (inhibiteurs de topoisomérase I) ont été développés par l'équipe du Pr. Pelinski (Unité de Catalyse et Chimie du Solide – Université de Lille). Leur toxicité a été testée dans notre laboratoire sur 5 lignées cellulaires cancéreuses via des tests MTS. La molécule appelée WN197 possédant les IC_{50} les plus faibles est une indénoisoquinoline à laquelle a été ajoutée une chaine latérale complexée à un atome de cuivre. Elle agit avec un IC_{50} de 0,144 µM sur la lignée MDA-MB-231 (cancer du sein triple négatif), de 0,644 µM sur la lignée MCF-7 (cancer du sein ER^+, PR^+, HER^-), de 0,22 µM sur la lignée HeLa (cancer du col de l'utérus), de 0,358 µM sur la lignée HT-29 (cancer du côlon), et de 0,162 µM sur la lignée DU-145 (cancer de la prostate). Le ligand sans molécule de cuivre, WN170, est utilisé comme contrôle pour déterminer l'apport du cuivre au complexe.

Dans ma thèse, trois adénocarcinomes ont été choisis en raison de leur taux d'incidence très élevé : le cancer du col de l'utérus (lignée HeLa), le cancer du sein triple négatif (MDA-MB-231) et le cancer du côlon (HT-29). Le projet de thèse vise à comprendre les mécanismes d'action de WN197 sur ces trois lignées, avec successivement la détermination précise de l'induction des dommages à l'ADN et du type d'inhibition sur les topoisomérases (type I et/ou II ; type poison ou catalytique), des impacts sur le cycle cellulaire et les acteurs moléculaires ciblés, du type de mort cellulaire activée, des potentielles résistances associées et de la toxicité sur des lignées cellulaires non cancéreuses ainsi que sur le développement embryonnaire du Xénope.

RESULTATS

I. Endommagement de l'ADN des lignées d'adénocarcinomes par le composé WN197

Les dommages à l'ADN induits par le composé WN197 ont été mis en évidence de manière indirecte par la présence du marqueur γH2AX en immunofluorescence et Western blot (Kinner *et al.*, 2008). Les cellules témoins (DMSO, 0,5%) ne présentent pas ou peu de marquage indiquant une absence de cassures de l'ADN. La doxorubicine, un inhibiteur des topoisomérases II utilisé comme témoin des cassures de l'ADN, provoque une importante formation de γH2AX nucléaire, reflet de nombreuses cassures. Après traitement avec WN197 (0,5 µM) 30 min ou 24 h, de nombreux *foci* (accumulations de marquage) sont retrouvés,

montrant que WN197 induit des dommages à l'ADN précocement après 30 min, de manière plus importante que pour le composé WN170 (sans atome de cuivre).

II. Effet de WN197 sur l'activité des topoisomérases

Des tests de mesure d'activité de la topoisomérase I (Top1) *in vitro* ont permis de démontrer que WN197 est un inhibiteur des Top1 à faible dose (0,2 µM), et que celui-ci agit à la manière d'un poison (formation d'un complexe ADN-Top1-inhibiteur → stabilisation d'ADN ébréché ; e.g. camptothécine). Des doses plus élevées de WN197 (0,5 µM, 1 µM et 2 µM) induisent une inhibition de la Top1 mais présentent un profil de migration d'ADN différent pouvant amener à penser à une intercalation dans l'ADN, au même titre que la doxorubicine à doses élevées.

Des tests d'inhibition *in vitro* des Top2α et β ont également été réalisés. En présence de Top2, l'ADN présente un profil relâché caractéristique après migration en gel d'agarose. En ajoutant de l'étoposide (VP-16 ; contrôle positif), le relâchement de l'ADN est perturbé et reste sous forme superenroulé. A partir de 2 µM de WN197, la présence d'ADN relâché diminue, montrant une perturbation de l'activité de la Top2α à 2 µM, et dès 1 µM pour la Top2β. Le DMSO (contrôle de solvant) n'inhibe pas l'activité des Top2.

III. Activation de la voie DDR des lignées d'adénocarcinomes

La voie DDR (DNA Damage Response) est une signalisation intracellulaire activée naturellement lorsque l'ADN subit des dommages pour dans un premier temps arrêter les cellules dans le cycle, ou induire la mort cellulaire si les dommages sont trop importants (Hakem, 2008). Des effecteurs de cette voie ont été analysés par Western blot : ATR et ATM sont les premières kinases activées après cassures simple ou double brin(s) respectivement. Elles activent les kinases Chk1 et Chk2, elles-mêmes suivies de p53 et p21. La phosphorylation activatrice d'ATR (S428) a été observée sur les 3 lignées d'adénocarcinomes. Une nette augmentation de l'activation d'ATR est constatée pour les cellules traitées avec WN197 comparées aux cellules non traitées. La même augmentation se retrouve pour la phosphorylation activatrice d'ATM (S1981). Les deux kinases suivantes de la signalisation, Chk1 et Chk2, sont également activées (S317 et T68 respectivement), ainsi que la phosphorylation de p53 (S15) et la quantité de p21, confirmant que la voie DDR est activée.

IV. Effet de WN197 sur le cycle cellulaire des lignées d'adénocarcinomes

La répartition des cellules MDA-MB-231, HeLa et HT-29 dans le cycle cellulaire a été analysée par cytométrie en flux. Les cellules non traitées montrent une répartition classique de la population cellulaire dans le cycle. Après 24 h de traitement avec WN197 à 0,5 µM, en moyenne, une accumulation de 70,51% des cellules en phase G2/M est observée.

Pour les doses-réponses, les cellules ont été exposées à des doses croissantes de WN197 pendant 24 h puis analysées par cytométrie en flux. Une accumulation significative des cellules en phase G2/M est retrouvée à partir de 0,5 µM pour les MDA-MB-231, et pour les HeLa et HT-29 à 0,25 µM, mais avec une baisse d'accumulation à 1 µM. Ceci indiquerait un mode d'action différent du composé à de plus fortes doses comme observé avec les tests topoisomérases *in vitro*. Pour les cinétiques, les cellules ont été exposées à 0,5 µM de WN197 de 4 h à 48 h. Une accumulation significative des cellules en G2/M est observée dès 8 h pour les MDA-MB-231, 12 h pour les HT-29, et un peu plus tardivement pour les HeLa à partir de 16 h. Une diminution de l'accumulation est observée après 48 h.

La cytométrie ne permettant pas de distinguer si les cellules sont bloquées en phase G2 ou M, l'arrêt en phase G2 du cycle cellulaire a été précisé sur les trois lignées par une analyse en Western blot de l'état de phosphorylation et/ou de la quantité de certains acteurs majeurs de la régulation de la transition G2/M : la kinase Cdk1, la cycline B, la phosphatase Cdc25C et l'histone H3. La kinase Cdk1 couplée à la cycline B forme un complexe appelé MPF. Lors de la transition G2/M, Cdk1 est activée par les déphosphorylations de ses résidus thréonine 14 et tyrosine 15 (phosphorylations inhibitrices) réalisées par Cdc25C, et par une phosphorylation activatrice de la thréonine 161 par la CAK (Hakem, 2008). Dans cet état, le MPF actif permet le passage des cellules de la phase G2 à la phase M du cycle cellulaire. La phosphorylation du résidu tyrosine 15 de Cdk1 augmente après traitement avec WN197 comparé au témoin sans traitement, ainsi que la quantité de cycline B, suggérant un défaut d'activation du MPF. Ce dernier serait la conséquence de l'inactivation de Cdc25C dans cette condition puisque les quantités de Cdc25C et de sa forme inactive phosphorylée sur le résidu sérine 216 (phosphorylation inhibitrice) en présence de WN197 étaient plus élevées que pour le témoin. Enfin, l'histone H3 phosphorylée sur la sérine 10, marqueur d'entrée en phase M du cycle cellulaire, n'est pas retrouvée après traitement avec WN197. Ces résultats démontrent que WN197 provoque un arrêt des cellules en phase G2 du cycle cellulaire plutôt qu'en phase M, en induisant une accumulation de Cdk1 inactive phosphorylée sur la tyrosine 15. Ce défaut d'activation de Cdk1 est accompagné d'une accumulation de cycline B et de l'absence de phosphorylation de l'histone H3 caractéristiques de la phase G2.

Quand Cdc25C est inactivée par phosphorylation sur la S216, 14-3-3 reconnait et s'associe à la phosphatase, puis l'exporte hors du noyau. Pour confirmer les résultats précédents liant WN197 et l'inactivation de Cdc25C, des immunoprécipitations (IP) de Cdc25C ou 14-3-3 ont été réalisées sur les trois lignées. Sans traitement, les deux molécules ne sont pas retrouvées couplées (absence de Cdc25C après IP de 14-3-3, et absence de 14-3-3 après IP de Cdc25C). En revanche, après traitement avec le cisplatine (témoin positif) ou WN197, les deux molécules sont immunoprécipitées. Ces résultats confirment que Cdc25C est inhibée et couplée à 14-3-3 après un traitement des cellules avec WN197.

V. Mort cellulaire induite par WN197 sur les lignées d'adénocarcinomes

Une des voies classiquement activées après des dommages à l'ADN est l'apoptose. Les formes clivées de la caspase 3 et de la PARP, marqueurs reconnus de ce type de mort cellulaire n'ont pas été retrouvées après un traitement avec WN197. De la même manière, le cytochrome *c* n'a pas été retrouvé dans le cytoplasme des cellules après traitement avec WN197, comparé au contrôle positif inducteur de l'apoptose, la doxorubicine. Les résultats ont été confirmés à l'aide de l'analyse annexine-V/iodure de propidium en cytométrie en flux. Un faible pourcentage de cellules est retrouvé en apoptose précoce et tardive avec une moyenne de 17% pour les MDA-MB-231, HeLa et HT-29. Ces résultats excluent donc une induction de l'apoptose par WN197. L'autophagie a ensuite été étudiée.

LC3, présent sous forme LC3-I dans les cellules, s'associe avec la phosphatidyléthanolamine pour former LC3-II lors du mécanisme d'autophagie (Kroemer *et al.*, 2009). Ce changement de conformation a été analysé dans les 3 lignées d'adénocarcinomes après 24 h de traitement. Après traitement avec la rapamycine (inducteur d'autophagie) une augmentation de LC3-II est détectée, de même qu'après un traitement avec 0,5 µM de WN170 ou WN197. Un deuxième marqueur, p62, dégradé lors de l'autophagie a été observé par WB. Après traitement avec la rapamycine, une perte de p62 est constatée, tout comme pour les traitements avec WN170 et WN197. Le troisième marqueur étudié est la protéine Beclin-1, synthétisée lors de l'autophagie. Celle-ci est retrouvée de manière plus élevée pour les trois lignées cancéreuses traitées avec WN197.

Lors de l'autophagie, la protéine RAPTOR (regulatory-associated protein of mTOR) est phosphorylée sur la serine 792 dans le complexe mTOR (Ma *et al.*, 2018). La présence de la forme phosphorylée de RAPTOR dans le complexe mTOR a été retrouvée par immunoprécipitation pour les trois lignées, après un traitement de 24 h avec la rapamycine ou WN197 (0,5 µM), contrairement au témoin et au contrôle négatif (doxorubicine, inducteur d'apoptose).

L'activation de l'autophagie a finalement été vérifiée par un marquage fluorescent et une quantification des autophagosomes. Ces autophagosomes sont plus abondants dans les cellules traitées à la rapamycine et avec WN197 comparés au contrôle DMSO (0,5%, moyenne de 7) avec une moyenne de 186 pour la rapamycine et de 66 pour WN197 dans les lignées MDA-MB-231 et HeLa.

L'ensemble de ces résultats démontrent que WN197 induit la mort des cellules cancéreuses par autophagie.

VI. Effet de WN197 sur des lignées du sein tumorigènes et non-tumorigènes.

Le composé WN197 a été testé sur une lignée de cellules non cancéreuses du sein MCF-10A par MTS. L'IC_{50} relevé est de 1,080 µM, une valeur significativement plus élevée de 3 à 7 fois en comparaison des IC_{50} déterminés sur les lignées cancéreuses.

Pour compléter les résultats obtenus sur les lignées mammaires (cancéreuses MDA-MB-231, MCF-7 ; et non-cancéreuse MCF-10A), des MTS ont été réalisés sur deux autres lignées triple-négatives : les BT-549 et le SUM-159. Les IC_{50} obtenus sont également faibles : sur la lignée BT-549 de 0,676 µM pour WN197 et 0,691 µM pour WN170 ; et sur la lignée SUM-159 de 0,679 µM pour WN197 et 0,689 µM pour WN170.

VII. Effet de WN197 sur la lignée multi-drug resistant H69AR

Le test de viabilité MTS a été réalisé sur la lignée multi-drug resistant (MDR) H69AR du poumon. Les IC_{50} obtenus sont de 0,683 µM pour WN197 et 4,966 µM pour WN170. Ces valeurs sont proches de celles obtenues sur les adénocarcinomes pour WN197 (moyenne de 0,306 µM), mais s'en éloignent pour WN170 (moyenne de 0,550 µM).

VIII. Effet de WN197 sur les ovocytes de *Xenopus laevis*

La cytotoxicité de WN197 a été déterminée sur le développement d'embryons de *Xenopus laevis* exposés au composé. Aucune variation de viabilité n'est observée après traitement avec WN197 en comparaison avec les contrôles non traités.

CONCLUSION ET PERSPECTIVES

Les résultats obtenus montrent que WN197 est un potentiel agent anti-cancéreux en inhibant les topoisomérases 1 à faibles doses (0,2 µM), autour des IC_{50}. Dans les lignées de cancer du sein MDA-MB-231, de cancer du col de l'utérus HeLa et du côlon HT-29, WN197 induit l'accumulation de dommages à l'ADN, suivi par l'activation de la voie DDR et par un arrêt des cellules en phase G2 du cycle cellulaire. Cet arrêt est caractérisé par l'accumulation de MPF sous forme inactive (Cdk1 phosphorylé sur la Y15), consécutivement à l'inactivation de Cdc25C *via* une phosphorylation sur S216 et son attachement à 14-3-3. L'accumulation des cassures de l'ADN irréparables conduisent à la mort des cellules par autophagie. Le composé WN197 a particulièrement de faibles IC_{50} sur les cellules cancéreuses (nM), et plus élevé (µM) sur la lignée non-cancéreuse MCF-10A. Le composé affecte aussi la viabilité cellulaire à ces faibles doses sur la lignée multi-drug resistant, H69AR. De plus, WN197 n'a pas d'effet sur le développement embryonnaire du Xénope. Ainsi, le composé WN197 est un candidat intéressant pour des études précliniques. Au préalable, des expériences seront réalisées sur des organoïdes et des études en modèle murin sont à envisager. Cette nouvelle molécule serait un atout pour des chimiothérapies ciblant les topoisomérases 1 seule ou en combinaison avec d'autres composés.

TABLE OF CONTENTS

LIST OF FIGURES AND TABLES

Introduction

Materials & Methods

Results

Conclusion & Perspectives

Appendices & Annexes

ABBREVIATIONS (PART 1/2)

Symbols

5-FU: 5-Fluorouracile

A

ABCG: ATP-Binding Cassette super-family G

AC: Adenocarcinoma

ALL: Acute Lymphoid Leukemia

AML: Acute Myeloid Leukemia

ASC: Adenosquamous carcinoma

ATM: Ataxia Telangiectasia Mutated

ATP: Adenosine Triphosphate

ATR: Ataxia Telangiectasia and Rad3-related protein

ATRIP: ATR-Interacting Protein

B

BCRP: Breast Cancer Resistance Protein

EGF/R: Epithelial Growth Factor / Receptor

EtBr: Ethidium Bromide

BSA: Bovine Serum Albumin

C

CAK: CDK-activating kinase

CDC25: Cell Division Control 25

Cdk: Cyclin Dependent Kinase

Chk: Checkpoint Kinase

Cis: Cisplatin

CML: Chronic Myeloid Leukemia

CPT: Camptothecin

Cu(II): Copper (II)

D

DAPI: 4,6-diamidino-2-phénylindole

DCFDA: Dichlorofluorescin Diacetate

DDR: DNA Damage Response

DMEM: Dulbecco's Modified Eagle's Medium

DMSO: Dimethylsulfoxyde

DNA-PK: DNA-dependent protein kinase

Doxo: Doxorubicin

DSB: Double Strand Break

E

ECL: Enhanced Chemiluminescence

EDTA: Ethylene Diamine Tetra-Acetic

ER: Estrogen Receptor

H

H2AX: Histone H2A family member X

HCl: Hydrogen chloride

HER: Human Epidermal growth factor Receptor

I

IARC: International Agency for Research on Cancer

IC_{50}: Half maximal inhibitory concentration

IF: Immunofluorescence

IPBS: Institut de Pharmacologie et de Biologie Structurale

K

KO: Knock-Out

L

$_L$DNA: linear DNA

M

MDR: Multi-drug resistance

ABBREVIATIONS (PART 2/2)

Mg^{2+}: Magnesium

MPF: Mitosis Promoting Factor

MRP: Multi-drug Resistance-associated Protein

mTOR: mechanistic Target of Rapamycin

MW: Molecular weight

N

NaCl: Sodium chloride

NaF: Sodium fluoride

$_N$DNA: nicked DNA

NHL: Non-Hodgkin Lymphoma

NP40: Nonyl Phenoxypolyethoxylethanol

NSCLC: Non-Small Cell Lung Cancer

P

PARP: Poly(ADP-Ribose) Polymerase

PBS: Phosphate Buffered Salin

PGP: Permeability-Glycoprotein

PE: Phosphatidylethanolamine

PI3K: Phosphatidylinositol 3-kinases

PR: Progesterone Receptor

R

$_R$DNA: relaxed DNA

RIPA: Radio Immuno-Precipitation Assay

ROS: Reactive Oxygen Species

RPA: Replication Protein A

RPM: Revolutions Per Minute

S

SCC: Squamous Cell Carcinoma

$_{SC}$DNA: supercoiled DNA

SCLC: Small Cell Lung Cancer

SDS: Sodium Dodecyl Sulfate

SSB: Single Strand Break

T

t-AML: therapy-related Acute Myeloid Leukemia

TBS: Tris-buffered Saline

TGS: Tris-Glycine-SDS

TK: Tyrosine Kinase

Top1/2/3: Topoisomerase 1/2/3

Top1mt: Mitochondrial Topoisomerase

TRIS: Tris(hydroxymethyl)aminomethane

U

UGSF: Unité de Glycobiologie Structurale et Fonctionnelle

V

VEGF/R: Vascular Endothelial Growth Factor / Receptor

VP-16: Etoposide

W

WB: Western Blot

WN170/197: Wambang Nathalie compound n°170/197

WW: Worldwide

Introduction

1 INTRODUCTION

1.1 SCIENTIFIC CONTEXT, CANCERS AND TOPOISOMERASES

1.1.1 Cancers

Nowadays, cancer is a major health problem with 19.3 million new cases and 9.96 million of deaths in 2020 in the world (GLOBOCAN 2020 – WHO – **Figure I**) and an estimation of 28.9 million new cases in 2040. 52% of the new cancer cases affected men and 48% women. The cancers with the most incidence in men include lung (14.3% of total cancer number), prostate (14%) and colorectal cancers (10.6%). In woman, cancer incidence is the highest for breast cancer (24.5%), followed by colorectal (9.4%) lung (8.3%) and cervical (6.5%). These four cancers were also the deadliest in women (15.5%, 9.5%, 13.7% and 7.7% respectively), and lung, liver and colorectal cancers were the deadliest in men (21.5%, 10.4% and 9.3% respectively).

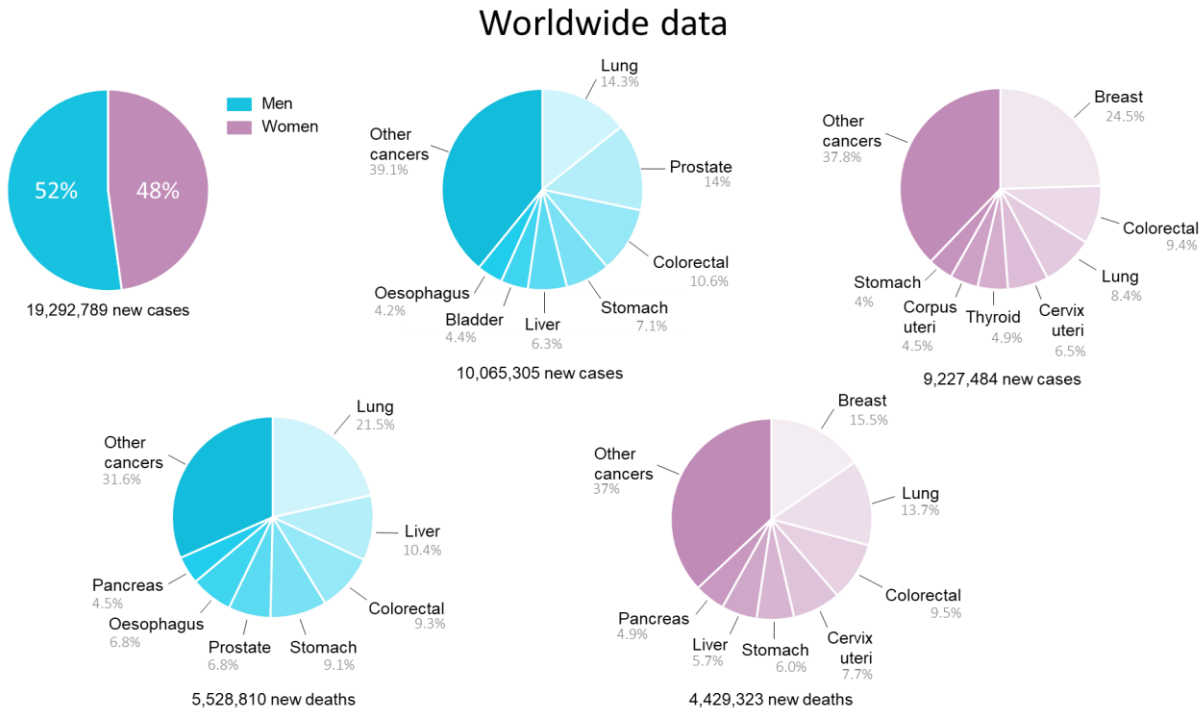

Figure I. Number of worldwide cancer new cases by gender (upper left), and distribution of new cases (upper middle and right) and new deaths (bellow) by gender (other cancers are listed in Appendice 1).

Cancers originate from various tissues. **Carcinoma** cancers originate from epithelial cells, **sarcomas** from non-hematopoietic mesenchymal cells (bone, muscle, fat, cartilage, tendons, nerves), **leukemias** and **lymphomas** from hematopoietic cells, either from bone marrow cells that mature in the bloodstream, or that mature in the lymphatic system. Less

common cancer includes **blastoma**, originating from precursor cells. Carcinomas are divided into various subgroups, determined by their histological aspects. Squamous cell carcinomas (SCC), also known as epidermoid carcinomas, arise from epitheliums covering both the outside of the body (skin) and the inside cavities. Adenocarcinomas (AC) arise from glandular cells and/or have glandular aspects. Mixtures of both types are called adenosquamous carcinomas (ASC). Anaplastic carcinomas are undifferentiated cells with excessive growth.

1.1.1.1 Breast cancer

Breast cancer is the most diagnosed cancer and the first cause of death by cancer among women with 58,500 new cases in France in 2018 and 12,100 deaths (with 1% of breast cancers in men) (INCa: France cancers panorama 2022). Most breast cancers arise from the gland duct (ductal carcinoma; 80%), but also from the lobules (lobular carcinoma) (**Figure II**) (Li *et al.*, 2005). Carcinoma can be *in situ* (not spread) or invasive (spread to other tissues).

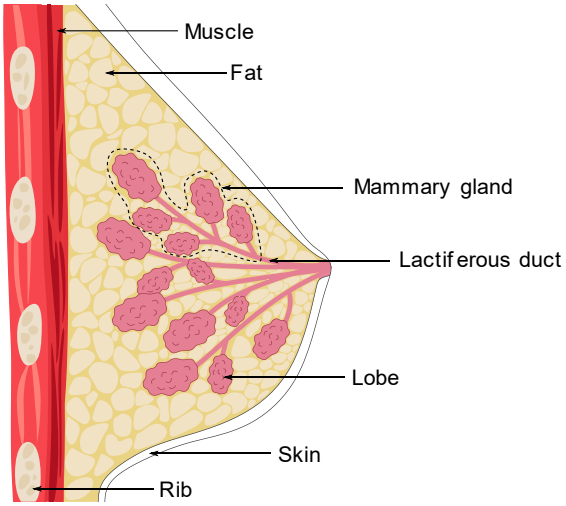

Figure II. Female breast anatomy.

Breast cancer cells can present receptors at their surface or not, classifying them hormono-dependent or -independent respectively. The three types of receptors present are the estrogen receptor (ER), the progesterone receptor (PR), and the human epidermal growth factor receptor 2 (HER2). Breast cancers can then be divided into three categories based on the receptors they express: luminal, HER2$^+$, or triple-negative (Phipps *et al.*, 2008; Waks and Winer, 2019). **Luminal A** tumor type represents cells expressing ERs and PRs but not HER2 (ER$^+$, PR$^+$, HER2$^-$), while **luminal B** type regroups cells expressing all three receptors (ER$^+$, PR$^+$, HER$^+$). **HER2$^+$** tumor type only expresses HER2 (ER$^-$, PR$^-$, HER2$^+$). The last category does not express any of the receptors and is called **triple-negative cancer** (ER$^-$, PR$^-$, HER2$^-$). Receptor-positive cancer cells can be treated with drugs inhibiting the receptors (hormonotherapy), while triple-negative cannot, rendering them more difficult to treat. Breast cancer incidence has increased by 0.6% each year between 2010 and 2018 (in France), but the number of deaths has diminished by 1.6% per year. The net standard survival rate for 5 years, representing the

people diagnosed and still alive 5 years later, is 87%. These cancers are detectable at early stages, and the widespread screening in the women's population explains the detection increase associated with the diminution of death. Yet, breast cancers aggressiveness depends on various factors including the expression of receptors (e.g. breast HER2$^+$ cancers are highly aggressive (Cossetti *et al.*, 2015)), the lack of receptor (triple-negative breast cancers) (Dent *et al.*, 2007), and the genetic aspect associated with the age of the patient (Kuchenbaecker *et al.*, 2017).

1.1.1.2 Cervical cancer

3,000 new cases of cervical cancers are diagnosed every year in France (INCa: France cancers panorama 2022). The cervix is covered by squamous cells on the outer surface (endocervix) and glandular cells on the inner surface (ectocervix) (**Figure III**).

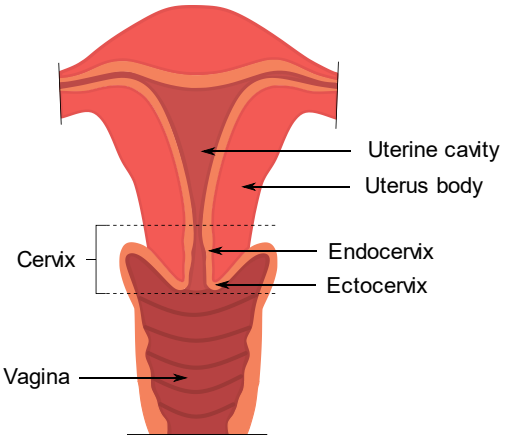

Figure III. Cervix anatomy.

Cervical cancers arise either from the squamous cells, causing a squamous cell carcinoma (SCC, about 70% of the cancer cases), or from the glandular cells, causing adenocarcinoma (AC, about 30% of the cancer cases) (Vizcaino *et al.*, 2000; Smith *et al.*, 2000). The cervical cancer incidence and the number of deaths decreased by 0.7% and 1.1% respectively every year between 2010 and 2018 (INCa: France cancers panorama 2022). The diminution can be explained by an increase of vaccination since the approval for the first vaccine in 2006 against the main infectious human papillomaviruses (HPV) (yet not all women and men eligible are vaccinated) (Cohen *et al.*, 2019). Moreover, pre-cancerous lesions of those cancers can be diagnosed by gynecologic screening. Nevertheless, the 5 years standardized survival rate for women diagnosed in 2010 is 63%, showing that those cancers remain difficult to treat.

1.1.1.3 Colorectal cancer

With 23,200 new cases in men and 20,100 in women in 2018, colorectal cancer is the second most frequent cancer among women and the third among men in France (INCa: France

cancers panorama 2022). It is also the third deadliest cancer among women and the second among men (9,200 deaths in men and 7,900 in women in France). Among colorectal cancers, an average of 60% is colon cancer, and 40% is rectum cancer. Because of the numerous glands of the colon, the majority of colon cancer are adenocarcinomas. They are either Lieberkühnian adenocarcinomas (carcinomas of the Lieberkühn glands, the most common) or mucinous adenocarcinomas (carcinomas of the epithelium tissue with abundant mucus secretion) (Fleming *et al.,* 2012). Colorectal cancers mainly arise from adenomatous polyps (benign tumor) (Cappell, 2005). A decrease of 1.4% number of cases per year is seen in men from 2010 to 2018, but no changes are reported for women. On the other side, the number of deaths has decreased for men and women, with 1.8% and 1.6% respectively. Those diminutions are explained by the increase of both immunologic tests to detect blood (hemoglobin) in feces, and high-risk factors in patients (polyps, genetics, inflammation) follow-up. However, the 5 years net survival rate after the established diagnosis is 63%, due to the high number of cancers detected at late stages and the lack of efficient treatments available.

1.1.2 Treatments

Several types of treatments are currently proposed to patients depending on the type and grade of cancer detected (**Table I**), but also the localization of the tumor, the age, and the health status given the medical and chirurgical antecedents, in addition to the side effects consequences of the treatments. The patient's choice is also considered, regarding his willingness to participate in therapeutic trials.

1.1.2.1 Surgery

Surgery of the primary tumor and surrounding tissues is the main treatment but is not sufficient to eradicate cancers that have reached the metastasis stage. Sometimes surgery can be preceded by neoadjuvant chemotherapy to diminish the size of the tumor, or after surgery with adjuvant chemotherapy to kill any remaining cancer cells and to avoid cancer recidivism (Lambert *et al.*, 2021; Kerr *et al*., 2022).

1.1.2.2 Radiotherapy

Radiotherapy is also given after surgery, to kill cancer cells that may have escaped the surgery, or before to reduce the tumor. It can also be proceeded after an adjuvant chemotherapy to complete the treatment. Radiotherapy can be realized internally, as brachytherapy (also known as curie therapy in French), or externally at determined doses (Ahmad *et al.*, 2012; De Ruysscher *et al.*, 2019). Both technics can be combined. Brachytherapy requires the implantation of the material next to the tumor (Chargari *et al.*, 2019). However, the ionizing radiations can also damage normal cells, leading to adverse effects (De Ruysscher *et al.*, 2019).

	Cancer type	Incidence (new cases) and deaths (2020 WW)	Risk factors	Treatments
Breast cancer	SCC, AC	2,261,419; 684,996	Alcohol, tobacco smoking, obesity, lack of physical activity, age (>50), menopause hormonotherapy, radiation, genetic predisposition/mutation (BRCA1/2…) familial or personal	Surgery *(tumorectomy or mastectomy)*, extern radiotherapy, brachytherapy, chemotherapy *(anthracyclines, taxanes, cyclophosphamide, 5-FU, carboplatin…)*, hormonotherapy (*tamoxifen, anastrozole, letrozole, exemestane…)*, targeted therapy *(trastuzumab, lapatinib, palbociclib, everolimus, alpelisib, olaparib…)*, immunotherapy (*pembrolizumab*)
Cervical cancer	SCC, AC	604,127; 341,831	HPV, tobacco smoking, extended use of hormonal contraceptives, immunosuppression	Surgery (*conization or hysterectomy*), extern radiotherapy, brachytherapy, chemotherapy (*carboplatin, cisplatin, paclitaxel, topotecan*), targeted therapy (*bevacizumab*), immunotherapy (*pembrolizumab*)
Colorectal cancer	AC	1,931,590; 935,173	Alcohol, tobacco smoking, obesity, lack of physical activity, age, alimentation (excessive red meat and insufficient fibers), familial background, polyps, Lynch syndrome (HNPCC), inflammatory diseases	Surgery (*hemicolectomy, colectomy, polypectomy, proctectomy*), extern radiotherapy, brachytherapy, chemotherapy (*oxaliplatin, capecitabine, irinotecan, raltitrexed, 5-FU*), targeted therapy (*bevacizumab, ramucirumab, ziv-aflibercept, cetuximab, panitumumab, encorafenib, regorafenib*) immunotherapy (*pembrolizumab, nivolumab, ipilimumab*)

Table I. Breast, cervical, and colorectal cancers and their cell types, incidences, associated deaths, risk factors, and treatments. AC: Adenocarcinoma; SCC: Squamous cell carcinoma; WW: Worldwide. References: GLOBOCAN 2020 – WHO; Waks and Winer, 2019; Cohen *et al.*, 2019; Ciombor *et al.*, 2014; Biller and Schrag, 2021.

1.1.2.3 Immunotherapy

Emerging therapies including **immunotherapy** can be proposed to patients, to help their immune system to fight cancer (monoclonal antibody inhibitors are discussed in targeted therapy §1.1.2.5.2, page 30). The first type of immunotherapy uses **immune checkpoint inhibitors**. Normal cells express immune checkpoint receptors on their surface, like PD-L1 or B7. These immune checkpoint receptors are recognized by specific ligands expressed on immune T cell surfaces, like PD-1 and CTLA-4 (Waldman *et al.*, 2020). They allow an inhibitory signal to be sent to the immune system cells to avoid their killing. Cancer cells have developed a mechanism to escape the immune system by expressing these receptors (Seidel *et al.*, 2018). Immune checkpoint inhibitors target these surface receptors to inhibit the escape signal, which induces cell destruction by the immune system (Wei et *al.*, 2018) (**Figure IV**). Actual treatments are composed of anti-PD-L1 (ex: atezolizumab), anti-PD-1 (ex: nivolumab), anti-CTLA-4 (ipilimumab), and anti-LAG-3 (relatlimab, in combination with nivolumab) antibodies (Hodi *et al.*, 2010; Seidel *et al.*, 2018; Wei et *al.*, 2018; Paik, 2022). Nonetheless, immune checkpoint inhibitors do not only target cancer cells, but also normal cells and are associated with auto-immune and infusion (allergic) reactions (Seidel *et al.*, 2018; Marin-Acevedo *et al.*, 2019).

The **T-cell transfer therapy** consists in the extraction and collection of patient T-cells (leukapheresis), called TIL (tumor-infiltrating lymphocytes). The most effective TIL against the patient tumor can be either collected and multiplied before a transfer into the patient's vain, called TIL therapy, or modified with the CAR (chimeric antigen receptor) gene (through a retrovirus) to produce the associated protein, called CAR T-cell therapy (Wang *et al.*, 2014; Houot *et al.*, 2015) (**Figure IV**). CARs recognize specific antigens on the cancer cell surface to improve the effectiveness of T-cells against the tumorigenic cells. The first CAR-T drug FDA approved was tisagenlecleucel in 2017 (O'Leary *et al.*, 2018), but the CAR-T treatments are rarely used or in clinical trials (Wang *et al.*, 2014; Houot *et al.*, 2015). Serious side effects can be induced by these treatments, such as cytokine release syndrome (fever, nausea, headache, rash, tachycardia, hypotension, dyspnea), and several deaths happened during clinical trials (Wang *et al.*, 2014). CAR-NK (Natural Killer) could be an alternative to CAR-T. They are highly cytotoxic by favoring antibody-dependent cell-mediated cytotoxicity and by activation and persistence of NK cells via IL-15 cytokine (Nguyen et al., 2021). At the moment, CAR-NK therapy is only at the pre-clinical stage or recruiting for phase 1.

Therapeutic **vaccination** with the use of dendritic cells is another approach to immunotherapy. Dendritic cells are a type of antigen-presenting cells in the immune system. For immunotherapy, dendritic cells of the patient are extracted and incubated with antigens expressed at the tumor cells' surface before reinfusion into the patient (Hammerstrom *et al.*, 2011). The dendritic cells will present the antigens to the immune system and activate an

adaptative immune response, that will target cancer cell antigens and destroy them (**Figure IV**). The sipuleucel-T is the first FDA-approved immunotherapy vaccine for the treatment of metastatic hormone-refractory prostate cancer (2010) (Hammerstrom *et al.*, 2011; Handy and Antonarakis, 2018). It uses a fusion protein (PA2024) composed of the prostatic acid phosphatase antigen, overexpressed in prostate cancer, associated with a granulocyte-macrophage colony-stimulating factor that helps the dendritic cells to mature. Another approach in vaccine immunotherapy is the use of oncolytic viruses *in situ* (tumor site). These viruses replicate in cancer cells and induce oncolysis. Talimogene laherparepvec (T-VEC), a herpes simplex virus variant, is used to treat inoperable melanomas since 2015 (Ott and Hodi, 2016). The vaccine immunotherapy is associated with side effects, known as flu-like symptoms or allergic reactions. Stroke has been linked to sipuleucel-T treatment, and tumor lysis syndrome to T-VEC (dying cancer cells liberating substances in the blood that can generate serious complications leading to death) (Greig, 2016; Zhang *et al.*, 2016; Handy and Antonarakis, 2018).

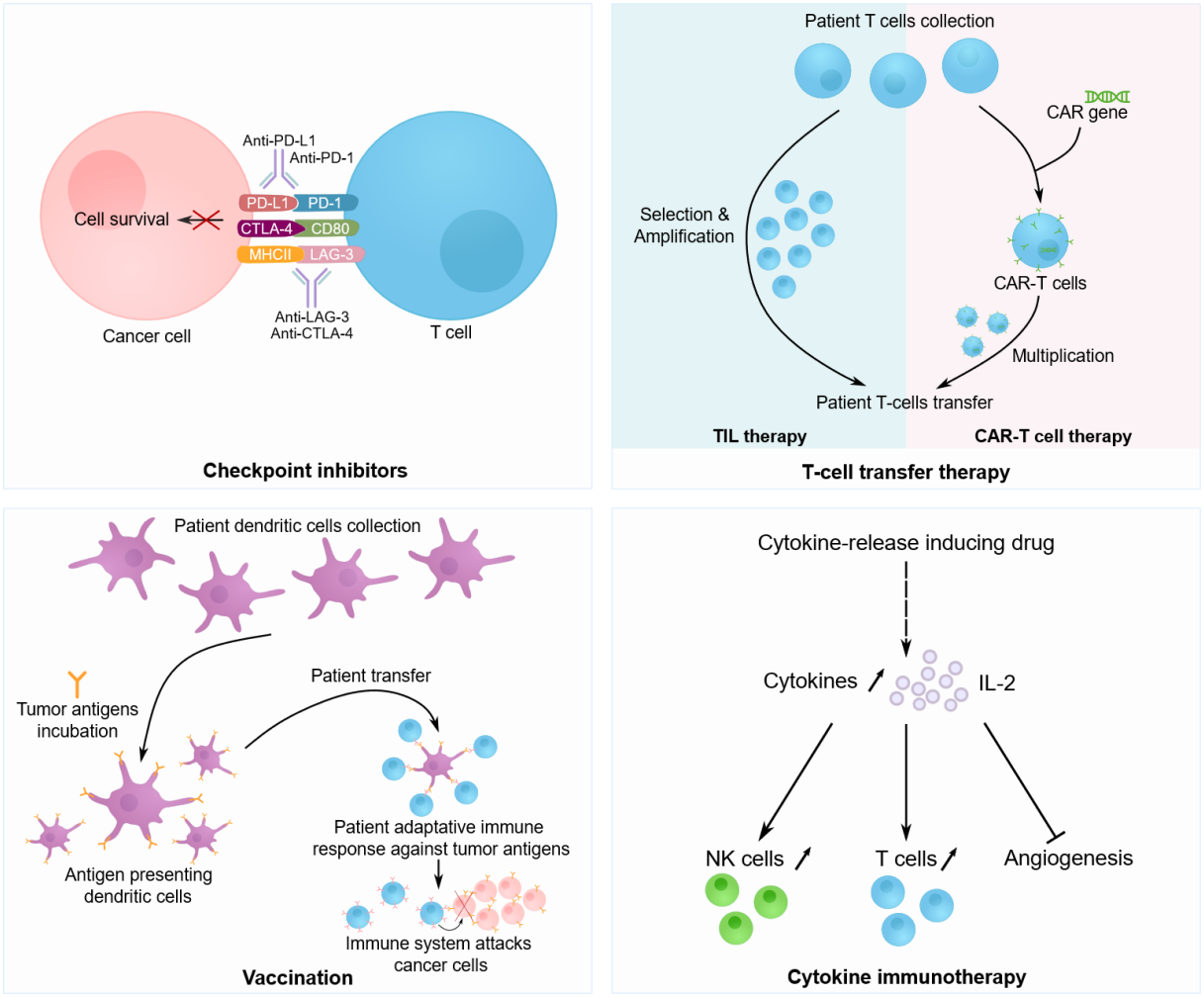

Figure IV. Four cancer immunotherapy approaches: checkpoint inhibitors, T-cell transfer therapy, vaccination, and cytokine immunotherapy. CAR: chimeric antigen receptor; IL: interleukines; NK: natural killer.

Cytokine immunotherapy can also be used to stimulate the immune system against cancer cells (**Figure IV**). Cytokine can be directly infused into the body with IL-α or IL-2, or increased *via* the use of drugs that allow cytokine production. These drugs cause a release of interleukin 2 (IL-2) that increases the activity of the immune T-cells and natural killer, and also works as an anti-angiogenesis factor (Berraondo *et al.*, 2018). Imiquimod acts by activating TLR7 that releases cytokines and is used against basal cell carcinoma (Testerman *et al.*, 1995). Flu-like symptoms are also related to these treatments, as long with serious side effects associated with the release of a large number of cytokines (severe allergic reactions, dyspnea, hypo and hypertension, blood clots, and organ damage). Cytokine release is also linked to troubles in behavior, and depression (Pollak & Yirmiya, 2002; Kovacs *et al.*, 2016).

1.1.2.4 Hormonotherapy

Hormonotherapy is used against various hormono-dependent cancers (breast, prostate principally, but also endometrium, thyroid, neuroendocrine cancers), (Weelden *et al.*, 2019; Grani *et al.*, 2019). The principle is to inhibit the stimulating action of female hormones (progesterone or estrogens) or male hormones (testosterone). The non-drug treatments stop hormone production by the body, using chirurgical approaches such as ovariectomy (ovarian ablation), pulpectomy (the external membrane of testicular is conserved), orchiectomy (testicular ablation), or radiotherapy. The systemic treatments use drugs to inhibit the hormonal receptor expressed at the cancer cell surfaces, damage these receptors, or inhibit hormonal production (**Figure V**).

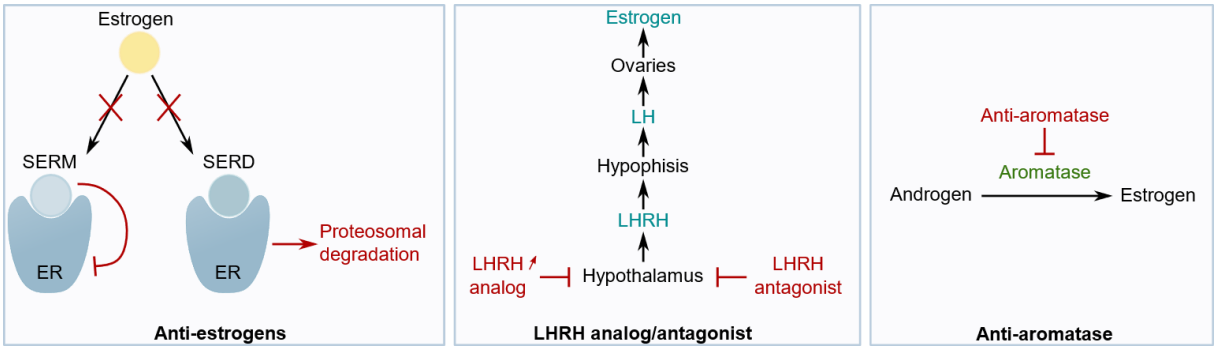

Figure V. Women hormonotherapies: anti-estrogens, LHRH analogs and antagonists, and anti-aromatases. ER: Estrogen Receptor; LH: Luteinizing Hormone; LHRH: Luteinizing Hormone Releasing Hormone; SERD: Selective Estrogen Receptor Degradation; SERM: Selective Estrogen Receptor Modulator.

For breast cancers, the most used hormonotherapy is the **anti-estrogens** treatment with tamoxifen (Waks and Winer, 2019). It acts as a competitive ligand for the estrogen receptors, and belongs to the drug class of SERM (Selective Estrogen Receptor Modulator). The other category of anti-estrogen is classified into SERD (Selective Estrogen Receptor Degradation), and includes fulvestrant that induces the degradation of the receptor (Iorfida *et al.*, 2020). **LHRH** (Luteinizing Hormone Releasing Hormone) **analogues** can also be used to inhibit the

hormone production by the ovaries. LHRH, produced by the hypothalamus, is responsible for the stimulation of the hypophysis (/pituitary gland) that produces LH (luteinizing hormone) that consequently stimulates estrogens secretion by the ovaries. The hypophysis is hyperstimulated by LHRH analogues, resulting in an arrest of ovary stimulation (Schally and Comaru-Schally, 2003). LHRH analogues and antagonists are goserelin and leuprorelin. Finally, **anti-aromatases** are prescribed to menopaused women. They compete with aromatase, the enzyme responsible for the transformation of androgen (produced by the adrenal gland) into estrogens. Anti-aromatases used in hormonotherapy are letrozole and anastrazol (Waks and Winer, 2019). Hormonotherapy lasts for three to five years and can be linked to recidivism after the arrest of the treatment (Haque and Desai, 2019). The main side effects of hormonotherapy are the menopause effects and a diminution in mineral bone density (Narayan *et al*., 2021).

Anti-androgens act by fixation to the testosterone receptors. Flutamide, bicalutamide, nilutamide and cyproterone acetate are mostly used (Pronzato and Rondini, 2005). They are generally used before **LHRH antagonists'/analogues'** treatments. The most common LHRH analogues are leuprorelin, goserelin, buserelin, triptorelin and histrelin (Shim *et al.*, 2019). The antagonist used is degarelix. The most common side effects are osteoporosis, gynecomastia, libido and mood troubles, and heat flashes (Tucci *et al*., 2018).

1.1.2.5 Chemotherapy

Chemotherapies are proceeded with diverse cytotoxic molecules, targeting a variety of cellular effectors: the mitotic spindle, extracellular receptors, cell cycle kinases, and/or DNA and its metabolism.

1.1.2.5.1 Mitotic spindle chemotherapy

The mitotic spindle is targeted by two main groups of drugs: **alkaloids** and **taxanes**, mainly originating from plants. Alkaloids prevent the assembly of the cell microtubules while the taxanes their disassembly, resulting in a cell cycle arrest, and cell death (Ballout *et al*., 2019). The first alkaloids used in chemotherapy were vincristine and vinblastine, extracted from the *Catharanthus roseus* (Madagascar periwinkle). Derivatives of these compounds were produced including vinorelbine, vindesine, and vinflunin. Original and derivative compounds are used to treat various carcinomas, sarcomas, lymphomas, and myelomas. Regarding taxanes, the first extracted drug was paclitaxel, from *Taxus brevifolia*, approved in 1993 (Ballout *et al*., 2019). Paclitaxel and its analogue docetaxel are used in chemotherapy alone or combined with other compounds mainly against carcinomas. The main side effects of these treatments are myelosuppression, and cardiovascular and gastrointestinal toxicities. Neurotoxicity can also occur as a chronic persistent side effect (Ho and Mackey, 2014).

1.1.2.5.2 Targeted therapy

Another type of emerging therapy is **targeted therapy**. Targeted therapy can either be the use of small molecules or monoclonal antibodies acting at different cellular levels: on growth factors, cell receptors, or regulatory enzymes (**Figure VI**). The drugs can either inhibit cancer cells growth and division, inhibit cancer cell angiogenesis, help the immune system to attack cancer cells, or induce cancer cell apoptosis. The main targets are VEGFR, EGFR, tyrosine kinase enzymes, and proteasome, but many other cell pathways can be targeted (Ma and Adjei, 2009; Tsimberidou, 2015; Zhong *et al.*, 2021). In some chemotherapies, drugs are carried to cancer cells using nanocarriers like liposomes, polymeric nanoparticles, or antibodies (Beltrán-Gracia *et al.*, 2019).

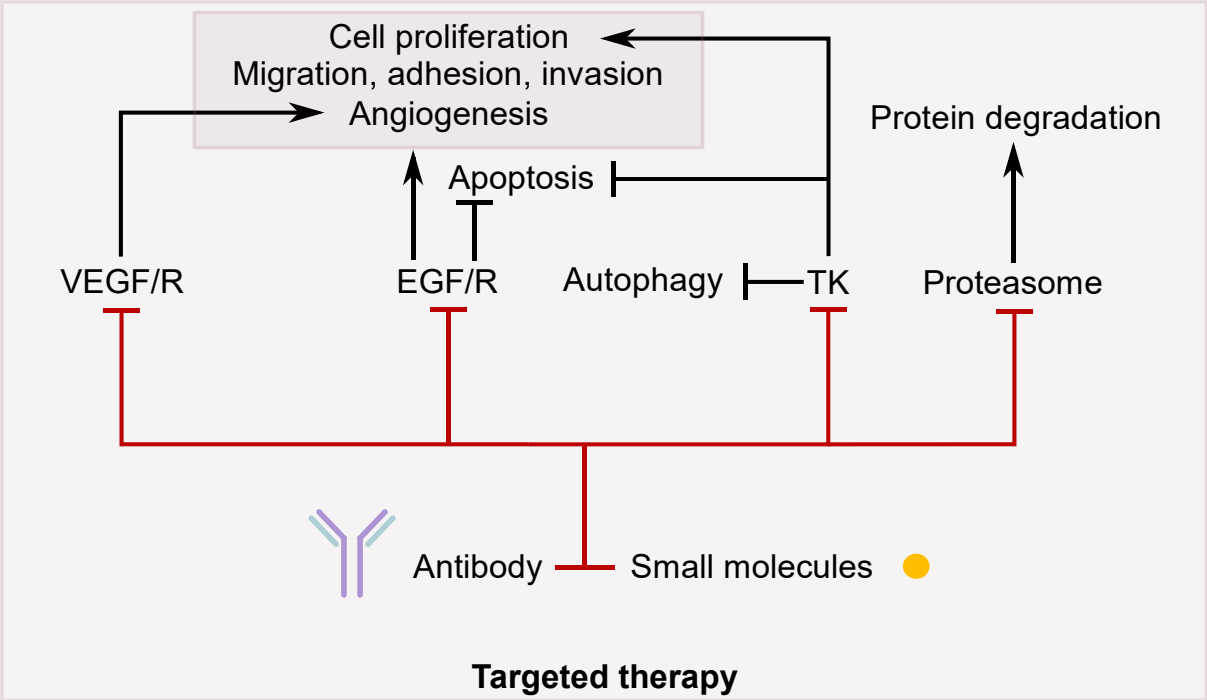

Figure VI. Major pathways targeted by antibodies or small molecules in anti-cancer strategies. EGF/R: Epidermal Growth Factor/Receptor; TK: tyrosine kinases; VEGF/R: Vascular Endothelial Growth Factor/Receptor.

Cancer cell growth can be targeted by **tyrosine-kinase inhibitors**. Tyrosine kinases encompass a multitude of proteins belonging to several signal transduction pathways (Pottier *et al.*, 2020). Imatinib (2001 approval) is an inhibitor of the Bcr-Abl oncoprotein (fusion protein from a translocation between chromosome 9 and 22, known as Philadelphia gene) targeting the tyrosine kinase domain by a competitive binding (Rossari *et al.*, 2018). As a consequence, the cell substrate cannot enter the kinase site for phosphorylation, resulting in an inactivation of the cancer proliferation signal. Imatinib also inhibits PDGFR (platelet-derived growth factor receptor), and c-kit (oncogene encoding for tyrosine-protein kinase KIT). The Bcr-Abl oncoprotein characterizes the chronic myeloid leukemia and is also found in various

percentage in other leukemias (Jabbour and Kantarjian, 2018). Imatinib is prescribed against these cancers, while dasatinib, nilotinib, bosutinib, and ponatinib are used in first- or second-line treatment depending on the patient's mutations and responsiveness to the previous treatment.

Another target is the **EGFR** (epidermal growth factor receptor) overexpressed in a number of carcinomas (Yarden and Pines, 2012). The EGFR signaling pathway activation results in cell growth, proliferation, invasion, metastasis, and angiogenesis (Cruijsen *et al*., 2006; Sigismund *et al*., 2017). EGFR inhibitors are both small molecules and monoclonal antibodies. Cetuximab is a chimeric monoclonal antibody approved by the FDA in 2009 against colon cancer (García-Foncillas *et al*., 2019). It is also administered to treat head and neck cancers. Other monoclonal antibodies are panitumumab and necitumumab. Small molecules inhibiting EGFR, like erlotinib (approval 2004), afatinib, and osimertinib are prescribed against metastatic NSCLC (non-small cell lung cancer), depending on the cancer cell mutations (Tagliamento *et al.*, 2018; Wu *et al*., 2020). **EGFR2/HER2** (Human Epidermal growth factor Receptor 2) is involved in the regulation, proliferation, and survival of epidermal cells. HER2 is a known amplificated and overexpressed oncogene in 15-20% of breast cancers associated with a poor prognosis. HER2 inhibitors pertuzumab, trastuzumab, and lapatinib are approved for the treatment of advanced or metastatic breast cancers associated with HER2 overexpression (Waks and Winer, 2019).

Some agents do not target receptors but proteins from their signaling pathways. In the **Ras/Raf pathway**, **BRAF** is a target of vemurafenib and dabrafenib approved by the FDA for the treatment of metastatic melanoma characterized by the *BRAF* mutation. *BRAF* mutations are found in 62–72% of patients with metastatic melanomas (Dong *et al*., 2003), making it an important effector for targeted therapy. **MEK1** and **MEK2** are targeted by trametinib, and also approved for the treatment of metastatic melanomas (Tsimberidou, 2015). **mTOR** from the **PI3K pathway** is also an interesting target for approved everolimus and temsirolimus to treat several carcinomas.

Cancer cells angiogenesis is inhibited using **VEGF** (vascular endothelial growth factor) inhibitors such as bevacizumab (2004 approval), a monoclonal antibody that binds to VEGF and inhibits its interaction with the VEGF receptor (VEGFR) (You *et al.,* 2020). Bevacizumab is used to treat metastatic colorectal and NSCL cancers, and breast cancer (Ferrara *et al*., 2020; Hey *et al.*, 2020). Ramucirumab is another antibody inhibitor used in advanced gastric cancer, but there are also small molecules targeting VEGFR like sorafenib, sunitinib, and pazopanib approved for advanced renal and hepatocellular cancers, and gastrointestinal stromal tumors (Escudier *et al.*, 2018; Zhong *et al.,* 2021).

CDK4/CDK6, kinases involved in cell cycle progression, are targeted by palbociclib, ribociclib, and abemaciclib approved in 2017 for the treatment of advanced/metastasis breast cancers in combination with fulvestrant (Waks and Winer, 2019).

Bortezomib, carfilzomib, and ixazomib are **proteasome inhibitors** used to treat multiple myeloma (Sherman and Li, 2020). They result in the downregulation of the NF-κB (nuclear factor kappa B) pathway, a major signaling pathway of cell survival in multiple myeloma (Annunziata *et al*., 2007). Moreover, the inhibition of NF-κB has been shown to restore chemosensitivity in pancreatic cancer (Li *et al*., 2018).

PARP is a major enzyme involved in DNA single strand break reparation. PARP inhibitors are actively studied, and some of them are in clinical trials (Zhong *et al.,* 2021). The inhibition of PARP alone is not sufficient to induce cell death, but the association with another treatment or given to patient bearing mutations results in the increased toxicity of the associated drugs against cancer cells. This phenomenon is called the synthetic lethality: the loss of one gene alone is not lethal, while the concomitant inactivation of two genes leads to cell death (Huang *et al.,* 2020). Olaparib has been approved in 2014 for patients with BRCA gene mutations in breast and ovarian cancers (Mateo *et al*., 2019), and metastatic prostate cancer. Talazoparib, FDA approved in 2018, is used against advanced breast cancer with BRCA mutations (Eskiler, 2019).

Targeted therapy is associated with classical side effects, like nausea, vomiting and fever, but also hypertension, myelosuppression, infusion reactions (Waks and Winer, 2019; Zhong *et al*., 2021), severe hepatotoxicity (Wang *et al*., 2021), and severe or fatal allergic reactions (Keramida *et al*., 2019). Sudden cardiac death has been associated with cetuximab treatments (Keramida *et al*., 2019). Additionally, treated cancer cells tend to develop resistance to these treatments (Mateo *et al*., 2019; Zhong *et al*., 2021).

Concerning the use of nanocarriers, few are FDA approved and most are in clinical trials (Beltrán-Gracia *et al*., 2019). Liposomes are molecules containing two layers of phospholipids that self-form vesicles in water. The first liposomes were approved by the FDA in 1995 and in Europe in 1997 and contain doxorubicin (Sanna *et al.,* 2014). They are used to treat metastatic breast cancer, ovarian cancer, multiple myeloma, and Kaposi's sarcoma. Liposomes carrying daunorubicin were approved in 1996 against Kaposi's sarcoma. Liposomes increase the half-life circulation time and maximize drug accumulation in tumor tissues. Nevertheless, the use of liposomes does not allow to control the kinetic profile and the drug localization. Further research about dosage regimen needs to be carried out, as the lipids could affect the efficiency of the drug or its formulation.

1.1.2.5.3 DNA targeting chemotherapies

Molecules targeting DNA act in different ways. **Alkylating agents** interact with DNA and attach alkyl groups to guanines, resulting in cytotoxic DNA crosslinks. They are separated into six classes. The class of nitrogen mustards were the first alkylating agent used in chemotherapy, with cyclophosphamide being the most used (Lehmann and Wennerberg, 2021). This class also includes ethylenamine and methylenamine derivatives (altretamine, thiotepa), alkyl sulfonates (busulfan), nitrosoureas (carmustine, lomustine, bedamustine), triazenes (dacarbazine, procarbazine) and platinum derivative compounds used against a large range of cancers (Dasari & Tchounwou, 2014). Cisplatin was the first platinum compound approved in 1978, currently used alongside carboplatin and oxaliplatin. Cisplatin and carboplatin work as inactive prodrugs. Their planar conformation and their metabolite diaquaplatin render them active (Chatelut, 2011). The main side effects associated with the use of alkylating agents are numerous and include immunosuppression, treatment-associated leukemia (t-AML), digestive troubles, hair loss, myelotoxicity, ototoxicity, renal toxicity, neuro and nephrotoxicity (Ma *et al.,* 2020).

Antimetabolites inhibit the DNA production by incorporating altered nucleotides, or by inhibiting the synthesis of new nucleotides. The incorporation of altered nucleotides or the absence of nucleotides incorporation lead to DNA damage and cell death, while the inhibition of nucleotides synthesis prevents cancer cell mitosis (Valenzuela *et al*., 2014). Anti-folate methotrexate is widely used to inhibit DHFR (dihydrofolate reductase), necessary for nucleotides synthesis (Chan and Cronstein, 2010). 5-fluorouracile is an anti-pyrimidine, used in 60% of the chemotherapies, that acts as an uracil substitute (Valenzuela *et al*., 2014). Side effects possible are cardiotoxicity, mucositis, and palmar-plantar erythrodesia (Fabian *et al.,* 1990; Alter *et al*., 2006; Ribeiro *et al.*, 2016). Fludarabine is an anti-purine used to treat chronic lymphoid leukemia (Ricci *et al*., 2009).

Topoisomerase inhibitors impede the replication/transcription of the DNA and induce DNA damage that result in cell death (Pommier *et al.,* 2010). They will be discussed in paragraph number 1.1.5, page 44.

1.1.3 DNA Damage Response, cell cycle, and cell death

DNA damage can be induced by a variety of endogenous or exogenous factors (O'Connor, 2015). The DNA damage response (DDR) pathway has evolved to protect the cells' genomic integrity. DDR includes a large network of proteins starting with sensors, and followed by transducers, mediators, and effectors. The DDR control mechanisms sense DNA damage, coordinate DNA repair with cell cycle arrest, and ensure cell death when repair is not possible (Pearl *et al.*, 2015; Molinaro *et al*., 2021) (**Figure VII**).

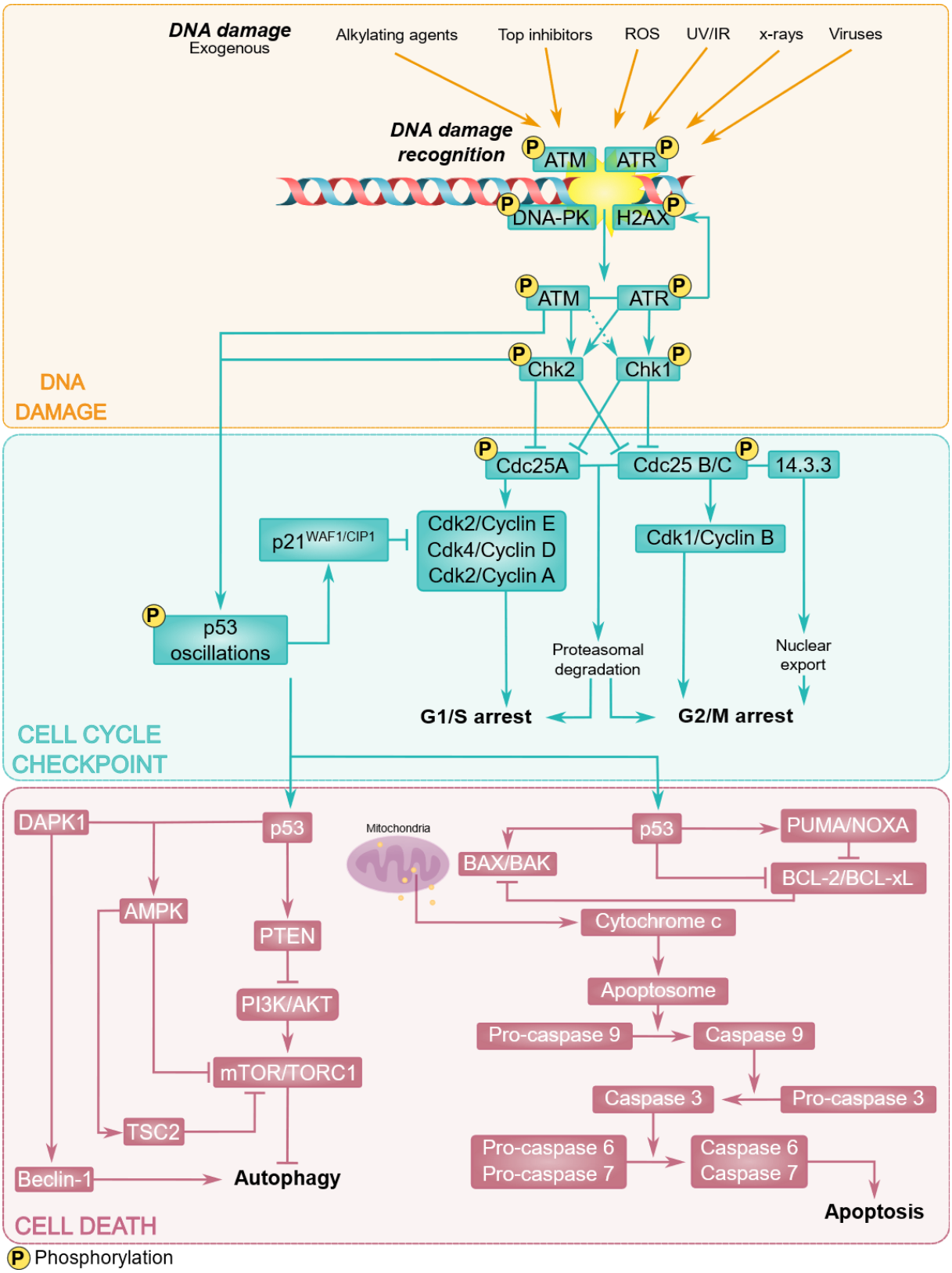

Figure VII. DNA damage response pathways.

The damage sensors allow the detection of DNA breaks and serve to recruit various protein complexes depending on the type of break (Molinaro *et al*., 2021). Classically, a series of kinases, PI3KK (phosphatidylinositol-3- kinase-related kinase), ATM (ataxia-telangiectasia mutated), ATR (ATM- and Rad3-related), and DNA-PKcs (DNA-dependent protein kinase, catalytic subunit) are activated (Schlam-Babayov *et al*., 2021). These kinases phosphorylate multiple substrates, firstly to allow a cell cycle arrest and then DNA repair. Notably, PI3KKs phosphorylate H2AX (γH2AX) to allow the early recruitment of repair effectors to the damaged DNA site, and Chk1/Chk2 to arrest the cell cycle (**Figure VII**) (Molinaro *et al*., 2021).

The cell cycle is composed of checkpoints to avoid multiplication of incorrect DNA. These checkpoints rely on several Cdk/Cyclin complexes that display phase-specific activity. The G2/M checkpoint is regulated by the Cyclin B/Cdk1 complex, called MPF (mitosis promoting factor). To allow the transition through the M phase, Cdk1 is activated through dephosphorylations of its threonine 14 and tyrosine 15 residues by Cdc25C, and by a threonine 161 phosphorylation by CAK (Cdk7/Cyclin H/Mat1 complex) (Hakem, 2008). After DNA damage, Chk1 and Chk2 inhibit Cdc25C by phosphorylation on serine 216, recognized by the 14-3-3 chaperon which exports Cdc25C to the cytoplasm. The MPF complex can not be activated and the cells are arrested in the G2 phase. Phosphorylated Chk1 and Chk2 can add a ubiquitination signal to Cdc25A for proteasomal degradation, resulting in a G1/S arrest due to the lack Cdk2/Cyclin A/E complexes activation (Donzelli & Draetta, 2003).

In parallel to the cell cycle arrest, DNA damage can be repaired by various mechanisms, depending on the type of damage (single- or double-strand breaks, adducts, interstrand crosslinks…) (Molinaro *et al*., 2021). The different types of damage are detected by different sensors that determine the type of repair. ROS-induced DNA damage are repaired by NER (nucleotide excision repair) or HR (homologous recombination). DNA damage induced by alkylating agents are repaired by NER, BER (base excision repair), MMR (mismatch repair), TLS (translesion synthesis process), HR, FA proteins (Fanconi anemia) or NER. X-rays, IR, and UV induced damage are repaired by TLS or HR, and the DNA damage induced by topoisomerase inhibitors are repaired by HR or NHEJ (non-homologous excision repair), with the proteins TDP1 and TDP2 (tyrosyl-DNA phosphodiesterases 1 and 2), eukaryotic enzymes involved in the aberrant topoisomerase activity reparation. TDP1 hydrolyzes phosphotyrosyl peptides emanating from the 3' DNA ends from trapped Top1, and TDP2 has the same role for Top2-induced 5'-phosphotyrosyl residues (Pommier *et al.,* 2014; Kawale and Povirk, 2018).

If the DNA damage are too extended or unrepairable, the DDR pathway leads to a cell death. The most common cell death induced is apoptosis, mediated by p53 (**Figure VII**). p53 and its target p21 are activated by ATM/ATR, Chk1 and Chk2. The p53 level oscillates and the oscillation numbers directly relate to the DSB (double-strand break) quantities and to the cell death outcome that also depends on the genetic context of the damaged cells (Reyes *et al*.,

2018). When p53 is mutated in high-grade serous carcinomas, its reliance on the G2/M checkpoint is increased (Ngoi *et al*., 2020). Otherwise, p53 (phosphorylated on S15 or S20) activates the transcription of various apoptosis genes, the pro-apoptotic BCL-2 members (PUMA, NOXA, BAX, BAK…), and inhibits the transcription of the anti-apoptotic BCL-2 members (BCL-2, BCL-XL…). In normal cells, cytochrome *c* is located in the mitochondria intermembrane space where it functions as an electron shuttle in the respiratory chain (Garrido *et al*., 2006). Upon apoptotic stimulus, BAX and BAK oligomerization at the mitochondria membrane forms pores and triggers membrane permeabilization, resulting in the cytochrome *c* release from the mitochondria to the cytosol and the activation of Apaf-1 (apoptosis protease activating factor 1). Apaf-1 and cytochrome *c* together form the apoptosome, and in combination with caspase 9, allow the cleavage of the procaspase 3. The activated caspases catalyze the cleavage of other key proteins, such as PARP (poly ADP ribose polymerase), a DNA repair enzyme, and procaspases 6 and 7, leading to cell death (Oda *et al*., 2000; Matt and Hofmann, 2016).

Autophagy can also be triggered after DNA damage. Autophagy is mediated by ATM/ATR and nuclear p53, which activates the transcription of PTEN (phosphatase and tensin homolog) and AMPK, to inhibit PI3K/AKT and by extension the autophagy inhibitor mTORC1 (Lorin *et al*., 2013) (**Figure VII**). At the same time, p53 activates DAPK1 to allow the activation of LC3, and the synthesis of Beclin-1 (Zalckvar *et al*., 2009). LC3-I is complexed with phosphatidyl-ethanolamine (forming LC3-II) at the membrane of the phagophore by ATG12-5-16. p62 associated with a ubiquitination signal ligates LC3-II on the inside of the membrane (Liu *et al*., 2016) to allow the formation of autophagosomes that fuse with lysosomes, generating autolysosomes that are further degraded.

1.1.4 Topoisomerases

Discovered by J.C. Wang in 1971 while working on *Escherichia coli*, topoisomerases are DNA interacting enzymes that regulate DNA topology, by increasing or decreasing the unwinding to allow replication, transcription, and chromosome segregation. These enzymes bind to DNA, form a cleavage complex (DNA-topoisomerase), generate transitory breaks, relax and religate the DNA before unbinding (Champoux, 2001; Pommier, 2013; Pommier *et al*., 2022) (**Figure VIII**). Type one topoisomerases (Top1) cut one strand of the DNA, while type two topoisomerases (Top2) cut both strands of the DNA.

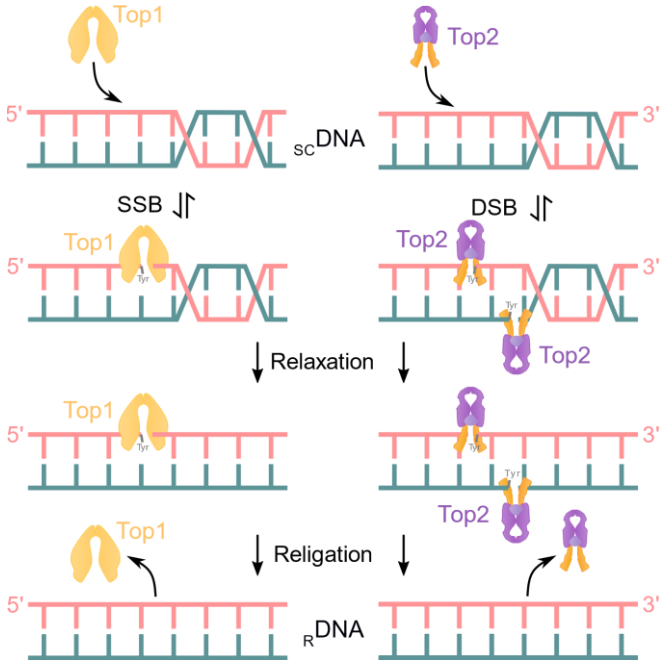

Figure VIII. Topoisomerases 1 and 2 mechanism of action. Top1 (left) or Top2 (right) act as monomer or dimer respectively, and bind to supercoiled DNA ($_{SC}$DNA). They cut one (Top1) or two strands (Top2) of the DNA *via* transesterification between the active tyrosine site of the enzyme and the phosphate group of the DNA, either on the 5' side (Top1) or 3' side (Top2). This creates transient single-strand breaks (SSB) or double-strand breaks (DSB), and allows the passage of one strand through the other to relax DNA ($_{R}$DNA). Topoisomerases rejoin the DNA strands by reverse transesterification, and finally detach from the DNA.

1.1.4.1 Topoisomerase classification

Human topoisomerases are classified into three sub-groups IA, IB, and IIA (**Figure IX; Table II**). Type IA regroups Top3α and Top3β. Their mechanisms of action were recently determined. Top3α acts during replication and removes negative supercoiling (Pommier *et al.*, 2016). Top3β acts during transcription and translation by removing R-loops on CpG sites in active promoters. Top3β KO is non-lethal (Joo *et al.*, 2020). Both Top3 enzymes require Mg^{2+} metal cofactor for their activity (Sissi and Palumbo, 2009) but are ATP-independent, and act as monomers, cleaving one strand of the DNA at the 5' end. Type IB includes nuclear Top1 and mitochondrial Top1mt. Top1 allows replication and transcription, while Top1mt allows specific mitochondrial DNA replication. They both remove positive and negative supercoiling and support fork movement during replication. They also act as monomers but do not require Mg^{2+} nor ATP for their activity. They cleave one strand of the DNA at the 3' end involving sequential transesterifications. Type IIA is composed of Top2α and Top2β. Top2α allows DNA replication and Top2β DNA transcription. Differently, Top2 acts as a heterodimer, cleaves both strands of the DNA at the 5' end, and requires both Mg^{2+} and ATP. Top2α relaxes positive supercoils faster than negative ones (> 10-fold), while Top2β relaxes both positive and negative

supercoils in the same way (McClendon, 2005). Top1, Top2, and Top3α are essential as their KOs are lethal (**Table II**) (Morham *et al.*, 1996; Li and Wang, 1998; Akimitsu *et al.*, 2003). Only one topoisomerase is expressed in germinal cells, Spo11, a type II topoisomerase acting as a dimer and required for meiosis recombination (Vrielynck *et al.*, 2016).

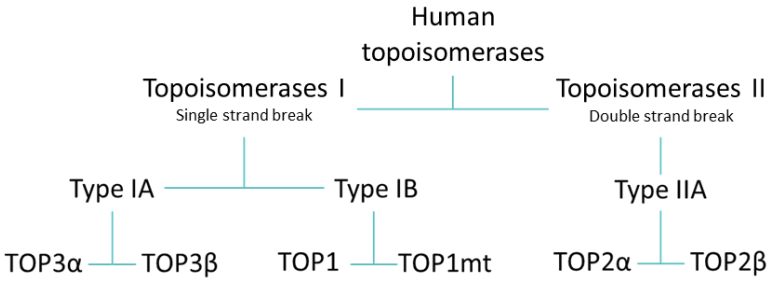

Figure IX. Human somatic cells topoisomerases repartition.

Type	Topoiso-merase	Strand break	Activity	Conformation	ATP	Mg^{2+}	KO
Type IA	Top3α	SSB	Replication, remove (-) supercoiling	Monomer	No	Yes	Lethal
	Top3β		Transcription, translation, remove CpGs' R-loops				Non-lethal
Type IB	Top1	SSB	Replication, transcription, remove (+) and (-) supercoiling	Monomer	No	No	Lethal
	Top1mt		mtDNA replication, remove (+) and (-) supercoiling				Non-lethal
Type IIA	Top2α	DSB	Replication, segregation, remove (+) and (-) supercoiling	Homodimer	Yes	Yes	Lethal
	Top2β		Transcription, remove (+) and (-) supercoiling				Lethal

Table II. Human somatic cells topoisomerases and their specificities. DSB: double-strand break; SSB: single-strand break.

1.1.4.2 Topoisomerase structures

Top1 is composed of 765 amino acids and contains four domains: a N-terminal domain, a DNA-binding region (core domain), a catalytic domain, and a C-terminal domain containing the catalytic tyrosine (**Figure X, XI**) (Redinbo *et al.*, 1998; Stewart *et al.*, 1998; McKinnon, 2016). Top1mt is composed of 601 amino acids with the same domains as Top1, with whom they share 71% of identity, reflecting high conservation between Top1 and Top1mt.

Top2α and Top2β share a 69% identity. They both share the same domains: ATPase and ATP-binding regions in the N-terminal, a core with TOPRIM domain and DNA-binding regions, and a low-complexity region in the C-terminus. Top2α and Top2β are composed of 1,531 and 1,626 amino acids, respectively (Berger *et al.*, 1996; Aravind *et al.*, 1998; McKinnon, 2016).

Regarding Top3α and Top3β, only 37% of the proteins are identical, with 1,001 amino acids for the first one and 862 for the second. Top3 is composed by four domains: the first domain (N-terminal) comprises the TOPRIM domain, responsible for Mg^{2+} binding, domains 2 and 4 (C-terminal) are winged-helix domains that form a single-strand DNA-binding groove, and the third domain is a β-barrel. Domains 1 and 3 form the enzyme active site (Garnier *et al.*, 2018).

Spo11, initiator of meiotic recombination by double-strand breaks in gametes, is the smallest topoisomerase with 396 amino acids. Spo11 has a C-terminal domain containing the TOPRIM domain, and a 5Y-CAP domain (catabolite gene activator protein) including the catalytic tyrosines (Baudat and Massy, 2004).

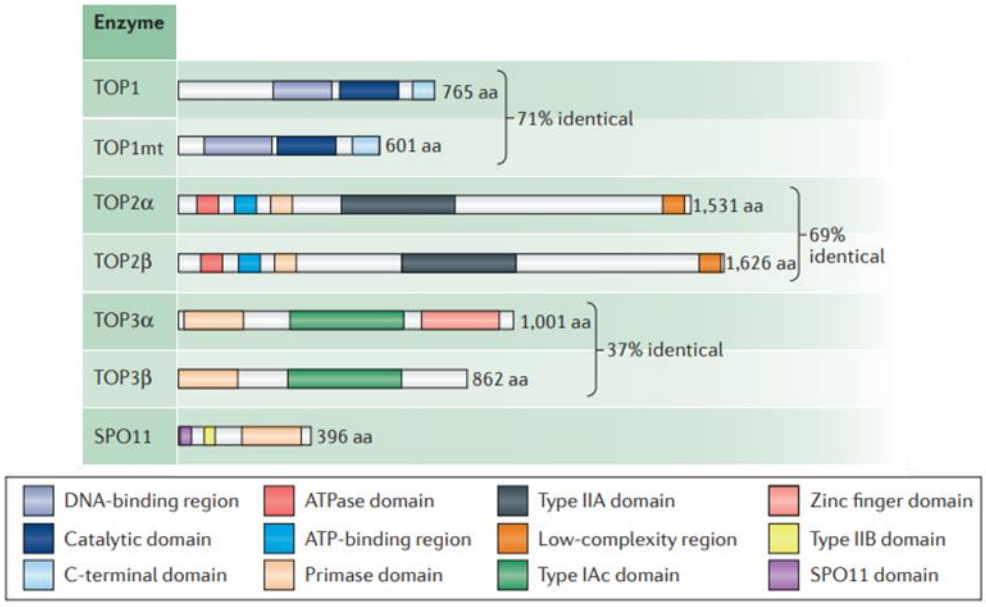

Figure X. Human topoisomerases and their protein domains. aa: amino acids. *Modified, from McKinnon, 2016*.

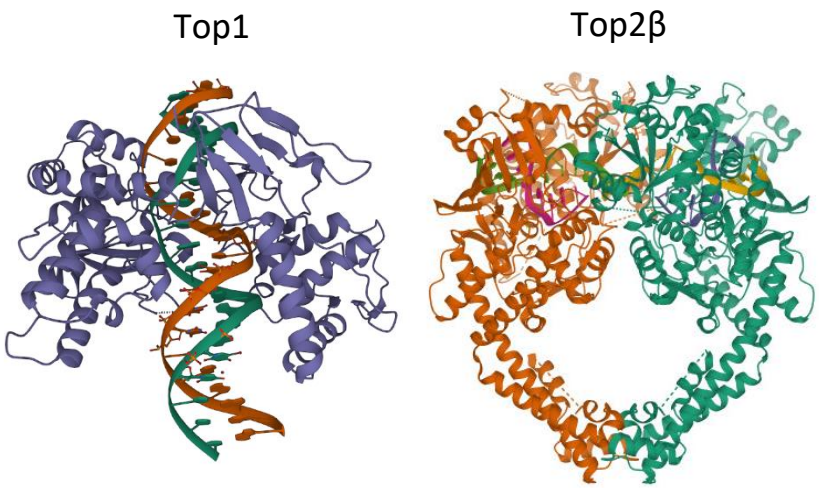

Figure XI. Overall structure and domains of human topoisomerases 1 and 2β. Left: structure of human Top1 (70 kDa; blue) in complex with a 22 base pairs DNA (green and brown) (PDB ID: 1A35; Redinbo *et al.*, 1998). Right: structure of human Top2β dimer (183 kDa; chain A of Top2β in orange; chain B of Top2β in green) in complex with DNA (pink/green and purple/orange) (PDB ID: 4J3N; Wu *et al.*, 2013).

1.1.4.3 Topoisomerases expression patterns and modifications

Tissue	Top2α	Top2β
Stomach		
Kidney		
Muscle		
Lung		
Heart		
Spleen		
Pancreas		
Intestine		
Uterus		
Bladder		
Ovary		
Lymph nodes		
Adrenal glands		
Eyes		
Marrow		
Testis		
Tongue		
Salivary glands		
Thymus		
Breast		
Brain		
Liver		

Interestingly, Top2α and β isoforms present different patterns of expression depending on the type of tissues. Northern blot analysis of expression pattern in mice tissues showed that the expression of Top2α is high in proliferating tissues, such as bone marrow and spleen, and undetectable in the other tissues, while Top2β expression is higher in quiescent cells, such as heart and lung with no expression of Top2α (Capranico *et al.*, 1992) (**Table III**). Some tissues do not express any Top2, like muscle and pancreas. On the opposite, Top1 has no tissue specificity and is expressed in every tissue, mainly at a high level except for adipose tissue, heart, smooth and skeletal muscles (Human Protein Atlas).

◂ Table III. Pattern of expression of Top2α/β in mice tissues according to Capranico *et al., 1992*. In blue: undetectable expression; green: low expression; yellow: intermediate expression; pink: high expression.

Top1 protein level does not fluctuate during the cell cycle (Heck *et al*., 1988), but Top1 endorses post-translational modifications that are involved in the regulation of the enzyme activity. c-Abl phosphorylates Top1 at Y268 in the core subdomain II, which upregulates Top1 activity, as shown *in vitro* and *in cellulo* (Yu *et al*., 2004) (**Table IV**). This phosphorylation by c-Abl was induced after cells' ionizing radiation. c-Abl-deficient cells are lacking the accumulation of the classical protein-linked DNA breaks, leading to camptothecin resistance (a Top1 inhibitor). These results shown that the phosphorylation of Top1 is important for its activity. Moreover, *in vitro* and *in vivo* studies have shown that Top1 is phosphorylated by casein kinase II on a serine residue, which stimulates its activity (Durban *et al*., 1985). Additionally, an increase in the *O*-GlcNAcylation of Top1 results in the augmentation of Top1 activity, and *vice versa* in the mouse kidney (Noach *et al*., 2007).

Unlikely, Top2α stability and level undergo a cell-cycle dependent fluctuation (**Table IV**). The expression of Top2α starts at the beginning of the S phase and continues through G2 and M phases, and shows a pike of expression between the G2 and M phase (Lee and Berger, 2019). Top2α is not expressed during the G1 phase. On the contrary, Top2β level does not fluctuate during the cell cycle (Woessner *et al*., 1991). Levels of expression and post-translational modifications are related to Top2α activity during the cell cycle. Indeed, during the DNA replication in S phase, Top2α decatenates newly-replicated sister chromosomes and relaxes supercoils that accumulate ahead of replication forks (Lee and Berger, 2019). During the G2 phase, Top2α plays a role in the decatenation equilibrium. During prophase, Top2α and condensin work together for chromosome condensation. Top2α localizes to centromere in metaphase, facilitated by its SUMOylation, but DNA is protected from Top2 activity by the cohesin protein. During anaphase, the release of cohesion by separase allows decatenation of the sister chromatids by Top2 for chromosome segregation. During this phase, Top2α starts to be ubiquitinylated by APC/Cdh1 and is degraded by the proteasome (Lee and Berger, 2019). Additionally, Top2α phosphorylation increases during the G2 and M phases due to a multitude of kinases (CK1/2, PKC, CamKII, Cdc7, PLK1), which have been demonstrated to enhance the enzyme activity (Gasser *et al*., 1992; Lee and Berger, 2019). Finally, Top2α acetylation on its catalytic domain was recently demonstrated, and supposed to modulate the enzyme's catalytic activity (Bedez *et al*., 2018).

Topoiso-merases	Tissue specificity	Cell cycle fluctuation	Post-translational modifications
Top1	No	No	• Phosphorylation increases its activity • *O*-GlcNAcylation increases its activity
Top2α	Yes (see **Table III**)	• Absence in G1 • Expression starting at S phase • Pike of expression between G2 and M phase	• Phosphorylation increases its activity (G2/M phases) • SUMOylation upon mitotic entry until anaphase (centromere localization) • Acetylation (catalytic activity) • Ubiquitination (anaphase)
Top2β	Yes (see **Table III**)	No	No data

Table IV. Topoisomerases 1 and 2α/β tissue specificities, cell cycle fluctuation and post-translational modifications.

1.1.4.4 Topoisomerase-associated diseases

Dysregulations of Top1 activity are associated with several human diseases, such as spinocerebellar ataxia disorders and autoimmune scleroderma (Li and Liu, 2016). Besides, in scleroderma, which autoimmune antibodies cause hardening of the skin and connective tissues, a high level of Top1 autoantibodies are found (Li and Liu, 2016), associated with a decrease in Top1 catalytic activity alongside an increase of its SUMOylation (Zhou *et al*., 2011). Top1 SUMOylation in scleroderma could lead to DNA damage and genome instability. In addition, topoisomerase mutations cause genomic instability in neurons associated with the early onset of neurodegeneration (Fragola *et al.,* 2020). The inhibition of Top1 not only counteracts tumorigenesis, but also some autism spectrum disorders by inhibiting a specific RNA transcript (*UBE3A-ATS* in Angelman syndrome) (Li and Liu, 2016), suppresses inflammatory genes, and protects from death by inflammation after a pathogen infection (Rialdi *et al*., 2016).

The involvement of topoisomerases in transcriptional regulation has become more in focus when several topoisomerases mutation, depletion or inactivation have been shown to be involved in neuronal diseases like schizophrenia and autism. In familial cases of schizophrenia, the *TOP3B* gene is directly inactivated (Stoll *et al*., 2013), suggesting the importance of Top3β in neuronal integrity. In the same way, Top3β has been shown to interact

with RNAs and has an RNA topoisomerase activity (Stoll *et al*., 2013; Xu *et al.,* 2013). It was demonstrated that Top3β can bind to mRNA encoded by genes linked to schizophrenia and autism. Autism causes a fragile X, resulting in the loss of the gene encoding for FMRP (fragile X mental retardation protein). Normally, FMRP functions in synapses to inhibit translation stimulated by metabotropic glutamate receptors (Bhakar *et al*., 2012). Top3β and FMRP can both interact with TDRD3 (tudor domain-containing protein 3), which acts as a scaffold to integrate Top3β and FMRP to transcribed genes through the binding of TDRD3 to histones (Yang *et al*., 2010; 2014). This suggests that the Top3β-TDRD3-FMRP complex ensures a correct mRNA translation, and that the loss of one of its components, like FMRP in autism, could lead to its inactivation, resulting in diseases.

Top2β activity is essential for neural development and transcription (Madabhushi, 2018). Recently, a missense *TOP2B* variant has been identified in two individuals with global developmental delay and autism spectrum disorder (Lam *et al*., 2017; Hiraide *et al*., 2020).

1.1.5 Topoisomerase inhibitors

Inhibition of topoisomerases is used as prime therapy to kill fast-growing cancer cells. Topoisomerase targeting compounds can act as poisons or catalytic inhibitors (Larsen *et al.*, 2003; Nitiss, 2009a; Pommier, 2013) against Top1, Top2α and Top2β. No Top3α/β or Top1mt inhibitors are yet known or developed at this point.

- ➔ **Poisons** ligate to DNA and topoisomerases, forming the ternary cleavage complex (DNA-topoisomerase-inhibitor) with cleaved DNA, called interfacial inhibition (**Figure XII**). This ligation is covalent, and inhibits the DNA religation, inducing SSB (type I topoisomerase) or DSB (type II topoisomerase) in the DNA. SSB and DSB induce the DNA damage response (DDR) pathway associated with a cell cycle arrest and a cell death if DNA damage are too extended as explained previously (§1.1.3, page 33) (Molinaro *et al.*, 2021; Pommier, 2009, 2013; Pommier *et al.* 2010; Young, 2015).
- ➔ **Catalytic inhibitors** act in three different ways: as DNA intercalators, avoiding the complexation of the topoisomerase within the site of interaction with DNA; as ATP competitor, rendering Top2 unable to cut DNA; or finally, as ATP hydrolysis inhibitor, impeding Top2 detachment from the DNA (**Figure XIII**) (Larsen *et al*., 2003; Nitiss, 2009).

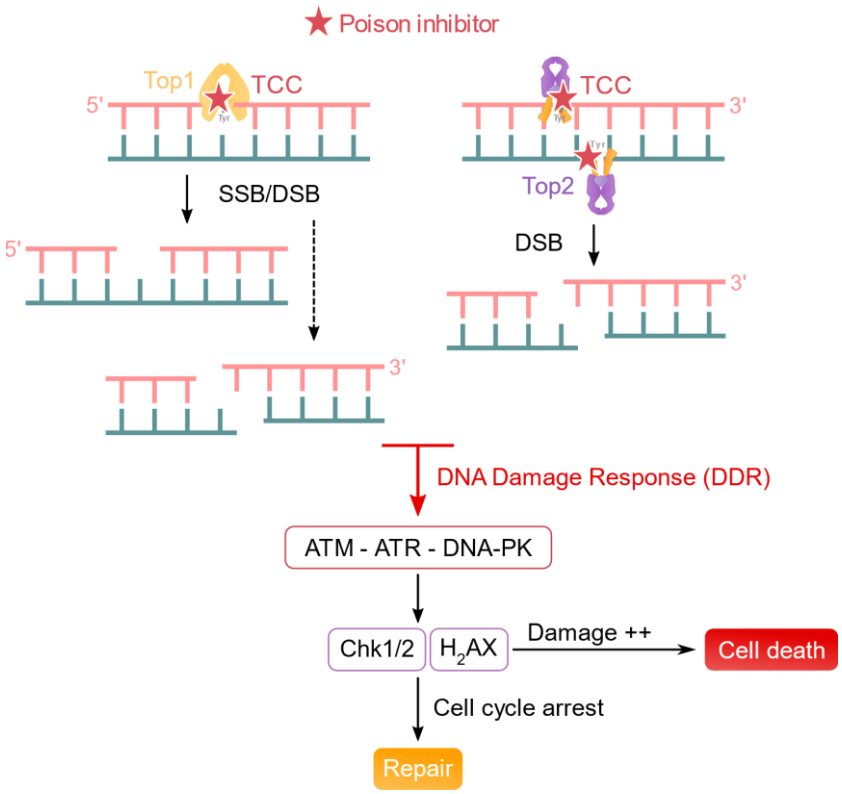

Figure XII. Mechanism of action of topoisomerases' poisons. After binding of the topoisomerase to the DNA and its cleavage, the poison interacts with the DNA and the topoisomerase, forming the ternary cleavage complex (TCC). This interaction generates single- and double-strand breaks (SSB and DSB), which induce the DNA damage response pathway (DDR). Three PI3K kinases, ATM, ATR, and DNA-PK, are activated, and trigger a signaling cascade. Some effectors are involved in cell cycle arrest to allow DNA repair, or cell death if the damage is too extended.

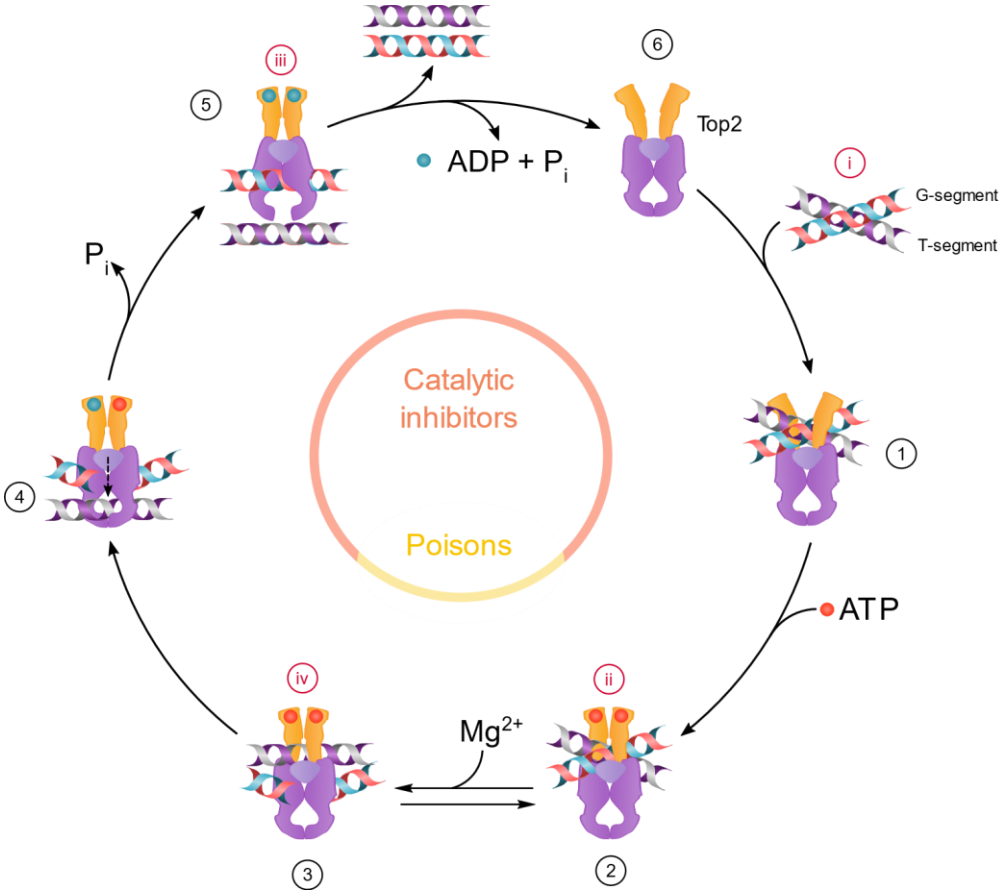

Figure XIII. Action mechanism of Top2 catalytic and poison inhibitors. (1): Top2 enzymes bind to two dsDNA segments, the G- and T-segments. (2): two ATP molecules bind to the ATPase domains of Top2, which induce their dimerization. (3): the addition of Mg^{2+} allows Top2 to cut both strands of the G-segment. (4): one molecule of ATP is hydrolyzed to allow the passage of the T-segment through the break of the G-segment. (5): the second ATP molecule is hydrolyzed to religate the DSB of the G-segment. (6): finally, the two ADP molecules dissociate, and the two dsDNA are released through the Top2 C-terminal end before the ATPase domain reopens to enable a new cycle of activity. Catalytic inhibitors (in sand pink) can (i) intercalate in the DNA, (ii) act as ATP competitors, or (iii) inhibit ATP hydrolysis. Poison inhibitors (iv) create DNA breaks accumulation by complexation with the broken DNA and Top2.

Top1 inhibitors reversibly bind to Top1 cleavage complexes, so the drugs do not directly damage DNA. However, the collision between the replication fork or the transcription machinery and the cleavage complex (Top1-DNA-inhibitor) causes irreversible Top1 covalent complexes associated with double-strand breaks (Pommier and Cushman, 2009).

Two **Top1 inhibitors** are used in chemotherapy to treat ovarian, cervical, SCLC, and colorectal cancers: **topotecan** and **irinotecan** (**Table V**) (Thomas and Pommier, 2019). They are derivatives of camptothecin, an alkaloid isolated from the *Camptotheca acuminata* tree in 1966 (Wall *et al.*, 1966). Camptothecin has a low solubility, is unstable (its open ring form is unable to inhibit Top1 when inactivated by lactone hydrolysis at physiologic pH), and induces

high toxicity (Thomas and Pommier, 2019), explaining why topotecan and irinotecan were developed in 1996 and 1998 respectively. Topotecan and irinotecan act as Top1 poisons. They bind to the DNA-Top1 cleavage complexes, avoiding DNA religation, leading to DNA breaks accumulation in the cell and therefore apoptotic cell death. Topotecan was firstly approved to treat ovarian cancer in 1996, then lately to treat cervical and SCLC in 2006 and 2007 respectively. Irinotecan was fully approved in 1998 to treat colorectal cancer. Side effects associated with topotecan and irinotecan are a severe myelosuppression, digestive troubles, and asthenia (persisting fatigue) (Thomas and Pommier, 2019). The myelosuppression in patients treated with topotecan is associated with sepsis, an inflammatory dysregulation associated with an infection that can lead to death (Pawel *et al.*, 2001). Specifically, the neutropenia induced by topotecan can lead to fatale neutropenic colitis (colon infection) (Takaoka *et al.,* 2006). Topotecan is also associated with interstitial pulmonary pathologies (pulmonary inflammations) (Shiozawa *et al.*, 2013; Meng *et al., 2019*), with rare cases being fatal. **Belotecan** is another camptothecin derivative, only approved in South Korea to treat ovarian and SCL cancers since 2003 (Hur *et al.*, 2021). More recently, new antibody-drug conjugates have been approved. Sacituzumab govitecan was fully approved in 2021 to treat triple-negative breast cancers. Sacituzumab is a monoclonal antibody design to bind Trop-2, a protein overexpressed on several solid cancers, responsible for cancer progression. Sacituzumab is linked to the small molecule govitecan (SN-38), which is the active metabolite of irinotecan, targeting Top1 (Syed, 2020). The binding of sacituzumab to cancer cells allows the uptake of govitecan to induce cell death, avoiding SN-38 toxicity to normal cells. Another antibody-drug conjugate is **trastuzumab deruxtecan**, accepted in 2019 in USA and 2021 in the European Union against unresectable or metastasis $HER2^+$ breast cancer (Keam, 2020). Deruxtecan is a derivative of the exatecan camptothecin analog and trastuzumab is an antibody directed against HER2 (de Langen *et al.*, 2018). However, the same side effects as the other camptothecin derivatives are observed: digestive trouble, fatigue, alopecia, neutropenia, leukopenia, and thrombopenia (Bartsch, 2020).

Diverse **Top2 inhibitors** are used in chemotherapy (**Table V**). Most of them are not specific to one Top2 but target both Top2α and Top2β. Some of them belong to the **anthracycline** family and were extracted from the bacteria genus *Streptomyces.* **Doxorubicin** was extracted in 1971, and is currently prescribed against carcinomas, sarcomas, leukemias, and lymphomas, alongside **daunorubicin** (1979), **epirubicin** (1984), and **idarubicin** (1990) (Pommier, 2013). Anthracyclines act as poisons at low doses and as catalytic inhibitors at higher doses due to DNA intercalation property (Pommier *et al.*, 2010; Pommier 2013). Nevertheless, associated side effects are high with hematological toxicity, vomiting, diarrhea, treatment-associated leukemias, and cardiotoxicity (Pommier 2013). The mechanisms responsible for doxorubicin's cardiotoxicity remain unclear. One possibility is that doxorubin targets Top2β, the topoisomerase highly expressed in cardiomyocytes, with absence of Top2α

and a low level of Top1 (Capranico et al., 1992; Zhang *et al*., 2012). Another possibility is the increased selective uptake of doxorubicin by cardiac tissue due to its daunosamine aminosugar moiety and the production of ROS (Evison *et al*., 2016). This cardiotoxicity prevents the treatment of patients with cardiac diseases or background, who must be given another treatment. **Mitoxantrone** is a doxorubicin analog developed in the 1980s (Fox, 2004). It was approved for the treatment of AML in 1987, hormone-refractory prostate cancer in 1996, breast cancer, and NHL (Non-Hodgkin Lymphoma). In comparison to doxorubicin, mitoxantrone shows less cardiotoxicity (Evison *et al*., 2016). Mitoxantrone targets both Top2α and β, but Top2β seems to be the most important target as an increase in Top2β -/- cells survival is observed under mitoxantrone treatment (Errington *et al*., 1999).

Another category of Top2 inhibitor is the **podophyllotoxins**, extracted from the rhizomes of the genus *Podophyllum* in 1966 (Pommier, 2013). **Etoposide** was developed in 1966 and FDA approved in 1983. It acts as a poison and is prescribed against lung, testicular and ovarian cancers, neuroblastoma, leukemia and lymphoma. It can also induce t-AML (Pommier *et al*., 2010; Pommier 2013). **Teniposide** (1992 FDA first approval) is another podophyllotoxin used to treat ALL (acute lymphocytic leukemia), Hodgkin's lymphoma, and brain tumors (Zia *et al*., 2018; Schor, 2019).

Regarding **catalytic inhibitors**, **dexrazoxane** is used as a complementary treatment, and as a cardioprotector of anthracycline treatments. It stabilizes the closed conformation of the enzyme around DNA by blocking its ATPase activity (Larsen *et al*., 2003). It is a derivative of EDTA that chelates iron and decreases the formation of superoxide radicals, partly responsible for anthracycline cardiotoxicity. **Novobiocin**, another catalytic inhibitor, binds to Top2 ATP sites before or after Top2 fixation to DNA (Larsen *et al*., 2003), but was not approved for treatment due to lack of efficiency.

In addition to toxicity, another problem related to the use of topoisomerase inhibitors is the rise of resistance mechanisms of cancer cells. Resistance occurs in diverse ways, one of them being the increased production of efflux transporters production (Pommier, 2009, 2013; Pommier *et al*., 2010). Efflux transporters are part of the MDR (multi-drug resistance) mechanisms, and involve specific members of the ABC transporter family. The ABC transporters are the largest family of transmembrane proteins divided into seven subfamilies (ABC-A to G). They include a majority of PGPs (P-glycoprotein/ABCB1), MRPs (multi-drug resistance-associated protein/ABCC1), and ABCG2s (ATP-binding cassette super-family G member 2). In cancer cells treated with a chemotherapeutic drug for a long period of time, transporters synthesis increases to expulse the treatment. Various MRPs are expressed differentially in function of the administered treatment (Sodani *et al*., 2012). It has been shown that MRP1,2,4 are responsible for camptothecins resistance, MRP1,2 and 6 for

anthracyclines resistance, and MRP1,2,3 and 6 for podophyllotoxins resistance (Tiwari *et al.*, 2011; Sodani *et al.*, 2012).

Family	Name	Target	Mechanism	Cancers
Camptothecins	Topotecan	Top1	Poison	Ovarian, cervical, SCLC
	Irinotecan			Colorectal
	(Trastuzumab) deruxtecan	Top1 and (EGFR)	Poison and (EGFRi)	Unresectable/metastasis $HER2^+$ breast cancer
	(Sacituzumab) govitecan	Top1 and (Trop-2)	Poison	Metastatic triple-negative breast cancer and urothelial cancer
Anthracyclines	Doxorubicin	Top2α/β	Poison (low doses) and Catalytic (intercalator; higher doses)	Various carcinomas, sarcomas, lymphoma, and leukemia
	Daunorubicin			AML, ALL, CML, Kaposi's sarcoma
	Epirubicin			Carcinomas, sarcomas, lymphoma
	Idarubicin			AML, ALL, CML
Anthracenedione	Mitoxantrone	Top2(α)/β	Poison, Catalytic (intercalator)	AML, prostate and breast cancers, NHL
Podophyllotoxins	Etoposide	Top2α/β	Poison	Lung, testicular, ovarian, neuroblastoma, leukemia, lymphoma
	Teniposide			Lymphoma, leukemia, brain tumor
EDTA derivative	Dexrazoxane	Top2	Catalytic inhibitor (ATP)	Following anthracycline treatment

Table V. Main approved topoisomerase inhibitors as chemotherapy drugs.

Additional resistance mechanisms are: the mutation of topoisomerases, that avoids the recognition of the enzyme by the inhibitor; a reduction in the topoisomerase level; a change in the topoisomerase subcellular localization; and Top2 phosphorylation (Nitiss 2009a,b). The reduction in the Top2α expression level responsible for cancer resistance is a consequence of intronic polyadenylation (Elton *et al.*, 2022). It results in truncated Top2α with altered biological activities. Recently, the CRISPR/Cas9 technology has been used to circumvent a specific topoisomerase inhibitor resistance in leukemia cells (Hernandez *et al.*, 2021, 2022). The technology allows the removal of an intron responsible for the truncated version of Top2α and restores the toxicity of Top2α-targeting drugs such as etoposide.

Due to their high proliferative activity, some cancers overexpress topoisomerases to allow a fast cell multiplication (Gouveris *et al.*, 2011; Pommier, 2013). Upon analysis of 24,262 patient solid tumors (26 types), 51% of the tumors showed overexpression of Top1 (Heestand

et al., 2017). From 230 breast cancer samples, Top2α expression was found in 0.6 to 39.4% of the carcinomas' cells (mean 10.6%±7.9%), whereas expression was undetectable in nonmalignant breast epithelium (Järvinen *et al*., 1996). More specifically, the Top2α gene is located close to the HER2 oncogene and is amplified or deleted in almost 90% of the $HER2^+$ breast tumors (Järvinen and Liu, 2003). Chemotherapies targeting topoisomerases are more efficient in cancers overexpressing topoisomerases (Gouveris *et al.*, 2011; Pommier, 2009, 2013). For example, patients with locally advanced or metastatic breast cancers had a better anthracycline response when they had Top2α amplification or overexpression (Coon *et al*., 2002; Cardoso *et al*., 2004; Arriola *et al*., 2007).

Biomarkers to predict clinical efficacy are under investigation to allow the selection of patients that could benefit from Top1 inhibitors chemotherapy the most. γH2AX (Furuta *et al.,* 2003; Rao *et al.,* 2007), and schlafen-11 (Murai *et al.,* 2019; Coleman *et al*., 2021; Bednarikova *et al*., 2022) are interesting candidate markers. A gene signature developed for sensitivity and resistance to topotecan and other chemotherapeutic drugs is also underway to determine the value in patient identification (Potti *et al*., 2006). Moreover, some genes hypermethylation involved in gene silencing are linked to drug sensitivity. Methylation of *WRN* (Werner Syndrome), *CHFR* (Checkpoint with Forkhead and Ring finger domains), and *SULF2* (sulfatase 2) gene promoters has been linked to a better response to irinotecan in colorectal, cervical, gastric and NSCL cancers (Tessema *et al*., 2011; Masuda *et al*., 2012; Wang *et al*., 2013; Cha *et al.,* 2019). WRN is a helicase that plays critical roles in DNA replication, recombination, repair, and telomere maintenance; CHFR is an E3 ubiquitin protein required for maintenance of the antephase checkpoint that regulates cell cycle entry into mitosis; and SULF2 is a heparan sulfate proteoglycan involved in cell signaling.

Altogether, despite the powerful effects of topoisomerase inhibitors to efficiently direct cancer cells to death, the limitations due to the side effects and the necessity to circumvent cancer cell resistance mechanisms require a constant development of new molecules.

1.1.6 Organometallics and Copper-complexes

The first discovery of an antitumoral metal-based agent arose in the 1960s with platinum, which opened a new era of chemotherapeutic drugs (Rosenburg, 1969). As described previously (§1.1.2.5.3, page 33), cisplatin is an alkylating agent widely used in chemotherapy to treat a variety of cancer, as long as its derivatives from second (carboplatin) and third generations (oxaliplatin). In cisplatin, the platinum (II) is located at the center of a squared planar structure and is coordinated with two chlorides and two ammonia molecules in a cis configuration.

In an attempt to circumvent the major problems associated with classical chemotherapeutics drugs including the severe side effects, a possible approach consists to design and develop new therapeutic metal-based anticancer drugs. Transition metals from the D-block of the periodic table (groups 3 to 12), such as essential trace metals, including copper and iron, can be used for the implementation of metal-based complexes in anticancer therapies. In this context, new organometallics containing iron have been developed and studied from preexisting compounds, including ferrocene species (originally derived from tamoxifen) with antiproliferative potential used due to their stable aromatic nature of ferrocene, associated with low toxicity and cost (Jaouen *et al*., 2015). The metal-based agent ferroquine, composed of the addition of an iron atom to the chloroquine core, was firstly used as an antimalarial drug and are now unveiled to be a promising agent to treat cancer (Kondratskyi *et al*., 2017).

Amongst metals use in the chemotherapeutic strategy, copper was shown to be an interesting candidate. Physiologically, copper has a central role in various cellular processes, being an essential micronutrient, an important cofactor of metalloenzymes involved in mitochondrial metabolism (cytochrome *c* oxidase) and cellular radical detoxification against reactive oxygen species (ROS) (superoxide dismutase) (Hordyjewska *et al*., 2014). Copper is essential for angiogenesis, proliferation, and migration of endothelial cells (Hu, 1998; Urso and Maffia, 2015).

A number of copper-complexes have been synthesized through the years, among them promising topoisomerase inhibitors (Molinaro *et al*., 2020), (**Table VI**). Many compounds have been newly designed and synthesized to enhance preexisting molecules. They have been added with diverse metals to improve their cytotoxicity against cancer cells. The copper complexes are mainly formed with a Cu(II) atom, a stable form of copper. Copper modifies the backbone of the complexed ligand and grants better DNA affinity (Krasnovskaya *et al*., 2020; Brissos *et al*., 2015). These compounds can either target Top1, such as the oxindolimine-Cu(II) or plumbagin-Cu(II) (Castelli *et al*., 2018; Chen *et al*., 2009), Top2α, such as thiazole-TSC-Cu-(II) or quinoline-TSC-Cu(II) (Lisic *et al*., 2018; Bisceglie *et al*., 2015), or are dual Top2α and β inhibitors such as bis-pyrazolyl-Cu(I) compound (Khan *et al*., 2017). Copper-complexes act as poison or catalytic inhibitors but are often associated with ROS production, which is the case for most metal-based drugs (Devi *et al*., 2018; Gulcin and Alwasel, 2022). ROS are radical and non-radical oxygen species formed by a partial reduction of the oxygen (e.g. superoxide anion (O2−), hydrogen peroxide (H2O2), or hydroxyl radical (HO•)). ROS production arises from mitochondria oxidative metabolism at a low and stationary level and have a role in cell signaling and homeostasis, but also in physiological functions such as aging, inflammation, and immune responses (Mirzaei *et al*., 2021). When accumulated at a high level by exogenous factors like chemotherapeutic drugs, ROS induce DNA damage which increases the toxicity against cancer cells, but also towards normal cells.

As a consequence of their induced activation of the DDR, copper-complexes arrest cancer cells in different phases of the cell cycle and trigger cell death, mainly apoptosis, and in some cases autophagy (Molinaro *et al.*, 2020). For example, pyrophosphate and tetrazolopyrimidine diimine copper complexes act with low IC_{50} under 1 µM (0.64 µM on an ovarian and 0.12 µM on a lung cancer lineage, respectively), with an induced apoptosis for tetrazolopyrimidine diimine (Ikotun *et al.*, 2009; Haleel *et al.*, 2016). The Cu(II)(GTSCHCl) complex acts with an IC_{50} of 1.45 µM on triple-negative breast cancer cell, 1.23 µM on colon cancer cell, and induces a G2/M arrest as long as apoptosis (Palanimuthu *et al.*, 2013). Copper complexes inhibitors of topoisomerase have been published in our review included page 187. All these results obtained with copper complexes encourage the expansion of this highly active anticancer type of drug targeting the topoisomerase family.

Ligand class of Cu-C	Targeted Top(s)	Cancer cell lines	IC_{50} (µM)	Cell cycle arrest/Cell death	Reference
Oxindolimine	Top1	Neuroblastoma SH-SY5Y		G2/M arrest	Castelli *et al.*, 2018
		Promonocytic U937		Apoptosis	Cerchiaro *et al.*, 2005
Hydrazone with triphenylphosphonium		Lung A549	4.2 ± 0.8		Chew *et al.*, 2014
		Prostatic PC-3	3.2 ± 0.2		
Plumbagin		Breast MCF-7	3.2 ± 1.1		Chen *et al.*, 2009
		Colon HCT116	5.9 ± 1.4		
		Hepatoma BEL7404	12.9 ± 3.6		
		Hepatoma HepG2	9.0 ± 0.7		
		Kidney 786-O	2.5 ± 0.9		
		Lung NCI-H460	2.0 ± 1.2		
		Nasopharyngeal cancer CNE2	11.8 ± 5.9		
Phenanthroline with amino acids		Nasopharyngeal cancer HK1	2.2 - 5.2	Apoptosis	Seng *et al.*, 2012
Pyrophosphate		Ovarian A2780/AD	0.64 ± 0.12		Ikotun *et al.*, 2009
Heterobimetallic Cu(II)-Sn2(IV) phenanthroline		Breast Zr-75–1	< 10 (GI50)		Tabassum *et al.*, 2012
		Cervix SiHa			
		Colon HCT15, SW620			
		Kidney 786-O, A498			
		Lung Hop-62, A569			
		Pancreatic MIA PaCa-2			
		Neuroblastoma SH-SY5Y	2 – 8	Apoptosis	Chauhan *et al.*, 2007
Tridentate chiral Schiff base		Hepatoma HuH7	25		Tbassum *et al.*, 2013; 2015
		Hepatoma HepG2	6.2 ± 10		

Table VI *part 1*. Copper-complexes inhibitors of human topoisomerases, toxicity on cancer cells (IC_{50}), and induced cell cycle arrests and/or cell deaths when determined (Molinaro *et al.*, 2020).

Ligand class of Cu-C	Targeted Top(s)	Cancer cell lines	IC_{50} (µM)	Cell cycle arrest/Cell death	Reference
Salicylidene	Top1	Prostatic PC-3 Breast MCF7 Colon HT29 Hepatoma HepG2 Lung A549 Ovary A2780 Prostatic LNCaP	7.3 ± 0.2 51.1 ± 1.6 16.6 ± 0.6 2.3 ± 0.1 16.8 ± 1.0 14.6 ± 0.2 25.4 ± 0.8		Lee *et al.*, 2014; 2016
Chalcone-derived Thiosemicarbazone		Breast MCF-7 Leukemia THP-1	0.16 ± 0.06 0.20 ± 0.06		Vutey *et al.*, 2016
Pyridyl-substituted tetrazolopyrimidine		Cervix HeLa Colon HCT-15 Lung A549	0.565 ± 0.01 0.358 0.733	Apoptosis	Haleel *et al.*, 2019
Tetrazolopyrimidine diimine		Cervical HeLa Colon HCT-15 Lung A549	0.620 ± 0.0013 0.540 ± 0.00015 0.120 ± 0.002	Apoptosis	Haleel *et al.*, 2016
Piperazine					Tabassum *et al.*, 2012
Elesclomol		Erythroleukemic K562	0.0075	Apoptosis Necrosis Oxidative stress	Hasinoff *et al.*, 2015
Cu(SBCM)2		Breast MCF7 Breast MDA-MB-231	27 18.7 ±3.1	G2/M arrest Apoptosis	Foo *et al.*, 2019
Pyridine-TSC	Top2α	Breast MDA-MB-231 Breast MCF7	1.01 0.0558		Conner *et al.*, 2016 Wilson *et al.*, 2016 Morris *et al.*, 2019
	Top2β				Keck *et al.*, 2019
Piperazine-TSC	Top2α	Breast MCF7 Breast SK-BR-3	4.7 ± 0.3 1.3 ± 0.3		Zeglis *et al.*, 2011
Thiazole-TSC		Breast MDA-MB-231 Breast MCF7 Breast HCC 70, HCC 1395, HCC 1500, and HCC 1806 Colon Caco-2, HCT-116 and HT-29	1.41 (EC50) 0.13 (EC50) 1 to 20 0.83 to 41.2		Lisic *et al.*, 2018 Morris *et al.*, 2019 Sandhaus *et al.*, 2016
L- and D-Proline-TSC		Ovarian carcinoma CH1	113 ± 16		Bacher *et al.*, 2013
Quinoline-TSC		Lymphoma U937	0.48-16.2		Bisceglie *et al.*, 2015
Naphthoquinone-TSC		Breast MCF7	3.98 ± 1.01	No apoptosis	Chen *et al.*, 2004

Table VI *part 2*. Copper-complexes inhibitors of human topoisomerases, toxicity on cancer cells (IC_{50}), and induced cell cycle arrests and/or cell deaths when determined (Molinaro *et al.*, 2020).

Ligand class of Cu-C	Targeted Top(s)	Cancer cell lines	IC_{50} (µM)	Cell cycle arrest/Cell death	Reference
Bis-TSC	Top2α	Breast MDA-MB-231 Colon HCT116 Keratinocyte HaCaT Colon HCT116	1.45 ± 0.07 1.23 ± 0.27 0.65 ± 0.07 Delayed mice xenograft	G2/M arrest Apoptosis	Palanimuthu *et al.*, 2013
Carbohydrazone		Breast MCF7 Breast MDA-MB-231 Breast HCC 1937 Breast MX1 Breast MDA-MB-436 Breast MX-1	9.916 7.557 3.278 4.534 5.249 Reducted mice xenograft (83%)	Apoptosis	Nair *et al.*, 2017
Chromone		Breast MCF7 Breast Zr-75-1 Colon HT29 Cervix SiHa Kidney A498 Lung A549 Ovary A2780	18.6 (GI 50) 25.2 (GI 50) >80 (GI 50) 34.6 (GI 50) 73.3 (GI 50) 31.7 (GI 50) 17.4 (GI 50)		Arjmand *et al.*, 2012
Quinolinone Shiff Base		Hepatic HepG2	17.9 ± 3.8		Duff *et al.*, 2012
Bis-pyrazolyl Carboxylate	Dual Top1/Top2	Hepatic HepG2	3.3 ± 0.02	Apoptosis	Khan *et al.*, 2017

Table VI *part 3*. Copper-complexes inhibitors of human topoisomerases, toxicity on cancer cells (IC_{50}), and induced cell cycle arrests and/or cell deaths when determined (Molinaro *et al.*, 2020).

1.2 RESEARCH CONTEXT, INDENOISOQUINOLINE COPPER-COMPLEXES

1.2.1 Indenoisoquinolines

A new Top1 inhibitor family of molecules, the indenoisoquinolines, was developed by Pommier and Cushman from 1998 at the National Cancer Institute (NCI) using a COMPARE algorithm to predict biological targets from data generated by the screen of 60 human cancer cell lines (NCI-60) (Nagarajan *et al.*, 2006; Pommier and Cushman, 2009). The indenoisoquinoline backbone is composed of four carbon cycles, including two aromatic cycles, one azote, and two oxygens (**Figure XIV**). Recently, modulation of the chemical nature of substituents on the indenoisoquinoline has resulted in additional biological targets with convincing evidence for the use of indenoisoquinolines for the treatment of many various diseases (Cushman, 2021).

These compounds are good protagonists for chemotherapy as they are chemically stable in the absence of e-ring compared to camptothecins (inactivated at physiologic pH) (Pommier et Cushman, 2009). In addition, the DNA-protein crosslinks (DPCs) induced by the indenoisoquinoline *via* the inhibition of Top1 are persistent at least 1 h after drug removal, while the DPCs are reversed less than 15 min after camptothecin or topotecan removal (Antony *et al*., 2007). Therefore, indenoisoquinoline chemotherapy requires shorter infusion times because the Top1 inhibitor complex is less likely to dissociate. Moreover, indenoisoquinolines are less or not substrates for PGP and ABCG2 efflux transporters responsible for MDR, in comparison to topotecan and irinotecan, and can circumvent established chemoresistance (Antony *et al*., 2007).

Co-crystal structures of indenoisoquinolines with Top1-DNA elucidated the structure of the ternary complex showing that they interact with DNA in a hydrophobic stacking interaction, and with Top1 by a network of hydrogen bonds, a common feature of interfacial inhibition (Marchand *et al*., 2006; Pommier, 2006).

Three indenoisoquinolines have been selected for clinical trials: indotecan (LMP-400), indimitecan (LMP-776), and LMP-744, and have completed or are in phase 1 to treat lymphoma and advanced solid tumors (Kummar *et al*., 2016; Pommier *et al*., 2018). They have good pharmacokinetics proprieties, including a good cell absorption, body diffusion, and excretion characteristics (Muzzio *et al*., 2015; Kummar *et al*., 2016). Myelosuppression has been linked to these treatments, without significant gastrointestinal problems (Kummar *et al*., 2016).

To enhance their efficiency towards cancer cells, new organometallic compounds derivative of indenoisoquinoline were synthetized by Pr. L. Pelinksi's team (Unité de Catalyse et Chimie du Solide – Lille University) (Wambang *et al.* 2016). Associated with the backbone of indenoisoquinoline, a carbonated chain was added linked to a metal from the D bloc of the periodic table such as: copper, zinc and ruthenium (**Figure XIV**).

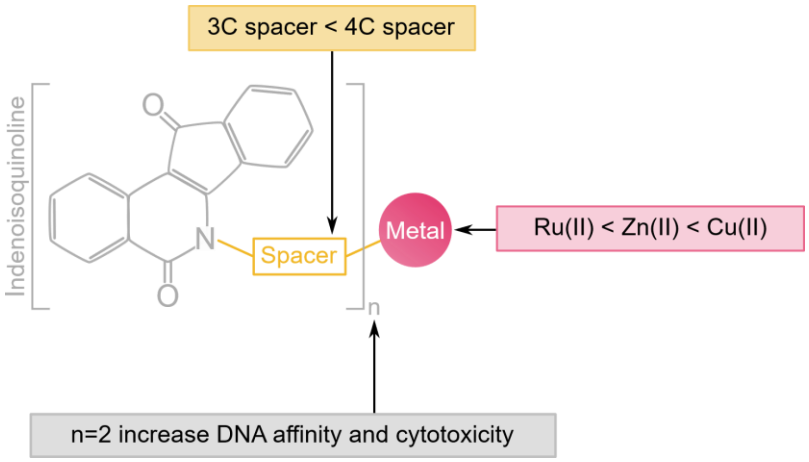

Figure XIV. Indenoisoquinoline organometallic derivative compounds skeleton. The derivatives are composed of the indenoisoquinoline backbone, a spacer (three or four carbons: 3C or 4C), and a metal (ruthenium: Ru, zinc: Zn or copper: Cu). Parameters including length of the carbon spacer and nature of the metal bound were tested for toxicity on cancer cells by MTS to classify the compounds according to their efficiency.

1.2.2 Metal complexes of indenoisoquinoline

Fourteen complexes were synthesized by Pr. L. Pelinski team, and their cytotoxicity were determined using MTS on five cancer cell lines, MDA-MB-231 (triple-negative breast cancer), MCF-7 (hormone-independent breast cancer), HeLa (cervix cancer), HT-29 (colon cancer), and DU-145 (prostate cancer) (**Figure XV**). The copper complexes came out to be efficient organometallic complexes, with the lowest IC_{50} on the five cell lines (mean of 0.455 µM for the copper complexes; mean of 0.556 µM for the zinc complexes; mean of 149.239 µM for the ruthenium complexes). Another piece of evidence that came out of the MTS tests was the high efficiency of a four-carbon spacer compared to shorter spacers. An additional interesting feature demonstrated an increased efficiency provided by two symmetrical molecules of indenoisoquinoline surrounding the copper atom (**Table VII**) (Wambang, 2016; Wambang *et al.*, 2016).

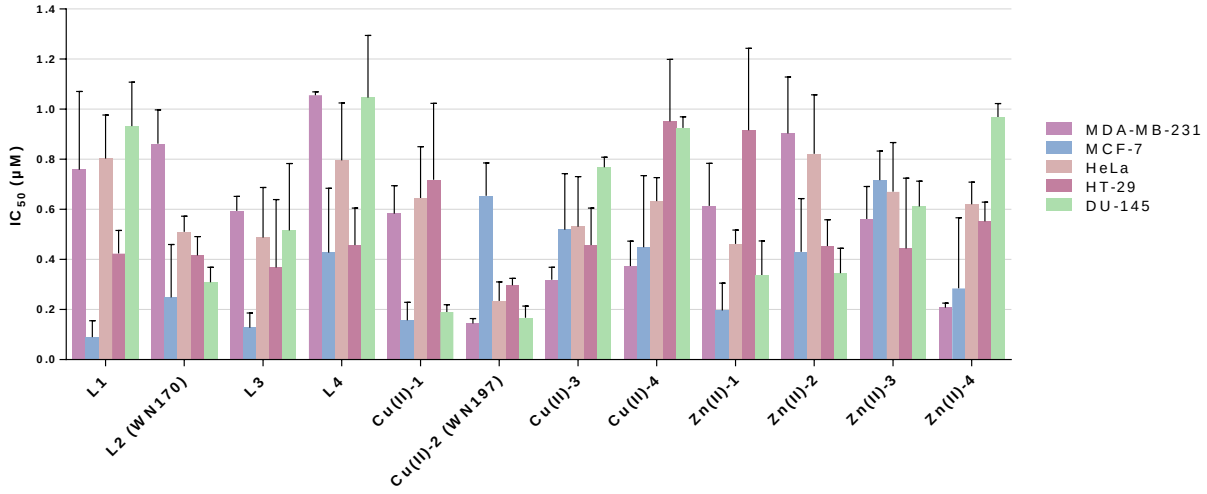

Figure XV. IC_{50} (in µM) of organometallic indenoisoquinoline derivatives on five cancer cell lines. L1 to L4 are derivative ligands without a metal atom. Roman numerals (II) correspond to the form of copper and zinc atoms (Cu(II) and Zn(II)), and Arabic numerals are their serial numbers.

	L2 (WN170)	L3	L4	Cu-1	Cu-2 (WN197)	Cu-3	Cu-4	Zn-1	Zn-2	Zn-3	Zn-4	Ru-1	Ru-2
L1	ns	ns	ns	ns	**	ns	ns	ns	ns	ns	ns	****	ns
L2 (WN170)		ns	*	ns	*	ns	*	ns	ns	ns	ns	****	ns
L3			**	ns	ns	ns	**	ns	ns	*	ns	****	ns
L4				*	****	ns	ns	*	ns	ns	ns	****	ns
Cu-1					*	ns	*	ns	ns	ns	ns	****	ns
Cu-2 (WN197)						**	****	*	**	****	**	****	ns
Cu-3							ns	ns	ns	ns	ns	****	ns
Cu-4								*	ns	ns	ns	****	ns
Zn-1									ns	ns	ns	****	ns
Zn-2										ns	ns	****	ns
Zn-3											ns	****	ns
Zn-4												****	ns
Ru-1													****

Table VII. Statistical comparison of synthesized organometallic compounds derived from indenoisoquinoline. L1 to L4 are derivative ligands without a metal atom. Numbers refer to different compounds: Cu-1 to Cu-4 are copper-complexes number 1 to 4; Zn-1 to Zn-4 are zinc-complexes number 1 to 4; Ru-1 and Ru-2 are ruthenium-complexes number 1 and 2. The Cu(II)-2 (WN197) copper-complex is the most cytotoxic. Statistical analyses were realized using ANOVA on the mean IC_{50} of the five cancer cell lines (*p<0.05; **p<0.01; ****p<0.001).

The compound with the lowest $IC_{50,}$ named WN197 (Cu-2 on the figure above), shows IC_{50} of 0.144 µM on MDA-MB-231, 0.644 µM on MCF-7, 0.220 µM on HeLa, 0.358 µM on HT-29 and 0.162 µM on DU-145. The WN197 IC_{50} mean was significantly higher compared to all other compounds except for L3 and Ru-2 (**Table VII**). WN197 is composed of a copper-core surrounded by two indenoisoquinolines connected with a four carbons chains. WN170 (L2 on the figure above) was studied as a control to understand the benefit of the copper addition. WN170 is composed of one indenoisoquinoline with a four carbons chain bound to the nitrogen atom (**Figure XVI**).

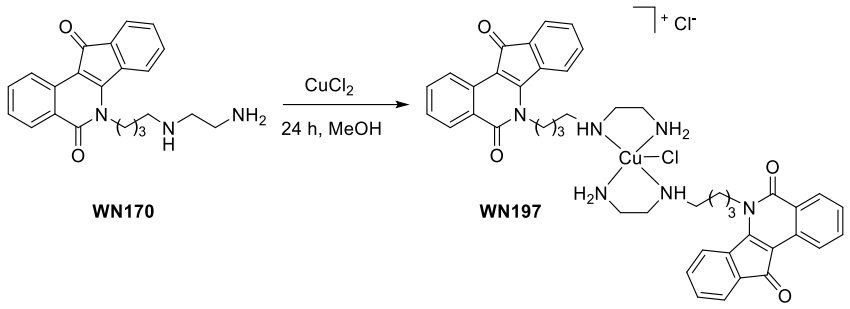

Figure XVI. Structure of WN197 and its precursor WN170.

1.2.3 Thesis objectives

The aim of my thesis was to determine the action mechanisms involved in the cytotoxic effect of WN197 on three adenocarcinoma representing cancers with a high prevalence and difficult to treat: MDA-MB-231, HeLa, and HT-29 cell lines. This research takes part in the context of effectiveness' determination of copper-complexes inhibitors of topoisomerases to envision new anticancer chemotherapies. In a first part, the determination of DNA damage and the action on topoisomerases with the type of inhibition (Type I and/or II topoisomerases targeted; and poison or catalytic inhibitor) were ascertained using DNA binding experiments and *in vitro* topoisomerases tests. In a second part, impacts of WN197 on the cell cycle and the targeted molecular actors were analyzed with flow cytometry, immunoprecipitation, and Western blots. In a third part, the type of cell death activated, the potential effects on resistant cancer cells, including a human cell-line and a vertebrate embryonic model system were investigated. Finally, the effects of WN197 compared to its ligand WN170 allowed us to conclude that WN197 is a promising tool in future cancer chemotherapies, alone or in combination with other compounds and types of therapies. The last part of the manuscript includes the main scientific articles and reviews I have published as main author.

Materials & Methods

2 MATERIALS & METHODS

2.1 CELLULAR MODEL

2.1.1 Cell lines

WN197 effect on cell viability and mechanism of action were determined on three adenocarcinoma cell lines: **MDA-MB-231** (breast cancer cells), **HeLa** (cervix cancer cells) and **HT-29** (colon cancer cells). MDA-MB-231 is a triple-negative breast cancer cell line (ER^-, PR^-, $HER2^-$) hormono-independent towards growth. These cells express a high level of mutated p53 and are tumorigenic in mice (Bartek *et al.*, 1990; Leroy *et al.*, 2014). The second epithelial cell line, HeLa, originated from Henrietta Lacks, and was the first immortalized human cell line (1951). The cells are HPV positive (HPV-18) and express wild-type p53, but the papillomavirus leads to p53 degradation (May *et al.*, 1991; Leroy *et al.*, 2014). The third cancer line is the colon cancer line HT-29. These epithelial cells were isolated from a primary tumor of a patient in 1964. They express a mutated p53 (Ikediobi *et al.*, 2006; Leroy *et al.*, 2014). The three cancer cell lines were selected for deepen research because a low IC_{50} was obtained with the WN197 compound on these cells but also based on the high incidence their cancer represents. **MCF-10A**, a breast non-cancerous cell line, is an epithelium cell line isolated from an anonymous woman mammary gland. **BT-549** is a triple-negative breast cancer cell line originating from a woman metastasized ductal tumor. **SUM-159** is a triple-negative breast cancer cell line derived from a mouse xenograft of a transplanted primary human invasive infiltrating ductal carcinoma metastatic nodule. **H69AR** is a small cell lung cancer (SCLC) cell line derivative from the NCI-H69. A treatement with increasing doses of doxorubicin (up to 0.8 µM) for 14 months created this multi-drug resistance (MDR) cell line, notably resistant to anthracyclines (Mirski *et al.*, 1987).

HeLa, MDA-MB-231, HT-29, H69AR, and MCF-10A, cell lines originate from ATCC (Manassas, VA, USA). BT-549 were gifted by Dr. Lagadec (CANTHER, Lille), and SUM-159 by Dr. Groux (UGSF, Villeneuve d'Ascq).

2.1.2 Cell Culture

Cell lines were maintained at 37°C in a humidified atmosphere with 5% CO_2 in DMEM medium (Lonza, Basel) for adenocarcinomas, or RPMI-1640 medium (Lonza, Basel) for H69AR, supplemented with 10% fetal bovine serum (Dutscher, Dernolsheim, France) for adenocarcinomas, or 20% for H69AR, 1% Zell Shield (Dutscher, Bernolsheim, France) and 1% non-essentials amino-acids (Lonza, Basel, Switzerland). MCF-10A were maintained in MEBM medium (Lonza, Basel, Switzerland) supplemented with MEGM (Lonza, Basel, Switzerland).

2.2 Chemical Reagents and Materials

All commercial reagents and solvents were used without further purification. Cisplatin was purchased from Alfa Aesar; rapamycin from Abcam; doxorubicin, nocodazole and DMSO from Sigma-Aldrich. Stock solutions were prepared in DMSO. Doxorubicin is a Top2 inhibitor that can intercalate in DNA, induce ROS production and apoptosis (Cappetta *et al.*, 2017; Sritharan and Sivalingam, 2021). Cisplatin is an alkylating agent that induces DNA damage and S phase arrest in the cell cycle as long as apoptosis (Dasari et Tchounwou, 2014). Nocodazole is a mitotic spindle poison, that induces a M phase arrest in the cell cycle (Blajeski *et al.*, 2002).

2.3 MTS assay

2.3.1 Principle

The MTS assay is a colorimetric test used to determine cell viability. MTS is a tetrazolium salt, reduced by viable cells *via* mitochondrial dehydrogenases into a colored formazan (Aqueous soluble tetrazolium/formazan MTS as an indicator of NADH- and NADPH-dependent dehydrogenase activity) (Kamiloglu *et al.*, 2020). The brown color is directly proportional to the percentage of viable cells.

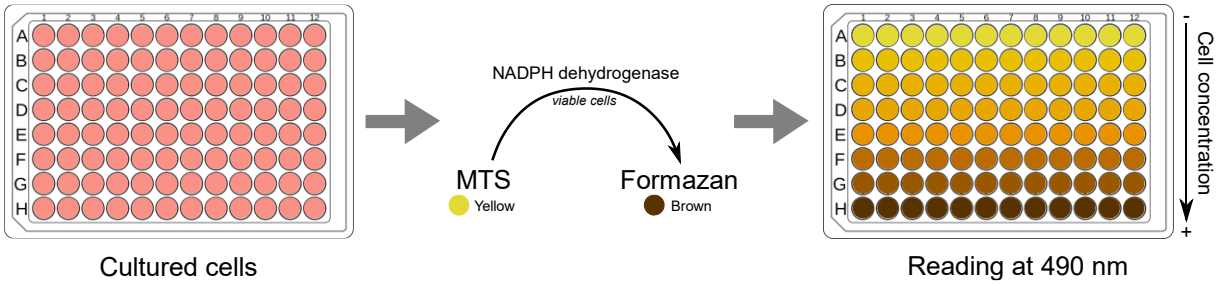

Figure A. Schematic representation of the MTS assay. Cells are treated or not with the compound of interest in a 96-well plate. After treatments, the yellow MTS compound is added to the wells, and incubation proceeded for 1 to 4 hours. The mitochondria of viable cells transform the yellow MTS into brown colored formazan quantified by spectrophotometry at 490 nm.

2.3.2 Protocol

Cell viability was determined using CellTiter 96® AQueous One Solution Cell Proliferation Assay (MTS, Promega). 2.10^3 cells per well were seeded in 96-well plate for 24 h before treatment for 72 h with 0 to 100 µM of WN197, WN170 or cisplatin. After an incubation of 2 h with 20 µL of CellTiter solution at 37°C in 5% CO2, the production of reduced MTS (3-(4,5-dimethylthiazol-2-yl)-5-(3-carboxymethoxyphenyl)-2-(4-sulfophenyl)-2H-tetrazolium) in formazan was measured at 490 nm (SPECTROstar Nano, BMG LABTECH). IC_{50} were calculated

using GraphPad Prism V6.0 software. Statistical differences between WN197 and WN170 were ascertained by a Student t-test (***p<0.005).

2.4 TOPOISOMERASE ACTIVITY *IN VITRO* TEST

2.4.1 Principle

Topoisomerase activity *in vitro* assay is based on the capacity of topoisomerase to relax supercoiled DNA ($_{SC}$DNA). Relaxed ($_{R}$DNA) and $_{SC}$DNA subjected to an electric current have different migration profiles in a 1% agarose gel. Topoisomerase inhibitors (poisons or catalytic inhibitors) impede DNA relaxation, altering the migration profiles of DNA. Differentiation between catalytic and poison inhibitors is determined by the ability of a poison to stop topoisomerase reaction after the DNA cleavage, leading to an accumulation of stabilized nicked or linear DNA ($_{N}$DNA or $_{L}$DNA) due to the formation of a ternary complex between the DNA, the topoisomerase, and the poison.

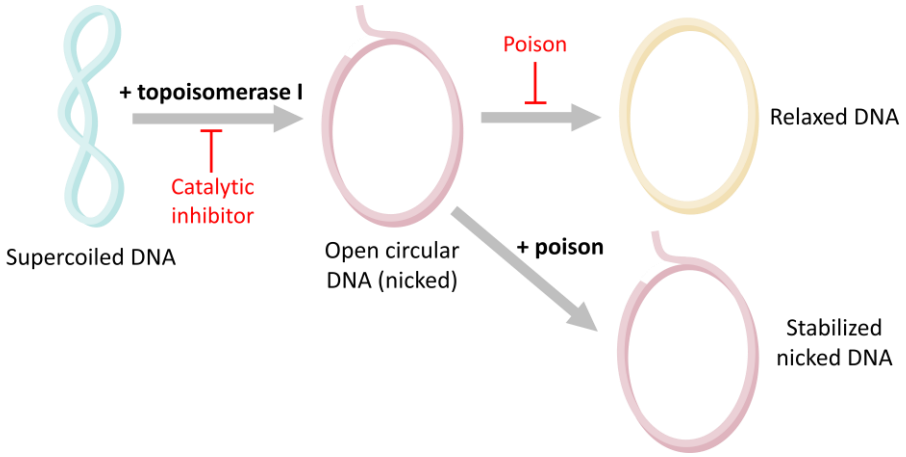

Figure B. Principle of topoisomerase 1 (Top1) *in vitro* activity test. One strand of the supercoiled DNA (in blue) is cleaved by Top1, leading to a transient open circular DNA (or nicked DNA) (in pink), and religated to form a relaxed DNA (in yellow). In the presence of a Top1 poison or a catalytic inhibitor, DNA stays supercoiled. More specifically, a Top1 poison intercalates between the topoisomerase and the cleaved DNA, stabilizing the DNA in a nicked form, detected on a 1% agarose gel.

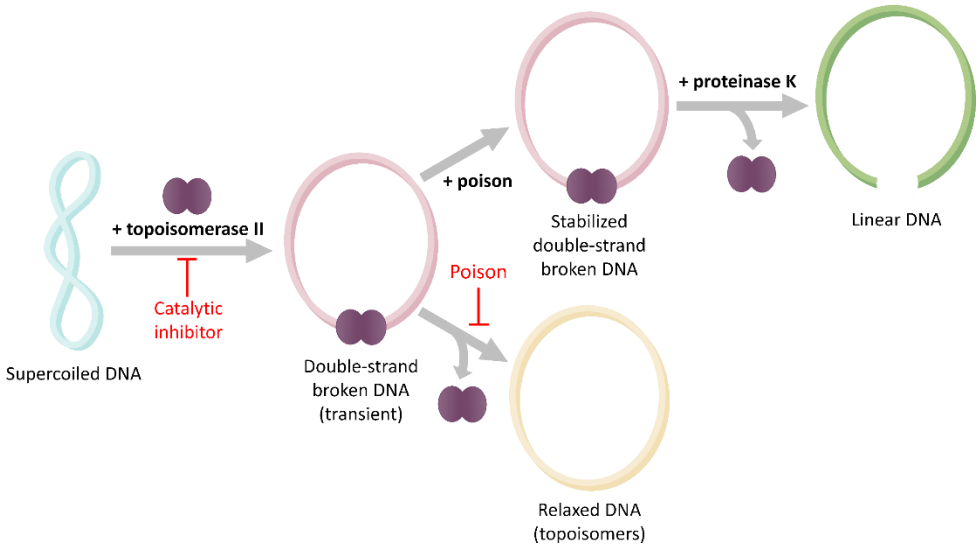

Figure C. Principle of topoisomerase 2 (Top2) *in vitro* activity test. Both DNA strands of supercoiled DNA (in blue) are cleaved by Top2, forming a transient double-strand broken DNA (in pink), and religated to form a relaxed DNA (in yellow). In the presence of a Top2 poison or a catalytic inhibitor, the DNA stays supercoiled. More specifically, a Top2 poison intercalates between the topoisomerase and the cleaved DNA, stabilizing the DNA in a double-strand break form. The addition of proteinase K in the assay allows the separation of the topoisomerase enzyme from the broken DNA and the liberation of a linear DNA (in green), visible after migration in a 1% agarose gel.

2.4.2 Protocol

Topoisomerase I (Top1) activity assay was performed using the drug screening kits protocol (TopoGEN, Inc.). The reaction mixture was composed of supercoiled plasmid DNA pHOT1 (250 ng), 10X TGS buffer (10 mM Tris-HCl pH 7.9, 1 mM EDTA), 5 units of Top1, the compound, and a final volume adjusted to 20 µL with H_2O. WN197 was tested at concentrations ranging from 0.2 to 2 µM. Camptothecin (CPT, 10 µM) was used as a positive control (poison inhibitor of Top1 activity), etoposide (VP-16, 100 µM) as negative control (inhibitor of Top2 activity), and 1% DMSO alone as vehicle control. Relaxed pHOT1 DNA (100 ng) was used as migration control. The addition of proteinase K (50 µg/mL) for 15 min at 37°C allowed Top1 degradation to visualize the cleavage products (nicked DNA). Reaction products were separated by electrophoresis in a 1% agarose gel containing ethidium bromide (0.5 µg/mL) for 1 h at 100 V in TAE (Tris-Acetate-EDTA; pH 8.3) buffer.

Topoisomerase II Relaxation Assay Kit (Inspiralis, Inc.) was used to measure topoisomerase II (Top2) activity. The reaction mixture was composed of supercoiled plasmid DNA pBR322 (1 µg), 10X assay buffer (50 mM Tris-HCl (pH 7.5), 125 mM NaCl, 10 mM MgCl2, 5 mM DTT, 100 µg/mL albumin), 30 mM ATP, 5 units of Top2α or Top2β, the compound, and a final volume adjusted with H_2O to 30 µL. Etoposide (VP-16, 100 µM) was used as positive

control, and camptothecin (10 µM) as negative control. The mixtures were incubated at 37 °C for 30 min and the reactions stopped by the addition of 5 µL 10% SDS. Reaction products were separated by electrophoresis in a 1% agarose gel for 1 h at 100 V in TAE buffer, and stained with ethidium bromide (0.5 µg/mL) for 15 min. After rinsing with water, the DNA migratory profiles were visualized under UV light (ChemiDocTM XRS+, BioRad).

2.5 FLUORESCENCE

2.5.1 Principle

DNA damage were analyzed by **immunofluorescence** localization of a marker protein. After DNA damage, the DDR pathway is activated, resulting in the activation of the ATM/ATR kinases. These proteins phosphorylate histone H2AX on serine 139 (γH2AX), on the DNA break sites (Hakem, 2008; Bonner, 2008; Kinner *et al.*, 2008). γH2AX is detectable by immunofluorescence as fluorescence dots (*foci*). The amount of γH2AX *foci* is directly related to the amount of DNA breaks, allowing to compare the number of breaks between different conditions.

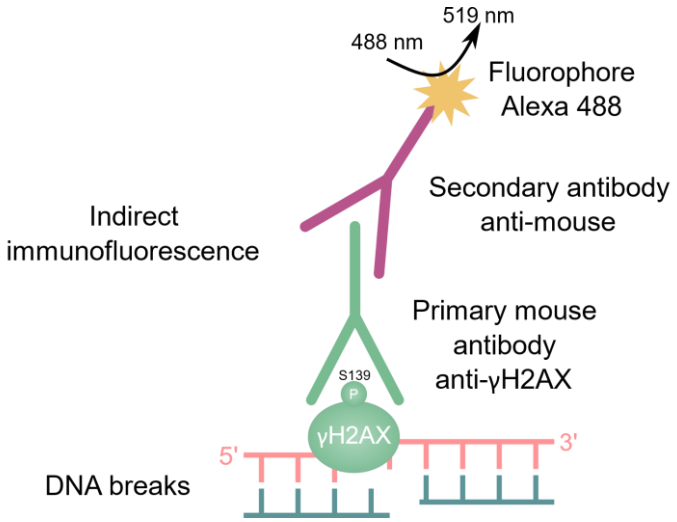

Figure D. Representative scheme of indirect immunofluorescence used to detect γH2AX. H2AX is phosphorylated on the DNA damaged sites, and recognized by the primary mouse antibody directed against the phosphorylated S139 form of H2AX. The secondary antibody coupled to Alexa 488 fluorophore emits a green fluorescence (519 nm) after excitation at 488 nm.

Autophagy was visualized by fluorescence, using the autophagy assay kit from Abcam (*ab139484*). The special dye allows a green fluorescent signal emission at 530 nm after excitation at 488 nm, specifically in the lysosomes, and with a higher intensity when incorporated into pre-autophagosomes, autophagosomes, and autolysosomes. The target(s) or physiological mechanism of the probe is not specified by the seller.

2.5.2 Protocol

For γH2AX detection, 2.10^5 cells seeded on glass coverslips in 6-well plate were treated with 0.5 µM of WN197 or WN170, 5 µM of doxorubicin, 20 µM of cisplatin as positive controls, or 0.1% DMSO as a solvent control for 30 min or 24 h. Cell fixation was performed with 4% paraformaldehyde (Sigma-Aldrich) for 5 min and followed by permeabilization with 0.1% Triton in PBS (Sigma-Aldrich) for 10 min and saturation of unspecific sites with 1% BSA in PBS (Sigma) for 1 h at room temperature. Cells were incubated overnight at 4°C with anti-γH2AX mouse antibody (S139, 1:1000, Cell Signaling, by Ozyme) and washed 3 times with 1% BSA/PBS. Cells were then incubated with secondary anti-mouse IgG (Alexa Fluor® 488, 1:2000, Thermo-Fisher Scientific Biosciences GMBH) for 1 h at room temperature in the dark, washed 3 times before *nuclei* were stained with DAPI (6-diamidino-2-phenylindole, 1 µg/mL, Molecular Probes, by Thermo Fisher Scientific Biosciences GMBH). Images were captured under a Leica fluorescent microscope (TISBIO platform, UGSF, Lille), and γH2AX *foci* were counted with ImageJ (Fiji Software, v1.52i) on 30 cells from 3 independent experiments and quantified with GraphPad Prism V6.0 software. Statistical significances (mean ± SD) were performed by a two-way ANOVA followed by Dunnett's multiple comparison test (*p<0.05; **p<0.01; ***p<0.001; ****p<0.0001).

For autophagy detection, the autophagy assay kit was used as described by the manufacturer (Abcam, ab139484). 2.10^5 cells were seeded on glass coverslips and treated for 24 h with 0.5 µM of WN197, rapamycin as positive control, or 0.1% of DMSO as a solvent control. Cells were rinsed twice with 1X assay buffer and incubated with the green detection reagent and Hoechst dye (20 mM, nucleus stain). Cells were fixed by 4% paraformaldehyde (Sigma-Aldrich) for 10 min and rinsed three times with 1X assay buffer. Images were captured under a Leica fluorescent microscope, and γH2AX green spots were counted with ImageJ (Fiji Software, v1.52i) on 30 cells from 3 independent experiments and quantified with GraphPad Prism V6.0 software. Statistical significances (mean ± SD) were performed by a two-way ANOVA followed by Dunnett's multiple comparison test (*p<0.05; ***p<0.001; ****p<0.0001).

2.6 FLOW CYTOMETRY

2.6.1 Principle

Flow cytometry works on the principle of light scattering and fluorescence emission by specific fluorescent probe-labeled cells as they pass one by one through a laser beam. The **cell cycle** analysis by flow cytometry consists of the detection of the quantity of fluorescent propidium iodide (PI) intercalated in the cell nucleus and allows a distinction between the different cell cycle phases. PI intercalates in the DNA, with an arbitrary quantity of n=1 in

G0/G1 phases leading to the emission of a low fluorescent signal, a quantity of n=2 in G2/M phases as a result of DNA duplication with a higher fluorescent signal emission, and with an intermediate quantity when DNA duplicates in S phase resulting in an intermediate emission of fluorescence between n=1 and n=2.

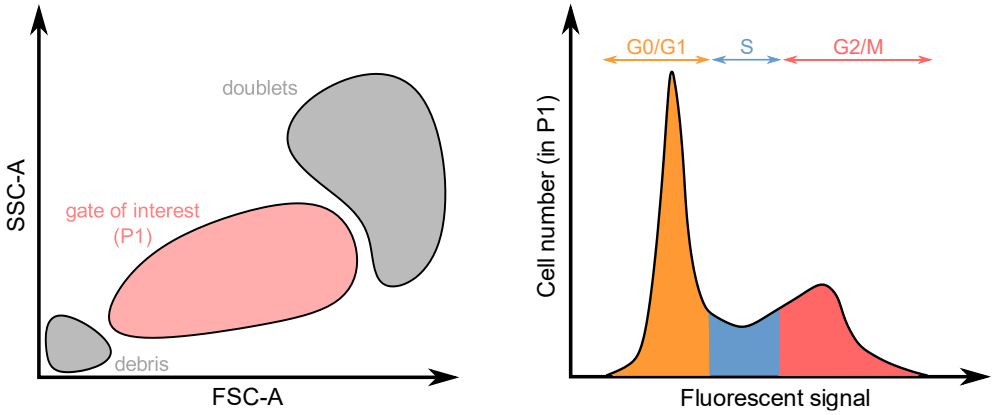

Figure E. Schematic representation of cell cycle analysis by flow cytometry. Labeled cells are flowing one by one in a laser beam that excites a fluorochrome. Each cell is sorted and its fluorescent emission is detected and quantified. Left: debris (low density (SSC) and height (FSC)) and cell doublets (high density and height) are excluded from the gate of interest (P1). Right: cells from the gate P1 are distributed according to the intensity of their fluorescent signal, and divided into three different pools corresponding to cell cycle phases (representation of the control distribution of a human proliferating cell population with cell cycle phases repartition as follow: ~45% in G0/G1, ~20% in S, ~35% in G2/M).

For **apoptosis detection**, annexin-V levels were measured by **flow cytometry**. During apoptosis, the phosphatidylserine (PS) is translocated early from the inner to the outer part of the membrane. Annexin V has a high affinity to PS, therefore, during apoptosis, cells exposing PS to the external environment are ligated to annexin V proteins. Annexin V binds to FITC (fluorescein isothiocyanate) detected by flow cytometry. Propidium iodide (PI) is used as a co-marker to differentiate cells in early *versus* late apoptosis since only dead cells have a permeabilized membrane. Therefore, annexin V^- PI^- cells are cells that don't proceed through apoptosis, annexin V^+ PI^- are cells in early apoptosis and annexin V^+ PI^+ are cells in late apoptosis. Annexin V^- PI^+ cells can also represent necrotic cells or cell debris as annexin V finally enters any damaged cell membrane.

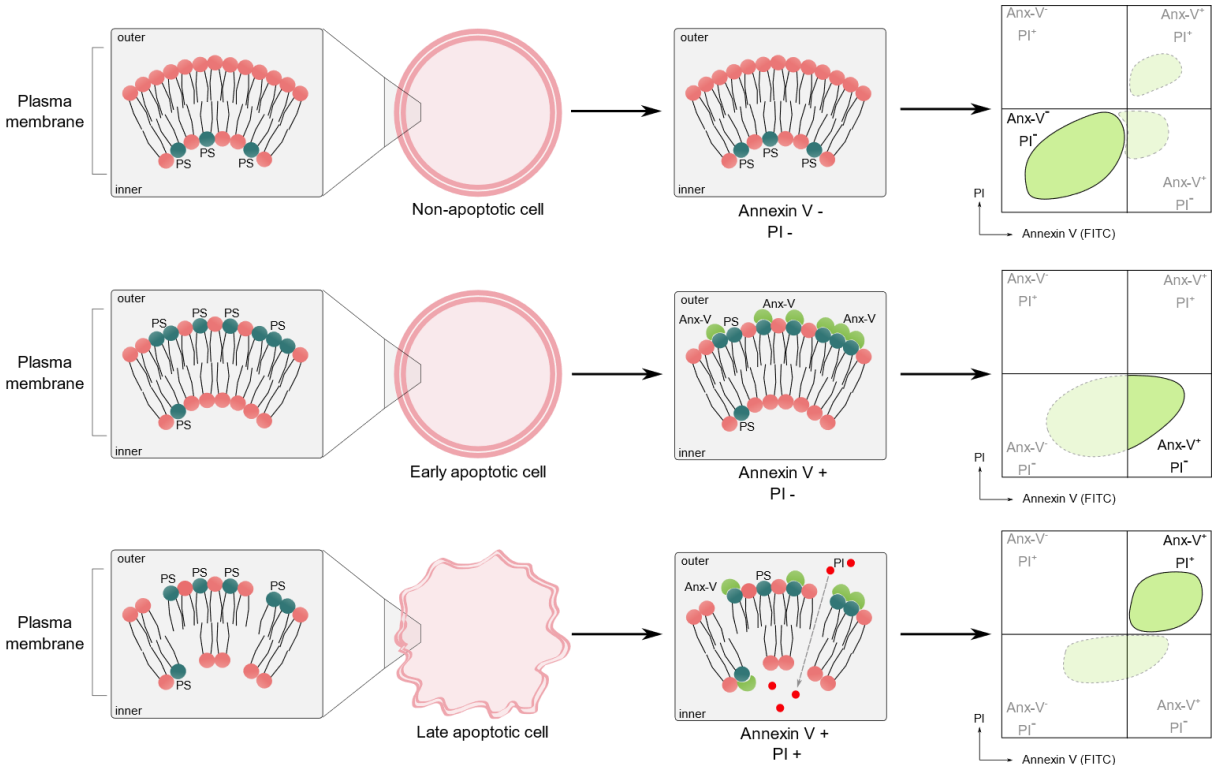

Figure F. Principle of annexin V-propidium iodide (PI) analysis by flow cytometry. **(Upper)** In normal cells, the phosphatidylserine (PS) sets on the inner side of the plasma membrane and the addition of annexin V and PI results in an absence of staining. In a cultured cell population, a basal level of apoptosis is often detected. **(Middle)** In early apoptotic cells, PS is present on the outer side of the cell plasma membranes, allowing the fixation of annexin V, and an annexin V positive staining is obtained. **(Bottom)** In late apoptotic cells, PS is detected on the outer side of the membrane, and the membrane is permeabilized, allowing PI entrance into the cells which results in positive staining for annexin V and PI.

2.6.2 Protocol

$7.5.10^5$ cells plated for 24 h were treated with 0.5 µM WN197 or WN170, 20 µM of cisplatin (S phase arrest control), 83 nM of nocodazole (M phase arrest control), or 0.1% DMSO (solvent control). For the dose titration experiments, cells were treated for 24 h with increasing concentrations of WN197. For kinetic experiments, cells were treated with 0.5 µM of WN197 or WN170 from 4 to 48 h. Cells were detached using trypsin (Biowest) for 5 min at 37°C, centrifuged at 1,000 G for 10 min, resuspended in PBS, and fixed with 70% ethanol at -20°C for 24 h, before they were centrifugated (1,000 G, 10 min), resuspended in PBS, and treated for 15 min at room temperature with RNase (200 µg/mL, Sigma). Finally, incubation with propidium iodide (10 µL/mL, Molecular Probes, by Thermo Fisher Scientific Biosciences GMBH) at 4°C for 30 min was performed before flow cytometry (BD FACSCalibur, Becton Dickinson) analysis. For each sample, 10,000 events (without cell doublets and cellular debris) were considered. The cell cycle repartition was analyzed with Graphpad Prism V6.0 software.

Statistical significances (mean ± SD) were determined by two-way ANOVA followed by Dunnett's multiple comparison test (*p<0.05; **p<0.01; ***p<0.005; ****p<0.001).

For apoptosis detection featured by annexin V-propidium iodide (PI), MDA-MB-231, HeLa, and HT-29 cells were cultivated to 80% of confluence ($7.5.10^5$ cells), incubated or not for 24 h with WN170 (0.5 µM), WN197 (0.5 µM), camptothecin (20 µM; CPT) or doxorubicin (5 µM; Doxo), trypsinized for 5 min at 37°C, and washed in ice-cold PBS. Cell suspensions were treated with 1:1 PI and annexin V-FITC reagent (Apoptosis Detection Kit, BD) and incubated for 15 min at RT in the dark. The binding buffer (1X) was added to each tube before they were analyzed by flow cytometry (CytoFLEX LX, Beckman Coulter) with Kaluza analysis software (v2.1.1).

2.7 WESTERN BLOTS AND IMMUNOPRECIPITATIONS

2.7.1 Principle

Following DNA damage, a kinases cascade initiates the activation of the DNA damage response (DDR) pathway, with ATM and ATR phosphorylating H2AX, Chk1 and Chk2 (Hakem, 2008; Bonner, 2008). ATM/ATR and Chk1/Chk2 interact with p53 and p21 to regulate their activity or transcription (**Figure G**). The phosphorylation state or quantity of seven proteins of the DDR pathway were analyzed by **Western blots**.

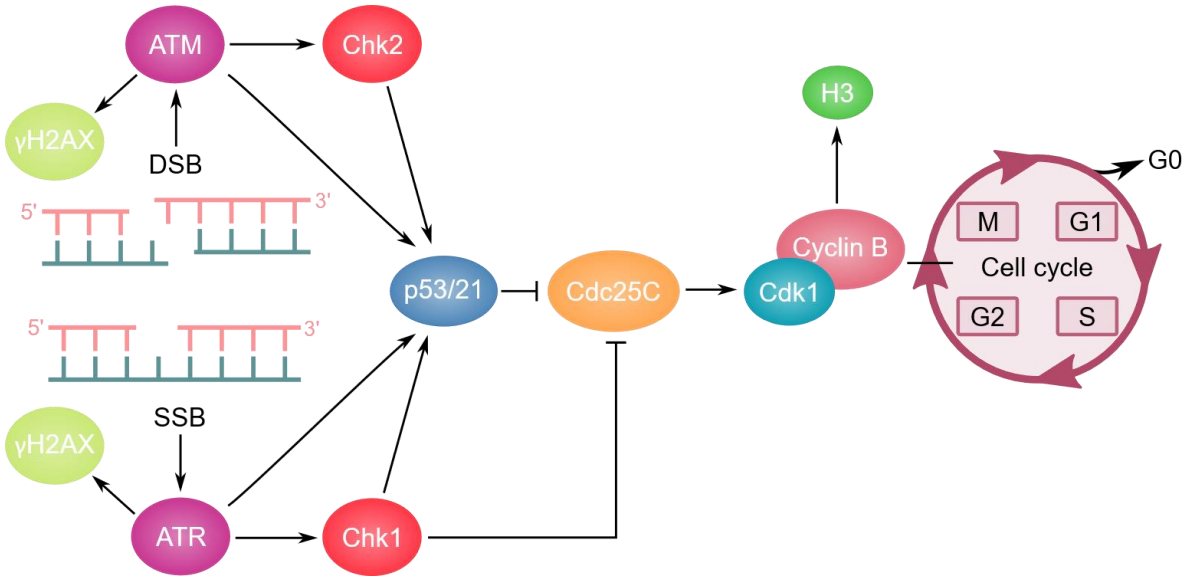

Figure G. DNA damage and cell cycle regulation. After DNA double- or single-strand breaks (DSB and SSB) an activation cascade is triggered. The ATM/ATR transducers activate Chk1/Chk2 and p53/p21 effectors. ATM is mostly recruited following DSB while ATR is after SSB. Chk1 and Chk2 subsequently inhibit proteins of the Cdc25 family involved in the activation of Cyclin/Cdk complexes activation, regulators of the different cell cycle phases. Consequently, cell cycle inhibition and arrest are possible in different phases, according to the targeted couple of Cyclin/Cdk checkpoint regulator. Here is represented the G2/M checkpoint blockage.

Cell cycle checkpoints are composed of a diversity of Cyclin/Cdk complexes (**Figure G**). Depending on the cell cycle phases, different Cdc25 are activated, and subsequently different Cyclin/Cdk couples. In our experiments, markers from the G2/M transition and M phase were analyzed by **Western blots** to refine the results obtained by flow cytometry: Cdc25C, Cdk1/Cyclin B, and histone H3. Histone H3 phosphorylation on S10 by active MPF is necessary for DNA condensation during mitosis, making it a suitable M phase marker (Hans et Dimitrov, 2001).

Cdc25C is phosphorylated on S216 before the M phase by the DNA damage cascades as seen in the introduction page 34-36, and can bind to the chaperon protein 14-3-3 (**Figure H**). This Cdc25C sequestration prevents it from dephosphorylating Cdk1, and therefore from activating the MPF complex and entry of cells in the M phase. Cdc25C **immunoprecipitations** were realized and **Western blots** were proceeded against 14-3-3 to verify the complexation of the two proteins.

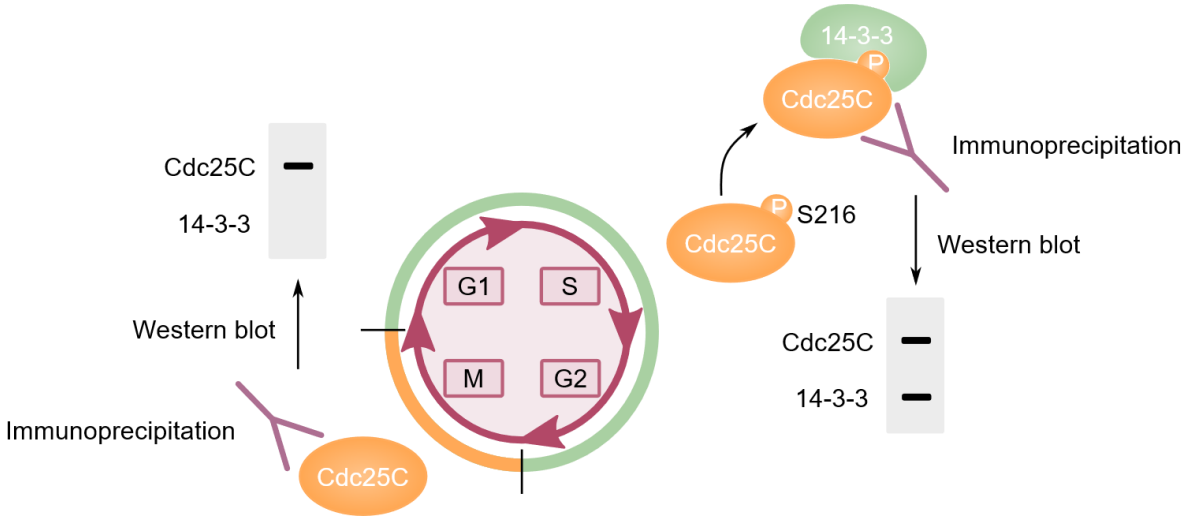

Figure H. Schematic representation of Cdc25C detection by immunoprecipitation and Western blot. During the M phase, active Cdc25C is not phosphorylated on S216 (inhibitory phosphorylation), which allows MPF (Cyclin B/Cdk1) activation. When cells are accumulated or stopped in the M phase, the Cdk1/Cyclin B complex is activated and no 14-3-3 protein is found on Western blots after a Cdc25C immunoprecipitation. In case of an arrest in the other phases of the cell cycle, Cdc25C is inactivated by phosphorylation on S216, and recognized by 14-3-3 to which it binds, allowing a detection of both partners after immunoprecipitation and Western blots.

Apoptosis markers analyzed by **Western blots** are: activated PARP (cleaved), activated caspase 3 (cleaved) and the cytosolic cytochrome *c*. For autophagy, markers including the degradation of p62, the synthesis of Beclin-1, and the switch from LC3-I to LC3-II (LC3-I coupled to phosphatidylethanolamine) (Kroemer *et al.*, 2009) were analyzed by **Western blots**. During autophagy, mTOR gets complexed to a phosphorylated form of RAPTOR (S792) in the rapamycin-sensitive mTOR complex 1 (mTORC1). After DNA damage, the mTORC1 complex is

inhibited by RAPTOR phosphorylation (on multiple sites including S792) in a negative feedback loop to induce autophagy (Dunlop *et al*., 2011; Ma *et al*., 2018). This activation is similar to the mTORC1 inhibitor rapamycin (Kim and Guan, 2015). **Immunoprecipitations** against mTOR from the mTORC1 complex were proceeded and **Western blots** against mTOR and phosphorylated RAPTOR were done.

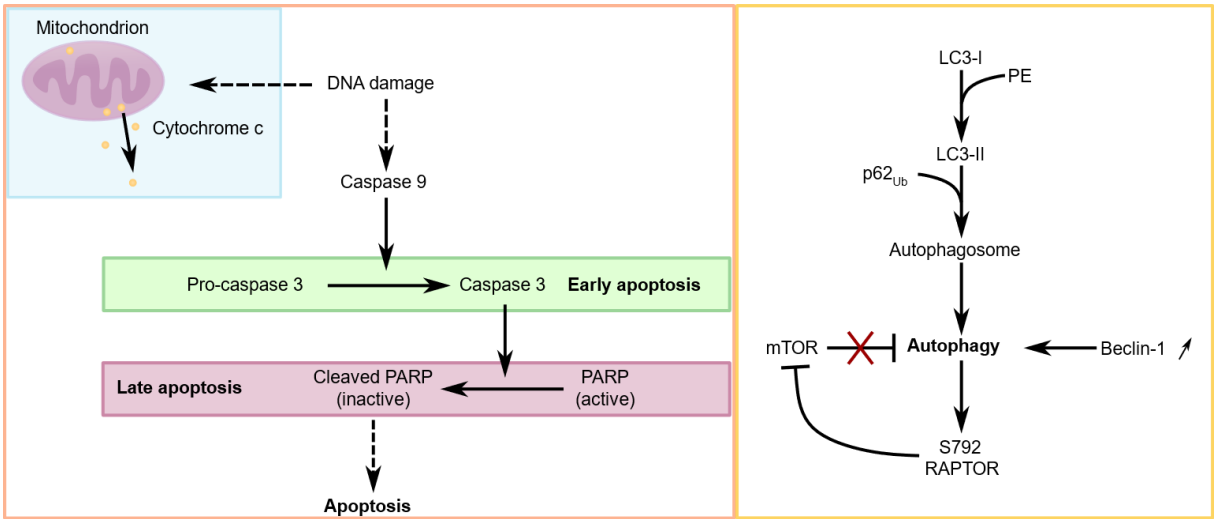

Figure I. Analyzed apoptosis and autophagy pathway effectors.

2.7.2 Protocol

$7.5.10^5$ cells were seeded in a 25 cm^3 flask for 24 h and treated with 0.5 µM of WN197 or WN170, 20 µM of cisplatin, 5 µM of doxorubicin, or 0.1% DMSO (solvent control). After 24 h, they were lysed in RIPA buffer (1% Triton X-100; 50 mM TRIS-HCl pH 4; NP40 2%; 0.4% Na-deoxycholate; 0.6% SDS; 150 mM NaCl; 150 mM EDTA; 50 mM NaF) supplemented with 1% of protease inhibitor cocktail (Sigma-Aldrich) and phosphatase inhibitors (Roche SAS by Merck). For cytochrome *c* analysis, $7.5.10^5$ cells were seeded for 24 h and treated for 3 h, 16 h, 24 h or 48 h with 0.5 µM of WN197, and for 24 h or 48 h with 5 µM of doxorubicin as a positive control. Cells were lysed in a glass grinder at 4°C in homogenization buffer (25 mM MOPS at pH 7.2, 60 mM b−glycerophosphate, 15 mM para-nitrophenylphosphate, 15 mM EDTA, 15 mM $MgCl_2$, 2 mM DTT, 1 mM sodium orthovanadate, 1 mM NaF, 1 mM phenylphosphate, 10 mg/mL leupeptin, 10 mg/mL aprotinin, 10 mg/mL soybean trypsin inhibitor, 10 mM benzamidine). Samples were centrifuged for 10 min at 12,000 G and the protein concentration of supernatants was determined using the Bradford assay (BioRad) and a spectrophotometer reading at 595 nm (SPECTROstar Nano, BMG LABTECH).

Proteins were denatured in 2X Laemmli buffer (65.8 mM TRIS- HCl pH 6.8; 26.3% glycerol; 2.1% SDS; 0.01% bromophenol blue; 4% β-mercaptoethanol, BioRad) at 75°C for 10 min. 15 µg of proteins were separated on 4-20% SDS PAGE gels (mini protean TGX, BioRad), for 1 h at 200 V in denaturing buffer (0.1% SDS; 0.3% TRIS base; 1.44% glycine). Proteins were transferred onto nitrocellulose membrane (Amersham Hybond, Dutscher) by wet transfer

(0.32% TRIS; 1.8% glycine; 20% methanol, Sigma-Aldrich), for 1 h at 100 V. Membranes were saturated with 5% low fat dry milk in TBS (15 mM de TRIS, 140 mM de NaCl: Sigma) added with 0.05% Tween (Sigma-Aldrich), and incubated overnight at 4°C with specific primary antibodies: rabbit polyclonal antibodies against ATM (Cell Signaling technology (CST, Ozyme), 1/1000), ATR (CST, 1/750), phosphorylated ATR (S428, CST, 1/1000), Beclin-1 (CST, 1/800), Cdc25C (CST, 1/1500), phosphorylated Cdc25C (S216, CST, 1/1000), phosphorylated Cdk1 (Y15, CST, 1/1500), phosphorylated Chk1 (S317, CST, 1/1000), phosphorylated Chk2 (T68, CST, 1/1000), cleaved caspase 3 (CST, 1/1000), phosphorylated H2AX (S139, CST, 1/750), histone H3 (CST, 1/1000), phosphorylated H3 (S10, CST, 1/1000), phosphorylated p53 (S15, CST, 1/1000), p53 (CST, 1/1000), p21 (CST, 1/1000), LC3 (CST, 1/50), mTOR (CST, 1/1200), RAPTOR (CST, 1:1500), phosphorylated RAPTOR (S792, CST, 1/1000); mouse monoclonal antibodies against phosphorylated ATM (S1981, Santa Cruz Biotechnology (SCB), 1/200), Chk1 (SCB, 1/1000), Chk2 (SCB, 1/ 200), Cdk1 (CST, 1/1000), 14-3-3 (SCB, 1/1000), cyclin B2 (CST, 1/1500), p62 (SCB, 1/100); goat polyclonal antibodies against β-actin (SCB, 1/1200); and cocktail antibodies against cleaved PARP (Abcam, cell cycle and apoptosis cocktail, 1/1500). After three washes of 10 min in TBS-Tween, nitrocellulose membranes were incubated for 1 h with the appropriate horseradish peroxidase-labeled secondary antibodies: anti-rabbit or anti-mouse antibodies (Invitrogen, Thermo Fisher Scientific Biosciences, 1/30,000) or anti-goat antibodies (SCB, 1/30,000). Secondary antibodies were washed in TBS-Tween three times for 10 min and the signals were revealed with a chemiluminescent assay (ECL Select, GE Healthcare, Dutscher) on hyperfilms (Amersham hyperfilm MP, Dutscher). β-actin or histone H3 were used as loading controls. Signals were quantified with Image J (Fiji Software, v1.52i), and normalized to respective loading control.

For immunoprecipitation, protein samples were pre-cleared with protein A sepharose (20 µL of 50% beads/200 µL of cell lysate, Sigma-Aldrich) for 1 h at 4°C under gentle rocking. After brief centrifugation, supernatants were incubated with antibodies against 14.3.3 (Santa Cruz Biotechnology), Cdc25C (Thermo Fisher Scientific Biosciences GMBH, 1/200) or mTOR (CST, 1/200) at 4°C for 1 h under rotation and followed by incubation with protein A sepharose (20 mL of 50% bead slurry, Sigma-Aldrich) for 1 h at 4°C under rotation. Samples were rinsed 3 times with RIPA buffer. Pellets were collected by brief centrifugation, resuspended in 2X Laemmli buffer, and heated at 100°C for 10 min before SDS-PAGE and Western blots were performed.

2.8 TOXICITY ON *XENOPUS LAEVIS* EMBRYOS

2.8.1 Principle

Xenopus laevis amphibian originates from South Africa. Xenopus eggs and embryos are easy to obtain (high number of gametes, and rapid external development), making them

perfect developmental models to study diverse aspects of embryogenesis and to assess the effects of various drugs and treatments (Ishibashi *et al*., 2017; Slaby *et al*., 2016). At the mid-blastula transition (after the 12th cell cycle, NF stage 9 (Nieuwkoop and Faber), and 7 h after fertilization), Xenopus embryos can activate large-scale zygotic transcription, zygotic cell cycle are modified, and multiple pathways are activated to respond to DNA damage (Finkielstein *et al*., 2001). WN197 toxicity was tested on Xenopus embryonic development.

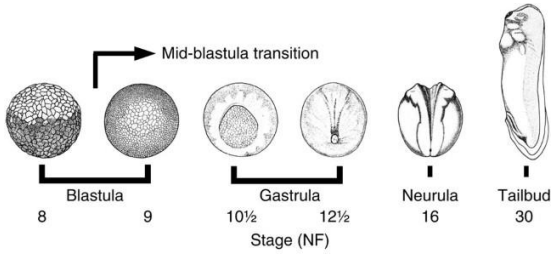

Figure J. Developmental stages of *Xenopus laevis* embryos. NF: Nieuwkoop and Faber. From Nieuwkoop and Faber, 1994.

2.8.2 Animals and embryos handling

All animal experiments were performed according to the rules of the European Community Council guidelines (86/609/EEC) for laboratory animal experimentation. The vertebrate animal protocol was approved by the local institutional review board (Comité d'Ethique en Expérimentation Animale, Hauts-de-France, G59-00913). Mature *Xenopus laevis* females, purchased from the CRB-University of Rennes I (Rennes, France) and housed in PHExMAR, at the University of Lille, were anesthetized by immersion in 1 g/L MS222 solution (tricaine methane sulfonate, Sigma Aldrich). After anesthesia in 3g/L MS222 solution, males were sacrificed, and testis were surgically removed and stored in MMR (Marc's modified Ringer's; 100 mM NaCl, 2 mM KCl, 1 mM $MgSO_4$, 2 mM $CaCl_2$, 0.1 mM EDTA, 5 mM HEPES, pH 7.8 at 4°C). Ovulation was induced by injection of human chorionic gonadotropin (hCG) ranging from 500 U to 700 U, into the dorsal lymph sac of the female frogs. After 20 h, smooth pressure was applied on the female ventral side to help the egg-laying process. For fertilization, eggs were collected, and immediately placed in contact with a piece of sliced testicle in sterile water with or without doxorubicin or WN197 at 0.5 or 5 µM under gentle agitation for 10 min. The eggs thick jelly coat was removed using an incubation under gentle rocking with L-cysteine (2%). Eggs were rinsed 3 times, exposed or not to doxorubicin or WN197 at 0.5 or 5 µM, and development was followed at 22°C. The number of dead embryos appearing as swollen structures with disorganized pigments was counted at different developmental stages: gastrula (NF stage 12), neurula (NF stage 16), and tailbud (NF stage 30) (**Figure L**). Statistical analyses were performed with Graphpad Prism V6.0 software, and significances (mean ± SD) were determined by two-way ANOVA followed by Dunnett's multiple comparison test (***p<0.005, ****p<0.001).

Results

3 RESULTS

3.1 EFFECT OF WN197 ON ADENOCARCINOMAS' DNA

To determine if WN197 induces DNA damage in the adenocarcinoma cell lines MDA-MB-231, HeLa, and HT-29, immunofluorescences detection of γH2AX (phosphorylated form) were proceeded. DNA breaks were visualized by γH2AX *foci* (dots) in the cell nucleus. In control with DMSO treatment (solvent control, 0.5%) for 24 h, MDA-MB-231 and HeLa presented no γH2AX *foci*, and HT-29 a very low quantity of dots in the range of the background noise (**Figures 1-3**). After doxorubicin (5 µM) or cisplatin (20 µM) treatments (positive controls) cell lines displayed a large amount of γH2AX *foci*. WN197 or WN170 addition at a concentration close to their IC_{50} (0.5 µM) produced γH2AX *foci*. A lower number of *foci* were observed for WN170 in MDA-MB-231 and HT-29 cells, and a small portion in the HeLa cells compared to WN197 that generated more γH2AX *foci* in the three cell lines.

γH2AX *foci* were quantified (**Figure 4A**). In the DMSO controls, a mean of 10, 9 and 7 *foci* per cell was obtained respectively for MDA-MB-231, HeLa, and HT-29. Doxorubicin and cisplatin induced a significant increase in the mean of *foci* per nucleus compared to the negative controls: 90 and 60 *foci* per cell in MDA-MB-231, 127 and 76 in HeLa, 70 and 30 in HT-29. In the WN170 condition, the mean of *foci* per cell was not significant compared to the control with 30 *foci* in MDA-MB-231, 25 in HeLa, and 15 in HT-29. After WN197 treatments, the mean of *foci* was significantly higher compared to the control and WN170, and equal to doxorubicin and cisplatin conditions: 100 γH2AX *foci* were obtained in MDA-MB-231, 98 in HeLa, and 70 in HT-29.

Western blots were performed to confirm the results obtained by immunofluorescence (**Figure 4B**). No γH2AX signal was visible in the control conditions for the three cell lines. On the contrary, γH2AX signals were detected in the doxorubicin and cisplatin positive control conditions. For WN170, a signal was obtained 1.9 times superior to the control in the MDA-MB-231 (quantification by densitometry), 2.6 times superior in HeLa, and 1.4 times superior in HT-29. With WN197, the signals were higher (2.8, 3.5, 4.8 respectively).

To determine if WN197 could induced early DNA damage in the cancer cells, immunofluorescence experiments against γH2AX were realized after 30 min of treatment and the *foci* quantified (**Figure 4C**). In the untreated conditions, a mean of 4 *foci* was obtained in MDA-MB-231, 31 in HeLa, and 3 in HT-29. A significant number of *foci* was observed after doxorubicin and WN197 treatments, with an average of 63 and 84 *foci* respectively in MDA-MB-231, 106 and 87 in HeLa, and 27 and 13 in HT-29.

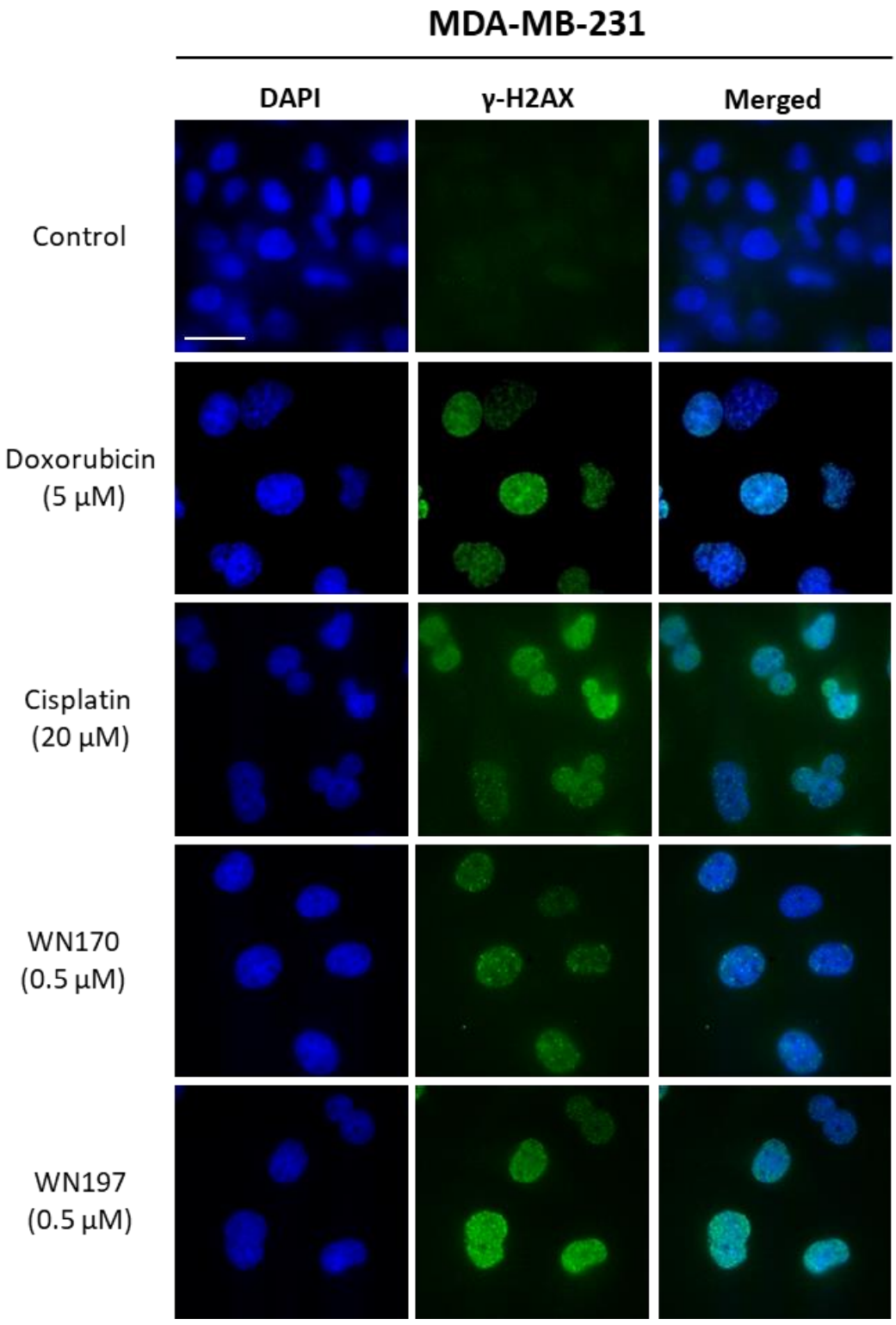

Figure 1: γH2AX detection by immunofluorescence in MDA-MB-231. Cells were treated with DMSO (0.5%, solvent control), doxorubicin (5 µM, positive control), cisplatin (20 µM, positive control), WN170 (0.5 µM) or WN197 (0.5 µM). After 24 h of treatment, the antibody against γH2AX (green) revealed DNA breaks staining as *foci* (dots). Nuclei were stained with DAPI (blue). Images were obtained on a Leica fluorescent microscope (x100) and were representative of three independent experiments. Scale bar: 20 µm.

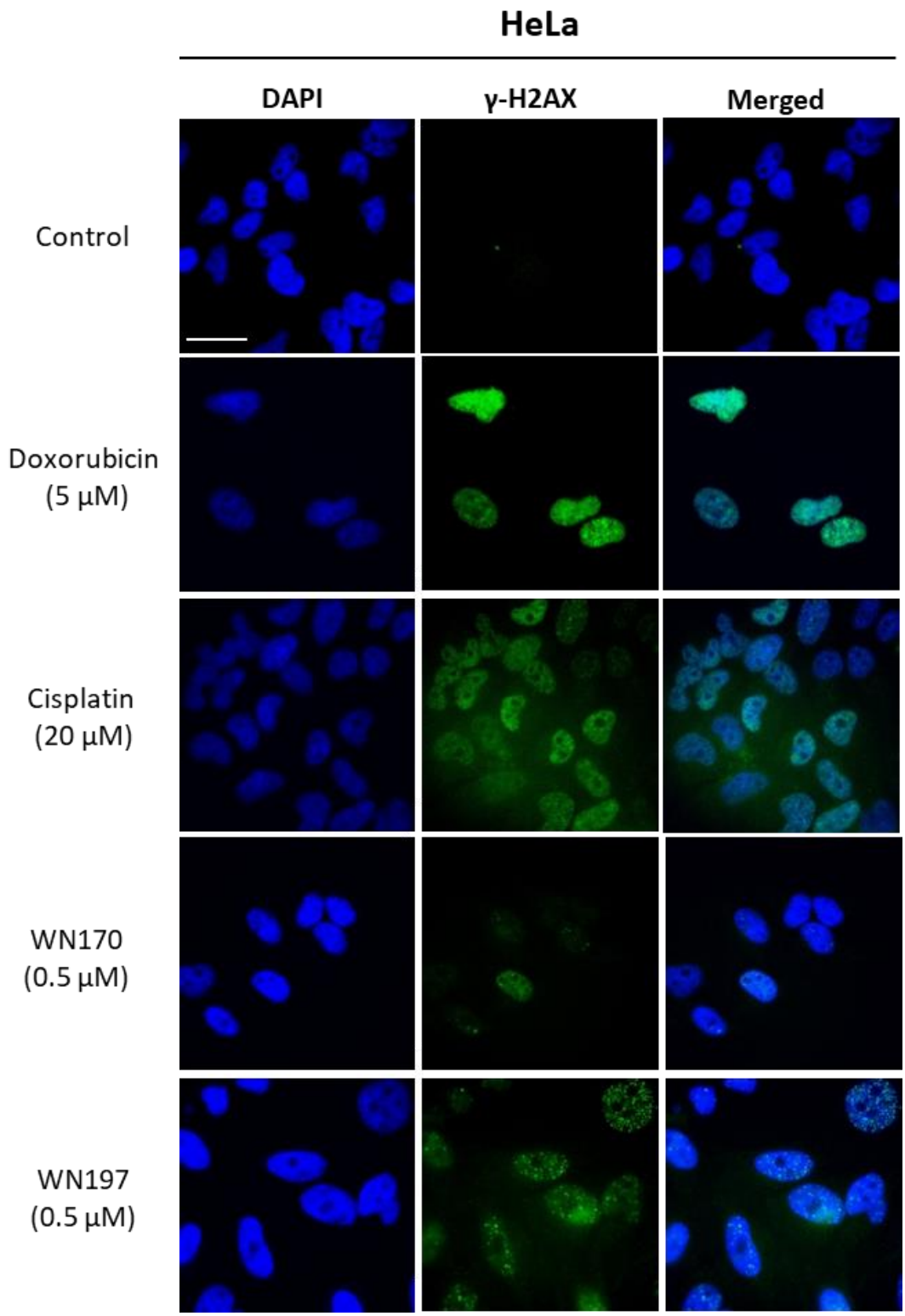

Figure 2: γH2AX detection by immunofluorescence in HeLa. Cells were treated with DMSO (0.5%, solvent control), doxorubicin (5 µM, positive control), cisplatin (20 µM, positive control), WN170 (0.5 µM) or WN197 (0.5 µM). After 24 h of treatment, the antibody against γH2AX (green) revealed DNA breaks staining as *foci* (dots). Nuclei were stained with DAPI (blue). Images were obtained on a Leica fluorescent microscope (x100) and were representative of three independent experiments. Scale bar: 20 µm.

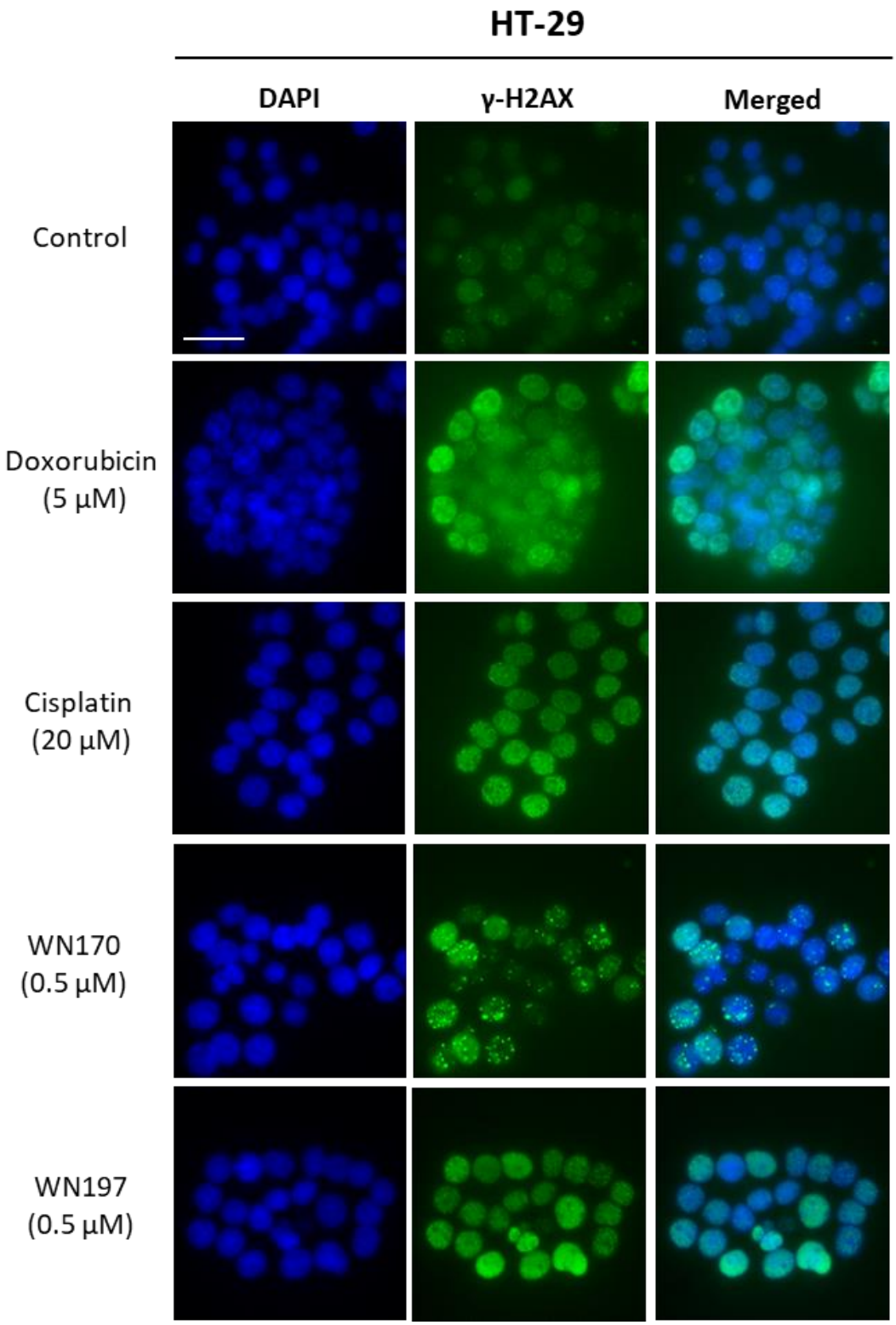

Figure 3: γH2AX detection by immunofluorescence in HT-29. Cells were treated with DMSO (0.5%, solvent control), doxorubicin (5 µM, positive control), cisplatin (20 µM, positive control), WN170 (0.5 µM) or WN197 (0.5 µM). After 24 h of treatment, the antibody against γH2AX (green) revealed DNA breaks staining as *foci* (dots). Nuclei were stained with DAPI (blue). Images were obtained on a Leica fluorescent microscope (x100) and were representative of three independent experiments. Scale bar: 20 µm.

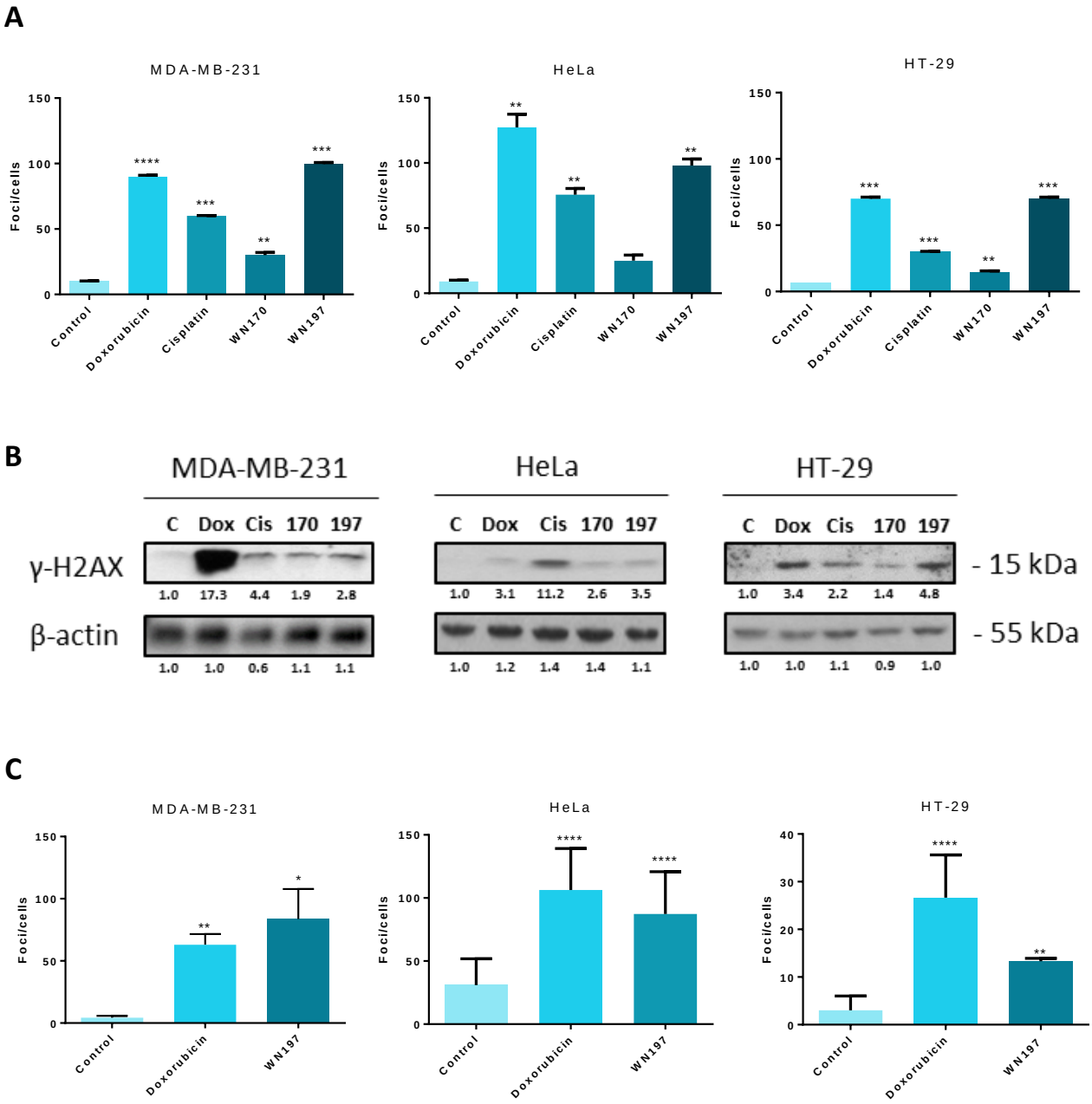

Figure 4: γH2AX *foci* quantification and Western blot analysis in three adenocarcinomas. MDA-MB-231, HeLa, and HT-29 cells were treated with DMSO (0.5%, solvent control), doxorubicin (5 µM, positive contro, Doxl), cisplatin (20 µM, positive control, Cis), WN170 (0.5 µM) or WN197 (0.5 µM). **(A)** Quantification of immunofluorescence γH2AX mean *foci* per cells after 24 h of treatment. **(B)** Western blot analysis of γH2AX after 24 h of treatments. β-actin was used as a loading control and relative γH2AX level was quantified by densitometry using Image J (Fiji Software, v1.52i). **(C)** Quantification of γH2AX mean *foci* per cells after 30 min of treatment based on immunofluorescence experiments. **(A, C)**, data were expressed as the mean ± SD for 30 nuclei of three independent experiments. Statistical analyses were based on a two-way ANOVA followed by a Dunnett's test (*p<0.05, **p<0.01, ***p<0.005 and ****p<0.001).

3.2 EFFECT OF WN197 ON HUMAN TOPOISOMERASE ACTIVITY

To determine whether WN197 was capable to inhibit topoisomerase 1 (Top1), *in vitro* topoisomerase activity tests were realized (**Figure 5A**). The test relies on the ability of Top1 to relax a supercoiled plasmid DNA ($_{SC}$DNA). In presence of Top1, $_{SC}$DNA had a relaxed profile on the agarose gel that migrated further compared to $_{R}$DNA (relaxed DNA). When camptothecin (CPT), a well-known Top1 inhibitor, was added to the enzymatic reaction, the relaxation of the DNA was disturbed and a part of the DNA remains supercoiled. Etoposide (VP-16), a Top2 inhibitor (negative control), and DMSO (solvent control) had no inhibitory effect on DNA relaxation. WN197 inhibited DNA relaxation from 0.2 µM to 2 µM, indicating a Top1 inhibition.

Top1 inhibitors can act as poison or catalytic inhibitors. A poison will prevent DNA religation by Top1, inducing the accumulation of a nicked DNA ($_{N}$DNA) (Pommier *et al.*, 2015). The addition of proteinase K into the reaction allowed the detection of $_{N}$DNA on an agarose gel. $_{N}$DNA was visible in presence of CPT, a Top1 poison (**Figure 5A**). $_{N}$DNA was also visible in presence of WN197 at 0.2 µM. At higher doses of WN197 (0.5 µM to 2 µM), the DNA migration profile was disturbed with no presence of $_{N}$DNA, showing that WN197 is not a poison at higher doses but could act as a catalytic inhibitor by intercalation in the DNA.

WN197 effect on Top2α and Top2β was also assayed (**Figure 5B and 5C**). In the presence of Top2α (**Figure 5B**) or Top2β (**Figure 5C**), a plasmid $_{SC}$DNA was relaxed (topoisomers). Etoposide (VP-16), a Top2 inhibitor, avoided the relaxation of DNA. DMSO (solvent control) and CPT (Top1 inhibitor) did not affect DNA relaxation by Top2α and Top2β. WN197 inhibited the relaxation of DNA by Top2α at 2 µM and had a Top2β inhibitory effect at 1 µM and 2 µM as no topoisomers (relaxed DNA) were visible, but the migration profile is disturbed. DNA intercalation of WN197 could explain this disturbed migration.

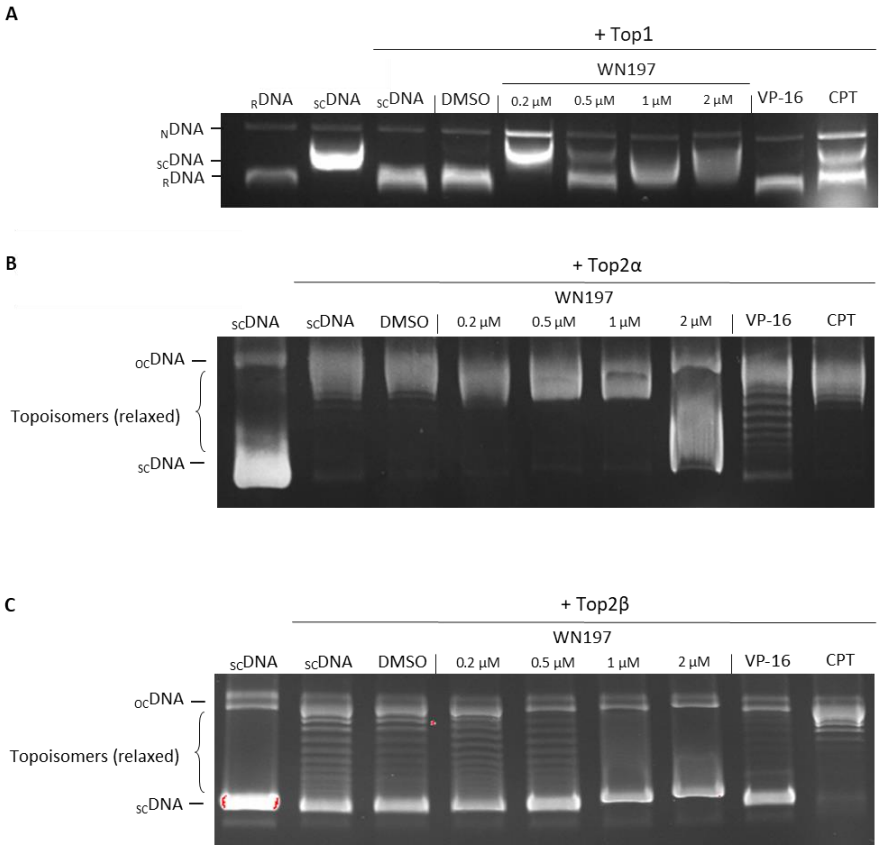

Figure 5: WN197 inhibits Top1 and Top2α/β in a dose-dependent manner. **(A)** *In vitro* Top1 activity assay. Relaxed DNA ($_{R}$DNA, lane 1) or supercoiled DNA ($_{SC}$DNA, lane 2) were used as migration controls. $_{SC}$DNA was used in all other reactions in presence of Top1. The Top1 activity control allowing the relaxation of $_{SC}$DNA is in lane 3. The Top1 activity was assayed in presence of either DMSO (5%, solvent control, lane 4), WN197 at different concentrations (0.2, 0.5, 1 and 2 µM, lanes 5-8), etoposide (VP-16, 50 µM; Top2 poison, lane 9) the negative control of Top1 activity inhibition, or camptothecin (CPT, 10 µM; Top1 poison, lane 10) the positive control of Top1 activity inhibition. The addition of proteinase K allowed the detection of nicked DNA ($_{N}$DNA), a witness of the single-strand broken DNA stabilization by a topoisomerase poison. **(B)** *In vitro* Top2α activity assay. The migration control of supercoiled DNA ($_{SC}$DNA) was performed in lane 1. Top2α was present in all other reactions. The Top2α activity control for the relaxation of $_{SC}$DNA is in lane 2, the first band corresponds to the transitional open circular DNA ($_{OC}$DNA) and topoisomers correspond to the diverse states of relaxed DNA. The Top2α activity was assayed in the presence of either DMSO (5%, solvent control) in lane 3, WN197 (concentrations of 0.2, 0.5, 1, and 2 µM) in lanes 4-7, etoposide (VP-16, 50 µM; Top2 poison) in lane 8, and camptothecin (CPT, 10 µM; Top1 poison) in lane 9. **(C)** *In vitro* Top2β activity assay. Migration control of $_{SC}$DNA was performed in lane 1. Top2β was present in all other reactions. The Top2β activity control for the relaxation of $_{SC}$DNA is in lane 2, DMSO (5%, solvent control) in lane 3, WN197 (concentrations of 0.2, 0.5, 1, and 2 µM) in lanes 4-7, etoposide (VP-16, 50 µM; Top2 poison) in lane 8, and camptothecin (CPT, 10 µM; Top1 poison) in lane 9. In **(A–C)** after topoisomerase reactions, DNA was run in a 1% agarose gel, stained with ethidium bromide (0.5 µg/mL), and visualized under UV light. Each test is representative of three independent experiments.

3.3 Effect of WN197 on the DNA Damage Response pathway of adenocarcinomas

After damage has been induced in DNA, the DNA Damage Response pathway (DDR) is activated (Surova and Zhivotovsky, 2007). Western blots of DDR effectors have been proceeded to verify its activation in MDA-MB-231, HeLa, and HT-29 (**Figure 6**). Activating phosphorylation of ATR (S428) and ATM (S1981) were found in the three cell lines treated with WN170, WN197, and the positive controls doxorubicin and cisplatin after 24 h of treatments, with higher signals compared to the untreated cells. The ATM and ATR signals were higher after WN197 treatment compared to WN170 and positive controls, except for ATM in doxorubicin treated HeLa. The downstream proteins of the DDR pathway, Chk1 and Chk2, were also activated (S317 and T68 phosphorylation respectively) in the cisplatin, WN170 and WN197 conditions in the three cell lines, to higher levels compared to the control. Subsequent phosphorylation on S15 of the effector p53 was also visualized: a higher signal was found after 24 h of treatment with WN197 in the three cell lines compared to the untreated controls. The same higher results were obtained for the quantities of p21, a target gene of p53. In doxorubicin and cisplatin treated cell lines, quantities of p53 and p21 were not increased except for p53 in MDA-MB-231 and p21 in HT-29 cells.

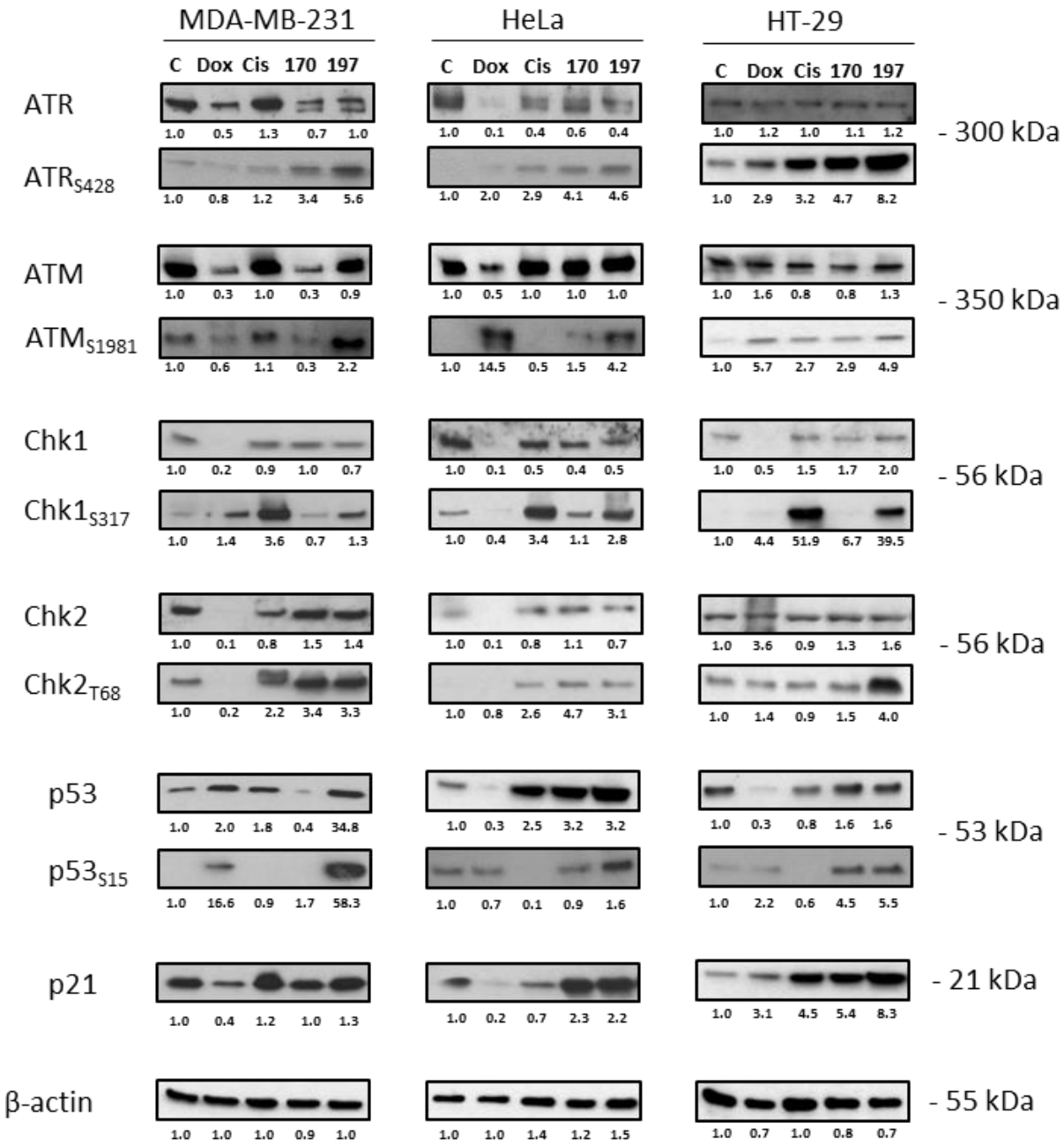

Figure 6: DNA Damage Response (DDR) pathway activation. MDA-MB-231, HeLa, and HT-29 were treated for 24 h with doxorubicin (5 µM, Dox), cisplatin (20 µM, Cis), WN170 (0.5 µM), or WN197 (0.5 µM). Western blots were performed to detect ATM, ATR, Chk1, Chk2, p53, and their active phosphorylated forms, and p21. β-actin was used as a loading control and relative protein levels were quantified by densitometry using Image J software (Fiji Software, v1.52i). Results are representative of three independent experiments.

3.4 Effect of WN197 on the adenocarcinomas' cell cycle

MDA-MB-231, HeLa, and HT-29 cells were exposed for 24 h to different treatments and analyzed by flow cytometry to investigate possible cell cycle phase accumulation (**Figure 7A**). Untreated cells showed a classical cell cycle repartition in the three cell lines with a mean of 50.52% cells in G0/G1 phases, 29.80% in the S phase, and 19.68% in the G2/M phases. Cisplatin, a well-known S phase blocking control (Wagner and Karnitz, 2009), induced significant accumulation of 79.79%, 59.61%, and 85.53% cells in S phase for MDA-MB-231, HeLa, and HT-29 cells, respectively. Nocodazole, a mitotic spindle poison and a control for M phase accumulation, induced 70.17%, 88.61%, and 39.68% cells in G2/M phase for MDA-MB-231, HeLa, and HT-29, respectively. After treatment with WN170, MDA-MB-231 did not present a perturbated cell cycle (21.08% of cells in the G2/M phase), while an accumulation in the G2/M phase was observed for the HeLa and HT-29 (54.19% and 48.06% respectively). An accumulation in the G2/M phase was also obtained after a WN197 treatment with 51.29% for the MDA-MB-231, 70.51% for the HeLa, and 74.40% for the HT-29, which was significantly higher compared to the untreated controls, WN170, and nocodazole in HT-29.

To determine the sufficient dose of WN197 to obtain the G2/M accumulation, MDA-MB-231, HeLa, and HT-29 were treated for 24 h with increasing doses of WN197 (**Figure 7B**). A significant accumulation in the G2/M phase was obtained from 0.5 µM to 1 µM in MDA-MB-231, 0.25 µM to 0.5 µM for the HeLa, and 0.25 µM to 1 µM for the HT-29.

A kinetic treatment with WN197 at 0.5 µM was realized on the three adenocarcinoma cell lines to determine the earliest-induced G2/M accumulation (**Figure 7C**). The G2/M accumulation is obtained from 8 h to 48 h in MDA-MB-231, 12 h to 48 h in HeLa, and 12 h to 24 h in HT-29.

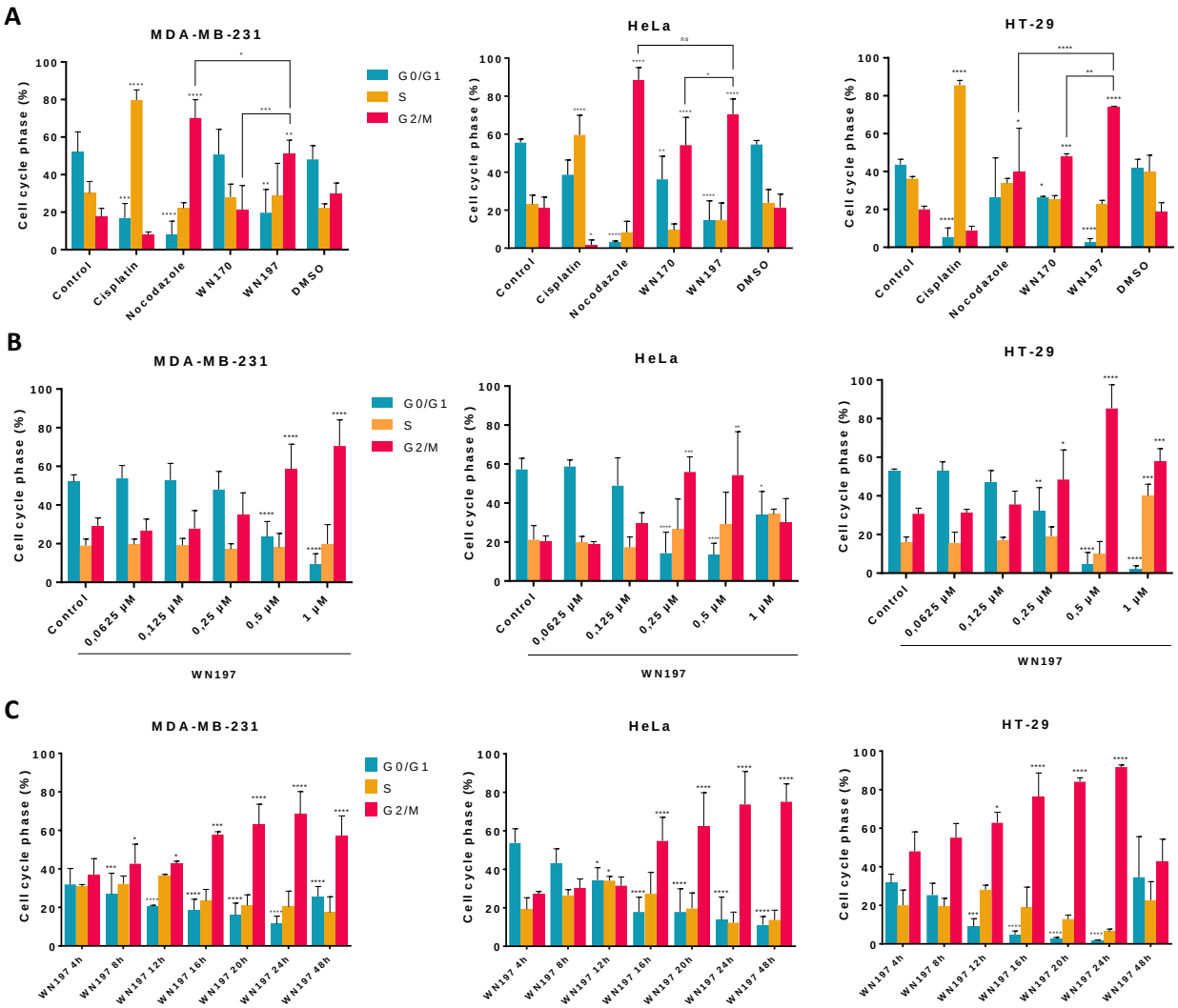

Figure 7: cell cycle repartition analysis of MDA-MB-231, HeLa, and HT-29 cells. (A) Flow cytometry analysis of MDA-MB-231, HeLa, and HT-29 cells repartition in the cell cycle 24 h after treatments with cisplatin (20 µM, S phase arrest control), nocodazole (84 nM, M phase arrest control), WN170 or WN197 (0.5 µM). *Raw data available in Appendice 2.* (B) Dose-response analysis by flow cytometry of the cell cycle repartition in the three cell lines 24 h after treatment with WN197 or untreated (control). (C) Time course analysis by flow cytometry of the cell cycle repartition in the three cell lines treated with WN197 (0.5 µM). Statistical analyses were based on two-way ANOVA followed by Dunnett's test (*p<0.05; **p<0.01; ***p<0.005; ****p<0.001) on three independent experiments.

The cell cycle arrest phase was further determined by Western blot analysis of major cell cycle regulators: Cdk1, cyclin B, Cdc25C phosphatase, and histone H3 (**Figure 8A**). The inhibitory phosphorylation on Cdk1's Y15 was increased after 24 h of treatment with cisplatin, WN170, and WN197 compared to the untreated controls in the three adenocarcinoma cell lines. No increase in the signal was obtained after doxorubicin treatment, while a decrease

was obtained in the three cell lines for nocodazole, and also in the doxorubicin condition for HeLa and HT-29. The cyclin B level was increased after a treatment with WN170 and WN197 in the three cell lines, with cisplatin in MDA-MB-231 and HeLa, with nocodazole in MDA-MB-231 and HT-29, but a decrease was observed in doxorubicin conditions. Cdc25C inhibitory phosphorylation on S216 was also assayed. The phosphorylation was enhanced by cisplatin and WN197 treatments compared to untreated conditions in the three cell lines, and was slighter compared with WN170. On the contrary, a decrease of this phosphorylation was obtained after doxorubicin and nocodazole treatments, except for HT-29. All cell cycle markers were increased to higher level in WN197 condition compared to WN170. Finally, the S10 phosphorylated form of histone H3, an M phase marker, was increased only in the nocodazole condition for the three adenocarcinoma cell lines.

Cdc25C complexation with 14-3-3 was assayed by immunoprecipitation and visualized by Western blots (**Figure 8B**). After a Cdc25C immunoprecipitation, no 14-3-3 is found bound to the protein in the untreated conditions, while it was after cisplatin and WN197 treatments in the three cell lines. 14-3-3 reverse immunoprecipitations were performed in HeLa to ascertain the results, and Cdc25C was also found in cisplatin and WN197 treatment conditions.

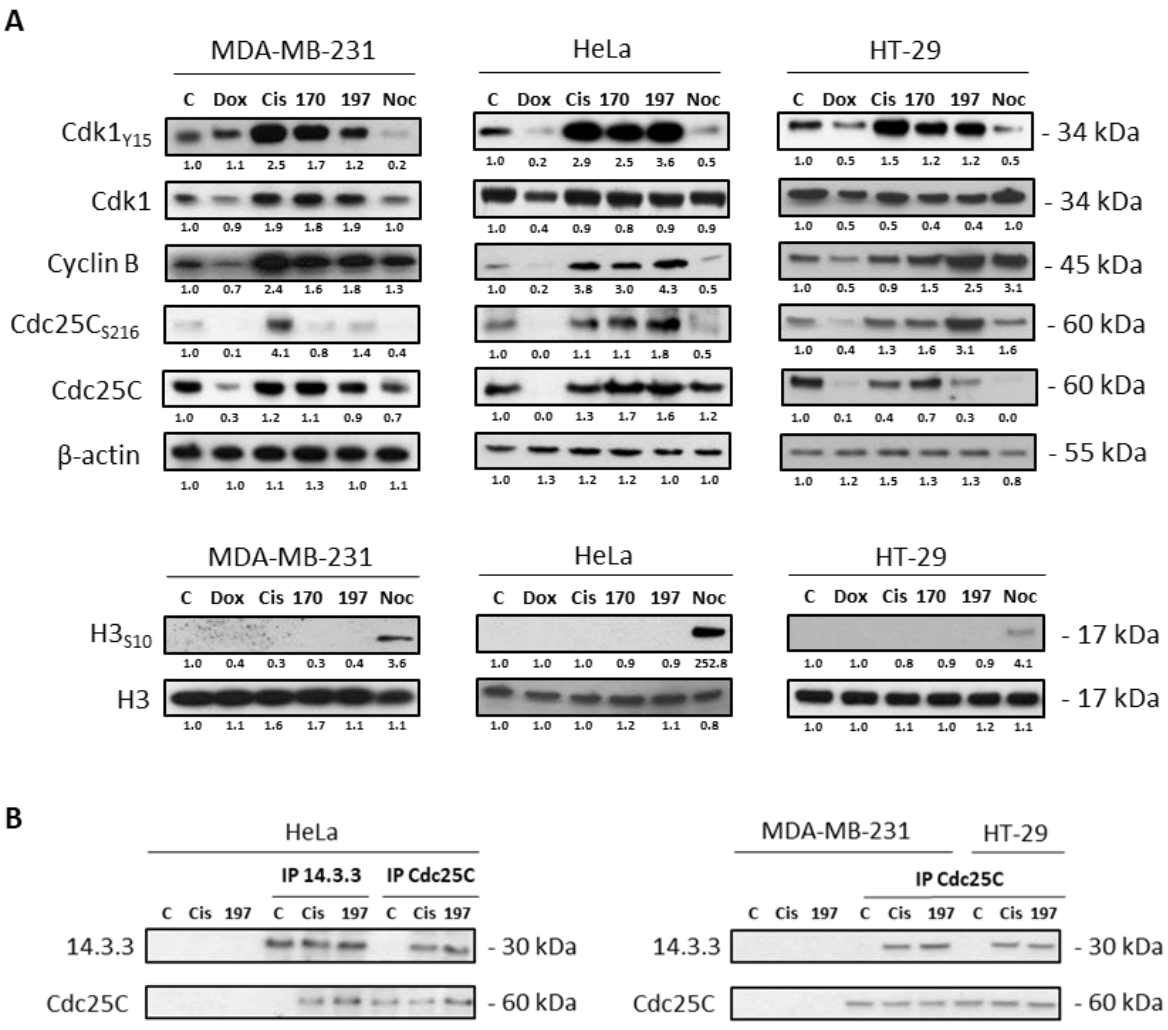

Figure 8: Western blot analysis of cell cycle markers in MDA-MB-231, HeLa, and HT-29 cells. (A) Cells were treated for 24 h with doxorubicin (5 µM), cisplatin (20 µM), WN170 (0.5 µM), WN197 (0.5 µM), or nocodazole (84 nM). β-actin was used as a loading control. For H3 S10 phosphorylation, respective H3 total levels were used as loading controls. Relative protein levels were expressed by densitometry using Image J software (Fiji Software, v1.52i). (B) 14-3-3 and Cdc25C immunoprecipitations were realized in cell lines treated for 24 h with cisplatin (20 µM) or WN197 (0.5 µM). Results are representative of three independent experiments.

3.5 Effect of WN197 on adenocarcinomas' cell death

Apoptosis, a classical induced cell death after DNA damage and topoisomerase inhibition, was assayed by Western blots (**Figure 9A-C**). The activated cleaved caspase 3 (early apoptosis marker) was found after 24 h of treatment with doxorubicin, cisplatin and nocodazole in MDA-MB-231, HeLa, and HT-29, while no signal was obtained in the untreated control, WN170 and WN197 conditions (**Figure 9A**). The inactivated cleaved PARP (late apoptosis marker) was only found in doxorubicin treated condition for the three cell lines. A time-course detection of cleaved PARP and cytochrome *c* release in the cytoplasm at 3, 16,

24, 48, and 72 h was proceeded, and no signal was obtained after WN197 treatments, compared to doxorubicin apoptosis positive control at 24 and 48 h (**Figures 9B, C**). In addition, annexin V-Propidium iodide (PI) tests were realized (**Figure 9D**): a low percentage of cells were found in the early and late apoptosis phases when untreated (controls) for the three cell lines, with a mean of 6.89% for MDA-MB-231, 18.44% in HeLa, and 25.72% in HT-29. After WN170 or WN197 treatments, a mean of respectively 8.6% and 13.6% cells were found in apoptosis in MDA-MB-231, 27.2% and 21.9% HeLa, and 20.5% and 23.4% in HT-29.

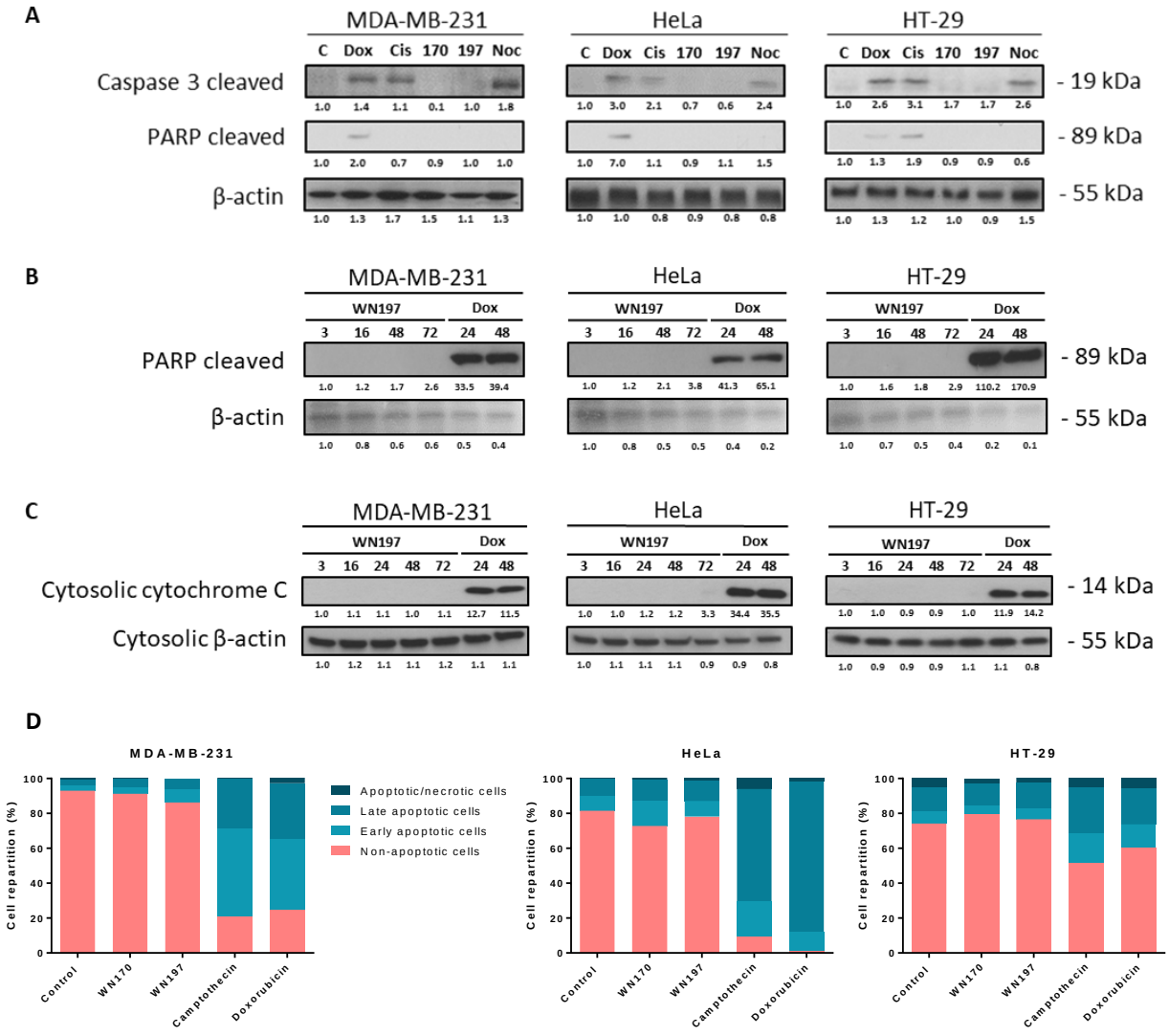

Figure 9: apoptosis analysis. Cells were treated for 24 h with doxorubicin (5 µM, Dox), cisplatin (20 µM, Cis), WN170 (0.5 µM), WN197 (0.5 µM), nocodazole (84 nM, Noc), or camptothecin (20 µM). **(A)** Cleaved caspase 3 and PARP analysis were realized after 24 h of treatment or untreated in controls. **(B)** Cleaved PARP and **(C)** cytosolic cytochrome *c* analysis after 3, 16, 24 (cytochrome *c* only), 48, and 72 h of treatment with WN197 or doxorubicin for 24 and 48 h. β-actin levels were used as a loading control. Relative protein levels were analyzed by densitometry using Image J software (Fiji Software, v1.52i). **(D)** Histogram representations of annexin V-Propidium iodide analysis by flow cytometry, showing the apoptotic cell repartition after 24 h of treatments. *Raw data available in Appendice 3*.

We then investigated whether autophagy was induced by WN197 and WN170. In the three adenocarcinoma cell lines, several autophagy markers were detected: p62 degradation, Beclin-1 synthesis, and LC3-II formation (**Figure 10A**). A p62 signal was obtained for the untreated cells but none after rapamycin (autophagy inducer), WN170 or WN197 treatments for 24 h in the three cell lines. On the contrary, Beclin-1 signal was obtained only in the treated cells. LC3-I associated to phosphatidyl-ethanolamine (LC3-II form) was not obtained in the untreated control cells or after treatment with WN170 in MDA-MB-231 and HeLa, but found after rapamycin and WN197 addition in the three cell lines, and only in HT-29 for WN170.

The complexation of mTOR to its phosphorylated (S792) RAPTOR partner occurs in the mTORC1 complex during autophagy and was visualized by immunoprecipitations (**Figure 10B**). In cells treated with doxorubicin (apoptosis inducer), or untreated, mTOR is not complexed with RAPTOR$_{S792}$. Differently, the two proteins are complexed after 24 h of treatment with rapamycin, an autophagy inducer, and after the treatment with WN197.

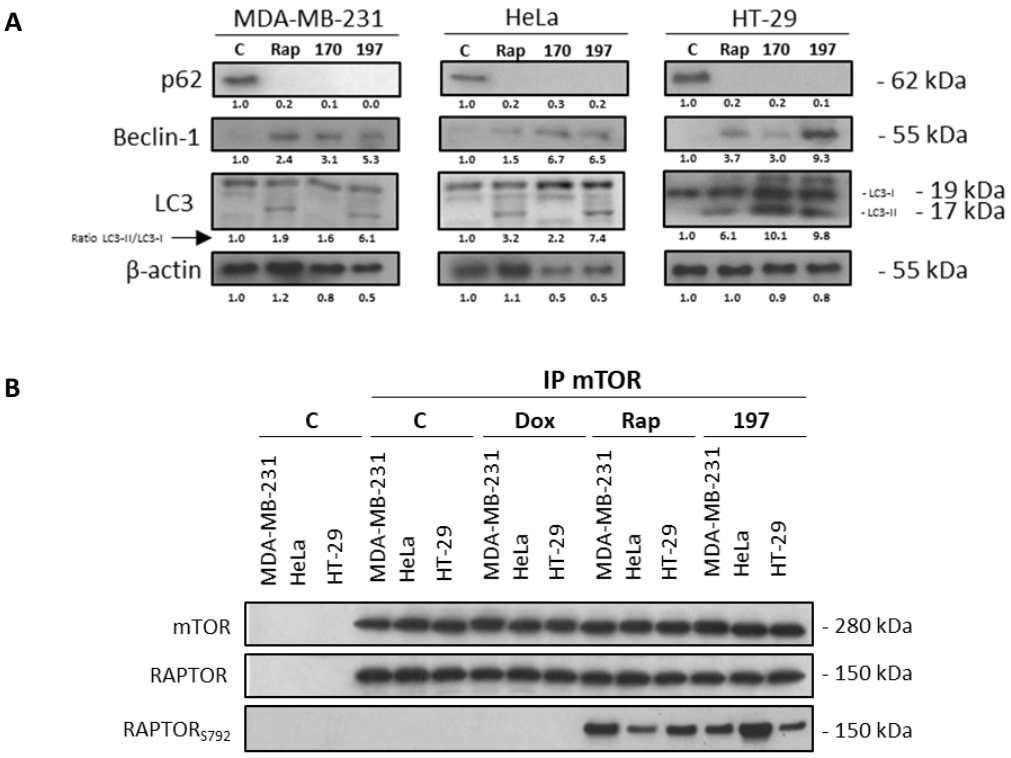

Figure 10: autophagy analysis by Western blots. MDA-MB-231, HeLa, and HT-29 cells were treated for 24 h with doxorubicin (5 µM, Dox), WN170 (0.5 µM), WN197 (0.5 µM), or rapamycin (0.5 µM, Rap). (A) p62, Beclin-1, and LC3 markers were analyzed, LC3 levels were expressed as the LC3-II/LC3-I ratio. β-actin levels were used as a loading control. (B) mTOR immunoprecipitations were realized in cell lines treated or not with doxorubicin (5 µM), rapamycin (0.5 µM) or WN197 (0.5 µM) for 24 h. Relative protein levels were expressed by densitometry using Image J software (Fiji Software, v1.52i).

Finally, autophagic vacuoles (lysosomes, phagosomes) were visualized by immunofluorescence and quantified (**Figure 11A, B**). In MDA-MB-231, a mean of 7 vacuoles per cell was obtained in the untreated control, while a significant number of vacuoles were obtained after 24 h of treatment with rapamycin or WN197, with a mean of 19 and 22 vacuoles per cell respectively. For HeLa, a mean of 8 vacuoles per cell was obtained in the control, 353 with rapamycin, and 111 with WN197, both significant results compared to the control. For HT-29, a mean of 2 vacuoles per cell was obtained, and 18 and 17 vacuoles per cell were scored after rapamycin and WN197 treatments respectively, also significant compared to the control.

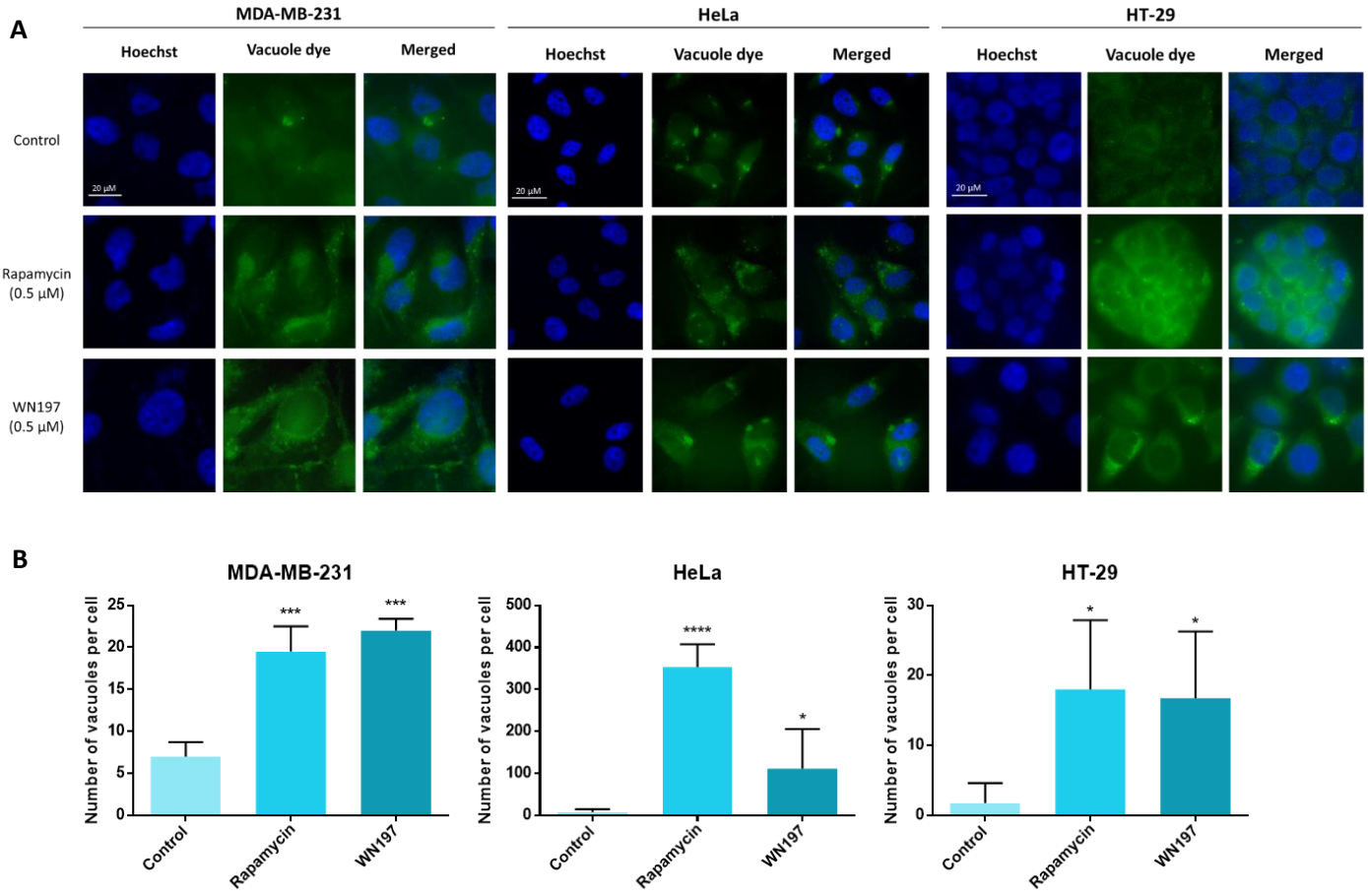

Figure 11: autophagic vacuoles detection by fluorescence. MDA-MB-231, HeLa, and HT-29 cells were treated for 24 h with DMSO (0.1%, solvent control), WN197 (0.5 µM), or rapamycin (0.5 µM). **(A)** After 24 h of treatment, the green dye revealed autophagic vacuoles (dots). Nuclei were stained with Hoechst 33342 (blue). Images were obtained on a Leica fluorescent microscope (x100) and were representative of three independent experiments. Scale bar: 20 µm. **(B)** Quantification of the mean vacuoles per cells were performed after 24 h of treatment.

3.6 Effect of WN197 on tumorigenic and non-tumorigenic breast cells

MTS viability assay was proceeded on non-cancerous MCF-10A cells (**Table 1**). The obtained IC_{50} for WN197 was 1.080 µM, compared to formerly obtained IC_{50} on adenocarcinomas with 0.144 µM, 0.22 µM, and 0.358 µM respectively for the MDA-MB-231, HeLa, and HT-29 cell lines. The concentration required to inhibit 50% of the MCF-10A viability is significantly higher compared to the mean obtained on the three adenocarcinomas IC_{50}.

Table 1. Half maximal inhibitory concentrations (IC_{50} in µM) for cell survival of MCF-10A.

Compound	IC_{50} (µM)
WN197	1.080 ± 0.037
Cisplatin	14.218 ± 7.157
Statistical difference (WN197 on adenocarcinomas vs. on MCF-10A)	***

*Data are expressed as the mean ± SD of three independent experiments. Statistics are based on Student's t-test of the difference between WN197 IC_{50} on adenocarcinomas and MCF-10A; ***p<0.001.*

To complete the results obtained on breast cells (cancerous MDA-MB-231, MCF-7 (see IC_{50} introduction §1.2.2, page 55); and non-cancerous MCF-10A), MTS viability assays were performed on two other triple-negative breast cancer cell lines: BT-549 and SUM-159 (**Table 2**). The IC_{50} obtained on BT-549 were 0.676 µM and 0.691 µM after WN197 and WN170 treatments respectively. The IC_{50} obtained on SUM-159 were 0.679 µM and 0.689 µM after WN197 and WN170 treatments respectively. No significative differences between the two compounds are obtained.

Table 2. Half maximal inhibitory concentrations (IC_{50} in µM) for cell survival of BT-549 and SUM-159.

Compound	BT-549	SUM-159
WN197	0.676 ± 0.063	0.679 ± 0.178
WN170	0.691 ± 0.308	0.689 ± 0.154
Cisplatin	3.546 ± 0.924	13.96 ± 4.837
Statistical difference (WN197/WN170)	*ns*	*ns*

Data are expressed as the mean ± SD of three independent experiments. Statistics are based on Student's t-test of the difference between WN197 and WN170 IC_{50}; ns: non-significative.

3.7 Effect of WN197 on multi-drug resistant H69AR

MTS viability assay was proceeded on the multi-drug resistant cancer cells H69AR (**Table 3**). IC_{50} were 0.683 µM for WN197, and 4.966 µM for WN170. The value obtained for WN170 was increased compared to the IC_{50} mean of non-resistant adenocarcinomas (mean of

0.550 µM), while this value stays close to the IC_{50} mean obtained for WN197 on non-resistant adenocarcinomas (mean of 0.306 µM).

Table 3. Half maximal inhibitory concentrations (IC_{50} in µM) for cell survival of H69AR.

Compound	IC_{50} (µM)
WN197	0.683
WN170	4.966
Cisplatin	15.10

Data are expressed as the mean of a triplicate.

3.8 Effect of WN197 on *Xenopus laevis* embryos

WN197 cytotoxicity was determined on *Xenopus laevis* embryos by comparing the course of early development after treatment or not (**Figure 12**). After treatments with 0.5 or 5 µM of doxorubicin, the treated embryo/control embryo ratio was significantly decreased at the neurula stage (mean of 0.38 and 0.41 respectively) compared to the control (mean of 0.77), and the tailbud stage (mean of 0.20 and 0.18 respectively) compared to the control (mean of 0.74). No significant decreases were obtained after treatments with 0.5 or 5 µM of WN197, with a mean ratio of 0.95 and 0.92 at the gastrula stage, 0.88 and 0.83 at the neurula stage, and 0.85 and 0.79 at the tailbud stage compared to the control mean of 0.86.

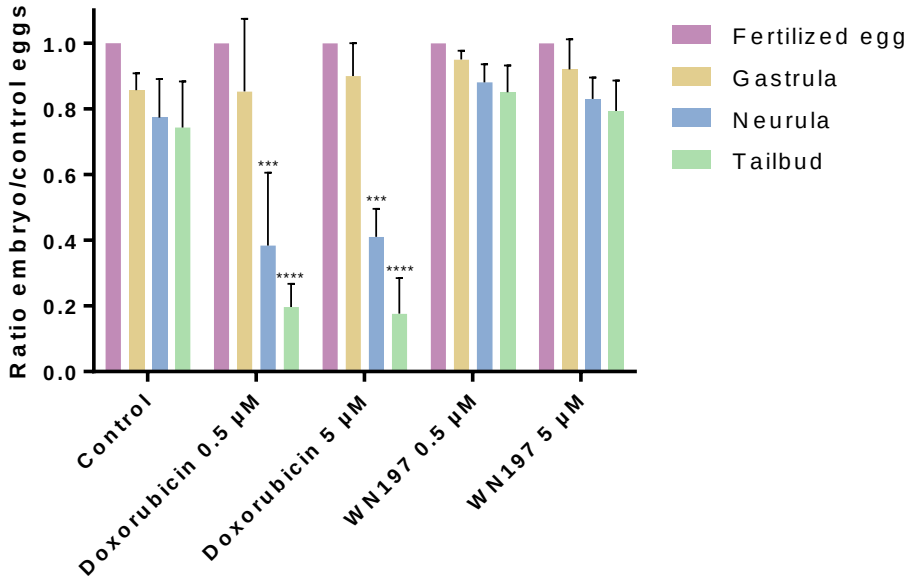

Figure 12: effect of WN197 on *Xenopus laevis* embryos. Fertilized oocytes were treated or not with 0.5 or 5 µM of doxorubicin, or WN197 and scored at indicated time as follow: fertilized egg (T=0, control eggs), gastrula (NF12, 14 h), neurula (NF16, 19 h), tailbud (NF30, 25 h) and their viability determined by visual observation under a stereomicroscope. Ratio for treated embryo/control embryo were calculated at each developmental stage. Data were expressed as the mean ± SD for 20 embryos from three independent experiments. Statistical analyses were based on a two-way ANOVA followed by a Dunnett's test (***p<0.005 and ****p<0.001).

Conclusion & Perspectives

4 CONCLUSION & PERSPECTIVES

4.1 CONCLUSION

I studied the properties of the WN197 organometallic compound derived from indenoisoquinolines during my thesis, and analyzed its effects on cancerous cells and in non-tumorigenic models, in regards to DNA damage, cell cycle arrest, cell death, and topoisomerase activity (**Figure i**).

The results obtained by immunofluorescence after 30 min and 24 h of treatment with WN197 showed a high number of γH2AX *foci*, in MDA-MB-231, HeLa, and HT-29 cancer cells, that highlights DNA breaks induced by WN197. Phosphorylation of H2AX histone was realised in particular after double-strand breaks (DSB), notably after topoisomerase inhibition by poisons, and served as a topoisomerase inhibitor marker (Pommier and Cushman, 2008). In addition, DNA breaks were higher in number after treatments with WN197 compared to WN170, and the results were confirmed by Western blots.

Parallelly, *in vitro* topoisomerase activity tests revealed that the WN197 compound inhibited topoisomerase 1 (Top1) at low doses, corresponding to the IC_{50} (0.2 µM), acting as a poison inhibitor, while at higher doses (> 1 µM) it behaved as a catalytic inhibitor. WN197 inhibited Top2α and Top2β as a catalytic inhibitor at higher doses (2 µM and 1 µM, respectively). In a previous research published in Nathalie Wambang's thesis, WN197 was demonstrated to intercalate in DNA by melting temperature measurement (ΔTm) and ethidium bromide (EtBr) competition test (K_{app}) (Wambang, 2016; Molinaro *et al.*, 2022). These results comforted that WN197 acted as a topoisomerase catalytic inhibitor, by intercalation in the DNA. The same mechanism was observed for anthracyclines, capable to switch from a poison activity to a catalytic inhibitory activity at high doses (Pommier *et al.*, 2010).

The activation of the DDR (DNA Damage Response) pathway was demonstrated by Western blots after treatment of the three cancer cells with WN197. ATM/ATR, Chk1/Chk2, p53 and p21 were activated by phosphorylation and p53 and p21 were upregulated. The DDR pathway was shown to induce a G2/M accumulation of the adenocarcinoma cells after WN197 treatments by flow cytometry. The G2/M accumulations were visible starting from 0.5 µM of WN197 for MDA-MB-231 and 0.25 µM for HeLa and HT-29. The cell accumulation in G2/M was lost at 1 µM of WN197 for HeLa and HT-29 and can be related to a different mechanism of action at high doses, due to the intercalation property of WN197. This dose correlated with the *in vitro* topoisomerase activity tests results. The G2/M accumulation was significative after 8 h of treatment with WN197 for MDA-MB-231, and 12 h for HeLa and HT-29 cell lines. WN170 induced a significant lower accumulation of cells in G2/M at the same dose (0.5 µM).

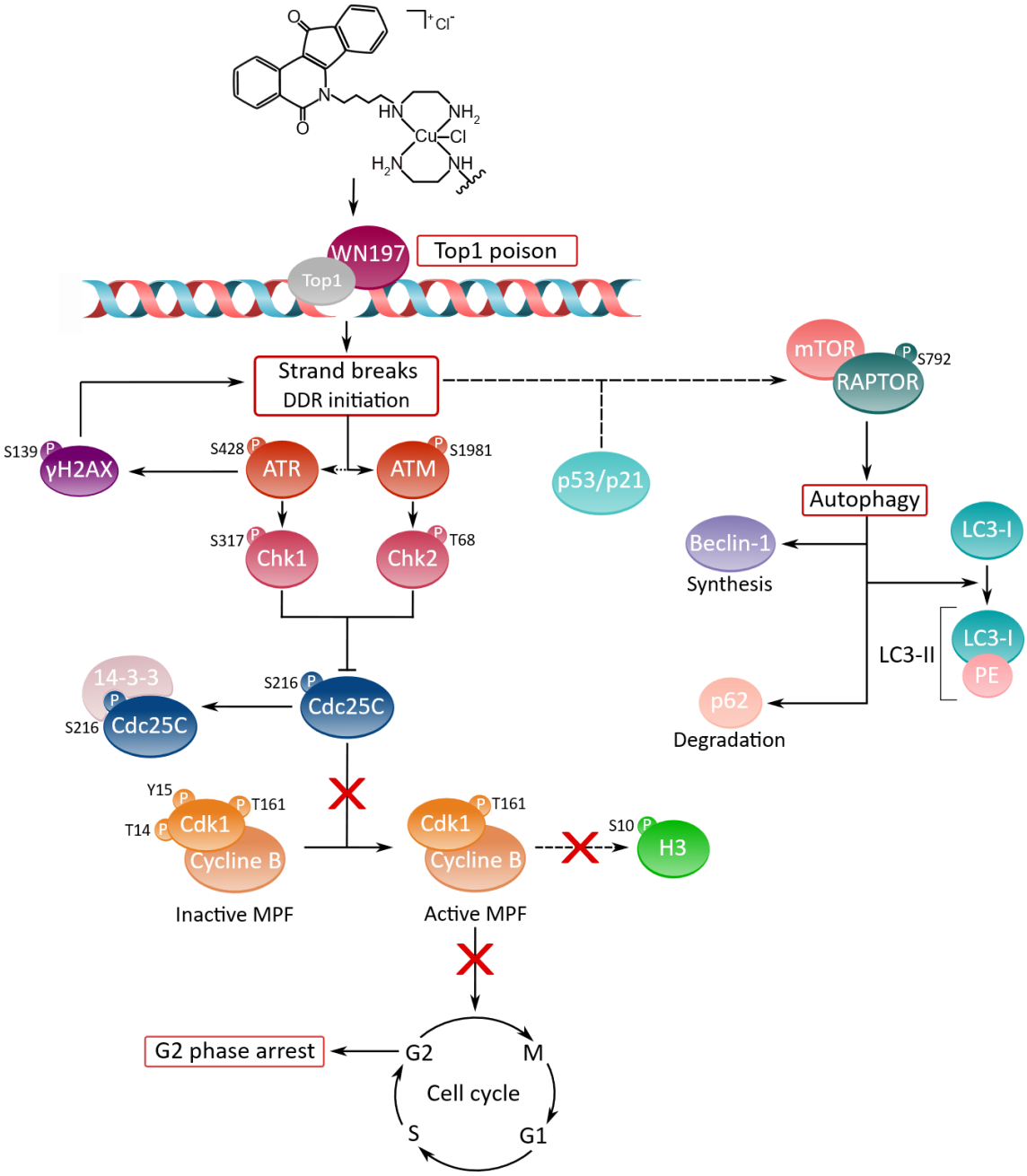

Figure i. Deciphering of the molecular mechanisms of the novel copper (II) indenoisoquinoline complex WN197. WN197 inhibits topoisomerase 1 at low doses in a poison mode and forms a ternary complex with the topoisomerase and DNA, leading to strand break accumulation. Phosphorylated H2AX (γH2AX) localizes at the DNA damage sites. The DNA damage response pathway is activated: ATM and ATR kinases are phosphorylated, and subsequently activate Chk1 and Chk2, leading to Cdc25C phosphorylation on serine 216 (S216) and its binding to 14-3-3. Consequently, Cdk1 remains phosphorylated on tyrosine 15 (Y15), impeding the activation of the MPF (Cdk1/Cyclin B) and the phosphorylation of H3 on serine 10 (S10). Cancer cells accumulate in the G2 phase of the cell cycle. The DDR also leads to an increase in p53 and p21 followed by an autophagic cell death characterized by the phosphorylation of RAPTOR on serine 792 (S792) in the mTORC1 complex, the synthesis of Beclin-1, the formation of LC3-II (complex LC3-I/PE), and the degradation of p62.

To understand the mechanisms involved in the cell cycle arrest, the amount and the phosphorylation state of the phosphatase Cdc25C were determined by Western blots. After 24 h of treatments with WN197, we observed an increase in the S216 inhibitory phosphorylation of Cdc25C. This phosphorylation allowed the recognition and binding by 14-3-3 verified by immunoprecipitations and prevented the MPF activation (Cdk1/Cyclin B). Indeed, as shown by Western blots, the inhibitory phosphorylation of Cdk1 (Y15) was maintained after treatment with WN197. In addition, an accumulation of Cyclin B was found. Cancer cells can no longer progress in the cell cycle. The histone H3 is only phosphorylated by active MPF in mitosis to allow DNA condensation, making it an M phase marker (Hans and Dimitrov, 2001). After 24 h of treatment with WN197, no histone H3 phosphorylation (S10) was observed, showing that cells were arrested in the G2 phase of the cell cycle.

When DNA breaks are too important, apoptosis is classically activated to induce cell death. Moreover, most of the topoisomerase inhibitors induce apoptosis (Larsen *et al*., 2003; Pommier, 2013; see §1.1.6, pages 49-53). We have determined by Western blots, immunoprecipitations, and annexin V-propidium iodide analyses that apoptosis is not activated after treatment with WN197, nor WN170. Only a few numbers of topoisomerase inhibitors induce autophagy (e.g. SN-38 in HSC-4 oral squamous cell carcinoma, Tamura *et al*., 2012) as WN197 did in the three adenocarcinomas MDA-MB-231, HeLa, and HT-29. Autophagy was shown by the degradation of p62, the synthesis of Beclin-1, the switch from the LC3-I to the LC3-II form, in addition to the complexation of mTOR to RAPTOR phosphorylated on S792 in the mTORC1 complex, and the formation of autophagic vacuoles visualized by fluorescence. Autophagy cell death has been discussed regarding the gain it could bring compared to apoptosis in cancer treatments leading to cytoprotective effects towards surrounding normal cells around a targeted tumor. However, contradictory opinions have been raised considering autophagy is also protecting cancer cells (Kondo Y and S., 2006), allows cells survival in nutrient deprived situation, and contribute to cancer resistance (Hippert *et al*., 2006; Smith and Macleod, 2019).

As patients bearing triple-negative breast cancer cannot undergo hormonotherapy, it was of prime importance to focus on this type of cancer and determine the toxicity of WN197 towards other breast cancerous cells and a non-cancerous cell line. The IC_{50} obtained on MDA-MB-231 for WN197 is the lowest with 0.144 µM in comparison to the four other cancer cell lines tested (Wambang, 2016, see §1.2.2, page 55). We also found low IC_{50} for BT-549 and SUM-159, two other triple-negative breast cell lines. Furthermore, the IC_{50} obtained on MCF-10A, a non-cancerous breast cell line, is significantly higher compared to all the adenocarcinomas' IC_{50} obtained, with 1.080 µM. These interesting results allow to envision WN197 as a possible treatment for breast cancer therapy, especially against triple-negative breast cancer, bypassing toxicity on surrounding healthy cells.

Another approach was to determine if WN197 was able to avoid cancer cell resistance, by testing the viability of H69AR by MTS, a pulmonary MDR (multi-drug resistant) cell line. The IC_{50} obtained, 0.683 µM, showed that WN197 kept its cytotoxicity on MDR cells, leading to the conclusion that WN197 could be used as a secondary treatment for patients to overcome multi-drug resistance. WN170 did not manage to keep its low cytotoxicity on H69AR, with an IC_{50} of 4.966 µM. This result, in addition to those obtained for WN170 on the DDR, cell cycle and cell death, showed that the symmetric indenoisoquinoline structural core containing copper atoms brings specificity and increases the activity of WN197 compared to WN170. Previous studies mentioning the presence of metal atoms like iron (Kondratskyi *et al.*, 2017), ruthenium (Wambang *et al.*, 2016), or platin (Dasari and Tchounwou, 2014), demonstrate their increased efficiency and raised interest of organometallic compounds in cancerology (see §1.1.6, page 49).

Finally, we showed that WN197 had no effect on *Xenopus laevis* embryonic development, that displays DDR and cell cycle proteins (Garner and Costanzo, 2009), compared to detrimental effects obtained with doxorubicin. This brings a promising future for WN197 as a chemotherapeutic drug.

4.2 PERSPECTIVES

4.2.1 Compound specificity

To confirm the effect of WN197 on topoisomerases, docking evaluations of the compound in complex with the DNA and the topoisomerase are underway in collaboration with Dr. De Ruyck (UGSF). Besides, cell lines with siRNA directed against Top1 have been produced by Dr. Calsou's team (IPBS) and could be used as another way to confirm that the organometallic compounds are specific and do not target other cellular effectors. Indeed, if WN197 cytotoxic effect on cancer cells is lost while Top1 has been silenced, it means no other molecular effectors are targeted.

Although WN197 inhibits Top1 and induces DNA breaks shown by the phosphorylation of H2AX, this mechanism is not exclusive. Other mechanisms can be parallelly activated to provoke DNA breaks, like ROS (Reactive Oxygen Species). ROS production is induced by Top2 inhibitors like anthracyclines, in addition to their poison activity (Pommier et al., 2010; Pommier 2013), but also by other Top1 and Top2 inhibitors (see compounds from Table IV in the introduction). Furthermore, organometallic compounds tend to induce ROS production (§1.1.6, page 49). Nevertheless, ROS is mainly related to apoptosis (Simon *et al.*, 2000). The fact that no apoptosis is found after treatment with WN197 might be a clue about ROS production, but other deaths can be linked to ROS, including autophagy (Gibson, 2010). Potential ROS production after treatments with WN197 will be measured with oxidizable

probs, like CellROX™ that gets oxidized in presence of ROS, and emits measurable fluorescence (Soares *et al*., 2015).

4.2.2 Cancer resistances

We have shown with the results on H69AR cells that WN197 is keeping its cytotoxic effect on cancer cells that have developed a resistance to previous chemotherapeutic agents (adriamycin, daunomycin, epirubicin, menogaril, mitoxantrone, acivicin, etoposide, gramicidin D, colchicine, vincristine, and vinblastine). Nevertheless, H69AR cells do not overexpress MDR transporters responsible for a part of cancer resistance (Cole *et al*., 1992). A cell line overexpressing P-glycoproteins could further be used to test the capability of WN197 to overpass this resistance (Peng *et al*., 2012).

4.2.3 Combined anticancer therapies

To enhance the cytotoxicity of drugs in chemotherapy and ensure a response to the drugs, the association of WN197 to other compounds, such as PARP inhibitors and the use of synthetic lethality action mode is another perspective. PARP is required for DNA repair, and the combination of PARP inhibitors like olaparib with the Top1 inhibitor SN-38 showed an interesting synergic effect (Tahara *et al*., 2014). Another synergic effect is obtained when veliparib, a PARP inhibitor, is associated with irinotecan (Murai *et al*., 2014). A phase I trial showed that the combination of the PARP inhibitor veliparib with topotecan was effective but not tolerated by patients due to hematological toxicities (Kummar *et al*., 2011). Another phase I clinical trial showed that the combination of veliparib with etoposide was well tolerated in SCLC (Owonikoko *et al*., 2015). An additional phase I trial showed that olaparib PARP inhibitor in combination with the pegylated liposomal doxorubicin could generate good response in patients with ovarian cancer with good tolerance, with only 2 patients out of 44 exhibiting high-grade dose-limiting toxicity (Del Conte *et al*., 2014).

The combination of topoisomerase inhibitors with ATR inhibitors has also been tested to inhibit the DDR that could repair the DNA damage induced by topoisomerase inhibitors. The ATR inhibitor M6620 in combination with topotecan is in a current phase II clinical trial against SCLC (Thomas *et al*., 2018).

Combination of WN197 to TDP1/2 inhibitors is also an interesting prospect. TDP1 and TDP2 are enzymes responsible for the reparation of DNA breaks induced by topoisomerase inhibitors (Pommier 2016). They act by cleaving the Top1 (TDP1) or Top2 (TDP2) tyrosyl–DNA covalent bond, and leave a 3’ or 5’-phosphatase ends repaired by polynucleotide kinase phosphatase, DNA polymerases, and ligases (Pommier 2014; Kawale and Povirk, 2018). Inhibitors of TDP1 and TDP2 exist, such as neomycin, rolitetracycline, and deazaflavin (Huang *et al*., 2012; Kawale and Povirk, 2018). The combination of TDP inhibitors alongside

topoisomerase inhibitors could have a synergic effect by inducing DNA damage and inhibiting their reparation.

For all these reasons, synergetic effects could be tested for WN197 with additional inhibitors described hereby.

4.2.4 Organoids models of cancer

To pursue the research of WN197 as an anti-cancerous compound, tests on organoids can be proceeded. In an ongoing effort to develop alternatives and reduce animal experimentations, organoids are good compromise because they possess a topology and cell to cell interaction alike *in vivo* tissues. The WN197 compound can be tested on cancerous organoids but also non-cancerous organoids. Preliminary results were obtained on cancerous colon organoids (TraCo2) and non-cancerous colon organoids (Col). Organoids were treated with 1 µM of WN197 or 0,1% DMSO (solvent control) for 72 h and pictures were taken every 3 h. The results showed that the cancerous colon had a dead morphology after treatment with WN197, while the non-cancerous colon did not present a dead morphology (**Appendice 4**). The results will be confirmed with further experiments at various doses and times.

Prospects for organoids experiments are the development of colorimetric assays with tetrazolium salt like MTS or CCK-8 to evaluate organoids viability (Zeng *et al*., 2021). After the treatment of organoids with various doses of WN197 for various times, the tetrazolium salt can be used and measured by spectrophotometry at the corresponding wave length to determine IC_{50}. The other prospect on organoids is to determine the presence of apoptosis or autophagy proteins after WN197 treatment. However, adjustments will be necessary as these experiments remain difficult to carry out in a context where the organoids are cultured in small quantities in a surrounding matrix.

4.2.5 Structural enhancement

Structural modifications of WN197 could be undertaken to enhance its efficiency. For example, the addition of sugar bounds that could increase the drug permeability. The addition of a carbohydrate chain has been previously shown to enhance the antiproliferative activity of indenoisoquinoline (Beck *et al*, 2014).

Another possible approach would be the addition of a light-activating unit to the drug. The topoisomerase 1 inhibitor, SN-38, has been modified with the addition of a photo-triggered moiety (nitrovanillin) and a cancer targeting unit (biotin). This drug, PT-1 (phototherapeutic agent 1), is activated upon light excitation and therefore permits the activation of the topoisomerase inhibitor at determined location to limit side effects (Shin *et al*., 2016).

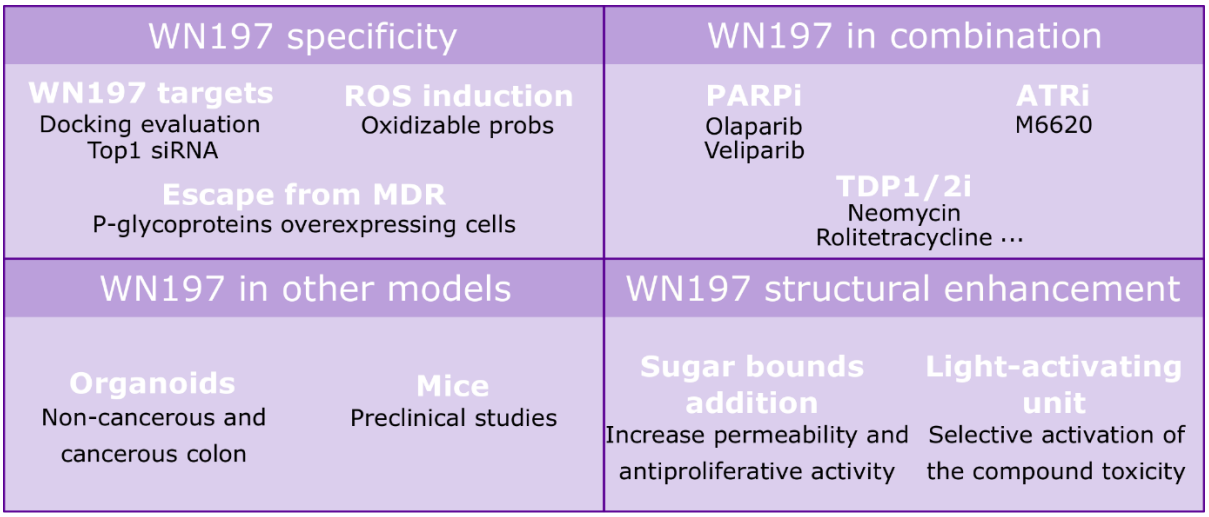

Figure ii. Furture research on the WN197 organometallic compound. Upper left: docking evaluation of WN197 with DNA and topoisomerase 1, and the use of Top1 siRNA in cancer cell lines could confirm that WN197 has no other target. ROS production and P-glycoproteins escape could be verified. Upper right: examples of inhibitors that could be used in combination with WN197 to optimize the cytotoxic effects on cancer cells. Bottom left: for further development of WN197 as a chemotherapeutic agent, WN197 will be tested on colon organoids, and studies on mice could be performed. Bottom right: WN197 possible structural modifications to improve its permeability, toxicity, and selectivity.

Finally, my thesis results demonstrate that WN197 is a novel anti-cancerous agent by inhibiting topoisomerase 1 at low doses, less toxic for healthy cells, that could be an interesting candidate as a new chemotherapeutic drug for pre-clinical studies.

BIBLIOGRAPHY

A

Ahmad SS, Duke S, Jena R, Williams MV, Burnet NG. Advances in radiotherapy BMJ 2012 Dec 4; 345 :e7765 doi: 10.1136/bmj.e7765. PMID: 23212681.

Akimitsu N, Adachi N, Hirai H, Hossain MS, Hamamoto H, Kobayashi M, Aratani Y, Koyama H, Sekimizu K. Enforced cytokinesis without complete nuclear division in embryonic cells depleting the activity of DNA topoisomerase IIalpha. Genes Cells. 2003 Apr;8(4):393-402. doi: 10.1046/j.1365-2443.2003.00643.x. PMID: 12653966.

Alter P, Herzum M, Soufi M, Schaefer JR, Maisch B. Cardiotoxicity of 5-fluorouracil. Cardiovasc Hematol Agents Med Chem. 2006 Jan;4(1):1-5. doi: 10.2174/187152506775268785. PMID: 16529545.

Annunziata CM, Davis RE, Demchenko Y, Bellamy W, Gabrea A, Zhan F, Lenz G, Hanamura I, Wright G, Xiao W, Dave S, Hurt EM, Tan B, Zhao H, Stephens O, Santra M, Williams DR, Dang L, Barlogie B, Shaughnessy JD Jr, Kuehl WM, Staudt LM. Frequent engagement of the classical and alternative NF-kappaB pathways by diverse genetic abnormalities in multiple myeloma. Cancer Cell. 2007 Aug;12(2):115-30. doi: 10.1016/j.ccr.2007.07.004. PMID: 17692804; PMCID: PMC2730509.

Antony S, Agama KK, Miao ZH, Takagi K, Wright MH, Robles AI, Varticovski L, Nagarajan M, Morrell A, Cushman M, Pommier Y. Novel indenoisoquinolines NSC 725776 and NSC 724998 produce persistent topoisomerase I cleavage complexes and overcome multidrug resistance. Cancer Res. 2007 Nov 1;67(21):10397-405. doi: 10.1158/0008-5472.CAN-07-0938. Erratum in: Cancer Res. 2007 Dec 15;67(24):12034. PMID: 17974983.

Aravind L, Leipe DD, Koonin EV. Toprim--a conserved catalytic domain in type IA and II topoisomerases, DnaG-type primases, OLD family nucleases and RecR proteins. Nucleic Acids Res. 1998 Sep 15;26(18):4205-13. doi: 10.1093/nar/26.18.4205. PMID: 9722641; PMCID: PMC147817.

Arjmand F, Jamsheera A, Afzal M, Tabassum, S. Enantiomeric specificity of biologically significant Cu(II) and Zn(II) chromone complexes towards DNA. Chirality 2012, 24, 977–986. doi: 10.1002/chir.22081.

Arriola E, Rodriguez-Pinilla SM, Lambros MB, Jones RL, James M, Savage K, Smith IE, Dowsett M, Reis-Filho JS. Topoisomerase II alpha amplification may predict benefit from adjuvant anthracyclines in HER2 positive early breast cancer. Breast Cancer Res Treat. 2007 Dec;106(2):181-9. doi: 10.1007/s10549-006-9492-5. Epub 2007 Jan 27. PMID: 17260090.

B

Bacher F, Enyedy É, Nagy NV, Rockenbauer A, Bognár GM, Trondl R, Novak MS, Klapproth E, Kiss T, Arion VB. Copper(II) complexes with highly water-soluble L- and D-proline-thiosemicarbazone conjugates as potential inhibitors of Topoisomerase IIα. Inorg Chem. 2013 Aug 5;52(15):8895-908. doi: 10.1021/ic401079w. Epub 2013 Jul 5. PMID: 23829568.

Ballout F, Habli Z, Monzer A, Rahal ON, Fatfat M and Gali-Muhtasib H. “Anticancer Alkaloids: Molecular Mechanisms and Clinical Manifestations.” Bioactive Natural Products for the Management of Cancer: from Bench to Bedside 2019. doi: 10.1007/978-981-13-7607-8_1.

Baranello L, Wojtowicz D, Cui K, Devaiah BN, Chung HJ, Chan-Salis KY, Guha R, Wilson K, Zhang X, Zhang H, Piotrowski J, Thomas CJ, Singer DS, Pugh BF, Pommier Y, Przytycka TM, Kouzine F, Lewis BA, Zhao K, Levens D. RNA Polymerase II Regulates Topoisomerase 1 Activity to Favor Efficient Transcription. Cell. 2016 Apr 7;165(2):357-71. doi: 10.1016/j.cell.2016.02.036. PMID: 27058666; PMCID: PMC4826470.

Bartek J, Iggo R, Gannon J, Lane DP. Genetic and immunochemical analysis of mutant p53 in human breast cancer cell lines. Oncogene. 1990 Jun;5(6):893-9. PMID: 1694291.

Bartsch R. Trastuzumab-deruxtecan: an investigational agent for the treatment of HER2-positive breast cancer. Expert Opin Investig Drugs. 2020 Sep;29(9):901-910. doi: 10.1080/13543784.2020.1792443. Epub 2020 Jul 23. PMID: 32701032.

Baudat F, de Massy B. SPO11: une activité de coupure de l'ADN indispensable à la méiose [SPO11: an activity that promotes DNA breaks required for meiosis]. Med Sci (Paris). 2004 Feb;20(2):213-8. French. doi: 10.1051/medsci/2004202213. PMID: 14997442.

Beck DE, Agama K, Marchand C, Chergui A, Pommier Y, Cushman M. Synthesis and biological evaluation of new carbohydrate-substituted indenoisoquinoline topoisomerase I inhibitors and improved syntheses of the experimental anticancer agents indotecan (LMP400) and indimitecan (LMP776). J Med Chem. 2014 Feb 27;57(4):1495-512. doi: 10.1021/jm401814y. Epub 2014 Feb 11. PMID: 24517248; PMCID: PMC3983348.

Bedez C, Lotz C, Batisse C, Vanden Broeck A, Stote RH, Howard E, Pradeau-Aubreton K, Ruff M and Lamour V. Post-translational modifications in DNA topoisomerase 2α highlight the role of a eukaryote-specific residue in the ATPase domain. Sci Rep. 2018;8, 9272. doi: 0.1038/s41598-018-27606-8.

Bednarikova M, Hausnerova J, Ehrlichova L, Matulova K, Gazarkova E, Minar L, Weinberger V. Can Schlafen 11 Help to Stratify Ovarian Cancer Patients Treated with DNA-Damaging Agents? Cancers (Basel). 2022 May 10;14(10):2353. doi: 10.3390/cancers14102353. PMID: 35625957; PMCID: PMC9139752.

Beltrán-Gracia E, López-Camacho A, Higuera-Ciapara I, Velázquez-Fernández JB and Vallejo-Cardona AA. Nanomedicine review: clinical developments in liposomal applications. Cancer Nano. 2019;10, 11. doi: 10.1186/s12645-019-0055-y.

Berger JM, Gamblin SJ, Harrison SC, Wang JC. Structure and mechanism of DNA topoisomerase II. Nature. 1996 Jan 18;379(6562):225-32. doi: 10.1038/379225a0. Erratum in: Nature 1996 Mar 14;380(6570):179. PMID: 8538787.

Berraondo P, Sanmamed MF, Ochoa MC, Etxeberria I, Aznar MA, Pérez-Gracia JL, Rodríguez-Ruiz ME, Ponz-Sarvise M, Castañón E, Melero I. Cytokines in clinical cancer immunotherapy. Br J Cancer. 2019 Jan;120(1):6-15. doi: 10.1038/s41416-018-0328-y. Epub 2018 Nov 9. PMID: 30413827; PMCID: PMC6325155.

Bhakar AL, Dölen G, Bear MF. The pathophysiology of fragile X (and what it teaches us about synapses). Annu Rev Neurosci. 2012;35:417-43. doi: 10.1146/annurev-neuro-060909-153138. Epub 2012 Apr 5. PMID: 22483044; PMCID: PMC4327822.

Biller LH, Schrag D. Diagnosis and Treatment of Metastatic Colorectal Cancer: A Review. JAMA. 2021 Feb 16;325(7):669-685. doi: 10.1001/jama.2021.0106. PMID: 33591350.

Bisceglie F, Musiari A, Pinelli S, Alinovi R, Menozzi I, Polverini E, Tarasconi P, Tavone M, Pelosi G. Quinoline-2-carboxaldehyde thiosemicarbazones and their Cu(II) and Ni(II) complexes as topoisomerase IIa inhibitors. J Inorg Biochem. 2015 Nov;152:10-9. doi: 10.1016/j.jinorgbio.2015.08.008. Epub 2015 Aug 8. PMID: 26335598.

Blajeski AL, Phan VA, Kottke TJ, Kaufmann SH. G(1) and G(2) cell-cycle arrest following microtubule depolymerization in human breast cancer cells. J Clin Invest. 2002 Jul;110(1):91-9. doi: 10.1172/JCI13275. PMID: 12093892; PMCID: PMC151025.

Bonner WM, Redon CE, Dickey JS, Nakamura AJ, Sedelnikova OA, Solier S, Pommier Y. GammaH2AX and cancer. Nat Rev Cancer. 2008 Dec;8(12):957-67. doi: 10.1038/nrc2523. Epub 2008 Nov 13. PMID: 19005492; PMCID: PMC3094856.

Brissos RF, Caubet A, Gamez P. Possible DNA-interacting pathways for metal-based compounds exemplified with copper coordination compounds. Eur. J. Inorg. Chem. 2015, 16, 2633–2645. doi: 10.1002/ejic.201500175.

C

Cappell MS. The pathophysiology, clinical presentation, and diagnosis of colon cancer and adenomatous polyps. Med Clin North Am. 2005 Jan;89(1):1-42, vii. doi: 10.1016/j.mcna.2004.08.011. PMID: 15527807.

Cappetta D, De Angelis A, Sapio L, Prezioso L, Illiano M, Quaini F, Rossi F, Berrino L, Naviglio S, Urbanek K. Oxidative Stress and Cellular Response to Doxorubicin: A Common Factor in the Complex Milieu of Anthracycline Cardiotoxicity. Oxid Med Cell Longev. 2017;2017:1521020. doi: 10.1155/2017/1521020. Epub 2017 Oct 18. PMID: 29181122; PMCID: PMC5664340.

Capranico G, Tinelli S, Austin CA, Fisher ML, Zunino F. Different patterns of gene expression of topoisomerase II isoforms in differentiated tissues during murine development. Biochim Biophys Acta. 1992 Aug 17;1132(1):43-8. doi: 10.1016/0167-4781(92)90050-a. PMID: 1380833.

Cerchiaro G, Aquilano K, Filomeni G, Rotilio G, Ciriolo MR, Ferreira AM. Isatin-Schiff base copper(II) complexes and their influence on cellular viability. J Inorg Biochem. 2005 Jul;99(7):1433-40. doi: 10.1016/j.jinorgbio.2005.03.013. PMID: 15878622.

Cardoso F, Durbecq V, Larsimont D, Paesmans M, Leroy JY, Rouas G, Sotiriou C, Renard N, Richard V, Piccart MJ, Di Leo A. Correlation between complete response to anthracycline-based chemotherapy and topoisomerase II-alpha gene amplification and protein overexpression in locally advanced/metastatic breast cancer. Int J Oncol. 2004 Jan;24(1):201-9. PMID: 14654958.

Castelli S, Gonçalves MB, Katkar P, Stuchi GC, Couto RAA, Petrilli HM, da Costa Ferreira AM. Comparative studies of oxindolimine-metal complexes as inhibitors of human DNA topoisomerase IB. J Inorg Biochem. 2018 Sep;186:85-94. doi: 10.1016/j.jinorgbio.2018.05.012. Epub 2018 May 21. PMID: 29860208.

Cha Y, Kim SY, Yeo HY, Baek JY, Choi MK, Jung KH, Dong SM, Chang HJ. Association of CHFR Promoter Methylation with Treatment Outcomes of Irinotecan-Based Chemotherapy in Metastatic Colorectal Cancer. Neoplasia. 2019 Jan;21(1):146-155. doi: 10.1016/j.neo.2018.11.010. Epub 2018 Dec 15. PMID: 30562637; PMCID: PMC6297269.

Champoux JJ. DNA topoisomerases: structure, function, and mechanism. Annu Rev Biochem. 2001;70:369-413. doi: 10.1146/annurev.biochem.70.1.369. PMID: 11395412.

Chan ES, Cronstein BN. Methotrexate--how does it really work? Nat Rev Rheumatol. 2010 Mar;6(3):175-8. doi: 10.1038/nrrheum.2010.5. PMID: 20197777.

Chargari C, Deutsch E, Blanchard P, Gouy S, Martelli H, Guérin F, Dumas I, Bossi A, Morice P, Viswanathan AN, Haie-Meder C. Brachytherapy: An overview for clinicians. CA Cancer J Clin. 2019 Sep;69(5):386-401. doi: 10.3322/caac.21578. Epub 2019 Jul 30. PMID: 31361333.

Chatelut E. Pharmacologie des dérivés du platine : différences entre les trois composés et les facteurs de variabilité entre patients [Pharmacology of platinum compounds: differences between the three molecules and factors of interpatient variability]. Bull Cancer. 2011 Nov;98(11):1253-61. French. doi: 10.1684/bdc.2011.1464. PMID: 22024542.

Chauhan M, Banerjee K, Arjmand F. DNA binding studies of novel Copper(II) complexes containing L-tryptophan as chiral auxiliary: in vitro antitumor activity of Cu-Sn2 complex in human neuroblastoma cells. Inorg Chem. 2007 Apr 16;46(8):3072-82. doi: 10.1021/ic061753a. Epub 2007 Mar 23. PMID: 17378549.

Chen J, Huang YW, Liu G, Afrasiabi Z, Sinn E, Padhye S, Ma Y. The cytotoxicity and mechanisms of 1,2-naphthoquinone thiosemicarbazone and its metal derivatives against MCF-7 human breast cancer cells. Toxicol. Appl. Pharm. 2004, 197, 40–48.

Chen ZF, Tan MX, Liu LM, Liu YC, Wang HS, Yang B, Peng Y, Liu HG, Liang H, Orvig C. Cytotoxicity of the traditional chinese medicine (TCM) plumbagin in its copper chemistry. Dalton Trans. 2009 Dec 28;(48):10824-33. doi: 10.1039/b910133k. Epub 2009 Nov 16. PMID: 20023912.

Chew ST, Lo KM, Lee SK, Heng MP, Teoh WY, Sim KS, Tan KW. Copper complexes with phosphonium containing hydrazone ligand: Topoisomerase inhibition and cytotoxicity study. Eur. J. Med. Chem. 2014 Apr 9;76, 397–407. doi: 10.1016/j.ejmech.2014.02.049.

Ciombor KK, Wu C, Goldberg RM. Recent therapeutic advances in the treatment of colorectal cancer. Annu Rev Med. 2015;66:83-95. doi: 10.1146/annurev-med-051513-102539. Epub 2014 Oct 9. PMID: 25341011.

Cohen PA, Jhingran A, Oaknin A, Denny L. Cervical cancer. Lancet. 2019 Jan 12;393(10167):169-182. doi: 10.1016/S0140-6736(18)32470-X. PMID: 30638582.

Cole SP, Bhardwaj G, Gerlach JH, Mackie JE, Grant CE, Almquist KC, Stewart AJ, Kurz EU, Duncan AM, Deeley RG. Overexpression of a transporter gene in a multidrug-resistant human lung cancer cell line. Science. 1992 Dec 4;258(5088):1650-4. doi: 10.1126/science.1360704. Erratum in: Science. 1993 May 14;260(5110):879. PMID: 1360704.

Coleman N, Zhang B, Byers LA, Yap TA. The role of Schlafen 11 (SLFN11) as a predictive biomarker for targeting the DNA damage response. Br J Cancer. 2021 Mar;124(5):857-859. doi: 10.1038/s41416-020-01202-y. Epub 2020 Dec 16. PMID: 33328609; PMCID: PMC7921443.

Conner JD, Medawala W, Stephens MT, Morris WH, Deweese JE, Kent PL, Rice JJ, Jiang X, Lisic EC. Cu(II) benzoylpyridine thiosemicarbazone complexes: Inhibition of human topoisomerase IIα and activity against breast cancer cells. Open J. Inorg. Chem. 2016 Apr; 6, 146–154. doi: 10.4236/ojic.2016.62010.

Coon JS, Marcus E, Gupta-Burt S, Seelig S, Jacobson K, Chen S, Renta V, Fronda G, Preisler HD. Amplification and overexpression of topoisomerase IIalpha predict response to anthracycline-based therapy in locally advanced breast cancer. Clin Cancer Res. 2002 Apr;8(4):1061-7. PMID: 11948114.

Cossetti RJ, Tyldesley SK, Speers CH, Zheng Y, Gelmon KA. Comparison of breast cancer recurrence and outcome patterns between patients treated from 1986 to 1992 and from 2004 to 2008. J Clin Oncol. 2015 Jan 1;33(1):65-73. doi: 10.1200/JCO.2014.57.2461. Epub 2014 Nov 24. PMID: 25422485.

van Cruijsen H, Giaccone G, Hoekman K. Epidermal growth factor receptor and angiogenesis: Opportunities for combined anticancer strategies. Int J Cancer. 2005 Dec 20;117(6):883-8. doi: 10.1002/ijc.21479. PMID: 16152621.

Cushman M. Design and Synthesis of Indenoisoquinolines Targeting Topoisomerase I and Other Biological Macromolecules for Cancer Chemotherapy. J Med Chem. 2021 Dec 23;64(24):17572-17600. doi: 10.1021/acs.jmedchem.1c01491. Epub 2021 Dec 8. PMID: 34879200.

D

Dasari S, Tchounwou PB. Cisplatin in cancer therapy: molecular mechanisms of action. Eur J Pharmacol. 2014 Oct 5;740:364-78. doi: 10.1016/j.ejphar.2014.07.025. Epub 2014 Jul 21. PMID: 25058905; PMCID: PMC4146684.

Del Conte G, Sessa C, von Moos R, Viganò L, Digena T, Locatelli A, Gallerani E, Fasolo A, Tessari A, Cathomas R, Gianni L. Phase I study of olaparib in combination with liposomal doxorubicin in patients with advanced solid tumours. Br J Cancer. 2014 Aug 12;111(4):651-9. doi: 10.1038/bjc.2014.345. Epub 2014 Jul 15. PMID: 25025963; PMCID: PMC4134498.

Dent R, Trudeau M, Pritchard KI, Hanna WM, Kahn HK, Sawka CA, Lickley LA, Rawlinson E, Sun P, Narod SA. Triple-negative breast cancer: clinical features and patterns of recurrence. Clin Cancer Res. 2007 Aug 1;13(15 Pt 1):4429-34. doi: 10.1158/1078-0432.CCR-06-3045. PMID: 17671126.

De Ruysscher D, Niedermann G, Burnet NG, Siva S, Lee AWM, Hegi-Johnson F. Radiotherapy toxicity. Nat Rev Dis Primers. 2019 Feb 21;5(1):13. doi: 10.1038/s41572-019-0064-5. Erratum in: Nat Rev Dis Primers. 2019 Mar 4;5(1):15. PMID: 30792503.

Dong J, Phelps RG, Qiao R, Yao S, Benard O, Ronai Z, Aaronson SA. BRAF oncogenic mutations correlate with progression rather than initiation of human melanoma. Cancer Res. 2003 Jul 15;63(14):3883-5. PMID: 12873977.

Donzelli M, Draetta GF. Regulating mammalian checkpoints through Cdc25 inactivation. EMBO Rep. 2003 Jul;4(7):671-7. doi: 10.1038/sj.embor.embor887. PMID: 12835754; PMCID: PMC1326326.

Duff B, Thangella VR, Creaven BS, Walsh M, Egan DA. Anti-cancer activity and mutagenic potential of novel copper(II) quinolinone Schiff base complexes in hepatocarcinoma cells. Eur J Pharmacol. 2012 Aug 15;689(1-3):45-55. doi: 10.1016/j.ejphar.2012.06.004. Epub 2012 Jun 15. PMID: 22705894.

Dunlop EA, Hunt DK, Acosta-Jaquez HA, Fingar DC, Tee AR. ULK1 inhibits mTORC1 signaling, promotes multisite Raptor phosphorylation and hinders substrate binding. Autophagy. 2011 Jul;7(7):737-47. doi: 10.4161/auto.7.7.15491. Epub 2011 Jul 1. PMID: 21460630; PMCID: PMC3149699.

Durban E, Goodenough M, Mills J, Busch H. Topoisomerase I phosphorylation in vitro and in rapidly growing Novikoff hepatoma cells. EMBO J. 1985 Nov;4(11):2921-6. doi: 10.1002/j.1460-2075.1985.tb04024.x. PMID: 2998765; PMCID: PMC554599.

E

Elton TS, Hernandez VA, Carvajal-Moreno J, Wang X, Ipinmoroti D, Yalowich JC. Intronic Polyadenylation in Acquired Cancer Drug Resistance Circumvented by Utilizing CRISPR/Cas9 with Homology-Directed Repair: The Tale of Human DNA Topoisomerase IIα. Cancers (Basel). 2022 Jun 27;14(13):3148. doi: 10.3390/cancers14133148. PMID: 35804920; PMCID: PMC9265003.

Errington F, Willmore E, Tilby MJ, Li L, Li G, Li W, Baguley BC, Austin CA. Murine transgenic cells lacking DNA topoisomerase IIbeta are resistant to acridines and mitoxantrone: analysis of cytotoxicity and cleavable complex formation. Mol Pharmacol. 1999 Dec;56(6):1309-16. doi: 10.1124/mol.56.6.1309. PMID: 10570059.

Escudier B, Worden F, Kudo M. Sorafenib: key lessons from over 10 years of experience. Expert Rev Anticancer Ther. 2019 Feb;19(2):177-189. doi: 10.1080/14737140.2019.1559058. Epub 2018 Dec 21. PMID: 30575405.

Evison BJ, Sleebs BE, Watson KG, Phillips DR, Cutts SM. Mitoxantrone, More than Just Another Topoisomerase II Poison. Med Res Rev. 2016 Mar;36(2):248-99. doi: 10.1002/med.21364. Epub 2015 Aug 19. PMID: 26286294.

F

Fabian CJ, Molina R, Slavik M, Dahlberg S, Giri S, Stephens R. Pyridoxine therapy for palmar-plantar erythrodysesthesia associated with continuous 5-fluorouracil infusion. Invest New Drugs. 1990 Feb;8(1):57-63. doi: 10.1007/BF00216925. PMID: 2345070.

Ferrara R, Imbimbo M, Malouf R, Paget-Bailly S, Calais F, Marchal C, Westeel V. Single or combined immune checkpoint inhibitors compared to first-line platinum-based chemotherapy with or without bevacizumab for people with advanced non-small cell lung cancer. Cochrane Database Syst Rev. 2020 Dec 14;12(12):CD013257. doi: 10.1002/14651858.CD013257.pub2. Update in: Cochrane Database Syst Rev. 2021 Apr 30;4:CD013257. PMID: 33316104; PMCID: PMC8094159.

Finkielstein CV, Lewellyn AL, Maller JL. The midblastula transition in Xenopus embryos activates multiple pathways to prevent apoptosis in response to DNA damage. Proc Natl Acad Sci U S A. 2001 Jan 30;98(3):1006-11. doi: 10.1073/pnas.98.3.1006. PMID: 11158585; PMCID: PMC14699.

Fleming M, Ravula S, Tatishchev SF, Wang HL. Colorectal carcinoma: Pathologic aspects. J Gastrointest Oncol. 2012 Sep;3(3):153-73. doi: 10.3978/j.issn.2078-6891.2012.030. PMID: 22943008; PMCID: PMC3418538.

Foo JB, Ng LS, Lim JH, Tan PX, Lor YZ, Loo JSE, Low ML, Chan LC, Beh CY, Leong SW, Saiful Yazan L, Tor YS, How CW. Induction of cell cycle arrest and apoptosis by copper complex Cu(SBCM)2 towards oestrogen-receptor positive MCF-7 breast cancer cells. RSC Adv. 2019 Jun 11;9(32):18359-18370. doi: 10.1039/c9ra03130h. PMID: 35515266; PMCID: PMC9064738.

Fox EJ. Mechanism of action of mitoxantrone. Neurology. 2004 Dec 28;63(12 Suppl 6):S15-8. doi: 10.1212/wnl.63.12_suppl_6.s15. PMID: 15623664.

Fragola G, Mabb AM, Taylor-Blake B, Niehaus JK, Chronister WD, Mao H, Simon JM, Yuan H, Li Z, McConnell MJ, Zylka MJ. Deletion of Topoisomerase 1 in excitatory neurons causes genomic instability and early onset neurodegeneration. Nat Commun. 2020 Apr 23;11(1):1962. doi: 10.1038/s41467-020-15794-9. PMID: 32327659; PMCID: PMC7181881.

Furuta T, Takemura H, Liao ZY, Aune GJ, Redon C, Sedelnikova OA, Pilch DR, Rogakou EP, Celeste A, Chen HT, Nussenzweig A, Aladjem MI, Bonner WM, Pommier Y. Phosphorylation of histone H2AX and activation of Mre11, Rad50, and Nbs1 in response to replication-dependent DNA double-strand breaks induced by mammalian DNA topoisomerase I cleavage complexes. J Biol Chem. 2003 May 30;278(22):20303-12. doi: 10.1074/jbc.M300198200. Epub 2003 Mar 25. PMID: 12660252.

G

García-Foncillas J, Sunakawa Y, Aderka D, Wainberg Z, Ronga P, Witzler P, Stintzing S. Distinguishing Features of Cetuximab and Panitumumab in Colorectal Cancer and Other Solid Tumors. Front Oncol. 2019 Sep 20;9:849. doi: 10.3389/fonc.2019.00849. PMID: 31616627; PMCID: PMC6763619.

Garner E, Costanzo V. Studying the DNA damage response using in vitro model systems. DNA Repair (Amst). 2009 Sep 2;8(9):1025-37. doi: 10.1016/j.dnarep.2009.04.015. Epub 2009 May 23. PMID: 19482562.

Garnier F, Debat H, Nadal M. Type IA DNA Topoisomerases: A Universal Core and Multiple Activities. Methods Mol Biol. 2018;1703:1-20. doi: 10.1007/978-1-4939-7459-7_1. PMID: 29177730.

Garrido C, Galluzzi L, Brunet M, Puig PE, Didelot C, Kroemer G. Mechanisms of cytochrome c release from mitochondria. Cell Death Differ. 2006 Sep;13(9):1423-33. doi: 10.1038/sj.cdd.4401950. Epub 2006 May 5. PMID: 16676004.

Gasser SM, Walter R, Dang Q, Cardenas ME. Topoisomerase II: its functions and phosphorylation. Antonie Van Leeuwenhoek. 1992 Aug;62(1-2):15-24. doi: 10.1007/BF00584459. PMID: 1332607.

Gibson SB. A matter of balance between life and death: targeting reactive oxygen species (ROS)-induced autophagy for cancer therapy. Autophagy. 2010 Oct;6(7):835-7. doi: 10.4161/auto.6.7.13335. Epub 2010 Oct 16. PMID: 20818163.

Grani G, Ramundo V, Verrienti A, Sponziello M, Durante C. Thyroid hormone therapy in differentiated thyroid cancer. Endocrine. 2019 Oct;66(1):43-50. doi: 10.1007/s12020-019-02051-3. Epub 2019 Oct 15. PMID: 31617165.

Greig SL. Talimogene Laherparepvec: First Global Approval. Drugs. 2016 Jan;76(1):147-54. doi: 10.1007/s40265-015-0522-7. PMID: 26620366.

Globocan 2020. [Online]. Available at: https://gco.iarc.fr/ (consulted September 1st 2022).

Gouveris, P., Skopelitis, E.E., & Tsavaris, N.B. Topoisomerase I and II Expression in Recurrent Colorectal Cancer Cells: A Dubious Matter. 2011 Aug 1. doi: 10.5772/INTECHOPEN.84014.

Gulcin İ, Alwasel SH. Metal Ions, Metal Chelators and Metal Chelating Assay as Antioxidant Method. Processes. 2022 Jan 10;10, 132. doi: 10.3390/pr10010132.

Guney Eskiler G. Talazoparib to treat BRCA-positive breast cancer. Drugs Today (Barc). 2019 Jul;55(7):459-467. doi: 10.1358/dot.2019.55.7.3015642. PMID: 31347614.

H

Hakem R. DNA-damage repair; the good, the bad, and the ugly. EMBO J. 2008 Feb 20;27(4):589-605. doi: 10.1038/emboj.2008.15. PMID: 18285820; PMCID: PMC2262034.

Haleel A, Mahendiran D, Veena V, Sakthivel N, Rahiman AK. Antioxidant, DNA interaction, VEGFR2 kinase, topoisomerase I and in vitro cytotoxic activities of heteroleptic copper(II) complexes of tetrazolo[1,5-a]pyrimidines and diimines. Mater Sci Eng C Mater Biol Appl. 2016 Nov 1;68:366-382. doi: 10.1016/j.msec.2016.05.120. Epub 2016 May 30. PMID: 27524032.

Haleel AK, Mahendiran D, Rafi UM, Veena V, Shobana S, Rahiman AK. Tetrazolo[1,5-a]pyrimidine-based metal(II) complexes as therapeutic agents: DNA interaction, targeting topoisomerase I and cyclin-dependent kinase studies. Inorg. Nano Met. Chem. 2019 Feb 26;48, 569–582. doi: 10.1080/24701556.2019.1571514.

Hammerstrom AE, Cauley DH, Atkinson BJ, Sharma P. Cancer immunotherapy: sipuleucel-T and beyond. Pharmacotherapy. 2011 Aug;31(8):813-28. doi: 10.1592/phco.31.8.813. PMID: 21923608; PMCID: PMC4159742.

Handy CE, Antonarakis ES. Sipuleucel-T for the treatment of prostate cancer: novel insights and future directions. Future Oncol. 2018 Apr;14(10):907-917. doi: 10.2217/fon-2017-0531. Epub 2017 Dec 20. PMID: 29260582; PMCID: PMC5925432.

Hans F, Dimitrov S. Histone H3 phosphorylation and cell division. Oncogene. 2001 May 28;20(24):3021-7. doi: 10.1038/sj.onc.1204326. PMID: 11420717.

Haque MM, Desai KV. Pathways to Endocrine Therapy Resistance in Breast Cancer. Front Endocrinol (Lausanne). 2019 Aug 21;10:573. doi: 10.3389/fendo.2019.00573. PMID: 31496995; PMCID: PMC6712962.

Hasinoff BB, Wu X, Yadav AA, Patel D, Zhang H, Wang DS, Chen ZS, Yalowich JC. Cellular mechanisms of the cytotoxicity of the anticancer drug elesclomol and its complex with Cu(II). Biochem Pharmacol. 2015 Feb 1;93(3):266-76. doi: 10.1016/j.bcp.2014.12.008. Epub 2014 Dec 27. PMID: 25550273.

Heestand GM, Schwaederle M, Gatalica Z, Arguello D, Kurzrock R. Topoisomerase expression and amplification in solid tumours: Analysis of 24,262 patients. Eur J Cancer. 2017 Sep;83:80-87. doi: 10.1016/j.ejca.2017.06.019. Epub 2017 Jul 17. PMID: 28728050; PMCID: PMC5613945.

Heck MM, Hittelman WN, Earnshaw WC. Differential expression of DNA topoisomerases I and II during the eukaryotic cell cycle. Proc Natl Acad Sci U S A. 1988 Feb;85(4):1086-90. doi: 10.1073/pnas.85.4.1086. PMID: 2829215; PMCID: PMC279709.

Hernandez VA, Carvajal-Moreno J, Papa JL, Shkolnikov N, Li J, Ozer HG, Yalowich JC, Elton TS. CRISPR/Cas9 Genome Editing of the Human Topoisomerase IIα Intron 19 5' Splice Site Circumvents Etoposide Resistance in Human Leukemia K562 Cells. Mol Pharmacol. 2021 Mar;99(3):226-241. doi: 10.1124/molpharm.120.000173. Epub 2021 Jan 14. PMID: 33446509; PMCID: PMC7919865.

Hernandez VA, Carvajal-Moreno J, Wang X, Pietrzak M, Yalowich JC, Elton TS. Use of CRISPR/Cas9 with homology-directed repair to silence the human topoisomerase IIα intron-19 5' splice site: Generation of etoposide resistance in human leukemia K562 cells. PLoS One. 2022 May 26;17(5):e0265794. doi: 10.1371/journal.pone.0265794. PMID: 35617303; PMCID: PMC9135202.

Hey SP, Gyawali B, D'Andrea E, Kanagaraj M, Franklin JM, Kesselheim AS. A Systematic Review and Meta-Analysis of Bevacizumab in First-Line Metastatic Breast Cancer: Lessons for Research and Regulatory Enterprises. J Natl Cancer Inst. 2020 Apr 1;112(4):335-342. doi: 10.1093/jnci/djz211. PMID: 31651981; PMCID: PMC7156929.

Hippert MM, O'Toole PS, Thorburn A. Autophagy in cancer: good, bad, or both? Cancer Res. 2006 Oct 1;66(19):9349-51. doi: 10.1158/0008-5472.CAN-06-1597. PMID: 17018585.

Hiraide T, Watanabe S, Matsubayashi T, Yanagi K, Nakashima M, Ogata T, Saitsu H. A de novo TOP2B variant associated with global developmental delay and autism spectrum disorder. Mol Genet Genomic Med. 2020 Mar;8(3):e1145. doi: 10.1002/mgg3.1145. Epub 2020 Jan 17. PMID: 31953910; PMCID: PMC7057084.

Ho MY, Mackey JR. Presentation and management of docetaxel-related adverse effects in patients with breast cancer. Cancer Manag Res. 2014 May 27;6:253-9. doi: 10.2147/CMAR.S40601. PMID: 24904223; PMCID: PMC4041377.

Hodi FS, O'Day SJ, McDermott DF, Weber RW, Sosman JA, Haanen JB, Gonzalez R, Robert C, Schadendorf D, Hassel JC, Akerley W, van den Eertwegh AJ, Lutzky J, Lorigan P, Vaubel JM, Linette GP, Hogg D, Ottensmeier CH, Lebbé C, Peschel C, Quirt I, Clark JI, Wolchok JD, Weber JS, Tian J, Yellin MJ, Nichol GM, Hoos A, Urba WJ. Improved survival with ipilimumab in patients with metastatic melanoma. N Engl J Med. 2010 Aug 19;363(8):711-23. doi: 10.1056/NEJMoa1003466. Epub 2010 Jun 5. Erratum in: N Engl J Med. 2010 Sep 23;363(13):1290. PMID: 20525992; PMCID: PMC3549297.

Hordyjewska A, Popiołek Ł, Kocot J. The many "faces" of copper in medicine and treatment. Biometals. 2014 Aug;27(4):611-21. doi: 10.1007/s10534-014-9736-5. Epub 2014 Apr 20. PMID: 24748564; PMCID: PMC4113679.

Houot R, Schultz LM, Marabelle A, Kohrt H. T-cell-based Immunotherapy: Adoptive Cell Transfer and Checkpoint Inhibition. Cancer Immunol Res. 2015 Oct;3(10):1115-22. doi: 10.1158/2326-6066.CIR-15-0190. PMID: 26438444.

Hu GF. Copper stimulates proliferation of human endothelial cells under culture. J Cell Biochem. 1998 Jun 1;69(3):326-35. doi: 10.1002/(sici)1097-4644(19980601)69:3<326::aid-jcb10>3.0.co;2-a. PMID: 9581871.

Huang A, Garraway LA, Ashworth A, Weber B. Synthetic lethality as an engine for cancer drug target discovery. Nat Rev Drug Discov. 2020 Jan;19(1):23-38. doi: 10.1038/s41573-019-0046-z. Epub 2019 Nov 11. PMID: 31712683.

Human Protein Atlas TOP1 [Online]. Available at: https://www.proteinatlas.org/ENSG00000198900-TOP1/tissue (consulted November 1st 2022).

Hur J, Ghosh M, Kim TH, Park N, Pandey K, Cho YB, Hong SD, Katuwal NB, Kang M, An HJ, Moon YW. Synergism of AZD6738, an ATR Inhibitor, in Combination with Belotecan, a Camptothecin Analogue, in Chemotherapy-Resistant Ovarian Cancer. Int J Mol Sci. 2021 Jan 27;22(3):1223. doi: 10.3390/ijms22031223. PMID: 33513721; PMCID: PMC7865398.

I

Ikediobi ON, Davies H, Bignell G, Edkins S, Stevens C, O'Meara S, Santarius T, Avis T, Barthorpe S, Brackenbury L, Buck G, Butler A, Clements J, Cole J, Dicks E, Forbes S, Gray K, Halliday K, Harrison R, Hills K, Hinton J, Hunter C, Jenkinson A, Jones D, Kosmidou V, Lugg R, Menzies A, Mironenko T, Parker A, Perry J, Raine K, Richardson D, Shepherd R, Small A, Smith R, Solomon H, Stephens P, Teague J, Tofts C, Varian J, Webb T, West S, Widaa S, Yates A, Reinhold W, Weinstein JN, Stratton MR, Futreal PA, Wooster R. Mutation analysis of 24 known cancer genes in the NCI-60 cell line set. Mol Cancer Ther. 2006 Nov;5(11):2606-12. doi: 10.1158/1535-7163.MCT-06-0433. Epub 2006 Nov 6. PMID: 17088437; PMCID: PMC2705832.

Ikotun OF, Higbee EM, Ouellette W, Doyle RP. Pyrophosphate-bridged complexes with picomolar toxicity. J Inorg Biochem. 2009 Sep;103(9):1254-64. doi: 10.1016/j.jinorgbio.2009.07.010. Epub 2009 Jul 17. PMID: 19666193.

INCa; Institut National du Cancer. France cancer panorama 2022 edition. [Online] available at: https://www.e-cancer.fr/Expertises-et-publications/Catalogue-des-publications/Panorama-des-cancers-en-France-Edition-2022#:~:text=Cette%20brochure%20synth%C3%A9tise%20les%20donn%C3%A9es,pendant%20et%20apr%C3%A8s%20la%20maladie (consulted august 1st 2022).

Iorfida M, Mazza M, Munzone E. Fulvestrant in Combination with CDK4/6 Inhibitors for HER2-Metastatic Breast Cancers: Current Perspectives. Breast Cancer (Dove Med Press). 2020 Mar 18;12:45-56. doi: 10.2147/BCTT.S196240. PMID: 32256106; PMCID: PMC7090187.

Ishibashi S., Saldanha Y.L. F., Amaya E. Xenopus as a Model Organism for Biomedical Research. Basic Science Methods for Clinical Researcher. Academic Press, 2017, Chapter 14, Pages 263-290. doi: 10.1016/B978-0-12-803077-6.00022-9.

J

Jabbour E, Kantarjian H. Chronic myeloid leukemia: 2018 update on diagnosis, therapy and monitoring. Am J Hematol. 2018 Mar;93(3):442-459. doi: 10.1002/ajh.25011. PMID: 29411417.

Jaouen G, Vessières A, Top S. Ferrocifen type anti-cancer drugs. Chem. Soc. Rev. 2015 Oct 21;44, 8802–8817. doi: 10.1039/C5CS00486A.

Järvinen TA, Kononen J, Pelto-Huikko M, Isola J. Expression of topoisomerase IIalpha is associated with rapid cell proliferation, aneuploidy, and c-erbB2 overexpression in breast cancer. Am J Pathol. 1996 Jun;148(6):2073-82. PMID: 8669491; PMCID: PMC1861630.

Järvinen TA, Liu ET. HER-2/neu and topoisomerase IIalpha in breast cancer. Breast Cancer Res Treat. 2003 Apr;78(3):299-311. doi: 10.1023/a:1023077507295. PMID: 12755489.

Joo Y, Xue Y, Wang Y, McDevitt RA, Sah N, Bossi S, Su S, Lee SK, Peng W, Xie A, Zhang Y, Ding Y, Ku WL, Ghosh S, Fishbein K, Shen W, Spencer R, Becker K, Zhao K, Mattson MP, van Praag H, Sharov A, Wang W. Topoisomerase 3β knockout mice show transcriptional and behavioural impairments associated with neurogenesis and synaptic plasticity. Nat Commun. 2020 Jun 19;11(1):3143. doi: 10.1038/s41467-020-16884-4. PMID: 32561719; PMCID: PMC7305123.

K

Kamiloglu S., Sari G., Ozdal T., Capanoglu E. Guidelines for cell viability assays. Food Front. 2020 Sept 16;1(3), 332-349. doi: 10.1002/fft2.44.

Kawale AS, Povirk LF. Tyrosyl-DNA phosphodiesterases: rescuing the genome from the risks of relaxation. Nucleic Acids Res. 2018 Jan 25;46(2):520-537. doi: 10.1093/nar/gkx1219. PMID: 29216365; PMCID: PMC5778467.

Keam SJ. Trastuzumab Deruxtecan: First Approval. Drugs. 2020 Apr;80(5):501-508. doi: 10.1007/s40265-020-01281-4. PMID: 32144719.

Keck JM, Conner JD, Wilson JT, Jiang X, Lisic EC, Deweese JE. Clarifying the Mechanism of Copper(II) α-(N)-Heterocyclic Thiosemicarbazone Complexes on DNA Topoisomerase IIα and IIβ. Chem Res Toxicol. 2019 Oct 21;32(10):2135-2143. doi: 10.1021/acs.chemrestox.9b00311. Epub 2019 Sep 20. PMID: 31512855.

Keramida K, Charalampopoulos G, Filippiadis D, Tsougos E, Farmakis D. Cardiovascular complications of metastatic colorectal cancer treatment. J Gastrointest Oncol. 2019 Aug;10(4):797-806. doi: 10.21037/jgo.2019.03.04. PMID: 31392061; PMCID: PMC6657319.

Kerr AJ, Dodwell D, McGale P, Holt F, Duane F, Mannu G, Darby SC, Taylor CW. Adjuvant and neoadjuvant breast cancer treatments: A systematic review of their effects on mortality. Cancer Treat Rev. 2022 Apr;105:102375. doi: 10.1016/j.ctrv.2022.102375. Epub 2022 Mar 4. PMID: 35367784; PMCID: PMC9096622.

Khan RA, Usman M, Dhivya R, Balaji P, Alsalme A, AlLohedan H, Arjmand F, AlFarhan K, Akbarsha MA, Marchetti F, Pettinari C, Tabassum S. Heteroleptic Copper(I) Complexes of "Scorpionate" Bis-pyrazolyl Carboxylate Ligand with Auxiliary Phosphine as Potential Anticancer Agents: An Insight into Cytotoxic Mode. Sci Rep. 2017 Mar 24;7:45229. doi: 10.1038/srep45229. PMID: 28338061; PMCID: PMC5364558.

Kim YC, Guan KL. mTOR: a pharmacologic target for autophagy regulation. J Clin Invest. 2015 Jan;125(1):25-32. doi: 10.1172/JCI73939. Epub 2015 Jan 2. PMID: 25654547; PMCID: PMC4382265.

Kinner A, Wu W, Staudt C, Iliakis G. Gamma-H2AX in recognition and signaling of DNA double-strand breaks in the context of chromatin. Nucleic Acids Res. 2008 Oct;36(17):5678-94. doi: 10.1093/nar/gkn550. Epub 2008 Sep 4. PMID: 18772227; PMCID: PMC2553572.

Kondo Y, Kondo S. Autophagy and cancer therapy. Autophagy. 2006 Apr-Jun;2(2):85-90. doi: 10.4161/auto.2.2.2463. Epub 2006 Apr 29. PMID: 16874083.

Kondratskyi A, Kondratska K, Vanden Abeele F, Gordienko D, Dubois C, Toillon RA, Slomianny C, Lemière S, Delcourt P, Dewailly E, Skryma R, Biot C, Prevarskaya N. Ferroquine, the next generation antimalarial drug, has antitumor activity. Sci Rep. 2017 Nov 21;7(1):15896. doi: 10.1038/s41598-017-16154-2. PMID: 29162859; PMCID: PMC5698296.

Kovacs D, Kovacs P, Eszlari N, Gonda X, Juhasz G. Psychological side effects of immune therapies: symptoms and pathomechanism. Curr Opin Pharmacol. 2016 Aug;29:97-103. doi: 10.1016/j.coph.2016.06.008. Epub 2016 Jul 22. PMID: 27456240.

Krasnovskaya O, Naumov A, Guk D, Gorelkin P, Erofeev A, Beloglazkina E, Majouga A. Copper Coordination Compounds as Biologically Active Agents. Int J Mol Sci. 2020 May 31;21(11):3965. doi: 10.3390/ijms21113965. PMID: 32486510; PMCID: PMC7312030.

Kuchenbaecker KB, Hopper JL, Barnes DR, Phillips KA, Mooij TM, Roos-Blom MJ, Jervis S, van Leeuwen FE, Milne RL, Andrieu N, Goldgar DE, Terry MB, Rookus MA, Easton DF, Antoniou AC. BRCA1 and BRCA2 Cohort Consortium, McGuffog L, Evans DG, Barrowdale D, Frost D, Adlard J, Ong KR, Izatt L, Tischkowitz M, Eeles R, Davidson R, Hodgson S, Ellis S, Nogues C, Lasset C, Stoppa-Lyonnet D, Fricker JP, Faivre L, Berthet P, Hooning MJ, van der Kolk LE, Kets CM, Adank MA, John EM, Chung WK, Andrulis IL, Southey M, Daly MB, Buys SS, Osorio A, Engel C, Kast K, Schmutzler RK, Caldes T, Jakubowska A, Simard J, Friedlander ML, McLachlan SA, Machackova E, Foretova L, Tan YY, Singer CF, Olah E, Gerdes AM, Arver B, Olsson H. Risks of Breast, Ovarian, and Contralateral Breast Cancer for BRCA1 and BRCA2 Mutation Carriers. JAMA. 2017 Jun 20;317(23):2402-2416. doi: 10.1001/jama.2017.7112. PMID: 28632866.

Kummar S, Chen A, Ji J, Zhang Y, Reid JM, Ames M, Jia L, Weil M, Speranza G, Murgo AJ, Kinders R, Wang L, Parchment RE, Carter J, Stotler H, Rubinstein L, Hollingshead M, Melillo G, Pommier Y, Bonner W, Tomaszewski JE, Doroshow JH. Phase I study of PARP inhibitor ABT-888 in combination with topotecan in adults with refractory solid tumors and lymphomas. Cancer Res. 2011 Sep 1;71(17):5626-34. doi: 10.1158/0008-5472.CAN-11-1227. Epub 2011 Jul 27. PMID: 21795476; PMCID: PMC3166628.

Kummar S, Chen A, Gutierrez M, Pfister TD, Wang L, Redon C, Bonner WM, Yutzy W, Zhang Y, Kinders RJ, Ji J, Allen D, Covey JM, Eiseman JL, Holleran JL, Beumer JH, Rubinstein L, Collins J, Tomaszewski J, Parchment R, Pommier Y, Doroshow JH. Clinical and pharmacologic evaluation of two dosing schedules of indotecan (LMP400), a novel indenoisoquinoline, in patients with advanced solid tumors. Cancer Chemother Pharmacol. 2016 Jul;78(1):73-81. doi: 10.1007/s00280-016-2998-6. Epub 2016 May 11. PMID: 27169793; PMCID: PMC5199138.

L

Lam CW, Yeung WL, Law CY. Global developmental delay and intellectual disability associated with a de novo TOP2B mutation. Clin Chim Acta. 2017 Jun;469:63-68. doi: 10.1016/j.cca.2017.03.022. Epub 2017 Mar 23. PMID: 28343847.

Lambert A, Schwarz L, Ducreux M, Conroy T. Neoadjuvant Treatment Strategies in Resectable Pancreatic Cancer. Cancers (Basel). 2021 Sep 21;13(18):4724. doi: 10.3390/cancers13184724. PMID: 34572951; PMCID: PMC8469083.

de Langen AJ, Jebbink M, Hashemi SMS, Kuiper JL, de Bruin-Visser J, Monkhorst K, Thunnissen E, Smit EF. Trastuzumab and paclitaxel in patients with EGFR mutated NSCLC that express HER2 after progression on EGFR TKI treatment. Br J Cancer. 2018 Aug;119(5):558-564. doi: 10.1038/s41416-018-0194-7. Epub 2018 Jul 31. PMID: 30061586; PMCID: PMC6162232.

Larsen AK, Escargueil AE, Skladanowski A. Catalytic topoisomerase II inhibitors in cancer therapy. Pharmacol Ther. 2003 Aug;99(2):167-81. doi: 10.1016/s0163-7258(03)00058-5. PMID: 12888111.

Lee JH, Berger JM. Cell Cycle-Dependent Control and Roles of DNA Topoisomerase II. Genes (Basel). 2019 Oct 30;10(11):859. doi: 10.3390/genes10110859. PMID: 31671531; PMCID: PMC6896119.

Lee SK, Tan KW, Ng SW. Zinc, copper and nickel derivatives of 2-[2-bromoethyliminomethyl]phenol as topoisomerase inhibitors exhibiting anti-proliferative and anti-metastatic properties. RSC Adv. 2014 Nov 5;4, 60280-60292. doi: 10.1039/C4RA09256B.

Lee SK, Tan KW, Ng SW. Topoisomerase I inhibition and DNA cleavage by zinc, copper, and nickel derivatives of 2-[2-bromoethyliminomethyl]-4-[ethoxymethyl]phenol complexes exhibiting anti-proliferation and anti-metastasis activity. J Inorg Biochem. 2016 Jun;159:14-21. doi: 10.1016/j.jinorgbio.2016.02.010. Epub 2016 Feb 11. PMID: 26901628.

Lehmann, F, Wennerberg, J. Evolution of Nitrogen-Based Alkylating Anticancer Agents. Processes 2021 Feb 19;9, 377. doi: 10.3390/pr9020377.

Leroy B, Girard L, Hollestelle A, Minna JD, Gazdar AF, Soussi T. Analysis of TP53 mutation status in human cancer cell lines: a reassessment. Hum Mutat. 2014 Jun;35(6):756-65. doi: 10.1002/humu.22556. Epub 2014 May 6. PMID: 24700732; PMCID: PMC4451114.

Li CI, Uribe DJ, Daling JR. Clinical characteristics of different histologic types of breast cancer. Br J Cancer. 2005 Oct 31;93(9):1046-52. doi: 10.1038/sj.bjc.6602787. PMID: 16175185; PMCID: PMC2361680.

Li M, Liu Y. Topoisomerase I in Human Disease Pathogenesis and Treatments. Genomics Proteomics Bioinformatics. 2016 Jun;14(3):166-171. doi: 10.1016/j.gpb.2016.02.004. Epub 2016 May 12. PMID: 27181710; PMCID: PMC4936607.

Li Q, Yang G, Feng M, Zheng S, Cao Z, Qiu J, You L, Zheng L, Hu Y, Zhang T, Zhao Y. NF-κB in pancreatic cancer: Its key role in chemoresistance. Cancer Lett. 2018 May 1;421:127-134. doi: 10.1016/j.canlet.2018.02.011. Epub 2018 Feb 10. PMID: 29432846.

Li W, Wang JC. Mammalian DNA topoisomerase IIIalpha is essential in early embryogenesis. Proc Natl Acad Sci U S A. 1998 Feb 3;95(3):1010-3. doi: 10.1073/pnas.95.3.1010. PMID: 9448276; PMCID: PMC18654.

Lisic EC, Rand VG, Ngo L, Kent P, Rice J, Gerlach D, Papish ET, Jiang X. Cu(II) propionyl-thiazole thiosemicarbazone complexes: Crystal structure, inhibition of human topoisomerase IIα, and activity against breast cancer cells. Open J. Med. Chem. 2018 Jun, 8, 30–46. doi: 10.4236/ojmc.2018.82004.

Liu WJ, Ye L, Huang WF, Guo LJ, Xu ZG, Wu HL, Yang C, Liu HF. p62 links the autophagy pathway and the ubiqutin-proteasome system upon ubiquitinated protein degradation. Cell Mol Biol Lett. 2016 Dec 13;21:29. doi: 10.1186/s11658-016-0031-z. PMID: 28536631; PMCID: PMC5415757.

Lorin S, Hamaï A, Mehrpour M, Codogno P. Autophagy regulation and its role in cancer. Semin Cancer Biol. 2013 Oct;23(5):361-79. doi: 10.1016/j.semcancer.2013.06.007. Epub 2013 Jun 27. PMID: 23811268.

M

Ma WW, Adjei AA. Novel agents on the horizon for cancer therapy. CA Cancer J Clin. 2009 Mar-Apr;59(2):111-37. doi: 10.3322/caac.20003. Erratum in: CA Cancer J Clin. 2010 Jan-Feb;60(1):62. PMID: 19278961.

Ma Y, Vassetzky Y, Dokudovskaya S. mTORC1 pathway in DNA damage response. Biochim Biophys Acta Mol Cell Res. 2018 Sep;1865(9):1293-1311. doi: 10.1016/j.bbamcr.2018.06.011. Epub 2018 Jun 22. PMID: 29936127.

Ma Z, Xu L, Liu D, Zhang X, Di S, Li W, Zhang J, Reiter RJ, Han J, Li X, Yan X. Utilizing Melatonin to Alleviate Side Effects of Chemotherapy: A Potentially Good Partner for Treating Cancer with Ageing. Oxid Med Cell Longev. 2020 May 21;2020:6841581. doi: 10.1155/2020/6841581. PMID: 32566095; PMCID: PMC7260648.

Madabhushi R. The Roles of DNA Topoisomerase IIβ in Transcription. Int J Mol Sci. 2018 Jun 29;19(7):1917. doi: 10.3390/ijms19071917. PMID: 29966298; PMCID: PMC6073266.

Marchand C, Antony S, Kohn KW, Cushman M, Ioanoviciu A, Staker BL, Burgin AB, Stewart L, Pommier Y. A novel norindenoisoquinoline structure reveals a common interfacial inhibitor paradigm for ternary trapping of the topoisomerase I-DNA covalent complex. Mol Cancer Ther. 2006 Feb;5(2):287-95. doi: 10.1158/1535-7163.MCT-05-0456. PMID: 16505102; PMCID: PMC2860177.

Marin-Acevedo JA, Chirila RM, Dronca RS. Immune Checkpoint Inhibitor Toxicities. Mayo Clin Proc. 2019 Jul;94(7):1321-1329. doi: 10.1016/j.mayocp.2019.03.012. PMID: 31272574.

Masuda K, Banno K, Yanokura M, Tsuji K, Kobayashi Y, Kisu I, Ueki A, Yamagami W, Nomura H, Tominaga E, Susumu N, Aoki D. Association of epigenetic inactivation of the WRN gene with anticancer drug sensitivity in cervical cancer cells. Oncol Rep. 2012 Oct;28(4):1146-52. doi: 10.3892/or.2012.1912. Epub 2012 Jul 13. PMID: 22797812; PMCID: PMC3583574.

Mateo J, Lord CJ, Serra V, Tutt A, Balmaña J, Castroviejo-Bermejo M, Cruz C, Oaknin A, Kaye SB, de Bono JS. A decade of clinical development of PARP inhibitors in perspective. Ann Oncol. 2019 Sep 1;30(9):1437-1447. doi: 10.1093/annonc/mdz192. PMID: 31218365; PMCID: PMC6771225.

Matt S, Hofmann TG. The DNA damage-induced cell death response: a roadmap to kill cancer cells. Cell Mol Life Sci. 2016 Aug;73(15):2829-50. doi: 10.1007/s00018-016-2130-4. Epub 2016 Jan 20. PMID: 26791483.

May E, Jenkins JR, May P. Endogenous HeLa p53 proteins are easily detected in HeLa cells transfected with mouse deletion mutant p53 gene. Oncogene. 1991 Aug;6(8):1363-5. PMID: 1886712.

McClendon AK, Rodriguez AC, Osheroff N. Human topoisomerase IIalpha rapidly relaxes positively supercoiled DNA: implications for enzyme action ahead of replication forks. J Biol Chem. 2005 Nov 25;280(47):39337-45. doi: 10.1074/jbc.M503320200. Epub 2005 Sep 27. PMID: 16188892.

McKinnon PJ. Topoisomerases and the regulation of neural function. Nat Rev Neurosci. 2016 Nov;17(11):673-679. doi: 10.1038/nrn.2016.101. Epub 2016 Sep 15. PMID: 27630045; PMCID: PMC5209242.

Meng L, Deng B, Liu B, Majeed U, Wang W. A Rare Case of Irinotecan-induced Interstitial Pulmonary Disease and Diffuse Alveolar Hemorrhage in a Patient with Pancreatic Cancer. Cureus. 2019 Jun 29;11(6):e5041. doi: 10.7759/cureus.5041. PMID: 31501733; PMCID: PMC6721880.

Mirski SE, Gerlach JH, Cole SP. Multidrug resistance in a human small cell lung cancer cell line selected in adriamycin. Cancer Res. 1987 May 15;47(10):2594-8. PMID: 2436751.

Mirzaei S, Hushmandi K, Zabolian A, Saleki H, Torabi SMR, Ranjbar A, SeyedSaleh S, Sharifzadeh SO, Khan H, Ashrafizadeh M, Zarrabi A, Ahn KS. Elucidating Role of Reactive Oxygen Species (ROS) in Cisplatin Chemotherapy: A Focus on Molecular Pathways and Possible Therapeutic Strategies. Molecules. 2021 Apr 19;26(8):2382. doi: 10.3390/molecules26082382. PMID: 33921908; PMCID: PMC8073650.

Molinaro C, Martoriati A, Pelinski L, Cailliau K. Copper Complexes as Anticancer Agents Targeting Topoisomerases I and II. Cancers (Basel). 2020 Oct 5;12(10):2863. doi: 10.3390/cancers12102863. PMID: 33027952; PMCID: PMC7601307.

Molinaro C, Martoriati A, Cailliau K. Proteins from the DNA Damage Response: Regulation, Dysfunction, and Anticancer Strategies. Cancers (Basel). 2021 Jul 29;13(15):3819. doi: 10.3390/cancers13153819. PMID: 34359720; PMCID: PMC8345162.

Morham SG, Kluckman KD, Voulomanos N, Smithies O. Targeted disruption of the mouse topoisomerase I gene by camptothecin selection. Mol Cell Biol. 1996 Dec;16(12):6804-9. doi: 10.1128/MCB.16.12.6804. PMID: 8943335; PMCID: PMC231683.

Morris WH, Ngo L, Wilson JT, Medawala W, Brown AR, Conner JD, Fabunmi F, Cashman DJ, Lisic EC, Yu T, Deweese JE, Jiang X. Structural and Metal Ion Effects on Human Topoisomerase IIα Inhibition by α-(N)-Heterocyclic Thiosemicarbazones. Chem Res Toxicol. 2019 Jan 22;32(1):90-99. doi: 10.1021/acs.chemrestox.8b00204. Epub 2018 Dec 11. PMID: 30484632.

Murai J, Zhang Y, Morris J, Ji J, Takeda S, Doroshow JH, Pommier Y. Rationale for poly(ADP-ribose) polymerase (PARP) inhibitors in combination therapy with camptothecins or temozolomide based on PARP trapping versus catalytic inhibition. J Pharmacol Exp Ther. 2014 Jun;349(3):408-16. doi: 10.1124/jpet.113.210146. Epub 2014 Mar 20. PMID: 24650937; PMCID: PMC4019318.

Murai J, Thomas A, Miettinen M, Pommier Y. Schlafen 11 (SLFN11), a restriction factor for replicative stress induced by DNA-targeting anti-cancer therapies. Pharmacol Ther. 2019 Sep;201:94-102. doi: 10.1016/j.pharmthera.2019.05.009. Epub 2019 May 23. PMID: 31128155; PMCID: PMC6708787.

Muzzio M, Hu SC, Holleran JL, Parise RA, Eiseman JL, Yellow-Duke AE, Covey JM, Glaze ER, Engelke K, Egorin MJ, McCormick DL, Beumer JH. Plasma pharmacokinetics of the indenoisoquinoline topoisomerase I inhibitor, NSC 743400, in rats and dogs. Cancer Chemother Pharmacol. 2015 May;75(5):1015-23. doi: 10.1007/s00280-015-2722-y. Epub 2015 Mar 17. PMID: 25776905; PMCID: PMC4420695.

N

Nagarajan M, Morrell A, Ioanoviciu A, Antony S, Kohlhagen G, Agama K, Hollingshead M, Pommier Y, Cushman M. Synthesis and evaluation of indenoisoquinoline topoisomerase I inhibitors substituted with nitrogen heterocycles. J Med Chem. 2006 Oct 19;49(21):6283-9. doi: 10.1021/jm060564z. PMID: 17034134; PMCID: PMC2526314.

Nair RS, Potti ME, Thankappan R, Chandrika SK, Kurup MR, Srinivas P. Molecular trail for the anticancer behavior of a novel copper carbohydrazone complex in BRCA1 mutated breast cancer. Mol Carcinog. 2017 May;56(5):1501-1514. doi: 10.1002/mc.22610. Epub 2017 Jan 18. PMID: 28052399.

Ngoi NY, Sundararajan V, Tan DS. Exploiting replicative stress in gynecological cancers as a therapeutic strategy. Int J Gynecol Cancer. 2020 Aug;30(8):1224-1238. doi: 10.1136/ijgc-2020-001277. Epub 2020 Jun 22. PMID: 32571890; PMCID: PMC7418601.

Nieuwkoop PD, Faber J. Normal table of Xenopus laevis (Daudin): A systematical and chronological survey of the development from the fertilized egg till the end of metamorphosis. 1994. New York: Garland Pub.

Nitiss JL. DNA topoisomerase II and its growing repertoire of biological functions. Nat Rev Cancer. 2009 May;9(5):327-37. doi: 10.1038/nrc2608. Epub 2009 Apr 20. PMID: 19377505; PMCID: PMC2730144. (a)

Nitiss JL. Targeting DNA topoisomerase II in cancer chemotherapy. Nat Rev Cancer. 2009 May;9(5):338-50. doi: 10.1038/nrc2607. Epub 2009 Apr 20. PMID: 19377506; PMCID: PMC2748742. (b)

Noach N, Segev Y, Levi I, Segal S, Priel E. Modification of topoisomerase I activity by glucose and by O-GlcNAcylation of the enzyme protein. Glycobiology. 2007 Dec;17(12):1357-64. doi: 10.1093/glycob/cwm105. Epub 2007 Oct 11. PMID: 17932134.

O

Oda K, Arakawa H, Tanaka T, Matsuda K, Tanikawa C, Mori T, Nishimori H, Tamai K, Tokino T, Nakamura Y, Taya Y. p53AIP1, a potential mediator of p53-dependent apoptosis, and its regulation by Ser-46-phosphorylated p53. Cell. 2000 Sep 15;102(6):849-62. doi: 10.1016/s0092-8674(00)00073-8. PMID: 11030628.

O'Leary MC, Lu X, Huang Y, Lin X, Mahmood I, Przepiorka D, Gavin D, Lee S, Liu K, George B, Bryan W, Theoret MR, Pazdur R. FDA Approval Summary: Tisagenlecleucel for Treatment of Patients with Relapsed or Refractory B-cell Precursor Acute Lymphoblastic Leukemia. Clin Cancer Res. 2019 Feb 15;25(4):1142-1146. doi: 10.1158/1078-0432.CCR-18-2035. Epub 2018 Oct 11. PMID: 30309857.

Ott PA, Hodi FS. Talimogene Laherparepvec for the Treatment of Advanced Melanoma. Clin Cancer Res. 2016 Jul 1;22(13):3127-31. doi: 10.1158/1078-0432.CCR-15-2709. Epub 2016 May 4. PMID: 27146699.

Owonikoko TK, Dahlberg SE, Khan SA, Gerber DE, Dowell J, Moss RA, Belani CP, Hann CL, Aggarwal C, Ramalingam SS. A phase 1 safety study of veliparib combined with cisplatin and etoposide in extensive stage small cell lung cancer: A trial of the ECOG-ACRIN Cancer Research Group (E2511). Lung Cancer. 2015 Jul;89(1):66-70. doi: 10.1016/j.lungcan.2015.04.015. Epub 2015 May 8. PMID: 25985977; PMCID: PMC4539011.

P

Paik J. Nivolumab Plus Relatlimab: First Approval. Drugs. 2022 Jun;82(8):925-931. doi: 10.1007/s40265-022-01723-1. PMID: 35543970.

Palanimuthu D, Shinde SV, Somasundaram K, Samuelson AG. In vitro and in vivo anticancer activity of copper bis(thiosemicarbazone) complexes. J Med Chem. 2013 Feb 14;56(3):722-34. doi: 10.1021/jm300938r. Epub 2013 Jan 30. PMID: 23320568.

Pearl LH, Schierz AC, Ward SE, Al-Lazikani B, Pearl FM. Therapeutic opportunities within the DNA damage response. Nat Rev Cancer. 2015 Mar;15(3):166-80. doi: 10.1038/nrc3891. PMID: 25709118.

Peng XX, Tiwari AK, Wu HC, Chen ZS. Overexpression of P-glycoprotein induces acquired resistance to imatinib in chronic myelogenous leukemia cells. Chin J Cancer. 2012 Feb;31(2):110-8. doi: 10.5732/cjc.011.10327. Epub 2011 Nov 18. PMID: 22098951; PMCID: PMC3777469.

Phipps AI, Malone KE, Porter PL, Daling JR, Li CI. Reproductive and hormonal risk factors for postmenopausal luminal, HER-2-overexpressing, and triple-negative breast cancer. Cancer. 2008 Oct 1;113(7):1521-6. doi: 10.1002/cncr.23786. PMID: 18726992; PMCID: PMC2587413.

Pollak Y, Yirmiya R. Cytokine-induced changes in mood and behaviour: implications for 'depression due to a general medical condition', immunotherapy and antidepressive treatment. Int J Neuropsychopharmacol. 2002 Dec;5(4):389-99. doi: 10.1017/S1461145702003152. PMID: 12466037.

Pommier Y. Topoisomerase I inhibitors: camptothecins and beyond. Nat Rev Cancer. 2006 Oct;6(10):789-802. doi: 10.1038/nrc1977. PMID: 16990856.

Pommier Y. DNA topoisomerase I inhibitors: chemistry, biology, and interfacial inhibition. Chem Rev. 2009 Jul;109(7):2894-902. doi: 10.1021/cr900097c. PMID: 19476377; PMCID: PMC2707511.

Pommier Y. Drugging topoisomerases: lessons and challenges. ACS Chem Biol. 2013 Jan 18;8(1):82-95. doi: 10.1021/cb300648v. Epub 2013 Jan 4. PMID: 23259582; PMCID: PMC3549721.

Pommier Y, Cushman M. The indenoisoquinoline noncamptothecin topoisomerase I inhibitors: update and perspectives. Mol Cancer Ther. 2009 May;8(5):1008-14. doi: 10.1158/1535-7163.MCT-08-0706. Epub 2009 Apr 21. PMID: 19383846; PMCID: PMC2888777.

Pommier Y, Cushman M, Doroshow JH. Novel clinical indenoisoquinoline topoisomerase I inhibitors: a twist around the camptothecins. Oncotarget. 2018 Dec 18;9(99):37286-37288. doi: 10.18632/oncotarget.26466. PMID: 30647868; PMCID: PMC6324668.

Pommier Y, Huang SY, Gao R, Das BB, Murai J, Marchand C. Tyrosyl-DNA-phosphodiesterases (TDP1 and TDP2). DNA Repair (Amst). 2014 Jul;19:114-29. doi: 10.1016/j.dnarep.2014.03.020. Epub 2014 May 22. PMID: 24856239; PMCID: PMC4090310.

Pommier Y, Kiselev E, Marchand C. Interfacial inhibitors. Bioorg Med Chem Lett. 2015 Sep 15;25(18):3961-5. doi: 10.1016/j.bmcl.2015.07.032. Epub 2015 Jul 18. PMID: 26235949; PMCID: PMC7747010.

Pommier Y, Leo E, Zhang H, Marchand C. DNA topoisomerases and their poisoning by anticancer and antibacterial drugs. Chem Biol. 2010 May 28;17(5):421-33. doi: 10.1016/j.chembiol.2010.04.012. PMID: 20534341; PMCID: PMC7316379.

Pommier Y, Nussenzweig A, Takeda S, Austin C. Human topoisomerases and their roles in genome stability and organization. Nat Rev Mol Cell Biol. 2022 Jun;23(6):407-427. doi: 10.1038/s41580-022-00452-3. Epub 2022 Feb 28. PMID: 35228717; PMCID: PMC8883456.

Pommier Y, Sun Y, Huang SN, Nitiss JL. Roles of eukaryotic topoisomerases in transcription, replication and genomic stability. Nat Rev Mol Cell Biol. 2016 Nov;17(11):703-721. doi: 10.1038/nrm.2016.111. Epub 2016 Sep 21. PMID: 27649880; PMCID: PMC9248348.

Potti A, Dressman HK, Bild A, Riedel RF, Chan G, Sayer R, Cragun J, Cottrill H, Kelley MJ, Petersen R, Harpole D, Marks J, Berchuck A, Ginsburg GS, Febbo P, Lancaster J, Nevins JR. Genomic signatures to guide the use of chemotherapeutics. Nat Med. 2006 Nov;12(11):1294-300. doi: 10.1038/nm1491. Epub 2006 Oct 22. Retraction in: Potti A, Dressman HK, Bild A, Riedel RF, Chan G, Sayer R, Cragun J, Cottrill H, Kelley MJ, Petersen R, Harpole D, Marks J, Berchuck A, Ginsburg GS, Febbo P, Lancaster J, Nevins JR. Nat Med. 2011 Jan;17(1):135. Erratum in: Nat Med. 2007 Nov;13(11):1388. Erratum in: Nat Med. 2008 Aug;14(8):889. PMID: 17057710.

Pottier C, Fresnais M, Gilon M, Jérusalem G, Longuespée R, Sounni NE. Tyrosine Kinase Inhibitors in Cancer: Breakthrough and Challenges of Targeted Therapy. Cancers (Basel). 2020 Mar 20;12(3):731. doi: 10.3390/cancers12030731. PMID: 32244867; PMCID: PMC7140093.

Pronzato P, Rondini M. Hormonotherapy of advanced prostate cancer. Ann Oncol. 2005 May;16 Suppl 4:iv80-84. doi: 10.1093/annonc/mdi913. PMID: 15923436.

R

Rao VA, Agama K, Holbeck S, Pommier Y. Batracylin (NSC 320846), a dual inhibitor of DNA topoisomerases I and II induces histone gamma-H2AX as a biomarker of DNA damage. Cancer Res. 2007 Oct 15;67(20):9971-9. doi: 10.1158/0008-5472.CAN-07-0804. PMID: 17942930.

Redinbo MR, Stewart L, Kuhn P, Champoux JJ, Hol WG. Crystal structures of human topoisomerase I in covalent and noncovalent complexes with DNA. Science. 1998 Mar 6;279(5356):1504-13. doi: 10.1126/science.279.5356.1504. PMID: 9488644.

Reyes J, Chen JY, Stewart-Ornstein J, Karhohs KW, Mock CS, Lahav G. Fluctuations in p53 Signaling Allow Escape from Cell-Cycle Arrest. Mol Cell. 2018 Aug 16;71(4):581-591.e5. doi: 10.1016/j.molcel.2018.06.031. Epub 2018 Jul 26. Erratum in: Mol Cell. 2019 Mar 21;73(6):1306. PMID: 30057196; PMCID: PMC6282757.

Rialdi A, Campisi L, Zhao N, Lagda AC, Pietzsch C, Ho JSY, Martinez-Gil L, Fenouil R, Chen X, Edwards M, Metreveli G, Jordan S, Peralta Z, Munoz-Fontela C, Bouvier N, Merad M, Jin J, Weirauch M, Heinz S, Benner C, van Bakel H, Basler C, García-Sastre A, Bukreyev A, Marazzi I. Topoisomerase 1 inhibition suppresses inflammatory genes and protects from death by inflammation. Science. 2016 May 27;352(6289):aad7993. doi: 10.1126/science.aad7993. Epub 2016 Apr 28. PMID: 27127234; PMCID: PMC5193222.

Ribeiro RA, Wanderley CW, Wong DV, Mota JM, Leite CA, Souza MH, Cunha FQ, Lima-Júnior RC. Irinotecan- and 5-fluorouracil-induced intestinal mucositis: insights into pathogenesis and therapeutic perspectives. Cancer Chemother Pharmacol. 2016 Nov;78(5):881-893. doi: 10.1007/s00280-016-3139-y. Epub 2016 Sep 2. PMID: 27590709.

Ricci F, Tedeschi A, Morra E, Montillo M. Fludarabine in the treatment of chronic lymphocytic leukemia: a review. Ther Clin Risk Manag. 2009 Feb;5(1):187-207. doi: 10.2147/tcrm.s3688. Epub 2009 Mar 26. PMID: 19436622; PMCID: PMC2697528.

Rosenberg B, VanCamp L, Trosko JE, Mansour VH. Platinum compounds: a new class of potent antitumour agents. Nature. 1969 Apr 26;222(5191):385-6. doi: 10.1038/222385a0. PMID: 5782119.

Rossari F, Minutolo F, Orciuolo E. Past, present, and future of Bcr-Abl inhibitors: from chemical development to clinical efficacy. J Hematol Oncol. 2018 Jun 20;11(1):84. doi: 10.1186/s13045-018-0624-2. PMID: 29925402; PMCID: PMC6011351.

S

Sandhaus S, Taylor R, Edwards T, Huddleston A, Wooten Y, Venkatraman R, Weber RT, González-Sarrías A, Martin PM, Cagle P, Tse-Dinh YC, Beebe SJ, Seeram N, Holder AA. A novel copper(II) complex identified as a potent drug against colorectal and breast cancer cells and as a poison inhibitor for human topoisomerase IIα. Inorg Chem Commun. 2016 Feb;64:45-49. doi: 10.1016/j.inoche.2015.12.013. PMID: 26752972; PMCID: PMC4704796.

Sanna V, Pala N, Sechi M. Targeted therapy using nanotechnology: focus on cancer. Int J Nanomedicine. 2014 Jan 15;9:467-83. doi: 10.2147/IJN.S36654. PMID: 24531078; PMCID: PMC3896284.

Schally AV, Comaru-Schally AM. Mode of Action of LHRH Analogs. In: Kufe DW, Pollock RE, Weichselbaum RR, et al., editors. Holland-Frei Cancer Medicine. 6th edition. Hamilton (ON): BC Decker; 2003. Available from: https://www.ncbi.nlm.nih.gov/books/NBK12517/

Schlam-Babayov S, Bensimon A, Harel M, Geiger T, Aebersold R, Ziv Y, Shiloh Y. Phosphoproteomics reveals novel modes of function and inter-relationships among PIKKs in response to genotoxic stress. EMBO J. 2021 Jan 15;40(2):e104400. doi: 10.15252/embj.2020104400. Epub 2020 Nov 20. PMID: 33215756; PMCID: PMC7809795.

Seidel JA, Otsuka A, Kabashima K. Anti-PD-1 and Anti-CTLA-4 Therapies in Cancer: Mechanisms of Action, Efficacy, and Limitations. Front Oncol. 2018 Mar 28;8:86. doi: 10.3389/fonc.2018.00086. PMID: 29644214; PMCID: PMC5883082.

Seng HL, Wang WS, Kong SM, Alan Ong HK, Win YF, Raja Abd Rahman RN, Chikira M, Leong WK, Ahmad M, Khoo AS, Ng CH. Biological and cytoselective anticancer properties of copper(II)-polypyridyl complexes modulated by auxiliary methylated glycine ligand. Biometals. 2012 Oct;25(5):1061-81. doi: 10.1007/s10534-012-9572-4. Epub 2012 Jul 27. PMID: 22836829.

Seo YH. Dual Inhibitors Against Topoisomerases and Histone Deacetylases. J Cancer Prev. 2015 Jun;20(2):85-91. doi: 10.15430/JCP.2015.20.2.85. PMID: 26151040; PMCID: PMC4492363.

Sherman DJ, Li J. Proteasome Inhibitors: Harnessing Proteostasis to Combat Disease. Molecules. 2020 Feb 5;25(3):671. doi: 10.3390/molecules25030671. PMID: 32033280; PMCID: PMC7037493.

Shim M, Bang WJ, Oh CY, Lee YS, Cho JS. Effectiveness of three different luteinizing hormone-releasing hormone agonists in the chemical castration of patients with prostate cancer: Goserelin versus triptorelin versus leuprolide. Investig Clin Urol. 2019 Jul;60(4):244-250. doi: 10.4111/icu.2019.60.4.244. Epub 2019 May 21. PMID: 31294133; PMCID: PMC6607074.

Shin W, Han J, Kumar R, Lee GG, Sessler JL, Kim JH and Kim JS. Programmed activation of cancer cell apoptosis: A tumor-targeted phototherapeutic topoisomerase I inhibitor. Sci Rep. 2016 July 4;6, 29018. doi: 10.1038/srep29018.

Shiozawa T, Tadokoro J, Fujiki T, Fujino K, Kakihata K, Masatani S, Morita S, Gemma A, Boku N. Risk factors for severe adverse effects and treatment-related deaths in Japanese patients treated with irinotecan-based chemotherapy: a postmarketing survey. Jpn J Clin Oncol. 2013 May;43(5):483-91. doi: 10.1093/jjco/hyt040. Epub 2013 Mar 27. PMID: 23536639; PMCID: PMC3638635.

Shobha Devi C, Thulasiram B, Aerva RR, Nagababu P. Recent Advances in Copper Intercalators as Anticancer Agents. J Fluoresc. 2018 Sep;28(5):1195-1205. doi: 10.1007/s10895-018-2283-7. Epub 2018 Aug 31. PMID: 30171479.

Schor NF. Neuroblastoma; Current Pharmacotherapy for Neuroblastoma. Academic Press. P. 203–211. doi:10.1016/B978-0-12-812005-7.00012-6.

Sigismund S, Avanzato D, Lanzetti L. Emerging functions of the EGFR in cancer. Mol Oncol. 2018 Jan;12(1):3-20. doi: 10.1002/1878-0261.12155. Epub 2017 Nov 27. PMID: 29124875; PMCID: PMC5748484.

Simon HU, Haj-Yehia A, Levi-Schaffer F. Role of reactive oxygen species (ROS) in apoptosis induction. Apoptosis. 2000 Nov;5(5):415-8. doi: 10.1023/a:1009616228304. PMID: 11256882.

Sissi C, Palumbo M. Effects of magnesium and related divalent metal ions in topoisomerase structure and function. Nucleic Acids Res. 2009 Feb;37(3):702-11. doi: 10.1093/nar/gkp024. Epub 2009 Feb 2. PMID: 19188255; PMCID: PMC2647314.

Slaby S, Lemière S, Hanotel J, Lescuyer A, Demuynck S, Bodart JF, Leprêtre A, Marin M. Cadmium but not lead exposure affects Xenopus laevis fertilization and embryo cleavage. Aquat Toxicol. 2016 Aug;177:1-7. doi: 10.1016/j.aquatox.2016.05.003. Epub 2016 May 9. PMID: 27218424.

Smith AG, Macleod KF. Autophagy, cancer stem cells and drug resistance. J Pathol. 2019 Apr;247(5):708-718. doi: 10.1002/path.5222. Epub 2019 Feb 4. PMID: 30570140; PMCID: PMC6668344.

Smith HO, Tiffany MF, Qualls CR, Key CR. The rising incidence of adenocarcinoma relative to squamous cell carcinoma of the uterine cervix in the United States--a 24-year population-based study. Gynecol Oncol. 2000 Aug;78(2):97-105. doi: 10.1006/gyno.2000.5826. PMID: 10926787.

Soares J, Raimundo L, Pereira NA, dos Santos DJ, Pérez M, Queiroz G, Leão M, Santos MM, Saraiva L. A tryptophanol-derived oxazolopiperidone lactam is cytotoxic against tumors via inhibition of p53 interaction with murine double minute proteins. Pharmacol Res. 2015 May-Jun;95-96:42-52. doi: 10.1016/j.phrs.2015.03.006. Epub 2015 Mar 23. PMID: 25814188.

Sodani K, Patel A, Kathawala RJ, Chen ZS. Multidrug resistance associated proteins in multidrug resistance. Chin J Cancer. 2012 Feb;31(2):58-72. doi: 10.5732/cjc.011.10329. Epub 2011 Nov 18. PMID: 22098952; PMCID: PMC3777468.

Sritharan S, Sivalingam N. A comprehensive review on time-tested anticancer drug doxorubicin. Life Sci. 2021 Aug 1;278:119527. doi: 10.1016/j.lfs.2021.119527. Epub 2021 Apr 20. PMID: 33887349.

Stewart L, Redinbo MR, Qiu X, Hol WG, Champoux JJ. A model for the mechanism of human topoisomerase I. Science. 1998 Mar 6;279(5356):1534-41. doi: 10.1126/science.279.5356.1534. PMID: 9488652.

Stoll G, Pietiläinen OPH, Linder B, Suvisaari J, Brosi C, Hennah W, Leppä V, Torniainen M, Ripatti S, Ala-Mello S, Plöttner O, Rehnström K, Tuulio-Henriksson A, Varilo T, Tallila J, Kristiansson K, Isohanni M, Kaprio J, Eriksson JG, Raitakari OT, Lehtimäki T, Jarvelin MR, Salomaa V, Hurles M, Stefansson H, Peltonen L, Sullivan PF, Paunio T, Lönnqvist J, Daly MJ, Fischer U, Freimer NB, Palotie A. Deletion of TOP3β, a component of FMRP-containing mRNPs, contributes to neurodevelopmental disorders. Nat Neurosci. 2013 Sep;16(9):1228-1237. doi: 10.1038/nn.3484. Epub 2013 Aug 4. PMID: 23912948; PMCID: PMC3986889.

Suntharalingam M, Winter K, Ilson D, Dicker AP, Kachnic L, Konski A, Chakravarthy AB, Anker CJ, Thakrar H, Horiba N, Dubey A, Greenberger JS, Raben A, Giguere J, Roof K, Videtic G, Pollock J, Safran H, Crane CH. Effect of the Addition of Cetuximab to Paclitaxel, Cisplatin, and Radiation Therapy for Patients With Esophageal Cancer: The NRG Oncology RTOG 0436 Phase 3 Randomized Clinical Trial. JAMA Oncol. 2017 Nov 1;3(11):1520-1528. doi: 10.1001/jamaoncol.2017.1598. Erratum in: JAMA Oncol. 2017 Nov 1;3(11):1589. PMID: 28687830; PMCID: PMC5710193.

Surova O, Zhivotovsky B. Various modes of cell death induced by DNA damage. Oncogene. 2013 Aug 15;32(33):3789-97. doi: 10.1038/onc.2012.556. Epub 2012 Dec 3. PMID: 23208502.

Syed YY. Sacituzumab Govitecan: First Approval. Drugs. 2020 Jul;80(10):1019-1025. doi: 10.1007/s40265-020-01337-5. PMID: 32529410; PMCID: PMC7288263.

T

Tabassum S, Zaki M, Arjmand F, Ahmad I. Synthesis of heterobimetallic complexes: in vitro DNA binding, cleavage and antimicrobial studies. J Photochem Photobiol B. 2012 Sep 3;114:108-18. doi: 10.1016/j.jphotobiol.2012.05.017. Epub 2012 Jun 13. PMID: 22762922.

Tabassum S, Al-Asbahy WM, Afzal M, Arjmand F, Bagchi V. Molecular drug design, synthesis and structure elucidation of a new specific target peptide based metallo drug for cancer chemotherapy as topoisomerase I inhibitor. Dalton Trans. 2012 Apr 28;41(16):4955-64. doi: 10.1039/c2dt12044e. Epub 2012 Mar 9. PMID: 22407358.

Tabassum S, Ahmad A, Khan RA, Hussain Z, Srivastav S, Srikrishna S, Arjmand F. Chiral heterobimetallic complexes targeting human DNA-topoisomerase Iα. Dalton Trans. 2013 Aug 30;42, 16749–16761. doi: 10.1039/C3DT51209F.

Tabassum S, Asim A, Khan RA, Arjmand F, Rajakumar D, Balaji P, Akbarsha AM. A multifunctional molecular entity CuII–SnIV heterobimetallic complex as a potential cancer chemotherapeutic agent: DNA binding/cleavage, SOD mimetic, topoisomerase Ia inhibitory and in vitrocytotoxic activities. RSC Adv. 2015 May 5; 5, 47439–47450. doi: 10.1039/C5RA07333B.

Tagliamento M, Genova C, Rijavec E, Rossi G, Biello F, Dal Bello MG, Alama A, Coco S, Boccardo S, Grossi F. Afatinib and Erlotinib in the treatment of squamous-cell lung cancer. Expert Opin Pharmacother. 2018 Dec;19(18):2055-2062. doi: 10.1080/14656566.2018.1540591. Epub 2018 Nov 3. Erratum in: Expert Opin Pharmacother. 2018 Dec;19(18):9. PMID: 30392436.

Tahara M, Inoue T, Sato F, Miyakura Y, Horie H, Yasuda Y, Fujii H, Kotake K, Sugano K. The use of Olaparib (AZD2281) potentiates SN-38 cytotoxicity in colon cancer cells by indirect inhibition of Rad51-mediated repair of DNA double-strand breaks. Mol Cancer Ther. 2014 May;13(5):1170-80. doi: 10.1158/1535-7163.MCT-13-0683. Epub 2014 Feb 27. PMID: 24577941.

Takaoka E., Kawai K., Ando S., Shimazui T., Akaza H., Neutropenic Colitis during Standard Dose Combination Chemotherapy with Nedaplatin and Irinotecan for Testicular Cancer. Japanese Journal of Clinical Oncology. Volume 36, Issue 1, January 2006, Pages 60–63. doi: 10.1093/jjco/hyi219.

Tamura N, Hirano K, Kishino K, Hashimoto K, Amano O, Shimada J, Sakagami H. Analysis of type of cell death induced by topoisomerase inhibitor SN-38 in human oral squamous cell carcinoma cell lines. Anticancer Res. 2012 Nov;32(11):4823-32. PMID: 23155248.

Tessema M, Yingling CM, Thomas CL, Klinge DM, Bernauer AM, Liu Y, Dacic S, Siegfried JM, Dahlberg SE, Schiller JH, Belinsky SA. SULF2 methylation is prognostic for lung cancer survival and increases sensitivity to topoisomerase-I inhibitors via induction of ISG15. Oncogene. 2012 Sep 13;31(37):4107-16. doi: 10.1038/onc.2011.577. Epub 2011 Dec 12. PMID: 22158045; PMCID: PMC3307938.

Testerman TL, Gerster JF, Imbertson LM, Reiter MJ, Miller RL, Gibson SJ, Wagner TL, Tomai MA. Cytokine induction by the immunomodulators imiquimod and S-27609. J Leukoc Biol. 1995 Sep;58(3):365-72. doi: 10.1002/jlb.58.3.365. PMID: 7665993.

Thomas A, Redon CE, Sciuto L, Padiernos E, Ji J, Lee MJ, Yuno A, Lee S, Zhang Y, Tran L, Yutzy W, Rajan A, Guha U, Chen H, Hassan R, Alewine CC, Szabo E, Bates SE, Kinders RJ, Steinberg SM, Doroshow JH, Aladjem MI, Trepel JB, Pommier Y. Phase I Study of ATR Inhibitor M6620 in Combination With Topotecan in Patients With Advanced Solid Tumors. J Clin Oncol. 2018 Jun 1;36(16):1594-1602. doi: 10.1200/JCO.2017.76.6915. Epub 2017 Dec 18. PMID: 29252124; PMCID: PMC5978471.

Thomas A, Pommier Y. Targeting Topoisomerase I in the Era of Precision Medicine. Clin Cancer Res. 2019 Nov 15;25(22):6581-6589. doi: 10.1158/1078-0432.CCR-19-1089. Epub 2019 Jun 21. PMID: 31227499; PMCID: PMC6858945.

Tiwari AK, Sodani K, Dai CL, Ashby CR Jr, Chen ZS. Revisiting the ABCs of multidrug resistance in cancer chemotherapy. Curr Pharm Biotechnol. 2011 Apr;12(4):570-94. doi: 10.2174/138920111795164048. PMID: 21118094.

Tsimberidou AM. Targeted therapy in cancer. Cancer Chemother Pharmacol. 2015 Dec;76(6):1113-32. doi: 10.1007/s00280-015-2861-1. Epub 2015 Sep 21. PMID: 26391154; PMCID: PMC4998041.

Tucci M, Leone G, Buttigliero C, Zichi C, DI Stefano RF, Pignataro D, Vignani F, Scagliotti GV, DI Maio M. Hormonal treatment and quality of life of prostate cancer patients: new evidence. Minerva Urol Nefrol. 2018 Apr;70(2):144-151. doi: 10.23736/S0393-2249.17.03066-1. Epub 2017 Dec 14. PMID: 29241313.

U

Urso E, Maffia M. Behind the Link between Copper and Angiogenesis: Established Mechanisms and an Overview on the Role of Vascular Copper Transport Systems. J Vasc Res. 2015;52(3):172-96. doi: 10.1159/000438485. Epub 2015 Oct 21. PMID: 26484858.

V

Valenzuela MM, Neidigh JW, Wall NR. Antimetabolite Treatment for Pancreatic Cancer. Chemotherapy (Los Angel). 2014 Dec;3(3):137. doi: 10.4172/2167-7700.1000137. PMID: 26161298; PMCID: PMC4494102.

Vizcaino AP, Moreno V, Bosch FX, Muñoz N, Barros-Dios XM, Borras J, Parkin DM. International trends in incidence of cervical cancer: II. Squamous-cell carcinoma. Int J Cancer. 2000 May 1;86(3):429-35. doi: 10.1002/(sici)1097-0215(20000501)86:3<429::aid-ijc20>3.0.co;2-d. PMID: 10760834.

Vrielynck N, Chambon A, Vezon D, Pereira L, Chelysheva L, De Muyt A, Mézard C, Mayer C, Grelon M. A DNA topoisomerase VI-like complex initiates meiotic recombination. Science. 2016 Feb 26;351(6276):939-43. doi: 10.1126/science.aad5196. PMID: 26917763.

Vutey V, Castelli S, D'Annessa I, Sâmia LB, Souza-Fagundes EM, Beraldo H, Desideri A. Human topoisomerase IB is a target of a thiosemicarbazone copper(II) complex. Arch Biochem Biophys. 2016 Sep 15;606:34-40. doi: 10.1016/j.abb.2016.07.009. Epub 2016 Jul 16. PMID: 27431056.

W

Wagner JM, Karnitz LM. Cisplatin-induced DNA damage activates replication checkpoint signaling components that differentially affect tumor cell survival. Mol Pharmacol. 2009 Jul;76(1):208-14. doi: 10.1124/mol.109.055178. Epub 2009 Apr 29. PMID: 19403702; PMCID: PMC2701464.

Waks AG, Winer EP. Breast Cancer Treatment: A Review. JAMA. 2019 Jan 22;321(3):288-300. doi: 10.1001/jama.2018.19323. PMID: 30667505.

Waldman AD, Fritz JM, Lenardo MJ. A guide to cancer immunotherapy: from T cell basic science to clinical practice. Nat Rev Immunol. 2020 Nov;20(11):651-668. doi: 10.1038/s41577-020-0306-5. Epub 2020 May 20. PMID: 32433532; PMCID: PMC7238960.

Wall ME, Wani MC, Cook CE, Palmer KH, McPhail AT and Sim GA. Journal of the American Chemical Society. 1966 Aug 1;88(16), 3888-3890. doi: 10.1021/ja00968a057.

Wambang N. Nouveaux Complexes Organométalliques d'Indéno[1,2- c]isoquinoléines Anticancéreux : Synthèse, Caractérisation et Evaluation Biologique en tant que Ligands de l'ADN et Inhibiteurs de Topoisomérase. Thèse de Doctorat en chimie, sous la direction de Lydie Pelinski et Peter Teke, Université de Yaoundé I, 2016, 219 p.

Wambang N, Schifano-Faux N, Martoriati A, Henry N, Baldeyrou B, Bal-Mahieu C, Bousquet T, Pellegrini S, Meignan S, Cailliau K, Goossens JF, Bodart JF, Ndifon PT, and Pélinski L. Synthesis, Structure, and Antiproliferative Activity of Ruthenium(II) Arene Complexes of Indenoisoquinoline Derivatives. Organometallics. 2016 Aug 19, 35(17): 2868–2872. doi: 10.1021/acs.organomet.6b00440.

Wang L, Xie L, Wang J, Shen J, Liu B. Correlation between the methylation of SULF2 and WRN promoter and the irinotecan chemosensitivity in gastric cancer. BMC Gastroenterol. 2013 Dec 23;13:173. doi: 10.1186/1471-230X-13-173. PMID: 24359226; PMCID: PMC3877991.

Wang M, Yin B, Wang HY, Wang RF. Current advances in T-cell-based cancer immunotherapy. Immunotherapy. 2014;6(12):1265-78. doi: 10.2217/imt.14.86. PMID: 25524383; PMCID: PMC4372895.

Wang Z, Wang X, Wang Z, Feng Y, Jia Y, Jiang L, Xia Y, Cao J, Liu Y. Comparison of Hepatotoxicity Associated With New BCR-ABL Tyrosine Kinase Inhibitors vs Imatinib Among Patients With Chronic Myeloid Leukemia: A Systematic Review and Meta-analysis. JAMA Netw Open. 2021 Jul 1;4(7):e2120165. doi: 10.1001/jamanetworkopen.2021.20165. PMID: 34292334; PMCID: PMC8299317.

van Weelden WJ, Massuger LFAG; ENITEC, Pijnenborg JMA, Romano A. Anti-estrogen Treatment in Endometrial Cancer: A Systematic Review. Front Oncol. 2019 May 7;9:359. doi: 10.3389/fonc.2019.00359. PMID: 31134155; PMCID: PMC6513972.

Wei SC, Duffy CR, Allison JP. Fundamental Mechanisms of Immune Checkpoint Blockade Therapy. Cancer Discov. 2018 Sep;8(9):1069-1086. doi: 10.1158/2159-8290.CD-18-0367. Epub 2018 Aug 16. PMID: 30115704.

Wilson JT, Jiang X, McGill BC, Lisic EC, Deweese JE. Examination of the Impact of Copper(II) α-(N)-Heterocyclic Thiosemicarbazone Complexes on DNA Topoisomerase IIα. Chem Res Toxicol. 2016 Apr 18;29(4):649-58. doi: 10.1021/acs.chemrestox.5b00471. Epub 2016 Mar 23. PMID: 26982206.

Woessner RD, Mattern MR, Mirabelli CK, Johnson RK, Drake FH. Proliferation- and cell cycle-dependent differences in expression of the 170 kilodalton and 180 kilodalton forms of topoisomerase II in NIH-3T3 cells. Cell Growth Differ. 1991 Apr;2(4):209-14. PMID: 1651102.

Wu CC, Li YC, Wang YR, Li TK, Chan NL. On the structural basis and design guidelines for type II topoisomerase-targeting anticancer drugs. Nucleic Acids Res. 2013 Dec;41(22):10630-40. doi: 10.1093/nar/gkt828. Epub 2013 Sep 14. PMID: 24038465; PMCID: PMC3905874.

Wu YL, Tsuboi M, He J, John T, Grohe C, Majem M, Goldman JW, Laktionov K, Kim SW, Kato T, Vu HV, Lu S, Lee KY, Akewanlop C, Yu CJ, de Marinis F, Bonanno L, Domine M, Shepherd FA, Zeng L, Hodge R, Atasoy A, Rukazenkov Y, Herbst RS; ADAURA Investigators. Osimertinib in Resected EGFR-Mutated Non-Small-Cell Lung Cancer. N Engl J Med. 2020 Oct 29;383(18):1711-1723. doi: 10.1056/NEJMoa2027071. Epub 2020 Sep 19. PMID: 32955177.

X

Xu D, Shen W, Guo R, Xue Y, Peng W, Sima J, Yang J, Sharov A, Srikantan S, Yang J, Fox D 3rd, Qian Y, Martindale JL, Piao Y, Machamer J, Joshi SR, Mohanty S, Shaw AC, Lloyd TE, Brown GW, Ko MS, Gorospe M, Zou S, Wang W. Top3β is an RNA topoisomerase that works with fragile X syndrome protein to promote synapse formation. Nat Neurosci. 2013 Sep;16(9):1238-47. doi: 10.1038/nn.3479. Epub 2013 Aug 4. PMID: 23912945; PMCID: PMC3853347.

Y

Yang Y, Lu Y, Espejo A, Wu J, Xu W, Liang S, Bedford MT. TDRD3 is an effector molecule for arginine-methylated histone marks. Mol Cell. 2010 Dec 22;40(6):1016-23. doi: 10.1016/j.molcel.2010.11.024. PMID: 21172665; PMCID: PMC3090733.

Yang Y, McBride KM, Hensley S, Lu Y, Chedin F, Bedford MT. Arginine methylation facilitates the recruitment of TOP3B to chromatin to prevent R loop accumulation. Mol Cell. 2014 Feb 6;53(3):484-97. doi: 10.1016/j.molcel.2014.01.011. PMID: 24507716; PMCID: PMC3959860.

Yarden Y, Pines G. The ERBB network: at last, cancer therapy meets systems biology. Nat Rev Cancer. 2012 Jul 12;12(8):553-63. doi: 10.1038/nrc3309. PMID: 22785351.

You XH, Jiang YH, Fang Z, Sun F, Li Y, Wang W, Xia ZJ, Wang XZ, Ying HQ. Chemotherapy plus bevacizumab as an optimal first-line therapeutic treatment for patients with right-sided metastatic colon cancer: a meta-analysis of first-line clinical trials. ESMO Open. 2020 Mar;4(Suppl 2):e000605. doi: 10.1136/esmoopen-2019-000605. PMID: 32132090; PMCID: PMC7064070.

Yu D, Khan E, Khaleque MA, Lee J, Laco G, Kohlhagen G, Kharbanda S, Cheng YC, Pommier Y, Bharti A. Phosphorylation of DNA topoisomerase I by the c-Abl tyrosine kinase confers camptothecin sensitivity. J Biol Chem. 2004 Dec 10;279(50):51851-61. doi: 10.1074/jbc.M404396200. Epub 2004 Sep 24. PMID: 15448168.

Z

Zalckvar E, Berissi H, Eisenstein M, Kimchi A. Phosphorylation of Beclin 1 by DAP-kinase promotes autophagy by weakening its interactions with Bcl-2 and Bcl-XL. Autophagy. 2009 Jul;5(5):720-2. doi: 10.4161/auto.5.5.8625. Epub 2009 Jul 2. PMID: 19395874.

Zeglis BM, Divilov V, Lewis JS. Role of metalation in the topoisomerase IIα inhibition and antiproliferation activity of a series of α-heterocyclic-N4-substituted thiosemicarbazones and their Cu(II) complexes. J Med Chem. 2011 Apr 14;54(7):2391-8. doi: 10.1021/jm101532u. Epub 2011 Mar 10. PMID: 21391686; PMCID: PMC4151564.

Zeng L, Zou Q, Huang P, Xiong L, Cheng Y, Chen Q, Li Y, He H, Yi W, Wei W. Inhibition of autophagy with Chloroquine enhanced apoptosis induced by 5-aminolevulinic acid-photodynamic therapy in secondary hyperparathyroidism primary cells and organoids. Biomed Pharmacother. 2021 Oct;142:111994. doi: 10.1016/j.biopha.2021.111994. Epub 2021 Aug 16. PMID: 34411921.

Zhang L, Steele MB, Jenks N, Grell J, Behrens M, Nace R, Naik S, Federspiel MJ, Russell SJ, Peng KW. Robust Oncolytic Virotherapy Induces Tumor Lysis Syndrome and Associated Toxicities in the MPC-11 Plasmacytoma Model. Mol Ther. 2016 Dec;24(12):2109-2117. doi: 10.1038/mt.2016.167. Epub 2016 Sep 26. PMID: 27669655; PMCID: PMC5167781.

Zhang S, Liu X, Bawa-Khalfe T, Lu LS, Lyu YL, Liu LF, Yeh ET. Identification of the molecular basis of doxorubicin-induced cardiotoxicity. Nat Med. 2012 Nov;18(11):1639-42. doi: 10.1038/nm.2919. Epub 2012 Oct 28. PMID: 23104132.

Zhong L, Li Y, Xiong L, Wang W, Wu M, Yuan T, Yang W, Tian C, Miao Z, Wang T, Yang S. Small molecules in targeted cancer therapy: advances, challenges, and future perspectives. Signal Transduct Target Ther. 2021 May 31;6(1):201. doi: 10.1038/s41392-021-00572-w. PMID: 34054126; PMCID: PMC8165101.

Zhou X, Lin W, Tan FK, Assassi S, Fritzler MJ, Guo X, Sharif R, Xia T, Lai S, Arnett FC. Decreased catalytic function with altered sumoylation of DNA topoisomerase I in the nuclei of scleroderma fibroblasts. Arthritis Res Ther. 2011 Aug 9;13(4):R128. doi: 10.1186/ar3435. PMID: 21827649; PMCID: PMC3239368.

Zia MK, Siddiqui T, Ali SS, Rehman AA, Ahsan H, Khan FH. Chemotherapeutic Drugs and Plasma Proteins: Exploring New Dimensions. Curr Protein Pept Sci. 2018;19(10):937-947. doi: 10.2174/1389203718666171002115547. PMID: 28969563.

Appendices & Annexes

APPENDICES

Appendix 1. Number of new worldwide cancer cases for both sexes in 2020: Non-Hodgkin lymphoma (544,352), Leukemia (474,519), Kidney (431,288), Lip/oral cavity (377,713), Melanoma of skin (324,635), Ovary (313,959), Brain/Central nervous system (308,102), Larynx (184,615), Multiple myeloma (176,404), Nasopharynx (133,354), Gallbladder (115,949), Oropharynx (98,412), Hypopharynx (84,254), Hodgkin lymphoma (83,087), Testis (74,458), Salivary gland (53,583), Vulva (45,240), Penis (36,068), Kaposi sarcoma (34,270), Mesothelioma (30,870), Vagina (17,908).

Appendix 2. Raw data of cell cycle analysis by flow cytometry of MDA-MB-231, HeLa, and HT-29 after 24 h of treatments or not with cisplatin (20 µM), nocodazole (84 nM), WN170 and WN197 (0.5 µM). The first red peak represents the cell population in the G0/G1 phase, the second red peak the cell population in the G2/M phase, and the blue proportion the cell population in the S phase.

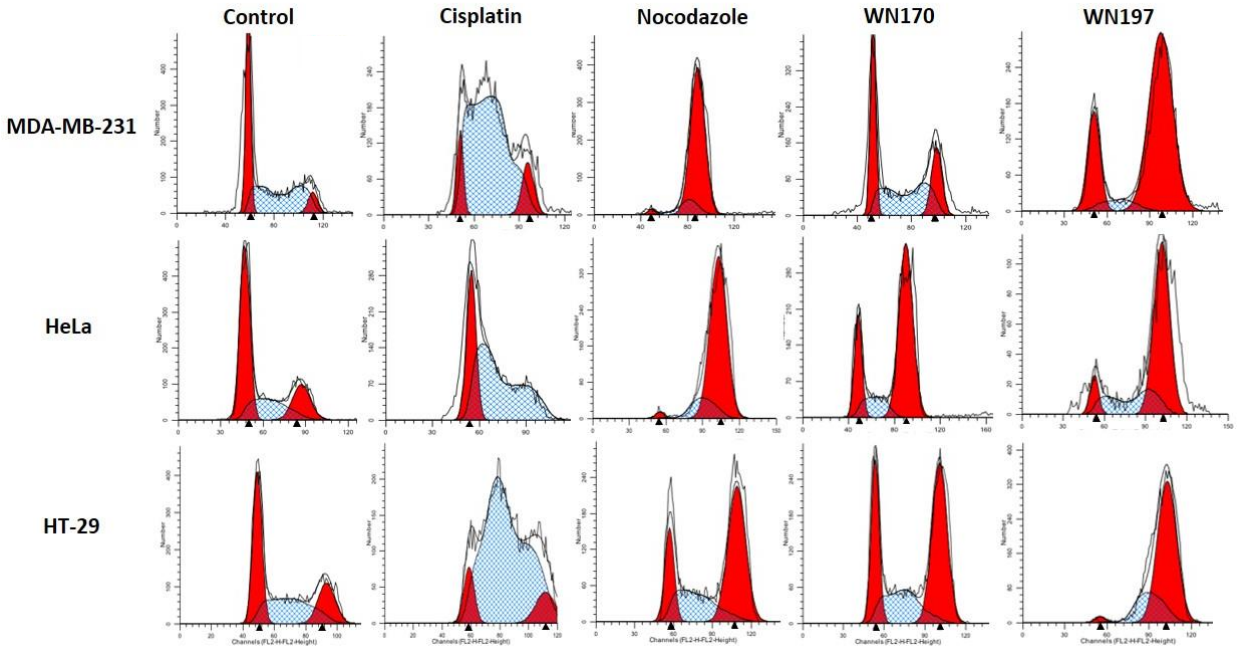

Appendix 3. Raw data of annexin V-Propidium iodide analysis by flow cytometry of MDA-MB-231, HeLa, and HT-29 after 24 h of treatments or not with WN170, WN197 (0.5 µM), camptothecin (20 µM, CPT), or doxorubicin (5 µM, Doxo).

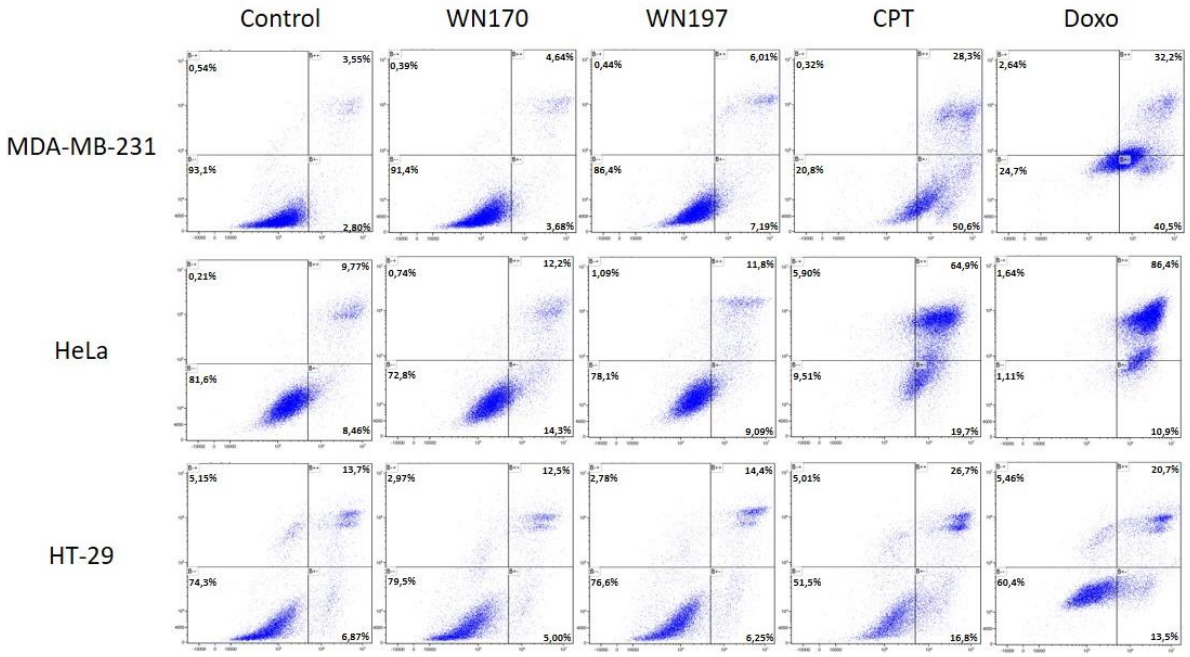

Appendix 4. Premilinary results obtained on colon cancerous (TraCo2) and non-cancerous (Col) organoids. Cells were treated for 72 h with 0,1% DMSO (control) or 1 µM of 197. *Collaboration with Stéphan Hardivillé (UGSF).*

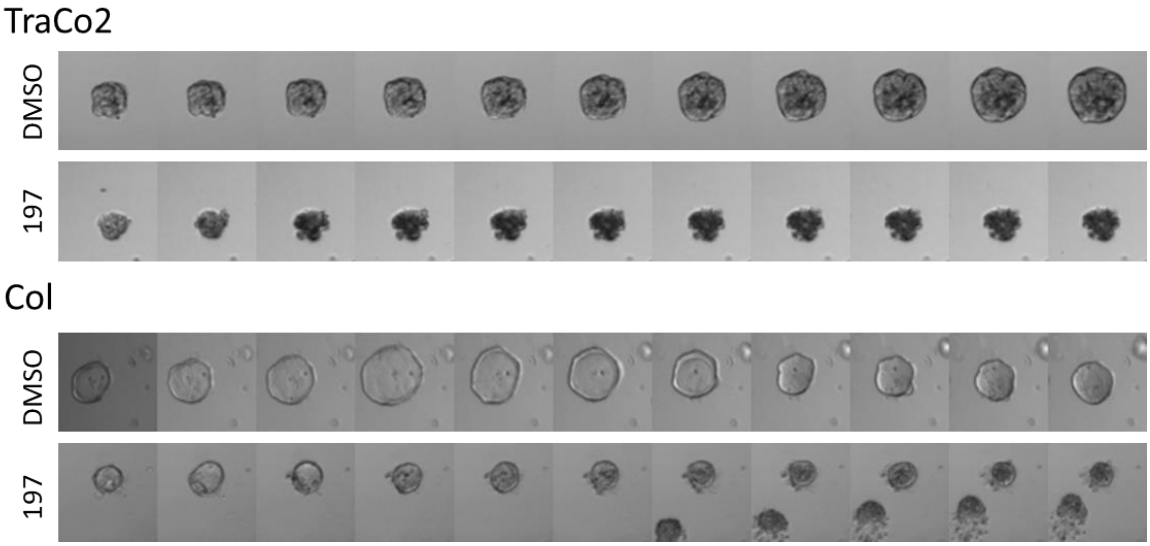

PUBLICATION LIST:

First author

1. **Molinaro C.**, Wambang N., Bousquet T., Vercoutter-Edouart AS., Pélinski L., Cailliau K., Martoriati A. A Novel Copper(II) Indenoisoquinoline Complex Inhibits Topoisomerase I, Induces G2 Phase Arrest, and Autophagy in Three Adenocarcinomas. *Front Oncol.* 2022 Feb 24;12:837373. doi: 10.3389/fonc.2022.837373. [SEE PAGE 127]
2. **Molinaro C.**, Martoriati A., Lescuyer A., Fliniaux I., Tulasne D., Cailliau K. 3-phosphoinositide-dependent protein kinase 1 (PDK1) mediates crosstalk between Src and Akt pathways in MET receptor signaling. *FEBS Lett.* 2021 Nov;595(21):2655-2664. doi: 10.1002/1873-3468.14195.
3. **Molinaro C.**, Martoriati A., Cailliau K. Proteins from the DNA Damage Response: Regulation, Dysfunction, and Anticancer Strategies. *Cancers* 2021, 13, 3819. doi: 10.3390/cancers13153819 [SEE PAGE 147]
4. **Molinaro C.,** Martoriati A., Pelinski L., Cailliau K. Copper-complexes as anticancer agents targeting topoisomerases I and II. *Cancers.* 2020 Oct 5;12(10):E2863. doi: 10.3390/cancers12102863 [SEE PAGE 187]

In progress: Molinaro C, Wambang C, Bousquet T, Cailliau K, Martoriati A and Pélinski L. Synthesis and biological activity of a new indenoisoquinoline copper derivative as a topoisomerase I inhibitor.

Collaboration

1. Fliniaux I, Marchand G, **Molinaro C**, Decloquement M, Martoriati A, Marin M, Bodart JF, Harduin-Lepers A, Maggio Cailliau K. Diversity of Sialic Acids and Sialoglycoproteins in Gametes and at Fertilization. *Front. Cell Dev. Biol.* 2022 doi: 10.3389/fcell.2022.982931
1. Marchand G., Wambang N., Pellegrini S., **Molinaro C.**, Martoriati A., Bousquet T., Markey A., Lescuyer-Rousseau A., Bodart JF., Cailliau K., Pelinski L., Marin M. Effects of Ferrocenyl 4-(Imino)-1,4-Dihydro-quinolines on Xenopus laevis Prophase I - Arrested Oocytes: Survival and Hormonal-Induced M-Phase Entry. *Int J Mol Sci.* 2020 Apr 26;21(9):3049. doi: 10.3390/ijms21093049.
2. Gelaude A., Slaby S., Cailliau K., Marin M., Lescuyer-Rousseau A., **Molinaro C.**, Nevoral J., Kučerová-Chrpová V., Sedmikova M., Petr J., Martoriati A., Bodart JF. Hydrogen Sulfide Impairs Meiosis Resumption in *Xenopus laevis* Oocytes. *Cells.* 2020 Jan 17;9(1):237. doi: 10.3390/cells9010237.

In progress: Martoriati A, **Molinaro C**, Marchand G, Fliniaux I, Marin M, Bodart JF, Lefevbre T, Dehennaut V, Cailliau K. Follicular cells protect Xenopus oocyte from abnormal maturation through adaptor Grb7 *O*-GlcNAcylation avoiding EGF receptor/integrin complex formation.

Communications

1. **Caroline Molinaro**, Nathalie Wambang, Till Bousquet, Anne-Sophie Vercoutter-Edouary, Lydie Pelinski, Katia Cailliau, Alain Martoriati. A Novel Copper(II) Indenoisoquinoline Complex Inhibits Topoisomerase I, Induces G2 Phase Arrest, and Autophagy in three Adenocarcinomas. *École de criblage ETC 2022*. **Poster and talk**.
2. **Caroline Molinaro**, Nathalie Wambang, Lydie Pélinski, Katia Cailliau and Alain Martoriati. A new organometallic compound inhibitor of topoisomerases: action on the cell cycle and cell death of adenocarcinomas. *Journée Andrée Verbert 2021*. **Talk**. **Jury's prize**.

3. **Caroline Molinaro**, Nathalie Wambang, Lydie Pélinski, Katia Cailliau and Alain Martoriati. Un nouveau composé organométallique inhibiteur de la croissance des adénocarcinomes : action sur le cycle cellulaire et sur l'activité des topoisomérases. *Séminaire UGSF 2021*. **Talk**.
4. **Caroline Molinaro**, Nathalie Wambang, Till Bousquet, Arlette Lescuyer, Katia Cailliau, Lydie Pelinski, Alain Martoriati. Un composé organométallique inhibiteur des topoisomérases : action sur le cycle et la mort cellulaire de lignées d'adénocarcinomes. *Cancéropôle Nord-Ouest 2020*. **Poster**.

Publication (research paper 1)

A Novel Copper(II) Indenoisoquinoline Complex Inhibits Topoisomerase I, Induces G2 Phase Arrest, and Autophagy in Three Adenocarcinomas

frontiers in Oncology

ORIGINAL RESEARCH
published: 24 February 2022
doi: 10.3389/fonc.2022.837373

A Novel Copper(II) Indenoisoquinoline Complex Inhibits Topoisomerase I, Induces G2 Phase Arrest, and Autophagy in Three Adenocarcinomas

Caroline Molinaro[1], Nathalie Wambang[2], Till Bousquet[3], Anne-Sophie Vercoutter-Edouart[1], Lydie Pélinski[3], Katia Cailliau[1†] and Alain Martoriati[1†]*

[1] Univ. Lille, CNRS, UMR 8576-UGSF-Unité de Glycobiologie Structurale et Fonctionnelle, Lille, France, [2] AGAT Laboratories, Intertek, Montréal, QC, Canada, [3] Univ. Lille, CNRS, Centrale Lille, Univ. Artois, UMR 8181-UCCS-Unité de Catalyse et Chimie du Solide, Lille, France

Topoisomerases, targets of inhibitors used in chemotherapy, induce DNA breaks accumulation leading to cancer cell death. A newly synthesized copper(II) indenoisoquinoline complex WN197 exhibits a cytotoxic effect below 0.5 μM, on MDA-MB-231, HeLa, and HT-29 cells. At low doses, WN197 inhibits topoisomerase I. At higher doses, it inhibits topoisomerase IIα and IIβ, and displays DNA intercalation properties. DNA damage is detected by the presence of γH2AX. The activation of the DNA Damage Response (DDR) occurs through the phosphorylation of ATM/ATR, Chk1/2 kinases, and the increase of p21, a p53 target. WN197 induces a G2 phase arrest characterized by the unphosphorylated form of histone H3, the accumulation of phosphorylated Cdk1, and an association of Cdc25C with 14.3.3. Cancer cells die by autophagy with Beclin-1 accumulation, LC3-II formation, p62 degradation, and RAPTOR phosphorylation in the mTOR complex. Finally, WN197 by inhibiting topoisomerase I at low concentration with high efficiency is a promising agent for the development of future DNA damaging chemotherapies.

Keywords: indenoisoquinoline, copper(II) complex, adenocarcinoma, topoisomerase, cell cycle, autophagy

OPEN ACCESS

Edited by:
Xuesen Dong,
University of British Columbia, Canada

Reviewed by:
Bertrand Liagre,
Université de Limoges, France
Alexander Tikhomirov,
Russian Academy of Medical Sciences, Russia

****Correspondence:***
Alain Martoriati
alain.martoriati@univ-lille.fr

†These authors have contributed equally to this work

Specialty section:
This article was submitted to Cancer Molecular Targets and Therapeutics, a section of the journal Frontiers in Oncology

Received: *16 December 2021*
Accepted: *26 January 2022*
Published: *24 February 2022*

Citation:
Molinaro C, Wambang N, Bousquet T, Vercoutter-Edouart A-S, Pélinski L, Cailliau K and Martoriati A (2022) A Novel Copper(II) Indenoisoquinoline Complex Inhibits Topoisomerase I, Induces G2 Phase Arrest, and Autophagy in Three Adenocarcinomas. Front. Oncol. 12:837373. doi: 10.3389/fonc.2022.837373

Abbreviations: ATM, ataxia telangiectasia mutated; ATR, ataxia telangiectasia related; BSA, bovine serum albumin; Cdc25, cell division cycle 25; Cdk1, cyclin dependent kinase 1; Chk1/2, checkpoint kinases 1/2; c-IAP1, cellular inhibitor of apoptosis protein 1; DDR, DNA damage response; DNA-PK, DNA-dependent protein kinase; DSB, double strand break; H2AX, H2A histone family member X; IC_{50}, half maximal inhibitory concentration; Kapp, apparent dissociation constant; mTOR, mammalian target of rapamycin; MTS, 3-(4,5-dimethylthiazol-2-yl)-5-(3-carboxymethoxyphenyl)-2-(4-sulfophenyl)-2H-tetrazolium; $_N$DNA, nicked DNA; PBS, phosphate-buffered saline; RAPTOR, regulatory-associated protein of mTOR; $_R$DNA, relaxed DNA; $_{SC}$DNA, supercoiled DNA; SDS, sodium dodecyl sulfate; SSB, single strand break; t-AML, therapy-related acute myeloid leukemia; TLC, thin-layer chromatography; Tm, temperature of melting; Top, Topoisomerase; VP-16, etoposide.

INTRODUCTION

Adenocarcinomas are the most diagnosed cancers. Among them, breast and cervix, respectively the first and fourth most represented cancers in women, and colorectal cancers the second and third most represented cancers respectively in women and men (1). Current treatments include chemotherapy with agents that generate DNA damage to trigger cancer cell division arrest and associated programmed cell death of tumours (2, 3).

Topoisomerases (Top) regulate DNA topology during replication, transcription, and chromosomal segregation (4–6). To relieve torsional strain, these DNA-interacting enzymes cleave one or two DNA strands before the religation step (7, 8). Human Top are subdivided into three subgroups including IA (Top3α and Top3β), IB (Top1 nuclear and Top1 mitochondrial), and IIA (Top2α and Top2β), type I Top cause single-strand breaks (SSB) while type II Top generate double-strand breaks (DSB) (9). In anticancer therapy, inhibition of Top allows DNA cleavage, prevents the religation reaction, and leaves cancer cells with DNA breaks. Top1 and Top2 are mainly targeted due to their overexpression in many cancers including breast, cervix, and colorectal cancers (10–13). The increased quantity and activity of Top in highly dividing cells directly correlate with positive responses to Top inhibitory treatments (12, 14, 15). The primary cytotoxic lesions in cancer cells result from collisions between the trapped Top and the replication forks (16–18). DNA breaks further trigger the activation of DNA Damage Response (DDR) pathways, leading to cell cycle arrest and to death if DNA damage is too severe (19, 20). The DDR pathways start with the recruitment and the phosphorylation of histone H2AX on serine 139 (γH2AX) by phosphoinositide 3-kinase related kinase family members ATM, ATR, and DNA-PK (21, 22). Consecutively, Chk1 and Chk2 kinases are activated, inhibit phosphatase Cdc25 (23), and induce a cell cycle arrest followed in most cases by apoptosis (20).

Top inhibitors display different action mechanisms. Poisons target the DNA/topoisomerase cleavage complex, form a ternary complex (interfacial inhibition) inhibiting DNA religation, and result in persistent DNA breaks (24). Catalytic inhibitors either intercalate into DNA in the Top fixation site or are ATP competitors or hydrolysis inhibitors to provoke an antineoplastic effect (25). A small number of Top inhibitors are approved for clinical use. The Top2 poison doxorubicin and its isomer epirubicin from the anthracycline family are first-line antineoplastic agents used against many different types of solid tumors, leukemias, and lymphomas (26, 27), with main side effects including cardiotoxicity and t-AML (treatment-related acute myelogenous leukemia) (28–30). At high doses (up to 10 μM), doxorubicin becomes a DNA intercalator and contributes to increase DNA breaks (31, 32). Top2 poison etoposide (VP-16) also induces t-AML (9). The Top1 poison camptothecin derivatives, topotecan and irinotecan, are used to treat solid tumors including ovary, cervix, pancreatic, lung, and colorectal cancers (33). However, their use in chemotherapy is limited by their instability, the need for long-term chemotherapies, and by severe side effects including hematotoxicity, vomiting and diarrhea (34). Unlike camptothecins, the Top1 inhibitors indenoisoquinolines are chemically stable, are not substrates for drug efflux transporters and as such are promising Top inhibitors (35, 36). Indenoisoquinoline derivatives (LMP400, LMP776, and LMP744) are in phase I/II clinical trials (35, 36).

Since the discovery of platinum anticancer properties and the use of cisplatin, a platinum-based alkylating agent, and its derivatives in chemotherapy (37–39), other metal-based drugs have been designed and developed for their cytotoxic effects on tumour cells (40–42). Transition metals from the d-block of the periodic table (groups 3 to 12) (43–46) are particularly suitable for this purpose as they adopt a wide variety of coordination geometries (47). Among them, copper modifies the backbone of the complexed ligand and grants better DNA affinity (48–50). Copper derivatives interact with DNA using noncovalent interactions with the major or the minor DNA grooves, intercalation, or electrostatic binding to enhance DNA damage, and display antitumor activity (51). Some copper complexes inhibit either or both Top1 and Top2 and results in severe DNA damage, cell cycle arrest, and death in cancer cells (52, 53).

As a part of an ongoing effort to develop new efficient anticancer organometallic drugs and to palliate limitations in drug resistances and/or side effects, the synthesis of a novel copper(II) complex of indenoisoquinoline ligand, named WN197, is established based on previous studies (54, 55). This organo-copper complex effects were investigated on breast triple-negative MDA-MB-231, cervix HeLa, and colon HT29 cell lines representative of three most prevalent adenocarcinomas, and associated with poor prognostics. WN197 exerts a specific cytotoxic effect at low concentration (IC_{50} below 0.5 μM) on the three cell lines and significantly below the value of human non-tumorigenic epithelial cell line MCF-10A (IC_{50} 1.08 μM). WN197 acts as a Top1 poison and displays DNA intercalation properties. The action mechanism of WN197 is further deciphered to bring insights into its efficiency. DNA damage is detected by the presence of a rapid increase in nuclear phosphorylated H2AX (after 30 min of treatment with 0.5 μM) and the main DDR kinases are activated by phosphorylations. Cell cycle arrest in the G2 phase is confirmed by the inhibitory phosphorylation of Cdk1 on tyrosine 15, an accumulation of cyclin B, and the unphosphorylated form of histone H3. Furthermore, the cell cycle is halted in G2 by inhibitory phosphorylation of Cdc25C on serine 216 associated with a binding to the 14.3.3 chaperon. Cancer cells halt in G2, die by autophagy detected through an increase in Beclin-1, and a decrease in the LC3-I/LC3-II ratio and the p62 marker. Moreover, the RAPTOR component in the mTORC1 complex is phosphorylated on serine 792, a feature of autophagic-induced cell death.

MATERIALS AND METHODS

Chemical Reagents and Materials

All commercial reagents and solvents were used without further purification. Cisplatin is purchased from Alfa Aesar (Heysham, UK); rapamycin from Abcam (Cambridge, UK); doxorubicin, nocodazole and DMSO from Sigma-Aldrich (Saint-Quentin-Fallavier, France). Stock solutions were prepared in DMSO. Melting points were determined with a Barnstead Electrothermal (BI 9300) capillary melting point apparatus and are uncorrected. Elemental analyses were performed with a

varioMICRO analyser. Thin layer chromatography (TLC) was carried out on aluminium-baked (Macherey-Nagel GmbH, Düren, Germany) silica gel 60. Column chromatography was performed on silica gel (230-400 mesh). The electronic absorption spectra were acquired on a UV-Vis double beam spectrophotometer SPECORD® PLUS (Analytik Jena GmbH, Germany). The molar conductance measurement was carried out using a CDRV 62 Tacussel electronic bridge, employing a calibrated 10^{-2} M KCl solution and 10^{-3} M solutions of compounds in DMSO. Purities of all tested compounds were ≥95%, as estimated by HPLC analysis. High Resolution Mass Spectrum (HR-MS) was measured at REALCAT (Université de Lille) on a Synapt G2Si (Waters) equipped with an ion mobility cell.

WN197 Copper(II) Indenoisoquinoline Complex Synthesis

WN170 was synthesized according to the literature procedure (56). To a solution of WN170 (160 mg, 0.443 mmol) in dry methanol (8 mL) was added dropwise a solution of $CuCl_2$ (59 mg, 0.443 mmol) in MeOH (7 mL). After stirring at room temperature for 10 h, the reaction mixture was filtered off to yield an orange precipitate which was washed with MeOH and dried under vacuum (8 h at 100°C). Yield: 132 mg (70%). Decomposition at 194°C. Anal. Calcd. for $C_{44}H_{54}Cl_2CuN_6O_8$ (%): C, 56.86; H, 5.86; N, 9.04: Found C, 56.76; H, 5.89; N, 9.22. FT-IR (neat) (νmax, cm^{-1}): 1650 (C=O), 1549 (C=C), 490 (Cu-N). UV-vis in DMSO-H_2O (19/01), λ/nm (ϵ/$M^{-1}cm^{-1}$): 625 (156), 463 (4500) (9800), 353 (17620), 350 (18100), 328 (16440). Λ_M (1 mM, DMSO) (S cm^2 mol^{-1}): 24. HRMS (ESI) m/z: calcd for $[M]^+$ $C_{44}H_{46}ClCuN_6O_4$ 820.2565; Found 820.2332.The equations should be inserted in editable format from the equation editor.

Cell Culture

HeLa, MDA-MB-231, HT-29 and MCF-10A cell lines originate from ATCC (Manassas, VA, USA), and were maintained at 37°C in a humidified atmosphere with 5% CO_2 in DMEM medium (Lonza, Basel, Switzerland) supplemented with 10% fetal bovine serum (Dutscher, Dernolsheim, France), 1% Zell Shield (Dutscher, Bernolsheim, France) and 1% non-essentials amino-acids (Lonza, Basel, Switzerland). MCF-10A were maintained in MEBM medium (Lonza, Basel, Switzerland) supplemented with MEGM (Lonza, Basel, Switzerland). All cell lines culture media were added with 1% Zell Shield (Dutscher, Bernolsheim, France).

Cell Viability Assay

Cell viability was determined using CellTiter 96® AQ_{ueous} One Solution Cell Proliferation Assay (MTS, Promega, Charbonnières-les-Bains, France). 2.10^3 cells well were seeded in 96-well plate for 24 h before treatment with 0 to 100 µM of WN197, WN170 or cisplatin for 72 h. After a 2 h incubation with 20 µL of CellTiter solution at 37°C in 5% CO_2, the production of reduced MTS (3-(4,5-dimethylthiazol-2-yl)-5-(3-carboxymethoxyphenyl)-2-(4-sulfophenyl)-2H-tetrazolium) in formazan was measured at 490 nm (SPECTROstar Nano, BMG LABTECH, Ortenberg, Germany). IC_{50} were calculated using GraphPad Prism V6.0 software. Statistical differences between WN197 and WN170 were ascertained by a Student *t*-test (**p<0.01 and ****p<0.0001).

Immunofluorescence for Nuclei *Foci*

2.10^5 cells seeded on glass coverslips were treated with 0.5 µM of WN197 or WN170, 5 µM of doxorubicin, 20 µM of cisplatin as positive controls, or 0.1% DMSO as a solvent control for 30 min or 24 h. Fixation was performed with 4% paraformaldehyde (Sigma-Aldrich, Saint-Quentin-Fallavier, France) for 5 min and followed by permeabilization with 0.1% Triton in PBS (Sigma-Aldrich, Saint-Quentin-Fallavier, France) for 10 min and saturation of unspecific sites with 1% BSA in PBS (Sigma) for 1 h at room temperature. Anti-γH2AX mouse antibody (S139, 1:1000, Cell Signalling, by Ozyme, Saint-Cyr-L'École, France) was incubated overnight at 4°C, washed 3 times with 1% BSA/PBS. Cells were incubated with secondary anti-mouse IgG (Alexa Fluor® 488, 1:2000, Thermo-Fisher Scientific Biosciences GMBH, Villebon-sur-Yvette, France) for 1 h at room temperature in the dark, washed 3 times before nuclei were stained with DAPI (6-diamidino-2-phenylindole, 1 µg/mL, Molecular Probes, by Thermo Fisher Scientific Biosciences GMBH, Villebon-sur-Yvette, France). Images were captured under a Leica fluorescent microscope, and γH2AX *foci* were counted with ImageJ (Fiji Software, v1.52i) on 30 cells from 3 independent experiments and quantified with GraphPad Prism V6.0 software. Statistical significances (mean ± SD) were performed by a two-way ANOVA followed by Dunnett's multiple comparison test (**p<0,01; ***p<0,001; ****p<0,0001).

Electrophoresis and Western Blot

$7.5.10^5$ cells were seeded for 24 h and treated with 0.5 µM of WN197 or WN170, 20 µM of cisplatin, 5 µM of doxorubicin, or 0.1% DMSO (solvent control). After 24 h, they were lysed in RIPA buffer (1% Triton X-100; 50 mM TRIS-HCl pH 4; NP40 2%; 0.4% Na-deoxycholate; 0.6% SDS; 150 mM NaCl; 150 mM EDTA; 50 mM NaF) supplemented with 1% of protease inhibitor cocktail (Sigma-Aldrich, Saint-Quentin-Fallavier, France) and phosphatase inhibitors (Roche SAS by Merck, Kenilworth, NJ, USA).

For cytochrome C analysis, $7.5.10^5$ cells were seeded for 24 h and treated for 3 h, 16 h, 24 h or 48 h with 0.5 µM of WN197, and for 24 h or 48 h with 5 µM of doxorubicin as positive control. Cells were lysed in a glass grinder at 4°C in homogenization buffer (25 mM MOPS at pH 7.2, 60 mM β–glycerophosphate, 15 mM para-nitrophenylphosphate, 15 mM EDTA, 15 mM MgCl2, 2 mM DTT, 1 mM sodium orthovanadate, 1 mM NaF, 1 mM phenylphosphate, 10 µg/mL leupeptin, 10 µg/mL aprotinin, 10 µg/mL soybean trypsin inhibitor, 10 µM benzamidine).

Samples were centrifuged for 10 min at 12,000 G and protein concentration of supernatants were determined using the Bradford assay (BioRad, Marnes-la-Coquette, France) at 595 nm (SPECTROstar Nano, BMG LABTECH, Ortenberg, Germany). Proteins were denatured in 2X Laemmli buffer (65.8 mM TRIS-HCl pH 6.8; 26.3% glycerol; 2.1% SDS; 0.01% bromophenol blue; 4% β-mercaptoethanol, BioRad, Marnes-la-Coquette, France) at 75°C for 10 min. 15 µg of proteins were separated on 4-20% SDS PAGE gels (mini protean TGX, BioRad, Marnes-la-Coquette,

France), for 1 h at 200 V in denaturing buffer (0.1% SDS; 0.3% TRIS base; 1.44% glycine). Proteins were transferred onto nitrocellulose membrane (Amersham Hybond, Dutscher, Bernolsheim, France) by wet transfer (0.32% TRIS; 1.8% glycine; 20% methanol, Sigma-Aldrich, Saint-Quentin-Fallavier, France), for 1 h at 100 V. Membranes were saturated with 5% low fat dry milk in TBS added with 0.05% Tween (Sigma-Aldrich, Saint-Quentin-Fallavier, France), and incubated overnight at 4°C with specific primary antibodies: rabbit polyclonal antibodies were against ATM (Cell Signaling technology (CST, by Ozyme, Saint-Cyr-L'École, France), 1/1000), ATR (CST, 1/750), phosphorylated ATR (S428, CST, 1/1000), Beclin-1 (CST, 1/800), Cdc25C (CST, 1/1500), phosphorylated Cdc25C (S216, CST, 1/1000), phosphorylated Cdk1 (Y15, CST, 1/1500), phosphorylated Chk1 (S317, CST, 1/1000), phosphorylated Chk2 (T68, CST, 1/1000), cleaved caspase 3 (CST, 1/1000), phosphorylated H2AX (S139, CST, 1/750), histone H3 (CST, 1/1000), phosphorylated H3 (S10, CST, 1/1000), phosphorylated p53 (S15, CST, 1/1000), p53 (CST, 1/1000), p21 (CST, 1/1000), LC3 (CST, 1/50), mTOR (CST, 1/1200), RAPTOR (CST, 1:1500), phosphorylated RAPTOR (S792, CST, 1/1000); mouse monoclonal antibodies against phosphorylated ATM (S1981, Santa Cruz Biotechnology (SCB), Santa Cruz, CA, USA, 1/200), Chk1 (SCB, 1/1000), Chk2 (SCB, 1/200), Cdk1 (CST, 1/1000), 14-3-3 (SCB, 1/1000), cyclin B2 (CST, 1/1500), p62 (SCB, 1/100); goat polyclonal antibodies against β-actin (SCB, 1/1200); and cocktail antibodies against cleaved PARP (Abcam, Cambridge, UK, cell cycle and apoptosis cocktail, 1/1500). After three washes of 10 min in TBS-Tween, nitrocellulose membranes were incubated 1 h with the appropriate horseradish peroxidase-labeled secondary antibodies: anti-rabbit or anti-mouse antibodies (Invitrogen, by Thermo Fisher Scientific Biosciences GMBH, Villebon-sur-Yvette, France, 1/30,000) or anti-goat antibodies (SCB, 1/30,000). Secondary antibodies were washed in TBS-Tween three times for 10 min and the signals were revealed with a chemiluminescent assay (ECL Select, GE Healthcare, Dutscher, Bernolsheim, France) on hyperfilms (Amersham hyperfilm MP, Dutscher, Bernolsheim, France). β-actin or histone H3 were used as loading controls. Signals were quantified with Image J (Fiji Software, v1.52i), and normalized to respective loading control. The means of 3 independent experiments were calculated.

In Vitro Activities of Human Topoisomerases I and II

Topoisomerase activities were examined in assays based on the relaxation of a supercoiled DNA into its relaxed form. Topoisomerase I (Top1) activity was performed using the drug screening kits protocol (TopoGEN, Inc., Buena Vista, CO, USA). The reaction mixture was composed of supercoiled pHOT1 DNA (250 ng), 10X TGS buffer (10 mM Tris-HCl pH 7.9, 1 mM EDTA), 5 units of Top1, a variable amount of compound to be tested, and a final volume adjusted to 20 µL with H2O. WN197 was tested at concentrations ranging from 0.2 to 2 µM. Camptothecin (10 µM) was used as a positive control (poison inhibitor of Top1 activity), etoposide (100 µM) as negative control (inhibitor of Top2 activity), and 1% DMSO alone as vehicle control. Relaxed pHOT1 DNA (100 ng) was used as migration control. The addition of proteinase K (50 µg/mL) for 15 min at 37°C allowed Top1 degradation to visualize the cleavage products (nicked DNA). Reaction products were separated by electrophoresis in a 1% agarose gel containing ethidium bromide (0.5 µg/mL) for 1 h at 100 V in TAE (Tris-Acetate-EDTA; pH 8.3) buffer.

Topoisomerase II Relaxation Assay Kit (Inspiralis, Inc., Norwich, UK) was used to measure topoisomerase II (Top2) activity. The reaction mixture was composed of supercoiled pBR322 DNA (1 µg), 10X assay buffer (50 mM Tris-HCl (pH 7.5), 125 mM NaCl, 10 mM MgCl2, 5 mM DTT, 100 µg/mL albumin), 30 mM ATP, 5 units of Top2α or Top2β, variable amount of compound to be tested, and a final volume adjusted with H2O to 30 µL. Etoposide (VP-16, 100 µM) was used as positive control, and camptothecin (10 µM) as negative control. The mixtures were incubated at 37 °C for 30 min and the reactions stopped by the addition of 5 µL 10% SDS. Reaction products were separated by electrophoresis in a 1% agarose gel for 1 h at 100 V in TAE buffer, and stained with ethidium bromide (0.5 µg/mL) for 15 min. After destaining in water, the DNA migratory profiles were visualized under UV light (ChemiDocTM XRS+, BioRad, Marnes-la-Coquette, France).

Melting Temperature Measurement

Melting temperatures were obtained as described (54, 55). 20 µM solutions of WN170 or WN197 were prepared in 1 mL of BPE buffer (2 mM NaH_2PO_4, 6 mM Na_2PO_4, 1 mM EDTA, pH 7.1) in the presence or not of 20 µM DNA from calf thymus (42% GC bp, Merck, Kenilworth, NJ, USA). Absorbances were measured at 260 nm (Uvikon 943 coupled to Neslab RTE111) every minute over the range of 20 to 100°C with an increment of 1°C per minute. All spectra were recorded from 230 to 500 nm. Tested compound results are referenced against the same DNA concentration in the same buffer. The Tm values were obtained from the first derived plots.

Ethidium Bromide Competition Test

Fluorescence titrations were determined as described (54, 55). Ethidium bromide/WN170 or WN197 molar ratio of 12.6/10 at concentrations ranging from 0.05 to 10 µM were used in a BPE buffer (pH 7.1). The excitation wavelength was set at 546 nm and the emission was monitored over the range of 560 to 700 nm (SPEX Fluorolog). IC_{50} values for ethidium bromide (EB) displacement were calculated using a fitting function incorporated into GraphPad Prism 6.0 software. The apparent binding constants were calculated using the equation $K_{app} = (1.26\ (K_{app}(EB)/IC_{50})$ with $K_{app}(EB) = 10^7\ M^{-1}$ and IC_{50} in µM.

Flow Cytometry

$7.5.10^5$ cells plated for 24 h were treated with 0.5 µM WN197 or WN170, 20 µM of cisplatin (S phase arrest control), 83 nM of nocodazole (M phase arrest control), or 0.1% DMSO (solvent control). For the dose titration experiments, cells were treated for 24 h with increasing concentrations of WN197. For kinetic experiments, cells were treated with 0.5 µM of WN197 or WN170 from 4 to 48 h. Cells were detached using trypsin

(Biowest, Nuaillé, France), centrifuged at 1,000 G for 10 min, resuspended in PBS, and fixed with 70% ethanol at -20°C for 24 h, before they were centrifugated (1,000 G, 10 min), resuspended in PBS, and treated for 15 min at room temperature with RNase (200 µg/mL, Sigma). Finally, incubation with propidium iodide (10 µL/mL, Molecular Probes, by Thermo Fisher Scientific Biosciences GMBH, Villebon-sur-Yvette, France) at 4°C for 30 min was performed before flow cytometry (BD FACSCalibur, Becton Dickinson, Le Pont-de-Claix, France) analysis. For each sample, 10,000 events (without cell doublets and cellular debris) were considered. The cell cycle repartition was analyzed with Graphpad Prism V6.0 software. Statistical significances (mean ± SD) were determined by two-way ANOVA followed by Dunnett's multiple comparison test (****p<0,0001).

Immunoprecipitation

Cell lysates were obtained as described in the Western blot section. Samples were pre-cleared with protein A sepharose (20 µL of 50% beads/200 µL of cell lysate, Sigma-Aldrich, Saint-Quentin-Fallavier, France) for 1 h at 4°C under gentle rocking. After brief centrifugation, supernatants were incubated with antibodies against 14.3.3 (Santa Cruz Biotechnology, Santa Cruz, CA, USA, 1/200), Cdc25C (Thermo Fisher Scientific Biosciences GMBH, Villebon-sur-Yvette, France, 1/200) or mTOR (CST, 1/200) at 4°C for 1 h under rotation and followed by incubation with protein A sepharose (20 µL of 50% bead slurry, Sigma-Aldrich, Saint-Quentin-Fallavier, France) for 1 h at 4°C under rotation. Samples were rinsed 3 times with RIPA buffer. Pellets were collected by brief centrifugation, resuspended in 2X Laemmli buffer, and heated at 100°C for 10 min before SDS-PAGE and Western blots were performed.

RESULTS

Organocopper Synthesis

The synthesis of WN197 is described in **Figure 1**. Indenoisoquinoline WN170 was first obtained in a four-step reaction. Condensation of the benzo[d]indeno[1,2-b]pyran-5,11-dione with a primary aminoalcohol was followed by tosylation of the alcohol function. The substitution of the tosyl group by the protected ethylenediamine and the consecutive deprotection of the Boc group led to WN170 in 68% global yield. Complex WN197 was then synthesized by reacting methanolic solutions of indenoisoquinoline derivative WN170 and $CuCl_2$. After purification, WN197 was obtained in 70% yield.

WN197 Displays a Cytotoxic Activity on Three Adenocarcinoma Cell Lines at Low Doses

Cells viability was assayed on the triple-negative breast cancer cells (MDA-MB-231), the cervix cancer cells (HeLa), and the colorectal cancer cells (HT-29) (**Table 1**). IC_{50} obtained are respectively 0.144 µM, 0.22 µM, and 0.358 µM for WN197 below the cisplatin IC_{50} values ranging from 10 to 40 µM. The copper-free indenoisoquinoline ligand, WN170, affected cell viability at higher doses (0.875 µM for MDA-MB-231, 0.630 µM for HeLa, and 0.479 µM for HT-29 cells), showing that the presence of the copper metal significantly enhances the anticancer effect of the indenoisoquinoline core for MDA-MB-231 and HeLa cell lines. A significantly higher IC_{50} (1.080 µM) is obtained on MCF-10A compared to the adenocarcinoma cell lines (**Table 2**).

WN197 Induces DNA Damage

To determine whether WN197 affects DNA integrity, detection of γH2AX DNA break marker was performed by immunofluorescence. γH2AX *foci* were visualized in the nucleus at 0.5 µM of WN197, a concentration close to the IC_{50} determined previously, in MDA-MB-231, HeLa, and HT-29. After 24 h of treatment, the average number of γH2AX *foci* per cell were respectively 99, 98, and 70 for MDA-MB-231, HeLa, and HT-29 cells (**Figure 2A**). The number of γH2AX *foci* was close to the result obtained for the Top2 inhibitor, doxorubicin, (average of 95 *foci* per cell), and higher than the number of γH2AX *foci* triggered by an alkylating agent, cisplatin (average of 55 *foci* per cell). WN197 induced more DNA damage than the indenoisoquinoline WN170 (average of 23 *foci* per cell). Controls with DMSO solvent showed a low number of *foci* (average of 9 *foci* per cell for the 3 adenocarcinomas) compared to treated conditions (**Figure 2B**).

These results were further confirmed by Western blot analysis (**Figure 2C**). Untreated cells showed a low γH2AX signal while a

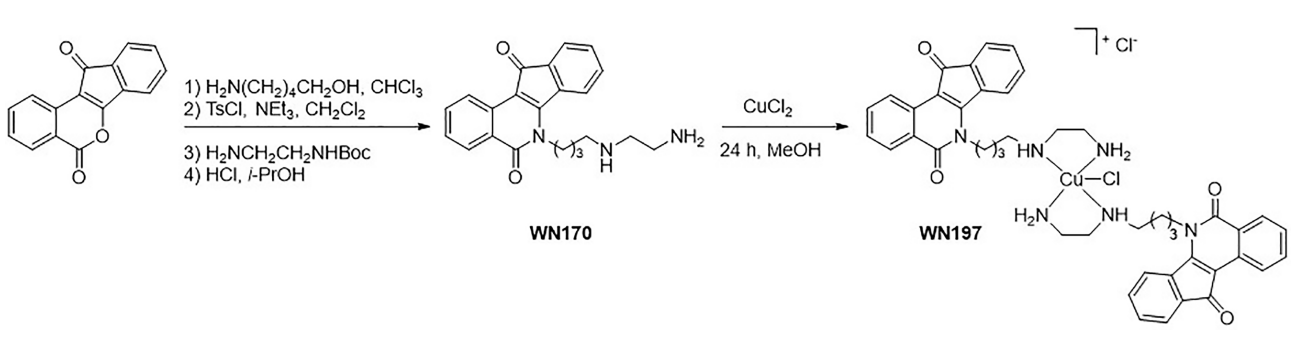

FIGURE 1 | WN197 synthesis.

TABLE 1 | Half maximal inhibitory concentrations (IC_{50} in μM) for cell survival.

	MDA-MB-231	HeLa	HT-29
WN197	0.144 ± 0.01	0.220 ± 0.01	0.358 ± 0.07
WN170	0.875 ± 0,01	0.630 ± 0.09	0.479 ± 0.07
Cisplatin	33.802 ± 1.27	19.287 ± 5.323	21.313 ± 7.475
Statistical difference (WN197/WN170)	****	**	*ns*

*Data are expressed as the mean ± SD of three independent experiments. Statistics were based on Student's t-test of the difference between WN197 and WN170; ns, non-significative, **p<0.01 and ****p<0.0001.*

strong signal was observed after doxorubicin, cisplatin, and WN197 treatments. As observed by immunofluorescence, the γH2AX signal is weaker in the WN170 condition compared to the WN197 condition, indicating that the WN197 compound induces more DNA damage than WN170 at the same concentration (0.5 μM).

Foci were detected as soon as 30 min after treatment (**Figure 2D**). The number of γH2AX *foci* was close to the result obtained at 24 h with an average of *foci* per cell of 84, and 87 for MDA-MB-231, HeLa, and lower to 13 for HT-29 cells after WN197 treatment.

WN197 Is a Concentration-Dependent Topoisomerase Inhibitor

To determine whether the Cu(II)-complex WN197 is a topoisomerase inhibitor, *in vitro* human topoisomerase activity tests were realized. The topoisomerase I (Top1) test relies on the ability of Top1 to relax supercoiled DNA, and the absence of relaxed DNA implies inhibition of Top1 activity. In the presence of Top1, supercoiled DNA showed a relaxed profile (**Figure 3A**). Camptothecin, a well-known Top1 inhibitor, disturbed DNA relaxation in the reaction, and part of the DNA remained supercoiled. Increasing doses of WN197 from 0.2 to 2 μM showed a decrease quantity of relaxed DNA, indicating disruption of Top1 activity. The solvent control, DMSO, and VP-16 (etoposide, a Top2 inhibitor) displayed no effect on Top1-induced DNA relaxation showing no inhibitory effect on Top1 activity.

Top1 inhibitors can act either as catalytic inhibitors by DNA intercalation at the Top1 fixation site or as poisons, forming a ternary complex (DNA + Top1 + compound) (24, 25), preventing DNA religation and inducing accumulation of nicked DNA. The addition of proteinase K to the Top1-DNA relaxation test allows the release of nicked DNA that can be resolved and detected on agarose gel. The short half-life of the nicked DNA is stabilized and detectable after addition of a Top1 poison, camptothecin (**Figure 3A**). Nicked DNA was also observed in presence of 0.2 μM of WN197, indicating a Top1 poison activity (**Figure 3A**). At higher concentrations (0.5 μM, 1 μM, 2 μM), the inhibition of Top1 activity without nicked DNA accumulation indicates that WN197 does not act as a Top1 poison.

The effect of WN197 on Top2α and Top2β activities were also assayed. The same principle based on the inhibition of topoisomerase-induced DNA relaxation was used (**Figure 3B**). In the presence of Top2α or Top2β, the supercoiled DNA is relaxed (topoisomers). VP-16 (etoposide, Top2 inhibitor) disturbed DNA relaxation in the reaction, as seen by the presence of supercoiled DNA in the gel, while camptothecin had no inhibitory effect, as expected. WN197 disrupted the Top2α-induced DNA relaxation only at 2 μM, and the Top2β at 1 and 2 μM, higher doses than the concentration necessary to inhibit Top1 activity, indicating a concentration-dependent mechanism of action.

TABLE 2 | Half maximal inhibitory concentrations (IC_{50} in μM) for cell survival of MCF-10A.

Compound	IC_{50} (μM)
WN197	1.080 ± 0.037
Cisplatin	14.218 ± 7.157
Statistical difference (WN197 on adenocarcinomas vs. on MCF-10A)	***

*Data are expressed as the mean ± SD of three independent experiments. Statistics were based on Student's t-test of the difference between WN197 IC_{50} on adenocarcinomas and MCF-10A; ***p<0.001.*

WN197 Intercalates in DNA

Melting curves and fluorescence measurements were performed to comfort results obtained in **Figure 3**, and ascertain WN197 intercalation in DNA.

Drugs ability to protect calf thymus DNA (CT DNA, 42% GC bp) against thermal denaturation was used as an indicator of the capacity of indenoisoquinoline derivatives to bind and stabilize the DNA double helix. The Cu(II) indenoisoquinoline complex WN197 displayed a slightly higher ΔTm value compared to the metal-free indenoisoquinoline WN170 (respectively 16.6°C and 16.1°C, drug/DNA ratio 0.5), showing a better binding affinity with DNA (**Table 3**).

The binding affinities, determined using a fluorescence quenching assay based on DNA binding competition between the intercalating drug ethidium bromide and the tested molecules, were used to gain insight into the DNA binding affinity. The apparent DNA binding constant Kapp value of the Cu(II) complex (15.005 ± 0.290 10^7 M^{-1}) is higher compared to the original ligand value (2.436 ± 0.883 10^7 M^{-1}). These results are in agreement with the ΔTm values showing that the complexation of indenoisoquinoline ligand by copper allows a stronger interaction with DNA (**Table 3**).

WN197 Activates the DNA Damage Response Pathway

The activation of molecular effectors of the DDR pathways involved in SSB and DSB was analysed by Western blot (**Figure 4**). Activating phosphorylation of ATR (S428) and ATM (S1981) occurred in the three cell lines MDA-MB-231, HeLa, and HT-29 treated with WN197 compared to the untreated cells. The subsequent activating phosphorylation of Chk1 (S317) and Chk2 (T68) were observed,

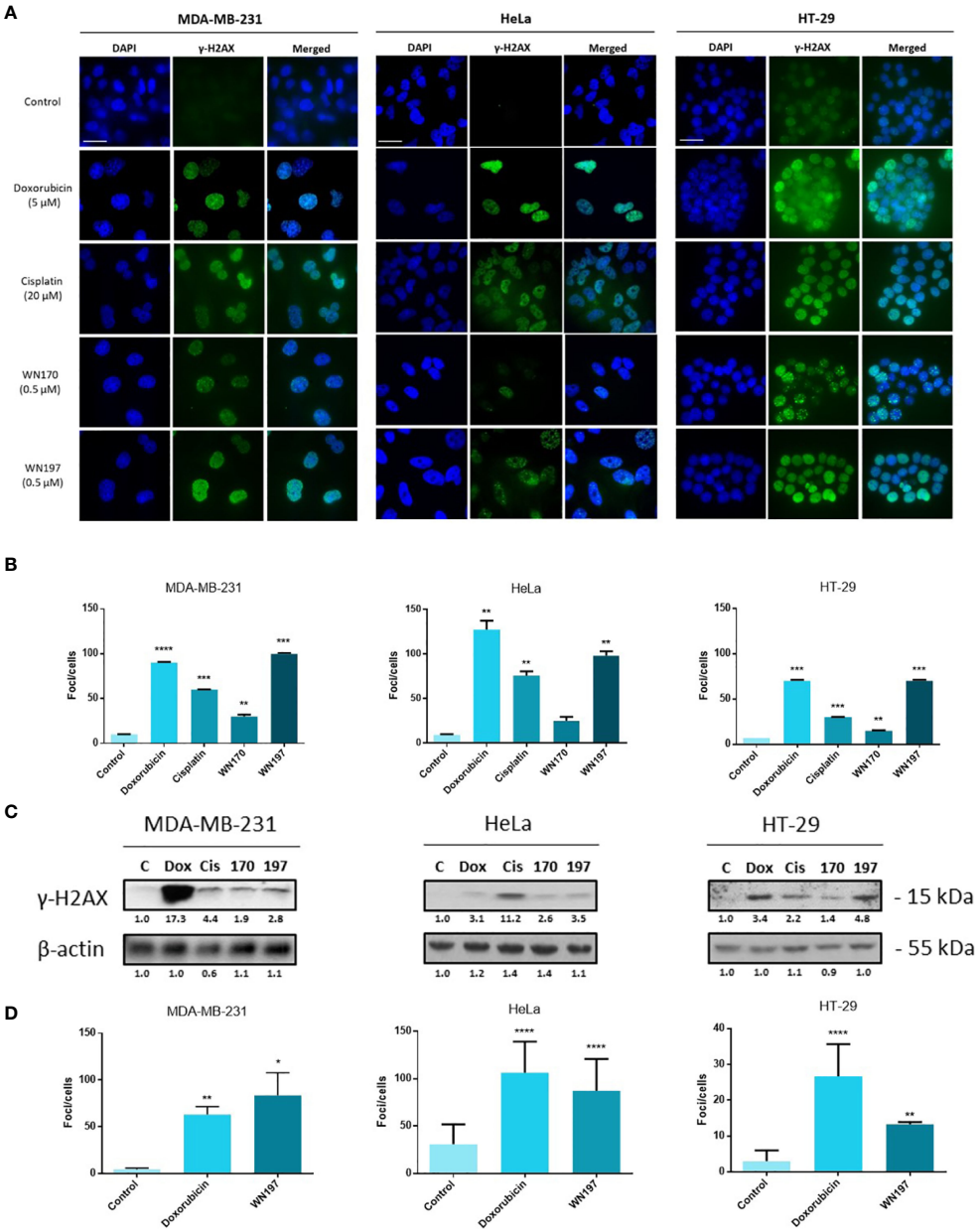

FIGURE 2 | The copper complex WN197 induced DNA damage in cancer cells. MDA-MB-231, HeLa and HT-29 cells were treated with DMSO (0.5%, solvent control), doxorubicin (5 μM, Top2 inhibitor inducing DNA breaks), cisplatin (20 μM, alkylating agent inducing DNA breaks), WN170 (0.5 μM, indenoisoquinoline without metal) or WN197 (0.5 μM). **(A)** Immunofluorescence of the DNA breaks marker γH2AX was visualized as green *foci* in nuclei stained with DAPI (blue) on a Leica fluorescent microscope 24 h after treatments. Images were representative of three independent experiments. Scale bar: 20 μm **(B)** Quantification of γH2AX *foci* number per cells. **(C)** Western blot analysis of γH2AX 24 h after treatments. β-actin was used as a loading control and relative γH2AX level was quantified by densitometry using Image J (Fiji Software, v1.52i). **(D)** Quantification of γH2AX *foci* number per cells 30 min after treatments, based on immunofluorescence experiments. In B and D, data were expressed as the mean ± SD for 30 nuclei of three independent experiments. Statistical analyses were based on a two-way ANOVA followed by a Dunnett's test (*p<0.05, **p<0,01, ***p<0,005 and ****p<0,001).

confirming the DDR pathway activation. In the doxorubicin, cisplatin, and WN170 these phosphorylations also occurred while in untreated controls they were always lower or absent.

p53 facilitates cell cycle arrest by targeting $p21^{WAF1/CIP1}$. After WN197 treatment, p53 and phosphorylated p53 were increased in MDA-MB-231, HeLa and HT-29 cells (respectively by factors 34.8, 3.2, and 1.6 for p53 and by 58.3, 1.6 and 5.5 for phosphorylated p53), while p21 was highly increased in HT-29 cells (by a factor 8.3) compared to MDA-MB-231 and HeLa (respectively 1.3 and 2.2). The WN170 values are slightly

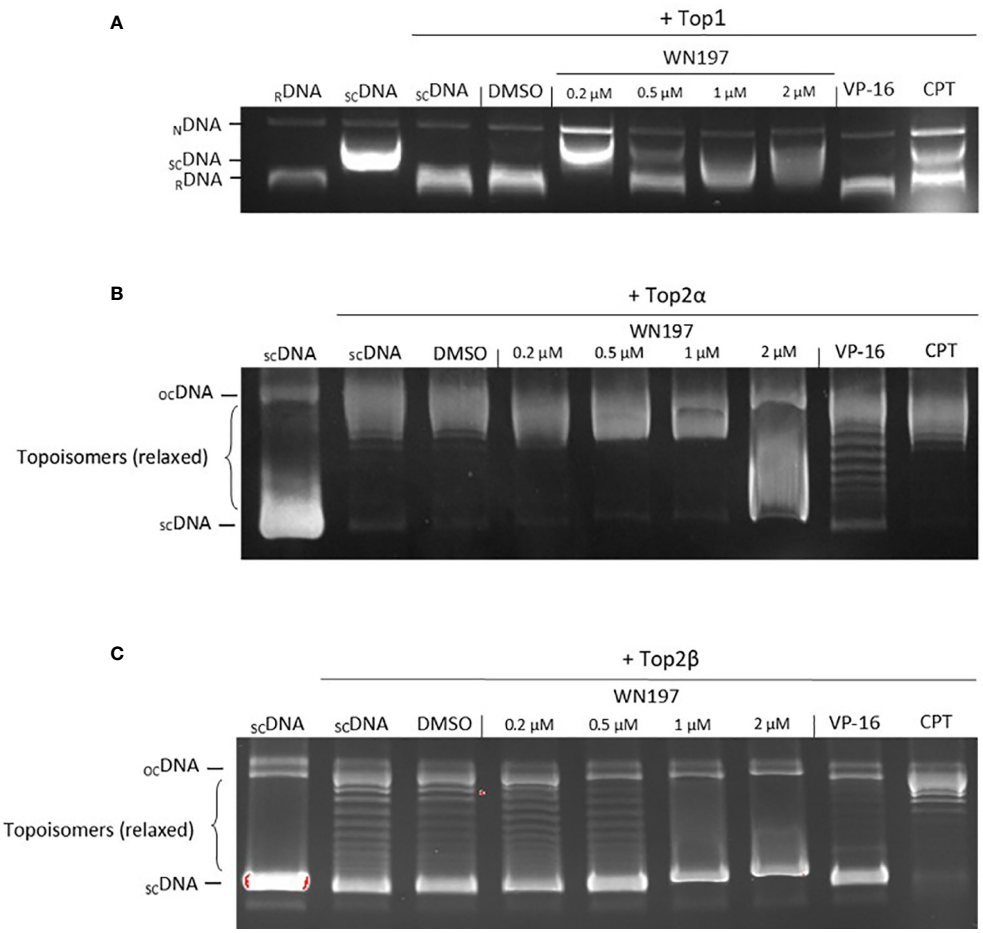

FIGURE 3 | WN197 inhibited human topoisomerase activity in a dose-dependent manner. **(A)** Top1 activity was determined by *in vitro* assays after addition of either DMSO (5%, solvent control, lane 4), WN197 at different concentrations (0.2, 0.5, 1 and 2 μM, lanes 5-8), etoposide (VP-16, 50 μM; Top2 poison, lane 9) the negative control of Top1 activity inhibition, or camptothecin (CPT, 10 μM; Top1 poison, lane 10) the positive control of Top1 activity inhibition. Relaxed DNA ($_R$DNA, lane 1) or supercoiled DNA ($_{SC}$DNA, lane 2) were used as migration controls. $_{SC}$DNA was used in all other reactions in presence of Top1. The Top1 activity control allowing the relaxation of $_{SC}$DNA is in lane 3. The addition of proteinase K allowed detection of nicked DNA ($_N$DNA), a witness of the single-strand broken DNA stabilization by a topoisomerase poison. **(B)** Top2α activity inhibition assay. Migration control of supercoiled DNA ($_{SC}$DNA) was performed in lane 1. Top2α was present in all other reactions. The Top2α activity control for the relaxation of $_{SC}$DNA is in lane 2, the first band corresponds to the transitional open circular DNA ($_{OC}$DNA) and topoisomers correspond to the relaxed DNA. DMSO (5%, solvent control) in lane 3, WN197 (concentrations of 0.2, 0.5, 1 and 2 μM) in lanes 4-7, etoposide (VP-16, 50 μM; Top2 poison) in lane 8, and camptothecin (CPT, 10 μM; Top1 poison) in lane 9. **(C)** Top2β activity inhibition assay. Migration control of $_{SC}$DNA was performed in lane 1. Top2β was present in all other reactions. The Top2β activity control for the relaxation of $_{SC}$DNA is in lane 2, DMSO (5%, solvent control) in lane 3, WN197 (concentrations of 0.2, 0.5, 1 and 2 μM) in lanes 4-7, etoposide (VP-16, 50 μM; Top2 poison) in lane 8, and camptothecin (CPT, 10 μM; Top1 poison) in lane 9. In **(A–C)** after topoisomerase reactions, DNA was run in a 1% agarose gel, stained with ethidium bromide (0.5 μg/mL), and visualized under UV light.

identical except for p53 and p21 in MDA-MB-231 (respectively factors 0.4 and 1.0). In doxorubicin and cisplatin treated cell lines, p53 and p21 were not increased except for p53 in MDA-MB-231 and p21 in HT-29 cells.

WN197 Induces a Cell Cycle Arrest in G2 Phase

The cell cycle repartition following the DDR pathway activation was monitored by flow cytometry in cells exposed for 24 h to

TABLE 3 | Melting curves and fluorescence measurements were determined for WN197 and WN170.

Compound	ΔTm (°C)	Kapp (10^7 M-1)	EtBr displacement
WN197	16.6	15.005 ± 0.290	90%
WN170	16.1	2.436 ± 0.883	87%

Variations in melting temperature (ΔTm=Tm drug–DNA complex–Tm DNA alone) were performed at a ratio of 0.5. Apparent binding constant were measured by fluorescence using [EB]/[DNA] = 1.26. Data were the mean of at least three independent experiments.

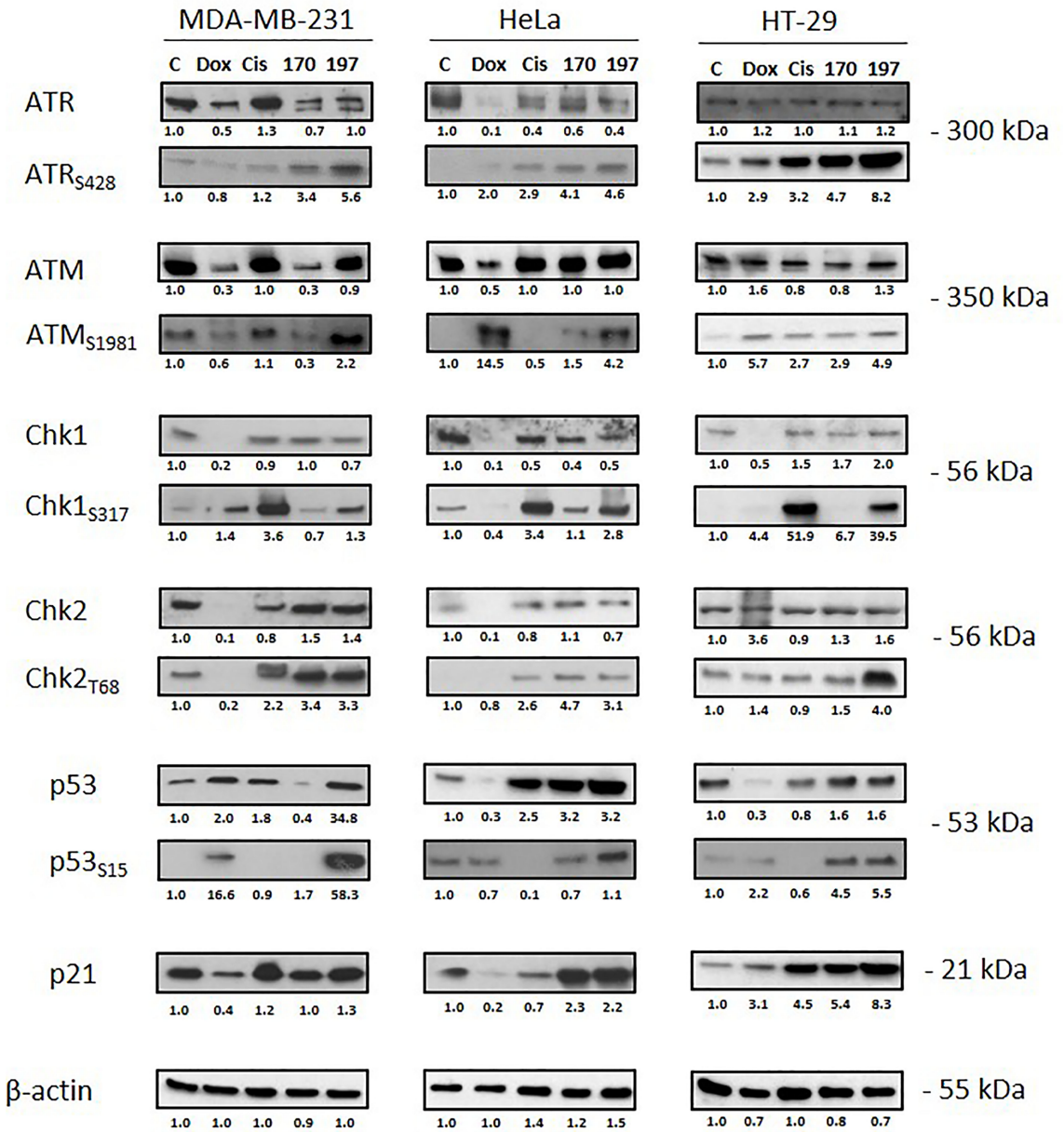

FIGURE 4 | Activation of the DNA Damage Response (DDR) pathway. Cells were treated for 24 h with doxorubicin (5 μM), cisplatin (20 μM), WN170 (0.5 μM), or WN197 (0.5 μM). Western blots were performed to detect ATM, ATR, Chk1, Chk2, p53 and their phosphorylated forms, and p21. β-actin was used as a loading control and relative protein levels were quantified by densitometry using Image J software (Fiji Software, v1.52i). Results were representative of three independent experiments.

different treatments (**Figures 5A, B**). Untreated cells showed a classical cell cycle repartition in the 3 cell lines with averages of 50.52% cells in G0/G1 phases, 29.80% in the S phase and 19.68% in the G2/M phases. Cisplatin, known to promote the accumulation of cells in the S phase (57, 58), induced 79.79%, 59.61%, and 85.53% cells in S phase for MDA-MB-231, HeLa, and HT-29 cells, respectively. The mitotic spindle poison, nocodazole, led to an arrest in mitosis with 70.17%, 88.61%, and 39.68% cells in G2/M phase for MDA-MB-231, HeLa, and HT-29, respectively. WN170 did not modified the cell cycle repartition of MDA-MB-231 cells and induced a G2/M accumulation of HeLa and HT-29 cell lines. Treatments with WN197 triggered a G2/M phase accumulation. WN197 had the capacity to induce a higher percentage of cells accumulation in the G2/M phase compared to WN170 respectively with 51.29% and 21.08% for MDA-MB-231 cells, 70.51% and 54.19% for HeLa cells, and 74.4% and 48.06% for HT-29 cells. Sub-G1 peaks were not observed in WN197 treated cells, while they were

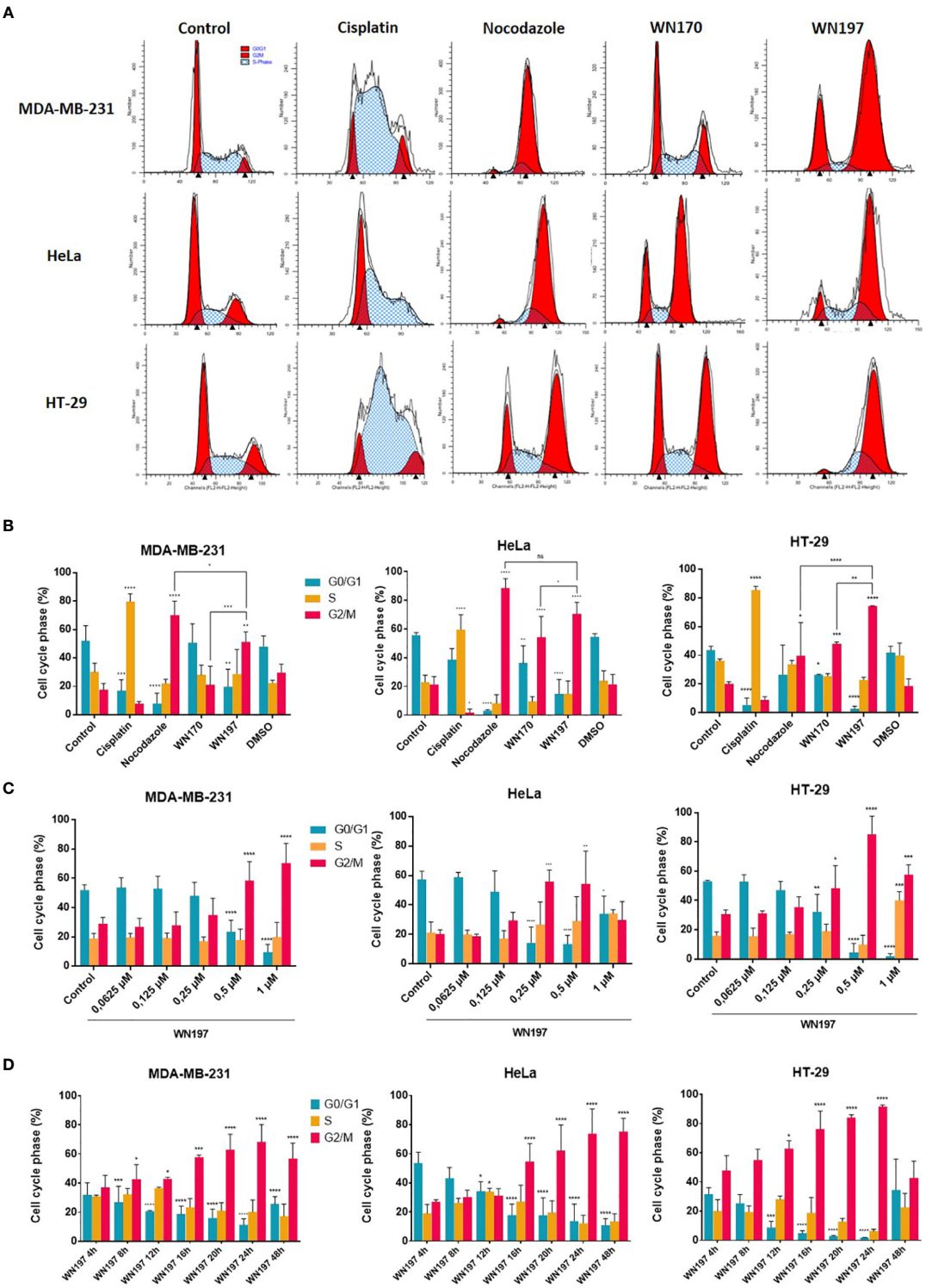

FIGURE 5 | WN197 induced cell cycle accumulation in the G2/M phase. **(A)** Cytograms (G0/G1 and G2/M first and second peaks respectively), and **(B)** flow cytometry analysis of MDA-MB-231, HeLa, and HT-29 cells repartition in the cell cycle 24 h after treatments with cisplatin (20 µM, S phase arrest control), nocodazole (84 nM, M phase arrest control), WN170 or WN197 (0.5 µM). **(C)** Dose-response analysis by flow cytometry of G2/M phase accumulation 24 h after treatments with WN197. **(D)** Time course analysis by flow cytometry of the cell cycle repartition in cell lines untreated (control) or treated with WN197 (0.5 µM). Statistic were based on two-way ANOVA followed by Dunnett's test (*p<0,05, **p<0,01, ***p<0,005 and ****p<0,001) on three independent experiments.

present after doxorubicin treatment (positive apoptotic control) in **Supplementary Figure S1**.

To determine the lower dose necessary to induce a G2/M phase accumulation, flow cytometry experiments were performed with increasing concentrations of WN197 and results are shown in **Figure 5C**. A G2/M phase accumulation was significantly induced by WN197 from 0.5 to 1 μM for MDA-MB-231, 0.25 to 0.5 μM for HeLa and 0.25 to 1 μM for HT-29.

A kinetic of treatment with WN197 (0.5 μM) was realized on the three adenocarcinoma cell lines by flow cytometry to determine the earliest-induced G2/M accumulation (**Figure 5D**). After 8 h of treatments, the cell cycle was modified for MDA-MB-231 with a significant accumulation in G2/M. A later effect after 12 h and 16 h of treatment was observed respectively for HT-29 and HeLa.

Cell cycle arrest phase was further determined by Western blot analysis of major cell cycle regulators: Cdk1, cyclin B, Cdc25C phosphatase, and histone H3 (**Figure 6A**). The Cdk1/cyclin B complex that forms the also called MPF (M-phase Promoting Factor) is required for the transition from G2 to M phase of the cell cycle. During the G2/M transition, Cdk1 is activated by dephosphorylation of its threonine 14 and tyrosine 15 residues (inhibitory phosphorylations) by the active Cdc25C phosphatase that requires prerequisite dephosphorylation on threonine 161 (59, 60). In comparison to the untreated control, the phosphorylation of Cdk1 on tyrosine 15 was increased after cisplatin, WN170 or WN197 treatments in the three adenocarcinoma cell lines, while it decreased after treatments with doxorubicin or nocodazole in HeLa and HT-29 and was slightly identical in MDA-MB-231 treated with doxorubicin. The cyclin B amount was increased after WN197 treatment in the three cell lines. Cdc25C was decreased in MDA-MB-231 and HT-29, and increased in HeLa after treatments with WN197 compared to untreated conditions. The inhibitory phosphorylation of Cdc25C on serine 216 was enhanced by WN197 treatments compared to untreated conditions in the three cell lines. On the contrary, a decrease of this phosphorylation was obtained after nocodazole treatments, consistent with the former detection of an activated form of MPF except for HT-29. Finally, histone H3 phosphorylation on serine 10 is involved in mitotic chromatin condensation and is a marker for entry in the M phase after activation of the Cdk1/Cyclin B complex (61). In WN197 treated cells, histone H3 was

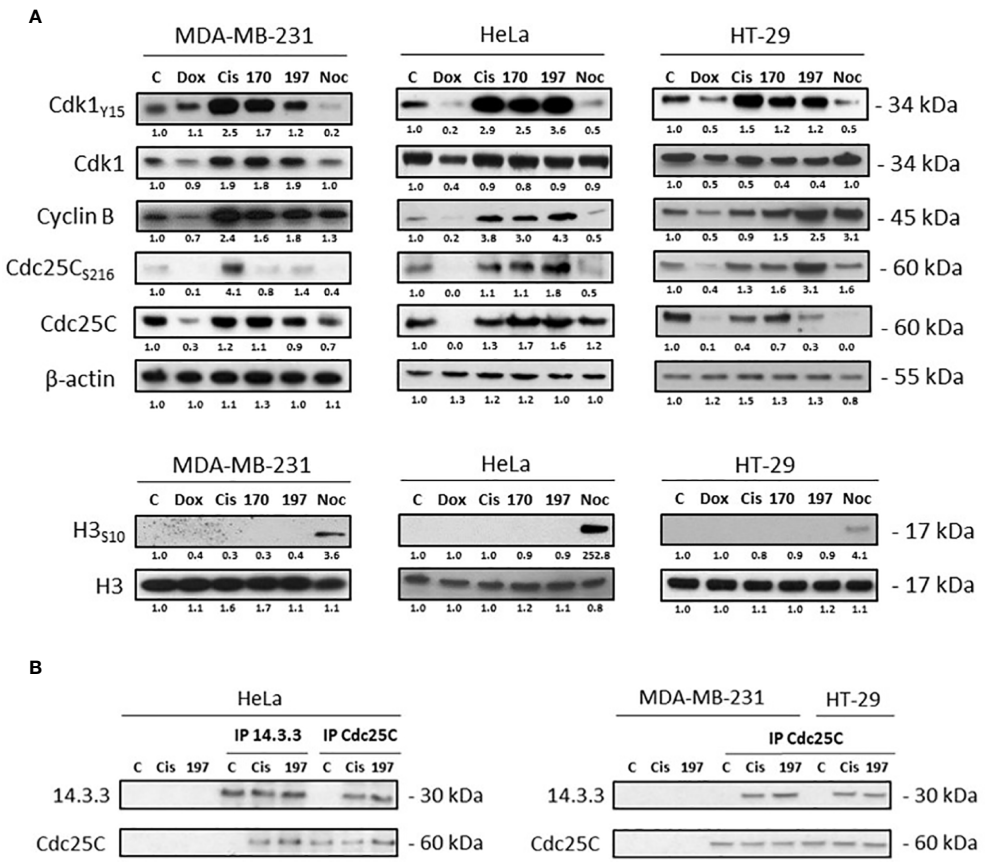

FIGURE 6 | WN197 arrested the cell cycle in G2. **(A)** Western Blot analysis of cells treated for 24 h with doxorubicin (5 μM), cisplatin (20 μM), WN170, WN197 (0.5 μM), or nocodazole (84 nM). β-actin was used as a loading control. For H3 phosphorylation, respective H3 total levels were used as loading controls. **(B)** 14-3-3 and Cdc25C immunoprecipitations were realized in cell lines treated for 24 h with cisplatin (20 μM) or WN197 (0.5 μM). Relative protein levels were expressed by densitometry using Image J software (Fiji Software, v1.52i). Results were representative of three independent experiments.

not phosphorylated on serine 10, showing that cancer cells were stopped in the G2 phase before they could reach the M phase. On the contrary in nocodazole treated adenocarcinoma lines in which an arrest in the M phase occurs, histone H3 was phosphorylated on serine 10.

Furthermore, as seen in **Figure 6B**, Cdc25C phosphorylated on serine 216 was trapped by 14-3-3 as shown by Cdc25C or 14-3-3 immunoprecipitations realized in HeLa, and Cdc25C immunoprecipitations in MDA-MB-231 and HT-29 cells after 24 h of treatment with 0.5 μM of WN197. The binding was observed after cisplatin treatment but not in untreated controls.

WN197 Induces Autophagy

Apoptosis is often activated after DNA damage (25, 62). However, the early apoptosis marker cleaved caspase 3 and the late apoptosis marker cleaved PARP were not detected after treatments with WN197 and WN170 in contrast to doxorubicin and cisplatin treatments (**Figure 7A**). A time-course detection of cleaved PARP and cytochrome C release in the cytoplasm at 3, 16, 24, 48, and 72 h compared to doxorubicin apoptosis positive control at 24 and 48 h (**Figures 7B, C**) and annexin V tests (**Figure S2**) confirm apoptosis is not triggered by WN197. These data indicate that apoptosis is not the programmed cell death activated.

We then determined whether WN197 and WN170 could induce autophagy. In the three adenocarcinoma cell lines, several autophagy markers (63) were detected. p62/sequestosome-1 was degraded, Beclin-1 was synthesized and LC3-I association with phosphatidyl-ethanolamine that forms LC3-II was increased as shown by accumulation of LC3-II after 24h of treatment with 0.5 μM of WN197 and WN170 (**Figure 7D**). The same changes were observed with the inhibitor of mTOR pathway, rapamycin which is known to activate the autophagy process. Moreover, immunoprecipitation carried on the mTOR complex showed that the RAPTOR component was phosphorylated on serine 792 after treatment with 0.5 μM of WN197, as seen in positive controls treated with 500 nM of rapamycin, and compared to negative controls treated with doxorubicin (**Figure 7E**).

DISCUSSION

This study aims to develop and understand the molecular properties of a new organometallic compound WN197, derived from the topoisomerase 1 inhibitor indenoisoquinoline. Previous studies highlighted action specifically correlated to the presence of a metallic atom like copper (53), iron [e.g. ferrocen/ferroquine (43, 64)], ruthenium [e.g. indenoisoquinoline (55) and various complexes (65, 66)], or platin [e.g. cisplatin (67)], and demonstrate the interest of these organometallic compounds in cancerology. More recently, a class of topoisomerase inhibitor, the indenoisoquinoline derivatives, were developed and selected for their high stability and non-drug substrate for efflux transporters involved in cell resistance (35, 68). These promising compounds are in phase I/II clinical trials (36, 68). However, constant efforts are made to increase their efficiency. The addition of a carbohydrate moiety to indenoisoquinoline derivatives significantly improves the binding affinity to DNA due to a stronger interaction through hydrogen bonds (69). Hereby, we synthesised a new copper indenoisoquinoline derivative. The copper(II) addition to the indenoisoquinoline backbone significantly enhance the toxicity on triple-negative breast MDA-MB-231 and cervix HeLa cancer cell lines. Those two cell lines are related to breast and cervix cancers with high mortality rates in women. In addition, the toxicity is obtained at lower doses compared to human non-tumorigenic epithelial cell line MCF-10A. The use of low doses in chemotherapy could be of particular interest and represent an advantage with less risk of adverse side effects. Further experiments will help to determine if WN197 has specificity at the cellular level.

The viability assays showed that low doses are necessary to induce cell death in breast, cervix, and colon cancer cell lines, from three of the most prevalent adenocarcinomas. The IC_{50} are under the values obtained for most other Top1 inhibitors that usually range from concentration of 1 to 10 μM except for thiosemicarbazone or pyrimidine-derived compounds (53). The medium value of 0.5 μM, close to the IC_{50} for the three adenocarcinoma cell lines, was further chosen to decipher the molecular pathways involved in the anti-proliferative effect of WN197. Topoisomerases are overexpressed in M phase in cancer cells and generate a high number of DNA breaks under the action of Top inhibitors (12, 14, 15). Cells overexpressing topoisomerases have shown better responses to Top inhibitors (70, 71). Using low doses of the compound could be useful to avoid unwanted normal cell death. Such strategies of low minimal but necessary anti-tumorigenic doses are often employed for anthracycline to limit cardiotoxicity (72, 73).

We determined the extent of DNA damage induced by the new compound, with immunofluorescence and Western blot analysis of a front-line activated marker of DNA breaks, the γH2AX histone. The recruitment of γH2AX normally occurs at the site of DNA breaks after exposition to Top1 or Top2 poisons (74, 75). Higher level of DNA breaks is observed with WN197 compared to the control copper-free compound WN170, proving that the presence of a metal atom increases the efficiency to induce DNA damage. DNA breaks appear early around 30 min after addition of the product. In parallel, *in vitro* tests reveal that WN197 inhibits Top1 at low doses, corresponding to the IC_{50}, and Top2 at higher doses up to 1 μM showing a dose-dependent action. The copper complex WN197 is a Top1 poison that forms a ternary complex with the DNA (interfacial inhibition) as indenoisoquinoline derivatives (24).

After DNA damage is induced, DDR effectors are activated, as shown in Western blot experiments. The upstream kinases ATM, ATR, Chk1, and Chk2 are phosphorylated after 24 h of treatment with 0.5 μM of WN197, a prerequisite for their activation (76, 77). Both SSB (ATR, Chk1) and DSB (ATM, Chk2) markers are detected at a concentration capable to inhibit Top1. Top1 are known to generate SSB and Top2 DSB. However, Top1 poisons produce SSB that can be converted into DSB, the most dangerous type of DNA break, at the replication fork stalling (78, 79) explaining the activation of

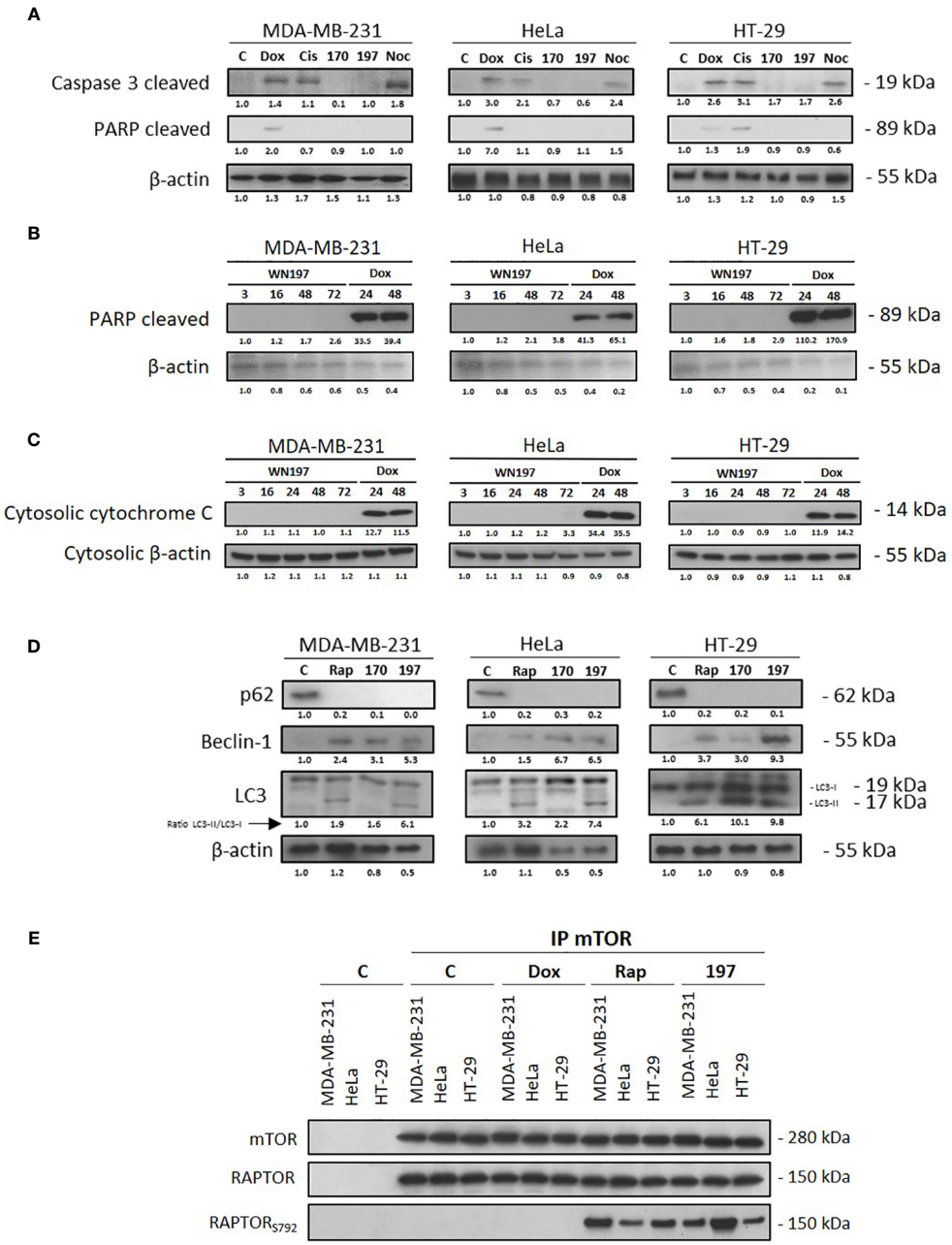

FIGURE 7 | WN197-induced autophagy. Cells were treated for 24 h with doxorubicin (5 μM), cisplatin (20 μM), WN170, WN197 (0.5 μM), nocodazole (84 nM) or rapamycin (0.5 μM). **(A)** Cleaved caspase 3 and PARP analysis by Western blots. Western blot analysis, after 3, 16, (24 or not), 48 and 72 h of treatment with WN197 or doxorubicin for 24 and 48 h, of **(B)** cleaved PARP or **(C)** cytosolic cytochrome **(C, D)** p62, Beclin-1, and LC3 markers analysis by Western blot. LC3 levels were expressed upon the LC3-II/LC3-I ratio. β-actin levels were used as a loading control. Relative protein levels were expressed by densitometry using Image J software (Fiji Software, v1.52i). **(E)** mTOR immunoprecipitations were realized in cell lines untreated or treated with doxorubicin (5 μM), rapamycin (0.5 μM) or WN197 (0.5 μM) for 24 h and followed by Western blots.

both SSB and DSB markers in our experiments. The cell cycle arrest induced by 0.5 μM of WN197 occurs in the G2/M phase for all cancer cell lines analysed, as early as 8 h or 16 h with a maximal number of arrested cells after 24 h of treatment and is maintained at 48 h. Concentration values ranging from 0.25 μM to 1 μM of WN197 are necessary to trigger the G2/M arrest. This result is consistent with the dose-dependent inhibitory effect obtained in the *in vitro* topoisomerase inhibition tests where Top1 inhibition is obtained with values between 0.2 μM and 0.5 μM. Above 1 μM a different DNA migration profile is detected showing WN197 poison activity is lost for a different type of inhibition. A catalytic mode of inhibition could occur through

intercalation of WN197 into DNA. At doses above 1 μM, the compound exerts a dual Top1/Top2 inhibitory activity and intercalation properties as demonstrated by the melting curves and the fluorescence measurements. The planar indenoisoquinoline skeleton of WN197 displays an increased intercalation into DNA compared to WN170. The high affinity of the Cu(II) complex with DNA can be attributed to the π-cation interaction between the base pairs and the atom of Cu(II) coordinated with ligands, but also to the capability to increase the π-π interaction between the base pairs of DNA and a second ligand molecule (80, 81). At high doses, DNA intercalation could avoid topoisomerase access to its fixation site similarly to a catalytic inhibitor. Such mechanism is found with anthracyclines such as doxorubicin whose poison activity at low doses is lost for an intercalating catalytic inhibitory activity at high doses. Due to a strong affinity for DNA duplexes, those anthracycline compounds prevent Top2 binding to DNA (75, 82).

To determine the exact arrest phase in the cell cycle, analyses were further conducted. To allow the G2 to M phase transition, Cdc25C dephosphorylates on residues tyrosine 15 and threonine 14, leading to its activation (83, 84). Cdk1 activation in the MPF complex phosphorylates histone H3 on serine 10 to allow DNA condensation during mitosis (61). After 24 h of treatments, an increase in the inhibitory serine 216 phosphorylation of Cdc25C is detected. This phosphorylation is recognized by 14-3-3 (85) to form a complex with Cdc25C, as shown in the three adenocarcinomas, by immunoprecipitation. Sequestration of Cdc25C by 14.3.3 impedes Cdk1 dephosphorylation on tyrosine 15 and histone H3 phosphorylation does not occur on serine 10 in the three cell lines after treatment with WN197 for 24 h. The cancer cell lines lack the required MPF activation and H3 phosphorylation to allow an M phase entry and remain arrested in G2. In addition, cyclin B accumulates in our experiments concomitantly and is not destroyed by the proteasome as expected at the end of the M phase (86, 87). p53 and its target the cell cycle inhibitor p21 are increased after WN197 treatments. p53 is involved in cell-cycle arrest by a transcriptional activation of p21 capable to inhibit Cdk1/cyclin B and cell-cycle progression through mitosis (88–90). p53 also targets 14-3-3 and blocks G2/M transition (91). Altogether, the results demonstrate that WN197 at low doses with a Top1 poison activity arrest adenocarcinoma cells in G2. After DNA damage have been induced, activation of the DDR pathways normally ensures repairs but when damage is too extended, cells undergo a programmed death (92, 93). While most of the actual topoisomerase inhibitors induce apoptosis (25, 62), WN197 triggers autophagy. Among topoisomerase I inhibitors, a camptothecin derivative irinotecan and an indenoisoquinoline compound NSC706744 were reported to activate autophagy with the absence of apoptosis (94, 95). After 24 h of treatment with low doses of WN197 (0.5 μM), autophagy markers are detected by Western blots: synthesis of Beclin-1 (96), increase in LC3-II/LC3-I ratio (97), and degradation of p62 (98). It was previously shown, after DNA damage, that the mTORC1 complex was inhibited by RAPTOR phosphorylation (on multiple sites including serine 792) in a negative feedback loop to induce autophagy (99, 100). We further show autophagy is triggered through the phosphorylation of RAPTOR in the mTOR complex. This mechanism of activation is similar to the mTORC1 inhibitor rapamycin (101). Our results show that under WN197 treatment from 3 to 72 h, cells die by a caspase-independent mechanism as classical markers annexin V staining, caspase 3 and PARP cleavage, cytoplasmic cytochrome C released were not detected. It also has to be noted, no sub-G1 cells were detected after WN197 treatment while they were after doxorubicin known to induce apoptosis. Previous data on breast cancer cells have showed autophagy could mask and delay apoptosis but was associated with an early release of cytochrome C from mitochondria which is not the case in our experiments (102). Cytochrome C is not released when autophagy is triggered and mitochondria degraded in autophagosomes (103). Several studies have described autophagy as dependent on wild-type p53 depletion or inhibition (104). WN197 action is associated with an increase in p53 and p53 phosphorylation. However, the induced-autophagy does not dependent on the cell lines p53 status. HeLa cells express wild-type p53 that end up as functionally null when targeted to degradation by E6 endogenous papillomavirus protein, while MDA-MB-231 and HT-29 display p53 mutations resulting in positive gain of function (105). Nevertheless, WN197 induced-autophagy is in agreement with an increase of p21 level and the G2 arrest detected our experiments in cancer cells. Several anti-apoptotic effects of p21 can explain the choice of an autophagic cell death instead of apoptosis. High levels of p21 are known to block Cdk1/cyclin B and to inhibit apoptosis through down-regulation of caspase-2 (106), stabilization of anti-apoptotic cellular inhibitor of apoptosis protein-1, c-IAP1 (107), and inhibition of procaspase 3 activity (108). Another additional mechanism through Beclin-1 could play an important role in apoptosis inhibition and autophagy. Beclin-1 protein expression was shown necessary to block the apoptotic cascade after induced-DNA damage (102, 109) and to activate autophagy under low doses of chemotherapeutics (rapamycin, tamoxifen) in breast and ovarian cancers (110, 111).

CONCLUSION

Copper(II) indenoisoquinoline complex WN197 displays an anti-cancerous activity at low doses inhibiting Top1. MDA-MB-231 (triple negative breast cancer cells), HeLa (cervix cancer cells), and HT-29 (colon cancer cells), cancer cells accumulate DNA breaks and arrest in the G2 phase of the cell cycle. This arrest is characterized by the inactivation of the Cdc25C phosphatase through phosphorylation on serine 216 and binding to 14.3.3 that consequently leaves in its inactive form the MPF (a phosphorylated form of Cdk1 associated to accumulated cyclin B). Autophagy is further processed by the RAPTOR effector phosphorylation in the mTOR complex, and associated to p21 overexpression. WN197 appears as a new efficient drug to counteract cancer cells when used at low doses. The action mechanism of the copper complex is summarized in **Figure 8**. Its use in chemotherapy could particularly benefit patients with cancer cells overexpressing topoisomerases or sensitize cancer cells to other DNA modifying agents including DNA adducts inducer, methylating agents, or PARP inhibitors (112, 113).

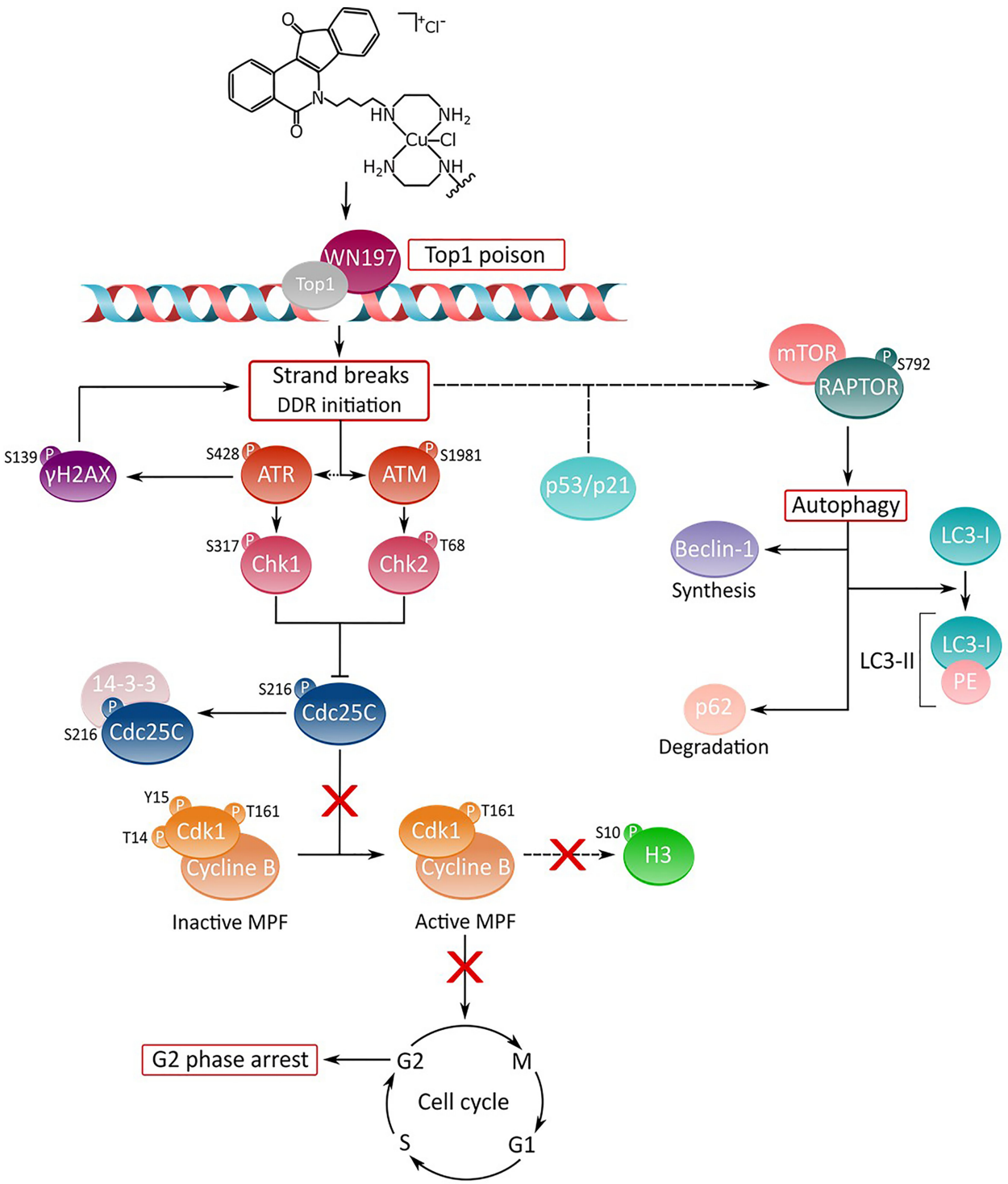

FIGURE 8 | Deciphering of the molecular mechanisms of the novel copper(II) indenoisoquinoline complex WN197. WN197 inhibits topoisomerases I at low doses in a poison mode and forms a ternary complex with the topoisomerase and DNA, leading to strand breaks accumulation. Phosphorylated H2AX (γH2AX) localizes at the sites of DNA damage. The DNA damage response pathway is activated: ATM and ATR kinases are phosphorylated, and subsequently activate Chk1 and Chk2, leading to Cdc25C phosphorylation on serine 216 (S216), and to its binding to 14-3-3. Consequently, Cdk1 remains phosphorylated on tyrosine 15 (Y15), impeding the activation of the MPF (Cdk1/Cyclin B) and the phosphorylation of H3 on serine 10 (S10). Cancer cells arrest in the G2 phase of the cell cycle. The DDR also leads to an increase in p53 and p21 followed by an autophagic cell death characterized by the phosphorylation of RAPTOR on serine 792 (S792) in the mTORC1 complex, the synthesis of Beclin-1, the formation of LC3-II (complex LC3-I/PE (phosphatidylethanolamine)), and the degradation of p62.

DATA AVAILABILITY STATEMENT

The raw data supporting the conclusions of this article will be made available by the authors, without undue reservation.

AUTHOR CONTRIBUTIONS

Conceptualization: CM, LP, KC, and AM. Performing experiments: CM, NW, TB, LP, KC, and AM. Manuscript reviewing: A-SV-E. Writing and editing: CM, LP, KC, and AM. All authors contributed to the article and approved the submitted version.

FUNDING

CM is a recipient of a doctoral fellowship from the French ministry. This work was supported by the CNRS, the University of Lille, and by grants from the "Ligue Contre le Cancer, Comités Nord et Aisne" (AM).

ACKNOWLEDGMENTS

We are sincerely indebted to Arlette Lescuyer (UMR-CNRS 8576) for helpful discussions, and Corentin Spriet (Univ. Lille, CNRS, Inserm, CHU Lille, Institut Pasteur de Lille, US 41 - UMS 2014 - PLBS, F-59000 Lille, France) for his help with microscopy. We acknowledge C. Delabre for HR-MS analysis and micronanalysis and Nathalie Jouy (IRCL, Lille) for annexin V analysis.

SUPPLEMENTARY MATERIAL

The Supplementary Material for this article can be found online at: https://www.frontiersin.org/articles/10.3389/fonc.2022.837373/full#supplementary-material

Supplementary Figure 1 | Cytograms obtained after flow cytometry analysis of MDA-MB-231 cells 24 h after treatments or not with WN197 (0.5 μM) or apoptosis positive control doxorubicin (5 μM, showing sub-G1 accumulation).

Supplementary Figure 2 | Detection of apoptosis feature by annexin V-propidium iodide (PI). MDA-MB-231, HeLa, and HT-29 cells were cultivated to 80% of confluence, incubated or not for 24 h with WN170 (0.5 μM), WN197 (0.5 μM), camptothecin (20 μM; CPT) or doxorubicin (5 μM; Doxo), trypsinized, and washed in ice-cold PBS. Cell suspensions were treated with PI and annexin V-FITC reagent (Apoptosis Detection Kit, BD) using the manufacturer's protocol before they were analysed by flow cytometry **(**CytoFLEX LX, Beckman Coulter**)** with Kaluza analysis software (v2.1.1). **(A)** Y-axis: number of PI-stained cells. X-axis: number of annexin V-FITC-stained cells. The lower left quadrant represents non-apoptotic cells (annexin V-FITC-negative and PI-negative cells; B–), the lower right quadrant represents early apoptotic cells (annexin V-FITC-positive and PI-negative cells; B+-), the upper right quadrant represents late apoptotic/necrotic cells (annexin V-FITC-positive and PI-positive cells; B++), and the upper left quadrant represents prenecrotic cells (annexin V-FITC-negative and PI-positive cells; B-+). **(B)** Representative histograms. Camptothecin and doxorubicin induced apoptosis in the three cancer cell lines, while WN170 and WN197 had no effect compared to the control.

REFERENCES

1. Bray F, Ferlay J, Soerjomataram I, Siegel RL, Torre LA, Jemal A. Global Cancer Statistics 2018: GLOBOCAN Estimates of Incidence and Mortality Worldwide for 36 Cancers in 185 Countries. *CA Cancer J Clin* (2018) 68:394–424. doi: 10.3322/caac.21492
2. Curtin NJ. DNA Repair Dysregulation From Cancer Driver to Therapeutic Target. *Nat Rev Cancer* (2012) 12:801–17. doi: 10.1038/nrc3399
3. O'Connor MJ. Targeting the DNA Damage Response in Cancer. *Mol Cell* (2015) 60:547–60. doi: 10.1016/j.molcel.2015.10.040
4. Fernández X, Díaz-Ingelmo O, Martínez-García B, Roca J. Chromatin Regulates DNA Torsional Energy *via* Topoisomerase II-Mediated Relaxation of Positive Supercoils. *EMBO J* (2014) 33:1492–501. doi: 10.15252/embj.201488091
5. Pommier Y, Sun Y, Huang SYN, Nitiss JL. Roles of Eukaryotic Topoisomerases in Transcription, Replication and Genomic Stability. *Nat Rev Mol Cell Biol* (2016) 17:703–21. doi: 10.1038/nrm.2016.111
6. Nielsen CF, Zhang T, Barisic M, Kalitsis P, Hudson DF. Topoisomerase IIa is Essential for Maintenance of Mitotic Chromosome Structure. *Proc Natl Acad Sci USA* (2020) 117:12131–42. doi: 10.1073/pnas.2001760117
7. Hanke A, Ziraldo R, Levene SD. DNA-Topology Simplification by Topoisomerases. *Molecules* (2021) 26:1–24. doi: 10.3390/molecules26113375
8. Spakman D, Bakx JAM, Biebricher AS, Peterman EJG, Wuite GJL, King GA. Unravelling the Mechanisms of Type 1A Topoisomerases Using Single-Molecule Approaches. *Nucleic Acids Res* (2021) 49:5470–92. doi: 10.1093/nar/gkab239
9. Pommier Y, Leo E, Zhang H, Marchand C. DNA Topoisomerases and Their Poisoning by Anticancer and Antibacterial Drugs. *Chem Biol* (2010) 17:421–33. doi: 10.1016/j.chembiol.2010.04.012
10. Branca M, Giorgi C, Ciotti M, Santini D, Di Bonito L, Costa S, et al. Over-Expression of Topoisomerase Iiα Is Related to the Grade of Cervical Intraepithelial Neoplasia (CIN) and High-Risk Human Papillomavirus (HPV), But Does Not Predict Prognosis in Cervical Cancer or HPV Clearance After Cone Treatment. *Int J Gynecol Pathol* (2006) 25:383–92. doi: 10.1097/01.pgp.0000209573.54457.32
11. Coss A, Tosetto M, Fox EJ, Sapetto-Rebow B, Gorman S, Kennedy BN, et al. Increased Topoisomerase Iiα Expression in Colorectal Cancer Is Associated With Advanced Disease and Chemotherapeutic Resistance *via* Inhibition of Apoptosis. *Cancer Lett* (2009) 276:228–38. doi: 10.1016/j.canlet.2008.11.018
12. Heestand GM, Schwaederle M, Gatalica Z, Arguello D, Kurzrock R. Topoisomerase Expression and Amplification in Solid Tumours: Analysis of 24,262 Patients. *Eur J Cancer* (2017) 83:80–7. doi: 10.1016/j.ejca.2017.06.019
13. Shigematsu H, Ozaki S, Yasui D, Yamamoto H, Zaitsu J, Taniyama D, et al. Overexpression of Topoisomerase II Alpha Protein Is a Factor for Poor Prognosis in Patients With Luminal B Breast Cancer. *Oncotarget* (2018) 9:26701–10. doi: 10.18632/oncotarget.25468
14. Villman K, Ståhl E, Liljegren G, Tidefelt U, Karlsson MG. Topoisomerase II-α Expression in Different Cell Cycle Phases in Fresh Human Breast Carcinomas. *Mod Pathol* (2002) 15:486–91. doi: 10.1038/modpathol.3880552
15. Lee YC, Lee CH, Tsai HP, An HW, Lee CM, Wu JC, et al. Targeting of Topoisomerase I for Prognoses and Therapeutics of Camptothecin-Resistant Ovarian Cancer. *PloS One* (2015) 10:1–19. doi: 10.1371/journal.pone.0132579
16. Cortez D. Replication-Coupled DNA Repair. *Mol Cell* (2019) 74:866–76. doi: 10.1016/j.molcel.2019.04.027
17. Toledo L, Neelsen KJ, Lukas J. Replication Catastrophe: When a Checkpoint Fails Because of Exhaustion. *Mol Cell* (2017) 66:735–49. doi: 10.1016/j.molcel.2017.05.001

18. Gan W, Guan Z, Liu J, Gui T, Shen K, Manley JL, et al. R-Loop-Mediated Genomic Instability Is Caused by Impairment of Replication Fork Progression. *Genes Dev* (2011) 25:2041–56. doi: 10.1101/gad.17010011
19. Surova O, Zhivotovsky B. Various Modes of Cell Death Induced by DNA Damage. *Oncogene* (2013) 32:3789–97. doi: 10.1038/onc.2012.556
20. Roos WP, Kaina B. DNA Damage-Induced Cell Death: From Specific DNA Lesions to the DNA Damage Response and Apoptosis. *Cancer Lett* (2013) 332:237–48. doi: 10.1016/j.canlet.2012.01.007
21. Sharma A, Singh K, Almasan A. Histone H2AX Phosphorylation: A Marker for DNA Damage. *Methods Mol Biol* (2012) 920:613–26. doi: 10.1007/978-1-61779-998-3_40
22. Smith HL, Southgate H, Tweddle DA, Curtin NJ. DNA Damage Checkpoint Kinases in Cancer. *Expert Rev Mol Med* (2020) 8:e2. doi: 10.1017/erm.2020.3
23. Liu K, Zheng M, Lu R, Du J, Zhao Q, Li Z, et al. The Role of CDC25C in Cell Cycle Regulation and Clinical Cancer Therapy: A Systematic Review. *Cancer Cell Int* (2020) 20:1–16. doi: 10.1186/s12935-020-01304-w
24. Pommier Y, Kiselev E, Marchand C. Interfacial Inhibitors. *Bioorganic Med Chem Lett* (2015) 25:3961–5. doi: 10.1016/j.bmcl.2015.07.032
25. Larsen AK, Escargueil AE, Skladanowski A. From DNA Damage to G2 Arrest: The Many Roles of Topoisomerase II. *Prog Cell Cycle Res* (2003) 5:295–300.
26. Eikenberry S. A Tumor Cord Model for Doxorubicin Delivery and Dose Optimization in Solid Tumors. *Theor Biol Med Model* (2009) 6:1–20. doi: 10.1186/1742-4682-6-16
27. Conte PF, Gennari A, Landucci E, Orlandini C. Role of Epirubicin in Advanced Breast Cancer. *Clin Breast Cancer* (2000) 1 Suppl 1:S46–51. doi: 10.3816/cbc.2000.s.009
28. Pendleton M, Lindsey RH Jr, Felix CA, Grimwade D, Osheroff N. Topoisomerase II and Leukemia MaryJean. *Ann NY Acad Sci* (2015) 1310:98–110. doi: 10.1111/nyas.12358
29. Kalyanaraman B. Teaching the Basics of the Mechanism of Doxorubicin-Induced Cardiotoxicity: Have We Been Barking Up the Wrong Tree? *Redox Biol* (2020) 29:101394. doi: 10.1016/j.redox.2019.101394
30. Zhang W, Gou P, Dupret JM, Chomienne C, Rodrigues-Lima F. Etoposide, an Anticancer Drug Involved in Therapy-Related Secondary Leukemia: Enzymes at Play. *Transl Oncol* (2021) 10:101169. doi: 10.1016/j.tranon.2021.101169
31. Cappetta D, De Angelis A, Sapio L, Prezioso L, Illiano M, Quaini F, et al. Oxidative Stress and Cellular Response to Doxorubicin: A Common Factor in the Complex Milieu of Anthracycline Cardiotoxicity. *Oxid Med Cell Longev* (2017) 2017:1521020–33. doi: 10.1155/2017/1521020
32. Sritharan S, Sivalingam N. A Comprehensive Review on Time-Tested Anticancer Drug Doxorubicin. *Life Sci* (2021) 278:119527. doi: 10.1016/j.lfs.2021.119527
33. Li F, Jiang T, Li Q, Ling X. Camptothecin Analogues and Their Molecular Targets. *Am J Cancer Res* (2017) 7:2350–94.
34. Holcombe RF, Kong KM, Wimmer D. Combined Topoisomerase I Inhibition for the Treatment of Metastatic Colon Cancer. *Anticancer Drugs* (2004) 15:569–74. doi: 10.1097/01.cad.0000132232.28888.21
35. Pommier Y, Cushman M, Doroshow JH. Novel Clinical Indenoisoquinoline Topoisomerase I Inhibitors: A Twist Around the Camptothecins. *Oncotarget* (2018) 9:37286–8. doi: 10.18632/oncotarget.26466
36. Thomas A, Pommier Y. Targeting Topoisomerase I in the Era of Precision Medicine. *Clin Cancer Res* (2019) 25:6581–9. doi: 10.1158/1078-0432.CCR-19-1089
37. Rosenberg B, VanCamp L, Trosko JE, Mansour VH. Platinum Compounds: A New Class of Potent Antitumour Agents. *Nature* (1969) 5191:385–6. doi: 10.1038/222385a0
38. Alderden RA, Hall MD, Hambley TW. The Discovery and Development of Cisplatin. *J Chem Educ* (2006) 83:728–34. doi: 10.1021/ed083p728
39. Dilruba S, Kalayda GV. Platinum-Based Drugs: Past, Present and Future. *Cancer Chemother Pharmacol* (2016) 77:1103–24. doi: 10.1007/s00280-016-2976-z
40. Komeda S, Casini A. Next-Generation Anticancer Metallodrugs. *Curr Top Med Chem* (2012) 12:219–35. doi: 10.2174/156802612799078964
41. Zhang P, Sadler PJ. Advances in the Design of Organometallic Anticancer Complexes. *J Organomet Chem* (2017) 839:5–14. doi: 10.1016/j.jorganchem.2017.03.038
42. Anthony EJ, Bolitho EM, Bridgewater HE, Carter OWL, Donnelly JM, Imberti C, et al. Metallodrugs Are Unique: Opportunities and Challenges of Discovery and Development. *Chem Sci* (2020) 11:12888–917. doi: 10.1039/d0sc04082g
43. Jaouen G, Vessières A, Top S. Ferrocifen Type Anti Cancer Drugs. *Chem Soc Rev* (2015) 44:8802–17. doi: 10.1039/c5cs00486a
44. Gasser G, Metzler-Nolte N. The Potential of Organometallic Complexes in Medicinal Chemistry. *Curr Opin Chem Biol* (2012) 16:84–91. doi: 10.1016/j.cbpa.2012.01.013
45. Szczepaniak A, Fichna J. Organometallic Compounds and Metal Complexes in Current and Future Treatments of Inflammatory Bowel Disease and Colorectal Cancer-A Critical Review. *Biomolecules* (2019) 9:398. doi: 10.3390/biom9090398
46. Ndagi U, Mhlongo N, Soliman ME. Metal Complexes in Cancer Therapy – An Update From Drug Design Perspective. *Drug Des Devel Ther* (2017) 11:599–616. doi: 10.2147/DDDT.S119488
47. Kostova I, Balkansky S. Metal Complexes of Biologically Active Ligands as Potential Antioxidants. *Curr Med Chem* (2013) 20:4508–39. doi: 10.2174/09298673113206660288
48. Santini C, Pellei M, Gandin V, Porchia M, Tisato F, Marzano C. Advances in Copper Complexes as Anticancer Agents. *Chem Rev* (2014) 114:815–62. doi: 10.1021/cr400135x
49. Denoyer D, Clatworthy SAS, Cater MA. Copper Complexes in Cancer Therapy. *Met Ions Life Sci* (2018) 18:469–506. doi: 10.1515/9783110470734-022
50. Marzano C, Pellei M, Tisato F, Santini C. Copper Complexes as Anticancer Agents. *Anticancer Agents Med Chem* (2012) 9:185–211. doi: 10.2174/187152009787313837
51. Shobha Devi C, Thulasiram B, Aerva RR, Nagababu P. Recent Advances in Copper Intercalators as Anticancer Agents. *J Fluoresc* (2018) 28:1195–205. doi: 10.1007/s10895-018-2283-7
52. Liang X, Wu Q, Luan S, Yin Z, He C, Yin L, et al. A Comprehensive Review of Topoisomerase Inhibitors as Anticancer Agents in the Past Decade. *Eur J Med Chem* (2019) 171:129–68. doi: 10.1016/j.ejmech.2019.03.034
53. Molinaro C, Martoriati A, Pelinski L, Cailliau K. Copper Complexes as Anticancer Agents Targeting Topoisomerases I and II. *Cancers (Basel)* (2020) 12:1–26. doi: 10.3390/cancers12102863
54. Wambang N, Schifano-Faux N, Aillerie A, Baldeyrou B, Jacquet C, Bal-Mahieu C, et al. Synthesis and Biological Activity of Ferrocenyl Indeno[1,2-C]Isoquinolines as Topoisomerase II Inhibitors. *Bioorganic Med Chem* (2016) 24:651–60. doi: 10.1016/j.bmc.2015.12.033
55. Wambang N, Schifano-Faux N, Martoriati A, Henry N, Baldeyrou B, Bal-Mahieu C, et al. Synthesis, Structure, and Antiproliferative Activity of Ruthenium(II) Arene Complexes of Indenoisoquinoline Derivatives. *Organometallics* (2016) 35:2868–72. doi: 10.1021/acs.organomet.6b00440
56. Ahn G, Lansiaux A, Goossens JF, Bailly C, Baldeyrou B, Schifano-Faux N, et al. Indeno[1,2-C]Isoquinolin-5,11-Diones Conjugated to Amino Acids: Synthesis, Cytotoxicity, DNA Interaction, and Topoisomerase II Inhibition Properties. *Bioorganic Med Chem* (2010) 18:8119–33. doi: 10.1016/j.bmc.2010.08.025
57. Lewis KA, Lilly KK, Reynolds EA, Sullivan WP, Kaufmann SH, Cliby WA. Ataxia Telangiectasia and Rad3-Related Kinase Contributes to Cell Cycle Arrest and Survival After Cisplatin But Not Oxaliplatin. *Mol Cancer Ther* (2009) 8:855–63. doi: 10.1158/1535-7163.MCT-08-1135
58. Wagner JM, Karnitz LM. Cisplatin-Induced DNA Damage Activates Replication Checkpoint Signaling Components That Differentially Affect Tumor Cell Survival. *Mol Pharmacol* (2009) 76:208–14. doi: 10.1124/mol.109.055178
59. Timofeev O, Cizmecioglu O, Settele F, Kempf T, Hoffmann I. Cdc25 Phosphatases Are Required for Timely Assembly of CDK1-Cyclin B at the G2/M Transition. *J Biol Chem* (2010) 285:16978–90. doi: 10.1074/jbc.M109.096552
60. Sur S, Agrawal DK. Phosphatases and Kinases Regulating CDC25 Activity in the Cell Cycle: Clinical Implications of CDC25 Overexpression and Potential Treatment Strategies. *Mol Cell Biochem* (2016) 416:33–46. doi: 10.1007/s11010-016-2693-2
61. Hans F, Dimitrov S. Histone H3 Phosphorylation and Cell Division. *Oncogene* (2001) 20:3021–7. doi: 10.1038/sj.onc.1204326

62. Pommier Y. Drugging Topoisomerases: Lessons and Challenges. *ACS Chem Biol* (2013) 8:82–95. doi: 10.1021/cb300648v
63. Molinaro C, Martoriati A, Cailliau K. Proteins From the DNA Damage Response: Regulation, Dysfunction, and Anticancer Strategies. *Cancers (Basel)* (2021) 13:3819. doi: 10.3390/cancers13153819
64. Kondratskyi A, Kondratska K, Vanden Abeele F, Gordienko D, Dubois C, Toillon RA, et al. Ferroquine, the Next Generation Antimalarial Drug, has Antitumor Activity. *Sci Rep* (2017) 7:1–15. doi: 10.1038/s41598-017-16154-2
65. Lee SY, Kim CY, Nam TG. Ruthenium Complexes as Anticancer Agents: A Brief History and Perspectives. *Drug Des Devel Ther* (2020) 14:5375–92. doi: 10.2147/DDDT.S275007
66. Pragti, Kundu BK, Mukhopadhyay S. Target Based Chemotherapeutic Advancement of Ruthenium Complexes. *Coord Chem Rev* (2021) 448:214169. doi: 10.1016/j.ccr.2021.214169
67. Dasari S, Bernard Tchounwou P. Cisplatin in Cancer Therapy: Molecular Mechanisms of Action. *Eur J Pharmacol* (2014) 740:364–78. doi: 10.1016/j.ejphar.2014.07.025
68. Marzi L, Sun Y, Huang SYN, James A, Difilippantonio S, Pommier Y. The Indenoisoquinoline LMP517: A Novel Antitumor Agent Targeting Both TOP1 and TOP2. *Mol Cancer Ther* (2020) 19:1589–97. doi: 10.1158/1535-7163.MCT-19-1064
69. Beck DE, Agama K, Marchand C, Chergui A, Pommier Y, Cushman M. Synthesis and Biological Evaluation of New Carbohydrate-Substituted Indenoisoquinoline Topoisomerase I Inhibitors and Improved Syntheses of the Experimental Anticancer Agents Indotecan (LMP400) and Indimitecan (LMP776). *J Med Chem* (2014) 57:1495–512. doi: 10.1021/jm401814y
70. Ali Y, Abd Hamid S. Human Topoisomerase II Alpha as a Prognostic Biomarker in Cancer Chemotherapy. *Tumor Biol* (2016) 37:47–55. doi: 10.1007/s13277-015-4270-9
71. Zhong W, Yang Y, Zhang A, Lin W, Liang G, Ling Y, et al. Prognostic and Predictive Value of the Combination of TOP2A and HER2 in Node-Negative Tumors 2 Cm or Smaller (T1N0) Breast Cancer. *Breast Cancer* (2020) 27:1147–57. doi: 10.1007/s12282-020-01142-8
72. Barrett-Lee PJ, Dixon JM, Farrell C, Jones A, Leonard R, Murray N, et al. Expert Opinion on the Use of Anthracyclines in Patients With Advanced Breast Cancer at Cardiac Risk. *Ann Oncol* (2009) 20:816–27. doi: 10.1093/annonc/mdn728
73. McGowan JV, Chung R, Maulik A, Piotrowska I, Walker JM, Yellon DM. Anthracycline Chemotherapy and Cardiotoxicity. *Cardiovasc Drugs Ther* (2017) 31:63–75. doi: 10.1007/s10557-016-6711-0
74. Kinders RJ, Hollingshead M, Lawrence S, Ji U, Tabb B, Bonner WM, et al. Development of a Validated Immunofluorescence Assay for γh2ax as a Pharmacodynamic Marker of Topoisomerase I Inhibitor Activity. *Clin Cancer Res* (2010) 16:5447–57. doi: 10.1158/1078-0432.CCR-09-3076
75. Marinello J, Delcuratolo M, Capranico G. Anthracyclines as Topoisomerase II Poisons : From Early Studies to New Perspectives. *Int J Mol Sci* (2018) 19:3480. doi: 10.3390/ijms19113480
76. Dai Y, Grant S. New Insights Into Checkpoint Kinase 1 in the DNA Damage Response Signaling Network. *Clin Cancer Res* (2010) 16:376–83. doi: 10.1158/1078-0432.CCR-09-1029
77. Smith J, Mun Tho L, Xu N, A. Gillespie D. The ATM-Chk2 and ATR-Chk1 Pathways in DNA Damage Signaling and Cancer. *Adv Cancer Res* (2010) 108:73–112. doi: 10.1016/B978-0-12-380888-2.00003-0
78. Kuzminov A. Single-Strand Interruptions in Replicating Chromosomes Cause Double-Strand Breaks. *Proc Natl Acad Sci USA* (2001) 98:8241–6. doi: 10.1073/pnas.131009198
79. Saleh-Gohari N, Bryant HE, Schultz N, Parker KM, Cassel TN, Helleday T. Spontaneous Homologous Recombination Is Induced by Collapsed Replication Forks That Are Caused by Endogenous DNA Single-Strand Breaks. *Mol Cell Biol* (2005) 25:7158–69. doi: 10.1128/MCB.25.16.7158-7169.2005
80. Deng JH, Luo J, Mao YL, Lai S, Gong YN, Zhong DC, et al. Π-π Stacking Interactions: Non-Negligible Forces for Stabilizing Porous Supramolecular Frameworks. *Sci Adv* (2020) 6:1–9. doi: 10.1126/sciadv.aax9976
81. Thakuria R, Nath NK, Saha BK. The Nature and Applications of π-π Interactions: A Perspective. *Cryst Growth Des* (2019) 19:523–8. doi: 10.1021/acs.cgd.8b01630
82. Atwal M, Swan RL, Rowe C, Lee KC, Armstrong L, Cowell IG, et al. Intercalating TOP2 Poisons Attenuate Topoisomerase Action at Higher Concentrations. *Mol Pharmacol* (2019) 2019:475–84. doi: 10.1124/mol.119.117259
83. Pines J. Four-Dimensional Control of the Cell Cycle. *Nat Cell Biol* (1999) 1:E73–9. doi: 10.1038/11041
84. Donzelli M, Draetta GF. Regulating Mammalian Checkpoints Through Cdc25 Inactivation. *EMBO Rep* (2003) 4:671–7. doi: 10.1038/sj.embor.embor887
85. Peng CY, Graves PR, Thoma RS, Wu Z, Shaw AS, Piwnica-Worms H. Mitotic and G2 Checkpoint Control: Regulation of 14-3-3 Protein Binding by Phosphorylation of Cdc25C on Serine-216. *Science* (1997) 277:1501–5. doi: 10.1126/science.277.5331.1501
86. Shabbeer S, Omer D, Berneman D, Weitzman O, Alpaugh A, Pietraszkiewicz A, et al. BRCA1 Targets G2/M Cell Cycle Proteins for Ubiquitination and Proteasomal Degradation. *Oncogene* (2013) 32:5005–16. doi: 10.1038/onc.2012.522
87. Bassermann F, Eichner R, Pagano M. The Ubiquitin Proteasome System - Implications for Cell Cycle Control and the Targeted Treatment of Cancer. *Biochim Biophys Acta* (2014) 1843:150–62. doi: 10.1016/j.bbamcr.2013.02.028
88. Bunz F, Dutriaux A, Lengauer C, Waldman T, Zhou S, Brown JP, et al. Requirement for P53 and P21 to Sustain G2 Arrest After DNA Damage. *Science* (1998) 282:1497–501. doi: 10.1126/science.282.5393.1497
89. Agarwal ML, Agarwal A, Taylor WR, Stark GR. P53 Controls Both the G2/M and the G1 Cell Cycle Checkpoints and Mediates Reversible Growth Arrest in Human Fibroblasts. *Proc Natl Acad Sci USA* (1995) 92:8493–7. doi: 10.1073/pnas.92.18.8493
90. Chen J. The Cell-Cycle Arrest and Apoptotic and Progression. *Cold Spring Harb Perspect Biol* (2016) 6:a026104. doi: 10.1101/cshperspect.a026104
91. Hermeking H, Lengauer C, Polyak K, He TC, Zhang L, Thiagalingam S, et al. 14-3-3sigma Is a P53-Regulated Inhibitor of G2/M Progression. *Mol Cell* (1997) 1:3–11. doi: 10.1016/s1097-2765(00)80002-7
92. Borges HL, Linden R, Wang JY. DNA Damage-Induced Cell Death: Lessons From the Central Nervous System. *Cell Res* (2008) 18:17–26. doi: 10.1038/cr.2007.110
93. Norbury CJ, Zhivotovsky B. DNA Damage-Induced Apoptosis. *Oncogene* (2004) 23:2797–808. doi: 10.1038/sj.onc.1207532
94. Cheng Y, Ren X, Hait WN, Yang JM. Therapeutic Targeting of Autophagy in Disease: Biology and Pharmacology. *Pharmacol Rev* (2013) 65:1162–97. doi: 10.1124/pr.112.007120
95. Kinders RJ, Dull AB, Wilsker D, LeBlanc A, Mazcko C, Hollingshead MG, et al. Antitumor Activity of Indenoisoquinoline Inhibitors of Topoisomerase 1 (TOP1) *via* Apoptosis and Autophagocytosis Pathways in Animal Models. *J Clin Oncol* (2017) 35:11588. doi: 10.1200/jco.2017.35.15_suppl.11588
96. Vega-Rubín-de-celis S. The Role of Beclin 1-Dependent Autophagy in Cancer. *Biol (Basel)* (2020) 9:1–13. doi: 10.3390/biology9010004
97. Kadowaki M, Karim MR. Cytosolic LC3 Ratio as a Quantitative Index of Macroautophagy. *Methods Enzymol* (2009) 451:199–213. doi: 10.1016/S0076-6879(08)03613-6
98. Bjørkøy G, Lamark T, Pankiv S, Øvervatn A, Brech A, Johansen T. Chapter 12 Monitoring Autophagic Degradation of P62/SQSTM1. *Methods Enzymol* (2009) 451:181–97. doi: 10.1016/S0076-6879(08)03612-4
99. Dunlop EA, Hunt DK, Acosta-Jaquez HA, Fingar DC, Tee AR. ULK1 Inhibits Mtorc1 Signaling, Promotes Multisite Raptor Phosphorylation and Hinders Substrate Binding. *Autophagy* (2011) 7:737–47. doi: 10.4161/auto.7.7.15491
100. Ma Y, Vassetzky Y, Dokudovskaya S. Mtorc1 Pathway in DNA Damage Response. *Biochim Biophys Acta - Mol Cell Res* (2018) 1865:1293–311. doi: 10.1016/j.bbamcr.2018.06.011
101. Young Chul K, Kun-Liang G. mTOR: A Pharmacologic Target for Autophagy Regulation. *J Clin Invest* (2015) 125:25–32. doi: 10.1172/JCI73939
102. Abedin MJ, Wang D, McDonnell MA, Lehmann U, Kelekar A. Autophagy Delays Apoptotic Death in Breast Cancer Cells Following DNA Damage. *Cell Death Differ* (2007) 14:500–10. doi: 10.1038/sj.cdd.4402039
103. Ma K, Chen G, Li W, Kepp O, Zhu Y, Chen Q. Mitophagy, Mitochondrial Homeostasis, and Cell Fate. *Front Cell Dev Biol* (2020) 24:467. doi: 10.3389/fcell.2020.00467

104. Tasdemir E, Maiuri MC, Galluzzi L, Vitale I, Djavaheri-Mergny M, D'Amelio M, et al. Regulation of Autophagy by Cytoplasmic P53. *Nat Cell Biol* (2008) 10:676–87. doi: 10.1038/ncb1730
105. Leroy B, Girard L, Hollestelle A, Minna JD, Gazdar AF, Soussi T. Analysis of TP53 Mutation Status in Human Cancer Cell Lines: A Reassessment. *Hum Mutat* (2014) 35:756–65. doi: 10.1002/humu.22556
106. Baptiste-Okoh N, Barsotti AM, Prives C. Caspase 2 is Both Required for P53-Mediated Apoptosis and Downregulated by P53 in a P21-Dependent Manner. *Cell Cycle* (2008) 7:1133–8. doi: 10.4161/cc.7.9.5805
107. Steinman RA, Johnson DE. P21waf1 Prevents Down-Modulation of the Apoptotic Inhibitor Protein C-IAP1 and Inhibits Leukemic Apoptosis. *Mol Med* (2000) 6:736–49. doi: 10.1007/BF03402190
108. Suzuki A, Tsutomi Y, Akahane K, Araki T, Miura M. Resistance to Fas-Mediated Apoptosis: Activation of Caspase 3 Is Regulated by Cell Cycle Regulator P21(WAF1) and IAP Gene Family ILP. *Oncogene* (1998) 17:931–9. doi: 10.1038/sj.onc.1202021
109. Pattingre S, Tassa A, Qu X, Garuti R, Liang XH, Mizushima N, et al. Bcl-2 Antiapoptotic Proteins Inhibit Beclin 1-Dependent Autophagy. *Cell* (2005) 122:927–39. doi: 10.1016/j.cell.2005.07.002
110. Bursch W, Ellinger A, Kienzl H, Torok L, Pandey S, Sikorska M, et al. Active Cell Death Induced by the Anti-Estrogens Tamoxifen and ICI 164 384 in Human Mammary Carcinoma Cells (MCF-7) in Culture: The Role of Autophagy. *Carcinogenesis* (1996) 17:1595–607. doi: 10.1093/carcin/17.8.1595
111. Ogier-Denis E, Codogno P. Autophagy: A Barrier or an Adaptive Response to Cancer. *Biochim Biophys Acta* (2003) 1603:113–28. doi: 10.1016/s0304-419x(03)00004-0
112. Eich M, Roos WP, Nikolova T, Kaina B. Contribution of ATM and ATR to the Resistance of Glioblastoma and Malignant Melanoma Cells to the Methylating Anticancer Drug Temozolomide. *Mol Cancer Ther* (2013) 12:2529–40. doi: 10.1158/1535-7163.MCT-13-0136
113. Jo U, Senatorov IS, Zimmermann A, Saha LK, Murai Y, Kim SH, et al. Novel and Highly Potent ATR Inhibitor M4344 Kills Cancer Cells With Replication Stress, and Enhances the Chemotherapeutic Activity of Widely Used DNA Damaging Agents. *Mol Cancer Ther* (2021) 20:1431–41. doi: 10.1158/1535-7163.MCT-20-1026

Conflict of Interest: Author NW was employed by AGAT Laboratories, Intertek.

The remaining authors declare that the research was conducted in the absence of any commercial or financial relationships that could be construed as a potential conflict of interest.

Publisher's Note: All claims expressed in this article are solely those of the authors and do not necessarily represent those of their affiliated organizations, or those of the publisher, the editors and the reviewers. Any product that may be evaluated in this article, or claim that may be made by its manufacturer, is not guaranteed or endorsed by the publisher.

Copyright © 2022 Molinaro, Wambang, Bousquet, Vercoutter-Edouart, Pélinski, Cailliau and Martoriati. This is an open-access article distributed under the terms of the Creative Commons Attribution License (CC BY). The use, distribution or reproduction in other forums is permitted, provided the original author(s) and the copyright owner(s) are credited and that the original publication in this journal is cited, in accordance with accepted academic practice. No use, distribution or reproduction is permitted which does not comply with these terms.

Publication (review 1)

Proteins from the DNA Damage Response: Regulation, Dysfunction, and Anticancer Strategies

cancers

MDPI

Review

Proteins from the DNA Damage Response: Regulation, Dysfunction, and Anticancer Strategies

Caroline Molinaro, Alain Martoriati and Katia Cailliau *

Univ. Lille, CNRS, UMR 8576-UGSF-Unité de Glycobiologie Structurale et Fonctionnelle, F-59000 Lille, France; caroline.molinaro@univ-lille.fr (C.M.); alain.martoriati@univ-lille.fr (A.M.)
* Correspondence: katia.cailliau-maggio@univ-lille.fr

Simple Summary: Cells respond to genotoxic stress through complex protein pathways called DNA damage response (DDR). These mechanisms ensure the preservation of genomic integrity and activate DNA repair, cell cycle regulation, and, ultimately, programmed cell death. When altered, the DDR protein network leads to several diseases, particularly cancers. In recent years, the vulnerabilities of the DDR network have been successfully exploited to improve cancer treatments using DNA damage strategies and therapies combination.

Abstract: Cells respond to genotoxic stress through a series of complex protein pathways called DNA damage response (DDR). These monitoring mechanisms ensure the maintenance and the transfer of a correct genome to daughter cells through a selection of DNA repair, cell cycle regulation, and programmed cell death processes. Canonical or non-canonical DDRs are highly organized and controlled to play crucial roles in genome stability and diversity. When altered or mutated, the proteins in these complex networks lead to many diseases that share common features, and to tumor formation. In recent years, technological advances have made it possible to benefit from the principles and mechanisms of DDR to target and eliminate cancer cells. These new types of treatments are adapted to the different types of tumor sensitivity and could benefit from a combination of therapies to ensure maximal efficiency.

Keywords: DNA damage response; DNA damage therapy; DNA repair; DDR inhibitors; cell cycle; cancers

check for updates

Citation: Molinaro, C.; Martoriati, A.; Cailliau, K. Proteins from the DNA Damage Response: Regulation, Dysfunction, and Anticancer Strategies. *Cancers* **2021**, *13*, 3819. https://doi.org/10.3390/cancers13153819

Academic Editor: Karen E. Pollok

Received: 24 June 2021
Accepted: 26 July 2021
Published: 29 July 2021

Publisher's Note: MDPI stays neutral with regard to jurisdictional claims in published maps and institutional affiliations.

Copyright: © 2021 by the authors. Licensee MDPI, Basel, Switzerland. This article is an open access article distributed under the terms and conditions of the Creative Commons Attribution (CC BY) license (https://creativecommons.org/licenses/by/4.0/).

1. Introduction

The genome is constantly harmed by spontaneous damage caused by endogenous factors produced by normal cellular physiological conditions such as bases alteration, aberrant DNA enzyme function or oxidation, and by a large variety of exogenous genotoxic factors [1]. Cells have evolved a complex network of hundreds of proteins, named the DNA damage response (DDR), to ensure genome integrity and the expression of dedicated proteins to each cell type. The quality control mechanisms of DDR senses DNA damage, coordinates DNA repair with cell cycle arrest, and ensures cell death when repairs are not possible [2]. The detection of DNA damage involves the recruitment of various repair protein complexes depending on the type of break. Classically, phosphatidylinositol-3-kinase-related kinases ATM (ataxia-telangiectasia mutated), ATR (ATM- and Rad3-related), and DNA-PKcs (DNA-dependent protein kinase, catalytic subunit) are activated [3]. These kinases phosphorylate numerous targets at the DNA damage sites including CHK1/2 (checkpoint kinases 1/2) and histone H2AX. Substrates of CHK kinases are effectors for DNA repair, transcription, and cell-cycle control, such as BRCA1, NBS1, P53, CDC25, and CDKs (cyclin-dependent kinase). The cellular outcome depends on the types but also on the severity of DNA damage, the cell cycle state, chromatin modifications, post-translational events, and non-coding RNA. Cells with excessive or unrepairable DNA

undergo an apoptotic P53-dependent death or another type of programmed cell death that does not rely on caspase activation.

Many natural cellular events rely on DNA breaks/repairs and use part of the DDR network to fulfill specific physiological functions. Despite physical and chemical agents, several biological agents induce severe DNA damage. When DDR processes are damaged or bypassed, DNA damage elicits mutations and heritable changes resulting in pathologies (e.g., immunodeficiency, inflammation, neurodegeneration, aging, cardiovascular diseases, and cancer). When and how the DDR complex signaling network of proteins is controlled to ensure the right cell outcome; and how the vulnerabilities are exploited in precision medicine to target and treat cancers (from single inhibitor to combined treatments) are hereby highlighted and updated in the present review.

2. DDR Proteins Activation Is Function of the Type of DNA Damage

Cells encounter tens of thousands of DNA lesions every day arising from endogenous cellular functions and exogenous environmental factors. Intracellular and external DNA damaging events create more than a single type of lesion. DNA damage inflicted to the DNA's double helix includes base damage that does not involve breakage of the phosphodiester backbone or single-strand DNA breaks (SSBs) and double-strand breaks (DSBs). Single base alterations are generated by depurination, deamination, alkylation (usually by guanine methylation), oxidation (production of 8-oxo-7, 8-dihydroguanine), hydrolysis or chemical bonds cleavage in DNA, base analog incorporation, and stable covalent DNA adducts formation. Two-base alterations are formed by a thymine-thymine dimer or by cross-linking under the effect of a bifunctional alkylating agent. DNA strand breaks arise from oxidative or DNA replication stress, transcriptional stalling, failure to repair processes, and abnormal high effectors activation [4,5]. SSBs are converted into DSB lesions during DNA replication [6] (Figure 1).

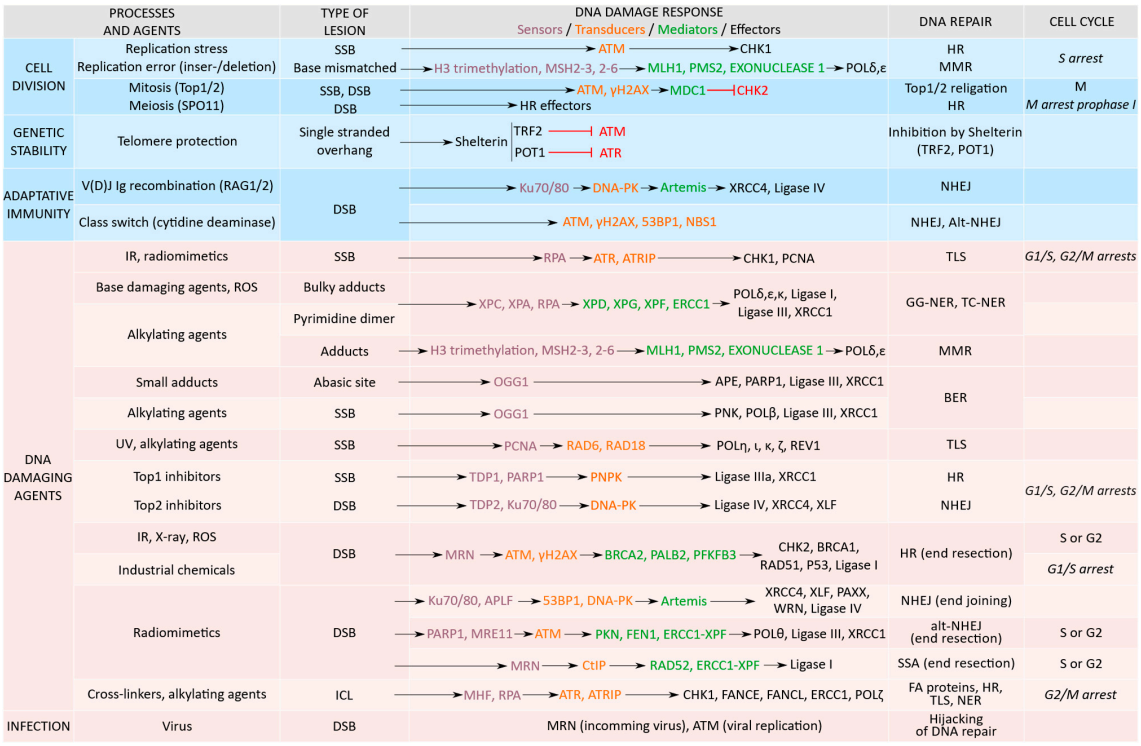

Figure 1. Classification of proteins from the DNA repair processes according to the DNA damaging agents, the type of DNA damage in relation with recruited effectors, repair mechanisms, and cell cycle phases occurrence or induced arrests. DNA damaged proteins are classified as sensors (violet), transducers (orange), mediators (green), and effectors (black). Natural processes, showed in the upper blue part, display a non-canonical DDR. They inhibit effectors, restrain the DNA repair in mitosis and protects telomere ends (inhibited proteins in red). Canonical DDR pathways are shown in the pink lower part.

2.1. Replication Stress and DNA Damage

DNA replication disturbances or the slowing/stalling of the replication fork progression during DNA synthesis generate replication stress. Replication stress is a source of massive DNA damage. It arises as a consequence of normal cellular reactions involving DNA, or upon exposure to external agents. Exogenous factors affecting DNA are numerous, ranging from physical agents such as ionizing radiation to genotoxic chemicals (organic compounds such as aromatic substances, or inorganic compounds such as heavy metals [7]) and biological agents including pathogens (bacteria, DNA, and RNA viruses), fungi, and plants [8–10]. Those agents also increase the ROS formation that enhances DNA damage [11].

The endogenous factors responsible for replication stress are numerous. DNA sequences can form special structures such as secondary hairpin loops, G-quadruplexes, display damage, or replication/transcription conflict, R-loops, topological stress constraints, or dysregulation of replicative proteins such as RPA, a natural barrier for replication forks [12]. Imbalance in the cellular pool of dNTPs also affect DNA polymerases inactivation and require two different RAD51-mediated pathways for restart and repair [13].

Damaged DNA bases, as a consequence of natural reactions such as depurination, base oxidation, and bulky adducts, are not recognized as templates by DNA polymerases, creating a source of replication stress [14]. On the contrary, interstrand crosslinks do not generate extensive areas of ssDNA (single stranded DNA) and are repaired by the FA (Fanconi Anemia) pathway [15].

Replication forks operate on genomic regions with special chromatin structures such as telomeres and centromeres that represent a challenge for the replisome. R-loops, formed by a DNA/RNA duplex and a ssDNA, arise during transcription and replication-transcription collision. They promote transcription-associated recombination and genome instability in mitotic and meiotic cell cycles [16] and the exposed ssDNA is processed into a DSB by transcription-coupled NER (nucleotide excision repair) [17].

Replication/transcription collisions can lead to transcription-associated recombination and chromosomal rearrangements. To minimize these encounters, both processes are temporally and spatially separated in different cell cycle phases S and G1 [18]. The THO/TREX (TRanscription-Export) and THSC/TREX-2 complexes that mediate the processing of mRNAs and nuclear export are required to avoid replication-transcription conflicts and may prevent R-loop formation [19].

2.2. Physiological DNA Breaks Involved in Normal Cellular Processes

Several natural events, necessary for cellular integrity, require programmed DNA lesions and a partial DDR recruitment [20] (Figure 1).

The replication stress checkpoint enables the DDR to act in coordination with the replisome to protect the stalled forks from degradation and to restart broken forks. Replication forks stalling triggers the activation of the ATR-CHK1 pathway for stabilization and is followed by the release of CHK1 from the chromatin, allowing for the phosphorylation and degradation of CDC25A and cell cycle S phase arrest [21–23].

During the course of the cell cycle, in the replicative and the mitosis phases, DNA is naturally cut and religated by topoisomerases (Top) to control DNA topology. To allow DNA or RNA polymerase action, topoisomerases (Top1 and 2) bind to DNA, cut the phosphate backbone of, respectively, one or two strands (SSB or DSB), and untangle DNA before the DNA backbone is resealed. Mitotic DDR functions to coordinate microtubule/kinetochore attachment and spindle assembly [24]. Top2 is necessary for chromosomal segregation before anaphase, and for chromosomal structure maintenance [25]. In mitosis, damage of condensed chromosomes activate initial upstream effectors such as H2AX-MDC1 (mediator of DNA damage checkpoint 1) platform, and the downstream signaling cascade is restrained (inhibition of CHK2), waiting for further progression into the cell cycle [26,27].

DNA lesions also occur through enzymatic reactions and chemical modifications from intracellular metabolism, the release of free radicals, reactive oxygen species (ROS), reactive nitrogen species (RNS), and reactive carbonyl species (RCS) that trigger a chain of reactions and result in a production of exocyclic adducts to DNA bases [28].

The production of male and female gametes for sexual reproduction involves a natural DSB formed during the meiotic recombination process by the SPO11 topoisomerase [29,30]. Meiotic DSBs occur in prophase from the leptotene to the pachytene stage of the first meiotic division. They are essential to allow chromosomal DNA exchange between non-homologous sister chromatids when they are paired to create genetic diversity [31]. A failure in this process directs germ cells to aneuploidy and leads to congenital disorder or pregnancy loss. During spermatogenesis, when histones are substituted by protamines, Top2 generates temporal DNA breaks to relax DNA that needs to be repaired properly before the end of spermiogenesis to avoid mature spermatozoa with fragmented DNA [32,33]. During meiotic sex chromosome inactivation (MSCI) in males, the sequestration of DDR factors (ATR and H2AX histone) to the XY chromatin away from the autosome is critical for meiosis progression [34].

The variable exon regions encoding the antigen recognition sites of B and T lymphocyte's receptors, respectively involved in humoral and cellular-mediated immunity, are generated by a V (variable), D (diversity), or J (joining) genes recombination during early development. In response to an antigen, class switch recombination modifies the immunoglobulin genes in B lymphocytes [35]. V(D)J recombination starts by the formation of a DSB in DNA by RAG1 and RAG2 (recombination activating gene 1/2) proteins and are repaired through the recruitment of the non-homologous end-joining (NHEJ) pathway composed by Ku70/80, DNA-PK, XRCC4 (X-ray repair cross-complementing protein 4)/DNA-ligase IV, and Artemis [36–38]. The class switch recombination (CSR) breaks are initiated in B-cells by a specific activation-induced cytidine deaminase (AID) that mediates DNA deamination. Unlike the V(D)J recombination, the CSR depends on non-canonical BER and MMR to generate DSBs that are finally joined by NHEJ for blunt ends and alt-NHEJ for staggered breaks. DDR factors such as H2AX, ATM, 53BP1, and NBS1 are also involved in CSR [39]. CSR and V(D)J recombination represent a paradigm to study regulations among the various DNA repair pathways. A SAGA deubiquitination module was recently shown to promote DNA repair and class switch recombination through DNA-PK and ATM-induced γH2AX formation [40]. These proteins were found to function upstream of various double-stranded DNA repair pathways. Interestingly, IgG were found to be produced in non-immune cells (spermatozoids) through CSR with RAG1/2 and AID, suggesting a role in fertilization, but also that gametes are far more complex in their DDR regulation [41].

Telomeres located at chromosomal ends protect chromosomes from end-to-end fusions and abnormal mitosis segregation. Telomeric DNA presents a single-stranded overhang protected by a specialized capping complex, called shelterin, composed by TRF1 and TRF2 (telomere repeat-binding factor 1 and 2), TIN2 (TRF1-interaction factor 2), RAP1 (repressor activator protein 1), TPP1, and POT1 (protection of telomere 1), that blocks the recognition by the DDR repair machinery [42]. After each replication, telomeres are partly deprotected, recruit a non-canonical DDR in the G2 phase of the cell cycle, and reconstruct the end protection complex. Only the MRN complex (MRE11/RAD50/NBS1) and the ATM kinase are activated, while the downstream diffusible DDR signaling proteins, CHK2 and P53, are not, avoiding downstream cell-cycle inhibition [43].

3. Structural Organization of the DDR

The type of ends and the structures of the DNA breaks dictate the selection and the recruitment of repair factors. The choice of the cell response and its outcome depends on factors from the DNA repair pathway, the cell cycle checkpoints, the expression level of effectors from the P53 family, the chromatin state, the genomic location of the break, the

post-translational modifications undergone by cytoplasmic or nuclear proteins, and RNA metabolism [44,45].

3.1. Selection of the Repair Mechanisms

After the detection of DNA damage, repair mechanisms are activated depending on the break types (Figure 1). The critical steps of the DNA repair process are the recognition and the signaling of the DNA lesions. DNA breaks can be repaired by direct reversal of the chemical reaction of the DNA damage using O^6-methylguanine methyltransferase (MGMT), or by removal and replacement of the damaged bases [46]. Repair processes involve an important number of effectors, multiple interactions, and post-translational modifications [47,48].

For SSBs, the following three main excision repair pathways exist: NER (nucleotide excision repair), BER (base excision repair), and MMR (mismatch repair). NER includes XPC/A key components for the recognition of the DNA lesion, ERCC1, ERCC4 (XPF), and XPG for excision (excision repair cross-complementation group 1/4/6), recruitment of PCNA (proliferating cell nuclear antigen) by RFC (replication factor C) to allow the copy of the undamaged strand by DNA polymerases (δ, ε, and/or κ), and finally ligated by the ligase-I or ligase-III-XRCC1 complex [49]. The repairs of the lesions throughout the genome are processed by GG-NER (global genome NER) and those blocking transcription by TC-NER (transcription coupled NER). BER is activated for bulky adducts. BER starts with OGG1 (8-Oxoguanine glycosylase), forming abasic (AP) sites cleaved by AP endonucleases, resulting in single-strand breaks further processed by single nucleotide replacement or synthesis and by the recruitment of PARP1/2, XRCC1, ends with polymerase β and ligase-I and III. The MMR, or strand-specific mechanism, recognizes and repairs erroneous insertion, deletion, or miss-paired bases, includes MSH (MutS Homolog) and MLH/PMS proteins. A translesion synthesis process (TLS) allows the DNA replication machinery to bypass DNA lesions such as AP sites or thymine dimers. In TLS, PCNA is ubiquitinated by RAD6 and RAD18 and allows the binding of polymerases (η, ι, κ, ζ, REV1) [50].

DSB repairs are processed by a non-homologous end joining (NHEJ), an alt-NHEJ also named micro-homology mediated end joining (MMEJ), single-strand annealing (SSA), or by a homologous directed repair (HDR) including the homologous recombination (HR). NHEJ mobilized in the G1 phase of the cell cycle requires the recognition of DNA damage by Ku70/80, the recruitment of APLF (Aprataxin and PNK-like factor), 53BP1 (P53-binding protein 1), DNA-PK, end processing by Artemis, the recruitment of PAXX (paralogue of XRCC4 and XLF) and polymerase δ, μ, and ligation by ligase-IV with partner XRCC4 and XLF (XRCC4-like factor). Alt-NHEJ/MMEJ is initiated by PARP1 and MRE11 nuclease to resect DNA-ends that generate single-stranded overhangs annealed at microhomologies and recruits polymerase θ. SSA requires RAD52 for annealing in addition to the ERCC1/4 endonucleases complex and ligase I. HR is activated in the S and G2 phases of the cell cycle and requires the ATM-MRN complex, CtIP (CtBP-interacting protein), RPA (replication protein A), BRCA1 (breast cancer 1), and PALB2 (partner and localizer of BRCA2) recruitment of BRCA2 that acts with RAD52 to mobilize RAD51 and PFKFB3 (6-phosphofructo-2-kinase/fructose-2,6-biphosphatase 3). In case of DSBs, CHK2 phosphorylates BRCA1, serving not only as a scaffold protein but also as a clock for HR repair [51]. The selection between the different DSB repair processes is, in part, driven by the length of the homologies [52,53].

Interstrand crosslinks (ICLs) are DNA strands linked with covalent bonds preventing the separation of DNA strands that are repaired by the FA (Fanconi anemia) pathway using FANCs proteins and effectors from the NER, TLS, HR, factors responsible for Fanconi anemia, and structure-specific endonucleases [54].

During gametogenesis, the DDR has a specific organization. In spermatogenesis, HR acts during the S phase to resolve the DNA damage and NHEJ in G1. Haploid spermatids use an Alt-NHEJ pathway due to the absence of the main components of the canonical NHEJ. Spermatozoa possess a truncated BER containing only the first enzyme, the 8-

oxoguanine DNA glycosylase, OGG1, to remove oxidized base adducts after oxidative damage (8-Oxoguanine lesions) [55]. Meiotic recombination in oocyte arrested in meiosis I uses HR, while oocytes in meiosis II accumulate transcripts from all the DNA repair pathways to be used after fertilization in the early embryo before transcription starts at the four-cell stage, and the canonical DDR is activated [56,57].

It was recently shown that during sleep, chromatin motion and dynamic in neuronal nuclei match DNA repairs but require a threshold of DNA damage. The general mechanism for this relationship remains to be deciphered. On the contrary, sleep deprivation affects NER, BER, HR repair processes and ERCC1, OGG1, and XRCC1 genes are decreased [58,59].

3.2. Cell Cycle Checkpoints

Checkpoint pathways arrest the cell cycle progression until DNA integrity is restored by the repair mechanisms [60]. Phosphatidylinositol 3′ kinase-related kinases (ATM, ATR, DNA-PK) phosphorylate multiple substrates. For example, a DSB allows the recruitment and the phosphorylation of the MRN (MRE11-RAD50-NBS1) complex and the ATM activation that further phosphorylates several targets: SMC1 (structural maintenance of chromosomes protein 1) activates the S-phase checkpoints and halts DNA replication, the BRCA proteins involved in HR repair, and NBS1 necessary for the ATM-dependent phosphorylation of CHK1 and CHK2. CHK1 and CHK2 phosphorylate phosphatases CDC25B/C and CDC25A promoting, respectively, a cell cycle arrest in G2/M and G1/S. These arrests involve the binding of CDC25 to 14-3-3 and a self-accelerated proteasomal degradation of CDC25. Therefore, the activation of the cyclin/CDK complexes by dephosphorylation on Thr14 and Tyr15 does not occur. Moreover, the phosphorylation of MDC1 (mediator of DNA damage checkpoint 1) by ATM, activates the S and G2/M cell cycle checkpoints and is facilitated by the phosphorylated histone H2AX (γH2AX). The phosphorylation of P53, by ATM and CHK2, activates $P21^{WAF1/CIP1}$ and Bax genes (BCL2 associated X protein), and, respectively, arrests cells in G1 or triggers apoptosis. Phosphoprotein phosphatases PP1, PP2A, PP2Cδ (WIP1), PP4, and PP6 restrain the response intensity with an action on several targets involved in recognition, signaling or recombination processes. PP5 has a contrasting activity by stimulating ATM signaling and restraining DNA-PK activity [61,62]. WIP1 is necessary for BRCA1 recruitment to the DNA lesion, 53BP1 dephosphorylation, and to promote HR repair [63] (Figure 2).

Cells are sensitive to DNA damage during mitosis and hypersensitive in antephase when they prepare to enter the M phase [64]. Even though the DDR is partially inactivated in mitosis, H2AX is phosphorylated, and the DNA-PK and MRN complexes, MDC1, and the DNA topoisomerase II binding protein 1 (TopBP1) are recruited [45]. After a DSB, mitosis progression is not halted unless a DNA break affects the centromeric or telomeric regions, while a reversible arrest is initiated in the G1 and G2 phases [65].

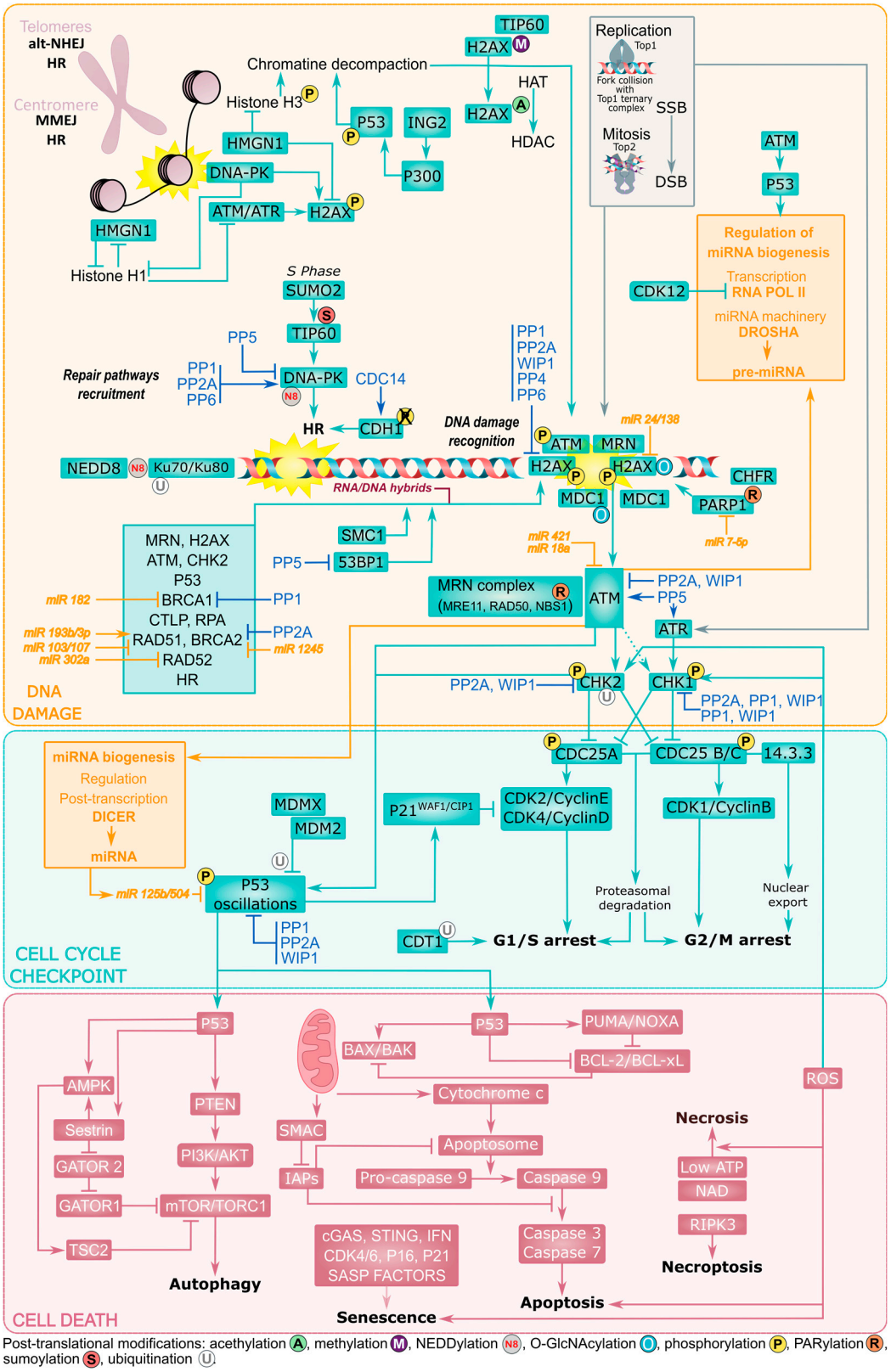

Figure 2. Regulation of the DNA damage signaling network of proteins. In the yellow panel: after DNA damage, induced for example by topoisomerases misregulation, repair pathways are selected, and major sensors/effectors are recruited to the damaged lesions. These recruitments are accompanied by many post-translational modifications of proteins with major impacts on the cell response to DNA damage, e.g., O-GlcNAcylation of H2AX and NDC1 at the DNA damage repair site, ubiquitination and NEDDylation of Ku70/80 from the NHEJ and/or PARylation of NBS1 in the MRN complex from HR, and

sumoylation of TIP60 in HR. The chromosomal state and the regions damaged mobilize different repair processes that are facilitated by chromatin decompaction through the action of HMGN1 on histone H3, histones methylation/acetylation, and ING proteins (e.g., ING2) action on phosphorylated P53. Topoisomerases misregulation induces persistent DNA breaks. The cell cycle phase controls the selected DSB repair process: HR acts in S phase. CDH1, a cofactor of APC/C (anaphase-promoting complex/cyclosome, a multi-subunit E3 ubiquitin ligase) involved in cyclin degradation, is activated by CDC14 and by DNA damage in G2, while normally inactive. CDK12 represses transcription by inhibition of RNA POLII (polymerase II). The replication factor CDT1 is proteolyzed in G1 providing a checkpoint control to avoid replication. In the blue panel: early signaling by PI3K (ATM, ATR, and DNA-PK) activates secondary kinases. CHK1 and CHK2 lead to cell cycle checkpoint regulation and arrest the cell cycle, respectively, in G2/M after CDC25C inactivation and G1/S after CDC25A inhibition. Another PI3K, PTEN, triggers cell death. Phosphatases tightly regulate phosphorylation at several levels of the signaling cascades, and counter-balance kinases. Recruited repair effectors, such as ATM, regulate miRNA biogenesis (orange) at the transcriptional and post-transcriptional levels. In return, miRNAs regulate other components of the signaling pathways. RNA/DNA hybrids facilitate the recruitment of DDR effectors to DSB. In the red panel: different cell death processes are triggered by different pathways. P53 oscillations initiate a caspase cleavage cascade and apoptosis, while the inhibition of the mTORC1 complex directs the cell outcome to autophagy. Levels of ATP and NAD dictate necrosis and senescence, and activation of the RIP3 kinase conducts to necroptosis. Senescence is only triggered when P21, P16, and CDK4/6 are activated with IFN-associated inflammatory background and results in the secretion of SASP (senescence-associated secretory phenotype) factors.

The cell cycle controls the competition between DSB resection-dependent repair pathways HR, SSA, Alt-NHEJ, and NHEJ. A DSB repair proceeds with a copy of the missing information from the sister chromatid during the S and G2 phases with the phosphorylation of the members of the MRN complex, BRCA1 and CtIP by the ATM kinase, favoring the three resection-dependent DSB repair pathways (HR, alt-NHEJ, or SSA). HR depends on CDK/cyclin and the phosphorylation of multiple substrates, including the MRN complex and CtIP. In the G1 phase, RIF1 and 53BP1 localize to the DSB, inhibit the recruitment of BRCA1, block the DNA end resection pathways, and promote NHEJ. The HR process competes with the NHEJ in interphase. The regulation of DNA-PK during the cell cycle determines the choice of the DNA repair pathway. After a DSB, in the G1 phase of the cell cycle, DNA-PK autophosphorylation on Ser2056 and activation is facilitated by its interaction with TIP60 histone acetyltransferase (HAT), and the repair process executes a NHEJ. In the S phase, the SUMO2 (small ubiquitin-related modifier 2) modification of TIP60 mediated by the PISA4-E3-ligase blocks the TIP60-induced DNA-PK activation, and HR repair is favored [58].

Cell cycle chromatin modifications regulate the coupling between DNA replication and mitosis. The initiation of DNA replication is controlled by CDT1 licensing factors. CDT1 accumulates from the M to the G1 phase and is degraded in the S phase (after poly-ubiquitination by Cullin-4-ring E3 ubiquitin ligase) to ensure a correct onset of DNA replication and prevent re-replication. In response to DNA damage, CDT1 is proteolyzed in G1 providing a checkpoint control [66].

3.3. Cell Death and P53 Signaling

The cellular outcome after the kinases cascades depends on the types and the severity of the DNA damage. Cells with excessive DNA damage or unrepairable DNA undergo a programmed cell death involving a P53-dependent mechanism such as apoptosis, or other types of cell death that do not rely on caspase-dependent activation (Figure 2).

P53 accumulates after a negative feedback loop involving an MDM2 (Murine double minute 2) inhibitor with a ubiquitin ligase activity and WIP1 phosphatase to induce cellular senescence or apoptosis. The P53 level oscillates and the oscillation numbers directly relate to the DSB quantities and to the cell death outcome that depends on the genetic context of the damaged cells [67]. A failure in these oscillations allows the cell to escape the G1 arrest. When P53 is mutated in a high-grade serous carcinoma, their reliance on the G2/M checkpoint is increased [68]. P53 maintains a cell arrest, initiates

senescence through the activation of $P21^{WAF1/CIP1}$, inhibits cyclin-dependent kinases, and the binding of retinoblastoma protein to E2F transcription factor to regulate the G1/S transition. P53 phosphorylation on Ser46 is specifically linked to the pro-apoptotic expression of PUMA and NOXA proteins, the release of mitochondrial cytochrome C, the cleavage of caspases, and apoptosis [69,70]. An exception is the mature spermatozoa that do not complete apoptosis as their nucleus and mitochondria are localized in different compartments [71]. Autophagy is mediated by ATM and nuclear P53, which activates the transcription of PTEN (phosphatase and tensin homolog), AMPK, and Sestrin that engages TSC2 (Tuberous Sclerosis Complex 2) and AKT to inhibit mTORC1. The inhibition of the DNA-PK or ATR/CHK1/RhoB-mediated lysosomal recruitment of a TSC complex also results in autophagy [72]. mTORC1 connects to the cell cycle checkpoint through the GATOR1 complex component NPRL2, which arrests the cell cycle in G1/S in P53 positive cells and in S or G2/M in P53 negative cells. mTORC1 also negatively controls ATM via S6K1/2 signaling by up-regulating two miRNAs (miR-18a and miR-421) targeting ATM mRNA [73,74]. The cellular depletion of ATP and NAD causes oxidative stress, activation of the RIPK3 (receptor-interacting protein kinase 3), and necroptosis [75]. In dividing cells, DNA lesions interfere with DNA synthesis (replication forks stalling) and the incompletely replicated DNA causes mitotic catastrophe when cells try to break through G2-arrest into the M phase [76].

Another member of the P53 family is involved in oocytes facing cumulative DNA damage when arrested in the prophase of the first meiosis division for many years in ovaries [77]. Prophase 1 oocytes in primordial follicles are unable to respond immediately to DNA damage, while all components necessary for the DNA repair including direct lesion reversal, NER, BER, MMR, HR, and NHEJ processes are present [56,78]. They depend on a G2/M DDR and P63, a member of the P53 family, activated by ATM and CHK1. During their meiotic arrest, DNA-damaged oocytes undergo a specific P63-dependent apoptotic death [79] only for severe DNA damage [80]. Later, in metaphase I and II oocytes of growing follicles, the DNA damage-induced arrest is overridden by the spindle assembly checkpoint (SAC) [81,82].

3.4. Chromatin State and Chromosomal Damage Location

The native chromatin state (heterochromatin, just transcribed DNA) and the type of damage (blunt end, overhang, adducts) influence the choice and the kinetic of the repair processes.

Chromatin compaction, such as heterochromatin, limits the accessibility of DNA damage response proteins to the DNA damage sites, making these regions difficult to repair. Chromatin local relaxation by histone H1 and high mobility group proteins (HMGs) is an early event of the DDR. HMGN1 binds to nucleosomes and reduces histone H3 phosphorylation on Ser10, a necessary site to maintain the chromatin condensed state in mitosis. TIP60 acetylates histone H2AX, a prerequisite to both its phosphorylation and ubiquitination. The phosphorylation of H2AX is mediated by ATM, ATR, or DNA-PK on the nucleosomes flanking accidental DSBs but also in natural processes of meiosis and the immune system during DNA recombination. This is an indirect effect of ING (inhibitor of growth) proteins, as ING2 on P53 is essential for the chromatin-induced decompaction allowing accessibility of the repair proteins to DNA damage sites and providing the necessary signal to translocate ATM and the MRN complex to the damaged DNA site [83]. A DSB in actively transcribed chromatin is preferentially halted and repaired by HR and end resection in G2, as they are absent in G1 [84,85]. Inactive lamina heterochromatin prefers alt-EJ [86]. Nuclear position dictates the DNA repair pathway choice. Transcriptionally active chromatin recruits HR at DNA DSBs. Open chromatin (in promoters and enhancers) is more permissive for end resection [87]. Specific chromatin locations have repair pathway preferences. Damage in the telomeres tends to inhibit NHEJ and to select alt-NHEJ or HR repair processes; centrosomes, the microtubules-organizing centers, rely on HR or MMEJ (resection mechanisms) [45,88].

3.5. Post-Translational Modifications

Proteins from the DDR are controlled by post-translational modifications, revealing a complex organizational response. Post-translational modifications modulate the chromatin structure and provide docking sites to recruit and accumulate DDR repair proteins at the DNA damage site. Phosphorylation is one of the central proteins post-translational modification and also the most studied in the initiation and the execution of the DDR response. Many different DDR proteins involved in checkpoint control and DNA repair are regulated by a cycle of phosphorylation/dephosphorylation and by the presence of DDR-kinase/phosphatase molecular switches. The kinases ATM/ATR/DNA-PK and CHK1/2 cascades are central networks in DDR activation.

Following DNA damage, several phosphatases participate in the DNA damage checkpoint activation and regulate several phosphorylations at multiple levels by dephosphorylating sensor kinases, ATM, ATR, and DNA-PK, transducer kinases CHK1/2, histones H2AX and H3, and effectors such as P53 and MDM2 [89]. PP1, PP2A, WIP1, and PP5 dephosphorylate ATM, allowing its recruitment to damaged sites [89,90]. PP5 is required for the ATR-dependent phosphorylation of CHK1 [91]. PP2A, PP5, and PP6 dephosphorylate DNA-PK on multiple sites to enhance its activity [92–94]. WIP1 dephosphorylates CHK1, promoting its release from chromatin and an increase in its kinase activity [95], and antagonizes CHK2 [96]. PP2A, PP4, PP6, and WIP1 dephosphorylate γH2AX, and PP1 dephosphorylates H3, leading to the transcriptional repression of cell cycle-regulated genes [62]. PP1 associates to PNUTS (protein phosphatase 1 nuclear-targeting subunit) [97] and WIP1 dephosphorylates and inactivates P53 [98]. PP1 dephosphorylates and positively regulates BRCA1 [99]. PP5 dephosphorylates 53BP1, leading to its release from DNA damage sites, while normally recruited to DNA damage to coordinate DDR factors localization and activation [100]. CDC14 triggers nuclear accumulation and the activation of YEN1 at anaphase to resolve recombination repair intermediates [101].

Distinct ways of regulation are used by phosphatases to regulate upstream DDR signals. WIP1 dampens the DDR with a feedback circuit, while PP2A provides fine-tuning and acts with P53 in a negative feedback loop [102] that is necessary for efficient DNA repair and post-repair restart of cell division [103]. PP2A keeps CHK2 inactive in normal conditions but, following DNA damage, CHK2 is released and followed by a late reconstitution of the PP2A/CHK2 interaction, increasing the threshold necessary for CHK2 activation [104]. Phosphatases are submitted to the DDR kinetic regulation working on different repair substrates during different time periods after DNA damage. Indeed, PP4 dephosphorylates and maintains RPA2 in a hypo-phosphorylated form immediately after DNA damage to avoid competition for ssDNA binding with other factors such as RPA1 [61,105,106].

Several other covalent modifications including ubiquitylation, sumoylation, poly-ADP-ribosylation (PARylation), neddylation, acetylation, and methylation facilitate protein recruitments to the damaged DNA [47]. SUMO and ubiquitin conjugates compete for lysine residues in target proteins [107]. The poly ADP-ribose polymerases (PARPs) modify proteins by linear or branched chains of ADP-ribose units originating from NAD rapidly after the induction of DNA breaks. More than 90% of PAR addition is mediated by PARP1. PARylated proteins are recruited through their PAR binding site. PARylation is capable of prime ubiquitination at the site of DNA lesions for mediators such as CHFR ubiquitin E3 ligases [108]. Neddylation is the link of the ubiquitin-like protein NEDD8 through its glycine carboxy-terminal to a lysine of the targeted protein, such as Ku70/80 and DNA-PK [109,110]. HATs (histone acetyltransferases) and HDACs (deacetylases) catalyze the addition or removal of acetyl groups on lysine residues, altering the chromatin structure and providing binding signals for proteins with recognition domains, to mediate key DDR activities [111]. Histone and non-histone lysine methylation can alter the protein's interaction with chromatin and recognition by reader proteins [112]. Similar to phosphorylation, the O-linked N-acetylglucosamine linkage (O-GlcNAcylation) is realized on serine or threonine residues [113]. OGT (O-GlcNAc transferase) relocates to a DNA-damaged site,

allowing for the O-GlcNAcylation of the H2AX histone and MDC1 and restrains the DDR to a specifically damaged site. The inhibition of OGT also delays DSB repair, reduces cell proliferation, and increases cell senescence [114].

3.6. ncRNAs as Emerging Regulators

Local RNA synthesis or processing, and non-coding RNA have emerged as novel pathways in the regulation of DDR. Transcription is globally impaired in response to DNA damage, with ATM/DNA-PK triggering the ubiquitination of RNAPII by NEDD4 ligase and proteasomal degradation but opening chromatin at the site of the DSB locally to allow RNA synthesis [115,116]. Moreover, DNA damage affects mRNA splicing and stability, and mRNA splicing affects DDR. Serine/arginine-rich splicing factors (SRSFs) and heterogeneous nuclear ribonucleoproteins (hnRNP) are phosphorylated by ATM/ATR. HnRNP is co-recruited with the BCRCA1/PALB2/BRCA2 complex that further recruits Rad51 and regulates proper splicing at the DNA damaged site [117].

R-loops are three-stranded structures formed by an RNA/DNA hybrid and a displaced single-stranded DNA that plays multiple roles in gene expression, DNA replication, immunoglobulin CSR, and DNA repair [118]. In normal conditions, several mechanisms prevent the deleterious effects of an accumulation of deregulated R-loops. The THO/TREX (TRanscription-EXport) and TREX-2 mRNA export complexes function in proper packaging of mRNA into export-competent mRNPs, minimizing the possibility for a nascent mRNA to re-hybridize with the strand of transcribed DNA [19]. DNA topoisomerases relax DNA-negative supercoils and SRSF1 packs nascent mRNA into ribonucleoprotein complexes in a topoisomerase 1-dependent manner [119,120]. An SR protein, the alternative splicing factor/splicing factor 2 (ASF/SF2), regulates the formation of R-loops [121]. However, the accumulation of diverse RNA-containing structures, including RNA/DNA hybrids, generates DNA damage. It has been accepted that R-loops present a block for the replication fork progression, and constitute a major cause of replication stress that gives rise to genetic instability and chromosome fragility [122,123]. R-loop-mediated genomic instability is caused by the impairment of replication fork progression [124] and a deficiency in the molecular factors responsible for R-loops prevention. On the contrary, other studies have shown that RNA/DNA hybrids are involved in DSB repair processes in HR or NHEJ [125–127]. Hybrids protect DNA 3'overhangs, preventing an excess of resection [125,128], and contribute to the recruitment of DNA repair factors such as BRCA1 [129], 53BP1 [130], RPA [131], and FA pathway proteins, including FANCD2, FANCA, and FANCM. Senataxin, in complex with BRCA1, is recruited to R-loop-rich termination regions [129]. The R-loop-driven ATR pathway acts at centromeres to promote faithful chromosome segregation [132].

DNA damage induces the production and the control of a variety of non-coding RNA (ncRNA), as follows: microRNA (miRNA), and small or long ncRNA (s/lncRNA). P53 induces lncRNA expression that controls gene expression, cell cycle, and apoptosis; DSB-induced small RNA contributes to HDR; ATM, BRCA1, and P53 regulate miRNA expression; DROSHA/DICER-dependent RNA are involved in the formation of DNA repair foci [133]. A class of sncRNA, the DNA damage response RNAs, generated in a DROSHA/DICER-dependent manner are required to recruit secondary DDR factors at the chromosomal and the telomeres DSBs [134]. Several DNA damage-induced effectors control the transcription processes of non-coding RNA by the regulation of RNA interference factors DROSHA/DICER, and RNA polymerase II [115]. On the reverse, ncRNA plays various roles in damage signaling and repair by a regulation of the quantity of DNA repair proteins, by guiding or by providing a template for the DNA reparation (Figure 2). Nearly all primary DDR-induced effectors are regulated by miRNA and interact through their RNA-binding motifs in response to DSBs [126]. MiRNAs regulate, for example, H2AX (miRNA 24 and 138 [135,136]), PARP1 (miRNA-7-5p [137]), ATM (miRNA 18a and 421 [138]), ATM and DNA-PK (miRNA 101 [139]), BRCA1 (miRNA 182 [140]), RAD51 (miRNA 193b, 103 and 107 [141]), BRCA2 (miRNA 1245 [142]), RAD52 (miRNA 302a [143]), and P53 (miRNA 125b and 504 [144,145]). Actual models propose that ncRNAs facilitate

DNA repair, either by the hybridization of sncRNA to broken DNA via DDX1 and DHX9 (dead-box helicases) to form specific sequences propagating repair pathways or by the hybridization of lncRNA via RAD52-strand invasion, generating a template for high-fidelity repair [146,147].

LncRNA has proven regulatory modulation of DDR. They attenuate ATM activation and HR repair, sensitizing genotoxic treatment in cancers [53]. MiRNAs and lncRNAs cooperate with $P21^{WAF1/CIP1}$ (CDK inhibitor) to affect protein expression [148]. This generates cross-signatures in glioma and could serve malignancy diagnosis and prognosis [149]. In actively transcribed regions, lncRNA serve as template for NHEJ-mediated DSB repair to allow for the faithful transfer of missing information [150].

4. DDR Alterations and Associated Diseases

The alterations of many DDR members are associated with a range of diverse diseases, including immunodeficiency, inflammation, neurodegeneration, premature aging, cardiovascular or metabolic diseases, and cancers. However, there are reciprocal interactions between DNA damaged/repairing responses. For example, under viral infection, immunity directly relates to inflammation that underlies premature aging, and a high risk of cancer (Figure 3).

4.1. Immune Diseases and Inflammation

Immunodeficiencies are associated with DNA repair defects in the process of V(D)J genes and immunoglobulin class-switch recombinations. In immunoglobulin class switch recombination, a DSB is induced by the activation of a cytidine deaminase before broken ends are repaired by NHEJ or MMR. Any deficiency in one of the effectors of these repair complexes impairs the generation of IgG diversity to fight foreign antigens (acquired immunity), and leads to immunodeficiency at various degrees or hyper-IgM syndrome [151].

Different components of the DDR activate the innate immune system through the expression of ligands for the immune cell receptors and promote the production of proinflammatory mediators [152,153]. ATM, ATR, and CHK1 upregulate the formation of a ligand for the NKG2D immune receptor triggered by the stalled DNA replication fork [154].

The association of pre-existing DNA-repair defects (e.g., PARP1 or XRCC1/4) with DNA-damaging antibodies is highly genotoxic. In autoimmune diseases, such as systemic lupus erythematosus, anti-DNA autoantibodies circulate in the blood, cross cell membranes through mechanisms independent of their Fc region, and translocate in the nucleus to inhibit DNA repair and even damage DNA [155–157].

DNA damage effectors detect aberrant DNA structures in the nucleus and the cytoplasm, leading to immune signaling activation. For instance, Ku70 and DNA-PK, which are involved in the NHEJ, act as pathogenic DNA-recognition receptors in the cytoplasm and activate proinflammatory interferon, respectively, directly by IRF3 (IFN regulatory factor 3) or indirectly via STING (stimulator of interferon genes) signaling [158]. PARP1 upon genotoxic stress or the ATM activation of IκB kinases in DSBs both induce the translocation of NF-κB into the nucleus and promote the proinflammatory interferon and cytokine mediator's production. A loss of ATM impairs the innate inflammasome-dependent antibacterial immunity due to oxidative stress [159].

Moreover, an infection causes inflammation and enhances the production of ROS and oxidative DNA damage, creating a positive feedback loop that promotes genomic instability, cellular transformation, and carcinogenesis [160]. In the innate immune response, the cGAS–cGAMP–STING pathway senses cytoplasmic DNA, including microbial DNA or DNA released by DNA damage, and allows the production of more interferon and cytokines, the hallmarks of inflammation [161]. This pathway is also involved in the detection of DNA damage induced by autoantibodies in the systemic lupus erythematosus and directly connects this disease to inflammation by chronic interferon release [162].

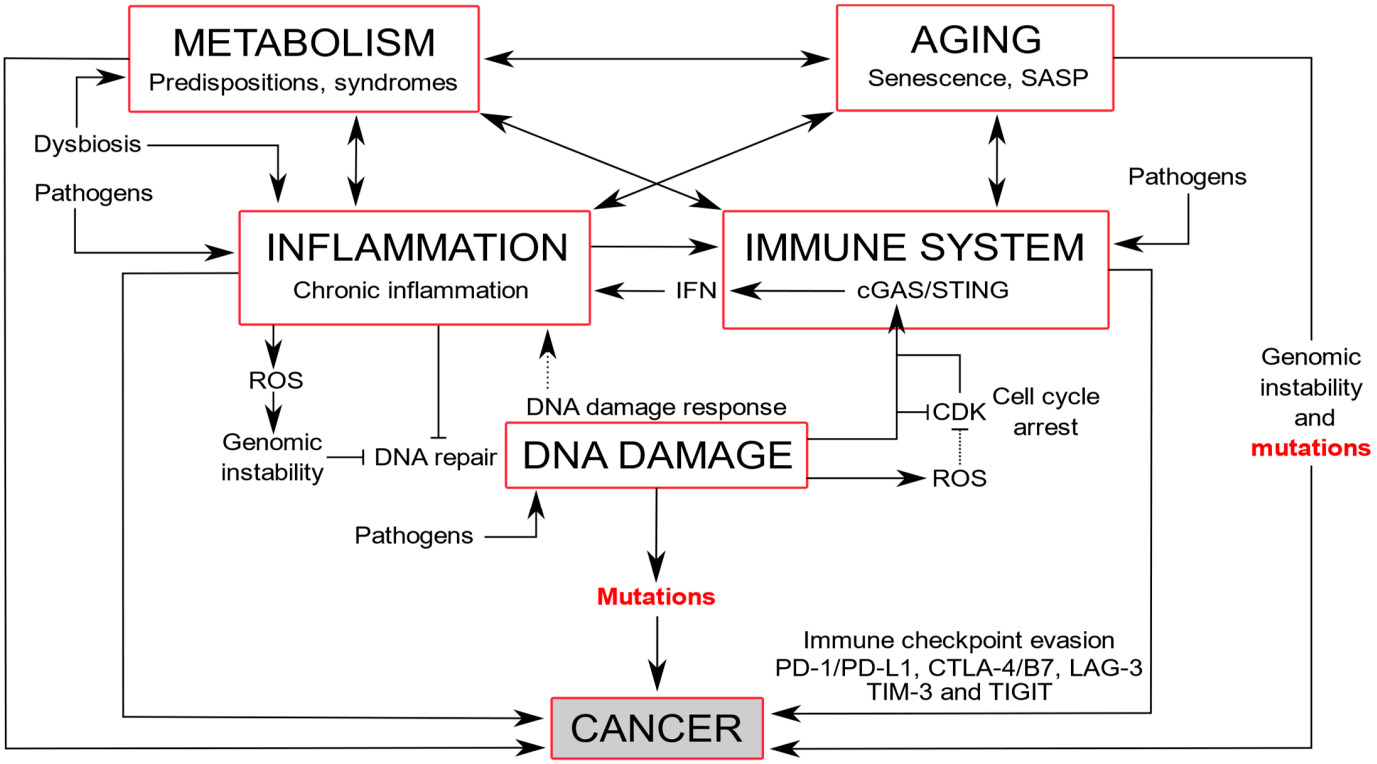

Figure 3. DNA damage induces inflammation and immunity that connect to metabolism and aging, with the genesis of mutations leading to cancer formation. The DNA damage response is activated upon DNA damage, arresting the cell cycle by CDK inhibition, and triggering an inflammatory response. cGAS, a cytosolic DNA sensor, triggers an innate immune response that activates STING. In mitosis, the CDK1-cyclin B complex phosphorylates and inhibits cGAS, but upon mitotic exit, dephosphorylation of cGAS by PP1 enables DNA cytoplasmic sensing [163]. cGAS connects DNA damage to the immune system, and subsequent inflammation by the production of interferon (IFN) and cytokines, but also to senescence and cancer [164]. Chronic inflammation can lead to an impairment of the immune system and generate ROS that counteracts DNA repair mechanisms [165]. Immunity triggers an inflammatory process that increases blood pressure, stimulating organ and metabolism damage [166,167]. Metabolism shifts with increased oxygen consumption and the generation of reactive nitrogen and oxygen intermediates are associated with inflammatory and immune responses [168]. Dysbiosis produces inflammation and metabolism syndromes that contribute to senescence. Pathogens can induce DNA damage and trigger immune and inflammatory responses. Aging is associated with adaptative immune and inflammatory responses and cumulative DNA damage and genomic instability that increase mutations [169,170]. Cancer cells evade detection by the immune system using immune checkpoints PD-1/PD-L1 (programmed cell death protein 1/programmed cell death ligand 1) and CTLA-4 (anti-cytotoxic T lymphocyte-associated antigen-4), LAG-3 (lymphocyte activation gene-3), TIM-3 (T cell immunoglobulin and mucin domain containing-3), and TIGIT (T cell immunoglobulin and ITIM domain) [171].

4.2. Neurodegeneration and Premature Aging

Neuronal dysfunction and neurodegenerative diseases occur with higher frequency when a persistent DDR is set up in neurons in association with an enhanced cholesterol biosynthesis and impaired Wnt or insulin (GSK3β increase) pathways [172]. In Huntington's, Parkinson's, and Alzheimer's diseases, PARP1 is increased. In Huntington's disease, NHEJ is defective and elevated PARP1 leads to increased AMPK activation, decreasing the CREB (C-AMP response element-binding protein) transcription factor necessary for the survival factor BNFD (brain-derived neurotrophic factor) and, finally, promotes necrotic cell death. In Parkinson's disease, increased levels of PARP1 accelerates the fibrillization and cytotoxicity of α-synuclein, which further activates ATM, H2AX, 53BP1, and NHEJ. In Alzheimer's disease, P53 stabilized by PARylation causes the upregulation of pro-apoptotic protein [173]. Moreover, Tau hyperphosphorylation, and abundant neurofibrillaries down-

regulate DNA damage/repair pathways with abnormal BRCA1 location and cell cycle re-entry inhibition [174].

Due to germline mutations in relevant genes, specific syndromes linked to DNA repair defects are hereditary. Distinct chromosomal instability disorders ataxia telangiectasia, Bloom syndrome, Cockayne syndrome, Fanconi anemia, Nijmegen breakage syndrome, trichothiodystrophy, Werner syndrome, and xeroderma pigmentosum display hypersensitive cells to particular genotoxic compounds. They also share clinical features of growth retardation, neurological disorders, premature aging, and skin alterations [175]. In ataxia telangiectasia, ataxia with oculomotor apraxia 1 and 2, and spinocerebellar ataxia with axonal neuropathy 1, the cerebellum is particularly affected. Neurodegeneration in xeroderma pigmentosum, Cockayne syndrome, and trichothiodystrophy is associated with NER deficiency [176]. These progeroid syndromes feature some aspects associated with physiological aging at an early age.

4.3. Aging

Several lines of evidence indicate that the aging process is an association of DNA damage accumulation due to decreased efficiency in repair processes, mitochondrial dysfunction, metabolism alteration, free radical accumulation, and telomeres shortening [177–179]. The persistence of DNA modifications affects DNA polymerization, resulting in the collapse of the replication fork, an arrest in transcription, and the genesis of mutagenic templates during the synthesis of nucleic acid leading to cellular aging [180]. Aged cells accumulate extranuclear DNA, which triggers inflammation initiated by cGAS-STING and senescence [181]. Senescence is associated with the inhibition of mitophagy [182]. The loss of sirtuin NAD-deacetylase activity due to lower NAD+ levels inhibits mitophagy and results in persistent dysfunctional mitochondria and aging [183]. Moreover, proteins from the DDR lack deacetylation, such as ATM, XA, WRN helicase, and Ku70, impairing the repair processes [184].

DNA repair proteins become less efficient with age, especially in germline cells where DNA damage accumulates within the genome [185]. After remaining in the prophase of the first meiotic division for years, the quality of oocytes declines with age. An increasing number of primordial follicles accumulate severe DSBs and are submitted to apoptosis that diminishes the ovarian reserve [186]. In the mid-30s, in the remaining oocytes, aneuploidy increases due to a decreased efficiency in BRCA1 and ATM that is necessary for the regulation of sister chromatid cohesion by a control of the ATM-regulated SMC1 cohesin complex [185] and ROS vulnerability [187]. During the menopause, DNA damage accumulates in oocyte due to the reduction in DNA repair capacities, such as a decrease in BRCA1 [185]. However, human oocytes submitted to potent DNA damaging agents applied chronically at high concentrations extrude their polar body and complete meiosis I, and have a higher acceptance of DNA-damage compared to other species [80].

4.4. Cardiovascular and Metabolic Diseases

DNA damage is a hallmark in cardiovascular and metabolism disorders. In failing hearts and cardiovascular diseases, oxidative stress (redox imbalance) and DNA damage are enhanced [123,188]. The BRCA1-deficient cardiomyocytes that have an impaired DSB repair activate p53-mediated proapoptotic signaling, whereas P53 deletion rescues BRCA1-deficient mice from cardiac failure. In addition, ischemia induces DSBs and upregulates BRCA1 expression in adult and fetal cardiac tissues [189]. An SSB was shown to cause heart failure by activating the DDR and increasing the expression of inflammatory cytokines via NF-κB signaling. Heart failure was more severe in the mice lacking XRCC1, but was inhibited by the genetic deletion of ATM [190].

In atherosclerosis, where the atherosclerotic plaque instability is associated with inflammatory cells, multiple DNA damage markers are present, including early induced DNA repair enzymes and the phosphorylated forms of ATM and H2AX [191]. The vascular smooth muscle cells show a defective repair of oxidative DNA damage, due to the

increased degradation of the BER enzyme, OGG1 [192]. In atherosclerotic cardiovascular diseases such as the Werner or Hutchinson-Gilford progeria syndromes, DSB repairs are defective [193]. Both syndromes are also, respectively, associated with diabetes and lipodystrophy symptoms. The metabolic changes in type 1 and type 2 diabetes increase the levels of genotoxic ROS and dicarbonyls that further form glycation adducts and reduce DNA repair [194].

Chronic diabetic type 2 β-cells have a greater extended DSB [195]. A compromised DNA repair is responsible for diabetes-associated fibrosis in various organs [194].

In obesity, oxidative stress and inflammation induce DNA damage, inhibit DNA repair, alter gene expression to set up metabolism disturbances, and further promote resistance to apoptosis and predispose to cancer [196]. Adipocytes' metabolic and secretory functions are strongly altered by DNA damage [197]. On the contrary, weight loss may prevent obesity and other adverse health effects due to a reduction in DNA damage with a decrease in pro-inflammatory cytokines and insulin levels [198].

4.5. Cancers

Various mechanisms related to DNA damage including dysregulation of the DDR pathways and a high level of replication stress are responsible for genomic instability, and linked to pretumor and tumor formation [44]. Aberrant copy numbers of genes correlate with the expression levels of mRNA [199]. Various primary cancers also display mitochondrial DNA mutations involved in ROS production, apoptosis inhibition, DNA repair anomalies, and cell cycle misregulation in the mitotic spindle and the G2/M checkpoint [200,201].

More than 450 proteins from the DDR [2] are related to familial cancer predispositions through diverse somatic mutations or inactivating germline mutations (Table 1). BRCA1 and BRCA2 are associated with a family history of breast and ovarian cancers. ATM is associated with a family history of breast and ovarian cancers with 1.7 times higher risk [202,203]. MSH2/6 is associated with a family history of colon/endometrial cancers. The "ICGC/TCGA Pan-Cancer Analysis of Whole Genomes Project Consortium 2020" has shown that somatic mutations of DDR-related genes were found in a third of cancers [204]. Multiple processes generate somatic mutations in the genome and determine a mutational signature for each type of cancer. These studies have identified defective components from the DNA damage repair, replication, the DNA-maintenance processes [204], and associated mutations, for instance, CDK12 (transcriptional modulator of DDR genes and mRNA processing) with DNA duplicated tandem stretches, or truncated variants of the MMR enzyme MBD4 (methyl-CpG-binding domain protein 4) with a mutational signature of CpG sites [205].

Moreover, interconnections are present between chronic inflammation or infection and generate genotoxic stress and tumor initiation/progression [206,207]. The risk of colorectal cancer is underlined by faster DNA damage in inflammatory bowel disease [208]. Tumor cell proliferation is also linked to the remodeling of the immune microenvironment through the deregulation of rhythmic expression of cyclin genes and the $P21^{WAF/CIP1}$ cell cycle inhibitor when the circadian rhythm is disrupted [209]. A virus such as the human papillomavirus reinitiates DNA replication by abrogating the cell cycle checkpoint proteins P53 and Rb (retinoblastoma protein), leading to an unscheduled S phase entry, followed by replication stress, DDR, and carcinogenesis [210].

Table 1. DDR-proteins mutations associated to various cancers.

DDR Proteins	DDR Signaling Pathways	Protein Activity/Function	Cancer-Associated Mutations *
ATM	Cell cycle regulators	Kinases	Breast, colon, endometrial, leukemia, lung, lymphoma, pancreatic, prostate
ATR			Breast, colon, endometrial, gastric, lung, lymphoma
CHK2	Cell cycle	Phosphatases	Bladder, breast, colon, endometrial, lung
APC-C/CDH1			Breast, gastric, lung
PTEN	Cell death	Phosphatase	Breast, endometrial, gastric
P53		Transcription factor	Found in 39.52% of all cancers *(AACR)*
DNA repair proteins	**DNA repair pathways**		
Ku70/Ku80	NHEJ	Helicases	Breast, colorectal, lung, melanoma
DNA-PK		Kinase	Breast, colon, glioma, oesophagal, lung
NBS1	HR	MRN complex	Breast, colon, esophageal, head and neck, hepatoma, liver, lung, lymphoma, prostate
MRE11			Breast
RAD50			Colon, gastrointestinal, lung
BRCA1		E3 ubiquitin-ligase	Breast, colon, gastrointestinal, haematological, lung, melanoma, ovarian, pancreatic, prostate
BRCA2		RAD51 binding to DNA	
PALB2/FANCN		Recruitment of BRCA2 and RAD51	Breast, colon, head and neck, lung, ovarian
FANCA, FANCB		FA repair complex	Breast, colon, leukemia, liver, lung
FANCO/RAD51C		DNA-dependent ATPase	Breast, colon, lung, ovarian, prostate
RAD51D			Breast, lung, ovarian
BLM		Helicases	Breast, colon, endometrial, leukemia, lung, lymphoma, melanoma
WRN			Colorectal, endometrial, lung, melanoma, pancreatic, thyroid
ERCC1	NER	Nuclease	Colorectal, glioma, lung, skin
XPA, XPC		Scaffold protein	Bladder, colon, lung, skin
XPD/ERCC2		Helicase	
XPG/ERCC5		Endonuclease	
OGG1	BER	Glycosylase	Breast, lung, renal
PARP1		ADP-ribosyltransferase	Breast, colon, endometrial, lung
XRCC1		Scaffold protein	Non-small cell lung
MLH1	MMR	ATPase	Brain, breast, colorectal, endometrial, hepatobiliary, lung, ovarian, pancreatic, skin, stomach, upper urinary
MSH2, MSH6		Scaffold protein	
MGMT	DR	Methyltransferase	Gliomas

Notes for Table 1: ATM, ATR, CHK1/2, and APC/C-CDH1 are involved in cell cycle regulation; PTEN and P53 in programmed cell death. In NHEJ, the ATP dependent helicases Ku70 and Ku80 form a heterocomplex with DNA-ends, and Ku80 C terminus recruits DNA-PK, a phosphatidylinositol 3-kinase related serine/threonine kinase [211]. In HR, two NBS1 subunits (phosphopeptide-binding Nijmegen breakage syndrome protein 1) are associated with two MRE11 subunits (meiotic recombination 11 homolog 1), and two ATP-binding cassette (ABC)-ATPase (RAD50) to compose the MRN complex [212]. BRCA1, an E3 ubiquitin ligase, and BRCA2 facilitate response to DNA damage. PALB2/FANCN (partner and localizer of BRCA2) has a critical role through the recruitment of BRCA2 and RAD51 to DNA breaks [213]. FANCA and FANCB are associated with other FANC (Fanconi Anaemia) and FAAP (FA-associated proteins) (FANCC, FANCE, FANCF, FANCG, FANCL, FANCM and FAAP20, FAAP24, and FAAP100). They form the FA core complex carrying an E3 ligase

activity to monoubiquitinate FANCI and FANCD2 [214], and initiate DNA repair by forming a platform to recruit additional proteins. RAD51C forms distinct complexes, one with a related DNA-dependent ATPase paralog, RAD51D, forming the BCDX2 complex (RAD51B-RAD51C-RAD51D-XRCC2), and one with the CX3 complex (RAD51C-XRCC3) [215]. BLM (Bloom syndrome protein) and WRN (Werner syndrome ATP-dependent helicase) are members of the RecQ helicase family. WRN also displays a 3′ to 5′ exonuclease activity [216]. In NER, ERCC1 has a nuclease activity involved in DNA excision repair. XPD/ERCC2 is a 5′–3′ DNA helicase, XPG/ERCC5 an endonuclease involved in DNA excision repair, and XPA (Xeroderma pigmentosum complementation group A) a zing finger protein involved in nucleotide excision repair [217]. In BER, OGG1 is a 8-Oxoguanine glycosylase and the primary enzyme of the process [218]. PARP1 the poly(ADP-ribose) polymerase 1 binds to damaged chromatin and recruits XRCC1 (X-ray repair cross-complementing protein 1) that interacts with DNA ligase III acting as a scaffold protein [219]. MMR is initiated by MutS α (MSH2–MSH6) or MutS β (MSH2–MSH3) binding to a dsDNA mismatch, before MLH MutL alpha (MLH1-PMS2) is recruited to the heteroduplex. MSH2 seems to act as a scaffold, MSH6 has a DNA-dependent ATPase activity, and MLH1 has a nucleotide-binding capability [220]. The O-6-méthylguanine-DNA-méthyltransférase, MGMT, carries out direct repair (DR) of alkylated DNA *: [204,221].

5. DDR Targets in Anticancer Therapies

5.1. Targeting DDR Proteins to Induce Deficiencies

Several categories of DDR proteins are targeted in anticancer monotherapies to elicit cell death [222,223] (Figure 4). DNA damage signaling inhibitors target kinases: ATM and DNA-PK are among the first activated kinases upon a DSB and, respectively, execute checkpoint signaling or DNA repair, while ATR is recruited by replication stress to facilitate fork stabilization and restart. ATR and ATM, respectively, activate the kinases CHK1 and CHK2, and WEE1. ATM and CHK2 are G1/S checkpoint DDR protein targets, ATR, CHK1, DNA-PK, and WEE1 are S phase regulators, and CHK1 and WEE1 are G2/M checkpoint regulators. Clinical trials are still currently running for this category of inhibitors, such as the trial in phase I for an oral ATR inhibitor BAY-1895344 against an advanced solid tumor [222,224,225].

Another category of inhibitors targets proteins involved in DNA repair such as RAD51 and POLQ, respectively from the HR and MMEJ processes, or PARP and MTH1 [226–229]. The discovery of PARP inhibitors was a milestone for anticancer chemotherapies directed against DDR proteins. Initially evaluated in patients with BRCA-mutated breast tumors, the inhibition of PARP eliminates its trapping on DNA and elicits death [230].

A third class of inhibitors is raised against proteins involved in DNA metabolism such as inhibitors for RNR (ribonucleotide reductase) that catalyzes a rate-limiting step in the production of deoxyribonucleotides and PFKFB3 (6-phosphofructo-2-kinase/fructose-2,6-biphosphatase 3) that converts fruc-tose-6-phosphate to indirectly stimulate glycolysis [231,232].

A fourth category of inhibitors is directed against chromatin regulation. DNA methylation or histone methylation/acetylation are epigenetic modifications that affect DNA repair ability. Histone deacetylase (HDAC) inhibitors lower DNA damage repair proteins from the NHEJ and the HR through the inhibition of ATM and MRN [233,234]. DNA methyltransferase 1 (DNMT1) inhibition induces the depletion of multiple repair protein in the MMR [235].

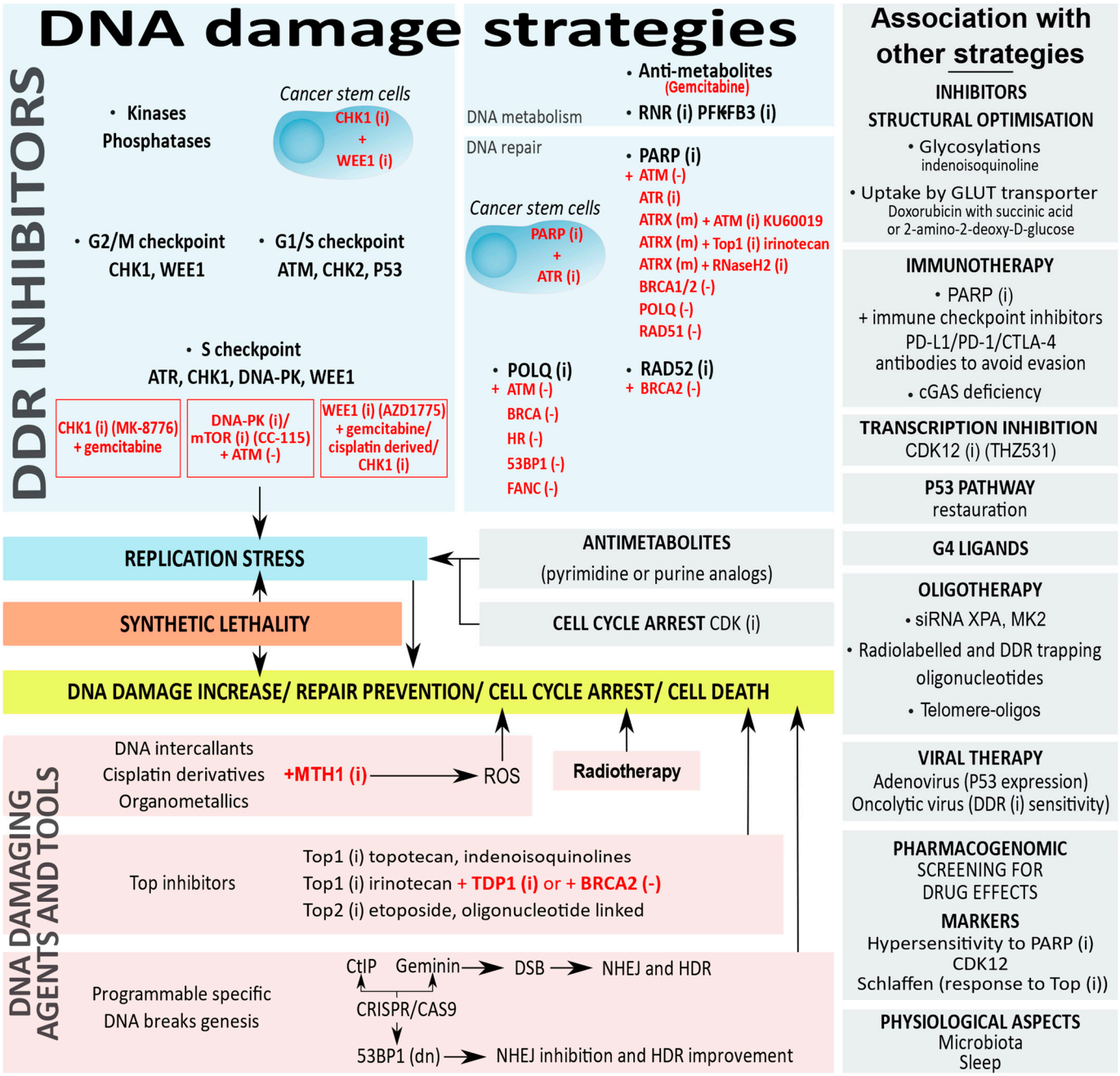

Figure 4. DNA damage strategies in cancer chemotherapies and possible combined therapies. Synthetic lethality is in red. Deficiency (-), dominant negative (dn), inhibitors (i), mutations (m).

5.2. Targeting the DDR Protein Network with Synthetic Lethality

By exploiting the defects in DNA repair, several categories of DDR proteins are targeted to take advantage of the concept of synthetic lethality and induce cell death. Cells usually repair DNA damage by switching from one alternative repair mechanism to another if a repair pathway is defective. Moreover, a loss of function targeting several DDR pathways renders these cells less susceptible to survival. The concept of synthetic lethality used to target DDR pathways occurs when deficiencies in independent genes are tolerated but when the combinations are lethal [230,236,237].

Several DDR inhibitors are investigated in ongoing clinical trials and the choice of the combination of inhibitors depends on the characteristic of the tumor [238]. Synthetic lethal vulnerabilities are exploited therapeutically by combining inhibitors against a tu-

mor deficiency in the DDR protein: CHK1 inhibitor (MK-8776) is used with gemcitabine (antimetabolite) in solid tumors [239], WEE1 Inhibitor (AZD-1775) with gemcitabine, cisplatin, or carboplatin (DNA damaging agents) in advanced solid tumors [240] or in combination with a checkpoint kinase CHK1 inhibitor (PF-0047736) in acute lymphoblastic leukemia [241], and a DNA-PK and mTOR dual inhibitor (CC-115) in hematopoietic and solid cancer cells [242].

Synthetic lethality is explored with PARP inhibitors in several cancers such as ATM-deficient tumors from breast and ovaries, aggressive prostate cancers in combination with ATR inhibitors [243,244], and high-risk neuroblastomas under ATR inhibition [245]. POLQ deficiency is synthetically lethal in combination with PARP inhibitors and associated with mutations of ATM, BRCA, Ku, 53BP1, and FA (Fanconi anaemia) [226,229,246]. Other synthetic lethalities include the ATM inhibitor, KU60019, or Top1 inhibitor, irinotecan, in ATRX-deleted neuroblastoma [247]. The application of synthetic lethality also depends on the RAD52 inhibition in cancer cells bearing BRCA1/2 mutations or the suppression of the BRCA1-RAD51 pathway [248]. Moreover, PARP controls the epigenetic modifications of chromatin at the level of DNA and histones, and changes in PARylation modify DNA methylation patterns and directly affect DNA repair [249]. PARP inhibitors show synergistic activity to allow a selective vulnerability with DNMT1 inhibition in acute myeloid leukemia and breast cancer [250], with HDAC inhibitors in triple-negative breast cancers [251], or with the inhibition of chromatin remodeling components of the SWI/SNF (switch/sucrose non-fermentable) complex in cancer cell lines [252].

Multiple components of the DDR are also targeted in cancer stem cells that are particularly resistant to DNA damage to increase their genetic lesions and boost their chemo- and radio-sensitivities [253]. Combining PARP and ATR inhibitors, or CHK1 and WEE1 inhibitors are efficient strategies for cancer stem cells sensitization [254–256].

5.3. Targeting Replication Stress

Replication stress arises when genomic stress affects the progression of DNA polymerase and uncouples DNA polymerization from DNA unwinding. New anti-cancer therapies targeting DNA damage repair mechanisms of the DDR are developed to exploit excessive unsustainable replication stress in cancer cells having a high proliferative index compared to normal cells [226,257]. The ATR–CHK1–WEE1 signaling pathway provides the possibility to enhance fork destabilization and replicative stress, and concomitantly lowers cell cycle checkpoint thresholds and pushes tumor cells into mitotic catastrophe and cell death. A high number of approved inhibitors against CDK, or DNA repair protein such as PARP are in clinical trials one and two against advanced ovarian cancer [68]. A novel target, WRNIP1 (Werner interacting protein 1), involved in an (ATM)-dependent phosphorylation of CHK1, is implicated in counteracting an aberrant R-loop accumulation capable of blocking the replication fork [258].

The antimetabolites that incorporate into DNA in place of thymidine during the S phase, preventing nucleobase addition and terminating chain elongation, also cause DNA replication failure. Antimetabolites are pyrimidine analogs (5-fluorouracil, gemcitabine, floxuridine, or capecitabine) and purine analogs (6-mercaptopurine, 8-azaguanine, fludarabine, and cladribine) that affect DNA and RNA metabolism and arrest cells in the S phase of the cell cycle. A transcriptomic analysis of colon cancer cells' response to 5-fluorouracil showed different cell fate phenotypes in the DNA-damage-induced genes' expression of apoptosis and cell-cycle checkpoints [259]. Similarly, the topoisomerase poisons (forming stable cleavage complex) described in the next paragraph hamper replication and are efficient agents to increase DNA damage.

5.4. Replication Stress and Telomere Deprotection

Several telomere-associated factors in the shelterin complex and the CST complex (CTC1–STN1–TEN1) ensure the prevention of replication stress by capping and by regulating telomerase and DNA polymerase alpha-primase [260,261].

Telomere deprotection contributes to replication stress, induces a SAC-dependent mitotic arrest through the activation of aurora B kinase and TRF2 that dissociates from chromosomal ends, triggers structural changes from telomere-loops to linear telomeres, exposes chromosome ends to ATM, and activates the mitotic telomere DDR [65,262–265]. Deprotected telomeres induce the transcription of tDDRNAs (telomeric small non-coding DNA damage response RNAs) and subsequent DDR. The depletion of tDDRNA by complementary antisense oligonucleotides results in the inhibition of the DDR at telomeres [266]. The strategy targeting tDDRNAs with oligonucleotides could be exploited as potential biomarkers to detect the DDR activation of telomeric damage or to modulate telomeres' function.

T-oligos (telomere homolog oligonucleotides) are homologous to the 3' single-stranded TTAGGG overhang involved in chromosome end stabilization. They trigger telomere uncapping, or mimic DNA damage and are also promising tools. Telomere overhang oligonucleotides decrease the proliferation of prostate cancer cells [267] and non-small cell lung cancer cells [268], and sensitize mammary tumor cells to radiation [269].

Telomeric DNA G-rich sequences allow for the formation of a G-quadruplex (G4) capable of impeding the progression of the replication fork and promoting telomere fragility and replication stress [260,261,270]. Several classes of G4 interacting agents affect telomere maintenance and are promising targets for cancer therapies [271,272]. G4 ligands alter telomeric chromatin, leading to POT1 dissociation and the consequent activation of the ATR-/ATM-dependent damage pathway at the telomeres [271]. G4 ligands have been successfully developed as favorable agents (tetracarboxymethyl porphyrins) for accurate probing [273] or as specific G4 telomeric porphyrin photosensitizers (TMPipEOPP) to discriminate G-quadruplex from duplex and ssDNA [274]. Employed in combination with PARP1 inhibitor, the RHPS4 G4 ligand reduces cell proliferation, avoids uncontrolled DNA replication, and induces cell death [275]. A basal level of DNA damage and telomere deprotection increase their sensitivity in cancer cells [276]. The CX-5461 G4 ligand, a quarfloxin derivative initially identified as a RNA-Pol I inhibitor [277], was recently shown to act at transcribed regions bearing G4 structures as a DNA structure-driven TOP2 poisons [278,279]. CX-5461 induces replication-dependent DNA damage through the stabilization of G4 DNA structures, which has entered phase I/II of clinical trials for patients with BRCA1/2 deficient tumors [280] and hematologic cancers [281].

5.5. Other Oligonucleotides, or Small Interfering RNA

In addition to telomere homolog oligonucleotides, other oligonucleotide therapeutics based on antisense RNAs and small interfering RNA (siRNA) modify the mRNA metabolism [282]. Using siRNA against repair protein XPA (NER) and co-targeting the synthetic lethal relationship with the cell cycle checkpoints, kinase MK2 enhances the antitumor response in P53-deficient cancers [283]. In myeloma, ILF2 antisense oligonucleotide (Interleukin Enhancer Binding Factor, a key modulator of the DNA repair pathway) is a synthetic lethal target with DNA2 (DNA replication helicase/nuclease 2) [284]. A radiolabeled oligonucleotide that targets the RNA-associated telomerase promotes radiation-induced genomic DNA damage in telomerase-positive cancer cells [285]. A short, double-stranded oligonucleotide linked to a cholesterol molecule, AsiDNA™, acts as a decoy, mimics DSBs, and triggers a false DNA break signal to activate and attract DNA repair proteins, preventing their recruitment to the site of genomic DNA damage. The oligonucleotide acts by the overactivation of false signaling of DNA damage through DNA-PK and PARP enzymes and depletion of the DDR. The tumor DNA breaks are not repaired, accumulate damage, and drive cancer cells to death at the onset of replication [286]. The inhibition of ncRNAs overexpressing or the replacement of tumor-suppressive ncRNAs is a strategy if the inflammatory response they produce is bypassed [287].

5.6. Topoisomerase Inhibitors

Interference with protein-DNA complexes alters DNA structure and triggers DDR-associated cell death. Topoisomerases (Top) are involved in replication and transcription. Top1 and Top2 relax DNA superhelical tension with, respectively, SSB or DSB cleavages to allow for strand rotation before resealing the DNA. A collision between the replication fork and the cleavage complex of Top1 produces DSBs. Top covalently attaches DNA, forming reversible DNA-Top cleavage complexes during the cleavage step. From the three subgroups of human Top (type IA, IB, and IIA), types IB and IIA are particularly overexpressed in certain cancers [288]. Top inhibitors are either poisons that bind to the DNA-topoisomerase cleavage complex (interfacial inhibition) and form a ternary DNA-topoisomerase-inhibitor complex preventing the religation of the two strands of DNA; or catalytic inhibitors including DNA intercalators, ATP competitors, and inhibitors of ATP hydrolysis [289,290]. When targeted by Top poisons, the stabilization of the DNA-Top cleavage complex blocks DNA replication and generates deleterious DSBs, inducing cell death. The initial inhibitors were camptothecin (Top1 inhibitor, poison), etoposide (Top2 inhibitor, poison), and doxorubicin (Top2 inhibitor, poison) an anthracycline that intercalates, alkylates and crosslinks DNA, producing free radicals, or interferes with the helicase function. Top1 inhibitors, indenoisoquinoline derivatives LMP400 (Indotecan) and LMP776 (Indimitecan) have reached the clinical trial phase [290,291]. The only dual Top1/2 inhibitor used in therapy is aclarubicin, but other dual inhibitors exist against Top2 and other targets such as kinases or proteasome [292]. Tyrosyl-DNA phosphodiesterase 1/2 (TDP1/2) resolve Top-DNA complexes by liberating Top1 or Top2 (respectively TDP1 and TDP2) from the DNA after the degradation of the cleavage complexes. A combination of inhibitors such as the Top1 inhibitor irinotecan with a TDP1 inhibitor also improves the treatment of glioblastoma [293]. A higher response to irinotecan (Top1 inhibitor) is obtained in BRCA2-mutated cancer with acquired resistance to olaparib (PARP inhibitor) showing the downregulation of TDP1 [294]. To render the Top2 inhibitor etoposide specific for cancer cells, a covalent link was realized with a single-stranded oligonucleotide displaying a complementary sequence to a translocated cleavable DNA region only present in promyelocytic leukemia [295].

The structural optimization of Top inhibitors by glycosylation is an option to enhance the DNA damaging efficiency [296]. The addition of a carbohydrate moiety to indenoisoquinoline enhances the binding affinity of the Top1 drug to DNA due to a stronger hydrogen bonding interaction [297]. The covalent conjugation of galactose on doxorubicin increases its effect on liver cancer cells with less myocardial damage [298]. Doxorubicin uptake by the GLUT1 glucose transporters is increased by the conjugation of 2-amino-2-deoxy-D-glucose or succinic acid within cancer cells that overexpress GLUT1 and are dependent on glucose metabolism (the Warburg effect) [299].

5.7. DNA Damaging Drugs

The concept of increasing DNA breaks to activate the DDR protein pathway and promote cancer cell death inspired the development of various anticancer drugs. Anticancer compounds that chemically modify DNA bases, intercalate, or crosslink DNA include alkylating agents such as nitrogen mustard or platinum-derived compounds and agents that target the minor groove of DNA instead of the major groove compared to most of the alkylants [300]. Alkylating agents such as estramustine for the treatment of prostate cancer [301] or bifunctional cyclophosphamide [302] result in the covalent transfer of alkyl-groups to DNA, induce bulky DNA damage, and block transcription and replication. The anticancer activity of alkylating agents such as cyclophosphamide is in close interplay with miRNA to determine the outcome of an applied therapy [303]. Platinums such as cisplatin and its derivatives such as carboplatin, oxaliplatin, and picoplatin bind to guanine and adenine residues to form DNA adducts after the aquation of the platinum chloride group. Recently, a map of the sites of cisplatin damage and repairs for the entire human genome were obtained at a single-nucleotide resolution to better understand cancer sensitivity and resis-

tance [304]. Other non-traditional alkylators are methylating agents, such as temozolomide used to treat glioblastoma [305]. Numerous metal-derived compounds, organometallics, are developed to generate severe DNA alterations [306,307]. Some ruthenium-containing compounds such as polynuclear ruthenium induce DNA damage and recruit DNA repair effectors such as XPC (Xeroderma Pigmentosum complementation group C) [308]. Certain organometallics target enzymes involved in DNA topology (Top1) [309]. Most metallo-glycopeptides are interesting DNA damaging drugs such as bleomycin that require a metal ion (Fe (II)) to be activated and cleave a DNA-specific sequence in 5'GT and 5'GC dinucleotides [310].

Most metal-containing compounds also belong to the class of ROS-inducing drugs that disrupt redox homeostasis, causing various types of death. Besides doxorubicin and cisplatin, a number of prooxidative drugs are used such as 2-methoxyestradiol, buthionine, or sulfoximine [311]. Cancer cells have an accelerated metabolism compared to normal cells, which generates a high level of ROS and makes them depend on MTH1 (MutT homolog 1), a repair enzyme that hydrolyzes oxidized nucleotides to corresponding monophosphates. The selective inhibition of MTH1 suppresses cancer growth through an accumulation of oxidative damage [312].

5.8. DNA Damaging Tools

Molecular tools are capable of introducing programmable DNA breaks. The CRISPR/Cas9 (clustered regularly interspaced palindromic repeats/associated protein 9) system provides the ability to add or remove specific DNA sequences in the genome to perform site-specific gene editing. In this plasmid-based technology, Cas9 endonuclease works guided by a single-stranded RNA at a specific site on a 20 base pair sequence among the human genome to create DSBs followed by endogenous DDR repair mechanisms NHEJ (error-prone) and HDR (high fidelity) [313]. To control DNA repair, outcomes for genome editing strategies have been developed to locally or globally inhibit or activate DNA repair effectors and favor a high-fidelity repair [314]. The fusion of DNA repair factors such as the HDR enhancer element of CtIP or Geminin to Cas9 ensures a rapid, efficient HDR [315]. Geminin inhibits the replication factor CDT1 during the S and G2 phases to avoid re-replication. The fusion of Cas9 to a dominant-negative 53BP1 inhibits NHEJ and improves HDR frequency [316]. DSB repair factors fused with Cas9 favored MMEJ and HDR in hematopoietic cells [317].

Ionizing radiation creates high levels of clustered DNA damage (including DSB, covalent crosslinking, base damage) that are difficult to repair and exploitable in radiation therapy. Over the years, radiotherapy has been improved by intensity modulation, image guided, and internal access [318,319]. The radiation efficiency is enhanced using drugs that target DNA repair machinery [320]. A new class of drugs, named radiopharmaceuticals, delivers radiation therapy specifically and directly to cancer cells. Despite the exploitation of the natural affinity of radioactive iodine to treat thyroid cancer or radium 223 to treat cancers that have spread to bones, new radiopharmaceuticals target surface molecules specifically present on cancer cells. A radiolabeled somatostatin analog compound, lutetium 177-dotatate, that targets surface receptors, is approved for the treatment of certain neuroendocrine tumors affecting the digestive tract [321], and small molecules such as PSMA (prostate-specific membrane antigen) inhibitors deliver radiotherapeutic nuclides in prostate cancer [322]. A combined strategy with an oncolytic adenovirus that inhibits the DDR, renders external beam radiation therapy more efficient [323].

6. Drugging DDR Proteins in Association with Other Therapies

6.1. Inhibition of Cell Cycle Progression and Transcription

Cancer cells are rapidly dividing cells and highly susceptible to DNA damage. Despite the fact CDKs activate the DNA damage checkpoint and initiate the DNA repair, they also interfere with the DDR. CDKs inhibition compromises CHK1 function in the DNA damage and the stalled replication [324]. The inhibition of CDK4/6 that commits the

G1 and S phases' transition inactivates the retinoblastoma tumor suppressor protein and arrests the cell cycle in G1. The CDK4/6 inhibitor, palbociclib, in combination with PARP inhibitors, added to endocrine therapy, suppresses the DNA damage repair to treat BRCA-mutated ER+ (estrogen receptor-positive) breast cancers [325]. In addition to their cell cycle regulatory functions, CDKs, especially CDK7, 8, 9, 12, and 13 phosphorylate and regulate RNA polymerase II-mediated transcription. Their inhibition can deeply affect the expression of DDR genes. CDK12 inhibitor THZ531 induces the RNA Pol II elongation defect and the premature cleavage and polyadenylation of long DDR genes followed by apoptosis in neuroblastoma cells [326]. SR-4835, a CDK12/13 inhibitor, acts in synergy with PARP inhibitors in triple-negative breast cancers [327].

6.2. Restoration of the P53 Pathway

P53 is the most frequently mutated gene in more than 50% of all cancers, leading to P53 protein loss or disfunction. Several strategies have been developed to reactivate P53. Murine double minute 2 (MDM2) is an E3 ubiquitin ligase responsible for P53 ubiquitination and inactivation by proteasomal degradation. MDM2 heterodimerizes with MDMX to enhance P53 ubiquitination and degradation.

Some compounds inhibit MDM2 interaction with P53, such as small molecules [328] that act as MDM2 antagonists, inhibit E3 ubiquitination of P53, or stabilize P53 and restore its conformation and DNA-binding ability [329,330]. PRIMA-1 and its analog (APR-246) restore mutated P53 proteins to a normal conformation and re-establish P53 transcriptional activity. The expression of PUMA, NOXA, and BAX are increased. PRIMA-1 is chemically converted intracellularly and binds the cysteine residues of mutated P53 protein, allowing a correct refolding [331,332]. Most P53 mutations are located in the DNA-binding core domain and create a destabilizing cavity that can be corrected by small molecules named PhiKan083 and PhiKan7088, restoring transactivation potential inducing P21 and NOXA expression with the consequent cell cycle arrest and apoptosis [333,334]. Many of those inhibitors have entered clinical trials against hematological malignancies or advanced solid tumors [335].

WIP1 phosphatase is a negative regulator of P53 after the completion of DNA repair [336]. The inhibition of WIP1 suppresses the proliferation of cancer cells by the activation of the P53 pathway. WIP1 depletion by RNA interference sensitizes cancer cells to DNA damage-inducing chemotherapy [337], and WIP1 inhibitor GSK2830371 potentiates the cytotoxic effect of doxorubicin in neuroblastoma [338].

The cell-cycle checkpoint abrogation is also a possible strategy to bypass a mutation in P53. Compared to normal cells, P53 mutated cancer cells lack a normal G1 checkpoint and mostly rely on the G2 checkpoint. The loss of WEE1 activity sensitizes P53 deficient cells to DNA damaging agents and radio sensitization [339]. The inhibition of WEE1 induces a mitotic catastrophe and cell death [340]. WEE1 inhibitor MK1775 was recently reported to suppress tumor proliferation and to potentiate Top1 inhibitor irinotecan action in P53 mutant colonic cancer cell lines [341].

6.3. DDR Inhibition Strategies Associated to Cancer Immunotherapies

The expression of immunosuppressive surface proteins allows cancer cells to escape immune detection and destruction. Activated T cells recognize tumor antigens, but their PD-1 receptor engaged to tumor PD-L1 (programmed death-ligand 1) or their CTLA-4 (cytotoxic T-lymphocyte associated antigen 4) interaction with B7 antigen-presenting cells inhibit T cells cytotoxicity. Consequently, antibodies against PD-1, PD-L1, or CTLA-4 are immune checkpoint blockers that potentiate anti-tumorigenic immune responses [342]. Combining a PD-L1 inhibitor with a PARP inhibitor or PARP/PD-L1 dual inhibitors [224] in breast cancers [343] allows a stronger antitumor activity compared to separate agents. In non-small cell lung cancer, pembrolizumab (anti-PD1 antibody) co-administrated with chemo- or radiotherapy showed a marked clinical benefit [344,345]. Regardless of the cancers' tissue of origin, a large proportion of mutant neoantigens in MMR-deficient cancers

are sensitive to an immune checkpoint blockade [346]. Around 200 clinical trials are testing a combination of immune checkpoint inhibitors with DNA damaging chemotherapies [226].

DNA fragments are recognized by cGAS sensor (innate immunity), followed by cGAMP synthesis, STING activation, and translocation to the Golgi, where it recruits IKKA (inhibitor of nuclear factor kappa-B kinase subunit alpha) and TBK1 (TANK-binding kinase 1) to induce the transcriptional activation of interferon and chemokines CXCL10 (chemokine (C-X-C motif) ligand 10). In addition to cytosolic DNA detection, cGAS is involved in the control of the replication dynamic by decelerating the replication fork. cGAS-deficient cells are exposed to an acceleration of the replication fork, and to replication stress that renders them hypersensitive to radiation and chemotherapy [347,348].

6.4. Pharmacogenomic and Predictive Markers in DDR Strategies

Cancer pharmacogenomic relates the interaction between genetic predisposition and therapeutic drugs responses [349,350]. Genome mapping of chemotherapeutic effects is performed to determine compounds selectivity for genomic regions: topotecan (Top1 inhibitor) and etoposide (Top2 inhibitor) induce similar DNA damage in transcriptional active genomic regions, daunorubicin (anthracycline) evicts histones, while aclarubicin evicts histones from heterochromatin. This different genomic specificity of DNA damage-inducing drugs has consequences for compound activity in different tumor types [351]. A prognostic signature related to the DDR pathway and a gene signature of RNA binding proteins was determined to promote an individualized treatment strategy in prostate cancer [352]. When mutated, 73 genes from the HR, FA components, and ATM/ATR kinases determine a hypersensitivity to PARP inhibitors [353]. Single nucleotide polymorphisms in ERCC1 predict the response to DNA damaging platinum chemotherapy for patients with non-small cell lung cancer [354].

The identification of markers is also important to select patients for proper therapy. A polymorphism study on CDK12, which modulates the transcription elongation of RNA polymerase II and affects the expression of DDR genes, reveals it is a possible prognostic biomarker in late-stage ovarian cancer treated with platinum [355]. Markers that predict sensitivity or resistance to induced DNA damage therapy such as the Schlaffen biomarker are useful to predict the accurate response to Top1 and Top2 inhibitors, in colon and ovarian cancers [356]. However, using a single marker to perform personalized therapy is limited and it appears necessary to integrate genomic data of several markers regarding the disease progression. The use of circulating tumor DNA (ctDNA), an emerging field in multiple cancer types, allows the evolutionary dynamics of tumors such as early stage lung cancer [357] or in bladder cancer to be tracked to follow the development of resistance in real-time using a liquid biopsy [358]. DNA-repair gene mutations are highly prevalent in ctDNA from myeloma [359]. The pharmacodynamic activation of the DDR pathway can confirm target engagement in tumors following anticancer treatment. DNA damage recognition and repair proteins (γH2AX, pS343-NBS1, and RAD51) are biomarkers detected in preclinical and clinical treatment with a quantitative multiplex immunofluorescence assay [360]. Mutation and neoantigen burden are developed as potential clinical biomarkers. The microsatellite-instability–high (MSI-H) that results from a defect in MMR in germline or somatic genes was recently approved as an indicator for immune checkpoint inhibitors [346]. Tumors with microsatellite instability respond better to PD-1 blockade with pembrolizumab in a phase two study [361]. The expression of major DDR kinases including ATM, ATR, CHK1/2, and WEE1 tailor anticancer treatment, such as systemic treatment with PD-L1-targeting monoclonal antibodies (checkpoint inhibitors). PD-L1 expression is upregulated in cancer cells in response to DSBs under genotoxic stress, such as radiotherapy or PARP inhibition. The inhibition of ATR downregulates PD-L1 in a proteasome-dependent manner, attenuates the interaction of PD-L1/PD-1, and sensitizes cancer cells to T-cell-mediated killing [362]. Using siRNA library screen targeting DNA repair genes, PD-L1 induction was shown to be dependent on the ATM/ATR/CHK1 pathway [363].

6.5. Viral Therapies to Boost the DDR

Viruses are actively involved in manipulating the DDR pathway targeting the MRN sensor complex of proteins for degradation and providing a rationale for their use in therapies [364]. Viral vectors have high efficiencies for gene transfer and expression. Adenoviral and retroviral vectors are primary used with tissue-specific promoters, facilitating tumor killing [365]. An adenovirus was used to express P53 (gendicine) to treat patients affected by head and neck carcinoma and is now applied to other cancers as gene therapy with adenovirus serotype-5 being the prevalent adenovirus used in clinical trials [366]. The combination of the potent Ad5/35 chimeric virus with either DNA damaging therapies (radiation or chemotherapy) leads to significant increase in the survival of aggressive tumors [367].

Oncolytic viruses such as Enadenotucirev formed as a chimera of two group B adenoviruses, Ad3 and Ad11p, are promising due to their dual action by a direct intratumor spread and oncolysis, in addition to an increase in the antitumor T-cell response [323,368]. DNA-PK inhibition sensitizes cancer cells to oncolytic alphavirus M1 and improves therapeutic effects in refractory patient tumor samples. Infection triggers the transcription of IFN and the activation of an antiviral response that is abolished by pretreatment with DNA-PK inhibitors and results in an enhanced replication of the virus within malignancies. DNA-PK inhibition further promotes viral induced DDR and increases cell apoptosis [369].

The oncolytic herpes simplex lentivirus has a unique property to target multiple components of the DDR, irrespective of their mutation. This virus generates cancer-selective sensitivity to PARP inhibitors in glioblastoma. Infection induces a loss of RAD51 due to proteasome-dependent degradation that requires viral DNA replication. This synthetic lethal-like interaction is applicable to resistant tumors in which PARP inhibitor treatments block BER and activate DDR and S phase arrest through CHK1 activation, while viral infection induces DSBs, inhibits HR repair through the degradation of RAD51, and alters the cell cycle through CHK1 degradation [370].

7. Conclusions

The DDR network, guardian of the genome, contains numerous proteins connected by multiple regulatory interactions. Cancers and several other diseases are caused by inherited mutations in DNA or those generated by high levels of DNA damage and repair defects in DDR proteins. To kill cancer cells, the creation of DNA-damaging agents in chemotherapy alone or combined with other agents controls the DDR to optimize anticancer activity. Choosing the right inhibitor to administer with indications from the genomic profile, and/or associated with a predictive effect of the drug would fine-tune these therapies and could adapt to the evolving profiles of tumors.

Author Contributions: C.M. and K.C. wrote the manuscript and generated all figures with additional support from A.M. All authors have read and agreed to the published version of the manuscript.

Funding: This review was funded by "Université de Lille" and grant from the "Ligue Contre le Cancer" to A.M.

Acknowledgments: The authors are thankful to the "Centre National de la Recherche Scientifique", the "Université de Lille", and the "Ligue Contre le Cancer". C.M. is a recipient of a doctoral fellowship from the French ministry.

Conflicts of Interest: The authors declare no conflict of interest. The funders had no role in the design of the study; in the collection, analyses, or interpretation of data; in the writing of the manuscript, or in the decision to publish the results.

References

1. O'Connor, M.J. Targeting the DNA Damage Response in Cancer. *Mol. Cell* **2015**, *60*, 547–560. [CrossRef] [PubMed]
2. Pearl, L.H.; Schierz, A.C.; Ward, S.E.; Al-Lazikani, B.; Pearl, F.M.G. Therapeutic opportunities within the DNA damage response. *Nat. Rev. Cancer* **2015**, *15*, 166–180. [CrossRef]

3. Schlam-Babayov, S.; Bensimon, A.; Harel, M.; Geiger, T.; Aebersold, R.; Ziv, Y.; Shiloh, Y. Phosphoproteomics reveals novel modes of function and inter-relationships among PIKKs in response to genotoxic stress. *EMBO J.* **2021**, *40*, e104400. [CrossRef] [PubMed]
4. Hossain, M.A.; Lin, Y.; Yan, S. Single-strand break end resection in genome integrity: Mechanism and regulation by APE2. *Int. J. Mol. Sci.* **2018**, *19*, 2389. [CrossRef] [PubMed]
5. Ensminger, M.; Iloff, L.; Ebel, C.; Nikolova, T.; Kaina, B.; Löbrich, M. DNA breaks and chromosomal aberrations arise when replication meets base excision repair. *J. Cell Biol.* **2014**, *206*, 29–43. [CrossRef]
6. Kuzminov, A. Single-strand interruptions in replicating chromosomes cause double-strand breaks. *Proc. Natl. Acad. Sci. USA* **2001**, *98*, 8241–8246. [CrossRef]
7. Jadoon, S.; Malik, A. DNA Damage by Heavy Metals in Animals and Human Beings: An Overview. *Biochem. Pharmacol. Open Access* **2017**, *6*. [CrossRef]
8. Shah, G.A.; O'Shea, C.C. Viral and Cellular Genomes Activate Distinct DNA Damage Responses. *Cell* **2015**, *162*, 987–1002. [CrossRef]
9. Adam, M.A.A.; Tabana, Y.M.; Musa, K.B.; Sandai, D.A. Effects of different mycotoxins on humans, cell genome and their involvement in cancer (Review). *Oncol. Rep.* **2017**, *37*, 1321–1336. [CrossRef]
10. Virgilio, A.; Sinisi, A.; Russo, V.; Gerardo, S.; Santoro, A.; Galeone, A.; Taglialatela-Scafati, O.; Roperto, F. Ptaquiloside, the Major Carcinogen of Bracken Fern, in the Pooled Raw Milk of Healthy Sheep and Goats: An Underestimated, Global Concern of Food Safety. *J. Agric. Food Chem.* **2015**, *63*, 4886–4892. [CrossRef]
11. Srinivas, U.S.; Tan, B.W.Q.; Vellayappan, B.A.; Jeyasekharan, A.D. ROS and the DNA damage response in cancer. *Redox Biol.* **2019**, *25*, 101084. [CrossRef]
12. Muñoz, S.; Méndez, J. DNA replication stress: From molecular mechanisms to human disease. *Chromosoma* **2017**, *126*. [CrossRef]
13. Petermann, E.; Orta, M.L.; Issaeva, N.; Schultz, N.; Helleday, T. Hydroxyurea-Stalled Replication Forks Become Progressively Inactivated and Require Two Different RAD51-Mediated Pathways for Restart and Repair. *Mol. Cell* **2010**, *37*, 492–502. [CrossRef] [PubMed]
14. Schorr, S.; Schneider, S.; Lammens, K.; Hopfner, K.; Carell, T. Mechanism of replication blocking and bypass of Y-family polymerase η by bulky acetylamino- fluorene DNA adducts. *Proc. Natl. Acad. Sci. USA* **2010**, *107*, 20720–20725. [CrossRef] [PubMed]
15. Huang, M.; Kim, J.M.; Shiotani, B.; Yang, K.; Zou, L.; D'Andrea, A.D. The FANCM/FAAP24 complex is required for the DNA interstrand crosslink-induced checkpoint response. *Mol. Cell* **2010**, *39*, 259–268. [CrossRef] [PubMed]
16. Castellano-Pozo, M.; García-Muse, T.; Aguilera, A. R-loops cause replication impairment and genome instability during meiosis. *EMBO Rep.* **2012**, *13*, 923–929. [CrossRef]
17. Sollier, J.; Stork, C.T.; García-Rubio, M.L.; Paulsen, R.D.; Aguilera, A.; Cimprich, K.A. Transcription-Coupled Nucleotide Excision Repair Factors Promote R-Loop-Induced Genome Instability. *Mol. Cell* **2014**, *56*, 777–785. [CrossRef]
18. Helmrich, A.; Ballarino, M.; Tora, L. Collisions between Replication and Transcription Complexes Cause Common Fragile Site Instability at the Longest Human Genes. *Mol. Cell* **2011**, *44*, 966–977. [CrossRef]
19. Gómez-González, B.; García-Rubio, M.; Bermejo, R.; Gaillard, H.; Shirahige, K.; Marín, A.; Foiani, M.; Aguilera, A. Genome-wide function of THO/TREX in active genes prevents R-loop-dependent replication obstacles. *EMBO J.* **2011**, *30*, 3106–3119. [CrossRef] [PubMed]
20. Burgess, R.C.; Misteli, T. Not All DDRs Are Created Equal: Non-Canonical DNA Damage Responses. *Cell* **2015**, *162*, 944–947. [CrossRef]
21. Mailand, N.; Falck, J.; Lukas, C.; Syljuåsen, R.G.; Welcker, M.; Bartek, J.; Lukas, J. Rapid destruction of human Cdc25A in response to DNA damage. *Science* **2000**, *288*, 1425–1429. [CrossRef]
22. Moiseeva, T.N.; Yin, Y.; Calderon, M.J.; Qian, C.; Schamus-Haynes, S.; Sugitani, N.; Osmanbeyoglu, H.U.; Rothenberg, E.; Watkins, S.C.; Bakkenist, C.J. An ATR and CHK1 kinase signaling mechanism that limits origin firing during unperturbed DNA replication. *Proc. Natl. Acad. Sci. USA* **2019**, *116*, 13374–13383. [CrossRef]
23. Cortez, D. Replication-Coupled DNA Repair. *Mol. Cell* **2019**, *74*, 866–876. [CrossRef] [PubMed]
24. Thompson, R.; Gatenby, R.; Sidi, S. How Cells Handle DNA Breaks during Mitosis: Detection, signaling, repair, and fate choice. *Cells* **2019**, *8*, 1049. [CrossRef]
25. Nielsen, C.F.; Zhang, T.; Barisic, M.; Kalitsis, P.; Hudson, D.F. Topoisomerase IIa is essential for maintenance of mitotic chromosome structure. *Proc. Natl. Acad. Sci. USA* **2020**, *117*, 12131–12142. [CrossRef]
26. Lee, H.J.; Hwang, H.I.; Jang, Y.J. Mitotic DNA damage response: Polo-like kinase-1 is dephosphorylated through ATM-Chk1 pathway. *Cell Cycle* **2010**, *9*, 2389–2398. [CrossRef]
27. Lee, K.Y.; Dutta, A. Chk1 promotes non-homologous end joining in G1 through direct phosphorylation of ASF1A. *Cell Rep.* **2021**, *34*, 108680. [CrossRef] [PubMed]
28. Gentile, F.; Arcaro, A.; Pizzimenti, S.; Daga, M.; Paolo Cetrangolo, G.; Dianzani, C.; Lepore, A.; Graf, M.; Ames, P.R.J.; Barrera, G. DNA damage by lipid peroxidation products: Implications in cancer, inflammation and autoimmunity. *AIMS Genet.* **2017**, *4*, 103–137. [CrossRef]
29. Cheng, E.Y.; Hunt, P.A.; Naluai-Cecchini, T.A.; Fligner, C.L.; Fujimoto, V.Y.; Pasternack, T.L.; Schwartz, J.M.; Steinauer, J.E.; Woodruff, T.J.; Cherry, S.M.; et al. Meiotic recombination in human oocytes. *PLoS Genet.* **2009**, *5*, e1000661. [CrossRef]

30. Neale, M.J.; Pan, J.; Keeney, S. Endonucleolytic processing of covalent protein-linked DNA double-strand breaks. *Nature* **2005**, *436*, 1053–1057. [CrossRef]
31. Hinch, A.G.; Zhang, G.; Becker, P.W.; Moralli, D.; Hinch, R.; Davies, B.; Bowden, R.; Donnelly, P. Factors influencing meiotic recombination revealed by whole-genome sequencing of single sperm. *Science* **2019**, *363*, eaau8861. [CrossRef]
32. García-Rodríguez, A.; Gosálvez, J.; Agarwal, A.; Roy, R.; Johnston, S. DNA damage and repair in human reproductive cells. *Int. J. Mol. Sci.* **2019**, *20*, 31. [CrossRef]
33. Har-Vardi, I.; Mali, R.; Breietman, M.; Sonin, Y.; Albotiano, S.; Levitas, E.; Potashnik, G.; Priel, E. DNA topoisomerases I and II in human mature sperm cells: Characterization and unique properties. *Hum. Reprod.* **2007**, *22*, 2183–2189. [CrossRef]
34. Abe, H.; Alavattam, K.G.; Hu, Y.C.; Pang, Q.; Andreassen, P.R.; Hegde, R.S.; Namekawa, S.H. The Initiation of Meiotic Sex Chromosome Inactivation Sequesters DNA Damage Signaling from Autosomes in Mouse Spermatogenesis. *Curr. Biol.* **2020**, *30*, 408–420.e5. [CrossRef]
35. Lorenz, M.; Jung, S.; Radbruch, A. Switch transcripts in immunoglobulin class switching. *Science* **1995**, *67*, 1825–1828. [CrossRef]
36. Rivera-Munoz, P.; Soulas-Sprauel, P.; Le Guyader, G.; Abramowski, V.; Bruneau, S.; Fischer, A.; Pâques, F.; De Villartay, J.P. Reduced immunoglobulin class switch recombination in the absence of Artemis. *Blood* **2009**, *114*, 3601–3609. [CrossRef] [PubMed]
37. Björkman, A.; Du, L.; Felgentreff, K.; Rosner, C.; Pankaj Kamdar, R.; Kokaraki, G.; Matsumoto, Y.; Davies, E.G.; van der Burg, M.; Notarangelo, L.D.; et al. DNA-PKcs Is Involved in Ig Class Switch Recombination in Human B Cells. *J. Immunol.* **2015**, *195*, 5608–5615. [CrossRef]
38. Soulas-Sprauel, P.; Le Guyader, G.; Rivera-Munoz, P.; Abramowski, V.; Olivier-Martin, C.; Goujet-Zalc, C.; Charneau, P.; De Villartay, J.P. Role for DNA repair factor XRCC4 in immunoglobulin class switch recombination. *J. Exp. Med.* **2007**, *204*, 1717–1727. [CrossRef]
39. Chi, X.; Li, Y.; Qiu, X. V(D)J recombination, somatic hypermutation and class switch recombination of immunoglobulins: Mechanism and regulation. *Immunology* **2020**, *160*, 233–247. [CrossRef] [PubMed]
40. Ramachandran, S.; Haddad, D.; Li, C.; Le, M.X.; Ling, A.K.; So, C.C.; Nepal, R.M.; Gommerman, J.L.; Yu, K.; Ketela, T.; et al. The SAGA Deubiquitination Module Promotes DNA Repair and Class Switch Recombination through ATM and DNAPK-Mediated γH2AX Formation. *Cell Rep.* **2016**, *15*, 1554–1565. [CrossRef] [PubMed]
41. Yan, M.; Zhang, X.; Pu, Q.; Huang, T.; Xie, Q.; Wang, Y.; Li, J.; Wang, Y.; Gu, H.; Huang, T.; et al. Immunoglobulin G Expression in Human Sperm and Possible Functional Significance. *Sci. Rep.* **2016**, *6*, 20166. [CrossRef] [PubMed]
42. Bandaria, J.N.; Qin, P.; Berk, V.; Chu, S.; Yildiz, A. Shelterin protects chromosome ends by compacting telomeric chromatin. *Cell* **2016**, *164*, 735–746. [CrossRef] [PubMed]
43. Deng, Y.; Guo, X.; Ferguson, D.O.; Chang, S. Multiple roles for MRE11 at uncapped telomeres. *Nature* **2009**, *460*, 914–918. [CrossRef] [PubMed]
44. Curtin, N.J. DNA repair dysregulation from cancer driver to therapeutic target. *Nat. Rev. Cancer* **2012**, *12*, 801–817. [CrossRef]
45. Krenning, L.; van den Berg, J.; Medema, R.H. Life or Death after a Break: What Determines the Choice? *Mol. Cell* **2019**, *76*, 346–358. [CrossRef]
46. Gutierrez, R.; O'Connor, T.R. DNA direct reversal repair and alkylating agent drug resistance. *Cancer Drug Resist.* **2021**. [CrossRef]
47. Dantuma, N.P.; Attikum, H. Spatiotemporal regulation of posttranslational modifications in the DNA damage response. *EMBO J.* **2016**, *35*, 6–23. [CrossRef] [PubMed]
48. Carusillo, A.; Mussolino, C. DNA Damage: From Threat to Treatment. *Cells* **2020**, *9*, 1665. [CrossRef]
49. Marteijn, J.A.; Lans, H.; Vermeulen, W.; Hoeijmakers, J.H.J. Understanding nucleotide excision repair and its roles in cancer and ageing. *Nat. Rev. Mol. Cell Biol.* **2014**, *15*, 465–481. [CrossRef]
50. Li, M.; Larsen, L.; Hedglin, M. Rad6/Rad18 Competes with DNA Polymerases η and δ for PCNA Encircling DNA. *Biochemistry* **2020**, *59*, 407–416. [CrossRef]
51. Parameswaran, B.; Chiang, H.C.; Lu, Y.; Coates, J.; Deng, C.X.; Baer, R.; Lin, H.K.; Li, R.; Paull, T.T.; Hu, Y. Damage-induced BRCA1 phosphorylation by Chk2 contributes to the timing of end resection. *Cell Cycle* **2015**, *14*, 437–448. [CrossRef] [PubMed]
52. Scully, R.; Panday, A.; Elango, R.; Willis, N.A. DNA double-strand break repair-pathway choice in somatic mammalian cells. *Nat. Rev. Mol. Cell Biol.* **2019**, *20*, 698–714. [CrossRef] [PubMed]
53. Zhao, K.; Wang, X.; Xue, X.; Li, L.; Hu, Y. A long noncoding RNA sensitizes genotoxic treatment by attenuating ATM activation and homologous recombination repair in cancers. *PLoS Biol.* **2020**, *18*, e3000666. [CrossRef]
54. Deans, A.J.; West, S.C. DNA interstrand crosslink repair and cancer. *Nat. Rev. Cancer* **2011**, *11*, 467–480. [CrossRef]
55. Smith, T.B.; Dun, M.D.; Smith, N.D.; Curry, B.J.; Connaughton, H.S.; Aitken, R.J. The presence of a truncated base excision repair pathway in human spermatozoa that is mediated by OGG1. *J. Cell Sci.* **2013**, *126*, 1488–1497. [CrossRef]
56. Khokhlova, E.V.; Fesenko, Z.S.; Sopova, J.V.; Leonova, E.I. Features of dna repair in the early stages of mammalian embryonic development. *Genes* **2020**, *11*, 1138. [CrossRef] [PubMed]
57. Ma, J.Y.; Yan, L.Y.; Wang, Z.B.; Luo, S.M.; Yeung, W.S.B.; Ou, X.H.; Sun, Q.Y.; Qiao, J. Meiotic chromatid recombination and segregation assessed with human single cell genome sequencing data. *J. Med. Genet.* **2019**, *56*, 156–163. [CrossRef]
58. Cheung, V.; Yuen, V.M.; Wong, G.T.C.; Choi, S.W. The effect of sleep deprivation and disruption on DNA damage and health of doctors. *Anaesthesia* **2019**, *74*, 434–440. [CrossRef] [PubMed]
59. Zada, D.; Bronshtein, I.; Lerer-Goldshtein, T.; Garini, Y.; Appelbaum, L. Sleep increases chromosome dynamics to enable reduction of accumulating DNA damage in single neurons. *Nat. Commun.* **2019**, *10*. [CrossRef]

60. Sadoughi, F.; Hallajzadeh, J.; Asemi, Z.; Mansournia, M.A.; Alemi, F.; Yousefi, B. Signaling pathways involved in cell cycle arrest during the DNA breaks. *DNA Repair* **2021**, *98*, 103047. [CrossRef]
61. Lee, D.H.; Chowdhury, D. What goes on must come off: Phosphatases gate-crash the DNA damage response. *Trends Biochem. Sci.* **2011**, *36*, 569–577. [CrossRef] [PubMed]
62. Ramos, F.; Villoria, M.T.; Alonso-Rodríguez, E.; Clemente-Blanco, A. Role of protein phosphatases PP1, PP2A, PP4 and Cdc14 in the DNA damage response. *Cell Stress* **2019**, *3*, 70–85. [CrossRef]
63. Burdova, K.; Storchova, R.; Palek, M.; Macurek, L. WIP1 Promotes Homologous Recombination and Modulates Sensitivity to PARP Inhibitors. *Cells* **2019**, *8*, 1258. [CrossRef]
64. Feringa, F.M.; Krenning, L.; Koch, A.; Van Den Berg, J.; Van Den Broek, B.; Jalink, K.; Medema, R.H. Hypersensitivity to DNA damage in antephase as a safeguard for genome stability. *Nat. Commun.* **2016**, *7*, 12618. [CrossRef]
65. Hayashi, M.T.; Cesare, A.J.; Fitzpatrick, J.A.J.; Lazzerini-Denchi, E.; Karlseder, J. A telomere-dependent DNA damage checkpoint induced by prolonged mitotic arrest. *Nat. Struct. Mol. Biol.* **2012**, *19*, 387–394. [CrossRef]
66. Kanellou, A.; Giakoumakis, N.N.; Panagopoulos, A.; Tsaniras, S.C.; Lygerou, Z. The licensing factor cdt1 links cell cycle progression to the DNA damage response. *Anticancer Res.* **2020**, *40*, 2449–2456. [CrossRef]
67. Reyes, J.; Chen, J.Y.; Stewart-Ornstein, J.; Karhohs, K.W.; Mock, C.S.; Lahav, G. Fluctuations in p53 Signaling Allow Escape from Cell-Cycle Arrest. *Mol. Cell* **2018**, *71*, 581–591.e5. [CrossRef] [PubMed]
68. Ngoi, N.Y.L.; Sundararajan, V.; Tan, D.S.P. Exploiting replicative stress in gynecological cancers as a therapeutic strategy. *Int. J. Gynecol. Cancer* **2020**, *30*, 1224–1238. [CrossRef] [PubMed]
69. Matt, S.; Hofmann, T.G. The DNA damage-induced cell death response: A roadmap to kill cancer cells. *Cell. Mol. Life Sci.* **2016**, *73*, 2829–2850. [CrossRef] [PubMed]
70. Oda, K.; Arakawa, H.; Tanaka, T.; Matsuda, K.; Tanikawa, C.; Mori, T.; Nishimori, H.; Tamai, K.; Tokino, T.; Nakamura, Y.; et al. p53AIP1, a potential mediator of p53-dependent apoptosis, and its regulation by ser-46-phosphorylated p53. *Cell* **2000**, *102*, 849–862. [CrossRef]
71. Cassina, A.; Silveira, P.; Cantu, L.; Montes, J.M.; Radi, R.; Sapiro, R. Defective human sperm cells are associated with mitochondrial dysfunction and oxidant production. *Biol. Reprod.* **2015**, *93*, 1–10. [CrossRef] [PubMed]
72. Liu, M.; Zeng, T.; Zhang, X.; Liu, C.; Wu, Z.; Yao, L.; Xie, C.; Xia, H.; Lin, Q.; Xie, L.; et al. ATR/Chk1 signaling induces autophagy through sumoylated RhoB-mediated lysosomal translocation of TSC2 after DNA damage. *Nat. Commun.* **2018**, *9*, 4139. [CrossRef]
73. Zhou, X.; Liu, W.; Hu, X.; Dorrance, A.; Garzon, R.; Houghton, P.J.; Shen, C. Regulation of CHK1 by mTOR contributes to the evasion of DNA damage barrier of cancer cells. *Sci. Rep.* **2017**, *7*, 1535. [CrossRef]
74. Shen, C.; Houghton, P.J. The mTOR pathway negatively controls ATM by up-regulating miRNAs. *Proc. Natl. Acad. Sci. USA* **2013**, *110*, 11869–11874. [CrossRef] [PubMed]
75. Weber, K.; Roelandt, R.; Bruggeman, I.; Estornes, Y.; Vandenabeele, P. Nuclear RIPK3 and MLKL contribute to cytosolic necrosome formation and necroptosis. *Commun. Biol.* **2018**, *1*, 6. [CrossRef] [PubMed]
76. Toledo, L.; Neelsen, K.J.; Lukas, J. Replication Catastrophe: When a Checkpoint Fails because of Exhaustion. *Mol. Cell* **2017**, *66*, 735–749. [CrossRef] [PubMed]
77. Stringer, J.M.; Winship, A.; Zerafa, N.; Wakefield, M.; Hutt, K. Oocytes can efficiently repair DNA double-strand breaks to restore genetic integrity and protect offspring health. *Proc. Natl. Acad. Sci. USA* **2020**, *117*, 11513–11522. [CrossRef] [PubMed]
78. Stringer, J.M.; Winship, A.; Liew, S.H.; Hutt, K. The capacity of oocytes for DNA repair. *Cell. Mol. Life Sci.* **2018**, *75*, 2777–2792. [CrossRef] [PubMed]
79. Gebel, J.; Tuppi, M.; Sänger, N.; Schumacher, B.; Dötsch, V. DNA Damaged Induced Cell Death in Oocytes. *Molecules* **2020**, *25*, 5714. [CrossRef] [PubMed]
80. Rémillard-Labrosse, G.; Dean, N.L.; Allais, A.; Mihajlović, A.I.; Jin, S.G.; Son, W.Y.; Chung, J.T.; Pansera, M.; Henderson, S.; Mahfoudh, A.; et al. Human oocytes harboring damaged DNA can complete meiosis I. *Fertil. Steril.* **2020**, *113*, 1080–1089.e2. [CrossRef]
81. Collins, J.K.; Jones, K.T. DNA damage responses in mammalian oocytes. *Reproduction* **2016**, *152*, R15–R22. [CrossRef]
82. Collins, J.K.; Lane, S.I.R.; Merriman, J.A.; Jones, K.T. DNA damage induces a meiotic arrest in mouse oocytes mediated by the spindle assembly checkpoint. *Nat. Commun.* **2015**, *6*, 8553. [CrossRef]
83. Archambeau, J.; Blondel, A.; Pedeux, R. Focus-ING on DNA integrity: Implication of ING proteins in cell cycle regulation and DNA repair modulation. *Cancers* **2020**, *12*, 58. [CrossRef]
84. Aymard, F.; Aguirrebengoa, M.; Guillou, E.; Javierre, B.M.; Bugler, B.; Rocher, V.; Iacovoni, J.S.; Biernacka, A.; Skrzypczak, M.; Ginalski, K.; et al. Genome-wide mapping of long-range contacts unveils clustering of DNA double-strand breaks at damaged active genes. *Nat. Struct. Mol. Biol.* **2017**, *24*, 353–361. [CrossRef] [PubMed]
85. Aymard, F.; Bugler, B.; Schmidt, C.K.; Guillou, E.; Caron, P.; Briois, S.; Iacovoni, J.S.; Daburon, V.; Miller, K.M.; Jackson, S.P.; et al. Transcriptionally active chromatin recruits homologous recombination at DNA double-strand breaks. *Nat. Struct. Mol. Biol.* **2014**, *21*, 366–374. [CrossRef] [PubMed]
86. Lemaître, C.; Grabarz, A.; Tsouroula, K.; Andronov, L.; Furst, A.; Pankotai, T.; Heyer, V.; Rogier, M.; Attwood, K.M.; Kessler, P.; et al. Nuclear position dictates DNA repair pathway choice. *Genes Dev.* **2014**, *28*, 2450–2463. [CrossRef]
87. van den Berg, J.; Joosten, S.E.; Kim, Y.; Manjón, A.G.; Krenning, L.; Koob, L.; Feringa, F.M.; Klompmaker, R.; van den Broek, B.; Jalink, K.; et al. DNA end-resection in highly accessible chromatin produces a toxic break. *bioRxiv* **2019**. [CrossRef]

88. Doksani, Y. The response to dna damage at telomeric repeats and its consequences for telomere function. *Genes* **2019**, *10*, 318. [CrossRef] [PubMed]
89. Campos, A.; Clemente-Blanco, A. Cell cycle and DNA repair regulation in the damage response: Protein phosphatases take over the reins. *Int. J. Mol. Sci.* **2020**, *21*, 446. [CrossRef]
90. Goodarzi, A.A.; Jonnalagadda, J.C.; Douglas, P.; Young, D.; Ye, R.; Moorhead, G.B.G.; Lees-Miller, S.P.; Khanna, K.K. Autophosphorylation of ataxia-telangiectasia mutated is regulated by protein phosphatase 2A. *EMBO J.* **2004**, *23*, 4451–4461. [CrossRef]
91. Zhang, J.; Bao, S.; Furumai, R.; Kucera, K.S.; Ali, A.; Dean, N.M.; Wang, X.-F. Protein Phosphatase 5 Is Required for ATR-Mediated Checkpoint Activation. *Mol. Cell. Biol.* **2005**, *25*, 9910–9919. [CrossRef] [PubMed]
92. Wang, Q.; Gao, F.; Wang, T.; Flagg, T.; Deng, X. A nonhomologous end-joining pathway is required for protein phosphatase 2A promotion of DNA double-strand break repair. *Neoplasia* **2009**, *11*, 1012–1021. [CrossRef] [PubMed]
93. Wechsler, T.; Chen, B.P.C.; Harper, R.; Morotomi-Yano, K.; Huang, B.C.B.; Meek, K.; Cleaver, J.E.; Chen, D.J.; Wabl, M. DNA-PKcs function regulated specifically by protein phosphatase 5. *Proc. Natl. Acad. Sci. USA* **2004**, *101*, 1247–1252. [CrossRef]
94. Mi, J.; Dziegielewski, J.; Bolesta, E.; Brautigan, D.L.; Larner, J.M. Activation of DNA-PK by ionizing radiation is mediated by protein phosphatase 6. *PLoS ONE* **2009**, *4*, e4395. [CrossRef]
95. Lu, X.; Nannenga, B.; Donehower, L. PPM1D dephosphorylates Chk1 and p53 and Abrogates Cell Cycle Checkpoints. *Genes Dev.* **2005**, 1162–1174. [CrossRef]
96. Oliva-Trastoy, M.; Berthonaud, V.; Chevalier, A.; Ducrot, C.; Marsolier-Kergoat, M.C.; Mann, C.; Leteurtre, F. The Wip1 phosphatase (PPM1D) antagonizes activation of the Chk2 tumour suppressor kinase. *Oncogene* **2007**, *26*, 1449–1458. [CrossRef] [PubMed]
97. Landsverk, H.B.; Mora-Bermúdez, F.; Landsverk, O.J.B.; Hasvold, G.; Naderi, S.; Bakke, O.; Ellenberg, J.; Collas, P.; Syljuåsen, R.G.; Küntziger, T. The protein phosphatase 1 regulator PNUTS is a new component of the DNA damage response. *EMBO Rep.* **2010**, *11*, 868–875. [CrossRef]
98. Macurek, L.; Lindqvist, A.; Voets, O.; Kool, J.; Vos, H.R.; Medema, R.H. Wip1 phosphatase is associated with chromatin and dephosphorylates γh2AX to promote checkpoint inhibition. *Oncogene* **2010**, *29*, 2281–2291. [CrossRef] [PubMed]
99. Yu, Y.M.; Pace, S.M.; Allen, S.R.; Deng, C.X.; Hsu, L.C. A PP1-binding motif present in BRCA1 plays a role in its DNA repair function. *Int. J. Biol. Sci.* **2008**, *4*, 352–361. [CrossRef]
100. Kang, Y.; Lee, J.H.; Hoan, N.N.; Sohn, H.M.; Chang, I.Y.; You, H.J. Protein phosphatase 5 regulates the function of 53BP1 after neocarzinostatin-induced DNA damage. *J. Biol. Chem.* **2009**, *284*, 9845–9853. [CrossRef]
101. Eissler, C.L.; Mazón, G.; Powers, B.L.; Savinov, S.N.; Symington, L.S.; Hall, M.C. The Cdk/Cdc14 Module Controls Activation of the Yen1 Holliday Junction Resolvase to Promote Genome Stability. *Mol. Cell* **2014**, *54*, 80–93. [CrossRef]
102. Batchelor, E.; Mock, C.S.; Bhan, I.; Loewer, A.; Lahav, G. A Mechanism for Triggering p53 Pulses in Response to DNA Damage. *Mol Cell.* **2008**, *53*, 277–289. [CrossRef]
103. Smolka, M. Fine-tuning the DNA damage response: Protein phosphatase 2A checks on CHK2. *Cell Cycle* **2010**, *9*, 861–869. [CrossRef]
104. Freeman, A.K.; Monteiro, A.N.A. Phosphatases in the cellular response to DNA damage. *Cell Commun. Signal.* **2010**, *8*, 27. [CrossRef]
105. Lee, D.H.; Pan, Y.; Kanner, S.; Sung, P.; Borowiec, J.A.; Chowdhury, D. A PP4 phosphatase complex dephosphorylates RPA2 to facilitate DNA repair via homologous recombination. *Nat. Struct. Mol. Biol.* **2010**, *17*, 365–372. [CrossRef] [PubMed]
106. Liu, Y.; Kvaratskhelia, M.; Hess, S.; Qu, Y.; Zou, Y. Modulation of replication protein A function by its hyperphosphorylation-induced conformational change involving DNA binding domain B. *J. Biol. Chem.* **2005**, *280*, 32775–32783. [CrossRef] [PubMed]
107. Morris, J.R.; Boutell, C.; Keppler, M.; Densham, R.; Weekes, D.; Alamshah, A.; Butler, L.; Galanty, Y.; Pangon, L.; Kiuchi, T.; et al. The SUMO modification pathway is involved in the BRCA1 response to genotoxic stress. *Nature* **2009**, *462*, 886–890. [CrossRef]
108. Liu, C.; Vyas, A.; Kassab, M.A.; Singh, A.K.; Yu, X. The role of poly ADP-ribosylation in the first wave of DNA damage response. *Nucleic Acids Res.* **2017**, *45*, 8129–8141. [CrossRef]
109. Brown, J.S.; Lukashchuk, N.; Sczaniecka-Clift, M.; Britton, S.; le Sage, C.; Calsou, P.; Beli, P.; Galanty, Y.; Jackson, S.P. Neddylation Promotes Ubiquitylation and Release of Ku from DNA-Damage Sites. *Cell Rep.* **2015**, *11*, 704–714. [CrossRef]
110. Guo, Z.; Wang, S.; Xie, Y.; Han, Y.; Hu, S.; Guan, H.; Xie, D.; Bai, C.; Liu, X.; Gu, Y.; et al. HUWE1-dependent DNA-PKcs neddylation modulates its autophosphorylation in DNA damage response. *Cell Death Dis.* **2020**, *11*. [CrossRef]
111. Gong, F.; Chiu, L.Y.; Miller, K.M. Acetylation Reader Proteins: Linking Acetylation Signaling to Genome Maintenance and Cancer. *PLoS Genet.* **2016**, *12*, e1006272. [CrossRef]
112. Chen, Y.; Zhu, W.G. Biological function and regulation of histone and non-histone lysine methylation in response to DNA damage. *Acta Biochim. Biophys. Sin.* **2016**, *48*, 603–616. [CrossRef]
113. Liu, C.; Li, J. O-GlcNAc: A Sweetheart of the Cell Cycle and DNA Damage Response. *Front. Endocrinol.* **2018**, *9*, 415. [CrossRef]
114. Efimova, E.V.; Appelbe, O.K.; Ricco, N.; Lee, S.S.Y.; Liu, Y.; Wolfgeher, D.J.; Collins, T.N.; Flor, A.C.; Ramamurthy, A.; Warrington, S.; et al. O-GlcN acylation enhances double-strand break repair, promotes cancer cell proliferation, and prevents therapy-induced senescence in irradiated tumors. *Mol. Cancer Res.* **2019**, *17*, 1338–1350. [CrossRef]
115. Burger, K.; Ketley, R.F.; Gullerova, M. Beyond the Trinity of ATM, ATR, and DNA-PK: Multiple Kinases Shape the DNA Damage Response in Concert With RNA Metabolism. *Front. Mol. Biosci.* **2019**, *6*, 61. [CrossRef]

116. Anindya, R.; Aygün, O.; Svejstrup, J.Q. Damage-Induced Ubiquitylation of Human RNA Polymerase II by the Ubiquitin Ligase Nedd4, but Not Cockayne Syndrome Proteins or BRCA1. *Mol. Cell* **2007**, *28*, 386–397. [CrossRef] [PubMed]
117. Naro, C.; Bielli, P.; Pagliarini, V.; Sette, C. The interplay between DNA damage response and RNA processing: The unexpected role of splicing factors as gatekeepers of genome stability. *Front. Genet.* **2015**, *6*, 142. [CrossRef] [PubMed]
118. García-Muse, T.; Aguilera, A. R Loops: From Physiological to Pathological Roles. *Cell* **2019**, *179*, 604–618. [CrossRef] [PubMed]
119. Olazabal-Herrero, A.; Green, A.M.; Chen, X.; Sung, P.; Pillai, M.M.; Kupfer, G.M. Binding of FANCD2 to SRSF1 Splicing Factor Prevents Genomic Instability through R Loop Regulation. *Blood* **2020**, *136*, 19. [CrossRef]
120. Tuduri, S.; Crabbé, L.; Conti, C.; Tourrière, H.; Holtgreve-Grez, H.; Jauch, A.; Pantesco, V.; De Vos, J.; Thomas, A.; Theillet, C.; et al. Topoisomerase I suppresses genomic instability by preventing interference between replication and transcription. *Nat. Cell Biol.* **2010**, *11*. Erratum in **2010**, *12*, 1122, doi:10.1038/ncb1110-1122. [CrossRef]
121. Li, X.; Manley, J.L. Inactivation of the SR protein splicing factor ASF/SF2 results in genomic instability. *Cell* **2005**, *122*, 365–378. [CrossRef]
122. Aguilera, A.; Huertas, P. Cotranscriptionally formed DNA:RNA hybrids mediate transcription elongation impairment and transcription-associated recombination. *Mol. Cell* **2003**, *12*, 711–721.
123. Gan, W.; Guan, Z.; Liu, J.; Gui, T.; Shen, K.; Manley, J.L.; Li, X. R-loop-mediated genomic instability is caused by impairment of replication fork progression. *Genes Dev.* **2011**, *25*, 2041–2056. [CrossRef] [PubMed]
124. Aguilera, A.; Gómez-González, B. DNA-RNA hybrids: The risks of DNA breakage during transcription. *Nat. Struct. Mol. Biol.* **2017**, *24*, 439–443. [CrossRef] [PubMed]
125. Ohle, C.; Tesorero, R.; Schermann, G.; Dobrev, N.; Sinning, I.; Fischer, T. Transient RNA-DNA Hybrids Are Required for Efficient Double-Strand Break Repair. *Cell* **2016**, *167*, 1001–1013.e7. [CrossRef]
126. Lu, W.T.; Hawley, B.R.; Skalka, G.L.; Baldock, R.A.; Smith, E.M.; Bader, A.S.; Malewicz, M.; Watts, F.Z.; Wilczynska, A.; Bushell, M. Drosha drives the formation of DNA:RNA hybrids around DNA break sites to facilitate DNA repair. *Nat. Commun.* **2018**, *9*. [CrossRef] [PubMed]
127. Mikolaskova, B.; Jurcik, M.; Cipakova, I.; Kretova, M.; Chovanec, M.; Cipak, L. Maintenance of genome stability: The unifying role of interconnections between the DNA damage response and RNA-processing pathways. *Curr. Genet.* **2018**, *64*, 971–983. [CrossRef] [PubMed]
128. Palancade, B.; Rothstein, R. The Ultimate (Mis)match: When DNA Meets RNA. *Cells* **2021**, *10*, 1433. [CrossRef]
129. Hatchi, E.; Skourti-Stathaki, K.; Ventz, S.; Pinello, L.; Yen, A.; Kamieniarz-Gdula, K.; Dimitrov, S.; Pathania, S.; McKinney, K.M.; Eaton, M.L.; et al. BRCA1 recruitment to transcriptional pause sites is required for R-loop-driven DNA damage repair. *Mol. Cell* **2015**, *57*, 636–647. [CrossRef] [PubMed]
130. Bhatia, V.; Valdés-Sánchez, L.; Rodriguez-Martinez, D.; Bhattacharya, S.S. Formation of 53BP1 foci and ATM activation under oxidative stress is facilitated by RNA:DNA hybrids and loss of ATM-53BP1 expression promotes photoreceptor cell survival in mice [version 1; peer review: 1 approved, 3 approved with reservations]. *F1000Research* **2018**, *7*, 1233. [CrossRef] [PubMed]
131. Nguyen, H.D.; Yadav, T.; Giri, S.; Saez, B.; Graubert, T.A.; Zou, L. Functions of Replication Protein A as a Sensor of R Loops and a Regulator of RNaseH1. *Mol. Cell* **2017**, *65*, 832–847.e4. [CrossRef]
132. Kabeche, L.; Nguyen, H.D.; Buisson, R.; Zou, L. A mitosis-specific and R loop-driven ATR pathway promotes faithful chromosome segregation. *Science* **2018**, *359*, 108–114. [CrossRef]
133. Ketley, R.F.; Gullerova, M. Jack of all trades? The versatility of RNA in DNA double-strand break repair. *Essays Biochem.* **2020**, *64*, 721–735. [CrossRef]
134. Gioia, U.; Francia, S.; Cabrini, M.; Brambillasca, S.; Michelini, F.; Jones-Weinert, C.W.; d'Adda di Fagagna, F. Pharmacological boost of DNA damage response and repair by enhanced biogenesis of DNA damage response RNAs. *Sci. Rep.* **2019**, *9*, 6460. [CrossRef]
135. Yuan, M.; Zhao, S.; Chen, R.; Wang, G.; Bie, Y.; Wu, Q.; Cheng, J. MicroRNA-138 inhibits tumor growth and enhances chemosensitivity in human cervical cancer by targeting H2AX. *Exp. Ther. Med.* **2019**, 630–638. [CrossRef] [PubMed]
136. Lal, A.; Pan, Y.; Navarro, F.; Dykxhoorn, D.M.; Moreau, L.; Meire, E.; Bentwich, Z.; Lieberman, J.; Chowdhury, D. MiR-24-mediated downregulation of H2AX suppresses DNA repair in terminally differentiated blood cells. *Nat. Struct. Mol. Biol.* **2009**, *16*, 492–498. [CrossRef]
137. Lai, J.; Yang, H.; Zhu, Y.; Ruan, M.; Huang, Y.; Zhang, Q. MiR-7-5p-mediated downregulation of PARP1 impacts DNA homologous recombination repair and resistance to doxorubicin in small cell lung cancer. *BMC Cancer* **2019**, *19*, 602. [CrossRef]
138. Rezaeian, A.H.; Khanbabaei, H.; Calin, G.A. Therapeutic potential of the miRNA–ATM axis in the management of tumor radioresistance. *Cancer Res.* **2020**, *80*, 139–150. [CrossRef]
139. Yan, D.; Ng, W.L.; Zhang, X.; Wang, P.; Zhang, Z.; Mo, Y.; Mao, H. Targeting DNA-PKcs and ATM with miR-101 Sensitizes Tumors to Radiation. *Plos ONE* **2010**, *5*, e11397. [CrossRef]
140. Jia, X.Q.; Chen, Z.P.; Jiang, J.; Li, Y.; Kang, Z.; Wen, Z.P.; He, W.S.; Bin, L.W.; Yan, Y. MiR-182 regulates proliferation and apoptosis by targeting FBW7 in glioma cells. *Int. J. Clin. Exp. Med.* **2017**, *10*, 16085–16094.
141. Huang, J.; Wang, Y.; Dhillon, K.K.; Calses, P.; Villegas, E. Systematic Screen Identi fi es miRNAs That Target RAD51 and RAD51D to Enhance Chemosensitivity. *Mol. Cancer Res.* **2013**, *11*, 1564–1574. [CrossRef]
142. Song, L.; Dai, T.; Xie, Y.; Wang, C.; Lin, C.; Wu, Z.; Ying, Z.; Wu, J.; Li, M.; Li, J. Up-regulation of miR-1245 by c-myc targets BRCA2 and impairs DNA repair. *J. Mol. Cell Biol.* **2012**, *4*, 108–117. [CrossRef]

143. Liu, X.; Heng, C.; Li, Y.; Yu, L. MiR-302a sensitizes leukemia cells to etoposide by targeting Rad52. *Oncotarget* **2017**, *8*, 73884–73891. [CrossRef]
144. Wang, Y.; Zeng, G.; Jiang, Y. The emerging roles of MiR-125b in cancers. *Cancer Manag. Res.* **2020**, *12*, 1079–1088. [CrossRef]
145. Szpechcinski, A.; Florczuk, M.; Duk, K.; Zdral, A.; Rudzinski, S.; Bryl, M.; Czyzewicz, G.; Rudzinski, P.; Kupis, W.; Wojda, E.; et al. The expression of circulating miR-504 in plasma is associated with EGFR mutation status in non-small-cell lung carcinoma patients. *Cell. Mol. Life Sci.* **2019**, *76*, 3641–3656. [CrossRef]
146. Cristini, A.; Groh, M.; Kristiansen, M.S.; Gromak, N. RNA/DNA Hybrid Interactome Identifies DXH9 as a Molecular Player in Transcriptional Termination and R-Loop-Associated DNA Damage. *Cell Rep.* **2018**, *23*, 1891–1905. [CrossRef]
147. Bader, A.S.; Hawley, B.R.; Wilczynska, A.; Bushell, M. The roles of RNA in DNA double-strand break repair. *Br. J. Cancer* **2020**, *122*, 613–623. [CrossRef]
148. Dimitrova, N.; Zamudio, J.R.; Jong, R.M.; Soukup, D.; Resnick, R.; Sarma, K.; Ward, A.J.; Raj, A.; Lee, J.T.; Sharp, P.A.; et al. LincRNA-p21 Activates p21 In cis to Promote Polycomb Target Gene Expression and to Enforce the G1/S Checkpoint. *Mol. Cell* **2014**, *54*, 777–790. [CrossRef]
149. Santoni, G.; Morelli, M.B.; Nabissi, M.; Maggi, F.; Marinelli, O.; Santoni, M.; Amantini, C. Cross-talk between microRNAs, long non-coding RNAs and $p21^{Cip1}$ in glioma: Diagnostic, prognostic and therapeutic roles. *J. Cancer Metastasis Treat.* **2020**, *2020*. [CrossRef]
150. Chakraborty, A.; Tapryal, N.; Venkova, T.; Horikoshi, N.; Pandita, R.K.; Sarker, A.H.; Sarkar, P.S.; Pandita, T.K.; Hazra, T.K. Classical non-homologous end-joining pathway utilizes nascent RNA for error-free double-strand break repair of transcribed genes. *Nat. Commun.* **2016**, *7*, 13049. [CrossRef]
151. Morio, T. Recent advances in the study of immunodeficiency and DNA damage response. *Int. J. Hematol.* **2017**, *106*, 357–365. [CrossRef]
152. Nakad, R.; Schumacher, B. DNA damage response and immune defense: Links and mechanisms. *Front. Genet.* **2016**, *7*, 147. [CrossRef]
153. Härtlova, A.; Erttmann, S.F.; Raffi, F.A.M.; Schmalz, A.M.; Resch, U.; Anugula, S.; Lienenklaus, S.; Nilsson, L.M.; Kröger, A.; Nilsson, J.A.; et al. DNA Damage Primes the Type I Interferon System via the Cytosolic DNA Sensor STING to Promote Anti-Microbial Innate Immunity. *Immunity* **2015**, *42*, 332–343. [CrossRef]
154. Soriani, A.; Zingoni, A.; Cerboni, C.; Iannitto, M.L.; Ricciardi, M.R.; Di Gialleonardo, V.; Cippitelli, M.; Fionda, C.; Petrucci, M.T.; Guarini, A.; et al. ATM-ATR—dependent up-regulation of DNAM-1 and NKG2D ligands on multiple myeloma cells by therapeutic agents results in enhanced NK-cell susceptibility and is associated with a senescent phenotype. *Blood J. Am. Soc. Hematol.* **2016**, *113*, 3503–3512. [CrossRef]
155. Noble, P.W.; Bernatsky, S.; Clarke, A.E.; Isenberg, D.A.; Ramsey-Goldman, R.; Hansen, J.E. DNA-damaging autoantibodies and cancer: The lupus butterfly theory. *Nat. Rev. Rheumatol.* **2016**, *12*, 429–434. [CrossRef]
156. Blatt, N.B.; Glick, G.D. Anti-DNA autoantibodies and systemic lupus erythematosus. *Pharmacol. Ther.* **1999**, *83*, 125–139. [CrossRef]
157. Hansen, J.E.; Chan, G.; Liu, Y.; Hegan, D.C.; Dalal, S.; Dray, E.; Kwon, Y.; Xu, Y.; Xu, X.; Peterson-roth, E.; et al. Targeting Cancer with a Lupus Autoantibody. *Sci. Transl. Med.* **2012**, *4*, 157ra142. [CrossRef] [PubMed]
158. Nastasi, C.; Mannarino, L.; D'Incalci, M. DNA Damage Response and Immune Defense. *Int J Mol Sci.* **2020**, *21*, 7504. [CrossRef] [PubMed]
159. Erttmann, S.F.; Härtlova, A.; Sloniecka, M.; Raffi, F.A.; Hosseinzadeh, A.; Edgren, T.; Rofougaran, R.; Resch, U.; Fällman, M.; Ek, T.; et al. Loss of the DNA Damage Repair Kinase ATM Impairs Inflammasome-Dependent Anti-Bacterial Innate Immunity. *Immunity* **2016**, *45*, 106–118. [CrossRef]
160. Sahan, A.Z.; Hazra, T.K.; Das, S. The Pivotal role of DNA repair in infection mediated-inflammation and cancer. *Front. Microbiol.* **2018**, *9*, 663. [CrossRef] [PubMed]
161. Bode, C.; Fox, M.; Tewary, P.; Steinhagen, A.; Ellerkmann, R.K.; Klinman, D.; Baumgarten, G.; Hornung, V.; Steinhagen, F. Human plasmacytoid dentritic cells elicit a Type I Interferon response by sensing DNA via the cGAS-STING signaling pathway. *Eur. J. Immunol.* **2016**, *46*, 1615–1621. [CrossRef] [PubMed]
162. Bennett, L.; Palucka, A.K.; Arce, E.; Cantrell, V.; Borvak, J.; Banchereau, J.; Pascual, V. Interferon and granulopoiesis signatures in systemic lupus erythematosus blood. *J. Exp. Med.* **2003**, *197*, 711–723. [CrossRef] [PubMed]
163. Zhong, L.; Hu, M.M.; Bian, L.J.; Liu, Y.; Chen, Q.; Shu, H.B. Phosphorylation of cGAS by CDK1 impairs self-DNA sensing in mitosis. *Cell Discov.* **2020**, *6*. [CrossRef] [PubMed]
164. Hwang, H.S.; Lee, M.H.; Choi, M.H. Induction of pro-inflammatory cytokines by 29-kDa FN-f via cGAS/STING pathway. *BMB Rep.* **2019**, *52*, 336–341. [CrossRef]
165. Rodriguez-iturbe, B.; Pons, H.; Johnson, R.J. Role of the immune system in hypertension. *Physiol. Rev.* **2017**, 1127–1164. [CrossRef]
166. Formanowicz, D.; Rybarczyk, A.; Radom, M. A Role of Inflammation and Immunity in Essential Hypertension—Modeled and Analyzed Using Petri Nets. *Int. J. Mol. Sci.* **2020**, *21*, 3348. [CrossRef]
167. Czopek, A.; Moorhouse, R.; Farrah, T.; Lenoir, O.; Owen, E.; Van Bragt, J.; Costello, H.M.; Menolascina, F.; Webb, D.J.; Kluth, D.C.; et al. A novel role for myeloid endothelin-B receptors in hypertension. *Eur. Heart J.* **2019**, *40*, 768–784. [CrossRef]
168. Kominsky, D.J.; Campbell, E.L.; Colgan, S.P. Metabolic Shifts in Immunity and Inflammation. *J. Immunol.* **2010**, *184*, 4062–4068. [CrossRef] [PubMed]

169. Fulop, T.; Larbi, A.; Dupuis, G.; Le Page, A.; Frost, E.H.; Cohen, A.A.; Witkowski, J.M.; Franceschi, C. Immunosenescence and inflamm-aging as two sides of the same coin: Friends or Foes? *Front. Immunol.* **2018**, *8*, 1960. [CrossRef]
170. Petr, M.A.; Tulika, T.; Carmona-Marin, L.M.; Scheibye-Knudsen, M. Protecting the Aging Genome. *Trends Cell Biol.* **2020**, *30*, 117–132. [CrossRef]
171. Qin, S.; Xu, L.; Yi, M.; Yu, S.; Wu, K.; Luo, S. Novel immune checkpoint targets: Moving beyond PD-1 and CTLA-4. *Mol. Cancer* **2019**, *18*, 155. [CrossRef] [PubMed]
172. Simpson, J.E.; Ince, P.G.; Minett, T.; Matthews, F.E.; Heath, P.R.; Shaw, P.J.; Goodall, E.; Garwood, C.J.; Ratcliffe, L.E.; Brayne, C.; et al. Neuronal DNA damage response-associated dysregulation of signalling pathways and cholesterol metabolism at the earliest stages of Alzheimer-type pathology. *Neuropathol. Appl. Neurobiol.* **2016**, *42*, 167–179. [CrossRef]
173. Abugable, A.A.; Morris, J.L.M.; Palminha, N.M.; Zaksauskaite, R.; Ray, S.; El-Khamisy, S.F. DNA repair and neurological disease: From molecular understanding to the development of diagnostics and model organisms. *DNA Repair* **2019**, *81*, 102669. [CrossRef]
174. Kurihara, M.; Mano, T.; Saito, Y.; Murayama, S.; Toda, T.; Iwata, A. Colocalization of BRCA1 with Tau aggregates in human tauopathies. *Brain Sci.* **2020**, *10*, 7. [CrossRef] [PubMed]
175. Taylor, A.M.R.; Rothblum-Oviatt, C.; Ellis, N.A.; Hickson, I.D.; Meyer, S.; Crawford, T.O.; Smogorzewska, A.; Pietrucha, B.; Weemaes, C.; Stewart, G.S. Chromosome instability syndromes. *Nat. Rev. Dis. Prim.* **2019**, *5*. [CrossRef]
176. McKinnon, P.J. DNA repair deficiency and neurological disease. *Nat. Rev. Neurosci.* **2009**, *10*, 100–112. [CrossRef]
177. Fang, E.F.; Scheibye-Knudsen, M.; Chua, K.F.; Mattson, M.P.; Croteau, D.L.; Bohr, V.A. Nuclear DNA damage signalling to mitochondria in ageing. *Nat. Rev. Mol. Cell Biol.* **2016**, *17*, 308–321. [CrossRef] [PubMed]
178. Whittemore, K.; Vera, E.; Martínez-Nevado, E.; Sanpera, C.; Blasco, M.A. Telomere shortening rate predicts species life span. *Proc. Natl. Acad. Sci. USA* **2019**, *116*, 15122–15127. [CrossRef]
179. Vizioli, M.G.; Liu, T.; Miller, K.N.; Robertson, N.A.; Gilroy, K.; Lagnado, A.B.; Perez-Garcia, A.; Kiourtis, C.; Dasgupta, N.; Lei, X.; et al. Mitochondria-to-nucleus retrograde signaling drives formation of cytoplasmic chromatin and inflammation in senescence. *Genes Dev.* **2020**, *34*, 428–445. [CrossRef]
180. Tiwari, V.; Wilson, D.M. DNA Damage and Associated DNA Repair Defects in Disease and Premature Aging. *Am. J. Hum. Genet.* **2019**, *105*, 237–257. [CrossRef] [PubMed]
181. Lan, Y.Y.; Heather, J.M.; Eisenhaure, T.; Garris, C.S.; Lieb, D.; Raychowdhury, R.; Hacohen, N. Extranuclear DNA accumulates in aged cells and contributes to senescence and inflammation. *Aging Cell* **2019**, *18*. [CrossRef]
182. Tyrrell, D.J.; Blin, M.G.; Song, J.; Wood, S.C.; Goldstein, D.R. Aging impairs mitochondrial function and mitophagy and elevates interleukin 6 within the cerebral vasculature. *J. Am. Heart Assoc.* **2020**, *9*. [CrossRef] [PubMed]
183. Fang, E.F.; Scheibye-Knudsen, M.; Brace, L.E.; Kassahun, H.; Sengupta, T.; Nilsen, H.; Mitchell, J.R.; Croteau, D.L.; Bohr, V.A. Defective mitophagy in XPA via PARP-1 hyperactivation and NAD +/SIRT1 reduction. *Cell* **2014**, *157*, 882–896. [CrossRef]
184. Patel, J.; Baptiste, B.A.; Kim, E.; Hussain, M.; Croteau, D.L.; Bohr, V.A. DNA damage and mitochondria in cancer and aging. *Carcinogenesis* **2020**, *41*, 1625–1634. [CrossRef] [PubMed]
185. Turan, V.; Oktay, K. BRCA-related ATM-mediated DNA double-strand break repair and ovarian aging. *Hum. Reprod. Update* **2020**, *26*, 43–57. [CrossRef]
186. Lin, F.; Ma, X.S.; Wang, Z.B.; Wang, Z.W.; Luo, Y.B.; Huang, L.; Jiang, Z.Z.; Hu, M.W.; Schatten, H.; Sun, Q.Y. Different fates of oocytes with DNA double-strand breaks in vitro and in vivo. *Cell Cycle* **2014**, *13*, 2674–2680. [CrossRef] [PubMed]
187. Sasaki, H.; Hamatani, T.; Kamijo, S.; Iwai, M.; Kobanawa, M.; Ogawa, S.; Miyado, K.; Tanaka, M. Impact of Oxidative Stress on Age-Associated Decline in Oocyte Developmental Competence. *Front. Endocrinol.* **2019**, *10*, 811. [CrossRef]
188. Shukla, P.C.; Singh, K.K.; Yanagawa, B.; Teoh, H.; Verma, S. DNA damage repair and cardiovascular diseases. *Can. J. Cardiol.* **2010**, *26*, 13A–16A. [CrossRef]
189. Shukla, P.C.; Singh, K.K.; Quan, A.; Al-Omran, M.; Teoh, H.; Lovren, F.; Cao, L.; Rovira, I.I.; Pan, Y.; Brezden-Masley, C.; et al. BRCA1 is an essential regulator of heart function and survival following myocardial infarction. *Nat. Commun.* **2011**, *2*. [CrossRef]
190. Higo, T.; Naito, A.T.; Sumida, T.; Shibamoto, M.; Okada, K.; Nomura, S.; Nakagawa, A.; Yamaguchi, T.; Sakai, T.; Hashimoto, A.; et al. DNA single-strand break-induced DNA damage response causes heart failure. *Nat. Commun.* **2017**, *8*. [CrossRef]
191. Uryga, A.; Gray, K.; Bennett, M. DNA Damage and Repair in Vascular Disease. *Annu. Rev. Physiol.* **2016**, *78*, 45–66. [CrossRef]
192. Shah, A.; Gray, K.; Figg, N.; Finigan, A.; Starks, L.; Bennett, M. Defective base excision repair of oxidative DNA damage in vascular smooth muscle cells promotes atherosclerosis. *Circulation* **2018**, *138*, 1446–1462. [CrossRef]
193. Ishida, T.; Ishida, M.; Tashiro, S.; Yoshizumi, M.; Kihara, Y. Role of DNA damage in cardiovascular disease. *Circ. J.* **2014**, *78*, 42–50. [CrossRef]
194. Kumar, V.; Agrawal, R.; Pandey, A.; Kopf, S.; Hoeffgen, M.; Kaymak, S.; Bandapalli, O.R.; Gorbunova, V.; Seluanov, A.; Mall, M.A.; et al. Compromised DNA repair is responsible for diabetes-associated fibrosis. *EMBO J.* **2020**, *39*, e103477. [CrossRef] [PubMed]
195. Tay, V.S.Y.; Devaraj, S.; Koh, T.; Ke, G.; Crasta, K.C.; Ali, Y. Increased double strand breaks in diabetic β-cells with a p21 response that limits apoptosis. *Sci. Rep.* **2019**, *9*, 19341. [CrossRef]
196. Włodarczyk, M.; Nowicka, G. Obesity, DNA damage, and development of obesity-related diseases. *Int. J. Mol. Sci.* **2019**, *20*, 1146. [CrossRef] [PubMed]
197. Vergoni, B.; Cornejo, P.J.; Gilleron, J.; Djedaini, M.; Ceppo, F.; Jacquel, A.; Bouget, G.; Ginet, C.; Gonzalez, T.; Maillet, J.; et al. DNA damage and the activation of the p53 pathway mediate alterations in metabolic and secretory functions of adipocytes. *Diabetes* **2016**, *65*, 3062–3074. [CrossRef]

198. Setayesh, T.; Mi, M.; Langie, S.A.S.; Godschalk, R.; Waldherr, M.; Bauer, T.; Leitner, S.; Bichler, C.; Prager, G.; Krupitza, G.; et al. Impact of Weight Loss Strategies on Obesity-Induced DNA Damage. *Mol. Nutr. Food Res.* **2019**, *63*, 1900045. [CrossRef] [PubMed]
199. Fehrmann, R.S.N.; Karjalainen, J.M.; Krajewska, M.; Westra, H.J.; Maloney, D.; Simeonov, A.; Pers, T.H.; Hirschhorn, J.N.; Jansen, R.C.; Schultes, E.A.; et al. Gene expression analysis identifies global gene dosage sensitivity in cancer. *Nat. Genet.* **2015**, *47*, 115–125. [CrossRef]
200. Caudron-Herger, M.; Diederichs, S. Mitochondrial mutations in human cancer: Curation of translation. *RNA Biol.* **2018**, *15*, 62–69. [CrossRef]
201. Yuan, Y.; Ju, Y.S.; Kim, Y.; Li, J.; Wang, Y.; Yoon, C.J.; Yang, Y.; Martincorena, I.; Creighton, C.J.; Weinstein, J.N.; et al. Comprehensive molecular characterization of mitochondrial genomes in human cancers. *Nat. Genet.* **2020**, *52*, 342–352. [CrossRef]
202. Kurian, A.W.; Hughes, E.; Handorf, E.A.; Gutin, A.; Allen, B.; Hartman, A.-R.; Hall, M.J. Breast and Ovarian Cancer Penetrance Estimates Derived From Germline Multiple-Gene Sequencing Results in Women. *JCO Precis. Oncol.* **2017**. [CrossRef]
203. Kurian, A.W.; Ward, K.C.; Howlader, N.; Deapen, D.; Hamilton, A.S. Genetic Testing and Results in a Population-Based Cohort of Breast Cancer Patients and Ovarian Cancer Patients. *J. Clin. Oncol.* **2021**, *37*, 1305–1316. [CrossRef] [PubMed]
204. Alexandrov, L.B.; Kim, J.; Haradhvala, N.J.; Huang, M.N.; Tian Ng, A.W.; Wu, Y.; Boot, A.; Covington, K.R.; Gordenin, D.A.; Bergstrom, E.N.; et al. The repertoire of mutational signatures in human cancer. *Nature* **2020**, *578*, 94–101. [CrossRef]
205. Cieslik, M.; Chinnaiyan, A.M. News & views Global cancer genomics project comes to fruition. *Nature* **2020**, *578*, 40.
206. Greten, F.R.; Grivennikov, S.I. Inflammation and Cancer: Triggers, Mechanisms, and Consequences. *Immunity* **2019**, *51*, 27–41. [CrossRef]
207. Kay, J.; Thadhani, E.; Samson, L.; Engelward, B. Inflammation-induced DNA damage, mutations and cancer. *DNA Repair* **2019**, *83*. [CrossRef]
208. Axelrad, J.E.; Lichtiger, S.; Yajnik, V. Inflammatory bowel disease and cancer: The role of inflammation, immunosuppression, and cancer treatment. *World J. Gastroenterol.* **2016**, *22*, 4794–4801. [CrossRef] [PubMed]
209. Aiello, I.; Mul Fedele, M.L.; Román, F.; Marpegan, L.; Caldart, C.; Chiesa, J.J.; Golombek, D.A.; Finkielstein, C.V.; Paladino, N. Circadian disruption promotes tumor-immune microenvironment remodeling favoring tumor cell proliferation. *Sci. Adv.* **2020**, *6*. [CrossRef] [PubMed]
210. Veena, M.S.; Raychaudhuri, S.; Basak, S.K.; Venkatesan, N.; Kumar, P.; Biswas, R.; Chakrabarti, R.; Lu, J.; Su, T.; Gallagher-Jones, M.; et al. Dysregulation of hsa-miR-34a and hsa-miR-449a leads to overexpression of PACS-1 and loss of DNA damage response (DDR) in cervical cancer. *J. Biol. Chem.* **2020**, *295*, 17169–17186. [CrossRef]
211. Fell, V.L.; Schild-Poulter, C. Ku Regulates Signaling to DNA Damage Response Pathways through the Ku70 von Willebrand A Domain. *Mol. Cell. Biol.* **2012**, *32*, 76–87. [CrossRef]
212. Bian, L.; Meng, Y.; Zhang, M.; Li, D. MRE11-RAD50-NBS1 complex alterations and DNA damage response: Implications for cancer treatment. *Mol. Cancer* **2019**, *18*, 169. [CrossRef] [PubMed]
213. Gudmundsdottir, K.; Ashworth, A. The roles of BRCA1 and BRCA2 and associated proteins in the maintenance of genomic stability. *Oncogene* **2006**, *25*, 5864–5874. [CrossRef] [PubMed]
214. Rajendra, E.; Oestergaard, V.H.; Langevin, F.; Wang, M.; Dornan, G.L.; Patel, K.J.; Passmore, L.A. The Genetic and Biochemical Basis of FANCD2 Monoubiquitination. *Mol. Cell* **2014**, *54*, 858–869. [CrossRef] [PubMed]
215. Sullivan, M.R.; Bernstein, K.A. RAD-ical new insights into RAD51 regulation. *Genes* **2018**, *9*, 629. [CrossRef]
216. Chen, L.; Huang, S.; Lee, L.; Davalos, A.; Schiestl, R.H.; Campisi, J.; Oshima, J. WRN, the protein deficient in Werner syndrome, plays a critical structural role in optimizing DNA repair. *Aging Cell* **2003**, *2*, 191–199. [CrossRef] [PubMed]
217. Shell, S.M.; Hawkins, E.K.; Tsai, M.S.; Hlaing, A.S.; Rizzo, C.J.; Chazin, W.J. Xeroderma pigmentosum complementation group C protein (XPC) serves as a general sensor of damaged DNA. *DNA Repair* **2013**, *12*, 947–953. [CrossRef]
218. Ba, X.; Boldogh, I. 8-Oxoguanine DNA glycosylase 1: Beyond repair of the oxidatively modified base lesions. *Redox Biol.* **2018**, *14*, 669–678. [CrossRef] [PubMed]
219. Leppard, J.B.; Dong, Z.; Mackey, Z.B.; Tomkinson, A.E. Physical and Functional Interaction between DNA Ligase IIIα and Poly(ADP-Ribose) Polymerase 1 in DNA Single-Strand Break Repair. *Mol. Cell. Biol.* **2003**, *23*, 5919–5927. [CrossRef]
220. O'Brien, V.; Brown, R. Signalling cell cycle arrest and cell death through the MMR System. *Carcinogenesis* **2006**, *27*, 682–692. [CrossRef] [PubMed]
221. Sweeney, S.M.; Cerami, E.; Baras, A.; Pugh, T.J.; Schultz, N.; Stricker, T.; Lindsay, J.; Del Vecchio Fitz, C.; Kumari, P.; Micheel, C.; et al. AACR project genie: Powering precision medicine through an international consortium. *Cancer Discov.* **2017**, *7*, 818–831. [CrossRef]
222. Yap, T.A.; Plummer, R.; Azad, N.S.; Helleday, T. The DNA Damaging Revolution: PARP Inhibitors and Beyond. *Am. Soc. Clin. Oncol. Educ. B* **2019**, 185–195. [CrossRef]
223. Reuvers, T.G.A.; Kanaar, R.; Nonnekens, J. DNA damage-inducing anticancer therapies: From global to precision damage. *Cancers* **2020**, *12*, 2098. [CrossRef] [PubMed]
224. Pilié, P.G.; Tang, C.; Mills, G.B.; Yap, T.A. State-of-the-art strategies for targeting the DNA damage response in cancer. *Nat. Rev. Clin. Oncol.* **2019**, *16*, 81–104. [CrossRef]
225. Zhou, P.; Wang, J.; Mishail, D.; Wang, C.-Y. Recent advancements in PARP inhibitors-based targeted cancer therapy. *Precis. Clin. Med.* **2020**, *3*, 187–201. [CrossRef] [PubMed]

226. Gourley, C.; Balmaña, J.; Ledermann, J.A.; Serra, V.; Dent, R.; Loibl, S.; Pujade-Lauraine, E.; Boulton, S.J. Moving from poly (ADP-ribose) polymerase inhibition to targeting DNA repair and DNA damage response in cancer therapy. *J. Clin. Oncol.* **2019**, *37*, 2257–2269. [CrossRef] [PubMed]
227. Laurini, E.; Marson, D.; Fermeglia, A.; Aulic, S.; Fermeglia, M.; Pricl, S. Role of Rad51 and DNA repair in cancer: A molecular perspective. *Pharmacol. Ther.* **2020**, *208*, 107492. [CrossRef]
228. Yin, Y.; Chen, F. Targeting human MutT homolog 1 (MTH1) for cancer eradication: Current progress and perspectives. *Acta Pharm. Sin. B* **2020**, *10*, 2259–2271. [CrossRef]
229. Schrempf, A.; Slyskova, J.; Loizou, J.I. Targeting the DNA Repair Enzyme Polymerase θ in Cancer Therapy. *Trends Cancer* **2021**, *7*, 98–111. [CrossRef]
230. Farmer, H.; McCabe, H.; Lord, C.J.; Tutt, A.H.J.; Johnson, D.A.; Richardson, T.B.; Santarosa, M.; Dillon, K.J.; Hickson, I.; Knights, C.; et al. Targeting the DNA repair defect in BRCA mutant cells as a therapeutic strategy. *Nature* **2005**, *434*, 917–921. [CrossRef]
231. Foskolou, I.P.; Jorgensen, C.; Leszczynska, K.B.; Olcina, M.M.; Tarhonskaya, H.; Haisma, B.; D'Angiolella, V.; Myers, W.K.; Domene, C.; Flashman, E.; et al. Ribonucleotide Reductase Requires Subunit Switching in Hypoxia to Maintain DNA Replication. *Mol. Cell* **2017**, *66*, 206–220.e9. [CrossRef]
232. Xiao, Y.; Jin, L.; Deng, C.; Guan, Y.; Kalogera, E.; Ray, U.; Thirusangu, P.; Staub, J.; Sarkar Bhattacharya, S.; Xu, H.; et al. Inhibition of PFKFB3 induces cell death and synergistically enhances chemosensitivity in endometrial cancer. *Oncogene* **2021**, *40*, 1409–1424. [CrossRef]
233. Karakaidos, P.; Karagiannis, D.; Rampias, T. Resolving DNA damage: Epigenetic regulation of DNA repair. *Molecules* **2020**, *25*, 2496. [CrossRef]
234. Thurn, K.T.; Thomas, S.; Raha, P.; Qureshi, I.; Munster, P.N. Histone deacetylase regulation of ATM-mediated DNA damage signaling. *Mol. Cancer Ther.* **2013**, *12*, 2078–2087. [CrossRef]
235. Loughery, J.E.P.; Dunne, P.D.; O'Neill, K.M.; Meehan, R.R.; McDaid, J.R.; Walsh, C.P. DNMT1 deficiency triggers mismatch repair defects in human cells through depletion of repair protein levels in a process involving the DNA damage response. *Hum. Mol. Genet.* **2011**, *20*, 3241–3255. [CrossRef]
236. Topatana, W.; Juengpanich, S.; Li, S.; Cao, J.; Hu, J.; Lee, J.; Suliyanto, K.; Ma, D.; Zhang, B.; Chen, M.; et al. Advances in synthetic lethality for cancer therapy: Cellular mechanism and clinical translation. *J. Hematol. Oncol.* **2020**, *13*, 118. [CrossRef] [PubMed]
237. Bryant, H.E.; Schultz, N.; Thomas, H.D.; Parker, K.M.; Flower, D.; Lopez, E.; Kyle, S.; Meuth, M.; Curtin, N.J.; Helleday, T. Specific killing of BRCA2-deficient tumours with inhibitors of poly(ADP-ribose) polymerase. *Nature* **2005**, *434*, 913–917. [CrossRef]
238. Sachdev, E.; Tabatabai, R.; Roy, V.; Rimel, B.J.; Mita, M.M. PARP Inhibition in Cancer: An Update on Clinical Development. *Target. Oncol.* **2019**, *14*, 657–679. [CrossRef]
239. Daud, A.I.; Ashworth, M.T.; Strosberg, J.; Goldman, J.W.; Mendelson, D.; Springett, G.; Venook, A.P.; Loechner, S.; Rosen, L.S.; Shanahan, F.; et al. Phase I dose-escalation trial of checkpoint kinase 1 inhibitor MK-8776 as monotherapy and in combination with gemcitabine in patients with advanced solid tumors. *J. Clin. Oncol.* **2015**, *33*, 1060–1066. [CrossRef] [PubMed]
240. Leijen, S.; Van Geel, R.M.J.M.; Pavlick, A.C.; Tibes, R.; Rosen, L.; Razak, A.R.A.; Lam, R.; Demuth, T.; Rose, S.; Lee, M.A.; et al. Phase I study evaluating WEE1 inhibitor AZD1775 as monotherapy and in combination with gemcitabine, cisplatin, or carboplatin in patients with advanced solid tumors. *J. Clin. Oncol.* **2016**, *34*, 4371–4380. [CrossRef] [PubMed]
241. Di Rorà, A.G.L.; Bocconcelli, M.; Ferrari, A.; Terragna, C.; Bruno, S.; Imbrogno, E.; Beeharry, N.; Robustelli, V.; Ghetti, M.; Napolitano, R.; et al. Synergism through WEE1 and CHK1 inhibition in acute lymphoblastic leukemia. *Cancers* **2019**, *11*, 1654. [CrossRef]
242. Munster, P.; Mita, M.; Mahipal, A.; Nemunaitis, J.; Massard, C.; Mikkelsen, T.; Cruz, C.; Paz-Ares, L.; Hidalgo, M.; Rathkopf, D.; et al. First-in-human phase i study of a dual mTOR kinase and DNA-PK inhibitor (CC-115) in advanced malignancy. *Cancer Manag. Res.* **2019**, *11*, 10463–10476. [CrossRef]
243. Jette, N.R.; Kumar, M.; Radhamani, S.; Arthur, G.; Goutam, S.; Yip, S.; Kolinsky, M.; Williams, G.J.; Bose, P.; Lees-Miller, S.P. ATM-deficient cancers provide new opportunities for precision oncology. *Cancers* **2020**, *12*, 687. [CrossRef]
244. Neeb, A.; Herranz, N.; Arce-Gallego, S.; Miranda, S.; Buroni, L.; Yuan, W.; Athie, A.; Casals, T.; Carmichael, J.; Rodrigues, D.N.; et al. Advanced Prostate Cancer with ATM Loss: PARP and ATR Inhibitors. *Eur. Urol.* **2021**, *79*, 200–211. [CrossRef]
245. Southgate, H.E.D.; Chen, L.; Tweddle, D.A.; Curtin, N.J. ATR Inhibition Potentiates PARP Inhibitor Cytotoxicity in High Risk Neuroblastoma Cell Lines by Multiple Mechanisms. *Cancers* **2020**, *12*, 1095. [CrossRef]
246. Higgins, G.S.; Prevo, R.; Lee, Y.F.; Helleday, T.; Muschel, R.J.; Taylor, S.; Yoshimura, M.; Hickson, I.D.; Bernhard, E.J.; McKenna, W.G. A small interfering RNA screen of genes involved in DNA repair identifies tumor-specific radiosensitization by POLQ knockdown. *Cancer Res.* **2010**, *70*, 2984–2993. [CrossRef] [PubMed]
247. George, S.L.; Lorenzi, F.; King, D.; Hartlieb, S.; Campbell, J.; Pemberton, H.; Toprak, U.H.; Barker, K.; Tall, J.; da Costa, B.M.; et al. Therapeutic vulnerabilities in the DNA damage response for the treatment of ATRX mutant neuroblastoma. *EBioMedicine* **2020**, *59*, 102971. [CrossRef] [PubMed]
248. Nogueira, A.; Fernandes, M.; Catarino, R.; Medeiros, R. RAD52 functions in homologous recombination and its importance on genomic integrity maintenance and cancer therapy. *Cancers* **2019**, *11*, 1622. [CrossRef] [PubMed]
249. Ciccarone, F.; Zampieri, M.; Caiafa, P. PARP1 orchestrates epigenetic events setting up chromatin domains. *Semin. Cell Dev. Biol.* **2017**, *63*, 123–134. [CrossRef]

250. Muvarak, N.E.; Chowdhury, K.; Xia, L.; Robert, C.; Choi, E.Y.; Cai, Y.; Bellani, M.; Zou, Y.; Singh, Z.N.; Duong, V.H.; et al. Enhancing the Cytotoxic Effects of PARP Inhibitors with DNA Demethylating Agents—A Potential Therapy for Cancer. *Cancer Cell* **2016**, *30*, 637–650. [CrossRef]
251. Marijon, H.; Lee, D.H.; Ding, L.W.; Sun, H.; Gery, S.; de Gramont, A.; Koeffler, H.P. Co-targeting poly(ADP-ribose) polymerase (PARP) and histone deacetylase (HDAC) in triple-negative breast cancer: Higher synergism in BRCA mutated cells. *Biomed. Pharmacother.* **2018**, *99*, 543–551. [CrossRef]
252. Park, Y.; Chui, M.H.; Rahmanto, Y.S.; Yu, Z.C.; Shamanna, R.A.; Bellani, M.A.; Gaillard, S.; Ayhan, A.; Viswanathan, A.; Seidman, M.M.; et al. Loss of ARID1A in tumor cells renders selective vulnerability to combined ionizing radiation and PARP inhibitor therapy. *Clin. Cancer Res.* **2019**, *25*, 5584–5593. [CrossRef]
253. Abad, E.; Graifer, D.; Lyakhovich, A. DNA damage response and resistance of cancer stem cells. *Cancer Lett.* **2020**, *474*, 106–117. [CrossRef]
254. Mir, S.E.; Hamer, P.C.D.W.; Krawczyk, P.M.; Balaj, L.; Claes, A.; Niers, J.M.; Van Tilborg, A.A.G.; Zwinderman, A.H.; Geerts, D.; Kaspers, G.J.L.; et al. Article In Silico Analysis of Kinase Expression Identifies WEE1 as a Gatekeeper against Mitotic Catastrophe in Glioblastoma. *Cancer Cell* **2010**, 244–257. [CrossRef]
255. Ahmed, S.U.; Carruthers, R.; Gilmour, L.; Yildirim, S.; Watts, C.; Chalmers, A.J. Selective Inhibition of Parallel DNA Damage Response Pathways Optimizes Radiosensitization of Glioblastoma Stem-like Cells. *Cancer Res.* **2015**, *75*, 4416–4428. [CrossRef] [PubMed]
256. Zhou, L.; Zhang, Y.; Chen, S.; Kmieciak, M.; Leng, Y.; Lin, H.; Rizzo, K.A.; Dumur, C.I.; Ferreira-Gonzalez, A.; Dai, Y.; et al. A regimen combining the Wee1 inhibitor AZD1775 with HDAC inhibitors targets human acute myeloid leukemia cells harboring various genetic mutations. *Leukemia* **2015**, *29*, 807–818. [CrossRef] [PubMed]
257. Jeggo, P.A.; Pearl, L.H.; Carr, A.M. DNA repair, genome stability and cancer: A historical perspective. *Nat. Rev. Cancer* **2016**, *16*, 35–42. [CrossRef] [PubMed]
258. Marabitti, V.; Lillo, G.; Malacaria, E.; Palermo, V.; Pichierri, P.; Franchitto, A. Checkpoint defects elicit a WRNIP1-mediated response to counteract R-loop-associated genomic instability. *Cancers* **2020**, *12*, 389. [CrossRef]
259. Park, S.R.; Namkoong, S.; Friesen, L.; Cho, C.S.; Zhang, Z.Z.; Chen, Y.C.; Yoon, E.; Kim, C.H.; Kwak, H.; Kang, H.M.; et al. Single-Cell Transcriptome Analysis of Colon Cancer Cell Response to 5-Fluorouracil-Induced DNA Damage. *Cell Rep.* **2020**, *32*, 108077. [CrossRef]
260. Sfeir, A.; Kosiyatrakul, S.T.; Hockemeyer, D.; MacRae, S.L.; Karlseder, J.; Schildkraut, C.L.; de Lange, T. Mammalian Telomeres Resemble Fragile Sites and Require TRF1 for Efficient Replication. *Cell* **2009**, *138*, 90–103. [CrossRef]
261. Parkinson, G.N.; Lee, M.P.H.; Neidle, S. Crystal structure of parallel quadruplexes from human telomeric DNA. *Nature* **2002**, *417*, 876–880. [CrossRef]
262. Masamsetti, V.P.; Low, R.R.J.; Mak, K.S.; O'Connor, A.; Riffkin, C.D.; Lamm, N.; Crabbe, L.; Karlseder, J.; Huang, D.C.S.; Hayashi, M.T.; et al. Replication stress induces mitotic death through parallel pathways regulated by WAPL and telomere deprotection. *Nat. Commun.* **2019**, *10*. [CrossRef] [PubMed]
263. Van Ly, D.; Low, R.R.J.; Frölich, S.; Bartolec, T.K.; Kafer, G.R.; Pickett, H.A.; Gaus, K.; Cesare, A.J. Telomere Loop Dynamics in Chromosome End Protection. *Mol. Cell* **2018**, *71*, 510–525.e6. [CrossRef] [PubMed]
264. Cesare, A.J.; Kaul, Z.; Cohen, S.B.; Napier, C.E.; Pickett, H.A.; Neumann, A.A.; Reddel, R.R. Spontaneous occurrence of telomeric DNA damage response in the absence of chromosome fusions. *Nat. Struct. Mol. Biol.* **2009**, *16*, 1244–1251. [CrossRef]
265. Cesare, A.J.; Hayashi, M.T.; Crabbe, L.; Karlseder, J. The Telomere deprotection response is functionally distinct from the Genomic DNA damage response. *Mol. Cell* **2013**, *51*, 141–155. [CrossRef] [PubMed]
266. Rossiello, F.; Aguado, J.; Sepe, S.; Iannelli, F.; Nguyen, Q.; Pitchiaya, S.; Carninci, P.; Di Fagagna, F.D.A. DNA damage response inhibition at dysfunctional telomeres by modulation of telomeric DNA damage response RNAs. *Nat. Commun.* **2017**, *8*. [CrossRef]
267. Rankin, A.M.; Forman, L.; Sarkar, S.; Faller, D.V. Enhanced cytotoxicity from deoxyguanosine-enriched T-oligo in prostate cancer cells. *Nucleic Acid Ther.* **2013**, *23*, 311–321. [CrossRef] [PubMed]
268. Puri, N.; Pitman, R.T.; Mulnix, R.E.; Erickson, T.; Iness, A.N.; Vitali, C.; Zhao, Y.; Salgia, R. Non-small cell lung cancer is susceptible to induction of DNA damage responses and inhibition of angiogenesis by telomere overhang oligonucleotides. *Cancer Lett.* **2014**, *343*, 14–23. [CrossRef] [PubMed]
269. Weng, D.; Cunin, M.C.; Song, B.; Price, B.D.; Eller, M.S.; Gilchrest, B.A.; Calderwood, S.K.; Gong, J. Radiosensitization of mammary carcinoma cells by telomere homolog oligonucleotide pretreatment. *Breast Cancer Res.* **2010**, *12*. [CrossRef]
270. Martínez, P.; Thanasoula, M.; Muñoz, P.; Liao, C.; Tejera, A.; McNees, C.; Flores, J.M.; Fernández-Capetillo, O.; Tarsounas, M.; Blasco, M.A. Increased telomere fragility and fusions resulting from TRF1 deficiency lead to degenerative pathologies and increased cancer in mice. *Genes Dev.* **2009**, *23*, 2060–2075. [CrossRef] [PubMed]
271. Casagrande, V.; Salvati, E.; Alvino, A.; Bianco, A.; Ciammaichella, A.; D'Angelo, C.; Ginnari-Satriani, L.; Serrilli, A.M.; Iachettini, S.; Leonetti, C.; et al. N-cyclic bay-substituted perylene g-quadruplex ligands have selective antiproliferative effects on cancer cells and induce telomere damage. *J. Med. Chem.* **2011**, *54*, 1140–1156. [CrossRef] [PubMed]
272. Kosiol, N.; Juranek, S.; Brossart, P.; Heine, A.; Paeschke, K. G-quadruplexes: A promising target for cancer therapy. *Mol. Cancer* **2021**, *20*, 40. [CrossRef]

273. Beniaminov, A.D.; Novikov, R.A.; Mamaeva, O.K.; Mitkevich, V.A.; Smirnov, I.P.; Livshits, M.A.; Shchyolkina, A.K.; Kaluzhny, D.N. Light-induced oxidation of the telomeric G4 DNA in complex with Zn(II) tetracarboxymethyl porphyrin. *Nucleic Acids Res.* **2016**, *44*, 10031–10041. [CrossRef] [PubMed]
274. Zhu, L.N.; Zhao, S.J.; Wu, B.; Li, X.Z.; Kong, D.M. A new cationic porphyrin derivative (TMPipEOPP) with large side arm substituents: A highly selective G-quadruplex optical probe. *PLoS ONE* **2012**, *7*, e35586. [CrossRef]
275. Salvati, E.; Leonetti, C.; Rizzo, A.; Scarsella, M.; Mottolese, M.; Galati, R.; Sperduti, I.; Stevens, M.F.G.; D'Incalci, M.; Blasco, M.; et al. Telomere damage induced by the G-quadruplex ligand RHPS4 has an antitumor effect. *J. Clin. Investig.* **2007**, *117*, 3236–3247. [CrossRef] [PubMed]
276. Salvati, E.; Rizzo, A.; Iachettini, S.; Zizza, P.; Cingolani, C.; D'Angelo, C.; Porru, M.; Mondello, C.; Aiello, A.; Farsetti, A.; et al. A basal level of DNA damage and telomere deprotection increases the sensitivity of cancer cells to G-quadruplex interactive compounds. *Nucleic Acids Res.* **2015**, *43*, 1759–1769. [CrossRef]
277. Haddach, M.; Schwaebe, M.K.; Michaux, J.; Nagasawa, J.; O'Brien, S.E.; Whitten, J.P.; Pierre, F.; Kerdoncuff, P.; Darjania, L.; Stansfield, R.; et al. Discovery of CX-5461, the first direct and selective inhibitor of RNA polymerase I, for cancer therapeutics. *ACS Med. Chem. Lett.* **2012**, *3*, 602–606. [CrossRef]
278. Bruno, P.M.; Lu, M.; Dennis, K.A.; Inam, H.; Moore, C.J.; Sheehe, J.; Elledge, S.J.; Hemann, M.T.; Pritchard, J.R. The primary mechanism of cytotoxicity of the chemotherapeutic agent CX-5461 is topoisomerase II poisoning. *Proc. Natl. Acad. Sci. USA* **2020**, *117*, 4053–4060. [CrossRef] [PubMed]
279. Bossaert, M.; Pipier, A.; Riou, J.F.; Noirot, C.; Nguyên, L.T.; Serre, R.F.; Bouchez, O.; Defrancq, E.; Calsou, P.; Britton, S.; et al. Transcription-associated topoisomerase 2α (TOP2A) activity is a major effector of cytotoxicity induced by G-quadruplex ligands. *Elife* **2021**, *10*, e65184. [CrossRef]
280. Xu, H.; Di Antonio, M.; McKinney, S.; Mathew, V.; Ho, B.; O'Neil, N.J.; Santos, N.D.; Silvester, J.; Wei, V.; Garcia, J.; et al. CX-5461 is a DNA G-quadruplex stabilizer with selective lethality in BRCA1/2 deficient tumours. *Nat. Commun.* **2017**, *8*. [CrossRef] [PubMed]
281. Khot, A.; Brajanovski, N.; Cameron, D.P.; Hein, N.; Maclachlan, K.H.; Sanij, E.; Lim, J.; Soong, J.; Link, E.; Blombery, P.; et al. First-in-human RNA polymerase I transcription inhibitor CX-5461 in patients with advanced hematologic cancers: Results of a phase I dose-escalation study. *Cancer Discov.* **2019**, *9*, 1036–1049. [CrossRef]
282. Liang, X.; Li, D.; Leng, S.; Zhu, X. RNA-based pharmacotherapy for tumors: From bench to clinic and back. *Biomed. Pharmacother.* **2020**, *125*, 109997. [CrossRef] [PubMed]
283. Kong, Y.W.; Dreaden, E.C.; Morandell, S.; Zhou, W.; Dhara, S.S.; Sriram, G.; Lam, F.C.; Patterson, J.C.; Quadir, M.; Dinh, A.; et al. Enhancing chemotherapy response through augmented synthetic lethality by co-targeting nucleotide excision repair and cell-cycle checkpoints. *Nat. Commun.* **2020**, *11*, 4124. [CrossRef]
284. Peaucellier, G.; Shartzer, K.; Jiang, W.; Maggio, K.; Kinsey, W.H. Anti-peptide Antibody Identifies a 57 kDa Protein Tyrosine Kinase in the Sea Urchin Egg Cortex: Tyrosine kinase/fertilization/src/egg/antibody. *Dev. Growth Differ.* **1993**, *35*. [CrossRef]
285. Jackson, M.R.; Bavelaar, B.M.; Waghorn, P.A.; Gill, M.R.; El-Sagheer, A.H.; Brown, T.; Tarsounas, M.; Vallis, K.A. Radiolabeled oligonucleotides targeting the RNA subunit of telomerase inhibit telomerase and induce DNA damage in telomerase-positive cancer cells. *Cancer Res.* **2019**, *79*, 4627–4637. [CrossRef]
286. Girard, P.M.; Berthault, N.; Kozlac, M.; Ferreira, S.; Jdey, W.; Bhaskara, S.; Alekseev, S.; Thomas, F.; Dutreix, M. Evolution of tumor cells during AsiDNA treatment results in energy exhaustion, decrease in responsiveness to signal, and higher sensitivity to the drug. *Evol. Appl.* **2020**, *13*, 1673–1680. [CrossRef] [PubMed]
287. Dragomir, M.P.; Kopetz, S.; Ajani, J.A.; Calin, G.A. Non-coding RNAs in GI cancers: From cancer hallmarks to clinical utility. *Gut* **2020**, *69*, 748–763. [CrossRef]
288. Heestand, G.M.; Schwaederle, M.; Gatalica, Z.; Arguello, D.; Kurzrock, R. Topoisomerase expression and amplification in solid tumours: Analysis of 24,262 patients. *Eur. J. Cancer* **2017**, *83*, 80–87. [CrossRef]
289. Pommier, Y.; Leo, E.; Zhang, H.; Marchand, C. DNA topoisomerases and their poisoning by anticancer and antibacterial drugs. *Chem. Biol.* **2010**, *17*, 421–433. [CrossRef]
290. Pommier, Y.; Cushman, M.; Doroshow, J.H. Novel clinical indenoisoquinoline topoisomerase I inhibitors: A twist around the camptothecins. *Oncotarget* **2018**, *9*, 37286–37288. [CrossRef]
291. Thomas, A.; Pommier, Y. Targeting topoisomerase I in the era of precision medicine. *Clin. Cancer Res.* **2019**, *25*, 6581–6589. [CrossRef]
292. Skok, Ž.; Zidar, N.; Kikelj, D.; Ilaš, J. Dual Inhibitors of Human DNA Topoisomerase II and Other Cancer-Related Targets. *J. Med. Chem.* **2020**, *63*, 884–904. [CrossRef]
293. Wang, W.; Rodriguez-Silva, M.; Acanda de la Rocha, A.M.; Wolf, A.L.; Lai, Y.; Liu, Y.; Reinhold, W.C.; Pommier, Y.; Chambers, J.W.; Tse-Dinh, Y.C. Tyrosyl-DNA phosphodiesterase 1 and topoisomerase I activities as predictive indicators for Glioblastoma susceptibility to genotoxic agents. *Cancers* **2019**, *11*, 1416. [CrossRef] [PubMed]
294. Kim, J.W.; Min, A.; Im, S.A.; Jang, H.; Kim, Y.J.; Kim, H.J.; Lee, K.H.; Kim, T.Y.; Lee, K.W.; Oh, D.Y.; et al. TDP1 and TOP1 modulation in Olaparib-resistant cancer determines the efficacy of subsequent chemotherapy. *Cancers* **2020**, *12*, 334. [CrossRef]
295. Lara, L.I.; Fenner, S.; Ratcliffe, S.; Isidro-Llobet, A.; Hann, M.; Bax, B.; Osheroff, N. Coupling the core of the anticancer drug etoposide to an oligonucleotide induces topoisomerase II-mediated cleavage at specific DNA sequences. *Nucleic Acids Res.* **2018**, *46*, 2218–2233. [CrossRef]

296. Molejon, M.I.; Weiz, G.; Breccia, J.D.; Vaccaro, M.I. Glycoconjugation: An approach to cancer therapeutics. *World J. Clin. Oncol.* **2020**, *11*, 110–120. [CrossRef] [PubMed]
297. Beck, D.E.; Agama, K.; Marchand, C.; Chergui, A.; Pommier, Y.; Cushman, M. Synthesis and biological evaluation of new carbohydrate-substituted indenoisoquinoline topoisomerase I inhibitors and improved syntheses of the experimental anticancer agents indotecan (LMP400) and indimitecan (LMP776). *J. Med. Chem.* **2014**, *57*, 1495–1512. [CrossRef]
298. Ma, Y.; Chen, H.; Su, S.; Wang, T.; Zhang, C.; Fida, G.; Cui, S.; Zhao, J.; Gu, Y. Galactose as broad ligand for multiple tumor imaging and therapy. *J. Cancer* **2015**, *6*, 658–670. [CrossRef] [PubMed]
299. Cao, J.; Cui, S.; Li, S.; Du, C.; Tian, J.; Wan, S.; Qian, Z.; Gu, Y.; Chen, W.R.; Wang, G. Targeted cancer therapy with a 2-deoxyglucose-based adriamycin complex. *Cancer Res.* **2013**, *73*, 1362–1373. [CrossRef]
300. Puyo, S.; Montaudon, D.; Pourquier, P. From old alkylating agents to new minor groove binders. *Crit. Rev. Oncol. Hematol.* **2014**, *89*, 43–61. [CrossRef]
301. Spitaleri, G.; Matei, D.V.; Curigliano, G.; Detti, S.; Verweij, F.; Zambito, S.; Scardino, E.; Rocco, B.; Nolè, F.; Ariu, L.; et al. Phase II trial of estramustine phosphate and oral etoposide in patients with hormone-refractory prostate cancer. *Ann. Oncol.* **2009**, *20*, 498–502. [CrossRef] [PubMed]
302. Hartmann, A.; Herkommer, K.; Glück, M.; Speit, G. DNA-damaging effect of cyclophosphamide on human blood cells in vivo and in vitro studied with the single-cell gel test (comet assay). *Environ. Mol. Mutagen.* **1995**, *25*, 180–187. [CrossRef]
303. Yuan, W.X.; Gui, Y.X.; Na, W.N.; Chao, J.; Yang, X. Circulating microRNA-125b and microRNA-130a expression profiles predict chemoresistance to R-CHOP in diffuse large B-cell lymphoma patients. *Oncol. Lett.* **2016**, *11*, 423–432. [CrossRef]
304. Hu, J.; Lieb, J.D.; Sancar, A.; Adar, S. Cisplatin DNA damage and repair maps of the human genome at single-nucleotide resolution. *Proc. Natl. Acad. Sci. USA* **2016**, *113*, 11507–11512. [CrossRef]
305. Woods, D.; Turchi, J.J. Chemotherapy induced DNA damage response Convergence of drugs and pathways. *Cancer Biol. Ther.* **2013**, *14*, 379–389. [CrossRef]
306. Zhang, P.; Sadler, P.J. Advances in the design of organometallic anticancer complexes. *J. Organomet. Chem.* **2017**, *839*, 5–14. [CrossRef]
307. Molinaro, C.; Martoriati, A.; Pelinski, L.; Cailliau, K. Copper complexes as anticancer agents targeting topoisomerases i and ii. *Cancers* **2020**, *12*, 2863. [CrossRef]
308. Fast, O.G.; Gentry, B.; Strouth, L.; Niece, M.B.; Beckford, F.A.; Shell, S.M. Polynuclear ruthenium organometallic compounds induce DNA damage in human cells identified by the nucleotide excision repair factor XPC. *Biosci. Rep.* **2019**, *39*, BSR20190378. [CrossRef]
309. Wambang, N.; Schifano-Faux, N.; Martoriati, A.; Henry, N.; Baldeyrou, B.; Bal-Mahieu, C.; Bousquet, T.; Pellegrini, S.; Meignan, S.; Cailliau, K.; et al. Synthesis, Structure, and Antiproliferative Activity of Ruthenium(II) Arene Complexes of Indenoisoquinoline Derivatives. *Organometallics* **2016**, *35*. [CrossRef]
310. Murray, V.; Chen, J.K.; Chung, L.H. The interaction of the metallo-glycopeptide anti-tumour drug bleomycin with DNA. *Int. J. Mol. Sci.* **2018**, *19*, 1372. [CrossRef] [PubMed]
311. Kim, S.J.; Kim, H.S.; Seo, Y.R. Understanding of ROS-Inducing Strategy in Anticancer Therapy. *Oxid. Med. Cell. Longev.* **2019**, *2019*. [CrossRef]
312. Magkouta, S.F.; Pappas, A.G.; Vaitsi, P.C.; Agioutantis, P.C.; Pateras, I.S.; Moschos, C.A.; Iliopoulou, M.P.; Kosti, C.N.; Loutrari, H.V.; Gorgoulis, V.G.; et al. MTH1 favors mesothelioma progression and mediates paracrine rescue of bystander endothelium from oxidative damage. *JCI Insight* **2020**, *5*, e134885. [CrossRef]
313. Doudna, J.A.; Charpentier, E. The new frontier of genome engineering with CRISPR-Cas9. *Science* **2014**, *346*. [CrossRef] [PubMed]
314. Yeh, C.D.; Richardson, C.D.; Corn, J.E. Advances in genome editing through control of DNA repair pathways. *Nat. Cell Biol.* **2019**, *21*, 1468–1478. [CrossRef]
315. Charpentier, M.; Khedher, A.H.Y.; Menoret, S.; Brion, A.; Lamribet, K.; Dardillac, E.; Boix, C.; Perrouault, L.; Tesson, L.; Geny, S.; et al. CtIP fusion to Cas9 enhances transgene integration by homology-dependent repair. *Nat. Commun.* **2018**, *9*, 1133. [CrossRef] [PubMed]
316. Jayavaradhan, R.; Pillis, D.M.; Goodman, M.; Zhang, F.; Zhang, Y.; Andreassen, P.R.; Malik, P. CRISPR-Cas9 fusion to dominant-negative 53BP1 enhances HDR and inhibits NHEJ specifically at Cas9 target sites. *Nat. Commun.* **2019**, *10*, 2866. [CrossRef]
317. Benitez, E.K.; Lomova Kaufman, A.; Cervantes, L.; Clark, D.N.; Ayoub, P.G.; Senadheera, S.; Osborne, K.; Sanchez, J.M.; Crisostomo, R.V.; Wang, X.; et al. Global and Local Manipulation of DNA Repair Mechanisms to Alter Site-Specific Gene Editing Outcomes in Hematopoietic Stem Cells. *Front. Genome Ed.* **2020**, *2*. [CrossRef]
318. Deutsch, E.; Chargari, C.; Galluzzi, L.; Kroemer, G. Optimising efficacy and reducing toxicity of anticancer radioimmunotherapy. *Lancet Oncol.* **2019**, *20*, e452–e463. [CrossRef]
319. Huang, R.X.; Zhou, P.K. DNA damage response signaling pathways and targets for radiotherapy sensitization in cancer. *Signal Transduct. Target. Ther.* **2020**, *5*. [CrossRef]
320. Biau, J.; Chautard, E.; Verrelle, P.; Dutreix, M. Altering DNA repair to improve radiation therapy: Specific and multiple pathway targeting. *Front. Oncol.* **2019**, *9*, 1009. [CrossRef] [PubMed]
321. de Jong, M.; Breeman, W.A.; Valkema, R.; Bernard, B.F.; Krenning, E.P. Combination radionuclide therapy using 177Lu- and 90Y-labeled somatostatin analogs. *J. Nucl. Med.* **2005**, *46* (Suppl. 1), 13S–17S.

322. Hofman, M.S.; Violet, J.; Hicks, R.J.; Ferdinandus, J.; Thang, S.P.; Akhurst, T.; Iravani, A.; Kong, G. Articles [^{177}Lu] -PSMA-617 radionuclide treatment in patients with metastatic castration-resistant prostate cancer (LuPSMA trial): A single-centre, single-arm, phase 2 study. *Lancet Oncol.* **2018**, *19*, 825–833. [CrossRef]
323. Pokrovska, T.D.; Jacobus, E.J.; Puliyadi, R.; Prevo, R.; Frost, S.; Dyer, A.; Baugh, R.; Rodriguez-Berriguete, G.; Fisher, K.; Granata, G.; et al. External beam radiation therapy and enadenotucirev: Inhibition of the DDR and mechanisms of radiation-mediated virus increase. *Cancers* **2020**, *12*, 798. [CrossRef]
324. Maude, S.L.; Enders, G.H. Cdk inhibition in human cells compromises Chk1 function and activates a DNA damage response. *Cancer Res.* **2005**, *65*, 780–786. [PubMed]
325. Militello, A.M.; Zielli, T.; Boggiani, D.; Michiara, M.; Naldi, N.; Bortesi, B.; Zanelli, P.; Uliana, V.; Giuliotti, S.; Musolino, A. Mechanism of action and clinical efficacy of CDK4/6 inhibitors in BRCA-mutated, estrogen receptor-positive breast cancers: Case report and literature review. *Front. Oncol.* **2019**, *9*, 759. [CrossRef]
326. Krajewska, M.; Dries, R.; Grassetti, A.V.; Dust, S.; Gao, Y.; Huang, H.; Sharma, B.; Day, D.S.; Kwiatkowski, N.; Pomaville, M.; et al. CDK12 loss in cancer cells affects DNA damage response genes through premature cleavage and polyadenylation. *Nat. Commun.* **2019**, *10*. [CrossRef] [PubMed]
327. Quereda, V.; Bayle, S.; Vena, F.; Frydman, S.M.; Monastyrskyi, A.; Roush, W.R.; Duckett, D.R. Therapeutic Targeting of CDK12/CDK13 in Triple-Negative Breast Cancer. *Cancer Cell* **2019**, *36*, 545–558.e7. [CrossRef]
328. Jiang, L.; Zawacka-Pankau, J. The p53/MDM2/MDMX-targeted therapies—A clinical synopsis. *Cell Death Dis.* **2020**, *11*, 9–12. [CrossRef] [PubMed]
329. Blandino, G.; Di Agostino, S. New therapeutic strategies to treat human cancers expressing mutant p53 proteins. *J. Exp. Clin. Cancer Res.* **2018**, *37*, 30. [CrossRef] [PubMed]
330. Haupt, Y.; Maya, R.; Kazaz, A.; Oren, M. Mdm2 promotes the rapid degradation of p53. *Nature* **1997**, *387*, 296–299. [CrossRef]
331. Lambert, J.M.R.; Gorzov, P.; Veprintsev, D.B.; Söderqvist, M.; Segerbäck, D.; Bergman, J.; Fersht, A.R.; Hainaut, P.; Wiman, K.G.; Bykov, V.J.N. PRIMA-1 Reactivates Mutant p53 by Covalent Binding to the Core Domain. *Cancer Cell* **2009**, *15*, 376–388. [CrossRef]
332. Aryee, D.N.T.; Niedan, S.; Ban, J.; Schwentner, R.; Muehlbacher, K.; Kauer, M.; Kofler, R.; Kovar, H. Variability in functional p53 reactivation by PRIMA-1 Met/APR-246 in Ewing sarcoma. *Br. J. Cancer* **2013**, *109*, 2696–2704. [CrossRef]
333. Liu, X.; Wilcken, R.; Joerger, A.C.; Chuckowree, I.S.; Amin, J.; Spencer, J.; Fersht, A.R. Small molecule induced reactivation of mutant p53 in cancer cells. *Nucleic Acids Res.* **2013**, *41*, 6034–6044. [CrossRef]
334. Bauer, M.R.; Jones, R.N.; Baud, M.G.J.; Wilcken, R.; Boeckler, F.M.; Fersht, A.R.; Joerger, A.C.; Spencer, J. Harnessing fluorine-sulfur contacts and multipolar interactions for the design of p53 mutant Y220C rescue drugs Harnessing Fluorine-Sulfur Contacts and Multipolar Interactions for the Design of p53 Mutant Y220C Rescue Drugs. *ACS Chem. Biol.* **2016**, *11*, 2265–2274. [CrossRef]
335. Gupta, A.; Shah, K.; Oza, M.J.; Behl, T. Reactivation of p53 gene by MDM2 inhibitors: A novel therapy for cancer treatment. *Biomed. Pharmacother.* **2019**, *109*, 484–492. [CrossRef]
336. Macurek, L.; Benada, J.; Müllers, E.; Halim, V.A.; Krejčíková, K.; Burdová, K.; Pecháčková, S.; Hodný, Z.; Lindqvist, A.; Medema, R.H.; et al. Downregulation of Wip1 phosphatase modulates the cellular threshold of DNA damage signaling in mitosis. *Cell Cycle* **2013**, *12*, 251–262. [CrossRef]
337. Kong, W.; Jiang, X.; Mercer, W.E. Downregulation of Wip-1 phosphatase expression in MCF-7 breast cancer cells enhances doxorubicin-induced apoptosis through p53-mediated transcriptional activation of Bax. *Cancer Biol. Ther.* **2009**, *8*, 555–563. [CrossRef] [PubMed]
338. Chen, Z.; Wang, L.; Yao, D.; Yang, T.; Cao, W.M.; Dou, J.; Pang, J.C.; Guan, S.; Zhang, H.; Yu, Y.; et al. Wip1 inhibitor GSK2830371 inhibits neuroblastoma growth by inducing Chk2/p53-mediated apoptosis. *Sci. Rep.* **2016**, *6*, 38011. [CrossRef]
339. Hirai, H.; Iwasawa, Y.; Okada, M.; Arai, T.; Nishibata, T.; Kobayashi, M.; Kimura, T.; Kaneko, N.; Ohtani, J.; Yamanaka, K.; et al. Small-molecule inhibition of Wee1 kinase by MK-1775 selectively sensitizes p53-deficient tumor cells to DNA-damaging agents. *Mol. Cancer Ther.* **2009**, *8*, 2992–3000. [CrossRef] [PubMed]
340. Wang, Y.; Li, J.; Booher, R.N.; Kraker, A.; Lawrence, T.; Leopold, W.R.; Sun, Y. Radiosensitization of p53 mutant cells by PD0166285, a novel G2 checkpoint abrogator. *Cancer Res.* **2001**, *61*, 8211–8217. [PubMed]
341. Yin, Y.; Shen, Q.; Tao, R.; Chang, W.; Li, R.; Xie, G.; Liu, W.; Zhang, P.; Tao, K. Wee1 inhibition can suppress tumor proliferation and sensitize p53 mutant colonic cancer cells to the anticancer effect of irinotecan. *Mol. Med. Rep.* **2018**, *17*, 3344–3349. [CrossRef] [PubMed]
342. Reisländer, T.; Groelly, F.J.; Tarsounas, M. DNA Damage and Cancer Immunotherapy: A STING in the Tale. *Mol. Cell* **2020**, *80*, 21–28. [CrossRef]
343. Jiao, S.; Xia, W.; Yamaguchi, H.; Wei, Y.; Chen, M.K.; Hsu, J.M.; Hsu, J.L.; Yu, W.H.; Du, Y.; Lee, H.H.; et al. PARP inhibitor upregulates PD-L1 expression and enhances cancer-associated immunosuppression. *Clin. Cancer Res.* **2017**, *23*, 3711–3720. [CrossRef] [PubMed]
344. Gandhi, L.; Rodríguez-Abreu, D.; Gadgeel, S.; Esteban, E.; Felip, E.; De Angelis, F.; Domine, M.; Clingan, P.; Hochmair, M.J.; Powell, S.F.; et al. Pembrolizumab plus Chemotherapy in Metastatic Non–Small-Cell Lung Cancer. *N. Engl. J. Med.* **2018**, *378*, 2078–2092. [CrossRef] [PubMed]
345. Shaverdian, N.; Lisberg, A.E.; Bornazyan, K.; Veruttipong, D.; Goldman, J.W.; Formenti, S.C.; Garon, E.B.; Lee, P. Articles Previous radiotherapy and the clinical activity and toxicity of pembrolizumab in the treatment of non-small-cell lung cancer: A secondary analysis of the KEYNOTE-001 phase 1 trial. *Lancet Oncol.* **2017**, *18*, 895–903. [CrossRef]

346. Le, D.T.; Le, D.T.; Durham, J.N.; Smith, K.N.; Wang, H.; Bartlett, B.R.; Aulakh, K.; Lu, S.; Kemberling, H.; Wilt, C.; et al. Mismatch-repair deficiency predicts response of solid tumors to PD-1 blockade. *Science* **2017**, *357*, 409–413. [CrossRef]
347. Brown, J.S.; Sundar, R.; Lopez, J. Combining DNA damaging therapeutics with immunotherapy: More haste, less speed. *Br. J. Cancer* **2018**, *118*, 312–324. [CrossRef]
348. Chen, H.; Chen, H.; Zhang, J.; Wang, Y.; Simoneau, A.; Yang, H.; Levine, A.S.; Zou, L.; Chen, Z.; Lan, L. Molecular biology cGAS suppresses genomic instability as a decelerator of replication forks. *Sci. Adv.* **2020**, *6*. [CrossRef]
349. Roden, D.M.; McLeod, H.L.; Relling, M.V.; Williams, M.S.; Mensah, G.A.; Peterson, J.F.; Van Driest, S.L. Pharmacogenomics. *Lancet* **2019**, *394*, 521–532. [CrossRef]
350. Khanna, K.K.; Duijf, P.H.G. Complexities of pharmacogenomic interactions in cancer. *Mol. Cell. Oncol.* **2020**, *7*. [CrossRef]
351. Pang, B.; De Jong, J.; Qiao, X.; Wessels, L.F.A.; Neefjes, J. Chemical profiling of the genome with anti-cancer drugs defines target specificities. *Nat. Chem. Biol.* **2015**, *11*, 472–480. [CrossRef] [PubMed]
352. Gao, L.; Meng, J.; Zhang, Y.; Gu, J.; Han, Z.; Wang, X.; Gao, S. Development and validation of a six-RNA binding proteins prognostic signature and candidate drugs for prostate cancer. *Genomics* **2020**, *112*, 4980–4992. [CrossRef]
353. Zimmermann, M.; Murina, O.; Reijns, M.A.M.; Agathanggelou, A.; Challis, R.; Tarnauskaite, Ž.; Muir, M.; Fluteau, A.; Aregger, M.; McEwan, A.; et al. CRISPR screens identify genomic ribonucleotides as a source of PARP-trapping lesions. *Nature* **2018**, *559*, 285–289. [CrossRef]
354. Hamilton, G.; Rath, B. Pharmacogenetics of platinum-based chemotherapy in non-small cell lung cancer: Predictive validity of polymorphisms of ERCC1. *Expert Opin. Drug Metab. Toxicol.* **2018**, *14*, 17–24. [CrossRef] [PubMed]
355. Guffanti, F.; Fruscio, R.; Rulli, E.; Damia, G. The impact of DNA damage response gene polymorphisms on therapeutic outcomes in late stage ovarian cancer. *Sci. Rep.* **2016**, *6*, 38142. [CrossRef] [PubMed]
356. Murai, J.; Thomas, A.; Miettinen, M.; Pommier, Y. Schlafen 11 (SLFN11), a restriction factor for replicative stress induced by DNA-targeting anti-cancer therapies. *Pharmacol. Ther.* **2019**, *201*, 94–102. [CrossRef]
357. Abbosh, C.; Birkbak, N.J.; Wilson, G.A.; Jamal-Hanjani, M.; Constantin, T.; Salari, R.; Le Quesne, J.; Moore, D.A.; Veeriah, S.; Rosenthal, R.; et al. Phylogenetic ctDNA analysis depicts early-stage lung cancer evolution. *Nature* **2017**, *545*, 446–451. [CrossRef]
358. Christensen, E.; Birkenkamp-Demtröder, K.; Sethi, H.; Shchegrova, S.; Salari, R.; Nordentoft, I.; Wu, H.T.; Knudsen, M.; Lamy, P.; Lindskrog, S.V.; et al. Early detection of metastatic relapse and monitoring of therapeutic efficacy by ultra-deep sequencing of plasma cell-free DNA in patients with urothelial bladder carcinoma. *J. Clin. Oncol.* **2019**, *37*, 1547–1557. [CrossRef]
359. Mithraprabhu, S.; Hocking, J.; Ramachandran, M.; Choi, K.; Klarica, D.; Khong, T.; Reynolds, J.; Spencer, A. DNA-repair gene mutations are highly prevalent in circulating tumour dna from multiple myeloma patients. *Cancers* **2019**, *11*, 917. [CrossRef]
360. Wilsker, D.F.; Barrett, A.M.; Dull, A.B.; Lawrence, S.M.; Hollingshead, M.G.; Chen, A.; Kummar, S.; Parchment, R.E.; Doroshow, J.H.; Kinders, R.J. Evaluation of pharmacodynamic responses to cancer therapeutic agents using DNA damage markers. *Clin. Cancer Res.* **2019**, *25*, 3084–3095. [CrossRef]
361. Skora, A.D.; Luber, B.S.; Azad, N.S.; Laheru, D.; Biedrzycki, B.; Donehower, R.C.; De Chapelle, A.; Koshiji, M.; Bhaijee, F.; Huebner, T.; et al. PD-1 Blockade in Tumors with Mismatch-Repair Deficiency. *N. Engl. J. Med.* **2015**, *372*, 2509–2520. [CrossRef]
362. Sun, L.-L.; Yang, R.-Y.; Li, C.-W.; Chen, M.-K.; Shao, B.; Hsu, J.-M.; Chan, L.-C.; Yang, Y.; Hsu, J.L.; Lai, Y.-J.; et al. Inhibition of ATR downregulates PD-L1 and sensitizes tumor cells to T cell-mediated killing. *Am. J. Cancer Res.* **2018**, *8*, 1307–1316.
363. Sato, H.; Niimi, A.; Yasuhara, T.; Bunga, T.; Permata, M.; Hagiwara, Y.; Isono, M.; Nuryadi, E.; Sekine, R.; Oike, T.; et al. DNA double-strand break repair pathway regulates PD-L1 expression in cancer cells. *Nat Commun.* **2017**, *8*, 1751. [CrossRef]
364. Luftig, M.A. Viruses and the DNA Damage Response: Activation and Antagonism. *Annu. Rev. Virol.* **2014**, *1*, 605–625. [CrossRef] [PubMed]
365. Stracker, T.H.; Carson, C.T.; Weitzman, M.D. Adenovirus oncoproteins inactivate the Mre11—Rad50—NBS1 DNA repair complex. *Nature* **2002**, *418*, 348–352. [CrossRef]
366. Zhang, W.W.; Li, L.; Li, D.; Liu, J.; Li, X.; Li, W.; Xu, X.; Zhang, M.J.; Chandler, L.A.; Lin, H.; et al. The First Approved Gene Therapy Product for Cancer Ad-p53 (Gendicine): 12 Years in the Clinic. *Hum. Gene Ther.* **2018**, *29*, 160–179. [CrossRef]
367. Ganesh, S.; Gibbons, D.; Ge, Y.; Vanroey, M.; Robinson, M.; Jooss, K. Combination therapy with radiation or cisplatin enhances the potency of Ad5/35 chimeric oncolytic adenovirus in a preclinical model of head and neck cancer. *Cancer Gene Ther.* **2009**, *16*, 383–392. [CrossRef]
368. Kuhn, I.; Harden, P.; Bauzon, M.; Chartier, C.; Nye, J.; Thorne, S.; Reid, T.; Ni, S.; Lieber, A.; Fisher, K.; et al. Directed Evolution Generates a Novel Oncolytic Virus for the Treatment of Colon Cancer. *PLoS ONE* **2008**, *3*, e2409. [CrossRef]
369. Xiao, X.; Liang, J.; Huang, C.; Li, K.; Xing, F.; Zhu, W.; Lin, Z.; Xu, W.; Wu, G.; Zhang, J.; et al. DNA-PK inhibition synergizes with oncolytic virus M1 by inhibiting antiviral response and potentiating DNA damage. *Nat. Commun.* **2018**, *9*. [CrossRef]
370. Ning, J.; Wakimoto, H.; Peters, C.; Martuza, R.L.; Rabkin, S.D. Rad51 degradation: Role in oncolytic virus-poly (ADP Ribose) polymerase inhibitor combination therapy in glioblastoma. *J. Natl. Cancer Inst.* **2017**, *109*. [CrossRef] [PubMed]

Publication (review 2)

Copper Complexes as Anticancer Agents Targeting Topoisomerases I and II

cancers

MDPI

Review

Copper Complexes as Anticancer Agents Targeting Topoisomerases I and II

Caroline Molinaro [1], Alain Martoriati [1], Lydie Pelinski [2] and Katia Cailliau [1,*]

[1] Univ. Lille, CNRS, UMR 8576-UGSF-Unité de Glycobiologie Structurale et Fonctionnelle, F-59000 Lille, France; caroline.molinaro@univ-lille.fr (C.M.); alain.martoriati@univ-lille.fr (A.M.)

[2] Univ. Lille, CNRS, Centrale Lille, Univ. Artois, UMR 8181-UCCS-Unité de Catalyse et Chimie du Solide, F-59000 Lille, France; lydie.pelinski@univ-lille.fr

* Correspondence: katia.maggio@univ-lille.fr

Received: 3 September 2020; Accepted: 29 September 2020; Published: 5 October 2020

Simple Summary: Organometallics, such as copper compounds, are cancer chemotherapeutics used alone or in combination with other drugs. One small group of copper complexes exerts an effective inhibitory action on topoisomerases, which participate in the regulation of DNA topology. Copper complexes of topoisomerase inhibitors work by different molecular mechanisms that have repercussions on the cell cycle checkpoints and death effectors. The expansion of this family of highly active anticancer drugs and their use in combination with other emerging cancer therapies opens new avenues for the treatment of cancers.

Abstract: Organometallics, such as copper compounds, are cancer chemotherapeutics used alone or in combination with other drugs. One small group of copper complexes exerts an effective inhibitory action on topoisomerases, which participate in the regulation of DNA topology. Copper complexes inhibitors of topoisomerases 1 and 2 work by different molecular mechanisms, analyzed herein. They allow genesis of DNA breaks after the formation of a ternary complex, or act in a catalytic mode, often display DNA intercalative properties and ROS production, and sometimes display dual effects. These amplified actions have repercussions on the cell cycle checkpoints and death effectors. Copper complexes of topoisomerase inhibitors are analyzed in a broader synthetic view and in the context of cancer cell mutations. Finally, new emerging treatment aspects are depicted to encourage the expansion of this family of highly active anticancer drugs and to expend their use in clinical trials and future cancer therapy.

Keywords: copper complexes; topoisomerase inhibitor; DNA damage response; cell cycle; cell death; chemotherapy

1. Introduction

Chemotherapy is a systemic treatment proposed to patients suffering from cancer. It is often a complementary approach to surgery or radiotherapy. The discovery of platinum's inhibitory effect on tumor cell growth in the 1960s [1] was a milestone for anticancer drug application in medicine [2]. Platinum (II) sets at the center of the squared planar structure of cisplatin and is coordinated with two chlorides and two ammonia molecules in a cis configuration. Cisplatin and its derivative drugs (carboplatin of second generation and oxaliplatin of third generation) are used worldwide in clinical applications and several other platinum analogs (lobaplatin, nedaplatin, and heptaplatin) are approved in several countries (Figure 1) [3,4]. However, serious side effects including toxicities on the kidney, heart, ear, and liver, decrease in immunity, hemorrhage, and gastrointestinal disorders limit the use of platinum derivatives [5–7]. The appearance of drug resistances, issuing from acquired or intrinsic

multiple genetic and epigenetic changes, has also limited the clinical use of platinum-derived drugs [8]. Platinum-based treatment efficiency is challenged by cross-resistance and multiple changes including a decreased accumulation of the drug, a reduction in DNA–drug adducts, a modification in cell survival gene expression, an alteration of DNA damage repair mechanisms, modifications of transporters, protein trafficking, and altered cell metabolism [9–14].

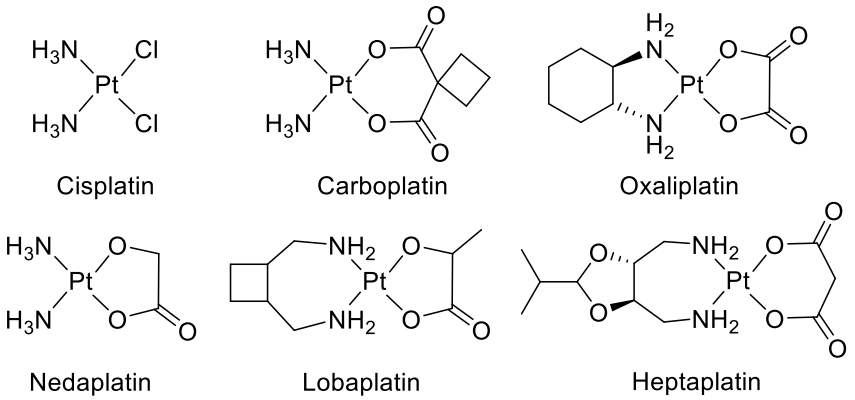

Figure 1. Platinum (II) complexes.

To circumvent drug resistance, a possible approach consists of designing and developing new therapeutic metal-based anticancer drugs [15–21]. Several transition metals from the d-block of the periodic table (groups 3 to 12) and particularly essential trace metals [15,22,23], such as copper [24–29], are useful for the implementation of metal-based complexes in anticancer therapies. Copper plays central roles in various cellular processes being an essential micronutrient and an important cofactor for several metalloenzymes involved in mitochondrial metabolism (cytochrome c oxidase), or cellular radical detoxification against reactive oxygen species (ROS) (superoxide dismutase) [30]. Copper is essential for angiogenesis, proliferation, and migration of endothelial cells [31–33]. Elevated copper favors tumor growth and metastasis. It is detected in several brain [34], breast [35], colon, prostate [36], and lung [37] tumors and serves as an indicator of the course of the disease [38]. The differences in tumor cells' responses to copper compared to normal cells laid the foundation of copper complexes' (CuC) evolution as anticancer agents. Numerous developed CuC contain different sets of N, S, or O ligands and demonstrate high cytotoxicity and efficient antitumor activity [25]. Different mechanisms are involved in copper drugs' anticancer effect. They act as chelators, and interact with and sequester endogenous copper, reducing its availability for tumor growth and angiogenesis [39]. On the contrary, ionophores trigger intracellular copper accumulation, cytotoxicity, and activate apoptosis inhibitor factor (XIAP) [24,40–46]. Other CuC are proteasome inhibitors [47,48]. Several CuC are actually on clinical trials: a number of copper/disulfiram-based drug combinations for therapy and as diagnostic tools (metastatic breast cancer and germ cell tumor), several casiopeínas compounds and elesclomol (leukemia), and thiosemicarbazone-based copper complexes labeled with a radioactive isotope for positron emission tomography imaging of hypoxia (in head and neck cancers) [49].

The cisplatin DNA-targeting principle of action also conditioned the development of anticancer copper-based drugs [4,23,50]. Antitumor activities of copper-based drugs are based on the interactive properties of both copper and the ligand. Copper toxicity results from its redox capacities (Cu(I) and Cu(II) redox states' interconversion in oxidation–reduction cycles), the property to displace other ions from the enzyme binding sites, a high DNA binding affinity, and the ability to promote DNA breaks [28,51]. In most cases, copper modifies the backbone of the complexed ligand and grants better DNA affinity, specificity, and stability [52]. Copper derivatives can interact with DNA without the formation of covalent adducts. The noncovalent interactions with DNA include binding along with the major or the minor DNA grooves, intercalation, or electrostatic binding. Some copper-based drugs generate reactive oxygen species (ROS) that overwhelm cellular antioxidant defenses to produce

oxidative damages in the cytoplasm, mitochondria, and DNA [53]. An important class of CuC, actually on focus for chemotherapy, inhibits topoisomerases (Top) 1 and 2, resulting in severe DNA damages, cell cycle arrest, and death [40,54–57]. Chemotherapeutics that target Top as poisons convert a transient DNA-enzyme complex into lethal DNA breaks [58–62]. However, topoisomerase inhibitors' activity and their multifaceted binding modes to DNA, the effects, and the modulations they produce on the control of cancer cell division necessitate better understanding to optimize their efficiency.

This review focuses on CuC targeting human Top1 and Top2, the molecular mechanism of induced DNA damages, cell cycle arrest, programmed cell death responses, and emerging research strategies.

2. Copper Complexes as Topoisomerases Inhibitors

DNA topoisomerases have been molecular targets for anticancer agents since their discovery in 1971 [63]. Topoisomerases regulate DNA winding and play essential functions in DNA replication and transcription [59,64]. Topoisomerase 1 (Top1) creates transient single-DNA nicks, while topoisomerases 2 (Top2α and Top2β) produce transient double-stranded DNA breaks. Both nuclear Top1 and Top2 are important targets for cancer chemotherapy, and Top inhibitors are used in therapeutic protocols [65–67]. Top inhibitors are classified into two groups: poisons and catalytic inhibitors. Top poisons (or interfacial poisons) stabilize the reversible cleavage complex formed between Top and DNA and form a ternary complex. Top2 catalytic inhibitors can prevent DNA strands cleavage through inhibition of the ATPase activity (novobiocin, merbarone), by impeding ATP hydrolysis to block Top dissociation from the DNA (ICRF-193), or by DNA intercalation at the Top fixation site (aclarubicinet) see [68]. In all cases, inhibitors convert the indispensable nuclear Top enzyme into a killing tool.

Top inhibitors' activity increases upon complexation with copper ion. Top1, Top2, or Top1/2 inhibitors synthesized in the form of copper complexes (CuC) are mostly mononuclear Cu(II) complexes associated with a variety of ligands (Table 1). Different strategies are currently proposed to design and develop Top inhibitory agents based on ligands' properties [69]. If both Top1 and Top2 inhibitors CuC primarily target DNA by a direct interaction through intercalation or cleavage, their antiproliferative activity is reinforced by ROS production and other molecular targets (Table 1) [25,52].

Table 1. Copper complexes inhibitors of topoisomerases: targeted top isoforms, cancer cell lines responses, and molecular mechanisms are summarized. * Tests were realized in vitro with human Top1 or Top2α/β unless specified. IC50: half-maximal inhibitory concentration. EC50: half-maximal effective concentration. GI50: half-average of growth inhibition.

Ligand Class of Cu-C	Compound Number	Targeted Top(s)	Inhibition of DNA Relaxation Total (μM) (minimal (μM))	Inhibition Mecanism	Cancer Cell Lines	IC50 (μM)	Cell Cycle Arrest	Cell Death Type	Other Specificity	Reference Number
Oxindolimine	**1**	Top1	50 (25)	Fixation in the DNA Top1 binding site	Neuroblastoma SH-SY5Y Promonocytic U937		G2/M arrest	Apoptosis	ROS induction	[70–73]
Hydrazone with triphenylphosphonium	**2**	Top1	40	DNA Binding Enzyme complex formation	Lung A549 Prostatic PC-3	4.2 ± 0.8 3.2 ± 0.2				[74]
Plumbagin	**3**	Top1	1.56	DNA intercalation	Breast MCF-7 Colon HCT116 Hepatoma BEL7404 Hepatoma HepG2 Kidney 786-O Lung NCI-H460 Nasopharyngeal cancer CNE2	3.2 ± 1.1 5.9 ± 1.4 12.9 ± 3.6 9.0 ± 0.7 2.5 ± 0.9 2.0 ± 1.2 11.8 ± 5.9				[75]
Phenanthroline with amino acids	**4**	Top1	50 (10)	DNA intercalation	Nasopharyngeal cancer HK1	2.2–5.2		Apoptosis		[76]
Pyrophosphate	**5**	Top1	500	DNA interaction	Ovarian A2780/AD	0.64 ± 0.12				[77]
Heterobimetallic Cu(II)-Sn2(IV) phenanthroline	**6**	Top1	20	DNA intercalation cleavage	Breast Zr-75–1 Cervix SiHa Colon HCT15, SW620 Kidney 786-O, A498 Lung Hop-62, A569 Pancreatic MIA PaCa-2	<10 (GI50)				[78]
					Neuroblastoma SH-SY5Y	2–8		Apoptosis		[79]
Analogs										[80]
Tridentate chiral Schiff base	**7**, **8**	Top1	25 (15)	DNA binding major groove	Hepatoma HuH7 Hepatoma HepG2	25 6.2 ± 10			ROS Cytokine TGFb mRNA upregulation	[81,82]

Table 1. *Cont.*

Ligand Class of Cu-C	Compound Number	Targeted Top(s)	Inhibition of DNA Relaxation Total (μM) (minimal (μM))	Inhibition Mecanism	Cancer Cell Lines	IC50 (μM)	Cell Cycle Arrest	Cell Death Type	Other Specificity	Reference Number
Salicylidene	**9**	Top1	(*E. coli*) *	DNA binding	Prostatic PC-3	7.3 ± 0.2			antimetastasis	[83]
				DNA cleavage	Breast MCF7 Colon HT29 Hepatoma HepG2 Lung A549 Ovary A2780 Prostatic LNCaP	51.1 ± 1.6 16.6 ± 0.6 2.3 ± 0.1 16.8 ± 1.0 14.6 ± 0.2 25.4 ± 0.8				[84]
Chalcone-derived Thiosemicarbazone	**10**	Top1	3 (0.75)	DNA binding DNA cleavage Religation inhibition	Breast MCF-7 Leukemia THP-1	0.16 ± 0.06 0.20 ± 0.06				[85]
Pyridyl-substituted tetrazolopyrimidie	**11**	Top1	(Molecular docking) *	DNA binding groove mode	Cervix HeLa Colon HCT-15 Lung A549	0.565 ± 0.01 0.358 0.733		Apoptosis	CDK receptor binding	[86]
Tetrazolopyrimidine Diimine		Top1	102 ± 1.1	DNA binding groove mode	Cervical HeLa Colon HCT-15 Lung A549	0.620 ± 0.0013 0.540 ± 0.00015 0.120 ± 0.002		Apoptosis	vEGF receptor binding	[87]
Piperazine	**12**	Top1	12.5 (5)	DNA binding minor groove					SOD mimic	[88]
Elesclomol	**13**	Top1	50	Poison	Erythroleukemic K562	0.0075		Apoptosis Necrosis Oxidative stress	Copper chelator Not a substrat for ABC transporters	[89]
Cu(SBCM)2	**14**	Top1	* (Molecular docking)	DNA intercalation DNA binding	Breast MCF7 Breast MDA-MB-231	27 18.7 ± 3.1	G2/M arrest	Apoptosis	p53 increase No ROS	[90] [91]
TSC and TSC CuC										[92–97]
Pyridine-TSC	**15**	Top2a	50 (10)		Breast MDA-MB-231 Breast MCF7	1.01 0.0558				[98]
			50	ATP hydrolysis inhibition						[99]
		Top2β	(5)	ATP hydrolysis inhibition						[100]

Table 1. *Cont.*

Ligand Class of Cu-C	Compound Number	Targeted Top(s)	Inhibition of DNA Relaxation Total (μM) (minimal (μM))	Inhibition Mecanism	Cancer Cell Lines	IC50 (μM)	Cell Cycle Arrest	Cell Death Type	Other Specificity	Reference Number
Piperazine-TSC	**16**	Top2a	0.9 ± 0.7	Potentially catalytic	Breast MCF7 Breast SK-BR-3	4.7 ± 0.3 1.3 ± 0.3				[101,102] [99]
Thiazole-TSC	**17**	Top2a	4 (2)		Breast MDA-MB-231 Breast MCF7	1.41 (EC50) 0.13 (EC50)				[103]
	17–18	Top2a	25 (10)	ATP hydrolysis inhibition + Poison	Breast HCC 70, HCC 1395, HCC 1500, and HCC 1806 Colon Caco-2, HCT-116 and HT-29	 1 to 20 0.83 to 41.2				[104,105]
L- and D-Proline-TSC	**19**	Top2a	300		Ovarian carcinoma CH1	113 ± 16				[106]
Quinoline-TSC	**20**	Top2a	0.48	Potentially catalytic	Lymphoma U937	0.48-16.2				[107]
Naphthoquinone-TSC	**21**	Top2α	1 mM		Breast MCF7	3.98 ± 1.01		No apoptosis		[108]
Bis-TSC	**22**	Top2a	100 (5)	Poison	Breast MDA-MB-231 Colon HCT116 Keratinocyte HaCaT Colon HCT116	1.45 ± 0.07 1.23 ± 0.27 0.65 ± 0.07 Delayed mice xenograft	G2/M arrest	Apoptosis	DNA synthesis inhibition No ROS	[109]
Carbohydrazone	**23**	Top2α	250 (25)	DNA binding major groove	Breast MCF7 Breast MDA-MB-231 Breast HCC 1937 Breast MX1 Breast MDA-MB-436 Breast MX-1	9.916 7.557 3.278 4.534 5.249 Reducted mice xenograft (83%)		Apoptosis		[110]

Table 1. *Cont.*

Ligand Class of Cu-C	Compound Number	Targeted Top(s)	Inhibition of DNA Relaxation Total (μM) (minimal (μM))	Inhibition Mecanism	Cancer Cell Lines	IC50 (μM)	Cell Cycle Arrest	Cell Death Type	Other Specificity	Reference Number
Chromone	**24**	Top2a	25 (15)	DNA binding major groove	Breast MCF7 Breast Zr-75-1 Colon HT29 Cervix SiHa Kidney A498 Lung A549 Ovary A2780	18.6 (GI 50) 25.2 (GI 50) >80 (GI 50) 34.6 (GI 50) 73.3 (GI 50) 31.7 (GI 50) 17.4 (GI 50)				[111]
Quinolinone Shiff Base	**25**	Top2α	9	No intercalation	Hepatic HepG2	17.9 ± 3.8			DNA synthesis inhibition Slight substrate for ABC transporter	[112]
Bis-pyrazolyl Carboxylate	**26**	Dual Top1/Top2	(Molecular docking) *	ATP entry (potentially) DNA religation inhibition (potentially)	Hepatic HepG2	3.3 ± 0.02		Apoptosis	DNA replication ROS	[113]

2.1. CuC Top1 Inhibitors

All the structures of CuC Top1 inhibitors are reported in Figure 2 and the main characteristics in Table 1. Oxindolimine-Cu(II) Top1 inhibitors such as **1** are planar copper compounds [70] that do not permit enzyme-DNA complex formation [71–73]. Besides, they produce ROS [70]. Cu(II) derivative complexes of the hydrazone ligand with triphenylphosphonium moiety **2** can bind DNA and the Top enzyme [74]. Plumbagin-Cu(II) **3** selectively intercalates into DNA [75]. The latter compound [75] and the phenanthroline-Cu(II) complexes modulated by amino acids **4** [**76**] can induce cancer cell apoptosis via mitochondrial signaling. Copper pyrophosphate-bridged binuclear complex **5** interacts with DNA, and based on the redox chemistry of copper, induces significant oxidative stress in cancer cell lines [77].

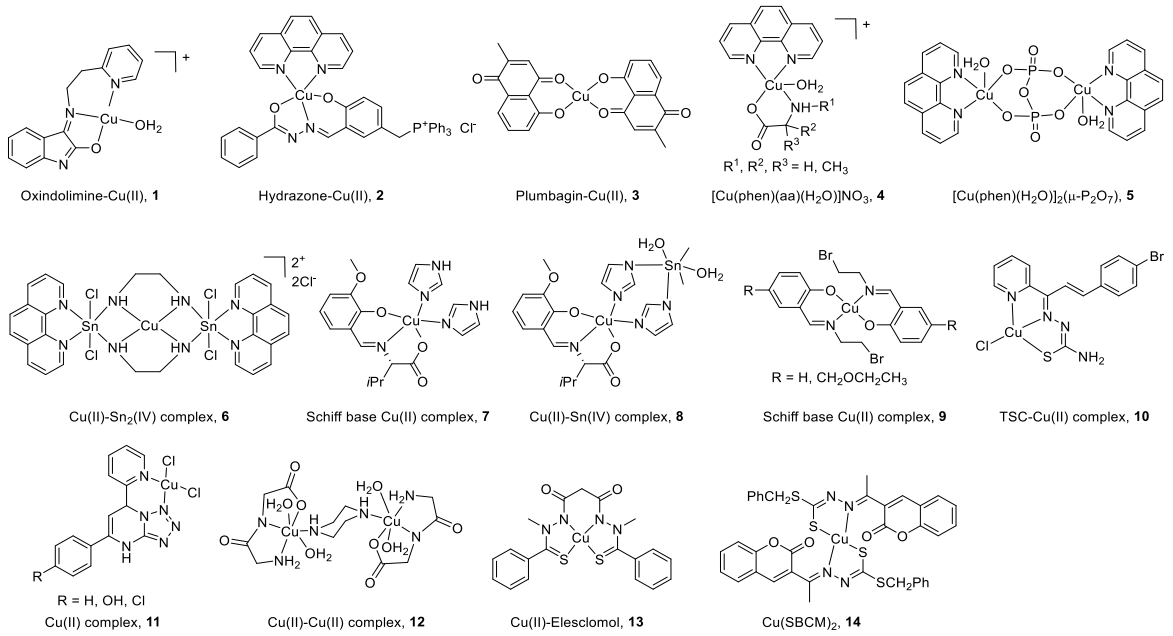

Figure 2. Structure of Cu(II) complexes as Top1 inhibitors.

In the heterobimetallic Cu(II)-Sn_2(IV) (copper/tin) complex **6**, the planar phenanthroline heterocyclic ring approaches the Top−DNA complex Cu(II)-Sn_2(IV) toward the DNA cleavage site and forms a stable complex with Top1 [78,79]. Other Cu(II)-Sn_2(IV) analogs induce apoptosis [80]. Chiral monometallic or heterobimetallic complexes **7** and **8** with tridentate chiral Schiff base–ONO-ligand are DNA groove binders and produce ROS [81,82].

Salicylidene-Cu(II) derivative **9** of 2-[2-bromoethyliminomethyl] phenol [83,84] is a bifunctional drug that inhibits both cancer cell growth and metastasis.

Chalcone-derived thiosemicarbazone (TSC) Cu(II) complex **10** prevents the DNA cleavage step of the Top1 catalytic cycle and DNA relegation [85].

Tetrazolo[1,5-*a*]pyrimidine-based Cu(II) complexes **11** have a square planar geometry, and despite their high capability to inhibit Top1, interact with CDK for **11** [86] and VEGF receptors for an analog of **11** [87]. Binuclear Cu(II) dipeptide piperazine-bridged complex **12** recognizes specific sequences in the DNA, oxidatively cleaves DNA, and displays superoxide dismutase (SOD) activity [88].

Derived from elesclomol (in clinical trials: phase 3 against melanoma and randomized phases 2 and 3 for the treatment of a variety of other cancers), the elesclomol-Cu(II) complex **13** inhibits Top1 and induces apoptosis in cancer cells [89].

As recently studied, Cu(II)$(SBCM)_2$ **14** derived from *S*-benzyldithiocarbazate and 3-acetylcoumarin intercalates into DNA, induces ROS production, and has an antiproliferative activity in breast cancer lines [90,91].

2.2. CuC Top2α Inhibitors

Due to its cell cycle phase dependence and its high expression in proliferating cells, the Top2α isoform is primarily targeted by copper complexes (CuC), whereas Top2β remains unchanged during the course of the cell cycle [66]. Another reason to limit the clinical application of Top2β inhibitors is the strong unwanted side effects produced (secondary leukemia, myelodysplastic syndrome (MDS), and cardiac toxicity [92,93]).

The main characteristics and structures of CuC Top2 inhibitors are reported in Figure 3 and Table 1. Several α-(*N*)-heterocyclic thiosemicarbazone (TSC) CuC [94,95] present a greater inhibitory effect on Top2α than corresponding TSC ligands alone [96,97] due to a square planar structure around the Cu(II) ion. A specific subset of pyridine-TSC CuC **15** inhibits Top2α [98] acting as ATP hydrolysis inhibitors in a non-competitive mode [94,99,100]. Another pyridine-TSC CuC inhibits Top2β [100]. Molecular modeling supports the binding of the complexes near but outside the ATP binding pocket in communication with the DNA cleavage/ligation site of Top2. Piperazine-TSCs based CuC **16** inhibit Top2α [101,102] by a strong interaction with the ATP-binding pocket residues [99] without ROS production [102]. Thiazole-TSC CuC **17** and **18** are Top2α catalytic inhibitors [103, 104] or poisons [105]. The highly water-soluble proline-TSC CuC series **19** inhibit Top2α and cell proliferation [106]. Quinoline-TSC CuC **20** interact with the DNA phosphate group preventing relegation. The presence of two methyl groups on the terminal nitrogen is responsible for high activity and confers a cationic nature responsible for easier passive access into the cell [107].

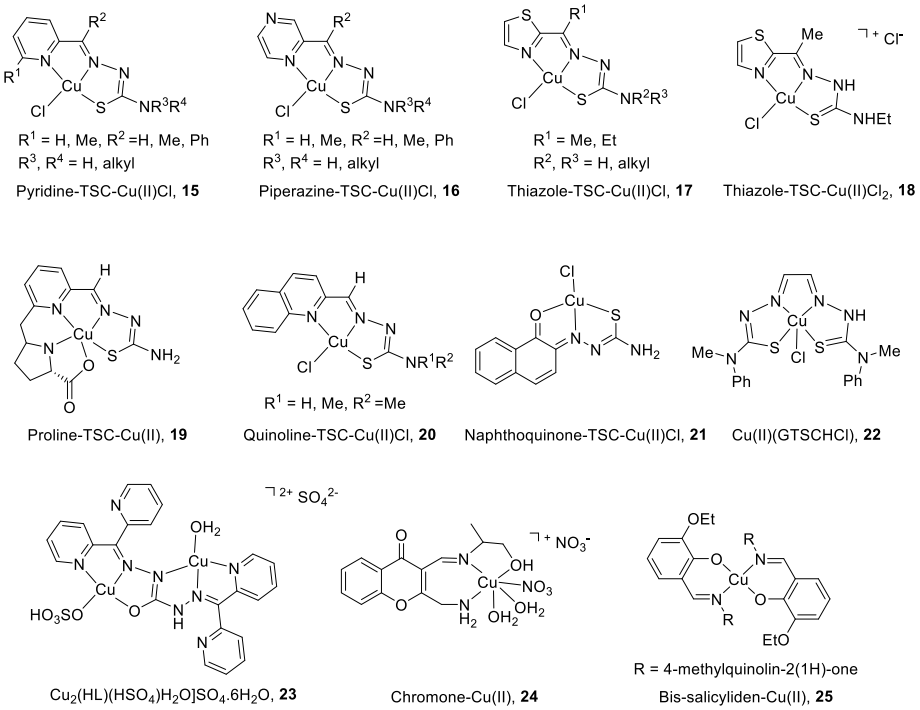

Figure 3. Structure of Cu(II) complexes as Top2 inhibitors.

Non-heterocycle naphthoquinone-TSC CuC **21** [108] and bis-TSC CuC **22** [109] are Top2α inhibitors acting as poisons [109]; they induce apoptosis in various human cancer cell lines and delay colorectal growth of carcinoma xenografts in mice [109]. Carbohydrazone CuC **23** [110] is a Top2α inhibitor that binds DNA, induces apoptosis, and reduces mice xenograft (83% after a treatment of 2 mg/kg). Chiral chromone Cu(II)/Zn(II) **24** [111] revealed catalytic inhibition of Top2α with DNA binding in the major groove. Quinolinone CuC **25** [112] inhibit Top2α and DNA synthesis without DNA intercalation and are only minimized PGP (P-glycoprotein efflux transporter) substrates.

2.3. CuC Dual Top1/Top2α Inhibitors

Heteroleptic Cu(I) complexes of the bis-pyrazolyl carboxylate ligand with auxiliary phosphine **26** (Figure 4) may inhibit Top1 by blocking the relegation step and inhibit Top2α by preventing ATP hydrolysis, as proposed by molecular docking analysis. They also perturb DNA replication, generate ROS, and induce apoptosis [113].

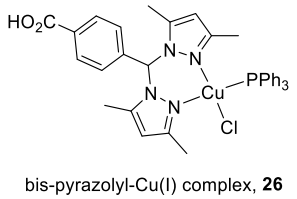

bis-pyrazolyl-Cu(I) complex, **26**

Figure 4. Structure of Cu(I) complex as a Top1/2α dual inhibitor.

3. Cell Cycle Regulation by Copper Complexes and Top Inhibitors

CuC inhibitors targeting Top1 [72,90] or Top2 [109] as DNA-damaging drugs or poisons arrest cancer cells in G2/M (Table 1). This common G2/M arrest involves the activation of two different cell cycle pathways: the DNA damage response (DDR) and the decatenation checkpoint.

Both Top1 and Top2 CuC inhibitors produce DNA damages. Top2 poisons prevent DNA relegation and stabilize an enzyme–DNA complex with the double-stranded cleaved DNA [114]. Top1 poisons induce single-stranded DNA breaks and associated signaling cascades. The collision between the Top1 cleavage complexes and the DNA replication forks ends up generating double-strand breaks [115] (Figure 5A). Top1- and Top2-induced DNA breaks trigger a DDR executed by ATM-, ATR-, and DNA-PK-related kinases, and an arrest of the cell cycle machinery [116–118]. ATM- and ATR-dependent phosphorylations of p53, Chk1, and Chk2 regulate the G1/S, S, or G2/M cell cycle checkpoints. Chk1 and Chk2 inhibit Cdc25 phosphatases (A,B,C) required for Cdks activation. Phosphorylated and ubiquitinated Cdc25A (Ser123) is degraded, leading to the absence of activation of the Cdk2/Cyclin E and the Cdk4/cyclin D complexes and followed by an arrest in G1/S. Phosphorylated Cdc25C (Ser216) binds to 14-3-3, prevents Cdk1/Cyclin B (MPF) activation, and induces a G2/M arrest (Figure 5A). Cdc25B inactivation also results in a G2 arrest [119,120]. The DNA damage-induced cell cycle arrest in G1 is dependent on p53 phosphorylation by ATM (Ser15) and Chk2 (Ser20) but arrest in S and G2 phases is p53-independent [121–124]. Phosphorylated p53 dissociates from MDM2 and activates the transcription of Cdk inhibitor p21WAF1 [125,126]. In several CuC (Top1 DNA binding CuC inhibitors [72,82,88] and a dual Top1/2 inhibitor with heteroleptic CuC [113]), Cu(II) exhibits a high redox potential and reinforces DDR activation by ROS production. ROS are also involved in a G2/M arrest through the decrease in Cdc25C [127] and Cdc25A levels [128], the activation of Chk1 [129] and Chk2 [130], and genomic instability through induced-DNA damages [131] (Figure 5A).

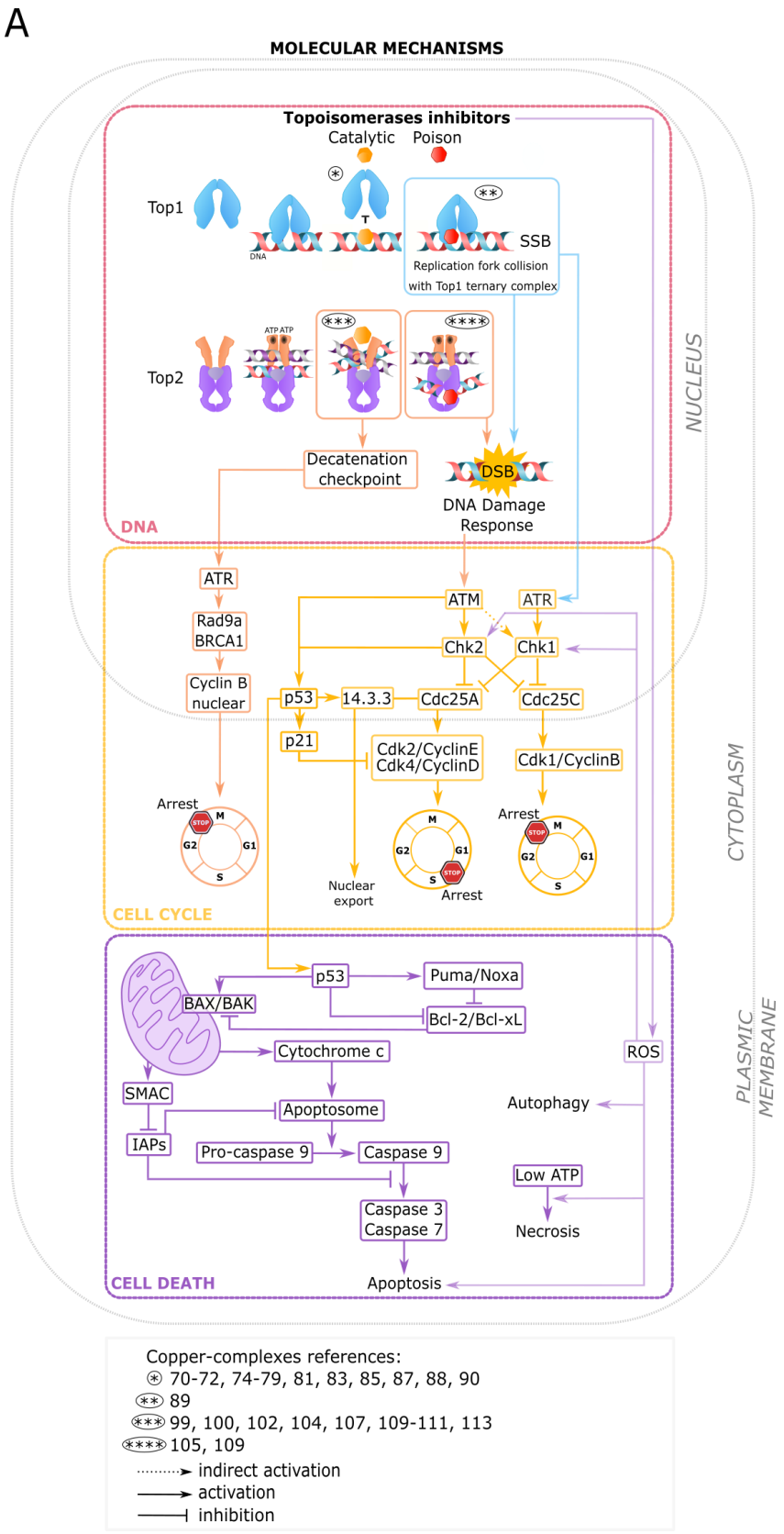

Figure 5. *Cont.*

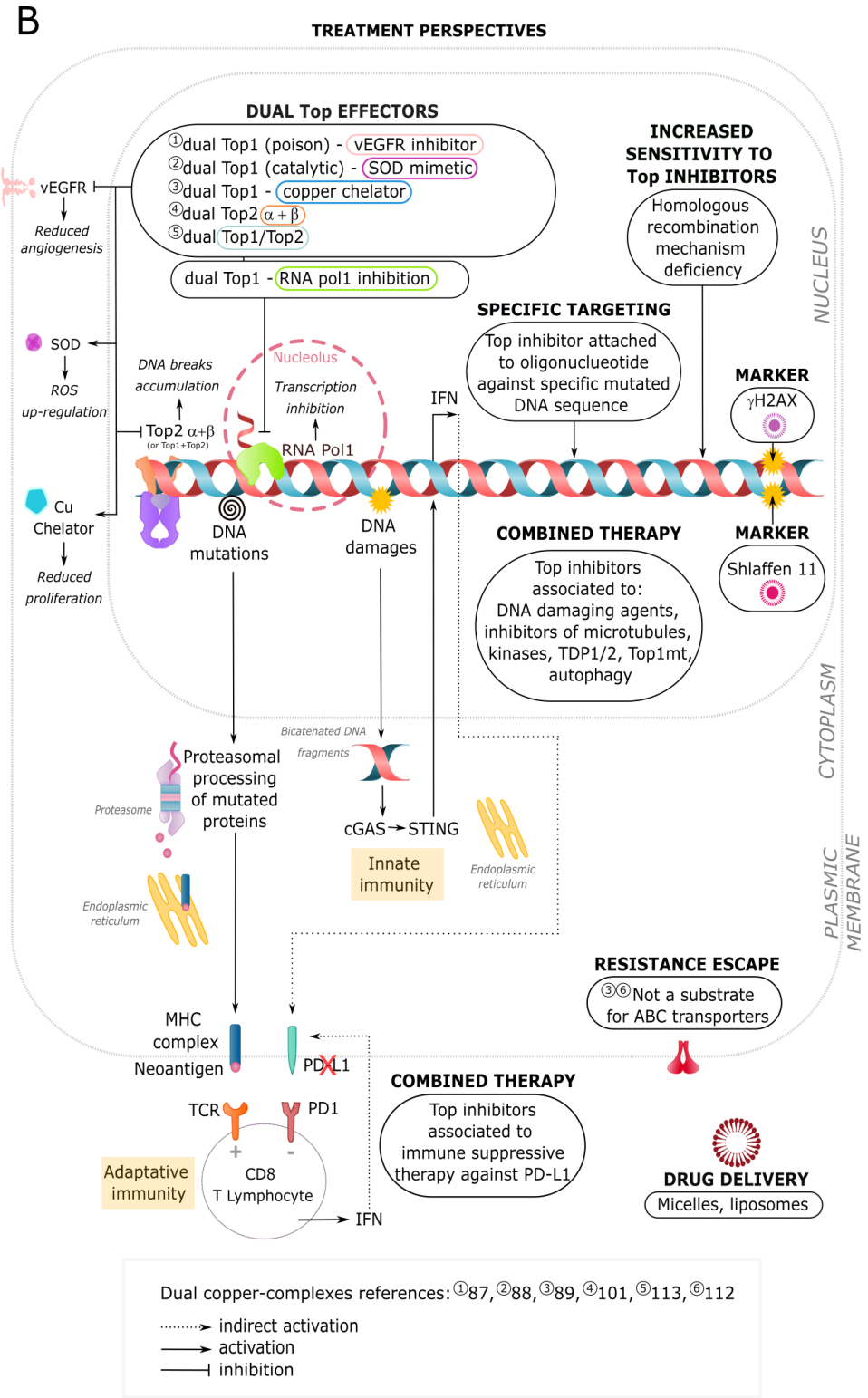

Figure 5. Molecular mechanisms and treatment perspectives for copper complexes (CuC) drugs. (**A**) Molecular checkpoints and networks involved in DNA damage (red), cell cycle regulation (yellow), and death response (violet) triggered by topoisomerase inhibitors (poison and catalytic), including CuC of topoisomerase inhibitors. (**B**) Treatment perspectives alone or in association with other chemotherapeutics (see text for more details).

By contrast to poisons, Top2 catalytic inhibitors do not form cleavable complexes. They function by enzymatic activity deprivation and cell cycle arrest in G2 through a decatenation checkpoint distinct from the DNA damage checkpoint. To delay the mitotic entry, an insufficient decatenation engages molecular components from the DDR and the spindle assembly checkpoint (SAC) (Rad9a, ATR, and BRCA1), SUMOylation and phosphorylation of Top2, the p38 and the MAPK pathways, and several decatenation checkpoint effectors but not p53 [66,132–136] (Figure 5A).

Cell cycle checkpoint effectors arrest DNA-damaged cells and induce their death providing that cell cycle regulatory networks are effective. Cell cycle checkpoint effectors integrity influences responses to Top2 inhibitors [137]. Besides, cancer disease is associated with multiple overexpression and mutations [138] in Cdc25 [139,140] and p53 [141,142], to a loss of Cdk inhibitors expression and/or overexpression of cell cycle-regulated protein [143,144], Top deregulation, and multidrug resistance [145–147]. Moreover, cell cycle variation of Top2α is regulated by post-translational modifications that represent potential targets. These alterations include ubiquitination by Cdk-1 [148], sumoylation [149], phosphorylation by polo-like kinase 1, Cdc7 [150], protein kinase C, Ca/calmodulin-dependent kinase II, and casein kinase [151], and the association with 14-3-3 [152]. Rewiring cellular pathways leading to cell death is a challenge that requires targeting specific molecular checkpoint effectors [153]. For example, a mutated p53 pathway arrests the cell cycle but avoids DDR-induced cell death [154]. Some anticancer therapeutic strategies (e.g., Chk1/2 pathways targeting drugs associated with DNA-damaging drugs) can force cancer cells to bypass S and G2/M arrest, enter mitosis with damaged DNA, and finally undergo a mitotic catastrophe and death [155]. ATR inhibition is another strategy to overcome the resistance of BRCA-deficient cancers [156].

4. Programmed Cell Death Engaged by Copper Complexes and Top Inhibitors

Multiple stress factors ranging from various cell damages, ATP levels, and specific pathways (e.g., caspases) determine the type of cell death [157]. Most Top1 CuC inhibitors that interact with DNA [70,76,79,86,87,90], Top1 poison [89], Top2α CuC poison [109], or dual Top1/Top2 inhibitor [113] trigger apoptotic programmed cell death. Genetic damages and oxidative stress activate an intrinsic mitochondrial response [158]. Pro-apoptotic members of the Bcl-2 family (Bid, Noxa, Puma, BAX, BAK) neutralize the anti-apoptotic members (Bcl-2, Bcl-xL, and Mcl-1), disrupt the mitochondrial outer membrane, and allow cytoplasmic cytochrome-c release. The binding of cytochrome c to the apoptotic protease activating factor-1 (Apaf-1), ATP, and the pro-caspase-9 create the apoptosome protein complex. Pro-caspase 9 is cleaved into its active caspase-9 form, which in turn cleaves pro-caspase-3 into caspase-3 effector, and the downstream executor caspase-7. SMAC (second mitochondria-derived activator of caspases), and Omi/HtrA2 (high-temperature requirement protein A2) are simultaneously released from mitochondria and deactivate the IAPs factors (inhibitors of apoptosis proteins). p53, activated by the DNA damage, contributes to apoptosis through the translation of several pro-apoptotic members of the Bcl-2 family (Bid, Puma) that inhibit the pro-survival action of Bcl-2 on BAX (Figure 5A). Most cancer cells evade apoptosis through caspase inhibition, upregulation of Bcl-2 (in more than 50% of all types of cancers), and loss of BAX/BAK and become resistant to anticancer drugs [159].

A Top1 DNA-damaging CuC inhibitor induces necrotic cell death. To facilitate cell destruction, necrosis is activated by ROS or ATP metabolic stresses in crosstalk with apoptosis [160]. When the intracellular energy/ATP level is low, the apoptotic cell death is converted into necrosis [161] (Figure 5A). However, necrosis releases pro-inflammatory and tumor-promoting cytokine HMGB1 [162] into the extracellular space reported to stimulate inflammation and angiogenesis, and promote tumor progression [163].

Apoptosis and necrosis often co-exist with another cell death with controversial pro-death and pro-survival functions: autophagy [164]. Up to the current study, no CuC Top inhibitors are involved in autophagic or necroptotic programmed cell death (Table 1). However, some CuC trigger stress-mediated protective autophagy in response to ROS that impedes apoptosis and creates survival

of malignant cells [165]. Moreover, topoisomerase inhibition-induced autophagy is associated with cancer resistance [166].

5. Future Strategies for Copper Complexes as Top Inhibitors in Cancer Cell Treatments

The development of new effective anticancer drugs is a major research area against the continuing increase in cancers worldwide. Top inhibitors used in chemotherapy are limited in number [61,167,168]. Top1 inhibitors' camptothecin derivatives used are irinotecan (colorectal [169], pancreatic (in combination) [170], and small cell lung cancers (in clinical trials and in combination) [171,172]), and topotecan (ovarian [173,174], cervical [175], and small cell lung cancers [176]). Top2 anticancer drugs commonly used are from the anthracycline group such as doxorubicin (acute leukemia [177], lymphomas [178], sarcomas [179,180], and solid tumors [181]), epirubicin (breast cancer [182]), valrubicin (bladder cancer [183]), and idarubicin (acute myeloid leukemia [184]), from the anthracenedione classes: mitoxantron and pixantron (lymphoma, [185–187]), and from the epipodopodophyllotoxins group such as etoposide (testicular [188] and small cell lung cancers [189]) and teniposide (brain [190] and small cell lung [191] cancers, acute lymphocytic leukemia [192]). Only a few numbers of Top1 inhibitors are in clinical trials including the promising indenoisoquinoline derivatives LMP400 (Indotecan), LMP776 (Indimitecan) (phase I), and LMP744 examined in a phase I study on lymphoma in dogs [193]. In addition to better stability, and milder side effects, they can escape ABC transporter efflux and the drug resistance mechanism, as Elesclomol-CuC Top complexes **13** [89] or Quinolinone-CuC **25** [112]. Perspectives to use CuC of Top inhibitors in clinical trials are summarized in Figure 5B. Development and optimization in CuC of Top inhibitors imply structure modifications that must encompass several specific strategies [194], such as scaffold hopping [195], pharmacophore hybridization [196], bioisosteric replacement [197], and conformational restrictions. Generally, a rigidification of the ligand heterocycle structure with a copper metal [78] provides a planar configuration that facilitates DNA intercalation and Top-DNA ternary complex formation compared to the molecular backbone alone.

Top inhibitors in clinical use and particularly Top poison display unwanted drawbacks, such as cumulative cardiotoxicity in long-term protocols, secondary malignancies, and drug resistance [198]. A therapeutic option would be to use preferentially catalytic Top agents that disturb the catalytic cycle without the formation of a ternary complex. CuC Top catalytic inhibitors, listed in Table 1, exhibit high antitumor effects on cancer cell lines and for some compounds on tumor growth in animal models, compared to their respective ligands (see Table 1). They constitute a reservoir of anticancer drugs. For example, TSC-based CuC Top2 inhibitors (Figure 3) [98,102,103,105,107] have demonstrated strong inhibition of tumor growth compared to TSC derivatives currently used in cancer chemotherapies [199].

Considering that cancer is a multigenetic and multifactorial disease that recruits numerous molecular effectors, monotherapies (based on Top inhibitors) do not provide the optimal curative effects. Combination therapy with a few numbers of therapeutics against two or more biotargets is the base of promising treatments such as the association of a Top 2 inhibitor (vosaroxin) with a DNA methyltransferase inhibitor (decitabine) in AML [200,201]. Inhibitors of Top1 and Top2, currently developed, also exert their effect against other cancer-related targets [202]. Dual Top inhibitors, e.g., Top 1/2 [203], Top2/microtubule [204], or Top2/histone deacetylase [205], may exert improved efficacy. Besides, Top1 inhibitors are nonspecific RNA polymerase inhibitors. An RNA Pol1-mediated ribosomal RNA gene increase is involved in cancer progression, through the control of cellular checkpoints and chromatin structure and is, therefore, an interesting co-target [206]. CuC dual Top inhibitors display a high antiproliferative activity. Particularly, some CuC and non-CuC are dual inhibitors of Top1 and superoxide dismutase agonist [88,207,208] or Cdk receptor, like VEGF inhibitors, involved in cancer cells proliferation [86,87,209,210] (Figure 5B). Another strategy to improve therapies is the association of a CuC with a TDP1/2 (tyrosyl-DNA-phosphodiesterase 1/2) inhibitor. TDP1/2 are enzymes responsible for the reparation of DNA breaks induced by topoisomerase poisons [57,211,212]. TDP1/2 inhibitors are capable of improving cancer cells' sensitivity to these poisons [213].

Autophagy, an essential mechanism for cell integrity and survival, is stimulated in cancer cells under several chemotherapeutic drugs and acts as an unwanted protective system towards tumor cells. Association of specific autophagic inhibitors with Cu-C treatment (disulfiram) in non-small cell lung cancer [214] has proven to be a novel efficient strategy to enhance apoptosis in cancer therapy.

Immunogenic cell death is an important mechanism used in chemotherapy. Association of CuC with immune checkpoint therapies is certainly a new avenue in cancer treatment. CuC and non-CuC Top inhibitors induce DNA damages and are linked to adaptive and innate immunities [215]. Top poisons promote immunogenicity in various ways [216]. Top1 poison camptothecin enhances the adaptive immune response [217]. Top inhibitors also increase chromosomal instability and mutations accumulated by cancer cells [59,218]. Consequently, due to their high number of mutations, tumors display more neoantigens presented at their surface by the major histocompatibility complex class I (MHCI) and recruit lymphocytes T harboring TCR (T cell receptor) and CD8 co-receptor (adaptive immunity). This response is counterbalanced by the overexpression of immune checkpoint modulators, such as the immune-suppressive ligand PD-L1 (programmed death-ligand 1) targeted in immune therapies [219] (Figure 5B). DNA-damaging agents such as Top2 poison anthracycline also interfere with the innate immune response. They enhance the malignant formation of cytosolic bicatenated DNA fragments that activate the cyclic GMP-AMP synthase-stimulator of the interferon (IFN) gene pathway (cGAS-STING) and initiate innate anti-cancer immunity. cGAS-STING agonist serves as a sensitizer in immunotherapies [220]. Top1-DNA covalent cleavage complex enables cGAS-mediated cytoplasmic chromatin recognition and immune checkpoint response [221] (Figure 5B). Top2 inhibitors teniposide and doxorubicin potentiate the therapeutic immune checkpoint blockade therapies based on anti-PD-1 (programmed cell death 1) in multiple types of mouse tumor models [222,223]. Besides, ROS produced by Top inhibitors alter the molecular pattern recognized as immunogenic structures and enhance apoptosis [224] (Figure 5B).

As DDR gene mutations exist in a large range of tumor types, the determination of tumor-specific mutations is another accurate strategy to generate chemotypes with beneficial efficacies superior to adverse effects [225,226]. In each tumor, the signaling components of the DDR exhibit numerous defects that result in a unique mutational signature [227]. Cancer cells with defects in their homologous recombination mechanism are more sensitive to Top2 inhibitory therapies that generate DNA double-strand breaks [228]. Moreover, the prediction of anticancer treatments determined by the clinical stage and the pathological features of the tumor does not always ascertain a cancer death response. Cellular biomarkers that may predict sensitivity or resistance to therapy based on DNA damage induced by Top inhibitors would be useful. Insights into the Top2 regulatory mechanisms have identified genetic markers to allow the prediction of an overcome treatment with a Top inhibitor. γ-H2AX is a DNA-damaged marker, recruited on DNA breaks after Top poison action, currently evaluated [229]. Schlaffen is also a promising marker for an accurate response to Top1 and Top2 inhibitors, especially for colon and ovarian adenocarcinomas [56,230] (Figure 5B).

Recently, cancer cells were targeted specifically by a Top2 inhibitor, etoposide, attached to a single-stranded oligonucleotide with a complementary sequence to a DNA cleavage hotspot corresponding to a translocated region only present in promyelocytic leukemia cells [231].

Finally, to overcome toxicity to normal cells, Top drugs could be attached to vehicles. Top2 inhibitors delivery has been optimized using liposomes [232], micelles [233], or functionalized nanoparticles [234] (Figure 5B).

Topoisomerases are present in mitochondria where they participate in mitochondrial DNA replication and transcription. Mitochondrial Top1 isoform (Top1mt) is involved in the metabolism of cancer cells providing energy to tumors surrounded by a nutrient-low microenvironment. Exposures to a Top1 inhibitor (lamellarin D) or Top2 inhibitors (doxorubicin or fluoroquinolones) exert mitochondrial toxicity [235]. However, the loss of Top1mt in liver cancers correlates with increased survival of hepatocellular carcinoma patients, showing that co-targeting Top1mt in addition to nuclear topoisomerases is another option for anticancer therapies [236].

6. Conclusions

In a multifactorial disease such as cancer, Top inhibitors are efficient anticancer compounds used in monotherapy or polypharmacological strategies. They certainly have to target closely related modulators of the cellular checkpoints' networks. CuC Top inhibitors are particularly adapted to fulfill this role. A perspective in anticancer strategy is to increase and to enlarge this family of highly active anticancer drugs.

Author Contributions: Writing—original draft preparation: C.M., K.C., A.M. and L.P. All authors have read and agreed to the published version of the manuscript.

Funding: C.M. is a recipient from a doctoral fellowship from the French ministry. The scientific supports were provided by the "Centre National de la Recherche Scientifique ", "Université de Lille ", and the "Ligue Contre le Cancer".

Acknowledgments: The authors are thankful to the Research Federation FRABio (FR 3688, FRABio, Biochimie Structurale et Fonctionnelle des Assemblages Biomoléculaires) and to E. Germain (Inserm U1003) for reading the manuscript.

Conflicts of Interest: The authors declare no conflict of interest.

References

1. Rosenberg, B.; VanCamp, L.; Trosko, J.E.; Mansour, V.H. Platinum compounds: A new class of potent antitumour agents. *Nature* **1969**, *222*, 385–386. [CrossRef] [PubMed]
2. Alderden, R.A.; Hall, M.D.; Hambley, T.W. The discovery and development of cisplatin. *J. Chem. Educ.* **2006**, *83*, 728–734. [CrossRef]
3. Dilruba, S.; Kalayda, G.V. Platinum-based drugs: Past, present and future. *Cancer Chemother. Pharm.* **2016**, *77*, 1103–1124. [CrossRef] [PubMed]
4. Bergamo, A.; Dyson, P.J.; Sava, G. The mechanism of tumour cell death by metal-based anticancer drugs is not only a matter of DNA interactions. *Coord. Chem. Rev.* **2018**, *360*, 17–33. [CrossRef]
5. Dasari, S.; Tchounwou, P.B. Cisplatin in cancer therapy: Molecular mechanisms of action. *Eur. J. Pharm.* **2014**, *740*, 364–378. [CrossRef]
6. Manohar, S.; Leung, N. Cisplatin nephrotoxicity: A review of the literature. *J. Nephrol.* **2018**, *31*, 15–25. [CrossRef]
7. Herradón, E.; González, C.; Uranga, J.A.; Abalo, R.; Martín, M.I.; López-Miranda, V. characterization of cardiovascular alterations induced by different chronic cisplatin treatments. *Front. Pharm.* **2017**, *8*, 196–211. [CrossRef]
8. Shen, D.W.; Pouliot, L.M.; Hall, M.D.; Gottesman, M.M. Cisplatin resistance: A cellular self-defense mechanism resulting from multiple epigenetic and genetic changes. *Pharm. Rev.* **2012**, *64*, 706–721. [CrossRef]
9. Chen, S.H.; Chang, J.Y. New insights into mechanisms of cisplatin resistance: From tumor cell to microenvironment. *Int. J. Mol. Sci.* **2019**, *20*, 4136. [CrossRef]
10. Obrist, F.; Michels, J.; Durand, S.; Chery, A.; Pol, J.; Levesque, S.; Joseph, A.; Astesana, V.; Pietrocola, F.; Wu, G.S.; et al. Metabolic vulnerability of cisplatin-resistant cancers. *EMBO J.* **2018**, *37*, e98597. [CrossRef]
11. Amable, L. Cisplatin resistance and opportunities for precision medicine. *Pharm. Res.* **2016**, *106*, 27–36. [CrossRef] [PubMed]
12. Galluzzi, L.; Senovilla, L.; Vitale, I.; Michels, J.; Martins, I.; Kepp, O.; Castedo, M.; Kroemer, G. Molecular mechanisms of cisplatin resistance. *Oncogene* **2012**, *31*, 1869–1883. [CrossRef] [PubMed]
13. Housman, G.; Byler, S.; Heerboth, S.; Lapinska, K.; Longacre, M.; Snyder, N.; Sarkar, S. Drug resistance in cancer: An overview. *Cancers* **2014**, *6*, 1769. [CrossRef] [PubMed]
14. Martinho, N.; Santos, T.; Florindo, H.F.; Silva, L.C. Cisplatin-membrane interactions and their influence on platinum complexes activity and toxicity. *Front. Physiol.* **2019**, *9*, 1898–1913. [CrossRef]
15. Zeng, L.; Gupta, P.; Chen, Y.; Wang, E.; Ji, L.; Chao, H.; Chen, Z.-S. The development of anticancer ruthenium(ii) complexes: From single molecule compounds to nanomaterials. *Chem. Soc. Rev.* **2017**, *46*, 5771–5804. [CrossRef]

16. Zhang, P.; Sadler, P.J. Advances in the design of organometallic anticancer complexes. *J. Org. Chem.* **2017**, *839*, 5–14. [CrossRef]
17. Jaouen, G.; Vessières, A.; Top, S. Ferrocifen type anti cancer drugs. *Chem. Soc. Rev.* **2015**, *44*, 8802–8817. [CrossRef]
18. Gianferrara, T.; Bratsos, I.; Alessio, E. A categorization of metal anticancer compounds based on their mode of action. *Dalton Trans.* **2009**, *37*, 7588–7598. [CrossRef]
19. Hartinger, C.G.; Dyson, P.J. Bioorganometallic chemistry from teaching paradigms to medicinal applications. *Chem. Soc. Rev.* **2009**, *38*, 391–401. [CrossRef]
20. Wambang, N.; Schifano-Faux, N.; Martoriati, A.; Henry, N.; Baldeyrou, B.; Bal-Mahieu, C.; Bousquet, T.; Pellegrini, S.; Meignan, S.; Cailliau, K.; et al. Synthesis, structure, and antiproliferative activity of ruthenium(ii) arene complexes of indenoisoquinoline derivatives. *Organometallics* **2016**, *35*, 2868–2872. [CrossRef]
21. Wambang, N.; Schifano-Faux, N.; Aillerie, A.; Baldeyrou, B.; Jacquet, C.; Bal-Mahieu, C.; Bousquet, T.; Pellegrini, S.; Ndifon, T.P.; Meignan, S.; et al. Synthesis and biological activity of ferrocenyl indeno[1,2-c]isoquinolines as topoisomerase II inhibitors. *Bioorg. Med. Chem.* **2016**, *24*, 651–660. [CrossRef] [PubMed]
22. Komeda, S.; Casini, A. Next-generation anticancer metallodrug. *Curr. Top. Med. Chem.* **2012**, *12*, 219–235. [CrossRef] [PubMed]
23. Mejía, C.; Ortega-Rosales, S.; Ruiz-Azuara, L. Mechanism of action of anticancer metallodrugs. In *Biomedical Applications of Metals*; Rai, M., Ingle, A., Medici, S., Eds.; Springer: Berlin/Heidelberg, Germany, 2018; Volume 10, pp. 213–234.
24. Denoyer, D.; Clatworthy, S.A.S.; Cater, M.A. Copper complexes in cancer therapy. *Met. Ions Life Sci.* **2018**, *18*, 469–506.
25. Santini, C.; Pellei, M.; Gandin, V.; Porchia, M.; Tisato, F.; Marzano, C. Advances in copper complexes as anticancer agents. *Chem. Rev.* **2014**, *114*, 815–862. [CrossRef] [PubMed]
26. Jungwirth, U.; Kowol, C.R.; Keppler, B.K.; Hartinger, C.G.; Berger, W.; Heffeter, P. Anticancer activity of metal complexes: Involvement of redox processes. *Antioxid. Redox Signal.* **2011**, *15*, 1085–1127. [CrossRef] [PubMed]
27. Tardito, S.; Marchiò, L. Copper compounds in anticancer strategies. *Curr. Med. Chem.* **2009**, *16*, 1325–1348. [CrossRef] [PubMed]
28. Marzano, C.; Pellei, M.; Tisato, F.; Santini, C. Copper complexes as anticancer agents. *Anticancer Agents Med. Chem.* **2009**, *9*, 185–211. [CrossRef] [PubMed]
29. Kellett, A.; Molphy, Z.; McKee, V.; Slator, C. Recent advances in anticancer copper compounds. In *Metal-Based Anticancer Agents*; Vessieres, I.A., Meier-Menches, S.M., Casini, A., Eds.; Royal Society of Chemistry, RSC Metallobiology: London, UK, 2019; Volume 14, pp. 91–119.
30. Hordyjewska, A.; Popiołek, L.; Kocot, J. The many "faces" of copper in medicine and treatment. *Biometals* **2014**, *27*, 611–621. [CrossRef] [PubMed]
31. Urso, E.; Maffia, M. Behind the link between copper and angiogenesis: Established mechanisms and an overview on the role of vascular copper transport systems. *J. Vasc. Res.* **2015**, *52*, 172–196. [CrossRef] [PubMed]
32. Lowndes, S.A.; Harris, A.L. The role of copper in tumour angiogenesis. *J. Mammary Gland. Biol. Neoplasia* **2005**, *10*, 299–310. [CrossRef] [PubMed]
33. Hu, G.F. Copper stimulates proliferation of human endothelial cells under culture. *J. Cell. Biochem.* **1998**, *69*, 326–335. [CrossRef]
34. Yoshida, D.; Ikeda, Y.; Nakazawa, S. Quantitative analysis of copper, zinc and copper/zinc ratio in selected human brain tumors. *J. Neurooncol.* **1993**, *16*, 109–115. [CrossRef] [PubMed]
35. Geraki, K.; Farquharson, M.J.; Bradley, D.A. Concentrations of Fe, Cu and Zn in breast tissue: A synchrotron XRF study. *Phys. Med. Biol.* **2002**, *47*, 2327–2339. [CrossRef] [PubMed]
36. Nayak, S.B.; Bhat, V.R.; Upadhyay, D.; Udupa, S.L. Copper and ceruloplasmin status in serum of prostate and colon cancer patients. *Indian J. Physiol. Pharm.* **2003**, *47*, 108–110.
37. Díez, M.; Arroyo, M.; Cerdàn, F.J.; Muñoz, M.; Martin, M.A.; Balibrea, J.L. Serum and tissue trace metal levels in lung cancer. *Oncology* **1989**, *46*, 230–234. [CrossRef]

38. Kaiafa, G.D.; Saouli, Z.; Diamantidis, M.D.; Kontoninas, Z.; Voulgaridou, V.; Raptaki, M.; Arampatzi, S.; Chatzidimitriou, M.; Perifanis, V. Copper levels in patients with hematological malignancies. *Eur. J. Intern. Med.* **2012**, *23*, 738–741. [CrossRef]
39. Baldari, S.; Di Rocco, G.; Toietta, G. Current biomedical use of copper chelation therapy. *Int. J. Mol. Sci.* **2020**, *21*, 1069. [CrossRef]
40. Denoyer, D.; Masaldan, S.; La Fontaine, S.; Cater, M.A. Targeting copper in cancer therapy: 'Copper That Cancer'. *Metallomics* **2015**, *7*, 1459–1476. [CrossRef]
41. Cater, M.A.; Pearson, H.B.; Wolyniec, K.; Klaver, P.; Bilandzic, M.; Paterson, B.M.; Bush, A.I.; Humbert, P.O.; La Fontaine, S.; Donnelly, P.S.; et al. Increasing intracellular bioavailable copper selectively targets prostate cancer cells. *ACS Chem. Biol.* **2013**, *8*, 1621–1631. [CrossRef]
42. Cater, M.A.; Haupt, Y. Clioquinol induces cytoplasmic clearance of the X-linked inhibitor of apoptosis protein (XIAP): Therapeutic indication for prostate cancer. *Biochem. J.* **2011**, *436*, 481–491. [CrossRef]
43. Cheriyan, V.T.; Wang, Y.; Muthu, M.; Jamal, S.; Chen, D.; Yang, H.; Polin, L.A.; Tarca, A.L.; Pass, H.I.; Dou, Q.P.; et al. Disulfiram suppresses growth of the malignant pleural mesothelioma cells in part by inducing apoptosis. *PLoS ONE* **2014**, *9*, e93711. [CrossRef] [PubMed]
44. Duan, L.; Shen, H.; Zhao, G.; Yang, R.; Cai, X.; Zhang, L.; Jin, C.; Huang, Y. Inhibitory effect of Disulfiram/copper complex on non-small cell lung cancer cells. *Biochem. Biophys. Res. Commun.* **2014**, *446*, 1010–1016. [CrossRef] [PubMed]
45. Jivan, R.; Damelin, L.H.; Birkhead, M.; Rousseau, A.L.; Veale, R.B.; Mavri-Damelin, D. Disulfiram/copper-disulfiram damages multiple protein degradation and turnover pathways and cytotoxicity is enhanced by metformin in oesophageal squamous cell carcinoma cell lines. *J. Cell. Biochem.* **2015**, *116*, 2334–2343. [CrossRef] [PubMed]
46. Safi, R.; Nelson, E.R.; Chitneni, S.K.; Franz, K.J.; George, D.J.; Zalutsky, M.R.; McDonnell, D.P. Copper signaling axis as a target for prostate cancer therapeutics. *Cancer Res.* **2014**, *74*, 5819–5831. [CrossRef]
47. Wang, F.; Jiao, P.; Qi, M.; Frezza, M.; Dou, Q.P.; Yan, B. Turning tumor-promoting copper into an anti-cancer weapon via high-throughput chemistry. *Curr. Med. Chem.* **2010**, *17*, 2685–2698. [CrossRef]
48. Zhang, Z.; Wang, H.; Yan, M.; Wang, H.; Zhang, C. Novel copper complexes as potential proteasome inhibitors for cancer treatment. *Mol. Med. Rep.* **2017**, *15*, 3–11. [CrossRef]
49. Krasnovskaya, O.; Naumov, A.; Guk, D.; Gorelkin, P.; Erofeev, A.; Beloglazkina, E.; Majouga, A. Copper Coordination Compounds as Biologically Active Agents. *Int. J. Mol. Sci.* **2020**, *21*, 3965. [CrossRef]
50. Brissos, R.F.; Caubet, A.; Gamez, P. Possible DNA-interacting pathways for metal-based compounds exemplified with copper coordination compounds. *Eur. J. Inorg. Chem.* **2015**, *16*, 2633–2645. [CrossRef]
51. Kagawa, T.F.; Geierstanger, B.H.; Wang, A.H.J.; Ho, P.S. Covalent modification of guanine bases in double-stranded DNA. *J. Biol. Chem.* **1991**, *266*, 20175–20184.
52. Ceramella, J.; Mariconda, A.; Iacopetta, D.; Saturnino, C.; Barbarossa, A.; Caruso, A.; Rosano, C.; Sinicropi, M.S.; Longo, P. From coins to cancer therapy: Gold, silver and copper complexes targeting human topoisomerases. *Bioorg. Med. Chem. Lett.* **2020**, *30*, 126905–126916. [CrossRef]
53. Shobha Devi, C.; Thulasiram, B.; Aerva, R.R.; Nagababu, P. Recent advances in copper intercalators as anticancer agents. *J. Fluoresc.* **2018**, *28*, 1195–1205. [CrossRef] [PubMed]
54. Liang, X.; Wu, Q.; Luan, S.; Yin, Z.; He, C.; Yin, L.; Zou, Y.; Yuan, Z.; Li, L.; Song, X.; et al. A comprehensive review of topoisomerase inhibitors as anticancer agents in the past decade. *Eur. J. Med. Chem.* **2019**, *171*, 129–168. [CrossRef] [PubMed]
55. Cuya, S.M.; Bjornsti, M.A.; van Waardenburg, R.C.A.M. DNA topoisomerase-targeting chemotherapeutics: What's new? *Cancer Chemother. Pharmacol.* **2017**, *80*, 1–14. [CrossRef] [PubMed]
56. Thomas, A.; Pommier, Y. Targeting topoisomerase I in the era of precision medicine. *Clin. Cancer Res.* **2019**, *25*, 6581–6589. [CrossRef] [PubMed]
57. Pommier, Y. Drugging topoisomerases: Lessons and challenges. *ACS Chem. Biol.* **2013**, *8*, 82–95. [CrossRef] [PubMed]
58. Bjornsti, M.A.; Kaufmann, S.H. Topoisomerases and cancer chemotherapy: Recent advances and unanswered questions. *F1000 Res.* **2019**, *8*. [CrossRef]
59. Pommier, Y.; Sun, Y.; Huang, S.N.; Nitiss, J.L. Roles of eukaryotic topoisomerases in transcription, replication and genomic stability. *Nat. Rev. Mol. Cell. Biol.* **2016**, *17*, 703–721. [CrossRef] [PubMed]

60. Pommier, Y.; Leo, E.; Zhang, H.; Marchand, C. DNA topoisomerases and their poisoning by anticancer and antibacterial drugs. *Chem. Biol.* **2010**, *17*, 421–433. [CrossRef]
61. Hevener, K.; Verstak, T.A.; Lutat, K.E.; Riggsbee, D.L.; Mooney, J.W. Recent developments in topoisomerase-targeted cancer chemotherapy. *Acta Pharm. Sin. B* **2018**, *8*, 844–861. [CrossRef]
62. Xu, Y.; Her, C. Inhibition of Topoisomerase (DNA) I (TOP1): DNA damage repair and anticancer therapy. *Biomolecules* **2015**, *5*, 1652. [CrossRef]
63. Wang, J.C. Interaction between DNA and an Escherichia coli protein omega. *J. Mol. Biol.* **1971**, *55*, 523–533. [CrossRef]
64. Madabhushi, R. The roles of DNA topoisomerase IIβ in transcription. *Int. J. Mol. Sci.* **2018**, *19*, 1917. [CrossRef] [PubMed]
65. Sakasai, R.; Iwabuchi, K. The distinctive cellular responses to DNA strand breaks caused by a DNA topoisomerase I poison in conjunction with DNA replication and RNA transcription. *Genes Genet. Syst.* **2016**, *90*, 187–194. [CrossRef] [PubMed]
66. Lee, J.H.; Berger, J.M. Cell cycle-dependent control and roles of DNA topoisomerase II. *Genes* **2019**, *10*, 859. [CrossRef] [PubMed]
67. Li, M.; Liu, Y. Topoisomerase I in human disease pathogenesis and treatments. *Genom. Proteom. Bioinform.* **2016**, *14*, 166–171. [CrossRef] [PubMed]
68. Larsen, A.K.; Escargueil, A.E.; Skladanowski, A. Catalytic topoisomerase II inhibitors in cancer therapy. *Pharm. Ther.* **2003**, *99*, 167–181. [CrossRef]
69. Hu, W.; Huang, X.S.; Wu, J.F.; Yang, L.; Zheng, Y.T.; Shen, Y.M.; Li, Z.Y.; Li, X. Discovery of novel topoisomerase II inhibitors by medicinal chemistry approaches. *J. Med. Chem.* **2018**, *61*, 8947–8980. [CrossRef] [PubMed]
70. Castelli, S.; Goncalves, M.B.; Katkar, P.; Stuchi, G.C.; Couto, R.A.A.; Petrilli, H.M.; da Costa Ferreira, A.M. Comparative studies of oxindolimine-metal complexes as inhibitors of human DNA topoisomerase IB. *J. Inorg. Biochem.* **2018**, *186*, 85–94. [CrossRef]
71. Katkar, P.; Coletta, A.; Castelli, S.; Sabino, G.L.; Alves Couto, R.A.; da Costa Ferreira, A.M.; Desideri, A. Effect of oxindolimine copper(ii) and zinc(ii) complexes on human topoisomerase I activity. *Metallomics* **2014**, *6*, 117–125. [CrossRef]
72. Cerchiaro, G.; Aquilano, K.; Filomeni, G.; Rotilio, G.; Ciriolo, M.R.; Ferreira, A.M. Isatin-Schiff base copper(II) complexes and their influence on cellular viability. *J. Inorg. Biochem.* **2005**, *99*, 1433–1440. [CrossRef]
73. Filomeni, G.; Cerchiaro, G.; Da Costa Ferreira, A.M.; De Martino, A.; Pedersen, J.Z.; Rotilio, G.; Ciriolo, M.R. Pro-apoptotic activity of novel Isatin-Schiff base copper(II) complexes depends on oxidative stress induction and organelle-selective damage. *J. Biol. Chem.* **2007**, *282*, 12010–12021. [CrossRef]
74. Chew, S.T.; Lo, K.M.; Lee, S.K.; Heng, M.P.; Teoh, W.Y.; Sim, K.S.; Tan, K.W. Copper complexes with phosphonium containing hydrazone ligand: Topoisomerase inhibition and cytotoxicity study. *Eur. J. Med. Chem.* **2014**, *76*, 397–407. [CrossRef] [PubMed]
75. Chen, Z.F.; Tan, M.X.; Liu, L.M.; Liu, Y.C.; Wang, H.S.; Yang, B.; Peng, Y.; Liu, H.G.; Liang, H.; Orvig, C. Cytotoxicity of the traditional chinese medicine (tcm) plumbagin in its copper chemistry. *Dalton Trans.* **2009**, *48*, 10824–10833. [CrossRef] [PubMed]
76. Seng, H.L.; Wang, W.S.; Kong, S.M.; Alan Ong, H.K.; Win, Y.F.; Raja Abd Rahman, R.N.Z.; Chikira, M.; Leong, W.K.; Ahmad, M.; Khoo, A.S.B.; et al. Biological and cytoselective anticancer properties of copper(II)-polypyridyl complexes modulated by auxiliary methylated glycine ligand. *BioMetals* **2012**, *25*, 1061–1081. [CrossRef] [PubMed]
77. Ikotun, O.F.; Higbee, E.M.; Ouellette, W.; Doyle, R.P. Pyrophosphate-bridged complexes with picomolar toxicity. *J. Inorg. Biochem.* **2009**, *103*, 1254–1264. [CrossRef]
78. Tabassum, S.; Afzal, M.; Arjmand, F. Synthesis of heterobimetallic complexes: In vitro DNA binding, cleavage and antimicrobial studies. *J. Photochem. Photobiol. B Biol.* **2012**, *114*, 108–118. [CrossRef]
79. Chauhan, M.; Banerjee, K.; Arjmand, F. DNA binding studies of novel copper(ii) complexes containing l-tryptophan as chiral auxiliary: in vitro antitumor activity of cu−sn2 complex in human neuroblastoma cells. *Inorg. Chem.* **2007**, *46*, 3072–3082. [CrossRef]
80. Afzal, M.; Al-Lohedan, H.A.; Usman, M.; Tabassum, S. Carbohydrate-based heteronuclear complexes as topoisomerase Iα inhibitor: Approach toward anticancer chemotherapeutics. *J. Biomol. Struct. Dyn.* **2019**, *37*, 1494–1510. [CrossRef]

81. Tabassum, S.; Ahmad, A.; Khan, R.A.; Hussain, Z.; Srivastav, S.; Srikrishna, S.; Arjmand, F. Chiral heterobimetallic complexes targeting human DNA-topoisomerase Iα. *Dalton Trans.* **2013**, *42*, 16749–16761. [CrossRef]
82. Tabassum, S.; Asim, A.; Khan, R.A.; Arjmand, F.; Rajakumar, D.; Balaji, P.; Akbarsha, A.M. A multifunctional molecular entity CuII–SnIV heterobimetallic complex as a potential cancer chemotherapeutic agent: DNA binding/cleavage, SOD mimetic, topoisomerase Ia inhibitory and in vitrocytotoxic activities. *RSC Adv.* **2015**, *5*, 47439–47450. [CrossRef]
83. Lee, S.K.; Tan, K.W.; Ng, S.W. Zinc, copper and nickel derivatives of 2-[2-bromoethyliminomethyl]phenol as topoisomerase inhibitors exhibiting anti-proliferative and antimetastatic properties. *RSC Adv.* **2014**, *4*, 60280–60292. [CrossRef]
84. Lee, S.K.; Tan, K.W.; Ng, S.W. Topoisomerase I inhibition and DNA cleavage by zinc, copper, and nickel derivatives of 2-[2-bromoethyliminomethyl]-4-[ethoxymethyl]phenol complexes exhibiting anti-proliferation and anti-metastasis activity. *J. Inorg. Biochem.* **2016**, *159*, 14–21. [CrossRef] [PubMed]
85. Vutey, V.; Castelli, S.; D'Annessa, I.; Sâmia, L.B.; Souza-Fagundes, E.M.; Beraldo, H.; Desideri, A. Human topoisomerase IB is a target of a thiosemicarbazone copper(II) complex. *Arch. Biochem. Biophys.* **2016**, *606*, 34–40. [CrossRef] [PubMed]
86. Haleel, A.K.; Mahendiran, D.; Rafi, U.M.; Veena, V.; Shobana, S.; Rahiman, A.K. Tetrazolo[1,5-a]pyrimidine-based metal(II) complexes as therapeutic agents: DNA interaction, targeting topoisomerase I and cyclin-dependent kinase studies. *Inorg. Nano Met. Chem.* **2019**, *48*, 569–582. [CrossRef]
87. Haleel, A.K.; Mahendiran, D.; Veena, V.; Sakthivel, N.; Rahiman, A.K. Antioxidant, DNA interaction, VEGFR2 kinase, topoisomerase I and in vitro cytotoxic activities of heteroleptic copper(II) complexes of tetrazolo[1,5-a]pyrimidines and diimines. *Mater. Sci. Eng. C Mater. Biol. Appl.* **2016**, *68*, 366–382. [CrossRef] [PubMed]
88. Tabassum, S.; Al-Asbahy, W.M.; Afzal, M.; Arjmand, F.; Bagchi, V. Molecular drug design, synthesis and structure elucidation of a new specific target peptide based metallo drug for cancer chemotherapy as topoisomerase I inhibitor. *Dalton Trans.* **2012**, *41*, 4955–4964. [CrossRef] [PubMed]
89. Hasinoff, B.B.; Wu, X.; Yadav, A.A.; Patel, D.; Zhang, H.; Wang, D.S.; Chen, Z.S.; Yalowich, J.C. Cellular mechanisms of the cytotoxicity of the anticancer drug elesclomol and its complex with Cu(II). *Biochem. Pharm.* **2015**, *93*, 266–276. [CrossRef] [PubMed]
90. Foo, J.B.; Ng, L.S.; Lim, J.H.; Tan, P.X.; Lor, Y.Z.; Loo, J.S.; Low, M.L.; Chan, L.C.; Beh, C.Y.; Leong, S.W.; et al. Induction of cell cycle arrest and apoptosis by copper complex Cu(SBCM)2 towards oestrogen-receptor positive MCF-7 breast cancer cells. *RSC Adv.* **2019**, *9*, 18359–18370. [CrossRef]
91. Foo, J.B.; Low, M.L.L.; Lim, J.H.; Lor, Y.Z.; Abidin, R.Z.; Dam, V.E.; Rahman, N.A.; Beh, C.Y.; Chan, L.C.; How, C.W.; et al. Copper complex derived fromS-benzyldithiocarbazate and 3-acetylcoumarin induced apoptosis in breast cancer cell. *Biometals* **2018**, *4*, 505–515. [CrossRef]
92. Yeh, E.T.H.; Ewer, M.; Moslehi, J.; Dlugosz-Danecka, M.; Banchs, J.; Chang, H.M.; Minotti, G. Mechanisms and clinical course of cardiovascular toxicity of cancer treatment I. Oncology. *Semin. Oncol.* **2019**, *46*, 397–402. [CrossRef]
93. Pendleton, M.; Lindsey, R.H., Jr.; Felix, C.A.; Grimwade, D.; Osheroff, N. Topoisomerase II and leukemia. *Ann. N. Y. Acad. Sci.* **2014**, *1310*, 98–110. [CrossRef]
94. West, D.X.; Thientanavanich, I.; Liberta, A.E. Copper(II) complexes of 6-methyl-2-acetylpyridine N(4)-substituted thiosemicarbazones. *Trans. Met. Chem.* **1995**, *20*, 303–308. [CrossRef]
95. Miller, M.C.; Bastow, K.F.; Stineman, C.N.; Vance, J.R.; Song, S.C.; West, D.X.; Hall, I.H. The Cytotoxicity of 2-Formyl and 2-Acetyl-(6-picolyl)-4 N-Substituted Thiosemicarbazones and Their Copper(II) Complexes. *Arch. Pharm. Pharm. Med. Chem.* **1998**, *331*, 121–127. [CrossRef]
96. Khan, T.; Rahmad, R.; Joshi, S.; Khan, A.R. Anticancer potential of metal thiosemicarbazone complexes: A review. *Chem. Sin.* **2015**, *6*, 1–11.
97. Huang, H.; Chen, Q.; Xin, K.; Meng, L.; Lin, L.; Wang, X.; Zhu, C.; Wang, Y.; Chen, Z.; Li, M.; et al. A series of α-heterocyclic carboxaldehyde thiosemicarbazones inhibit topoisomerase IIα catalytic activity. *J. Med. Chem.* **2010**, *53*, 3048–3064. [CrossRef] [PubMed]
98. Conner, J.D.; Medawala, W.; Stephens, M.T.; Morris, W.H.; Deweese, J.E.; Kent, P.L.; Rice, J.J.; Jiang, X.; Lisic, E.C. Cu(II) benzoylpyridine thiosemicarbazone complexes: Inhibition of human topoisomerase IIα and activity against breast cancer cells. *Open J. Inorg. Chem.* **2016**, *6*, 146–154. [CrossRef]

99. Wilson, J.T.; Jiang, X.; McGill, B.C.; Lisic, E.C.; Deweese, J.E. Examination of the impact of copper(ii) α-(n)-heterocyclic thiosemicarbazone complexes on dna topoisomerase IIα. *Chem. Res. Toxicol.* **2016**, *29*, 649–658. [CrossRef]
100. Keck, J.M.; Conner, J.D.; Wilson, J.T.; Jiang, X.; Lisic, E.C.; Deweese, J.E. Clarifying the mechanism of copper(II) α-(N)-heterocyclic thiosemicarbazone complexes on DNA topoisomerase IIα and IIβ. *Chem. Res. Toxicol.* **2019**, *32*, 2135–2143. [CrossRef]
101. Miller, M.C.; Stineman, C.N.; Vance, J.R.; West, D.X. Multiple Mechanisms for Cytotoxicity Induced by Copper(II) Complexes of 2-Acetylpyrazine-N-substituted Thiosemicarbazones. *Appl. Organometal. Chem.* **1999**, *13*, 9–19. [CrossRef]
102. Zeglis, B.M.; Divilov, V.; Lewis, J.S. Role of metalation in the topoisomerase IIα inhibition and antiproliferation activity of a series of α-heterocyclic-N4-substituted thiosemicarbazones and their Cu(II) complexes. *J. Med. Chem.* **2011**, *54*, 2391–2398. [CrossRef]
103. Lisic, E.C.; Rand, V.G.; Ngo, L.; Kent, P.; Rice, J.; Gerlach, D.; Papish, E.T.; Jiang, X. Cu(II) propionyl-thiazole thiosemicarbazone complexes: Crystal structure, inhibition of human topoisomerase IIα, and activity against breast cancer cells. *Open J. Med. Chem.* **2018**, *8*, 30–46. [CrossRef]
104. Morris, W.H.; Ngo, L.; Wilson, J.T.; Medawala, W.; Brown, A.R.; Conner, J.D.; Fabunmi, F.; Cashman, D.J.; Lisic, E.; Yu, T.; et al. Structural and metal ion effects on human topoisomerase IIα inhibition by α-(N)-heterocyclic thiosemicarbazones. *Chem. Res. Toxicol.* **2019**, *32*, 90–99. [CrossRef] [PubMed]
105. Sandhaus, S.; Taylor, R.; Edwards, T.; Huddleston, A.; Wooten, Y.; Venkatraman, R.; Weber, R.T.; González-Sarrías, A.; Martin, P.M.; Cagle, P.; et al. A novel copper(II) complex identified as a potent drug against colorectal and breast cancer cells and as a poison inhibitor for human topoisomerase IIα. *Inorg. Chem. Commun.* **2016**, *64*, 45–49. [CrossRef] [PubMed]
106. Bacher, F.; Enyedy, É.; Nagy, N.V.; Rockenbauer, A.; Bognár, G.M.; Trondl, R.; Novak, M.S.; Klapproth, E.; Kiss, T.; Arion, V.B. Copper(II) complexes with highly water-soluble L- and D-proline-thiosemicarbazone conjugates as potential inhibitors of Topoisomerase IIα. *Inorg. Chem.* **2013**, *52*, 8895–8908. [CrossRef] [PubMed]
107. Bisceglie, F.; Musiari, A.; Pinelli, S.; Alinovi, R.; Menozzi, I.; Polverini, E.; Tarasconi, P.; Tavone, M.; Pelosi, G. Quinoline-2-carboxaldehyde thiosemicarbazones and their Cu(II) and Ni(II) complexes as topoisomerase IIa inhibitors. *J. Inorg. Biochem.* **2015**, *152*, 10–19. [CrossRef]
108. Chen, J.; Huang, Y.W.; Liu, G.; Afrasiabi, Z.; Sinn, E.; Padhye, S.; Ma, Y. The cytotoxicity and mechanisms of 1,2-naphthoquinone thiosemicarbazone and its metal derivatives against MCF-7 human breast cancer cells. *Toxicol. Appl. Pharm.* **2004**, *197*, 40–48. [CrossRef]
109. Palanimuthu, D.; Shinde, S.V.; Somasundaram, K.; Samuelson, A.G. In vitro and in vivo anticancer activity of copper bis(thiosemicarbazone) complexes. *J. Med. Chem.* **2013**, *56*, 722–734. [CrossRef]
110. Nair, R.S.; Potti, M.E.; Thankappan, R.; Chandrika, S.K.; Kurup, M.R.; Srinivas, P. Molecular trail for the anticancer behavior of a novel copper carbohydrazone complex in BRCA1 mutated breast cancer. *Mol. Carcinog.* **2017**, *56*, 1501–1514. [CrossRef]
111. Arjmand, F.; Jamsheera, A.; Afzal, M.; Tabassum, S. Enantiomeric specificity of biologically significant Cu(II) and Zn(II) chromone complexes towards DNA. *Chirality* **2012**, *24*, 977–986. [CrossRef]
112. Duff, B.; Thangella, V.R.; Creaven, B.S.; Walsh, M.; Egan, D.A. Anti-cancer activity and mutagenic potential of novel copper(II) quinolinone Schiff base complexes in hepatocarcinoma cells. *Eur. J. Pharm.* **2012**, *689*, 45–55. [CrossRef]
113. Khan, R.A.; Usman, M.; Dhivya, R.; Balaji, P.; Alsalme, A.; AlLohedan, H.; Arjmand, F.; AlFarhan, K.; Akbarsha, M.A.; Marchetti, F.; et al. Heteroleptic copper(I) complexes of "scorpionate" bis-pyrazolyl carboxylate ligand with auxiliary phosphine as potential anticancer agents: An insight into cytotoxic mode. *Sci. Rep.* **2017**, *7*, 45229–45246. [CrossRef]
114. Ross, W.; Rowe, T.; Glisson, B.; Yalowich, J.; Liu, L. Role of topoisomerase II in mediating epipodophyllotoxin-induced DNA cleavage. *Cancer Res.* **1984**, *44*, 5857–5860. [PubMed]
115. Furuta, T.; Takemura, H.; Liao, Z.Y.; Aune, G.J.; Redon, C.; Sedelnikova, O.A.; Pilch, D.R.; Rogakou, E.P.; Celeste, A.; Chen, H.T.; et al. Phosphorylation of histone H2AX and activation of Mre11, Rad50, and Nbs1 in response to replication-dependent DNA double-strand breaks induced by mammalian DNA topoisomerase I cleavage complexes. *J. Biol. Chem.* **2003**, *278*, 20303–20312. [CrossRef] [PubMed]

116. Bonner, W.M.; Redon, C.E.; Dickey, J.S.; Nakamura, A.J.; Sedelnikova, O.A.; Solier, S.; Pommier, Y. Gamma H2AX and cancer. *Nat. Rev. Cancer* **2008**, *8*, 957–967. [CrossRef] [PubMed]
117. Sordet, O.; Redon, E.C.; Guirouilh-Barbat, J.; Smith, S.; Solier, S.; Douarre, C.; Conti, C.; Nakamura, J.A.; Das, B.B.; Nicolas, E.; et al. Ataxia telangiectasia mutated activation by transcription- and topoisomerase I-induced DNA double-strand breaks. *EMBO Rep.* **2009**, *10*, 887–893. [CrossRef]
118. Pilié, P.G.; Tang, C.; Mills, G.B.; Yap, T.A. State-of-the-art strategies for targeting the DNA damage response in cancer. *Nat. Rev. Clin. Oncol.* **2019**, *16*, 81–104. [CrossRef] [PubMed]
119. Hakem, R. DNA-damage repair; the good, the bad and the ugly. *EMBO J.* **2008**, *27*, 589–605. [CrossRef] [PubMed]
120. Donzelli, M.; Draetta, F.G. Regulating mammalian checkpoints through Cdc25 inactivation. *EMBO Rep.* **2003**, *4*, 671–677. [CrossRef]
121. Banin, S.; Moyal, L.; Shieh, S.; Taya, Y.; Anderson, C.W.; Chessa, L.; Smorodinsky, N.I.; Prives, C.; Reiss, Y.; Shiloh, Y.; et al. Enhanced phosphorylation of p53 by ATM in response to DNA damage. *Science* **1998**, *28*, 1674–1677. [CrossRef]
122. Canman, C.E.; Lim, D.S.; Cimprich, K.A.; Taya, Y.; Tamai, K.; Sakaguchi, K.; Appella, E.; Kastan, M.B.; Siliciano, J.D. Activation of the ATM kinase by ionizing radiation and phosphorylation of p53. *Science* **1998**, *281*, 1677–1679. [CrossRef]
123. Hirao, A.; Kong, Y.Y.; Matsuoka, S.; Wakeham, A.; Ruland, J.; Yoshida, H.; Liu, D.; Elledge, S.J.; Mak, T.W. DNA damage-induced activation of p53 by the checkpoint kinase Chk2. *Science* **2000**, *287*, 1824–1827. [CrossRef]
124. Shieh, S.Y.; Ahn, J.; Tamai, K.; Taya, Y.; Prives, C. The human homologs of checkpoint kinases Chk1 and Cds1 (Chk2) phosphorylate p53 at multiple DNA damage-inducible sites. *Genes Dev.* **2000**, *14*, 289–300. [PubMed]
125. Xiong, Y.; Hannon, G.J.; Zhang, H.; Casso, D.; Kobayashi, R.; Beach, D. p21 is a universal inhibitor of cyclin kinases. *Nature* **1993**, *366*, 701–704. [CrossRef] [PubMed]
126. Hengstschläger, M.; Braun, K.; Soucek, T.; Miloloza, A.; Hengstschläger-Ottnad, E. Cyclin-dependent kinases at the G1-S transition of the mammalian cell cycle. *Mutat. Res.* **1999**, *436*, 1–9. [CrossRef]
127. Xiao, D.; Herman-Antosiewicz, A.; Antosiewicz, J.; Xiao, H.; Brisson, M.; Lazo, J.S.; Singh, S.V. Diallyl trisulfide-induced G(2)-M phase cell cycle arrest in human prostate cancer cells is caused by reactive oxygen species-dependent destruction and hyperphosphorylation of Cdc 25 C. *Oncogene* **2005**, *24*, 6256–6268. [CrossRef] [PubMed]
128. Okoh, V.O.; Garba, N.A.; Penney, R.B.; Das, J.; Deoraj, A.; Singh, K.P.; Sarkar, S.; Felty, Q.; Yoo, C.; Jackson, R.M.; et al. Redox signalling to nuclear regulatory proteins by reactive oxygen species contributes to oestrogen-induced growth of breast cancer cells. *Br. J. Cancer* **2015**, *112*, 1687–1702. [CrossRef]
129. Macip, S.; Kosoy, A.; Lee, S.W.; O'Connell, M.J.; Aaronson, S.A. Oxidative stress induces a prolonged but reversible arrest in p53-null cancer cells, involving a Chk1-dependent G2 checkpoint. *Oncogene* **2006**, *25*, 6037–6047. [CrossRef]
130. He, L.; Nan, M.H.; Oh, H.C.; Kim, Y.H.; Jang, J.H.; Erikson, R.L.; Ahn, J.S.; Kim, B.Y. Asperlin induces G_2/M arrest through ROS generation and ATM pathway in human cervical carcinoma cells. *Biochem. Biophys. Res. Commun.* **2011**, *409*, 489–493. [CrossRef]
131. Tubbs, A.; Nussenzweig, A. Endogenous DNA damage as a source of genomic instability in cancer. *Cell* **2017**, *168*, 644–656. [CrossRef]
132. Deiss, K.; Lockwood, N.; Howell, M.; Segeren, H.A.; Saunders, R.E.; Chakravarty, P.; Soliman, T.N.; Martini, S.; Rocha, N.; Semple, R.; et al. A genome-wide RNAi screen identifies the SMC5/6 complex as a non-redundant regulator of a Topo2a-dependent G2 arrest. *Nucleic Acids Res.* **2019**, *47*, 2906–2921. [CrossRef]
133. Bower, J.J.; Zhou, Y.; Zhou, T.; Simpson, D.A.; Arlander, S.J.; Paules, R.S.; Cordeiro-Stone, M.; Kaufmann, W.K. Revised genetic requirements for the decatenation G2 checkpoint: The role of ATM. *Cell Cycle* **2010**, *9*, 1617–1628. [CrossRef]
134. Bower, J.J.; Karaca, G.F.; Zhou, Y.; Simpson, D.A.; Cordeiro-Stone, M.; Kaufmann, W.K. Topoisomerase IIalpha maintains genomic stability through decatenation G(2) checkpoint signaling. *Oncogene* **2010**, *29*, 4787–4799. [CrossRef] [PubMed]
135. Yoshida, C.; Hishiyama, K.; Miyazaki, K.; Watanabe, M.; Kanbe, M.; Yamada, Y.; Matsuzaki, K.; Miyashita, K.; Kitanaka, S.; Miyata, S. Analysis of inhibition of topoisomerase IIalpha and cancer cell proliferation by ingenolEZ. *Cancer Sci.* **2010**, *101*, 374–378. [CrossRef] [PubMed]

136. Dykhuizen, E.C.; Hargreaves, D.C.; Miller, E.L.; Cui, K.; Korshunov, A.; Kool, M.; Pfister, S.; Cho, Y.J.; Zhao, K.; Crabtree, G.R. BAF complexes facilitate decatenation of DNA by topoisomerase IIα. *Nature* **2013**, *497*, 624–627. [CrossRef] [PubMed]
137. D Arcy, N.; Gabrielli, B. Topoisomerase II inhibitors and poisons, and the influence of cell cycle checkpoints. *Curr. Med. Chem.* **2017**, *24*, 1504–1519. [CrossRef] [PubMed]
138. Hjaltelin, J.X.; Izarzugaza, J.; Jensen, L.J.; Russo, F.; Westergaard, D.; Brunak, S. Identification of hyper-rewired genomic stress non-oncogene addiction genes across 15 cancer types. *NPJ Syst. Biol. Appl.* **2019**, *5*, 27–37. [CrossRef]
139. Al-Matouq, J.; Holmes, T.R.; Hansen, L.A. CDC25B and CDC25C overexpression in nonmelanoma skin cancer suppresses cell death. *Mol. Carcinog.* **2019**, *58*, 1691–1700. [CrossRef]
140. Butz, H.; Németh, K.; Czenke, D.; Likó, I.; Czirják, S.; Zivkovic, V.; Baghy, K.; Korbonits, M.; Kovalszky, I.; Igaz, P.; et al. Systematic investigation of expression of G2/M transition genes reveals CDC25 alteration in nonfunctioning pituitary adenomas. *Pathol. Oncol. Res.* **2017**, *23*, 633–641. [CrossRef]
141. Mantovani, F.; Collavin, L.; Del Sal, G. Mutant p53 as a guardian of the cancer cell. *Cell Death Differ.* **2019**, *26*, 199–212. [CrossRef]
142. Hayman, L.; Chaudhry, W.R.; Revin, V.V.; Zhelev, N.; Bourdon, J.C. What is the potential of p53 isoforms as a predictive biomarker in the treatment of cancer? *Expert Rev. Mol. Diagn.* **2019**, *19*, 149–159. [CrossRef]
143. Lin, Z.P.; Zhu, Y.L.; Ratner, E.S. Targeting cyclin-dependent kinases for treatment of gynecologic cancers. *Front. Oncol.* **2018**, *8*, 303–314. [CrossRef]
144. Roskoski, R., Jr. Cyclin-dependent protein serine/threonine kinase inhibitors as anticancer drugs. *Pharm. Res.* **2019**, *139*, 471–488. [CrossRef] [PubMed]
145. Kachalaki, S.; Ebrahimi, M.; Mohamed Khosroshahi, L.; Mohammadinejad, S.; Baradaran, B. Cancer chemoresistance; biochemical and molecular aspects: A brief overview. *Eur. J. Pharm. Sci.* **2016**, *89*, 20–30. [CrossRef] [PubMed]
146. Gongora, C.; Vezzio-Vie, N.; Tuduri, S.; Denis, V.; Causse, A.; Auzanneau, C.; Collod-Beroud, G.; Coquelle, A.; Pasero, P.; Pourquier, P.; et al. New Topoisomerase I mutations are associated with resistance to camptothecin. *Mol. Cancer* **2011**, *10*, 64–77. [CrossRef] [PubMed]
147. Tsurutani, J.; Nitta, T.; Hirashima, T.; Komiya, T.; Uejima, H.; Tada, H.; Syunichi, N.; Tohda, A.; Fukuoka, M.; Nakagawa, K. Point mutations in the topoisomerase I gene in patients with non-small cell lung cancer treated with irinotecan. *Lung Cancer* **2002**, *35*, 299–304. [CrossRef]
148. Bassermann, F.; Eichner, R.; Pagano, M. The ubiquitin proteasome system–implications for cell cycle control and the targeted treatment of cancer. *Biochim. Biophys. Acta* **2014**, *1843*, 150–162. [CrossRef] [PubMed]
149. Lee, K.C.; Swan, R.L.; Sondka, Z.; Padget, K.; Cowell, I.G.; Austin, C.A. Effect of TDP2 on the Level of TOP2-DNA Complexes and SUMOylated TOP2-DNA Complexes. *Int. J. Mol. Sci.* **2018**, *19*, 2056. [CrossRef]
150. Gardner, L.; Malik, R.; Shimizu, Y.; Mullins, N.; ElShamy, W.M. Geminin overexpression prevents the completion of topoisomerase IIα chromosome decatenation, leading to aneuploidy in human mammary epithelial cells. *Breast Cancer Res.* **2011**, *13*, R53. [CrossRef]
151. Rozav, A.G.; Chikamori, K.; Kozuki, T.; Grabowski, D.R.; Bukowski, R.M.; Willard, B.; Kinter, M.; Andersen, A.H.; Ganapathi, R.; Ganapathi, M.K. Casein kinase I delta phosphorylates topoisomerase II at serine-1106 and modulates DNA cleavage activity. *Nucleic Acids Res.* **2009**, *37*, 382–392.
152. Kurz, E.U.; Leader, K.B.; Kroll, D.J.; Clark, M.; Gieseler, F. Modulation of human DNA topoisomerase II function by interaction with 14–3-3". *J. Biol. Chem.* **2000**, *275*, 13948–13954. [CrossRef]
153. Visconti, R.; Della Monica, R.; Grieco, D. Cell cycle checkpoint in cancer: A therapeutically targetable double-edged sword. *J. Exp. Clin. Cancer Res.* **2016**, *35*, 153–161. [CrossRef]
154. Allday, M.J.; Inman, G.J.; Crawford, D.H.; Farrell, P.J. DNA damage in human B cells can induce apoptosis, proceeding from G1/S when p53 is transactivation competent and G2/M when it is transactivation defective. *EMBO J.* **1995**, *14*, 4994–5005. [CrossRef] [PubMed]
155. Vitale, I.; Galluzzi, L.; Castedo, M.; Kroemer, G. Mitotic catastrophe: A mechanism for avoiding genomic instability. *Nat. Rev. Mol. Cell Biol.* **2011**, *12*, 385–392. [CrossRef] [PubMed]
156. Yazinski, S.A.; Comaills, V.; Buisson, R.; Genois, M.M.; Nguyen, H.D.; Ho, C.K.; Todorova Kwan, T.; Morris, R.; Lauffer, S.; Nussenzweig, A.; et al. ATR inhibition disrupts rewired homologous recombination and fork protection pathways in PARP inhibitor-resistant BRCA-deficient cancer cells. *Genes Dev.* **2017**, *31*, 318–332. [CrossRef] [PubMed]

157. Su, Z.; Yang, Z.; Xu, Y.; Chen, Y.; Yu, Q. Apoptosis, autophagy, necroptosis, and cancer metastasis. *Mol. Cancer* **2015**, *14*, 48–62. [CrossRef]
158. Singh, R.; Letai, A.; Sarosiek, K. Regulation of apoptosis in health and disease: The balancing act of BCL-2 family proteins. *Nat. Rev. Mol. Cell Biol.* **2019**, *20*, 175–193. [CrossRef]
159. Pfeffer, C.M.; Singh, A.T.K. Apoptosis: A target for anticancer therapy. *Int. J. Mol. Sci.* **2018**, *19*, 448. [CrossRef]
160. Lee, S.Y.; Ju, M.K.; Jeon, H.M.; Jeong, E.K.; Lee, Y.J.; Kim, C.H.; Park, H.G.; Han, S.I.; Kang, H.S. Regulation of tumor progression by programmed necrosis. *Oxid. Med. Cell. Longev.* **2018**, *2018*, 3537471–3537499. [CrossRef]
161. Eguchi, Y.; Shimizu, S.; Tsujimoto, Y. Intracellular ATP levels determine cell death fate by apoptosis or necrosis. *Cancer Res.* **1997**, *57*, 1835–1840.
162. Vakkila, J.; Lotze, M.T. Inflammation and necrosis promote tumour growth. *Nat. Rev. Immunol.* **2004**, *4*, 641–648. [CrossRef]
163. Kang, R.; Chen, R.; Zhang, Q.; Hou, W.; Wu, S.; Cao, L.; Huang, J.; Yu, Y.; Fan, X.G.; Yan, Z.; et al. MGB1 in health and disease. *Mol. Asp. Med.* **2014**, *40*, 1–116. [CrossRef]
164. Gomes, L.R.; Menck, C.F.M.; Leandro, G.S. Autophagy roles in the modulation of DNA repair pathways. *Int. J. Mol. Sci.* **2017**, *18*, 2351. [CrossRef] [PubMed]
165. Yang, Y.; Li, C.; Fu, Y.; Liu, Y.; Zhang, Y.; Zhang, Y.; Zhou, P.; Yuan, Y.; Zhou, S.; Li, S.; et al. Redox cycling of a copper complex with benzaldehyde nitrogen mustard-2-pyridine carboxylic acid hydrazone contributes to its enhanced antitumor activity, but no change in the mechanism of action occurs after chelation. *Oncol. Rep.* **2016**, *3*, 1636–1644. [CrossRef] [PubMed]
166. Chen, C.; Lu, L.; Yan, S.; Yi, H.; Yao, H.; Wu, D.; He, G.; Tao, X.; Deng, X. Autophagy and doxorubicin resistance in cancer. *Anticancer Drugs* **2018**, *29*, 1–9. [CrossRef] [PubMed]
167. Delgado, J.L.; Hsieh, C.M.; Chan, N.L.; Hiasa, H. Topoisomerases as anticancer targets. *Biochem. J.* **2018**, *475*, 373–398. [CrossRef]
168. Dehshahri, A.; Ashrafizadeh, M.; Ghasemipour Afshar, E.; Pardakhty, A.; Mandegary, A.; Mohammadinejad, R.; Sethi, G. Topoisomerase inhibitors: Pharmacology and emerging nanoscale delivery systems. *Pharm. Res.* **2020**, *151*, 104551–104563. [CrossRef]
169. Fujita, K.; Kubota, Y.; Ishida, H.; Sasaki, Y. Irinotecan, a key chemotherapeutic drug for metastatic colorectal cancer. *World J. Gastroenterol.* **2015**, *21*, 12234–12248. [CrossRef]
170. Woo, W.; Carey, E.T.; Choi, M. Spotlight on liposomal irinotecan for metastatic pancreatic cancer: Patient selection and perspectives. *Onco Targets Ther.* **2019**, *12*, 1455–1463. [CrossRef]
171. Kondo, R.; Watanabe, S.; Shoji, S.; Ichikawa, K.; Abe, T.; Baba, J.; Tanaka, J.; Tsukada, H.; Terada, M.; Sato, K.; et al. A Phase II Study of Irinotecan for Patients with Previously Treated Small-Cell Lung Cancer. *Oncology* **2018**, *94*, 223–232. [CrossRef]
172. Xu, F.; Ren, X.; Chen, Y.; Li, Q.; Li, R.; Chen, Y.; Xia, S. Irinotecan-platinum combination therapy for previously untreated extensive-stage small cell lung cancer patients: A meta-analysis. *BMC Cancer* **2018**, *18*, 808–820. [CrossRef]
173. Lihua, P.; Chen, X.Y.; Wu, T.X. Topotecan for ovarian cancer. *Cochrane Databse Syst. Rev.* **2008**, *2008*, CD005589.
174. Pignata, S.; Pisano, C.; Di Napoli, M.; Cecere, S.C.; Tambaro, R.; Attademo, L. Treatment of recurrent epithelial ovarian cancer. *Cancer* **2019**, *24*, 4609–4615. [CrossRef] [PubMed]
175. Rosen, V.M.; Guerra, I.; McCormack, M.; Nogueira-Rodrigues, A.; Sasse, A.; Munk, V.C.; Shang, A. Systematic review and network meta-analysis of bevacizumab plus first-line topotecan-paclitaxel or cisplatin-paclitaxel versus non-bevacizumab-containing therapies in persistent, recurrent, or metastatic cervical cancer. *Int. J. Gyn. Cancer* **2017**, *27*, 1237–1246. [CrossRef] [PubMed]
176. Qin, A.; Kalemkerian, G.P. Treatment options for relapsed small-cell lung cancer: What progress have we made? *J. Oncol. Pract.* **2018**, *14*, 369–370. [CrossRef] [PubMed]
177. Armenian, S.; Bhatia, S. Predicting and preventing anthracycline-related cardiotoxicity. *Am. Soc. Clin. Oncol. Educ. Book* **2018**, *38*, 3–12. [CrossRef] [PubMed]
178. Vu, K.; Ai, W. Update on the treatment of anaplastic large cell lymphoma. *Curr. Hematol. Malig. Rep.* **2018**, *13*, 135–141. [CrossRef] [PubMed]
179. Liu, W.; Jiang, Q.; Zhou, Y. Advances of systemic treatment for adult soft-tissue sarcoma. *Chin. Clin. Oncol.* **2018**, *7*, 42–55. [CrossRef]

180. D'Ambrosio, L.; Touati, N.; Blay, J.Y.; Grignani, G.; Flippot, R.; Czarnecka, A.M.; Piperno-Neumann, S.; Martin-Broto, J.; Sanfilippo, R.; Katz, D.; et al. European Organization for Research and Treatment of Cancer Soft Tissue and Bone Sarcoma Group. Doxorubicin plus dacarbazine, doxorubicin plus ifosfamide, or doxorubicin alone as a first-line treatment for advanced leiomyosarcoma: A propensity score matching analysis from the European Organization for Research and Treatment of Cancer Soft Tissue and Bone Sarcoma Group. *Cancer* **2020**, *126*, 2637–2647. [PubMed]
181. Carvalho, C.; Santos, R.X.; Cardoso, S.; Correia, S.; Oliveira, P.J.; Santos, M.S.; Moreira, P.I. Doxorubicin: The good, the bad and the ugly effect. *Curr. Med. Chem.* **2009**, *16*, 3267–3285. [CrossRef]
182. Banke, A.; Fosbøl, E.L.; Møller, J.E.; Gislason, G.H.; Andersen, M.; Bernsdorf, M.; Jensen, M.B.; Schou, M.; Ejlertsen, B. Long-term effect of epirubicin on incidence of heart failure in women with breast cancer: Insight from a randomized clinical trial. *Eur. J. Heart Fail.* **2018**, *20*, 1447–1453. [CrossRef]
183. Werntz, R.P.; Adamic, B.; Steinberg, G.D. Emerging therapies in the management of high-risk non-muscle invasive bladder cancer (HRNMIBC). *World J. Urol.* **2019**, *37*, 2031–2040. [CrossRef]
184. Ravandi, F.; Assi, R.; Daver, N.; Benton, C.B.; Kadia, T.; Thompson, P.A.; Borthakur, G.; Alvarado, Y.; Jabbour, E.J.; Konopleva, M.; et al. Idarubicin, cytarabine, and nivolumab in patients with newly diagnosed acute myeloid leukaemia or high-risk myelodysplastic syndrome: A single-arm, phase 2 study. *Lancet Haematol.* **2019**, *6*, e480–e488. [CrossRef]
185. Evison, B.J.; Sleebs, B.E.; Watson, K.G.; Phillips, D.R.; Cutts, S.M. Mitoxantrone, More than Just another topoisomerase II poison. *Med. Res. Rev.* **2016**, *36*, 248–299. [CrossRef] [PubMed]
186. Barrenetxea Lekue, C.; Grasso Cicala, S.; Leppä, S.; Stauffer Larsen, T.; Herráez Rodríguez, S.; Alonso Caballero, C.; Jørgensen, J.M.; Toldbod, H.; Leal Martínez, I.; D'Amore, F. Pixantrone beyond monotherapy: A review. *Ann. Hematol.* **2019**, *98*, 2025–2033. [CrossRef] [PubMed]
187. Minotti, G.; Han, H.; Cattan, V.; Egorov, A.; Bertoni, F. Pixantrone: Novel mode of action and clinical readouts. *Expert Rev. Hematol.* **2018**, *11*, 587–596. [CrossRef] [PubMed]
188. Alsdorf, W.; Seidel, C.; Bokemeyer, C.; Oing, C. Current pharmacotherapy for testicular germ cell cancer. *Expert Opin. Pharm.* **2019**, *20*, 837–850. [CrossRef] [PubMed]
189. Bernhardt, E.B.; Jalal, S.I. Small Cell Lung Cancer. *Cancer Treat. Res.* **2016**, *170*, 301–322. [PubMed]
190. Reveiz, L.; Rueda, J.R.; Cardona, A.F. Chemotherapy for brain metastases from small cell lung cancer. *Cochrane Databse Syst. Rev.* **2012**, *6*, CD007464. [CrossRef]
191. Li, J.; Chen, W.; Zhang, P.; Li, N. Topoisomerase II trapping agent teniposide induces apoptosis and G2/M or S phase arrest of oral squamous cell carcinoma. *World J. Surg. Oncol.* **2006**, *4*, 41–47. [CrossRef]
192. Joyce, M.J.; Pollock, B.H.; Devidas, M.; Buchanan, G.R.; Camitta, B. Chemotherapy for initial induction failures in childhood acute lymphoblastic leukemia: A Children's Oncology Group Study (POG 8764). *J. Pediatr. Hematol. Oncol.* **2013**, *35*, 32–35. [CrossRef]
193. Pommier, Y.; Cushman, M.; Doroshow, J.H. Novel clinical indenoisoquinoline topoisomerase I inhibitors: A twist around the camptothecins. *Oncotarget* **2018**, *9*, 37286–37288. [CrossRef]
194. Bailly, C. Contemporary challenges in the design of topoisomerase II inhibitors for cancer chemotherapy. *Chem. Rev.* **2012**, *112*, 3611–3640. [CrossRef] [PubMed]
195. Lovrics, A.; Pape, V.F.S.; Szisz, D.; Kalászi, A.; Heffeter, P.; Magyar, C.; Szakács, G. Identifying new topoisomerase II poison scaffolds by combining publicly available toxicity data and 2D/3D-based virtual screening. *J. Cheminform.* **2019**, *11*, 67–81. [CrossRef]
196. Ortega, J.A.; Riccardi, L.; Minniti, E.; Borgogno, M.; Arencibia, J.M.; Greco, M.L.; Minarini, A.; Sissi, C.; De Vivo, M. Pharmacophore hybridization to discover novel topoisomerase II poisons with promising antiproliferative activity. *J. Med. Chem.* **2018**, *61*, 1375–1379. [CrossRef] [PubMed]
197. Beck, D.E.; Abdelmalak, M.; Lv, W.; Reddy, P.V.; Tender, G.S.; O'Neill, E.; Agama, K.; Marchand, C.; Pommier, Y.; Cushman, M. Discovery of potent indenoisoquinoline topoisomerase I poisons lacking the 3-nitro toxicophore. *J. Med. Chem.* **2015**, *58*, 3997–4015. [CrossRef] [PubMed]
198. Nitiss, J.L. Targeting DNA topoisomerase II in cancer chemotherapy. *Nat. Rev. Cancer* **2009**, *9*, 338–350. [CrossRef]
199. Liu, T.; Karlsen, M.; Karlberg, A.M.; Redalen, K.R. Hypoxia imaging and theranostic potential of [64Cu][Cu(ATSM)] and ionic Cu(II) salts: A review of current evidence and discussion of the retention mechanisms. *Ejnmmi Res.* **2020**, *10*, 33–47. [CrossRef]

200. Kantarjian, H. Acute myeloid leukemia-Major progress over four decades and glimpses into the future. *Am. J. Hematol.* **2016**, *91*, 131–145.
201. Bornhäuser, M. Vosaroxin in acute myeloid leukaemia. *Lancet Oncol.* **2015**, *16*, 1000–1001. [CrossRef]
202. Skok, Ž.; Zidar, N.; Kikelj, D.; Ilaš, J. Dual inhibitors of human DNA topoisomerase II and other cancer-related targets. *J. Med. Chem.* **2020**, *63*, 884–904. [CrossRef]
203. Kim, S.O.; Sakchaisri, K.; Thimmegowda, N.R.; Soung, N.K.; Jang, J.H.; Kim, Y.S.; Lee, K.S.; Kwon, Y.T.; Asami, Y.; Ahn, J.S.; et al. STK295900, a dual inhibitor of topoisomerase 1 and 2, induces G(2) arrest in the absence of DNA damage. *PLoS ONE* **2013**, *8*, e53908. [CrossRef]
204. Yi, J.M.; Zhang, X.F.; Huan, X.J.; Song, S.S.; Wang, W.; Tian, Q.T.; Sun, Y.M.; Chen, Y.; Ding, J.; Wang, Y.Q.; et al. Dual targeting of microtubule and topoisomerase II by α-carboline derivative YCH337 for tumor proliferation and growth inhibition. *Oncotarget* **2015**, *6*, 8960–8973. [CrossRef]
205. Seo, Y.H. Dual inhibitors against topoisomerases and histone deacetylases. *J. Cancer Prev.* **2015**, *20*, 85–91. [CrossRef] [PubMed]
206. Ferreira, R.; Schneekloth, J.S., Jr.; Panov, K.I.; Hannan, K.M.; Hannan, R.D. Targeting the RNA polymerase I transcription for cancer therapy comes of age. *Cells* **2020**, *9*, 266. [CrossRef] [PubMed]
207. Li, X.; Chen, Y.; Zhao, J.; Shi, J.; Wang, M.; Qiu, S.; Hu, Y.; Xu, Y.; Cui, Y.; Liu, C.; et al. The specific inhibition of SOD1 selectively promotes apoptosis of cancer cells via regulation of the ROS signaling network. *Oxid. Med. Cell Longev.* **2019**, *2019*, 9706792–9706814. [CrossRef] [PubMed]
208. Huang, P.; Feng, L.; Oldham, E.A.; Keating, M.J.; Plunkett, W. Superoxide dismutase as a target for the selective killing of cancer cells. *Nature* **2000**, *407*, 390–395. [CrossRef]
209. Ceci, C.; Atzori, M.G.; Lacal, P.M.; Graziani, G. Role of VEGFs/VEGFR-1 signaling and its inhibition in modulating tumor invasion: Experimental evidence in different metastatic cancer models. *Int. J. Mol. Sci.* **2020**, *21*, 1388.
210. Roskoski, R., Jr. Properties of FDA-approved small molecule protein kinase inhibitors: A 2020 update. *Pharm. Res.* **2020**, *152*, 104609–104628. [CrossRef]
211. Yang, S.W.; Burgin, A.B., Jr.; Huizenga, B.N.; Robertson, C.A.; Yao, K.C.; Nash, H.A. A eukaryotic enzyme that can disjoin dead-end covalent complexes between DNA and type I topoisomerases. *Proc. Natl. Acad. Sci. USA* **1996**, *93*, 11534–11539. [CrossRef]
212. Cortes Ledesma, F.; El Khamisy, S.F.; Zuma, M.C.; Osborn, K.; Caldecott, K.W. A human 5′-tyrosyl DNA phosphodiesterase that repairs topoisomerase-mediated DNA damage. *Nature* **2009**, *461*, 674–678. [CrossRef]
213. Zakharenko, A.; Dyrkheeva, N.; Lavrik, O. Dual DNA topoisomerase 1 and tyrosyl-DNA phosphodiesterase 1 inhibition for improved anticancer activity. *Med. Res. Rev.* **2019**, *39*, 1427–1441. [CrossRef]
214. Wu, X.; Xue, X.; Wang, L.; Wang, W.; Han, J.; Sun, X.; Zhang, H.; Liu, Y.; Che, X.; Yang, J.; et al. Suppressing autophagy enhances disulfiram/copper-induced apoptosis in non-small cell lung cancer. *Eur. J. Pharm.* **2018**, *827*, 1–12. [CrossRef]
215. Marinello, J.; Delcuratolo, M.; Capranico, G. Anthracyclines as topoisomerase II poisons: From early studies to new perspectives. *Int. J. Mol. Sci.* **2018**, *19*, 3480. [CrossRef] [PubMed]
216. Brown, J.S.; Sundar, R.; Lopez, J. Combining DNA damaging therapeutics with immunotherapy: More haste, less speed. *Br. J. Cancer* **2018**, *118*, 312–324. [CrossRef] [PubMed]
217. Heinhuis, K.M.; Ros, W.; Kok, M.; Steeghs, N.; Beijnen, J.H.; Schellens, J.H.M. Enhancing antitumor response by combining immune checkpoint inhibitors with chemotherapy in solid tumors. *Ann. Oncol.* **2019**, *30*, 219–235. [CrossRef] [PubMed]
218. Kim, N.; Jinks-Robertson, S. The Top1 paradox: Friend and foe of the eukaryotic genome. *DNA Repair* **2017**, *56*, 33–41. [CrossRef] [PubMed]
219. Strickland, K.C.; Howitt, B.E.; Shukla, S.A.; Rodig, S.; Ritterhouse, L.; Liu, J.F.; Garber, J.E.; Chowdhury, D.; Catherine, J.; Andrea, A.D.D.; et al. Association and prognostic significance of BRCA1/2-mutation status with neoantigen load, number of tumorinfiltrating lymphocytes and expression of PD-1/PD-L1 in high grade serous ovarian cancer. *Oncotarget* **2016**, *7*, 1–12. [CrossRef]
220. Li, A.; Yi, M.; Qin, S.; Song, Y.; Chu, Q.; Wu, K. Activating cGAS-STING pathway for the optimal effect of cancer immunotherapy. *J. Hematol. Oncol.* **2019**, *12*, 35–47. [CrossRef]
221. Zhao, B.; Liu, P.; Fukumoto, T.; Fatkhutdinov, N.; Wu, S.; Lin, J.; Aird, K.M.; Tang, H.Y.; Liu, Q.; Speicher, D.W.; et al. Topoisomerase 1 cleavage complex enables pattern recognition and inflammation during senescence. *Nat. Commun.* **2020**, *11*, 908–919. [CrossRef]

222. Wang, Z.; Chen, J.; Hu, J.; Zhang, H.; Xu, F.; He, W.; Wang, X.; Li, M.; Lu, W.; Zeng, G.; et al. cGAS/STING axis mediates a topoisomerase II inhibitor-induced tumor immunogenicity. *J. Clin. Investig.* **2019**, *130*, 4850–4862. [CrossRef]
223. Wilkinson, R.D.A.; McCabe, N.; Parkes, E.E.; Barros, E.M.; Johnston, D.I.; Ali, R.M.M.; Lappin, K.; Greenberg, R.A.; Harkin, D.P.; McIntosh, S.A.; et al. Topoisomerase II inhibitors induce cGAS-STING dependent inflammation resulting in cytokine induction and immune checkpoint activation. *bioRxiv* **2019**. [CrossRef]
224. Srinivas, U.S.; Tan, B.; Vellayappan, B.A.; Jeyasekharan, A.D. ROS and the DNA damage response in cancer. *Redox Biol.* **2019**, *25*, 101084–101093. [CrossRef]
225. Corces, M.R.; Granja, J.M.; Shams, S.; Louie, B.H.; Seoane, J.A.; Zhou, W.; Silva, T.C.; Groeneveld, C.; Wong, C.K.; Cho, S.W.; et al. The chromatin accessibility landscape of primary human cancers. *Science* **2018**, *362*, eaav1898. [CrossRef] [PubMed]
226. Temko, D.; Tomlinson, I.P.M.; Severini, S.; Schuster-Böckler, B.; Graham, T.A. The effects of mutational processes and selection on driver mutations across cancer types. *Nat. Commun.* **2018**, *9*, 1857–1867. [CrossRef] [PubMed]
227. Alexandrov, L.B.; Alexandrov, L.B.; Nik-Zainal, S.; Wedge, D.C.; Aparicio, S.A.; Behjati, S.; Biankin, A.V.; Bignell, G.R.; Bolli, N.; Borg, A.; et al. Signatures of mutational processes in human cancer. *Nature* **2013**, *500*, 415–421. [CrossRef] [PubMed]
228. Helleday, T. Homologous recombination in cancer development, treatment and development of drug resistance. *Carcinogenesis* **2010**, *31*, 955–960. [CrossRef]
229. Palla, V.V.; Karaolanis, G.; Katafigiotis, I.; Anastasiou, I.; Patapis, P.; Dimitroulis, D.; Perrea, D. gamma-H2AX: Can it be established as a classical cancer prognostic factor? *Tumour Biol.* **2017**, *39*, 1010428317695931. [CrossRef]
230. Murai, J.; Thomas, A.; Miettinen, M.; Pommier, Y. Schlafen 11 (SLFN11), a restriction factor for replicative stress induced by DNA-targeting anti-cancer therapies. *Pharmacol. Ther.* **2019**, *201*, 94–102. [CrossRef]
231. Infante Lara, L.; Fenner, S.; Ratcliffe, S.; Isidro-Llobet, A.; Hann, M.; Bax, B.; Osheroff, N. Coupling the core of the anticancer drug etoposide to an oligonucleotide induces topoisomerase II-mediated cleavage at specific DNA sequences. *Nucleic Acids Res.* **2018**, *46*, 2218–2233. [CrossRef]
232. Ke, X.; Lin, W.; Li, X.; Wang, H.; Xiao, X.; Guo, Z. Synergistic dual-modified liposome improves targeting and therapeutic efficacy of bone metastasis from breast cancer. *Drug Deliv.* **2017**, *24*, 1680–1689. [CrossRef]
233. Asakura, T.; Yokoyama, M.; Shiraishi, K.; Aoki, K.; Ohkawa, K. Chemotherapeutic effect of CD147antibody-labeled micelles encapsulating doxorubicin conjugate targeting cd147-expressing carcinoma cells. *Anticancer Res.* **2018**, *38*, 1311–1316.
234. Shi, J.; Su, Y.; Liu, W.; Chang, J.; Zhang, Z. A nanoliposome-based photoactivable drug delivery system for enhanced cancer therapy and overcoming treatment resistance. *Int. J. Nanomed.* **2017**, *12*, 8257–8275. [CrossRef]
235. Goffart, S.; Hangas, A.; Pohjoismäki, J.L.O. Twist and Turn-Topoisomerase Functions in Mitochondrial DNA Maintenance. *Int. J. Mol. Sci.* **2019**, *20*, 2041. [CrossRef] [PubMed]
236. Baechler, S.A.; Factor, V.M.; Dalla Rosa, I.; Ravji, A.; Becker, D.; Khiati, S.; Miller Jenkins, L.M.; Lang, M.; Sourbier, C.; Michaels, S.A.; et al. The mitochondrial type IB topoisomerase drives mitochondrial translation and carcinogenesis. *Nat. Commun.* **2019**, *10*, 83–96. [CrossRef] [PubMed]

© 2020 by the authors. Licensee MDPI, Basel, Switzerland. This article is an open access article distributed under the terms and conditions of the Creative Commons Attribution (CC BY) license (http://creativecommons.org/licenses/by/4.0/).